LA--8775-C

DE83 006219

LA-8775-C
Conference

UC-34
Issued: March 1981

CONF-810115 --

Proceedings of the Workshop on Nuclear and Particle Physics at Energies up to 31 GeV: New and Future Aspects

Held at the Los Alamos National Laboratory

Los Alamos, New Mexico

January 5—8, 1981

Edited by

J. D. Bowman
L. S. Kisslinger *
R. R. Silbar

* Consultant. Carnegie-Mellon University, Pittsburgh, PA 15213

ABSTRACT

This report contains the proceedings of the LAMPF Workshop on Nuclear and Particle Physics at Energies up to 31 GeV, New and Future Aspects, held in Los Alamos, January 5-8, 1981. Included are invited talks and contributed papers covering recent developments in (a) weak and unified interactions (including discussions of neutrino oscillations), (b) the hadronic description of strong interactions, (c) the quark description of strong interactions, (d) hypernuclei, and (e) new facilities and proposed experiments. One of the motivations for the Workshop was to explore physics justifications for a future high-intensity proton accelerator in this energy regime. A general conclusion reached by many, if not most, of the participants in the Workshop was that there are many very interesting physics questions that can be profitably addressed by such a new facility.

ORGANIZATION COMMITTEE

J. David Bowman, Los Alamos National Laboratory
Ernest M. Henley, University of Washington
Leonard S. Kisslinger, Carnegie-Mellon University
Richard R. Silbar, Los Alamos National Laboratory

PREFACE

These proceedings are organized by subject rather than by the chronological order in which the papers were given, with the contributed papers placed according to the subject matter after the appropriate invited papers. The editors hope that this will make this volume more useful as a reference work. We did not attempt to include the discussion, although this was a valuable part of the workshop.

ACKNOWLEDGMENTS

The organizers of the workshop would like to thank L. Rosen for his encouragement and financial support. They would also like to thank their colleagues for their advice, Laura Shreffler for assistance in the preparation of the proceedings, and Alice Horpedahl for unstinting efforts in all phases of the organization.

WORKSHOP PARTICIPANTS

Aerts, Adrian, Los Alamos
Agnew, Lewis, Los Alamos
Allred, John C., Los Alamos
Amann, James, Los Alamos
Anderson, Herbert, Los Alamos
Ashery, Daniel, ANL
Bacher, Andrew, Indiana U.
Barnes, Peter D., Carnegie-Mellon U.
Black, Kevin, Yale U.
Blankenbecler, Richard, SLAC
Blecher, Marvin, VPI and SU
Boal, David, Simon Fraser U.
Bolsterli, Mark, Los Alamos
Bonner, Billy E., Los Alamos
Bosted, Peter, American U.
Boudrie, Richard L., Los Alamos
Bowman, J. David, Los Alamos
Bradbury, James N., Los Alamos
Britt, H. C., Los Alamos
Browman, Andrew, Los Alamos
Brown, B. Alex, Oxford
Brown, R. E., Los Alamos
Bryman, Douglas, TRIUMF
Burman, Robert, Los Alamos
Burleson, George, NMSU
Cabibbo, Nicola, U. of Rome
Carey, Tom, Los Alamos
Carruthers, Peter, Los Alamos
Chrien, Robert E., BNL
Cooper, Martin, Los Alamos
Cornelius, W. D., Los Alamos
Cortez, Bruce, Harvard U.
Craddock, M. K., TRIUMF/U. of B.C.
Cutkosky, R. E., Carnegie-Mellon U
Dalpiaz, Pietro, U. of Toronto
Deady, Matthew, MIT/Bates
Deutsch, Martin, MIT
DeVries, Ralph, Los Alamos
Domingo, John, SIN
Donahue, Joey B., Los Alamos
Dropesky, Bruce J., Los Alamos
Duck, Ian, Rice U.
Duong-Van, M., Los Alamos
Eisenstein, Robert A., Carnegie-Mellon
Feshbach, Herman, MIT
Flynn, Edward R., Los Alamos
Fortune, H. T., U. of Pennsylvania
Frank, James, Los Alamos
Funsten, Herbert, College of Wm & Mary
Gazzaly, M., U. of Minnesota
Gibson, Benjamin F., DOE
Gladisch, Michael, Yale U.
Glass, George, Fermilab
Goldman, Terry, Los Alamos
Greben, J. M., TRIUMF
Greene, Steven J., Los Alamos
Grenacs, Laslo, U. of Louvain
Hagerman, Donald, Los Alamos
Hahn, Alan A., SIN
Haji-Saeid, S. Mohammad, UCLA
Hargrove, Clifford, NRC of Canada
Harvey, Carol, U. of Texas
Haxton, Wick, Los Alamos
Heffner, Robert, Los Alamos
Heller, Leon, Los Alamos
Henley, Ernest, U. of Washington
Herczeg, Peter, Los Alamos
Highland, Virgil, Temple U.

Hintz, Norton, U. of Minnesota
Hoffman, Cyrus M., Los Alamos
Hoffman, Earl, Los Alamos
Hughes, Vernon, Yale U.
Hungerford, E. V., U. of Houston
Hwa, Rudolph, Oregon State U.
Hynes, Michael, Los Alamos
Igo, George, UCLA
Irom, Farokh, UCLA
Jackson, K. Peter, TRIUMF
Jacob, Richard J., Arizona State U.
Jarmer, John J., Los Alamos
Jarmie, Nelson, Los Alamos
Jovanovich, Jovan, U. of Manitoba
Johnson, Mikkel, Los Alamos
Kalogeropoulos, E. Ted, Syracuse U.
Kamae, Tuneyoshi, LBL/U. of Tokyo
Kapusta, Joe, Los Alamos
Kaufmann, William, Arizona State U.
Kelly, Robert L., LBL
Kenichi, Imai, ANL
Kerman, Arthur K., MIT
King, Nick, Los Alamos
Kinnison, W. Wayne, Los Alamos
Kisslinger, Leonard, Carnegie-Mellon U.
Kloet, W. M., Rutgers U.
Knapp, E. A., Los Alamos
Knowles, Brook, U. of New Mexico
Ko, Winston, U. of California, Davis
Kruse, Harold W., Los Alamos
Kyle, Gary, SIN
Kunselman, Ray, U. of Wyoming
Leitch, Michael J., Los Alamos
Leon, Melvin, Los Alamos
Liu, Lon-Chang, Los Alamos
Loman, Earle, MIT
Lowenstein, Derek I., BNL
Ma, Ernest, U. of Hawaii, Manoa
Macek, Robert, Los Alamos
Mann, Alfred, U. of Pennsylvania
Matis, Howard, Los Alamos
Matthews, June, MIT
May, Morgan, BNL
McClelland, John, Los Alamos
McDonald, W. John, LBL
McFarlane, W. K., Temple U.
McNaughton, M. W., Los Alamos
Miller, James, Boston U.
Mischke, Richard, Los Alamos
Moore, C. Fred, U. of Texas
Morgado, Richard E., Los Alamos
Morris, Chris, Los Alamos
Moses, John, Los Alamos
Moss, Joel, Los Alamos
Mottershead, Charles T., EG&G
Mulders, Peter J., Los Alamos
Mutchler, Gordon, Rice U.
Nagle, Darragh, Los Alamos
Nagamiya, Shoji, LBL
Nefkens, B.M.K., UCLA
Nieto, Michael M., Los Alamos
Ng, John, TRIUMF
Paciotti, Michael, Los Alamos
Pasierb, Elaine L., U. of CA, Irvine
Pauletta, Gianni, UCLA
Peng, Jen-Chieh, Los Alamos
Phillips, G. C., Rice U
Pile, Philip, Carnegie-Mellon U.
Piekarz, Henry, BNL
Rahbar, Ali A., UCLA
Ransome, Ronald, Los Alamos
Redwine, Robert, MIT

Remsberg, Louis P., BNL
Richardson, C. R., DOE
Riley, Peter, U. of Texas
Roberts, J. B., Rice U.
Rosen, Louis, Los Alamos
Rosen, S. Peter, Purdue U.
Rosenthal, A. S., Vancouver, BC
Rössle, Erwin, Freiburg
Sandberg, Vern, Los Alamos
Schroeder, Lee S., LBL
Seth, Kamal K., Northwestern U.
Serot, Brian, Stanford U.
Shera, E. Brooks, Los Alamos
Sierk, Arnold J., Los Alamos
Silbar, Richard R., Los Alamos
Simmons, James E., Los Alamos
Soni, A., U. of California, Irvine
Spinka, Harold, ANL
Stein, Nelson, Los Alamos
Stearns, Robert, Vassar College
Strottman, Daniel, Los Alamos
Sunier, Jules W., Los Alamos
Stephenson, Gerard, Los Alamos
Tabakin, Frank, U. of Pittsburgh
Talaga, Richard, Los Alamos
Thiessen, H. A., CERN/Los Alamos
Teng, Lee, Fermilab
Toevs, James W., Los Alamos
Tombrello, Thomas, Cal Tech/Los Alamos
Tripp, Robert D., LBL
Tzeng, Yihard, U. of Virginia
Turpin, Stephen, Rice U
Van Dyck, Olin, Los Alamos
Van Oers, Willem T.H., U. of Manitoba
Vieira, David, Los Alamos
Vogt, Erich, Vancouver, BC
Vuilleumier, Jean-Luc, Cal Tech/SIN
Walker, George, U. of Washington
Wallace, Stephen J., U. of Maryland
Werbeck, Richard, Los Alamos
Wang, Chu-Hsiang, Fermilab
Winstein, Bruce D., U. of Chicago
Wohlfahrt, Hans-Dieter, Los Alamos
Woloshyn, Richard, TRIUMF
Yang, Ming-Jen, Los Alamos
Yan, Wuguang, SLAC
Ye, Ming-Han, Princeton U.
Zeidman, Benjamin, ANL
zu Putlitz, Gisbert, U. of Heidelberg

Clinton P. Anderson Meson Physics Facility

PROGRAM

NUCLEAR AND PARTICLE PHYSICS AT ENERGIES UP TO 31 GeV: NEW AND FUTURE ASPECTS

Los Alamos National Laboratory
January 5—8, 1981

MONDAY, January 5	Los Alamos National Laboratory Study Center
	Session Chairman: V. Hughes, Yale University
8:15 - 8:45 a.m.	REGISTRATION
8:45 - 8:55	Welcome - L. Rosen/G. Bell, MP- and T-Division Leaders
8:55 - 9:05	*Introduction to the Workshop* - L. Kisslinger, Carnegie-Mellon University
9:05 - 9:50	N. Cabibbo, University of Rome *"New Directions in Weak Interactions"*
9:50 - 10:05	Contributed Paper
10:05 - 10:30	COFFEE BREAK
10:30 - 11:15	C. Hargrove, National Research Council of Canada *"Rare π and μ Decays"*
11:15 - 11:25	Contributed Paper
11:25 - 12:05	B. Winstein, Enrico Fermi Institute *"K Decays"*
12:05 - 12:20	Contributed Paper
12:20 - 1:30 p.m.	LUNCH
	Session Chairman:
1:30 - 2:20	R. Kelly, Lawrence Livermore Laboratory *"πN and NK Phenomenology"*
2:20 - 3:10	R. Eisenstein, Carnegie-Mellon University *"K and π Elastic and Inelastic Scattering from Nuclei"*
3:10 - 3:40	COFFEE BREAK
3:40 - 4:00	W. Kloet, Rutgers University *"Dibaryons — Theoretical"*
4:00 - 4:20	H. Spinka, Argonne National Laboratory *"Dibaryons — Experimental"*
4:20 - 5:15	Contributed Papers
5:15 - 6:30	DIRECTOR'S RECEPTION (Study Center)

TUESDAY, January 6	Los Alamos National Laboratory Study Center
	Session Chairman: H. Feshbach
8:15 - 9:15 a.m.	Colloquium — Vernon Hughes, Yale University *"Internal Spin Structure of the Proton"*
9:15 - 10:05	A. Kerman, Massachusetts Institute of Technology *"Quark Bags"*
10:05 - 10:20	Contributed Paper
10:20 - 10:45	COFFEE BREAK
10:45 - 11:35	R. Blankenbecler, SLAC *"Quark Structure of Nuclei"*
11:35 - 12:15	Contributed Papers
12:15 - 1:30 p.m.	LUNCH
	Session Chairman: Peter Rosen, Purdue University
1:30 - 2:15	A. Mann, University of Pennsylvania *"Neutrino Mass Oscillations"*
2:15 - 2:45	A. Hahn, SIN *"New Neutrino Oscillations Results from ILL"*
2:45 - 3:10	Contributed Paper
3:10 - 3:40	COFFEE BREAK
3:40 - 4:00	R. Tripp, Lawrence Berkeley Laboratory *"Antiproton Nucleon Experiments"*
4:00 - 4:50	P. Dalpiaz, University of Torino *"Research Program at LEAR"*
4:50 - 5:15	Contributed Papers
6:30 - 10:00	BANQUET AT BOCCACCIO'S

WEDNESDAY, January 7	Los Alamos National Laboratory Study Center
	Session Chairman: G. Keyworth, Los Alamos National Laboratory
8:45 - 9:35 a.m.	L. Teng, Fermi Laboratory *"A Fast Cycling Proton Synchrotron as a Kaon Factory"*
9:35 - 10:00	Contributed Papers
10:00 - 10:30	COFFEE BREAK
10:30 - 11:20	H. Thiessen, Los Alamos National Laboratory/CERN *"Nuclear Physics with High-Energy Pions"*
11:20 - 12:15	Contributed Papers
12:15 - 1:30 p.m.	LUNCH
	Free Afternoon. A tour of LAMPF will be available and skiing on Pajarito Mountain, conditions permitting.
5:30	COCKTAIL PARTY sponsored by LRS, Los Alamos Inn, Jemez Room

THURSDAY, January 8	Los Alamos National Laboratory Study Center
	Session Chairman: E. Vogt, University of British Columbia
8:45 - 9:35 a.m.	P. Barnes, Carnegie-Mellon University *"Hypernuclei"*
9:35 - 10:15	Contributed Papers
10:15 - 10:45	COFFEE BREAK
10:45 - 12:15	Contributed Papers
12:15 - 1:30 p.m.	LUNCH
	Session Chairman: P. Carruthers, Los Alamos National Laboratory
1:30 - 2:20	R. Hwa, Oregon University *"Implications of QCD for Soft Hadronic and Nuclear Physics"*
2:20	Conference Wrap-up: E. Henley, University of Washington *"Physics at a Future High-Intensity Facility of $E \leq 31$ GeV"*

TABLE OF CONTENTS

Page

III. STRONG INTERACTIONS: HADRONIC DESCRIPTION

IV. STRONG INTERACTIONS - QUARK DESCRIPTION

WELCOME

by

Louis Rosen
Director of the Los Alamos Meson Physics Facility

It is my pleasant privelege to welcome you this morning to Los Alamos and to this workshop; and while I'm at it to wish you all a very good new year. This is the third major workshop which has been held to explore activities associated with LAMPF. The first two had mainly to do with trying to understand the programs we were pursuing and where we should be going this year, next year, and perhaps the year or two after. The present workshop is different. It looks to the long range future. It will have an impact on what happens in nuclear physics and what happens with LAMPF not during this decade, but during the 1990's. In this connection, I should like to mention two or three factors of which you should be mindful as you deliberate and ponder the opportunities and the promises that are held out in the field of nuclear and particle physics at rather low energies, at up to 30 or so GeV. To make my point I'll tell you of two experiences. One year ago in Japan we were invited to give some talks and discuss with our Japanese colleagues where they are going in intermediate energy physics during the next five or ten years What impressed me greatly on that trip was a discussion I had with a very high official of the ministry of science and education. He told me about a disease which had already been noticeable in this country for some years. The disease he talked about was that the young people, the bright young people in Japan were opting out of the hard sciences and into the humanities, economics, business, industrial management, personnel management, activities which have to do with the equitable distribution of goods and services, rather than with how one produces them in the first place. That is the first thing I wanted to tell you about. The second thing occurred more recently, about two or three weeks ago, when I was in the Soviet Union on an official but different kind of mission having to do with scientific collaborations. And there I had a thirty minute talk with a prominent physicist whom I have known for many years. I was amazed when he told me the same story that I had heard in Japan, that in Russia the bright young people are now opting out of the basic science

and engineering disciplines and into what we would call the soft sciences. Now for this to happen in Russia is really amazing because the pressures on them to do quite the opposite are enormous. And so these two incidents tell me that workshops of this type have an even greater responsibility and can have an even greater impact than perhaps the organizers had in mind when first they envisioned this particular gathering. I think it is imperative that we worry about the scientific motivation of what we're going to do, even at the expense of how we might do it. There was a time when we worried about how you build a certain machine because we knew that if we could build it, we would find interesting things to do with it; and that may still be true if you talk about machines and energies beyond where people now are working. But when you start talking of an energy region that has been worked over at least once, then you have an enormous responsibility to envision what is the exciting science that might be done. A good way to judge whether the science to be done is really exciting is to ask the question, "will this attract some of the brightest young people, who might be looking at science in the years ahead, as a discipline that they might enjoy pursuing as their life work?" Well that is the brief message I have to relate to you this morning.

I hope you have very good meetings, and if there is anything any of us here at Los Alamos can do to make your stay more productive and more enjoyable, please let us know, and we will try! Thank you very much.

WELCOME

by

George I. Bell
Division Leader, Theoretical Division

On behalf of the Theoretical Division, I wish to join Louie in welcoming you to this workshop and I offer my personal apologies to those of you who may have brought skis or enthusiasm for powder skiing in the sunny southwest. At least we have sun today although the snow is probably better where you came from.

I might remark in following up Louie's comments, that Don Kerr, the Director of the laboratory, has organized a working group to review the merits and possibilities of upgrading the Los Alamos accelerator to reach the energy region you are going to be talking about. The working group is chaired by Peter Carruthers and Louie is a member, Gerry Stephenson is another member and if you have remarks or comments either in writing or in person, in depth or casually, I am sure the members of the committee would be delighted to have your input and to have some discussion with you on these matters.

I also want to make a couple of remarks about the Theoretical Division with which some of you may not be well acquainted. In addition to the nuclear and particle theory aspects of our division, which you will be encountering here and probably are already somewhat familiar with, we have a large group of people who are engaged in atomic and molecular theory, including theoretical chemistry with special applications to laser isotope separation, we have a group of applied mathematicians, and we have people who are engaged more in the engineering sciences, I think you would say, at least from an academic viewpoint; i.e., they work on things like fluid dynamics, transport theory, material properties. Since all of these activities are in one division, we have an interdisciplinary cooperative sort of atmosphere, we hope. Illustrative of the interdisciplinary nature of this division and also the laboratory in general, is the recent creation of the Center for Nonlinear Studies here which is intended to bring together academic people, theorists at the laboratory, and people involved in programmatic activities who are concerned with nonlinear problems that arise in their practical problems. The Center for Nonlinear Studies is just getting started and one

of the primary motivations is to increase our contacts and interactions with academic communities, so those of you who may be thinking of a sabbatical and have a deep interest in nonlinear studies might think about the possibility of spending some time at Los Alamos.

So with that commercial, I return you to the Program Chairman.

INTRODUCTION

by

Leonard S. Kisslinger
Carnegie-Mellon University
Pittsburgh, Pennsylvania

It seems fair that the organizers of this workshop should let you know of our objectives before we begin, although I might take the liberty of revising this introduction on Thursday afternoon.

About thirty years ago, the field of particle physics arose as an (almost) separate field out of nuclear physics. Nuclear structure physics proceeded with the study of the nuclear many-body problem, while particle physicists identified and classified the baryons, mesons, and leptons, and explored the nature of the fundamental dynamics. The area of medium energy physics started (or perhaps it might be better to say resumed) as the meson factories came into operation about 1970. It resumed as a branch of nuclear physics, but there has been a considerable overlap of interest with particle physics.

Meanwhile, the particle physicists not only clearly established that the baryons and mesons have structure, but also developed the quark model, which has made great progress in their description. Particle physics at medium energy, which has been engaged in discovering the baryon and meson modes and their interreactions, has thus become a quark many-body problem or at least quark few-body problem. This in turn has attracted nuclear structure physicists, who like nothing better than to study systems of particles in terms of the fundamental interactions. The fact that this is a relativistic field theoretical problem, with the concept of confinement not yet explained, does not seem to frighten away a courageous group of theorists.

The first purpose of the present workshop is to bring together the nuclear and particle physicists with related interests, and to discuss the work in progress relevant to medium energy.

The second purpose of the workshop is to evaluate the various problems in the light of what might be most interesting in, say, 1990. At that time, the meson factories will be about 20 years old, the ZGS will have been shut down for 10 years, and the AGS will have as its first priority the feeding of ISABELLE. The CERN accelerator and LEAR will be quite mature. Therefore, it is essential for us to immediately start planning for a future high intensity facility (LANAC)

if it is to be ready for the decade of the 1990s--for ourselves and for the next generation of physicists. We must do as much for the next generation as those who worked for the meson factories did for us (and themselves, since many are with us at this workshop).

The workshop starts out today with the relatively pure subject of weak interactions. Recent progress in theory and experiment will be reviewed, with particular attention to present and future experimental tests of weak interaction theories.*

Today we shall also learn of recent developments in strong interaction physics: meson-nucleon and meson-nucleus physics. The nature of the meson and baryon modes and their interactions with nuclei are basic questions for medium energy physics. Two other subjects of great current interest for the study of hadronic systems in terms of hadrons and of quark models, dibaryons and baryonium, are discussed this afternoon and tomorrow afternoon. The discussion of baryonium, a subject which has faded somewhat during the past year, is of considerable importance to this workshop as one aspect of planning for anti-protons at a new facility. Tomorrow's talk on the physics program at LEAR will review the proposed CERN program of $\bar{p}$ physics. In thinking about new directions in medium energy physics, the planners will be reaching a decision whether the LANAC should have the capability of producing high-intensity antiproton beams. I hope that this workshop can help in making such a decision.

On Thursday morning, hypernuclear physics will be reviewed. We know that this topic is central for the many-body nuclear physics of the present and the future. Current work on the nature of the baryon-baryon interactions is of particular interest, and the development of the Λ and Σ shell model is an important program. Current experimental research is centered at BNL and CERN. The future depends on more intense kaon beams.

A good deal of time will be devoted to quark models, with three major talks tomorrow morning and Thursday afternoon. A central theoretical problem for this decade is the understanding of the structure, and weak and strong interactions, of hadrons and nuclei in terms of quarks, gluons, gauge bosons, and maybe Higgs particles, in the fundamental theory--which now seems to be gauge field theories and QCD. Perhaps the most fundamental problem for medium energy physics for this

*On Tuesday afternoon there will be an extensive discussion of neutrino oscillation experiments and their theoretical implications.

decade will be the understanding of confinement. We shall hear a colloquium tomorrow morning on recent progress in experiments on nucleon structure, an important part of this subject.

At the present time, studies of grand unified theories of strong, weak, and electromagnetic interactions are not considered to be part of medium energy physics, but in the light of the great energy, or the very early cosmological times needed for direct tests, one should explore the possibility of tests of GUT's at medium energies. Discussions of this point are welcome.

Finally, on Wednesday morning there will be a session on new accelerators, beams, and detectors. The importance of this subject is manifest.

The organizers, Dave Bowman, Ernie Henley, Dick Silbar, and I, have tried to allow time for discussion. We hope that no chairman will be forced to halt discussion because of the schedule.

Those are our objectives. Now let's see how we do.

Perspectives on Weak Interactions

N. Cabibbo

New York University
and
Instituto di Fisica, University of Rome*

The past decade has been one of very successful developments in weak interaction physics as evidenced by the following discoveries:

- Weak neutral currents
- J/ψ and other charmonium states
- Charmed particles
- Upsilon states
- Bottom hadrons

just to mention some of the high points! It is easy, on the basis of widely accepted theoretical ideas, to formulate a shopping list for the following ten to fifteen years:

- $t\bar{t}$ states
- top hadrons
- W and Z bosons
- proton decay
- neutrino oscillations (?)
- the Higgs boson

---

*Permanent address.

The question is: Is this list complete? Most probably not.

Although it is important to specify goals on the basis of current theoretical ideas, it is equally important to realize that these ideas are far from complete (more on this point later) and that one should not leave any stone unturned. The advances in experimental facilities and methods offer new opportunities for pushing down the limits on theoretically unexpected phenomena. These opportunities are as important as those offered by conducting experiments that are suggested by current theory. In this talk, I will concentrate on the latter, and in particular on the possible contributions of experiments carried out at intermediate energies with high intensity facilities.

I intend to discuss three areas:

1) Precision tests of the Glashow-Salam-Weinberg (GSW) theory;

2) Quark mixing and CP-violation;

3) Grand unified theories and neutrino oscillations.

1) Precision tests of the GSW scheme.

One of the most striking predictions of GSW is that of a relation between low energy neutral current data, embodied in the parameter $\sin^2\theta_W$ and the masses of the Z and W bosons, namely:

$$M_W = M_o(\sin\theta_W)^{-1}\ (1+\delta_W) \qquad 1a)$$

$$M_Z = M_o(\sin\theta_W \cos\theta_W)^{-1}\ (1+\delta_Z) \qquad 1b)$$

where $M_o = (\alpha G_F)^{-1/2}$ and δ_W, δ_Z represent higher-order electromagnetic and weak corrections. These corrections have been computed to order α by different groups [1], and more recently, the leading logarithm

terms $(\alpha \ln(M_W/m_e))^n$ have also been computed to all orders.[2] These corrections are of the order of 3-4% for both M_Z and M_W. A verification of Eq. (1) at the 1% level would offer an important test of GSW beyond the lowest order.

An accurate measurement of M_Z ($\delta M/M<1\%$) is certainly possible at e^+e^- machines, so that a test of Eq. (1b) hinges on an equally accurate measurement of $\sin\theta_W$. This is clearly a problem for low and intermediate energy experimentalists to attack. A promising approach would be to look for effects which vanish near the presently accepted value, $\sin^2\theta_W = .22$. An example of this in neutrino physics is offered by νp and $\bar{\nu} p$ elastic scattering at low energies ($E_\nu \sim 1$GeV). It is easy to show that*

$$\frac{\sigma_{\nu p} - \sigma_{\bar{\nu} p}}{\sigma_{\nu p} + \sigma_{\bar{\nu} p}} \quad \propto \quad (1 - 4 \sin^2\theta_W) \tag{2}$$

which indeed vanishes at $\sin^2\theta_W = 0.25$. An accurate enough measurement of this quantity would probably require more intense neutrino beams than those presently available at the Brookhaven AGS or at the CERN PS. An accurate measurement of $\sin^2\theta_W$ is also important for testing Grand Unified theories, as will be noted later.

2) Quark-Mixing and CP-Violation

Kobayashi and Maskawa[3] (KM) pointed out in 1973 that if the

---

*After my talk, V. Hughes noted that another effect which is predicted to vanish similarly is parity violation in Möller scattering.

number of quarks is six or larger, then quark mixing can lead to CP-violation. The KM observation offers the basis for what is now (especially after the discovery of the b, the fifth quark) the widely accepted explanation for the violation of CP symmetry in the K^0-$\bar{K}^0$ system. A detailed verification of the scheme requires new experimentation not only at high energy (e.g., mass of the t-quark, decay properties of the b- and t-quarks) but also at lower energies.

Within a gauge theory, the weak charged current has the form:

$$J_\mu^W = \sum_{i,k} U_{ik}\, \bar{P}_i \tfrac{1}{2}\gamma_\mu(1+\gamma_5)\, N_k \quad ,$$

where $\{P_i\} = \{u,c,t,\ldots\}$ are the charge +2/3 quarks and $\{N_i\} = \{d,s,b\ldots\}$ are the charge -1/3 quarks. In order for J_μ^W to generate weak isospin, U has to be a unitary matrix. In the six quark case, its most general form is

P/N	d	s	b
u	CC_β	SC_β	S_β
c	$-S_\gamma S_\beta C - C_\gamma S e^{i\delta}$	$-S_\gamma S_\beta S + C_\gamma C e^{-i\delta}$	$S_\gamma C_\beta$
t	$-C_\gamma C_\beta S - S_\gamma C e^{i\delta}$	$-C_\gamma S_\beta S - S_\gamma C e^{-i\delta}$	$C_\gamma C_\beta$

I am using here the Maiani parametrization[4] which is more convenient than the original KM version. I also use the notation

$$\begin{aligned} C &= \cos\theta \quad , \quad S = \sin\theta \ , \\ C_\beta &= \cos\beta \quad , \quad S_\beta = \sin\beta \ , \\ C_\gamma &= \cos\gamma \quad , \quad S_\gamma = \sin\gamma \ , \end{aligned} \tag{4}$$

where θ is the usual weak interaction angle,* β and γ are two new mixing angles, and δ is a phase parameter leading to CP-violation. An analysis of available date [4,5] (involving a comparison of semi-leptonic and leptonic processes, the K_L-K_S mass difference, the rate for $K_L \to \mu^+\mu^-$, etc.) indicates that β must be fairly small, ($\beta < \theta/2$) while a larger range is possible for γ. Recent Cornell data [6] on B decays suggests that $\gamma > \beta$, since it is found that

$$\frac{\text{Branching Ratio (B-mesons} \to \text{charm)}}{\text{BR(B} \to \text{non-charm states)}} = \frac{\sin^2\gamma}{\tan^2\beta} > 1 \quad . \tag{5}$$

In the KM scheme, CP violation is natural (in that no new interaction must be postulated) but elusive. From the mixing matrix, it is clear that δ disappears (or can be eliminated by redefining the phases of P_i, N_i) whenever any one of S, S_β, S_γ equals zero. To see the relevance of this, consider the amplitude of any physical process:

$$A = a^+ + a^- \quad , \tag{6}$$

where a^+ is CP-conserving and a^- is CP-violating. Because of the above remark, we have:

$$a^- \propto \sin\beta \sin\gamma \sin\theta \sin\delta \tag{7}$$

The CP-violating amplitude is naturally small. The amount of CP-violation, given by

$$\text{CP-violation} = \frac{2a^-a^+}{(a^+)^2 + (a^-)^2} \quad , \tag{8}$$

---

* Ed. note: usually known as the "Cabibbo angle".

is also small, unless a is itself small. (But then the basic process will be rare).

As an example, in $K_L \to 2\pi$, we have

$$a^+ \propto \sin\Theta \ , \tag{9}$$

CP-violation $\propto \sin\beta \sin\gamma \sin\delta$.

Most of the effect is expected to arise from $K \leftrightarrow \bar{K}$ mixing, so that KM largely reproduces the results of Wolfenstein's superweak theory.[7] With the customary parametrization

$$\eta_{+-} = \varepsilon+\varepsilon' , \ \eta_{00} = \varepsilon-2\varepsilon' . \tag{10}$$

Superweak theory predicts $\varepsilon' \equiv 0$, whereas KM gives:[8]

$$1/200 \leqq |\varepsilon'/\varepsilon| \leqq 1/50 . \tag{11}$$

The uncertainty will be partly reduced by more information on β and γ and, hopefully, on the mass of the t-quark. Small as this is, it is still probably an easier target than the CP-violation effects expected in B decays[9] (which are at best $\sim$ 1%) and in D decays ($\sim 10^{-3}$ - 10^{-4}). An unambiguous value for ε' would require high precision studies of $K_L \to \pi\pi$ decay, suitable for a high intensity facility.

The ratio ε'/ε is particularly depressed by the fact that ε' proceeds through a $\Delta I = 3/2$ non-leptonic decay. It would be worthwhile to study other channels, such as $\pi^+\pi^-\pi^0$ (of both K_S and K_L), where CP-violation gives rise to an energy asymmetry

$$\frac{E_+ - E_-}{E_+ + E_-} \neq 0 \ , \tag{12}$$

and the contribution of terms not directly related to K_L -K_S mixing could be more important. (Again, a difficult, high statistics experiment is required.)

In conclusion, the differentiation between the KM and the super-weak schemes may be achieved with high statistics experiments. It is certainly a very important goal.

3) Grand Unified Theories - Neutrino Oscillations

It is widely believed that the presently known gauge symmetry, $SU(3)_{color} \times SU(2) \times U(1)$, which gives rise to the strong, weak and electromagnetic forces, is but a low energy remnant of a larger group structure, G. In the simpler, and so far more popular versions of grand unification, $G = SU(5)$ or $SO(10)$, the breakdown

$$G \rightarrow SU(3) \times SU(2) \times U(1) \qquad (13)$$

happens at a very large energy. One of the more striking consequences of these schemes is the prediction of proton instability, and the possible explanation of baryon asymmetry in the universe. Of more interest within the context of our discussion is a very definite prediction for the value of the Weinberg angle[10]. The most recent calculations lead to

$$\sin^2\theta_W = .210 \pm .005 \qquad (14)$$

This precise prediction (which will certainly be improved in the years to come) can be tested by precision neutrino experiments as discussed earlier.

Another consequence of grand unification schemes is that neutrino oscillations[11] have become a fully respectable possibility. Before grand unification, we lacked a mechanism to produce, in a natural way, the small neutrino masses required for oscillations. Grand unification provides such a natural mechanism. With some luck, neutrino mass

differences can lie in the range $\delta m^2 \geq 0.1(eV)^2$, where laboratory experiments are sensitive. If this is so, a very rich field will open up. Oscillations will be governed by a mixing matrix similar to that of quarks and will give rise to an intricate phenomenology. The values of the neutrino mixing angles can be relevant for different models of generation dynamics.[12] A different approach consists in assuming essentially a statistical origin of the mixing.[13] This can lead to substantial mixing and oscillation amplitudes.

The appearance of phase angles in the mixing matrix can give rise to CP-violation effects[14]. The transmutation pattern can be different for neutrinos and antineutrinos, e.g.,

$$P(\nu_\mu \to \nu_e) \neq P(\bar{\nu}_\mu \to \bar{\nu}_e) \ . \qquad (15)$$

Although many aspects of neutrino oscillations can be clarified through the study of reactor neutrinos, CP-violation effects require the use of higher energy neutrino and antineutrino beams of high intensity.

Concluding Remarks

I am convinced that the most exciting discoveries (at least to experimentalists) are those which are not predicted by the currently accepted theory. In spite of this, it is certainly important to recognize the existence of a body of significant and well-established physical problems that a new high intensity facility could help unravel. My list is certainly far from complete, but it is certainly encouraging. To tackle the problems I have indicated, the new facility should be able to provide high-quality beams of both kaons and neutrinos.

A final word on theory: The present model involves many arbitary parameters (15 to 25 depending on different hypotheses that one can make: massless or massive neutrinos, etc.) This number is not substantially changed by grand unification and thus gives a measure of the work yet to be done. We certainly need a little help from our friends*!

---

*The experimentalists, I mean.

References

(1) W. J. Marciano, Phys. Rev. D 20, 274 (1979); M. Veltman, Phys. Lett. 91B, 95 (1980).

(2) F. Antonelli and L. Maiani, to be published.

(3) M. Kobayashi and K. Maskawa, Prog. Theor. Phys. 49, 652 (1973).

(4) L. Maiani, Phys. Lett. 62B, 183 (1976).

(5) S. Pakvasa and H. Sugawara, Phys. Rev. D 14, 305 (1976); J. Ellis, M. K. Gaillard, and D. V. Nanopoulos, Nucl. Phys. B109, 213 (1976). For a good review, see M. K. Gaillard and L. Maiani, in Cargèse Lectures, 1979.

(6) Cornell B-Meson results, Madison conference, July 1980.

(7) L. Wolfenstein, Phys. Rev. Lett. 13, 562 (1964).

(8) See J. Ellis et al., ref. 5, and F. J. Gilman and M. B. Wise, SLAC-PUB-2341 (1979).

(9) See, e.g., V. Barger, W. F. Long, and S. Pakvasa, U. Wisc. COO-881-99 (1979); M. Bander, D. Silverman, and A. Soni, Phys. Rev. Lett. 43, 1242 (1979); and A. Carter and A. I. Sanda, Rockefeller preprint DOE/EK/2232B-205.

(10) T. Goldman and D. Ross, Phys. Lett. 84B, 208 (1979); W. J. Marciano, ref. 2.

(11) For a review by the originators of the concept, see S. M. Bilenky and B. Pontecorvo, Phys. Rep. 41C, 225 (1978).

(12) See, e.g., F. Wilczek and A. Zee, Phys. Rev. Lett. 42, 421 (1979).

(13) T. Goldman and G. J. Stephenson, LA-UR-80-3454.

(14) N. Cabibbo, Phys. Lett. 72B, 333 (1978).

EXPERIMENTS IN THE KAON SYSTEM

by

B. Winstein
University of Chicago

ABSTRACT

In this talk, we will review current experiments on kaon decays with a strong emphasis on those addressing the question of CP non-conservation. Experiments which could only be attempted with significantly more intense Kaon beams than now exist ("Kaon Factory" experiments) are also discussed. A point of view, currently ascribed to by the author, has been adopted for this talk: The Kobayashi-Maskawa model which links the CP non-conservation to the mass mixing among the quark doublets is most appealing and it is extremely important to test it against the superweak hypothesis.

I. Review of neutral Kaon phenomenology[1]

A. The mixing parameter ϵ and its measurement

Let us write

$\psi = \begin{pmatrix}\alpha\\ \beta\end{pmatrix}$, $\alpha = K^0$ amplitude

$\beta = \overline{K^0}$ amplitude

Then for the time development of the state ψ, we have

$$-\frac{d}{dt}\psi = i\left[\begin{pmatrix}M_{11} & M_{12}\\ M_{12}^* & M_{22}\end{pmatrix} + \frac{1}{2}\begin{pmatrix}\Gamma_{11} & \Gamma_{12}\\ \Gamma_{12}^* & \Gamma_{22}\end{pmatrix}\right]\psi$$

where M and Γ are Hermitian.

$M_{11} = M_{22}$; $\Gamma_{11} = \Gamma_{22}$ by CPT invariance.

M_{12}, Γ_{12} real if CP invariance is good.

Assuming CPT, and defining the eigenvalues (masses)

$$iM_S + \frac{1}{2}\Gamma_S \text{ and } iM_\ell + \frac{1}{2}\Gamma_\ell,$$

the eigenstates become

$$|K_S\rangle = \frac{1}{\sqrt{2}}\frac{1}{\sqrt{1+|\varepsilon|^2}}\{(1+\varepsilon)|K^0\rangle + (1-\varepsilon)|\overline{K^0}\rangle\}$$

$$|K_L\rangle = \frac{1}{\sqrt{2}}\frac{1}{\sqrt{1+|\varepsilon|^2}}\{(1+\varepsilon)|K^0\rangle - (1-\varepsilon)\overline{K^0}\rangle\}$$

or

$$|K_S\rangle = \frac{1}{\sqrt{1+|\varepsilon|^2}}\{|K_1\rangle + \varepsilon|K_2\rangle\}$$

$$|K_L\rangle = \frac{1}{\sqrt{1+|\varepsilon|^2}}\{|K_2\rangle + \varepsilon|K_1\rangle\}$$

where $\varepsilon = \dfrac{\text{Im } \Gamma_{12}/2 + i \text{ Im } M_{12}}{i(\Gamma_S - \Gamma_\ell)/2 - (M_S - M_\ell)}$.

It can be shown from the observed size of the parameter ε and the experimental limits on CP non-conservation in channels other than $K \to 2\pi$ that

$$\text{IM } \Gamma_{12}/2 << \text{Im } M_{12} \quad .$$

Additionally, the Kobayashi-Maskawa model would say[2]

$$\text{Im } \Gamma_{12}/2 \;/\; \text{Im } M_{12} \leq 10^{-4} \quad ,$$

which is indistinguishable from the superweak expectation of zero for this ratio. Thus from now on we will neglect Im Γ_{12}.

We see that the CP mixing can be described with just one parameter, ε, whose <u>phase</u> can be calculated in terms of the known quantities Γ_S, Γ_ℓ, and $\Delta m \equiv M_S - M_\ell$. The current value for this phase is given by (world average)

$$\phi_\varepsilon = 43.7^o \pm 0.2^o \quad . \quad \text{(calculated)}$$

How can $|\varepsilon|$ be measured? Since the K_L contains slightly more K^o than $\overline{K}^o$, and since the strangeness of the decaying Kaon is linked to the sign of the lepton in semileptonic decays, i.e., the K^o decays to positrons (here we assume the $\Delta S = \Delta Q$ rule), a measurement of the charge asymmetry in semileptonic decays can provide a measure of ε.

Letting N^+ and N^- be the number of detected leptons of plus and minus charge respectively, we find

$$2\mathrm{Re}\,\epsilon \equiv \delta = \frac{N^+ - N^-}{N^+ + N^-} \quad .$$

The most precise experiment (CERN-Heidelberg) obtains

$$\delta = (3.41 \pm 0.18)\ x10^{-3} \text{ from } Ke_3 \text{ decays}$$
$$= (3.13 \pm 0.29)\ x10^{-3} \text{ from } K\mu_3 \text{ decays.}$$

Averaging, we find

$$\mathrm{Re}\epsilon = (1.67 \pm 0.08) \times 10^{-3} \text{ (CERN-Heidelberg)}$$
$$= (1.64 \pm 0.06) \times 10^{-3} \text{ (World Average).}$$

From our value for $\phi\epsilon$, we can therefore deduce:

$$|\epsilon| = (2.27 \pm 0.08) \times 10^{-3} \text{ (from charge asymmetry)}$$

B. 2 decay modes

$$\text{Consider } K_L = \frac{1}{\sqrt{1+|\epsilon|^2}} \{|K_2> + \epsilon |K_1>\} \to 2\pi$$

The superweak hypothesis says that the 2π decay mode of the K_L comes solely from the ϵ admixture of the CP even state in the wave function, so that

$$\left.\begin{aligned} &\frac{\text{amp } K_L \to 2\pi}{\text{amp } K_S \to 2\pi} \equiv \begin{Bmatrix} \eta_{+-} \\ \eta_{oo} \end{Bmatrix} = \epsilon \\ &\text{amp } K_2 \to 2\pi = 0 \ , \\ &\text{amp } K^0 \to 2\pi = \text{amp } \overline{K^0} \to 2\pi \end{aligned}\right\} \text{ superweak}$$

As an experimental test of this hypothesis, consider the $\pi^+\pi^-$ decay distribution in an (initially) pure K^0 beam: $|K^0> \alpha\ |K_S> + |K_L>$
The rate of $\pi^+\pi^-$ decays as a function of proper time t is given by

$$R_{\pi^+\pi^-}(t) \propto \left| e^{i\Delta m t - t/2\tau_S} + \eta_{+-} e^{-t/2\tau_\ell} \right|^2$$

Thus a precision study of the interference of $K_{L,S} \to 2\pi$ can yield a measurement of η_{+-} (using Δm and $\tau_{S,\ell}$ from other determinations).

The results are

$$\eta_{+-} = (2.279 \pm 0.026) \times 10^{-3}\, e^{i(44.6^{o} \pm 1.2^{o})} \quad \text{(World Average)}$$

This is to be compared with

$$\varepsilon = (2.27 \pm 0.08) \times 10^{-3}\, e^{i(43.7^{\circ} \pm 0.2^{\circ})} \quad \text{(from charge asymmetry)}$$

Thus the hypothesis that

$$\eta_{+-} = \varepsilon$$

appears to be supported to remarkable accuracy. Why then are major new experimental efforts being launched to further study the $|K_2> \to 2\pi$ amplitude? To answer this question, we must look at the magnitude of the expected departures from the superweak model.

II. Theoretical Guidance: The Kobayashi-Maskawa model[3]

This highly appealing model relates CP nonconservation to the Cabibbo mixing among the quarks. The charged current weak interaction among the quarks is written as

$$J_{\mu}^{-} = (\bar{u}, \bar{c}, \bar{t})\, \gamma_u \begin{pmatrix} C_1 & -S_1C_3 & -S_1S_3 \\ S_1C_2 & C_1C_2C_3 - S_2S_3e^{i\delta} & C_1C_2S_3 + S_2C_3e^{i\delta} \\ S_1S_2 & C_1S_2C_3 + C_2S_3e^{i\delta} & C_1S_2S_3 - C_2C_3e^{i\delta} \end{pmatrix} \begin{pmatrix} d \\ s \\ b \end{pmatrix}$$

We note that with only 4 quarks, the CP violating phase factor $e^{i\delta}$ could not have been present. With the common notion that the mixing angles, like the Cabibbo angle θ_1, are small, the matrix reduces to

$$\begin{pmatrix} 1 & -S_1 & -S_1S_3 \\ S_1 & 1 - S_2S_3e^{i\delta} & S_3 + S_2e^{i\delta} \\ S_1S_2 & S_2 - S_3\, e^{i\delta} & S_2S_3 - e^{i\delta} \end{pmatrix}$$

In this model, the parameter ε arises from the imaginary part of the "box diagram"

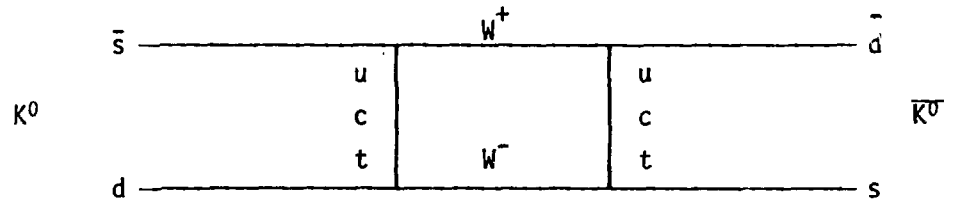

Calculations by Ellis, Gaillard, and Nanopoulos[2] and others yield

$$|\varepsilon| \simeq 2\, S_2 S_3 \sin\delta, \text{ assuming } m_t >> m_c$$

This relation can certainly be accommodated by experiment as neither S_2 nor S_3 are yet known with any precision.

The proposed model is a milliweak one in that CP violation occurs to first order in the weak interaction. Thus there are diagrams, for example, where $K \to 2\pi$ directly violates CP:

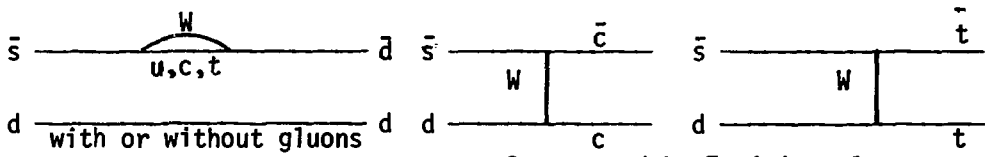

Suppressed by Zweig's rule

These diagrams (their imaginary part) will effectively induce a small phase difference between the $K \to 2\pi$ I=0 and I=2 transition amplitudes. (Note that if the $\Delta I = 1/2$ rule were exact for the $K \to 2\pi$ transitions, the final 2π state would be a pure I=0 state and therefore no CP violation in the direct decays could be observed. The known small size of the $\Delta I = 3/2$ transition, about 5% in amplitude, is partly responsible for the very small predicted direct effects, as we will see.)

Let

a_0 = $K \to 2\pi$ (I=0) transition amplitude

a_2 = $K \to 2\pi$ (I=2) transition amplitude

Then the $K_0 \to \pi^+\pi^-$ amplitude can be written as

$$\sqrt{\frac{1}{3}}\, a_0 e^{i\delta_0} + \sqrt{\frac{1}{6}}\, a_2 e^{i\delta_2}$$

$$= \sqrt{\frac{1}{3}}\, a_0 e^{i\delta_0} \left[1 + \frac{a_2}{\sqrt{2}a_0} e^{i(\delta_2 - \delta_0)}\right]$$

where $\delta_{2(0)}$ is the π-π phase shift in the I = 2(0) state.
We note, therefore, that there will be direct CP nonconservation in the decay of the K^0 provided a_2 and a_0 have different phases.

As a measure of the CP nonconservation in the $K \to 2\pi$ decay, the parameter ε' is defined by

$$\varepsilon' \equiv \frac{1}{\sqrt{2}} i \, \mathrm{Im} \left(\frac{a_2}{a_0}\right) e^{i(\delta_2 - \delta_0)}$$

In the superweak model, there is no direct decay, so $\varepsilon' = 0$. In the Kobayashi-Maskawa model, ε' has been evaluated by a number of authors and there is a great deal of uncertainty in its value. Estimates[4] are in the range

$$0.002 \lesssim \left|\frac{\varepsilon'}{\varepsilon}\right| \lesssim 0.02$$

The uncertainty is due in part to that in the mass of the top quark, the values of the two unknown Cabibbo angles, but mostly to uncertainties in the magnitudes of gluon corrections.
Note also that the phase of ε' is well determined from independent determinations[1] of δ_2 and δ_0 and, in fact, is accidentally very close to that of ε:

$$\phi(\varepsilon') = 37° \pm 5°$$

III. Experimental consequences of $\varepsilon' \neq 0$; current limits on $|\varepsilon'|$; future experiments.

A. A Gedanken Experiment

The Kobayashi-Maskawa model predicts a first order (milli-weak) CP violation in the direct decay of the K°. How can such an effect be detected?

In terms of our previously defined quantities, we have

$$\text{amp } K^\circ \to \pi^+\pi^- = \sqrt{\frac{1}{3}}\, a_0 e^{i\delta_0} \left[1 + \frac{1}{\sqrt{2}} \left(\frac{a_2}{a_0}\right) e^{i(\delta_2 - \delta_0)}\right]$$

$$\text{amp } \overline{K^\circ} \to \pi^+\pi^- = \sqrt{\frac{1}{3}}\, a_0^* e^{i\delta_0} \left[1 + \frac{1}{\sqrt{2}} \left(\frac{a_2}{a_0}\right)^* e^{i(\delta_2 - \delta_0)}\right]$$

Thus

$$\text{amp}\ \frac{K^\circ \to \pi^+\pi^-}{\overline{K^\circ} \to \pi^+\pi^-} = 1 + 2\varepsilon' \ ,$$

and

$$\frac{\text{Rate}\ K^\circ \to \pi^+\pi^-}{\text{Rate}\ \overline{K^\circ} \to \pi^+\pi^-} = 1 + 4\ \text{Re}\ \varepsilon'$$

The normalized time dependent decay curves will therefore look as follows:

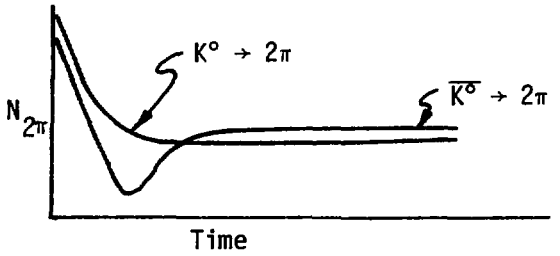

where the short time asymmetry is given by 4 Re ε' and that at long times by 4 Re ε. Thus in principle both mass mixing and direct CP effects could be revealed in such an experiment which only studies the $\pi^+\pi^-$ decays; in practice neither effect has yet been seen in this way.

B. Limits on ε' from charge asymmetry and $\pi^+\pi^-$ time distribution experiments

We note that $\eta_{+-} = \varepsilon + \varepsilon'$ which follows from our definition of ε'.

Thus

$$\text{Re}\ \frac{\eta_{+-}}{\varepsilon} = 1 + \text{Re}\ \frac{\varepsilon'}{\varepsilon} = 0.99 \pm 0.04$$

This implies $\left|\frac{\varepsilon'}{\varepsilon}\right| = .01 \pm .04$,

the result coming solely from measurements of η_{+-} and from the semi-leptonic charge asymmetry. The error is approaching the region of interest suggested by the Kobayashi-Maskawa model so that even more precise measurements of δ and η_{+-} could be contemplated.

C. Experiments on the $2\pi^0$ decay mode

It is clear that to detect the difference in K°, $\overline{K^\circ}$ decay amplitudes, the direct decay rate measurements are too "dilute" to see an $\simeq 10^{-5}$ effect. Ideally, one would like to prepare the state $K_2 = K_L - \varepsilon K_S$ which should not

decay to 2π unless $\varepsilon' \neq 0$. This is the essence of one of the ideas of the BNL-Yale group to which we will return. For now we will concentrate on the K_L decays themselves.

From the isospin decomposition, we find that

$$\eta_{oo} = \varepsilon - 2\,\varepsilon'$$

$$\eta_{+-} = \varepsilon + \varepsilon'$$

so that

$$\frac{\eta_{+-}}{\eta_{oo}} \simeq 1 + 3\varepsilon'/\varepsilon$$

$$R \equiv \left|\frac{\eta_{+-}}{\eta_{oo}}\right|^2 \simeq 1 + 6\varepsilon'/\varepsilon$$

There are three reasonably precise determinations of R:

R	$\sigma(\lvert\varepsilon'/\varepsilon\rvert)$	
1.00 ± 0.12	± 0.02	Holder et al. (1972)[5]
1.06 ± 0.14	± 0.023	Banner et al. (1972)[5]
1.00 ± 0.18	± 0.03	Christenson et al. (1979)[5]

(The latter group also obtained the most precise measurement of the phase of η_{oo}: $56° \pm 6°$)

Thus we see that the sum total of the data on K° decay, while of high quality and precision, and consistent with the superweak hypothesis, nevertheless barely probes the region of interest of the Kobayashi-Maskawa model: $|\varepsilon'/\varepsilon| = 0.002 - 0.02$.

D. New Experimental Determinations of ε'

The two most precise of the experiments quoted in the previous section were plagued by low statistics (about 300 $K \to 2\pi°$ events between them) and high backgrounds (from the dominant $K \to 3\pi°$ mode). Two new experiments have been approved and will run during the next year; some details can be found in the experimental proposals[6]. Both groups aim for high statistics ($\simeq$ 50K $2\pi°$ events), excellent mass and angle resolution, and very low background after analysis. The Chicago-Stanford group will convert one of the four gamma rays in the $2\pi°$ mode, tracking the resultant e^+e^- pair for good vertex resolution while the other three gammas are identified in a finely segmented

804-element lead glass detector. In addition, many systematic effects will be eliminated in the data taking as both decays of $K_L \to 2\pi^\circ$ (in one beam) and those of $K_S \to 2\pi^\circ$ (in another nearly parallel beam in which a regenerator is placed) are recorded simultaneously in identical environments. Although using only one beam with a regenerator cycling in and out periodically, the BNL-Yale group has a similar strategy.

Both experiments are aiming for a 1% measurement on the ratio of the directly measured quantity

$$R = \left|\frac{\eta_{+-}}{\eta_{oo}}\right|^2$$

This then would yield a determination of ε' with an uncertainty of .0017 ε. Thus the true sensitivity of the experiments is at the level of

$$\left|\frac{\varepsilon'}{\varepsilon}\right| \geq .004 \quad :$$

in this range, a non-zero effect can be "established" (to 2σ) or a 90% confidence limit set.

In addition, as suggested earlier, the BNL-Yale group plans to study the time dependence of 2π decays downstream of the regenerator.

The amplitude for $\pi^+\pi^-$ decays as a function of proper time t of the decay downstream of the regenerator is given by

$$A_{\pi^+\pi^-}(t) \propto \rho\, e^{i\Delta m t - t/2\tau_S} + \eta_{+-}$$

where ρ, the regeneration amplitude, depends upon properties of the regenerator and upon the Kaon momentum.

Suppose that we could "tune" ρ(e.g. by adjusting the length of the regenerator and the momentum) so that at some time t',

$$\rho\, e^{i\Delta m t' - t'/2\tau_S} = -\varepsilon \ .$$

Then we would have

$$A_{\pi^+\pi^-}(t') \propto -\varepsilon + \eta_{+-} = \varepsilon' \ ,$$

so that the observation of 2π decays at t' would directly rule out the superweak model! (It is clear that we have created a pure K_2 state at t=t'.) In practice, there is a momentum band, and ρ is not well enough known. How-

ever, by measuring both $\pi^+\pi^-$ and $\pi^0\pi^0$ near the minimum, one becomes insensitive to the exact value of ρ, and in fact the ratio of the two decay modes near the mi· shows a great deal of structure if $\varepsilon' \neq 0$. (The two decay distribu- ' are identical in shape if $\varepsilon' = 0$.)

While this effect is most interesting, it is not as statistically powerful as the "direct" measurement, although it may be freer of some systematic rors.

This concludes our discussion on $K \to 2\pi$ decays. To emphasize just how small the effect is, we show in the figure the range for the CP violating phase angle of the a_2 amplitude (in Kobayashi-Maskawa):

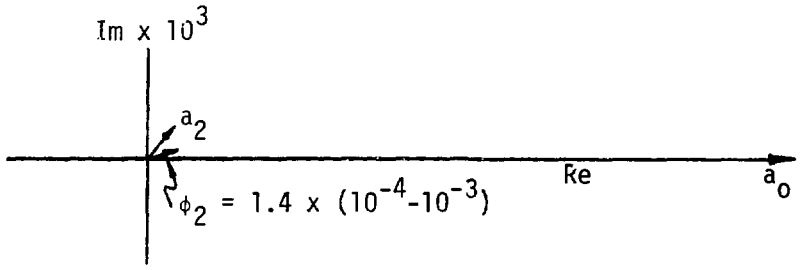

IV. Experimental Study of CP Violation in Semileptonic Decays

A. $K_L \to \pi^-\mu^+\nu$

A component of muon polarization lying normal to the decay plane, P_n, would be a measure of CP nonconservation, and the BNL-Yale group has published the results of the most recent search for such an effect.

If we let $A_{+(-)}$ = amplitude for muon production with positive (negative) helicity, then

$$P_t = 2 \text{ Re } (A_+A_-^*)/(|A_+|^2 + |A_-|^2) \text{ and}$$

$$P_n = 2 \text{ Im } (A_+A_-^*)/(|A_+|^2 + |A_-|^2)$$

where P_t is the transverse polarization of the muon in the decay plane.

The data are of high quality and the result[7] is

$P_t = 0.42$,

$P_n = 0.0021 \pm 0.0048$, which implies that

$\text{Im } \xi = \text{Im } f_-/f_+ = 0.012 \pm 0.026$.

Final state electromagnetic interactions would result in

$\text{Im } \xi \simeq 0.008$ (electromagnetic)

We note that the Kobayashi-Maskawa model predicts no effect to first order while the Weinberg model with extra Higgs would allow a non-zero value of P_n. Detailed calculations have yet to be performed.

B. $K^+ \to \pi^0 \mu^+ \nu$

The BNL-Yale group hopes to improve their sensitivity and as well eliminate final state interactions by studying the $K^+_{\mu 3}$ decay. Their (preliminary) result for the experiment in progress is

$$\text{Im } \xi = 0.015 \pm 0.055 \quad \text{(BNL-Yale } 2 \times 10^6 \text{ collected events)}$$

This can be compared with the world average of Im ξ = -0.09 ± 0.21. Their ultimate goal is to reach an error of ± 0.002.

V. Experimental Study of CP Non-conservation in $K \to 3\pi$

Consider the decay $K_S \to 3\pi$

$$|K_S\rangle = \frac{|K_1\rangle + \varepsilon |K_2\rangle}{\sqrt{1+|\varepsilon|^2}}$$

There are three contributions to the amplitude

$\varepsilon \cdot K_2 \to 3\pi$ (I=1) conserves CP in the decay: "state mixing"

$K_1 \to 3\pi$ (I=1) violates CP in the decay: "direct"

$K_1 \to 3\pi$ (I=2) conserves CP in the decay

The first (dominant) term contributes a factor ε to

$$\eta_{+-0} \equiv \text{Amp } (K_S \to \pi^+\pi^-\pi^0)/\text{Amp}(K_L \to \pi^+\pi^-\pi^0) .$$

The second is small with respect to ε in the KM model (and is zero in superweak) but could be large in other models while the third is suppressed by the angular momentum barrier (and in fact can be eliminated in the experiment under consideration).

Thus we expect $\eta_{+-0} \simeq \varepsilon$, which implies that

$$\text{Rate} \frac{K_S \to \pi^+\pi^-\pi^0}{K_L \to \pi^+\pi^-\pi^0} \simeq 4 \times 10^{-6}$$

Therefore the partial width is given by

$$\Gamma (K_S \to \pi^+\pi^-\pi^0) \simeq 10/\text{sec}$$

And thus for the branching ratio we expect

$$BR\ (K_S \to \pi^+\pi^-\pi^0) \approx 10^{-9}$$

To see how such a small branching ratio might be detected, consider the time evolution of a K^0 beam decaying to $\pi^+\pi^-\pi^0$.

$K^0 \alpha\ K_L + K_S$ so that for the rate of $\pi^+\pi^-\pi^0$ decays at proper time t, we have

$$\text{Rate}\ (K \to \pi^+\pi^-\pi^0) \propto \left| e^{-t/2\tau_\ell} + \eta_{+-0}\ e^{i\Delta m t - t/2\tau_S} \right|^2 \times \Gamma(K_L \to \pi^+\pi^-\pi^0)$$

Assuming $\eta_{+-0} = \varepsilon$, one has the following expectation:

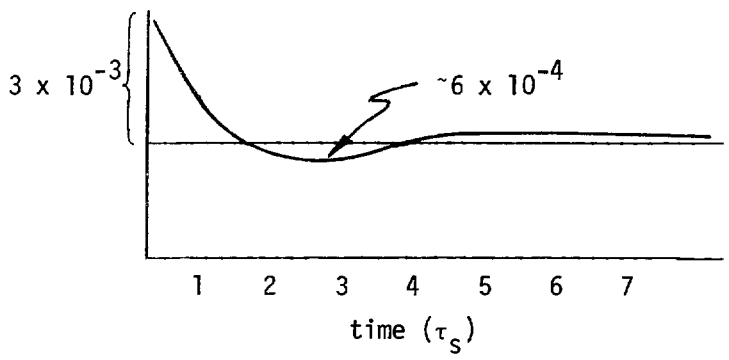

A CP violating effect shows itself in an interference term in the decay distribution which is first order in the amplitude. Thus the acceptance must be known to very high precision in order to isolate the expected 10^{-3} asymmetry. The RWMM[8] group at Fermilab plans to measure the acceptance variations with an additional production target located far upstream. They are planning a measurement to an accuracy of $\approx \varepsilon/4$ and need 150×10^6 events to attain that goal. Note that by having good acceptance over the Dalitz plot, the CP allowed $K_1 \to 3\pi(I=2)$ amplitude and the $K_2 \to 3\pi(I=1)$ amplitude have opposite symmetries with respect to pion interchange so their interference term cancels. Therefore, the observation of the interference term is a definite signature of CP nonconservation.

The difficulty of the experiment is evident when one quotes the current best determination[1]:

$$\left|\frac{\eta_{+-0}}{\varepsilon}\right| < 150.$$

Even less is known[1] about η_{000}:

$$\left|\frac{\eta_{000}}{\varepsilon}\right| < 230.$$

VI. CP Non-conservation in rare K decays

Here we rely heavily on the work done in Ref. 2 in applying the Kobayashi-Maskawa model to the rare K decays. Earlier work was done by Wolfenstein[9]. The paper of Gaillard and Lee[10] is most helpful. The relatively large effects arise from the fact that the heavier quarks can contribute without Zweig suppression. We will attempt to construct experiments to distinguish that model from the superweak hypothesis. It will be seen that these experiments can very likely be contemplated only in the context of a future Kaon factory, if at all.

A. $K \to \gamma\gamma$

For the case where the two gammas have positive CP the pattern of CP violation should reproduce that in 2π's in that the dominant contribution is found to be given the diagram

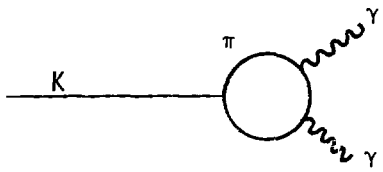

Then one finds $\dfrac{\text{amp } K_L \to \gamma\gamma(+)}{\text{amp } K_S \to \gamma\gamma(+)} = \varepsilon + \varepsilon'_{2\pi}$

where, as we recall in the KM model, $|\varepsilon'_{2\pi}/\varepsilon| = 1/500 - 1/50$

For the CP = - state of $\gamma\gamma$, the heavy quarks will contribute through the diagram

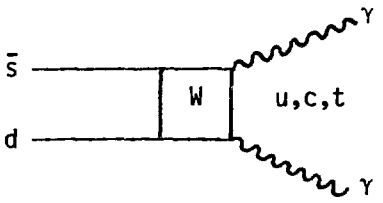

Writing $\dfrac{\text{amp } K_S \to \gamma\gamma(-)}{\text{amp } K_L \to \gamma\gamma(-)} = \varepsilon + \varepsilon'_{2\gamma(-)}$, the authors of Ref. 2 find

$$\frac{\varepsilon'_{2\gamma(-)}}{\varepsilon} \approx \frac{1}{15}$$

VI. CP Non-conservation in rare K decays

Here we rely heavily on the work done in Ref. 2 in applying the Kobayashi-Maskawa model to the rare K decays. Earlier work was done by Wolfenstein[9]. The paper of Gaillard and Lee[10] is most helpful. The relatively large effects arise from the fact that the heavier quarks can contribute without Zweig suppression. We will attempt to construct experiments to distinguish that model from the superweak hypothesis. It will be seen that these experiments can very likely be contemplated only in the context of a future Kaon factory, if at all.

A. $K \to \gamma\gamma$

For the case where the two gammas have positive CP the pattern of CP violation should reproduce that in 2π's in that the dominant contribution is found to be given the diagram

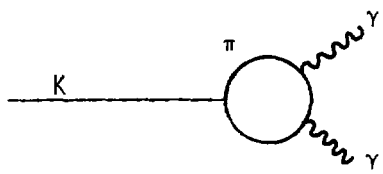

Then one finds $\dfrac{\text{amp } K_L \to \gamma\gamma(+)}{\text{amp } K_S \to \gamma\gamma(+)} = \varepsilon + \varepsilon'_{2\pi}$

where, as we recall in the KM model, $|\varepsilon'_{2\pi}/\varepsilon| = 1/500 - 1/50$

For the CP = - state of $\gamma\gamma$, the heavy quarks will contribute through the diagram

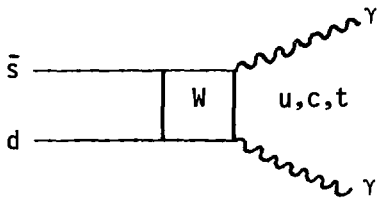

Writing $\dfrac{\text{amp } K_S \to \gamma\gamma(-)}{\text{amp } K_L \to \gamma\gamma(-)} = \varepsilon + \varepsilon'_{2\gamma(-)}$, the authors of Ref. 2 find

$$\frac{\varepsilon'_{2\gamma(-)}}{\varepsilon} \approx \frac{1}{15}$$

The following branching ratio table can then be constructed:

	$\gamma\gamma(+)$	$\gamma\gamma(-)$
K_L	$\underline{5 \times 10^{-9}}$	5×10^{-4}
K_S	2×10^{-6}	$\underline{5 \times 10^{-12}}$

where the underlined entries are CP violating and only the $K_L \to \gamma\gamma(-)$ has (presumably) been observed to date.

How can we observe such small CP violating effects? Consider, as we did for $K \to 3\pi$, the time distribution of 2γ decays in an initially pure K° beam:

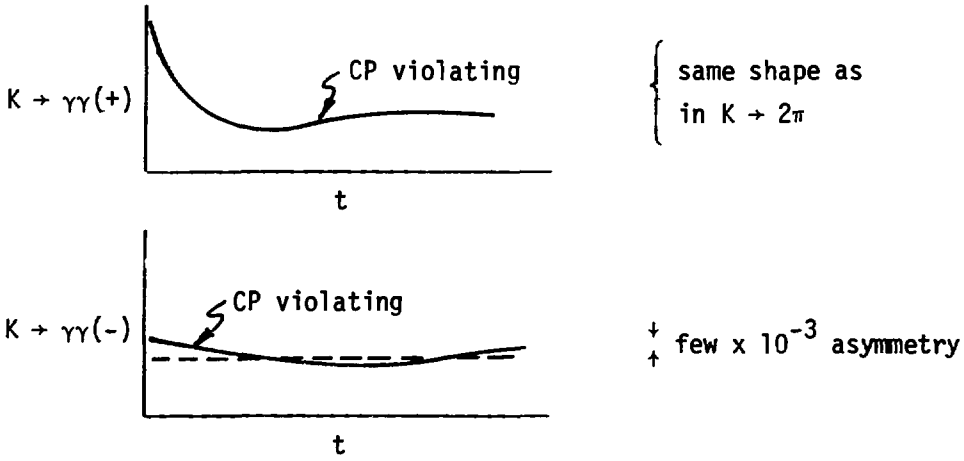

In both cases the CP violating amplitude is enhanced in interference with the corresponding CP conserving amplitude.

B. $\underline{K \to 2\mu}$

Here again the analysis of Ref. 2 is most useful. The dominant mechanism for $K_{L,S} \to 2\mu(+)$ is through the $2\gamma(+)$ state so that again the pattern of CP non-conservation in the $2\mu(+)$ final state ought to be the same as in $K_{L,S} \to 2\pi$.

For the $2\mu(-)$ final state, again short distance effects are found to be important:

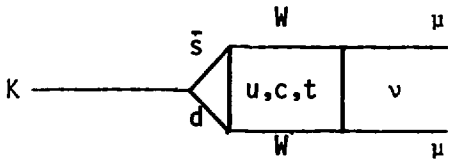

Deviations from superweak are very large: the heavier quarks can contribute relatively more due to the strong suppression of this amplitude by the

GIM cancellation mechanism.

Using the evaluation of Ref. 2, we find

$$\left|\frac{\epsilon'}{\epsilon}_{\mu\mu}\right| \geq 10$$

This is to be compared with

$$\left|\frac{\epsilon'}{\epsilon}_{2\pi}\right| \simeq \frac{1}{500}$$

so that in the 2μ channel, there are potentially very large direct CP violating effects. (We have evaluated the appropriate expression in Ref. 2 using $M_t \geq 20$ GeV.)

The following branching ratio table can then be constructed:

	$2\mu(+)$	$2\mu(-)$
K_L	$\underline{10^{-13}}$	10^{-8}
K_S	5×10^{-11}	$\underline{10^{-14}}$

where again the underlined entries are CP violating and only the $K_L \to 2\mu(-)$ has (presumably) been observed to date. Again consider the relevant interference patterns in an initially pure K° beam:

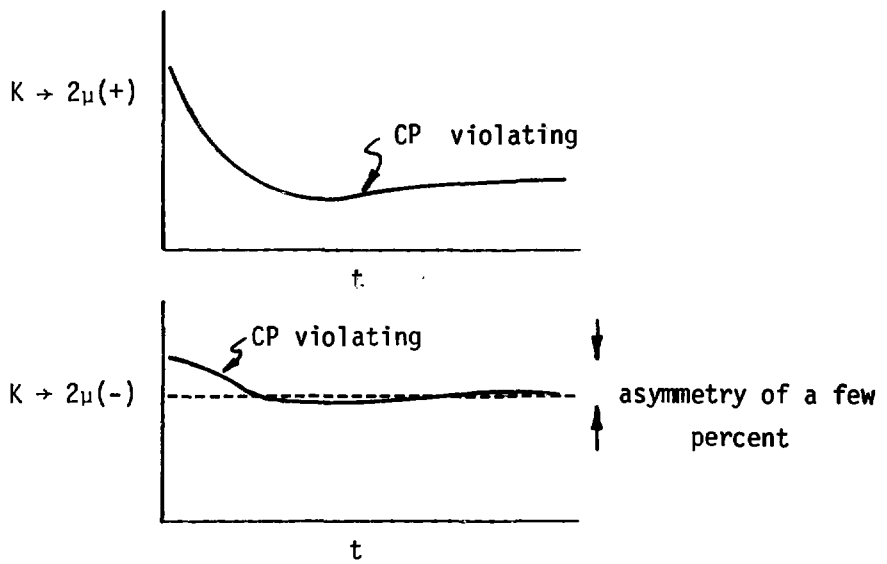

Note: all our estimates for these rare decays are made in the Kobayashi-Maskawa model. It would be most useful to have similar predictions for other models of CP nonconservation.

VII. Other rare Kaon decays

Finally, we briefly list a few other rare decays of some interest which could be studied at a future Kaon factory

Mode	Mechanism	Expected Branching Ratio
$K_L \to \pi^0 e^+ e^-$	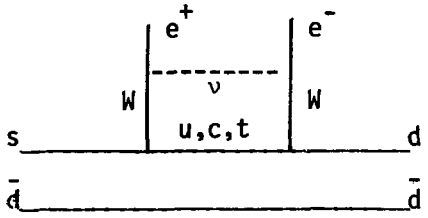	$\sim 10^{-11}$ (Ref. 11)
$K_L \to \pi^0 \nu\bar{\nu}$	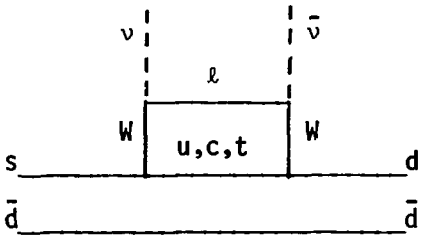	$\sim 10^{-13}$ (Ref. 12)

The above modes are clearly sensitive to higher order weak interactions.

$K_L \to (\pi^{\pm}\mu^{\mp})_{atom} + \nu$	$(1.0 \pm 0.1) \times 10^{-7}$

This branching ratio has recently been measured[13] at Fermilab. The atoms are formed (in S-States) at that spot on the $K\mu_3$ Dalitz plot where the π and the μ have negligible relative velocity. In principle, a study of the energy levels of this tightly bound atom can reveal information on the electromagnetic structure of the pion.

$K_L \to \mu e$	?
$K_L \to \pi\mu e$	?
$K^+ \to \pi^+\mu e$	?

These important lepton number violating decays, allowed in certain grand unified theories[14], are ideal for study at a new Kaon facility.

VIII. Conclusions

A. All existing data on K decays is consistent with the superweak model. There are many high quality-high precision results, yet the data does not significantly test the most appealing milliweak model--that of Kobayashi and Maskawa.

B. Currently planned experiments on $K \to 2\pi$ have a good chance of observing deviations from superweak. Expect results in 1982-1983.

C. A planned experiment on $K \to 3\pi$ could see CP nonconservation in that channel for the first time. Results in 1982-1983.

D. A currently running experiment is sensitive to CP nonconservation in $K^+_{\mu 3}$ decays. Nothing is expected, however, in the Kobayashi-Maskawa model. Results in 1981.

We now close with a speculation about the future. Suppose (and this is not a totally unlikely scenario) that between now and the late 1980's,

i) ε' remains consistent with zero
ii) η_{+-0} is not shown to differ from ε
iii) no CP violating polarization in $K^+_{\mu 3}$ is observed
iv) CP violation is not observed in D° or B° (or T°) systems
v) no better idea surfaces

then serious consideration will be given to:

1) studying interference effects in $K \to 2\gamma$ and $K \to 2\mu$
2) even better experiments to measure $|\eta_{00}/\eta_{+-}|$; and perhaps to
3) measuring Re η_{+-} and Re ε each to better than 0.1% accuracy, and
4) the Gedanken experiment described in Section III of directly looking at early times for a difference in decay rates of K° and $\overline{K^\circ}$ to the $\pi^+\pi^-$ final state.

The author would like to acknowledge stimulating and informative discussions with Jim Cronin, Chris Hill, Robert Sachs, and Michael Schmidt.

References

1. For a more complete discussion of items in this section, see the review article by K. Kleinknecht, ARNS 26, 1 (1976). The world average values for experimentally determined quantities are taken from Particle Data Group, N. Barash-Schmidt et al., Rev. Mod. Phys. 52, S1 (1980). For a valuable independent look at the current status, see CP Symmetry Violation--The Search for Its Origin, J.W. Cronin, to be published in Reviews of Modern Physics.

2. J. Ellis, M.K. Gaillard, and D.V. Nanopoulos, Nuc. Phys. B109 (1976), 213.

3. Prog. Theor. Phys. 49 (1973), 652.
4. Gilman and Wise, Phys. Lett. 83B 83, (1979) and for a recent review of estimates for ε', see L. Wolfenstein, Gauge Models of CP Violation, Carnegie-Mellon University preprint #C00-3066-139.

5. M. Holder et al., Phys. Letters 40B, 141 (1972).
M. Banner et al., Phys. Rev. Letters 21, 1103 (1968).
J.H. Christenson et al., Phys. Rev. Letters 43, 1209 (1979).

6. A Study of Direct CP Violation in the Decay of the Neutral Kaon via a Precision Measurement of $|\eta_{00}/\eta_{+-}|$, R. Bernstein et al., Fermilab Experiment #617 (Chicago-Stanford); A Measurement of Milliweak CP Violation in K_L-K_S Decays through the Determination of ε', R.C. Larson et al., Brookhaven Experiment #749 (BNL-Yale).

7. M.P. Schmidt et al., Phys. Rev. Lett. 43, 556 (1979). The author is grateful to Professor Schmidt for communicating his early result on the asymmetry in $K^+\mu 3$ decays.

8. A measurement of the CP Violation Parameter η_{+-0}, G. Thomson et al., Fermilab Experiment #621 (Rutgers, Wisconsin, Michigan, Minnesota).

9. CP-Violating Interference Effects in Radiative K° Decays, Sehgal and Wolfenstein, Phys. Rev. 162, 1362 (1967).

10. Rare Decay Modes of the K Mesons in Gauge Theories, Gaillard and Lee, Phys. Rev. D 10, 897 (1974).

11. See for example Gilman and Wise, Phys. Rev. D 21, 3150 (1980).

12. See for example Ma and Okada, Phys. Rev. D 18, 4219 (1978), as well as Reference 2.

13. A Measurement of the Rate of Formation of $\pi\mu$ Atoms in K_L Decay, to be submitted to Physical Review Letters (Chicago-Stanford-Wisconsin collaboration).

14. See for example Cahn and Harari, Nuc. Phys. B176 (1980), 135, and the talk of P. Herczeg, these proceedings.

RARE DECAYS OF PIONS & MUONS: A REVIEW

by

C.K. Hargrove

ABSTRACT

A general review of rare decays of pions and muons is given. The status of rare decays of pions and muons in the context of unified gauge theories is briefly discussed. The status of the experimental evidence is reviewed. Finally, an overview of current experiments is given.

It is very difficult to give a review of this topic at the present time because little has been reported since the Vancouver meeting of the Conference on High Energy Physics and Nuclear Structure. That is not to say that a lot is not happening. But, after the last flurry of activity in 1976-79 when incredibly low limits were placed on the branching ratios of the rare flavor changing decays, the groups have had to develop new techniques to push the limits to much lower levels. These efforts stimulated by the intense beams available at modern meson factories will bear fruit in the next few years. At present they are only gleams in the eyes of the experimenters driven by dreams and wild thoughts in the heads of theorists.

By the mid-thirties our world was a pretty tidy place. It was made up of the electron, the neutrino, the photon, the proton and neutron and the hypthesized pion. Also the theory, might have been said to be reasonable with the Dirac equation and Fermi's theory of weak interaction. The end of this simple picture was heralded by the discovery of the muon in 1936 by C.D. Anderson, S.H. Neddermeyer and others. It immediately raised the problem of the generation gap, characterized as the major problem in modern theories.

A question, as we learned more about the muon, was posed. Why should a heavy electron exist? The same question is still asked only we phrased it in a different jargon.

A new simple picture has evolved. The everyday world is made up of Leptons and Quarks.

$$\begin{pmatrix}\nu\\ e\end{pmatrix}_L \quad e_R \qquad \text{Leptons}$$

$$\begin{pmatrix}u\\ d\end{pmatrix}_L \quad u_R \; d_R \qquad \text{Quarks}$$

These particles interact Electroweakly through the Weinberg-Salam-Glashow (WSG)[1] $Su(2)_L \times u(1)$ unified Gauge theory of Electroweak interactions with their spin 1 gauge particles,

$$W^{\pm},\ Z^{o} \text{and } \gamma$$

Where the $W^{\pm}$ interact with the left-handed doublets. The Z^{o} interacts with the right-handed singlets and the doublets and the photon interacts with the charges. The Quarks interact strongly as explained by the theory called Quantum Chromodynamics (QCD) through its gauge particles called vector gluons.

This everyday world has had to be expanded, as was heralded by the discovery of the muon, to include the newly discovered massive repetitions of the ordinary particles

$$\begin{pmatrix}\nu_\mu\\ \mu\end{pmatrix}_L \begin{pmatrix}\nu_\tau\\ \tau\end{pmatrix}_L$$

$$\begin{pmatrix}c\\ s\end{pmatrix}_L \begin{pmatrix}t\\ b\end{pmatrix}_L$$

along with their right-handed singlets. These particles are all coupled to the same gauge bosons and all fit into the same WSG Electroweak theory and have the same strong QCD interactions among the quarks. The theory predicts quantitatively all Electroweak experimental tests.[2] They do not answer the fundamental questions that are raised by the existence of the higher generations.[3] Why do they exist? Why do they have their particular masses?

This problem is compounded by the fact that in the quark sector there is mixing between the gauge group eigenstates. The gauge states, d',s' and b', are related to the physical particles by the Kobayashi-Maskawa[4] parameterization

$$\begin{pmatrix}d'\\ s'\\ b'\end{pmatrix} = \begin{pmatrix}c_1 & s_1c_3 & s_1s_3\\ -s_1c_2 & c_1c_2c_3+s_2s_3e^{i\delta} & c_1c_2s_3-s_2c_3e^{i\delta}\\ -s_1s_2 & c_1s_2c_3-c_2s_3e^{i\delta} & c_1s_2s_3+c_2c_3e^{i\delta}\end{pmatrix}\begin{pmatrix}d\\ s\\ b\end{pmatrix},$$

where $c_1 = \cos\theta_1$, $s_1 = \sin\theta_1$, θ_1, θ_2 and θ_3 are real mixing angles and δ is a CP-violating phase parameter. In the limit $\theta_2 = \theta_3 = \delta = 0$, this reduces to the usual Cabibbo formalism for strangeness changing interactions.

In the minimal WSG theory the neutrinos are massless and such lepton flavor changing interactions cannot occur. However, the upper limit on the masses of the neutrinos has been supplemented by the recent measurements of the mass of the electron neutrino by Lyubimov, et al[5] who find a mass of 30±15 ev and also the possible observation of neutrino oscillations.[6] This being the case, it is possible that a mixing of the leptons similar to that of the quarks occurs and this will introduce four more parameters. It also means that separate conservation of electron, muon and τ-number will be violated. That is, already we are faced with the possible necessity of modifying the simplest WSG theory. There are many ways to do this and very little guidance from experiment on how to do it. However, the rare decays of muons and pions provide strong constraints on the theory and if the lepton non-conserving decays are observed they can be used crucially to define the type of modification required to the simple WSG theory.

There are almost as many ways to modify the theory as there are theorists. A list of the papers relative to lepton non-conservation can be found in the paper by Bjorken, Lane and Weinberg.[7]

At the present time, few of these extensions of the WSG theory have been ruled out. I might list a few of the more popular ones to give some idea of the type of thing being considered. The WSG theory requires the existence of at least one scalar Higgs doublet. It puts no constraint on the number, mass or couplings of these doublets. If more than one of these doublets exist then $\mu \to e$ can occur.[8] Weinberg has stated that the current limit on $\mu \to e\gamma$ requires a mass for such a second Higgs particles of 100 GeV. Further reduction on the limits of $\mu \to e\gamma$ will push the lower limit on the mass up to $\approx$500 GeV.[9] Another extension of the WSG theory is the addition of a massive right-handed vector boson, massive neutrinos, and the existence of right-handed doublets instead of the right-handed singlets.[10] Such a model explains baryon nonconservation and parity non-conservation in a "natural" way. This model can easily give a branching ratio of 3×10^{-13}. Other models which give lepton non-conservation include doubly charged leptons, heavy neutrinos, leptoquarks, etc. Thus the search for rare lepton number non-conserving decays of muons and kaons is one of the few ways, perhaps the only way, of looking for a deeper structure of the WSG model until the much higher energies of the future accelerators become available.

Let me now turn from the theoretical to the experimental situation. The decay modes and branching ratios (BR) of the muon are listed in Table I along with the references to the experiments and a statement of the type of physics addressed by each decay. I will now briefly discuss each of the entries in Table I and point out the present status and to my knowledge future plans for study of each of these reactions. Since so much emphasis has been put on generation changing reactions let me start with those and comment on them in some detail.

The first of these listed is the most famous decay $\mu^+ \to e^+\gamma$. Its absence, noticed in the fifties, was the first indication of the muon lepton quantum number since it was not obviously forbidden by any known physical law. Even early experiments showed to a high degree of forbiddenness that generation changing processes do not occur. The upper limit was driven down to a $\approx 3\times10^{-8}$ by the experiments referred to in the last three entries in Table I under $\mu \to e\gamma$. This very low limit combined with the discovery of the muon lepton number nonconservation to 10% and the general applicability of the Fermi theory which predicted an impossibly low branching ratio kept the effort minimal to push it much lower.

Almost simultaneously, realization that muon number nonconservation was easily included in the new unified gauge theory at this level and a rumoured observation of $\mu \to e\gamma$ burst on the scientific community. This stimulated a rush of theory papers and experiments at the three meson factories resulting in the other three $\mu \to e\gamma$ papers referred to in Table I. The TRIUMF and SIN experiments using two NaI counters in coincidence drove the ratio down to the 10^{-9} level. The LAMPF experimental apparatus, shown in Fig. 1, used a segmented NaI wall to detect the γ-ray, (this gave both position and energy of the γ ray) a magnetic spectrometer for the electron and a superb surface μ^+ beam (high intensity $2.5\times10^6 \mu^+$/sec, very small stopping range $\approx$50 mg/cm therefore very

small electron energy loss and straggling). Thus by combining spatial resolution and good energy resolution in the photon arm with good electron energy and spatial resolution they drove the upper limit with 90% confidence level down to $<1.9\times10^{-10}$, nearly an order of magnitude better than other measurements. This experiment has set a limit of >230 GeV on the mass of a second heavy Higgs scalar.

This group has shown in a LAMPF proposal[12] that improvements in the apparatus could achieve a BR limit of $\lesssim3\times10^{-13}$. Even though their present effort is on the Crystal Box, this proposal illustrates the techniques required to improve the BR. It uses a super-conducting magnet spectrometer to detect the electron with two NaI walls to detect the gamma ray. The comparison of this scheme with their previous experiment is shown in Table II. They have improved almost every aspect of the spectrometer by the factors shown in the last column and the product of these improvements is 1000 factors. They claim that it will require major improvements in meson factories beams to exceed their limit. That will remain to be seen but it certainly represents a tour du force in muon branching ratios. This experiment would reach the theoretical maximum allowable mass for a second Higgs of 1000 GeV.

Their current experiment on $\mu\to e\gamma$ uses the Crystal Box. Here the improvements in energy and spatial resolution are not as great as in the above proposal. However, this is compensated for by its simplicity and flexibility. It is possible for them to do $\mu\to3e$ and $\mu\to e\gamma\gamma$ simultaneously with $\mu\to e\gamma$ and still reach a BR limit of $\lesssim10^{-11}$ for $\mu\to e\gamma$.

This leads to the next entries in Table I, $\mu\to eee$ and $\mu\to e\gamma\gamma$. Since these are being tackled simultaneously in the Crystal Box at LAMPF, they will be discussed together. They are being done at the same time because both are three particle decays and require an apparatus which detects an electron in coincidence with either two photons or two electrons and therefore have similar kinematics.

Normally one would expect both of these decays to be less than $\mu\to e\gamma$ by a factor of α/π. However there are certain models which give a larger BR for $\mu\to eee$ or $\mu\to e\gamma\gamma$ than $\mu\to e\gamma$. For instance, $\mu\to e\gamma\gamma$, in a model where heavy doubly charged leptons exist, would have a higher BR than $\mu\to e\gamma$[13,14]. If there is more than one Higgs then the couplings of the second Higgs will determine which of the three of $\mu\to e\gamma$ and these two reactions is greater. Thus it is important to look for all three.

There are two proposals in the western world to do these experiments and they represent two rather different techniques. The first one is SINDRUM. Their layout is shown in Fig. 3. It is a copy of a similar apparatus being constructed by Korenchenko et al in Russia of which I have no documentation. They use a superconducting solenoid 1.1m diameter and 1.2m long with a field of 1.7T. There are two detection regions inside the magnet. One region, around the target, detects electrons, the other concentric with this is a pair spectrometer used to detect the photons. Each region has scintillators to trigger on the particles and multiwire proportional chambers to measure their trajectories. The pair spectrometer uses a cylinder of Pb .5mm thick to convert the

γ rays. They hope to reach a BR limit $\lesssim 10^{-12}$.

The Los Alamos proposal to measure these decays is titled the Crystal Box to distinguish it from the SLAC Crystal Ball. A view of of it is shown in Fig. 4. It is made of crystals of NaI $6.3x6.3x30cm^3$. Each face of the box has 88 crystals in an array of 11 x 8. Each corner is filled with 18 crystals for a total of 424. The specifications of the two systems are compared in Table III.

It is easy to see that both systems will make major improvements in the BR limits of these two decays. The simplicity of the Crystal Box is very appealing.

The next entry in Table I is $\mu^- Z \to e^- Z$. This branching ratio has been pushed to the lowest limit and in the more standard theories is the most probable since it is enhanced over the others by the coherent nature of the interaction with the nucleons of the nucleus. It's probability[15] increases with A up until $Z \doteqdot 75$. For models in which there is either lepton mixing or extra Higgs, it is by several orders of magnitude the most probable.[16] Further the probability has an isotopic dependence so that it should be done in several differing isospins.

The experiment has been done at SIN as referred to in Table I. Their apparatus is shown in Fig. 5. They had a streamer chamber sitting in the field of a super conducting Helmholtz coil with a sulpher target at the centre. It had a hodoscope outside which provided a rough determination of the sign and momentum of the particle, and all this was surrounded with a plastic scintillator calorimeter which provided an energy cut on the outgoing electron. The limit reached was $7x10^{-11}$.

There are two proposals to repeat this experiment. One is at TRIUMF and is in the final set up stage. The other is at LAMPF and is at a very early stage. The LAMPF proposal of Souder et al is shown in Fig. 6. It has a superconducting solenoid of 3.T with a drift chamber to detect electrons with momentum greater than 53 MeV/c. Not much detail has been given. They expect to reach a limit of $\lesssim 10^{-11}$.

The second proposal is the TPC experiment at TRIUMF. The layout of this experiment is shown in Fig. 7. The detector is a large volume drift chamber sitting in a magnetic field. The electric field is aligned with the magnetic field ($\vec{E} \times \vec{B} = 0$). The magnetic field does three things. First, the ionization electrons from fast charged particles are drifting along the magnetic field and therefore their diffusion transverse to it is reduced by a factor of 5. The fast particles are bent by the field allowing the measurement of their momentum. Finally the low energy muon decay electrons are bent enough so that they pass inside the trigger counters. When the drifting electrons, left in the gas by the passage of a fast charged particle, reach the end cap they are detected by proportional wires. These wires measure their time of arrival to give the axial position. Their position along the wire is given by the signal induced on pads equally spaced along the

wire and their radial position is given by the wire. Thus one measurement on each wire gives all three coordinates of a segment unambiguously. Further since we are only interested in one track, each pad in a sector is multiplexed to its corresponding pad in every other sector reducing the electronics by a factor of twelve. The parameters of the TPC and the SIN apparatus are listed in Table IV. The major improvements in the TPC experiment are the improved solid angle, beam and momentum resolution.

The TPC has now had two test runs and some preliminary results are shown in Figs. 8 and 9. Fig. 8 shows the x-y projection of a typical event. Fig. 9 shows the $\pi^+ \to e^+\nu$ peak and the $\mu^+ \to e^+\nu\nu$ spectrum with its 53 MeV end point. The $\pi \to e\nu$ peak intensity is so much greater than the $\mu \to e\nu\nu$ spectrum because of a narrow timing window and the cut-off provided by the magnetic field. The resolution of 5 MeV is mostly dominated by multiple scattering. This experiment has an inherent background due to μ-decay in orbit. Calculations of this[17] show it drops off rapidly and the limit possible is proportional to the resolution to the 6th power. This will limit our experiment to a BR of $\approx 2\times10^{-12}$. The experiment should take data during the summer of this year.

The experiments that look for $\mu \to e$ conversion also look for reaction 7 of Table I, $\mu^- \to e^+$ conversion. There are theories which allow this and the BR should be pushed as low as possible. In some of these theories it is more probable than $\mu^- \to e^-$ conversion.

Another method of measuring this is being developed by Backenstoss et al[20] at Basle. They are using chemical techniques in which the negative muons are stopped in a target and the daughter Z-2 radioactive atoms are separated chemically and their radioactivity is looked for. They have set a limit of 2×10^{-10} on this decay relative to μ^- capture. They hope to reach a much lower limit using this technique.

It is worth commenting on two experiments on normal μ^- decay. One is the recent proposal to TRIUMF by Strovink et al.[18] They propose to look at the decay from $\approx$100% polarised muons in the backward direction. The electron spectrum goes to zero in this direction at the 53 MeV end point. Any deviation from zero can be interpreted as due to a right-handed current and therefore a right-handed vector boson. This proposal hopes to improve the current precision of the measurement of the ξ-parameter of the Michel spectrum by a factor of 13. This would drive the minimum mass of such a boson up to 600 GeV from its present value of $\approx$200 GeV.

The second experiment is at Los Alamos and has been proposed by Anderson and Bowman et al. It is a high precision measurement of all the Michel parameters. The apparatus is shown in Fig. 10. This apparatus will be described in some detail in this workshop so only a brief description with emphasis on right-handed currents will be given here. The main characteristic of this apparatus is the use of the TPC technique. The "Perl Magnet", a high uniformity large volume magnet has been used to provide the field for the TPC. The surface muons, which are highly polarized, are accepted, one per pulse, and stopped in the gas of the TPC. The decay electron is then measured with good solid angle and

good momentum resolution. Since the electron energy varies from 0-53 MeV, and the resolution is a function of momentum due to the variation of the bending radius and the multiple scattering, one gets high precision by taking a large number of events $\approx 10^8$ with very small systematic errors ($L1 \times 10^{-4}$). The ultimate error on all the parameters will be improved by approximately ten. It would measure the ξ parameter to the same precision as the TRIUMF experiment and would raise the limit on the mass of a right-handed vector boson to 600 GeV. This experiment is also being carried out at SIN, but I have no documentation.

The final entry in Table I is the search for the decay $\mu^+ \to e^+ \nu_e \nu_\mu$. The so-called multiplicative law test. This decay was looked for at LAMPF and the limit is just above that which could be expected by several models.[19] Therefore, either a higher sensitivity experiment or an extension of this experiment is worth serious consideration.

I have concentrated most of this talk on muon decays which is perhaps appropriate, since it is the only "easily available", purely leptonic decay in nature. But to close out the discussion, let me now say something about rare pion decays. The BR of the charged and neutral pion decays are shown in Table V taken from Ref. 20.

The BR for the decay of the pion to an electron and its neutrino is one of the most important tests of muon-electron universality. It can be calculated within the framework of modern gauge theories to an accuracy of $\approx .2\%$, yet the best measurement to date is is that of Di Capua[21] done in 1964 and the calculation based on this by Bryman et al[22]. Their number has an error of 2%. Any deviation from the calculation would be evidence of new effects. It has been shown[23], that charged Higgs effects or mixing in the lepton sector can cause effects as large as 1%. Therefore, a precision measurement of this BR is a possible low energy probe of these effects. It can also be used as a probe for Lepto-quarks[24]. An experiment on this is under analysis at TRIUMF. The problems of reaching ½% demand much care in the experiment and the analysis. New results can be expected soon, but such a fundamental measurement deserves much more effort.

The experiment $\pi \to e\nu\gamma$ is used to measure the vector and axial vector form factors of the pion. It has been shown by Bernabeu et al[25] and Montemayor and Moreno[26] that unequal quark masses could cause isospin breaking effects which would be as great as 50 to 80%. Other estimates claim this is less than a few percent[20]. It is obvious that the experimental situation is limited by the number of events. There are experiments on this being carried out at TRIUMF and SIN. The experiment $\pi^+ \to e^+ \nu e^+ e^-$ is of the same nature, but is down by $\approx \alpha$. It might be seen in the Crystal Box.

Pion beta decay is another experiment that requires much more work. It has, to my knowledge, had no new measurements since that of Depommier et al[27]. (New results were presented by Highland et al at this workshop). Their branching ratio is $1.02 \pm .07 \times 10^{-8}$. The signature for this is so clean (an electron spectrum max ≤ 4.6MeV and a pair of γ rays from the final state π^0) that an apparatus like the Crystal Box should have a good chance of pushing the accuracy of this measurement much further. This experiment tests CVC and provides a limit on the couplings of charged Higgs. Even though

the branching ratio is so small the new instruments with their large solid angle and good energy resolution for γ rays and electrons should be able to considerably improve this measurement.

The decays of the neutral pion are listed in the second part of Table V. It seems to me that since all of these decays are electromagnetic, an instrument like the Crystal Box with a magnetic field would be a very powerful tool for their study. The major problem would be suppression of chance backgrounds from the 2γ decays. The most recent measurements of these decays are the search for the $\pi^0 \to 3\gamma$ by Highland et al[28] here at LAMPF and $\pi^0 \to e^+e^-$ by Fisher et al[29]. The first one is a test of C invariance. It should be possible to push this to a very much lower limit and again the Crystal Box is a likely candidate for an apparatus. The second experiment is a probe of $\pi^0\gamma\gamma$ vertex and a source of information on possible non-electromagnetic interactions. A more sensitive experiment would give a check on the decay amplitude calculations and also would test the Higgs meson exchange. Therefore, again a more precise determination of this decay, in say, the Crystal Box, would give useful information on the elusive Higgs sector.

Finally let us set out the conclusions of this survey.

1. The problem of the flavors is fundamental to current gauge theories. The searches for rare decays of the muon is one of the most important and sensitive probes of this problem. Therefore, it should be pursued with energy.
2. The Higgs sector of gauge theories is completely unknown. The rare decays of pions and muons are one of the few ways to look at this problem.
3. The high mass structure of the weak interactions can only be probed in these sensitive, high precision measurements of low energy decays at this time. Until much higher energies become available meson factories are the only probe of things like high mass right-handed vector mesons or Higgs particles.

Thus the continued high level efforts on these decays is crucial and can lead to a deeper understanding of nature. It is for the time being our only window into the high mass nature of the theory.

References

1. S. Weinberg, Phys. Rev. Lett. 19, 1264 (1967); A. Salam, Proc. 8th Nobel Sympos., ed. N. Svartholm (Almquist and Wiksells, Stockholm, 1968) p.367. S.L. Glashow, J. Iliopoulous and L. Maiani, Phys. Rev. D2, 1258 (1970).

2. For a Review with references see M.K. Gaillard, Proc. of the 1979 Int. Sympos. on Lepton and Photon Interactions at High Energies, Fermilab, Aug. 23-29, 1979.

3. M. Veltman, Proc. of 1979 Sympos. on Lepton and Photon Interactions at High Energies, Fermilab, Aug. 23-29, 1979.

4. M. Kobayashi and K. Maskawa, Prog. Theor. Phys. 49, 652 (1973).

5. V.A. Lyubimov, E.G. Novikov, V.Z. Nozik, E.F. Tretyakov, V.S. Kozik, ITEP Preprint 62.

6. F. Reines, H.W. Sobel and E. Pasierb, Phys, Rev. Lett. 45, 1307 (1980).

7. J.D. Bjorken, K. Lane and S. Weinberg, Phys. Rev. D16, 1474 (1977).

8. J.D. Bjorken and S. Weinberg, Phys. Rev. Lett. 38, 622 (1977).

9. S. Weinberg private communication.

10. R.E. Marshak, Riazzuddin and R.N. Mohapatra, to be published in Neutrino 80 and the Muon Physics Workshop (TRIUMF 1980). J.C. Pati and A. Salam, Phys. Rev. D10, 275 (1974); R.N. Mohapatra and J.C. Pati, Phys. Rev. D11, 566, 2559 (1975); G. Senjanovic and R.N. Mohapatra, Phys. Rev. D12, 1502 (1975).

11. S. Weinberg private communication and H.J. McKellar and P. Herzeg, Proc. of the Workshop on Program Options in Intermediate Energy Physics, Vol. I, LASL, Aug. 20-31, 1979.

12. H.L. Anderson et al, LAMPF Proposal #444, 1978.

13. F. Wilzek and A. Zee, Phys. Rev. Lett. 38, 531 (1977).

14. J.D. Bowman et al, Phys. Rev. Lett. 38, 531 (1977).

15. O. Shankar, Carnegie-Mellon University prepring (April 1979).

16. Alterelli et al, Nucl. Phys. B125, 285 (1977).

17. F. Herzog and K. Alder, Institut fur Physik, Universitat Basel preprint.

18. Strovink et al, Proposal to TRIUMF 1980.

19. E. Dermin, Phys. Lett 78B, 497 (1978).

20. P. Depommier. Edited by D.F. Measday and R.W. Thomas, Proc. of the Eighth International Conf. on High Energy Physics and Nuclear Structure, TRIUMF, Vancouver, 1979.

21. Di Capua et al, Phys. Rev. 133B, 1333 (1964).

22. D. Bryman et al, Phys. Rev. D11, 1337 (1975).

23. D. Bailin and N. Dombey, Phys. Lett. 64B, 304 (1976); C.W. Kim and J. Kim, Phys. Lett. 79B, 278 (1978); V.G. Vaks and B.L. Ioffe, Nuovo Cimento 10, 342 (1958).

24. J.D. Bjorken, E-P Workshop, Columbia University, Spring 1980 (unpublished).

25. J. Bernabeu, R. Tarrach and F.J. Yndurain, Phys. Lett. 79B, 464 (1978).

26. R. Montemayor and M. Moreno to be published.

27. P. Depommier et al, Nuclear Phys. B4, 189 (1968).

28. V. Highland et al, Phys. Rev. Lett. 44, 628 (1980) and Auerbach et al, Phys. Rev. Lett. 41, 275 (1979).

29. J. Fisher et al, Phys. Lett. 73B, 364 (1978).

TABLE I

MUON DECAYS

	Decay Mode	Branching Ratio	Physics
1.	$\mu^+ \to e^+ \nu_e \bar{\nu}_\mu$	.986 ± .004	Nature of the weak interaction and weak coupling constant.
2.	$\mu^+ \to e^+ \nu_e \bar{\nu}_\mu \gamma$	1.4×10^{-2}	Nature of the weak interaction.
3.	$\mu^+ \to e^+ \gamma$	$<1.9 \times 10^{-10}$	Lepton number non-conservation.
4.	$\mu^+ \to e^+ e^- e^+$	$<1.9 \times 10^{-}$	" " "
5.	$\mu^+ \to e^+ \gamma\gamma$	$<5.0 \times 10^{-}$	" " "
6.	$\mu^- (A,Z) \to e^- (A,Z)$	$<7.0 \times 10^{-11}$	" " "
7.	$\mu^- (A,Z) \to e^+ (A,Z-2)$	$<2.0 \times 10^{-10}$	" " "
8.	$\mu^+ \to e^+ \bar{\nu}_e \nu_\mu$	$<9.8 \times 10^{-2}$	

1. & 2. For a review see A.M. Sachs and A. Sirlin in "Muon Physics", Volume II, Section 2, edited by V.W. Hughes and C.S. Wu, Academic Press, New York (1977).

3. J.D. Bowman et al, Phys. Rev. Lett. 42, 556 (1978).
Povel et al, Phys. Lett. 72B, 183 (1977).
Depommier et al, Phys. Rev. Lett. 39, 1113 (1977).
Korenchenko et al, Sov. Journ. Nucl. Phys. 13, 190 (1971).
Parker et al, Phys. Rev. 133B, 768 (1964).
Frankel et al, Nuovo Cim. 27, 894 (1963).

4. Korenchenko et al, J.E.T.P. 43, 1 (1976).
Korenchenko et al, Sov. Journ. of Nucl. Phys. 13, 728 (1971).
Babaeke et al, J.E.T.P. 16, 1397 (1963).
Frankel et al, Phys. Rev. 130, 351 (1963).
Parker & Penman, Nuovo Cimento 23, 485 (1962).

5. J.D. Bowman et al, Phys. Rev. Lett. 41, 442 (1978).
(Using the data of Depommier et al from (3) above).
J.M. Poutissou et al. Nucl. Phys. B80, 221 (1974).
Frankel et al (see (3) above).

6. A. Badertschur et al, International Conference on High Energy Physics and Nuclear Structure, Vancouver, 1979.
(As reported by P. Depommier p. 106).
A. Badertscher et al, Phys. Rev. Lett. 39, 1385 (1977).
D. Bryman et al, Phys. Rev. Lett 28, 1469 (1972).

7. R. Abela et al, Eighth International Conference on High Energy Physics and Nuclear Structure, Vancouver, 1979 (as reported by Depommier p. 106).
A. Badertscher et al (see (6) above for two references).
D. Bryman et al (see (6) above).

8. S.E. Willis et al, Phys. Rev. Let. 44, 522 (1980) and eratta in Phys. Rev. Lett. 4 , 903 (1980) and Phys. Rev. 45, 1370 (1980).
Eichten et al, Phys. Lett 46B, 281 (1973).

TABLE II

	$\mu \to \gamma$ I	$\mu \to \gamma$ II	Improvement Factor
$\Delta E/E_\gamma$	8.0% (FWHM)	4% (FWHM)	2
ΔX_γ	5.2cm (FWHM)	2 cm (FWHM)	2.5
Δt	2.11ns (FWHM)	.7ns (FWHM)	3
$\Delta E/E_e$	8.7% (FWHM)	.6%	10
$\Delta\theta$	$(28)_{xy}$ (FWHM) $_{e-\gamma}$	$(20mr)_x (20mr)_y$	1.5
$\Delta\Omega/4\pi$	.018	.16	$\simeq$10
BR	1.9×10^{-10}	$\simeq 5 \times 10^{-13}$	$\pi f = 1000$

TABLE III

COMPARISON OF SINDRUM AND CRYSTAL BOX

	Sindrum		Crystal Box	
	$\mu \to 3e$	$\mu \to e\gamma$	$\mu \to 3e$	$\mu \to e\gamma\gamma$
Stop rate (10^7/s)	2.0	10	$\gtrsim .1$	$\gtrsim .1$
Target (mg/cm^2)	70	70	70	70
$\Delta E_\gamma / E_\gamma$		.03	.06	.06
ε_γ		.012	1	1
Energy Cutoff (MeV)	22(e^-)	-	15	-
$\Delta\Omega/4\pi$	.7	.5	.2	.2
$\Delta E_e/E_e$	.08	.02	.038	.038
$\Delta m/m_\mu$	.05			2.2
Δt(ns)	.8		1.0	1.0
Δz(cm)	.4		.4	.4
$\Delta\theta_e$ mr		25	20	20
$\Delta\theta_\gamma$ mr		8		80
Branching Ratio($\times 10^{-12}$)	1	1	7	7

TABLE IV

PARAMETERS OF $\mu \rightarrow e$ APPARATUS

	SIN	TPC	f
B(T)	3.5	.9	
$\Gamma \Delta \psi$ (mm)	-	.2	
ΔZ (mm)	-	2.0	
$\Delta\Omega/4\pi$ (including trigger eff.)	.05	.4	8
E/p (V/cm//Torr)	-	.2	
$\Delta p/p$ (FWHM)%	7.25	3.0	2
Beam rate (10^6/sec)	.3*	1.0	3
Branching ratio	$<7 \times 10^{-11}$	$\lesssim 2 \times 10^{-12}$	35

*Estimate of beam rate takes account of fifty per cent duty cycle.

TABLE V

Charged pion decays

Decay mode		Branching ratio		Physics
$\pi^+ \to \mu^+ \nu_\mu$		0.9999		Coupling constant f_π Muon-neutrino mass
$\pi^+ \to \mu^+ \nu_\mu \gamma$		1.24 ± 0.25	$\times 10^{-4}$	Muon-neutrino mass
$\pi^+ \to e^+ \nu_e$	(†)	1.267 ± 0.023	$\times 10^{-4}$	Muon-electron universality
$\pi^+ \to e^+ \nu_e \gamma$	(†)	3.0 for e^+, $\gamma > 48$ MeV	$\times 10^{-8}$	Axial-Vector form factor of pion Isospin breaking by quark masses?
$\pi^+ \to e^+ \nu_e e^+ e^-$		< 5.0	$\times 10^{-9}$	Axial-Vector form factor of pion Electromagnetic radius of pion ?
$\pi^+ \to \pi^o e^+ \nu_e$		1.02 ± 0.07	$\times 10^{-8}$	Conserved-Vector-Current theory

(†) Experiment in progress
all upper limits correspond to 90% confidence level

Neutral pion decays

Decay mode		Branching ratio		Physics
$\pi^o \to \gamma\gamma$		0.9885 ± 0.0005		Coloured quarks
$\pi^o \to \gamma e^+ e^-$		1.15 ± 0.05	$\times 10^{-2}$	Form factor of neutral pion
$\pi^o \to e^+ e^- e^+ e^-$		3.32	$\times 10^{-5}$	
$\pi^o \to \gamma\gamma\gamma$	(*)	< 3.3	$\times 10^{-7}$	C-violation in electromagnetic interactions of hadrons
$\pi^o \to \gamma\gamma\gamma\gamma$	(*)	< 4.4	$\times 10^{-6}$	
$\pi^o \to e^+ e^-$	(*)	$2.23 \; {}^{+2.4}_{-1.1}$	$\times 10^{-7}$	Second-order electromagnetic effect Weak neutral currents ?

(*) New result (< 2 years)
all upper limits correspond to 90% confidence level

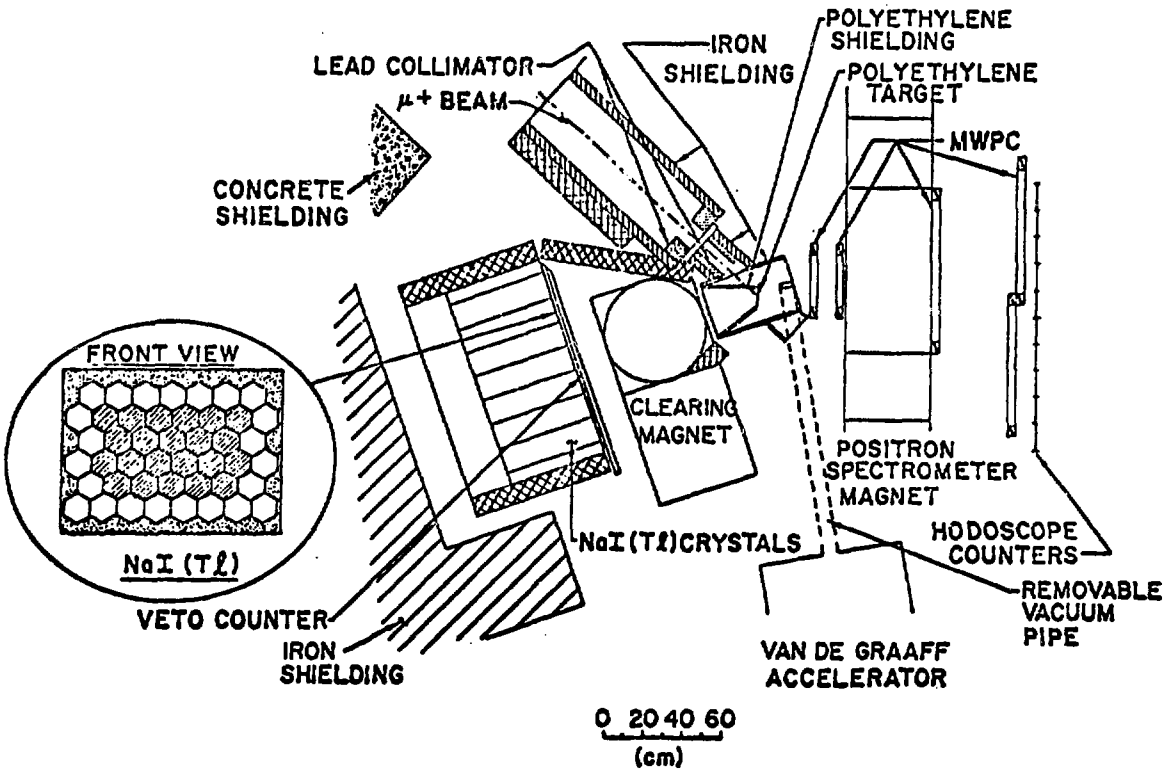

Fig. 1. The layout of LAMPF $\mu \to e\gamma$I experiment.

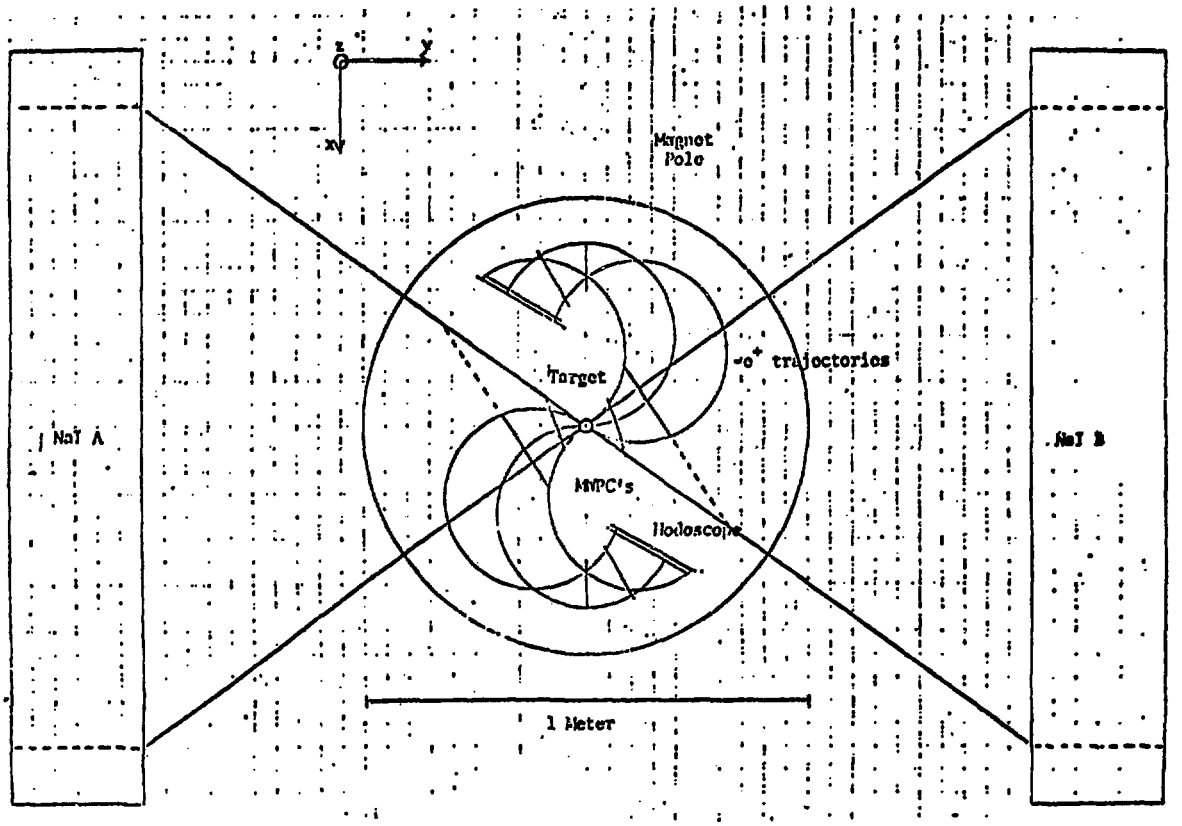

Fig. 2. The layout of $\mu \to e\gamma$II experiment.

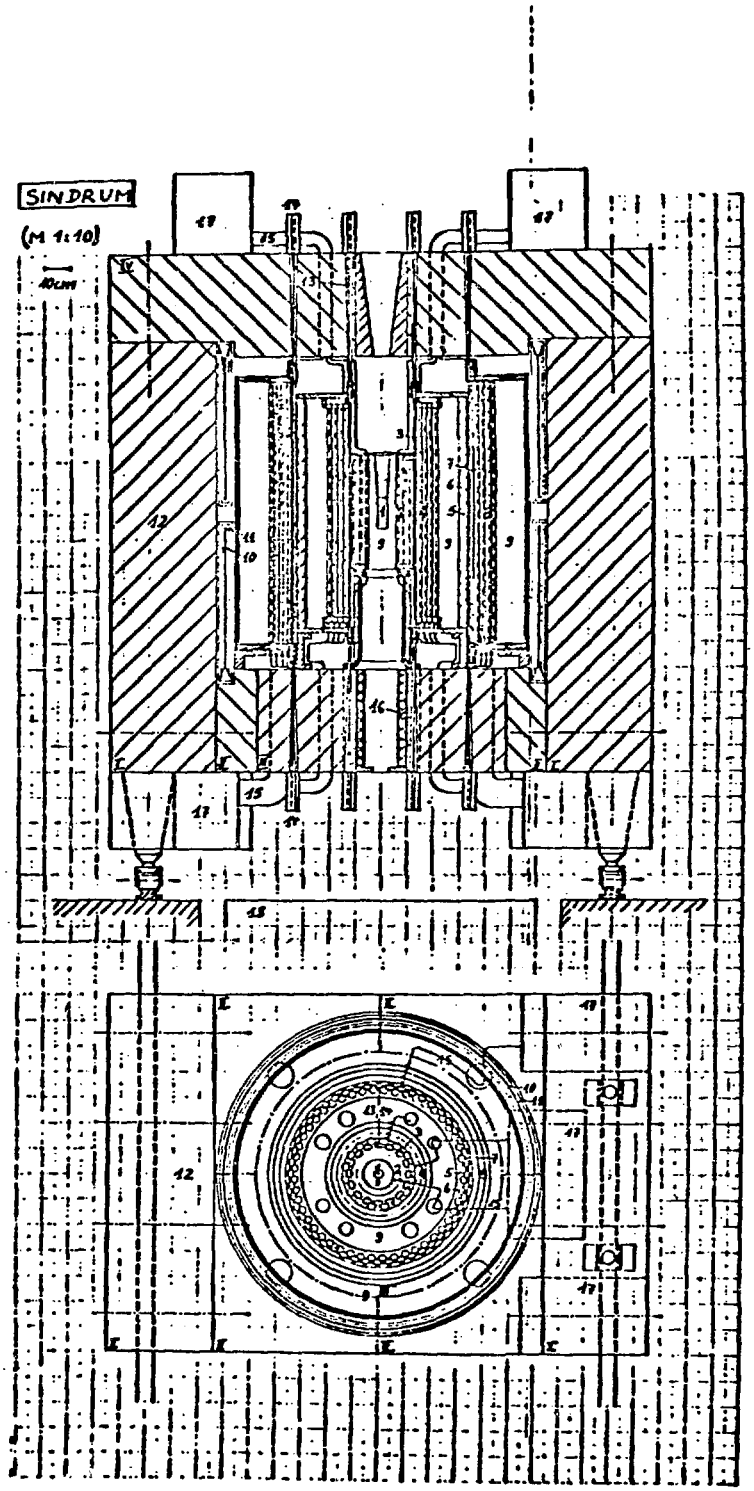

1 Target

2 Vertex detector
3 Prop. chambers
768 wires

3 32 Scintillators
80 • 45 • 0.3 cm³

4 e1-detector
4 Prop. chambers
2112 wires

5 3 cm CH_2

6 96 Scintillators
100 • 2.13 • 0.5 cm³

7 γ-converter
0.5 mm Pb
on Al-support

8 γ-detector
4 Prop. chambers
5040 wires

9 He-flushed cavities

10 Superconducting coil
4-17 kG; 1 cm thick;
200 A/mm²; 350 kg

11 Cryostat for coil

12 Magnet yoke
I 2 • 7.3 t
II 4 • 0.9 t
III 2.2 t
IV 9.2 t
} 30 t

13 Light guides (12 mm ϕ)
2 • 96 à 45 cm;
2 • 32 à 55 cm.

14 256 Photomultipliers
(Cathode 14 mm ϕ)

15 Wire chamber cables

16 Injection coil for 4 kG;
Fe-stub for 17 kG

17 Wire chamber electronics
+ - gas

18 Quadrupole

Fig. 3. The diagram of SINDRUM.

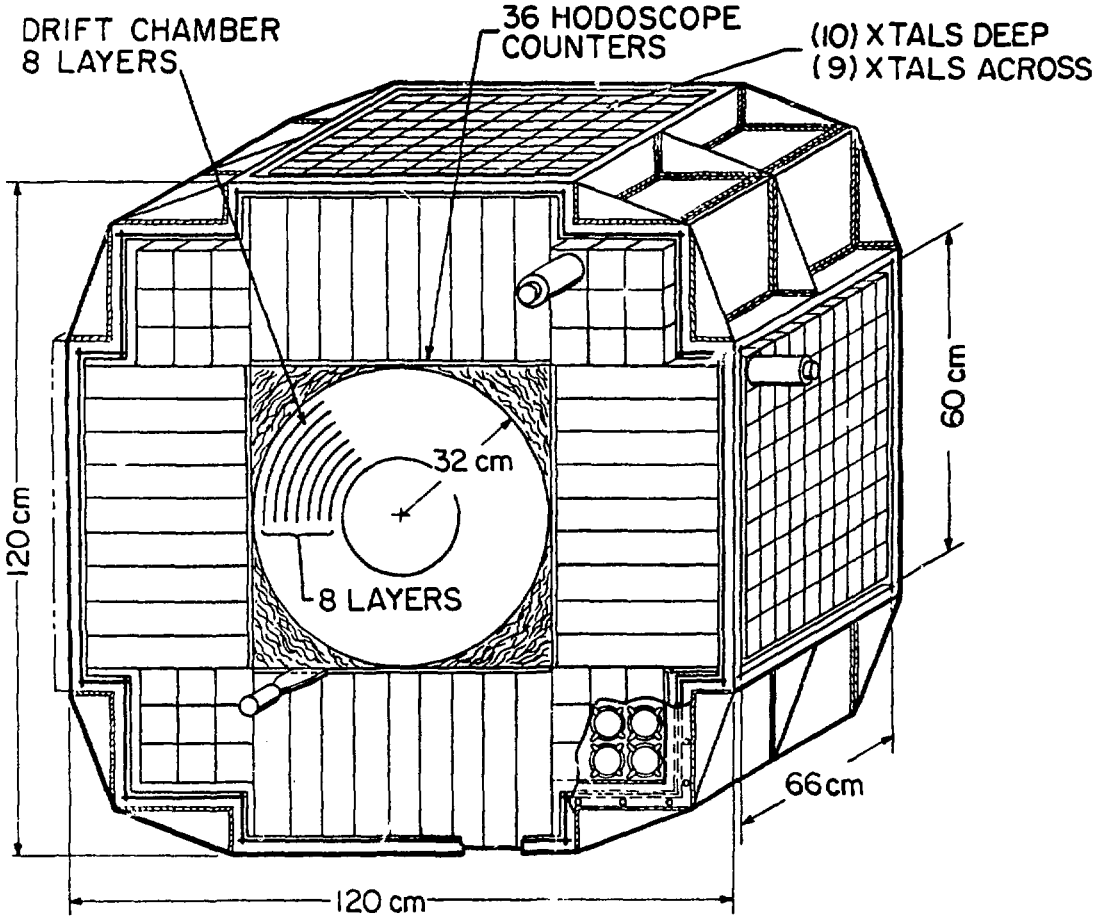

Fig. 4. The diagram of the crystal box.

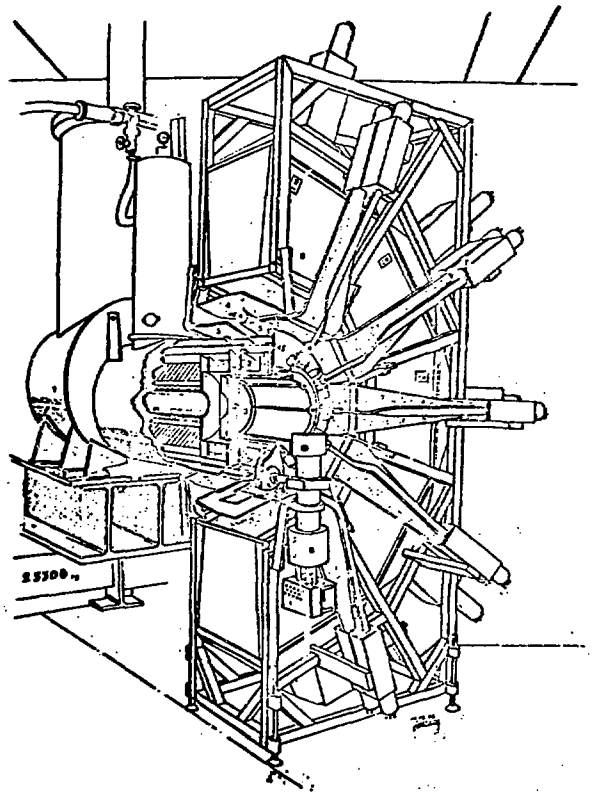

Fig. 5. The $\mu^- A \to e^{\pm} A$ apparatus at SIN.

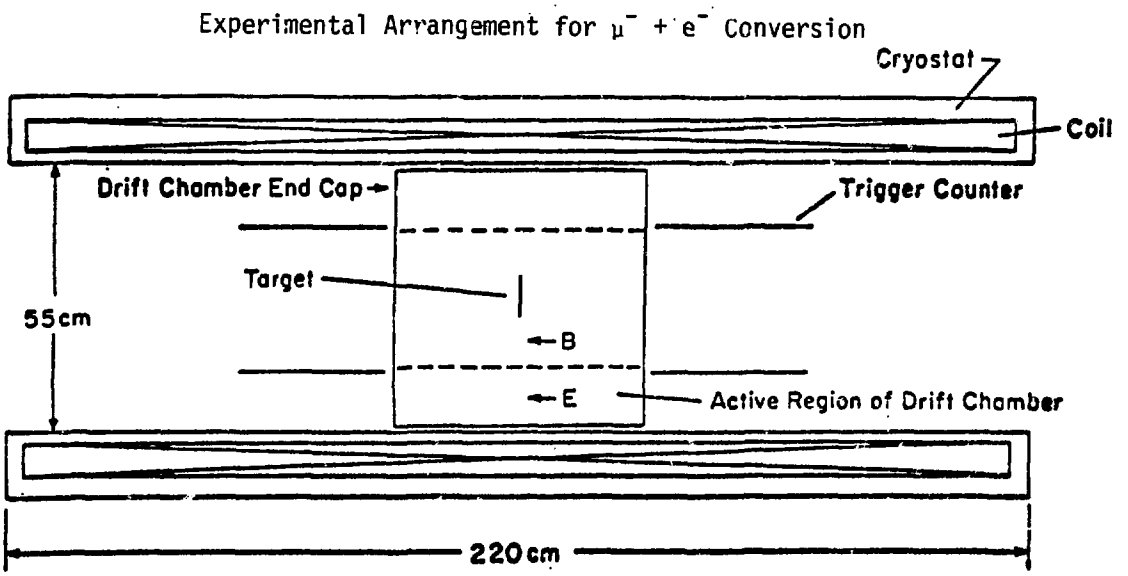

Fig. 6. The LAMPF $\mu^- A \to e^{\pm} A$ apparatus.

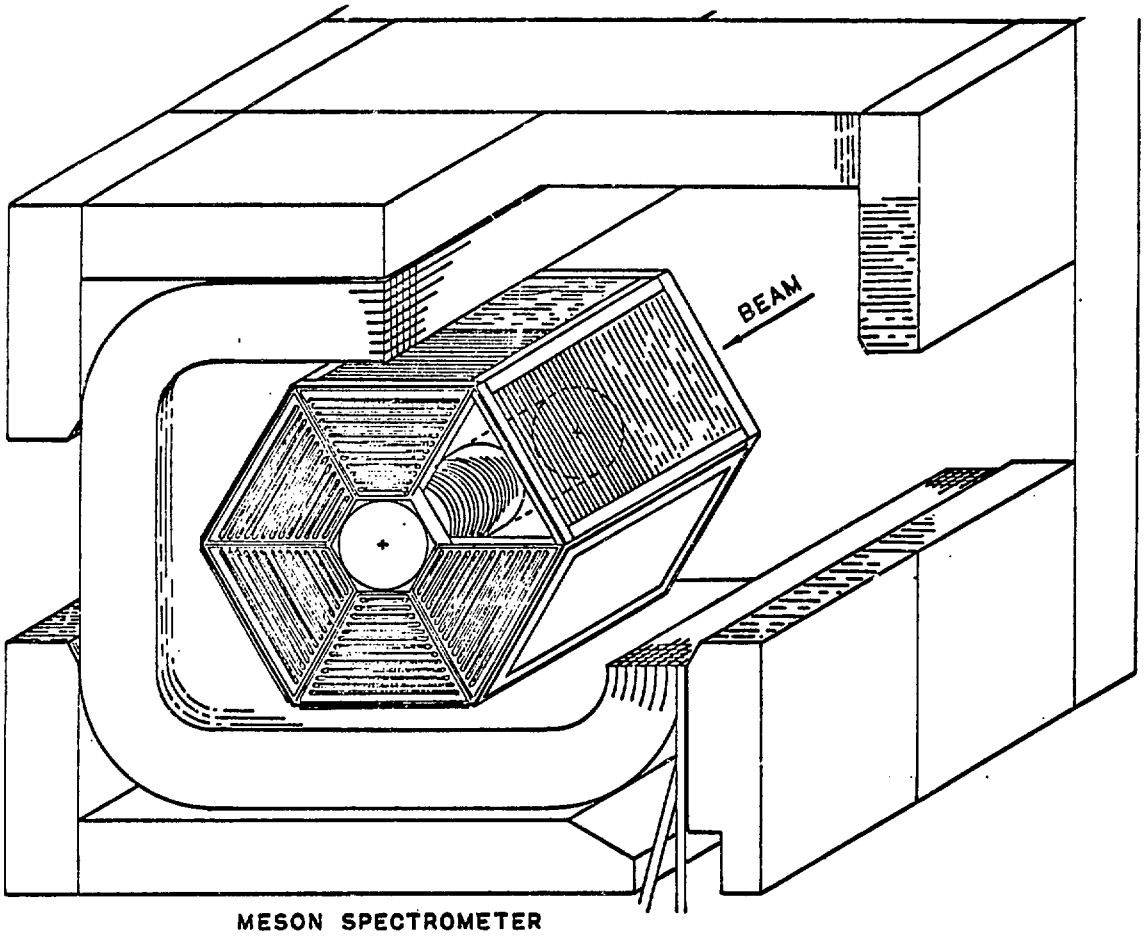

Fig. 7. The TRIUMF, TPC $e^{-}A \rightarrow e^{\pm}A$ apparatus.

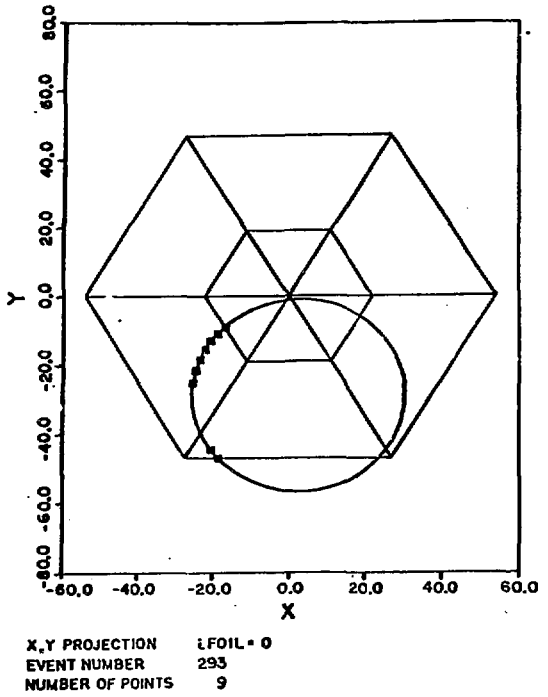

Fig. 8. A typical electron event in

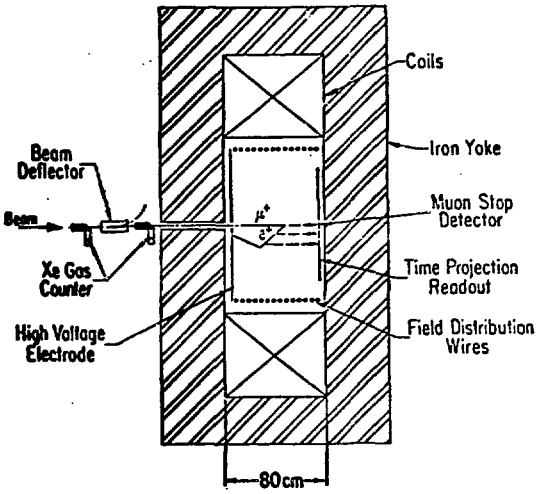

Fig. 10. The $\mu^+ \to e^+ \nu_e \bar{\nu}_\mu$ apparatus at LAMPF.

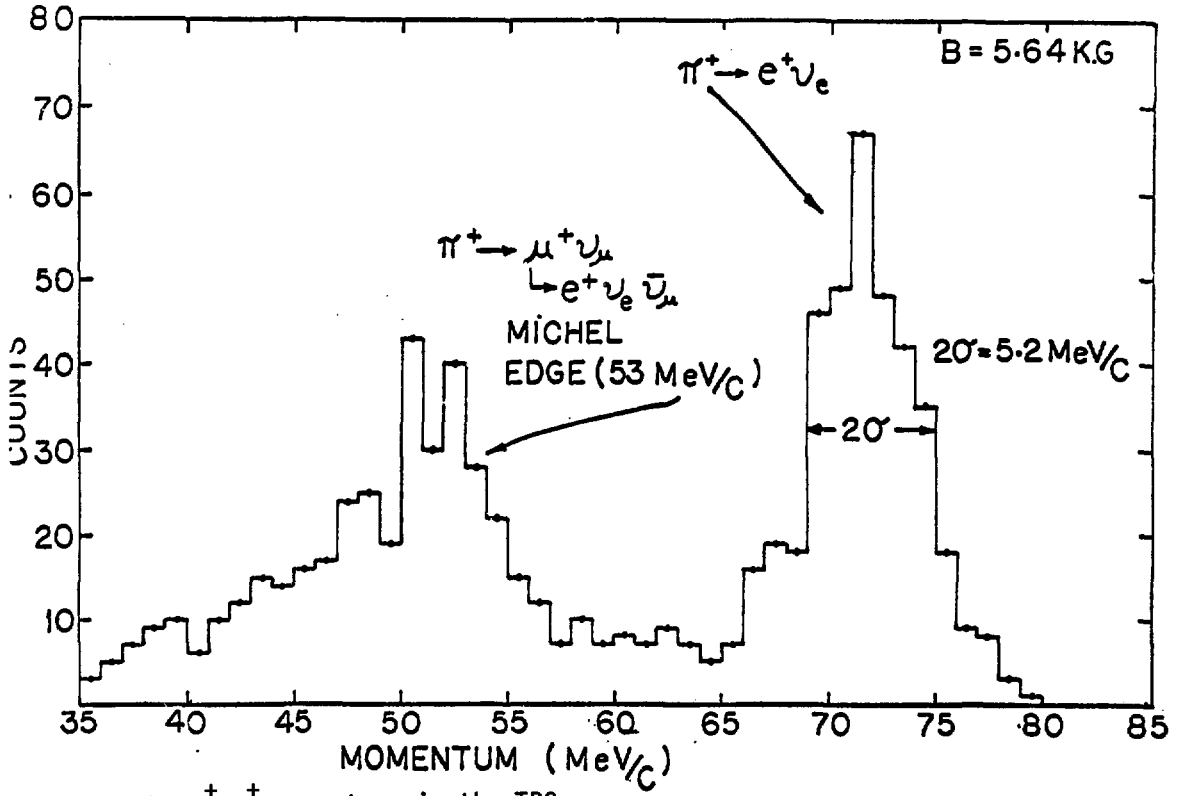

Fig. 9. The $\mu^+ \to e^+ \nu$ spectrum in the TPC.

ON MUON NUMBER VIOLATING KAON DECAYS*

by

P. Herczeg

Theoretical Division
Los Alamos National Laboratory
Los Alamos, New Mexico 87544

ABSTRACT

We discuss the decays $K_{L,S} \to \mu e$, $K_{L,S} \to \pi^0 \mu e$, and $K^{\pm} \to \pi^{\pm} \mu e$ in current theoretical schemes which imply the existence of neutral flavor-changing bosons. Possible patterns for the branching ratios of these decays are considered taking into account constraints imposed by pertinent data.

I. INTRODUCTION

Considering only decays which do not involve neutrinos and/or photons, and which contain no more than three particles in the final state, the following muon-number violating, lepton-number conserving decay modes of the charged and neutral kaons are possible:

$$K_L \to e^{\pm}\mu^{\mp}, \tag{1a}$$

$$K_S \to e^{\pm}\mu^{\mp}, \tag{1b}$$

$$K_L \to \pi^0 e^{\pm}\mu^{\mp}, \tag{1c}$$

$$K_S \to \pi^0 e^{\pm}\mu^{\mp}, \tag{1d}$$

$$K^{(\pm)} \to \pi^{(\pm)} e^{\pm}\mu^{\mp}. \tag{1e}$$

*Work supported by the U. S. Department of Energy

From the experimental point of view, the most accessible seems to be the decay $K_L \to e\mu$, followed by $K^{\pm} \to \pi^{\pm}\mu e$, $K_S \to \mu e$, $K_L \to \pi^0\mu e$, and $K_S \to \pi^0\mu e$, in increasing degree of difficulty.

The present experimental upper limits for the branching ratios (1a) and (1e) are

$$B(K_L \to e\mu) \equiv \Gamma(K_L \to \mu e)/\Gamma(K_L \to \text{all}) < 2 \times 10^{-9} \tag{2}$$

and

$$B(K^{\pm} \to \pi^{\pm}\mu e) \equiv \Gamma(K^{\pm} \to \pi^{\pm}\mu e)/\Gamma(K^{\pm} \to \text{all}) < 7 \times 10^{-9} \tag{3}$$

respectively.[1] No experimental information appears to be available as yet on the decays (1b), (1c), and (1d). To give some perspective concerning present and possible future experimental possibilities, with the existing facilities (such as, for example, the AGS at Brookhaven), one may be able to search for the branching ratios $B(K_L \to \mu e)$, $B(K^{\pm} \to \pi^{\pm}\mu e)$, $B(K_S \to \mu e)$, $B(K_L \to \pi^0\mu e)$, and $B(K_S \to \pi^0\mu e)$ with sensitivities of about 10^{-10}, 10^{-9}-10^{-10}, 10^{-7}, 10^{-5}, and 10^{-3}-10^{-4} respectively.[2] A facility with K-intensities two orders of magnitude higher than currently available might make it possible to increase the sensitivity for $K_L \to \mu e$ to better than 10^{-11}, and for $K^{\pm} \to \pi^{\pm}\mu e$ and $K_L \to \pi^0\mu e$ to about 10^{-10}-10^{-11} and 10^{-6} respectively.[2]

The decays (1a) - (1e), as well as other muon-number violating processes could occur via higher-order effects (e.g., when e, μ are coupled to intermixing neutral leptons), or at the tree level, either via neutral bosons which couple directly to (μe) and (sd) or via charged leptoquark bosons coupled to (μs), (ed) or (μd), (se).

In the sequential $SU(2)_L \times U(1)$ gauge theory of the electroweak interactions, with a single Higgs doublet and with fermions arranged in left-handed doublets and right-handed singlets (the "standard model"), there are no flavor-changing couplings of fermions to neutral gauge bosons or to the Higgs boson. Even so, muon-number conservation would not be expected to hold unless the neutrinos are all exactly massless (or degenerate). However, in view of the stringent experimental limits on the masses of ν_e, ν_μ, and ν_τ,

muon number violating processes could only occur at rates which would be too small to be detectable even in the next generation of experiments.[3] As a consequence, searches for muon-number violating processes probe the existence of new interactions and/or new leptons, beyond those of the three generation standard model.

Flavor-changing neutral gauge bosons might be encountered in gauge theories of the electroweak interactions based on a gauge group larger than $SU(2)_L \times U(1)$. Flavor-changing neutral couplings may appear even in the $SU(2)_L \times U(1)$ theory if further possible generations would not follow the left-handed doublet, right-handed singlet pattern.[4] While there is no experimental reason, nor theoretical need for such extensions of the standard model, a strong hint for the existence of new symmetries comes from the complete lack of understanding of the replication of fermion generations, each behaving identically with respect to $SU(2)_L \times U(1) \times SU(3)_C$, and also from the large number of undetermined parameters (masses, generalized Cabibbo angles) in the standard model. A possible resolution is to introduce symmetries (the so-called horizontal symmetries) which relate or distinguish the different generations.[5] These symmetries may be local gauge symmetries, in which case they lead to the existence of new gauge bosons and associated interactions. The total gauge group of the theory would become $G \times G_H$, G being the usual "vertical" group ($G = G_{electroweak} \times SU(3)_C$, or G = grand unification group) and G_H the horizontal group.[6] The gauge bosons associated with G_H are neutral and have flavor-changing couplings to fermions. They could be as light as experiment permits.[7] Flavor-changing neutral interactions appear also in extended technicolor schemes.[8] Still another possible source of muon-number violation is Higgs exchange. In the standard model, this would require the presence of more than one Higgs doublet.[9]

In this paper we investigate the ranges which the branching ratios for the decays (1a) - (1e) might attain in theoretical schemes involving neutral flavor-changing bosons.[10] In section 2, we consider muon-number violating K-decays in a gauge theory incorporating U(1)-type horizontal gauge interactions, first in a CP-invariant situation and then allowing for CP-violation. In Section 3, muon-number violation in horizontal models based on nonabelian gauge groups

is briefly reviewed and discussed. In Section 4, other possible sources of muon-number violation are briefly considered. Section 5 contains our conclusions.[11]

II. MUON-NUMBER VIOLATING K-DECAYS IN MODELS WITH HORIZONTAL INTERACTIONS

Considering flavor-changing effects, two general classes of horizontal interactions can be discerned: models where the horizontal bosons conserve flavor in the absence of generation mixing and models in which the horizontal bosons have flavor-nonconserving couplings even in the limit of no generation mixing. The first class consists of models based on horizontal gauge groups of the form U(1) x U(1)' x U(1)" x ... with an arbitrary number of U(1) factors; models of the second class are those based on horizontal gauge groups larger than U(1), i.e., SU(2), SU(3), ... The latter contain non-diagonal generators capable of connecting different representations of the vertical group.

Models of the type G x $U(1)_H$. CP-invariant case.

An additional U(1) factor is the simplest gauge group that can be added to the electroweak group to distinguish the fermion generations.[12] The new neutral (and hermitean) gauge boson Y_λ is coupled to a current of the general form[13]

$$
\begin{aligned}
J_Y^\lambda = {} & k_L \bar{d}_L' \gamma^\lambda d_L' + p_L \bar{s}_L' \gamma^\lambda s_L' + \ldots \\
& + k_R \bar{d}_R' \gamma^\lambda d_R' + p_R \bar{s}_R' \gamma^\lambda s_R' + \ldots \\
& + \ell_L \bar{e}_L' \gamma^\lambda e_L' + n_L \bar{\mu}_L' \gamma^\lambda \mu_L' + \ldots \\
& + \ell_R \bar{e}_R' \gamma^\lambda e_R' + n_R \bar{\mu}_R' \gamma^\lambda \mu_R' + \ldots
\end{aligned}
\tag{4}
$$

where d_L', d_R', ... e_L', e_R' ... are the vertical gauge group eigenstates ($d_L' = \frac{1}{2}(1-\gamma_5)d'$, $d_R' = \frac{1}{2}(1+\gamma_5)d'$, ...), and the numbers k_L, p_L, k_R, ... are determined by the $U(1)_H$ quantum number assignments. (d_L', s_L', ...),

$(d_R', s_R', \ldots)$, $(e_L', \mu_L', \ldots)$, $(e_R', \mu_R', \ldots)$ are related to the mass eigenstates $(d_L, s_L, \ldots)$, $(d_R, s_R, \ldots)$, $(e_L, \mu_L, \ldots)$, $(e_R, \mu_R, \ldots)$ by unitary transformations.

In terms of the mass eigenstates, the couplings of Y_λ to quarks and leptons are of the form (restricting ourselves only to terms involving the first two generations of $Q = -\frac{1}{3}$ quarks and $Q = -1$ leptons)

$$\begin{aligned} L_H = \tilde{g}(&\beta_V \bar{s}\gamma_\lambda d + \beta_A \bar{s}\gamma_\lambda\gamma_5 d + \xi_V \bar{d}\gamma_\lambda d + \xi_A \bar{d}\gamma_\lambda\gamma_5 d \\ &+ \zeta_V \bar{s}\gamma_\lambda s + \zeta_A \bar{s}\gamma_\lambda\gamma_5 s + \sigma_V \bar{\mu}\gamma_\lambda e + \sigma_A \bar{\mu}\gamma_\lambda\gamma_5 e + \rho_V \bar{e}\gamma_\lambda e + \rho_A \bar{e}\gamma_\lambda\gamma_5 e \\ &+ \kappa_V \bar{\mu}\gamma_\lambda \mu + \kappa_A \bar{\mu}\gamma_\lambda\gamma_5 \mu) Y^\lambda + \text{H.c.} \quad , \end{aligned} \tag{5}$$

where $\tilde{g}$ is the horizontal gauge group coupling constant and the quantities β_V, β_A, ξ_V,... depend, apart from the U(1) quantum number assignments, on the various unknown mixing angles and phase parameters. As discussed earlier, $\beta_V = \beta_A = \sigma_V = \sigma_A = 0$ in the limit of no generation mixing. Thus for small (as expected) mixing angles β_V, β_A, σ_V, and σ_A are proportional to combinations of mixing angles.

Let us assume that (5) is CP-invariant. Then all the quantities β_V, β_A, ξ_V,... are real. The branching ratios for the decays (1a) - (1e) are given by[14]

$$B(K_L \to \mu e) \equiv \Gamma(K_L \to \mu e)/\Gamma(K_L \to \text{all}) \tag{6a}$$

$$\simeq (4 \times 10^3)(m_w/m)^4(\tilde{g}/g)^4\beta_A^2(\sigma_V^2+\sigma_A^2)$$

$$B(K_S \to \mu e) \equiv \Gamma(K_S \to \mu e)/\Gamma(K_S \to \text{all}) \tag{6b}$$

$$\simeq (9 \times 10^{-9})B(K_L \to \mu e)$$

$$B(K_L \to \pi^0 \mu e) \equiv \Gamma(K_L \to \pi^0 \mu e)/\Gamma(K_L \to \text{all}) \tag{6c}$$

$$\simeq (3 \times 10^{-3})B(K_S \to \pi^0 \mu e)$$

$$B(K_S \to \pi^0 \mu e) \equiv \Gamma(K_S \to \pi^0 \mu e)/\Gamma(K_S \to \text{all}) \tag{6d}$$

$$\simeq (3 \times 10^{-1})(m_w/m)^4(\tilde{g}/g)^4\beta_V^2(\sigma_V^2+\sigma_A^2)$$

$$B(K \to \pi^{\pm}\mu e) \equiv \Gamma(K^{\pm} \to \pi^{\pm}\mu e)/\Gamma(K^{+} \to \text{all}) \tag{6e}$$

$$\simeq 40\ (m_w/m)^4(\tilde{g}/g)^4\beta_V^2(\sigma_V^2+\sigma_A^2)$$

In Eqs. (6a) - (6e), m denotes the mass of the horizontal boson and m_w is the mass of the usual charged weak boson.

Note that since $\beta_V^* = \beta_V$, $\beta_A^* = \beta_A$, the interaction (5) does not contain operators of the forms $\bar{s}\gamma_\lambda d - \bar{d}\gamma_\lambda s$ and $\bar{s}\gamma_\lambda\gamma_5 d - \bar{d}\gamma_\lambda\gamma_5 s$. Thus, $K_S \to \mu e$ and $K_L \to \pi^0\mu e$ can proceed only through the "wrong CP"-admixtures K_2 and K_1 in the K_S and K_L states, respectively.

The experimental limits (1a) and (1e) imply for m the lower limits

$$m \geq 94\ (\tilde{g}/g)|\beta_A|^{1/2}(\sigma_V^2+\sigma_A^2)^{1/4}\ \text{TeV} \tag{7}$$

and

$$m \geq 22\ (\tilde{g}/g)|\beta_V|^{1/2}(\sigma_V^2+\sigma_A^2)^{1/4}\ \text{TeV} \tag{8}$$

respectively. To assess the possible range of branching ratios for the decays (1a) - (1e), we have to investigate the lower bounds on m implied by other data. The most sensitive appear to be: the mass difference $\Delta m_{L,S} \equiv m_L - m_S \simeq 3.5 \times 10^{-6}$eV between K_L and K_S; the coherent muon-electron conversion rate in muon capture by ^{32}S, $R_{exp}^{coh} = \Gamma(\mu^- + S \to S + e^-)/\Gamma(\mu^- + S \to \text{capture})_{exp} < 7 \times 10^{-11}$ (Ref. 15), the decay $\mu \to 3e$ ($B(\mu \to 3e)_{exp} < 1.9 \times 10^{-9}$)[16], and the decay $K_L \to \mu\mu$ [17], ($B(K_L \to \mu\mu)_{exp} \equiv \Gamma(K_L \to \mu\mu)/\Gamma(K_L \to \text{all})_{exp} = (9.1 \pm 1.9) \times 10^{-9}$).[1] Demanding that the contribution of Y_λ to $\Delta m_{L,S}$, R^{coh}, $B(\mu \to 3e)$ and $B(K_L \to \mu\mu)$ would not exceed their experimental values, we obtain[18]

$$m \geq (1.5 \times 10^3)(\tilde{g}/g)|\beta|\ \text{TeV} \tag{9}$$

$$m \geq 230\ (\tilde{g}/g)|\xi_V|^{1/2}(\sigma_V^2+\sigma_A^2)^{1/4}\ \text{TeV} \tag{10}$$

$$m \geq 30\ (\tilde{g}/g)(\rho_V^2+\rho_A^2)^{1/4}(\sigma_V^2+\sigma_A^2)^{1/4}\ \text{TeV} \tag{11}$$

and

$$m \geq 90\ (\tilde{g}/g)|\beta_A|^{\frac{1}{2}}|\kappa_A|^{\frac{1}{2}}\ \text{TeV}\quad , \tag{12}$$

respectively.

In Table I we have exhibited the lower bounds on m implied by $B(K_L \to \mu e)$, $B(K^{\pm} \to \pi^{\pm}\mu e)$, $\Delta m_{L,S}$, R^{coh}, $B(K_L \to \mu\mu)$, and $B(\mu \to 3e)$ and the corresponding upper limits for the branching ratios (1a) - (1e) one would obtain with the arbitrary choice $\beta_V \simeq \beta_A \simeq \sigma_A \simeq \sigma_V \simeq \sin\theta_C$. ($\theta_C \equiv$ Cabibbo angle $\simeq 0.23$), $\xi_V \simeq \kappa_A \simeq \rho_V \simeq \rho_A \simeq 1$, and $\tilde{g} = g/2\sqrt{2}$ (i.e., $\tilde{g}^2/m^2 = (m_w/m)^2 G/\sqrt{2}$).[19] As seen from Table II, the most severe constraint on the branching ratios comes then from $\Delta m_{L,S}$. For $K_L \to \mu e$, $\Delta m_{L,S}$ implies

$$B(K_L \to \mu e) \leq (3 \times 10^{-14})(\sigma_V^2+\sigma_A^2)/\beta_A^2\quad . \tag{13}$$

The upper limit given in Table II corresponds to $(\sigma_V^2+\sigma_A^2)/\beta_A^2 \simeq 2$ leading to a branching ratio much below the experimental sensitivity one can hope for. However, $B(K_L \to \mu e)$ might be larger than 6×10^{-14}. One way this could happen is if β_A was much smaller than $\sin\theta_C$, while σ_V, $\sigma_A \simeq \sin\theta_C$. However, for too small β_A, the bound

$$B(K_L \to \mu e) \leq (2.5 \times 10^{-7})\beta_A^2/(\rho_V^2+\rho_A^2) \tag{14}$$

which follows from $B(\mu \to 3e)_{exp}$ would start to dominate over (13).[20] $\Delta m_{L,S}$ and $B(\mu \to 3e)_{exp}$ impose the same constraint (with $\rho_V \simeq \rho_A = 1$) on $B(K_L \to \mu e)$ for $\beta \simeq (2.3 \times 10^{-2})(\sigma_V^2+\sigma_A^2)^{\frac{1}{4}}$. Thus, we expect

$$B(K_L \to \mu e) \leq (6 \times 10^{-11})(\sigma_V^2+\sigma_A^2)^{\frac{1}{2}}\quad . \tag{15}$$

For $\sigma_V \simeq \sigma_A \simeq \sin\theta_C$, one would have

$$B(K_L \to \mu e) \leq 2 \times 10^{-11}\quad , \tag{16}$$

i.e., with possible future machines already in the measurable range.[21] A somewhat larger upper limit might be obtained if σ_V, $\sigma_A > \sin\theta_C$.[22]

Finally, one should note that the theoretical value for the K_L-K_S mass difference is uncertain and that in addition, the possibility of accidental cancellations among the various possible contributions to $\Delta m_{L,S}$ cannot be ruled out.

A further serious constraint may come from R_{exp}^{coh}. However, this will be of importance for $K_L \to \mu e$ only if the quarks have in addition to an axial vector coupling, also a vector coupling to Y_λ of strength not very much smaller than $\tilde{g}\beta_A$.

Concerning the remaining decay modes, for $\beta_V \simeq \beta_A$, $B(K^\pm \to \pi^\pm \mu e)$ (sensitive to a vector quark current) is smaller than $B(K_L \to \mu e)$ by a factor of 100. The chances for a measurable branching ratio for this decay is, therefore (and also because of the additional constraint from R_{exp}^{coh}) rather unlikely. The branching ratios for $K_S \to \mu e$, $K_L \to \pi^0 \mu e$, and also for $K_S \to \pi^0 \mu e$ are completely negligible.

For horizontal models involving several U(1) factors with CP-invariant interactions, the situation would remain qualitatively the same, since each gauge boson would make a contribution of the same sign to the effective $\Delta S = 2$ interaction.

Models of the type G x $U(1)_H$. CP-violating case.

So far we have been dealing with the case when the $U(1)_H$ horizontal interactions conserved CP. In general, the quantities β_V, β_A, ξ_V, ... are complex, giving rise to CP-violation.[23] A new feature will be the presence of operators of the form $\bar{s}\gamma_\lambda d - \bar{d}\gamma_\lambda s$, $\bar{s}\gamma_\lambda\gamma_5 d - \bar{d}\gamma_\lambda\gamma_5 s$, proportional to $\mathrm{Im}\beta_V$ and $\mathrm{Im}\beta_A$, respectively. As a consequence $B(K_1 \to \mu e)$ and $B(K_2 \to \pi^0 \mu e)$ will be different from zero. The $K_S \to \mu e$ and $K_L \to \pi^0 \mu e$ branching ratios are given by

$$B(K_S \to \mu e) \simeq 7\,(\tilde{g}/g)^4 (m_w/m)^4 (\mathrm{Im}\beta_A)^2 (|\sigma_V|^2 + |\sigma_A|^2) \qquad (17)$$

and

$$B(K_L \to \pi^0 \mu e) \simeq 170\,(\tilde{g}/g)^4 (m_w/m)^4 (\mathrm{Im}\beta_V)^2 (|\sigma_V|^2 + |\sigma_A|^2)\ . \qquad (18)$$

The lower bound on m implied by $\Delta m_{L,S}$ (Eq. 9) will become

$$m \geq (1.5 \times 10^3)(\tilde{g}/g)\left|(\mathrm{Re}\beta)^2 - (\mathrm{Im}\beta)^2\right|^{\frac{1}{2}} \text{ TeV} \quad . \tag{19}$$

The imaginary part of the $K^o \to \bar{K}^o$ amplitude will also receive a contribution, leading to the new bound [from the requirement $|\mathrm{ImA}(K^o \to \bar{K}^o)| \leq \sqrt{2}|\epsilon \Delta m_{L,S}|_{exp} \simeq \sqrt{2}\ (8 \times 10^{-9}\text{eV})$][24]

$$m \geq (3 \times 10^4)(\tilde{g}/g)\left|(\mathrm{Im}\beta)(\mathrm{Re}\beta)\right|^{\frac{1}{2}} \text{ TeV} \quad . \tag{20}$$

For $\mathrm{Im}\beta = \mathrm{Re}\beta \simeq \sin\theta_C$, there is no constraint from (19), but in view of the bound (20) all the branching ratios (1a) - (1e) would be completely negligible (about 10^{-5} times the values quoted under $\Delta m_{L,S}$ in Table I). Both constraints (19) and (20) would weaken for $\mathrm{Re}\beta$ and $\mathrm{Im}\beta$ sufficiently small and if simultaneously $\mathrm{Re}\beta \simeq \mathrm{Im}\beta$. However, $B(\mu \to 3e)$ would force then all the branching ratios (1a) - (1e) to be negligibly small. In the special case when $\mathrm{Re}\beta_A = 0$, $\mathrm{Im}\beta_A \neq 0$ the contribution to $\mathrm{ImA}(K^o \to \bar{K}^o)$ vanishes and the bound implied by $\Delta m_{L,S}$ is given by (9), with β replaced by $\mathrm{Im}\beta$. But now $B(K_2 \to \mu e) = 0$, $B(K_1 \to \pi^0 \mu e) = 0$, while $\Delta m_{L,S}$ leads to

$$B(K_S \to \mu e) \leq (5 \times 10^{-17})(|\sigma_V|^2+|\sigma_A|^2)/(\mathrm{Im}\beta_A)^2 \tag{21}$$

$$B(K_L \to \pi^0 \mu e) \leq (1.5 \times 10^{-15})(|\sigma_V|^2+|\sigma_A|^2)/(\mathrm{Im}\beta_V)^2 \tag{22}$$

and

$$B(K^{\pm} \to \pi^{\pm} \mu e) \leq (3 \times 10^{-16})(|\sigma_V|^2+|\sigma_A|^2)/(\mathrm{Im}\beta_V)^2 \quad . \tag{23}$$

For $|\mathrm{Im}\beta_{A,V}| \leq (2.3 \times 10^{-2})(|\sigma_V|^2+|\sigma_A|^2)^{\frac{1}{4}}$ more stringent constraints than (21), (22), and (23) are obtained from $B(\mu \to 3e)_{exp}$:

$$B(K_S \to \mu e) \leq 10^{-13}(|\sigma_V|^2+|\sigma_A|^2)^{\frac{1}{2}} \tag{24}$$

$$B(K_L \to \pi^0 \mu e) \leq (2.5 \times 10^{-12})(\sigma_V^2+\sigma_A^2)^{\frac{1}{2}} \tag{25}$$

and

$$B(K^{\pm} \to \pi^{\pm}\mu e) \leq (6 \times 10^{-13})(\sigma_V^2+\sigma_A^2)^{\frac{1}{2}} \quad . \tag{26}$$

Furthermore, R_{exp}^{coh} requires[18]

$$B(K_L \to \pi^0\mu e) \leq (2.5 \times 10^{-12})(Im\beta_V)^2/|\xi_V|^2 \tag{27}$$

$$B(K^{\pm} \to \pi^{\pm}\mu e) \leq (6 \times 10^{-13})(Im\beta_V)^2/|\xi_V|^2 \tag{28}$$

To summarize our discussion of the CP-violating $U(1)_H$-models, if $Im\beta$ is not negligible relative to $Re\beta$, the chances for any of the muon-number violating kaon decays to have detectable rates are remote. $Im\beta \ll Re\beta$ corresponds approximately to the CP-conserving case, of course.

In horizontal models based on a gauge group U(1) x U(1)' x U(1)" x ... involving more than one U(1) factors and with CP-invariant interactions, cancellations among the contributions of different gauge bosons to the $\Delta S = 2$ effective interaction is possible and consequently the branching ratios might turn out to be larger.

Nonabelian horizontal gauge models.

General features of muon-number violation in models based on a non-abelian horizontal gauge group[25] can be illustrated on the example of a CP-invariant $SU(2)_H$ model with two generations in which the fermions of given charge and chirality are assigned to $SU(2)_H$ doublets.[26] Thus, s_L', s_R', μ_L', μ_R', and d_L', d_R', e_L', e_R' are eigenstates of the third component of the "horizontal isospin" $\vec{H}$, with eigenvalues +1/2 and -1/2, respectively. The left-handed fields are related to the mass eigenstates as[27]

$$s_L' = -d_L\sin\theta + s_L\cos\theta$$

$$d_L' = d_L\cos\theta + s_L\sin\theta$$

$$\mu_L' = -e_L\sin\phi + \mu_L\cos\phi$$

$$e_L' = e_L\cos\phi + \mu_L\sin\phi \quad .$$

Identical relations hold for the right-handed fields, except for the angles, which will be in general different. The three hermitean bosons, Y_1, Y_2, and

Y_3 associated with the generators H_1, H_2, and H_3 will be assumed to coincide with the mass eigenstates. The interaction of s_L, d_L with the gauge bosons is given by

$$
\begin{aligned}
L = \tilde{g}\sqrt{2}\Big\{ & Y_1^\lambda[-\sin 2\theta\ \bar{d}_L\gamma_\lambda d_L + \sin 2\theta\ \bar{s}_L\gamma_\lambda s_L \\
& + \cos 2\theta\ (\bar{s}_L\gamma_\lambda d_L + \bar{d}_L\gamma_\lambda s_L)] \\
& - Y_2^\lambda[i(\bar{s}_L\gamma_\lambda d_L - \bar{d}_L\gamma_\lambda s_L)] \\
& + Y_3^\lambda[-\cos 2\theta\,\bar{d}_L\gamma_\lambda d_L + \cos 2\theta\ \bar{s}_L\gamma_L s_L - \sin 2\theta\ (\bar{s}_L\gamma_\lambda{}_L + \bar{d}_L\gamma_\lambda s_L)]\Big\}.
\end{aligned}
\tag{29}
$$

Interaction terms of the same form are contributed by (s_R, d_R), (μ_L, e_L), and (μ_R, e_R). The effective lagrangians for $\Delta S = 2$ transitions and for the decays (1a) - (1e) resulting from (29) and from an analogous term involving the left-handed leptons are

$$
L_{\text{eff}}^{\Delta S=2} = \tilde{g}^2\left[\frac{1}{m_1^2}\cos^2 2\theta - \frac{1}{m_2^2} + \frac{1}{m_3^2}\sin^2 2\theta\right]\bar{s}_L\gamma_\lambda d_L\,\bar{s}_L\gamma^\lambda d_L \tag{30}
$$

$$
\begin{aligned}
L_{\text{eff}}^{K_L \to \mu e,\ K_S \to \pi^0\mu e} = {} & 2\tilde{g}^2\left[\frac{1}{m_1^2}\cos 2\theta\ \cos 2\phi + \frac{1}{m_3^2}\sin 2\theta\ \sin 2\phi\right] \\
& \times (\bar{s}_L\gamma_\lambda d_L + \bar{d}_L\gamma_\lambda s_L)(\bar{e}_L\gamma^\lambda\mu_L + \bar{\mu}_L\gamma^\lambda e_L)
\end{aligned}
\tag{31}
$$

$$
L_{\text{eff}}^{K_S \to \mu e,\ K_L \to \pi^0\mu e} = -(2\tilde{g}^2/m_2^2)(\bar{s}_L\gamma^\lambda d_L - \bar{d}_L\gamma^\lambda s_L)(\bar{\mu}_L\gamma_\lambda e_L - \bar{e}_L\gamma^\lambda\mu_L) \tag{32}
$$

$$
L_{\text{eff}}^{K^\pm \to \pi^\pm\mu^\pm e^\mp} = 2\tilde{g}^2\left[\frac{1}{m_1^2}\cos 2\theta\ \cos 2\phi + \frac{1}{m_2^2} + \frac{1}{m_3^2}\sin 2\theta\ \sin 2\phi\right]\bar{s}_L\gamma_\lambda d_L\,\bar{e}_L\gamma^\lambda\mu_L + \text{H.c.} \tag{33}
$$

$$\mathcal{L}_{\text{eff}}^{K^{\pm} \to \pi^{\pm}\mu^{\mp}e^{\pm}} = 2\tilde{g}^2\left[\frac{1}{m_1^2}\cos2\theta\,\cos2\phi - \frac{1}{m_2^2} + \frac{1}{m_3^2}\sin2\theta\,\sin2\phi\right] \tag{34}$$
$$\times\left(\bar{s}_L\gamma_\lambda d_L\bar{\mu}_L\gamma^\lambda e_L\right) + \text{H.c.}$$

For each process there are three more terms of analogous form involving the right-handed fermions. As was expected, all these interaction terms survive in the limit $\theta = \phi = 0$. Also, $K_1 \to \mu e$ and $K_2 \to \pi^0\mu e$ are now allowed even in a CP-invariant theory. If the gauge bosons are degenerate (i.e., $m_1 = m_2 = m_3$), there will still be nonvanishing contributions for $\theta = \phi = 0$ to $K_{L,S} \to \mu e$, $K_{L,S} \to \pi^0\mu e$, and $K^{\pm} \to \pi^{\pm}\mu^{\pm}e^{\mp}$, while the contributions to $\Delta S = 2$ transitions and to the $K^{\pm} \to \pi^{\pm}\mu^{\mp}e^{\pm}$ amplitudes vanish.[28] This behavior is a consequence of global $SU(2)_H$ symmetry and the resulting conservation of H_3 which represents here the so-called generation-number G.[29] The $\Delta G = 0$ processes $K_{L,S} \to \mu e$, $K_{L,S} \to \pi^0\mu e$, and $K^{\pm} \to \pi^{\pm}\mu^{\pm}e^{\mp}$ are allowed, while $\Delta G = 2$ transitions such as (30) and (34) are forbidden. The conservation of the generation number, which is defined for unmixed states, is broken by generation mixing and by mass splittings among the bosons. $|\Delta G| = 1$ processes like $\mu \to 3e$, $\mu \to e\gamma$, $\mu^-Z \to e^-Z$, and $K_L \to \mu\mu$ are proportional to $\sin\theta$ or $\sin\phi$ (even for $m_1 \neq m_2 \neq m_3$).[29]

Let us consider now in this framework the decays (1a) - (1e) in some special cases:

(a) If the mass difference between Y_1 and Y_2 is comparable to m_1 and m_2, $(\Delta m_{L,S})_{\text{exp}}$ implies a lower bound for m_1, m_2 of about 530 TeV (assuming $\tilde{g} = g/2\sqrt{2}$). The contributions of Y_1 and Y_2 to any of the branching ratios (1a) - (1e) would then be too small to be detectable. For example, $B(K_L \to \mu e) < 10^{-13}$, $B(K^{\pm} \to \pi^{\pm}\mu^{\pm}e^{\mp}) < 2 \times 10^{-15}$.

The effects of Y_3 which is associated with the diagonal generator H_3 are the same as those of a horizontal gauge boson associated with a $U(1)_H$ group. The constraints from $|\Delta G| = 1$ processes are of the same order in the mixing angles as in the case of $U(1)_H$.

(b) If $m_1 \simeq m_2 (\equiv m)$, while $m_3 >> m$, Eq. (30) becomes

$$L_{\text{eff}}^{\Delta S = 2} \simeq -(\tilde{g}^2/m^2) \sin^2 2\theta \; \bar{s}_L \gamma_\lambda d_L \; \bar{s}_L \gamma^\lambda d_L \quad . \tag{35}$$

Consequently, for $\theta = 0$ (which corresponds to the case when the non-hermitean boson $Y_+ = (Y_1 - Y_2)/\sqrt{2}$ is coupled to $\bar{s}d$ but not to $\bar{d}s$), the contribution of Y_1, Y_2 to $\Delta m_{L,S}$ vanishes. In the presence of generation mixing, it is suppressed by $\sin^2 2\theta$.[30] At the same time the $\Delta G = 0$ transitions (31), (32), and (33) remain of the zeroth order in the mixing angles. $|\Delta G| = 1$ processes will be proportional to $\sin\theta$ or $\sin\phi$ as before.

In Table II, we show the lower bounds on m and the corresponding upper bounds on the branching ratios assuming $\theta = \phi = \theta_c$, $\tilde{g} = g/2\sqrt{2}$.[19,31] All the branching ratios could be much larger, however:

For $K_L \to \mu e$, $(\Delta m_{L,S})_{\text{exp}}$ implies

$$B(K_L \to \mu e) \leq (4 \times 10^{-15})/\theta^4 \quad . \tag{36}$$

For $\theta \simeq 4 \times 10^{-2}$, the branching ratio would be as large as the present experimental limit.

The constraint for $K_S \to \mu e$ from $(\Delta m_{L,S})_{\text{exp}}$ is

$$B(K_S \to \mu e) \leq (7 \times 10^{-18})/\theta^4 \tag{37}$$

which would allow, e.g., $B(K_S \to \mu e) \simeq 10^{-7}$ for $\theta \simeq 3 \times 10^{-3}$. However, $B(K_L \to \mu e)_{\text{exp}}$ demands $B(K_S \to \mu e) < 4 \times 10^{-12}$, independently on θ. Nevertheless, it is not impossible that in some more complicated models the operator $\bar{s}\gamma_\lambda\gamma_5 d + \bar{d}\gamma_\lambda\gamma_5 s$ is suppressed relative to $\bar{s}\gamma_\lambda\gamma_5 d - \bar{d}\gamma_\lambda\gamma_5 s$, allowing for a branching ratio larger than 4×10^{-12}.

For $\theta \geq 1.2 \times 10^{-2}$, $\theta \geq 2 \times 10^{-3}$, and $\theta \geq 2 \times 10^{-4}$, $(\Delta m_{L,S})_{\text{exp}}$ would allow $B(K^\pm \to \pi^\pm \mu^\pm e^\mp) \leq 7 \times 10^{-9}$ (i.e., the present experimental limit), $B(K_L \to \pi^0 \mu e) \leq 10^{-5}$ and $B(K_S \to \pi^0 \mu e) \leq 10^{-4}$ (i.e., branching ratios in the measurable range),[32] respectively. $B(K^\pm \to \pi^\pm \mu^\pm e^\mp)_{\text{exp}}$ requires $B(K_L \to \pi^0 \mu e) \leq 7 \times 10^{-9}$ and $B(K_S \to \pi^0 \mu e) \leq 10^{-11}$ but again, the possibility

that in a more complicated model, $\bar{s}\gamma^{\lambda}d$ is suppressed relative to $\bar{s}\gamma_{\lambda}d \pm \bar{d}\gamma_{\lambda}s$ cannot be excluded. $B(K^{\pm} \to \pi^{\pm}\mu^{\pm}e^{\mp})$, $B(K_L \to \pi^0\mu e)$, and $B(K_s \to \pi^0\mu e)$ have to respect yet the constraints from R_{exp}^{coh}. For values of θ quoted above, they are $B(K^{\pm} \to \pi^{\pm}\mu^{\pm}e^{\mp}) \leq 4 \times 10^{-9}$, $B(K_L \to \pi^0\mu e) \leq 2 \times 10^{-7}$, and $B(K_s \to \pi^0\mu e) \leq 3 \times 10^{-8}$, which would render $B(K_L \to \pi^0\mu e)$ and $B(K_s \to \pi^0\mu e)$ too small to be observable.[2] It should be noted, however, that the relationships between various processes would presumably become less tight when the third generation is included, in view of the presence of more mixing angles. In addition, one has to remember the uncertainties involved in the estimate of R^{coh}.[18]

The constraints from $\mu \to 3e$ and $K_L \to \mu\mu$ need not be effective, since the angle associated with the $\mu \to \mu$ and $e \to e$ vertices could be small.

(c) For $m_1 = m_2 = m$, and m_3 arbitrary, Eq. (30) reads

$$L^{\Delta S = 2} = \tilde{g}^2 \sin^2 2\theta \left(\frac{1}{m_3^2} - \frac{1}{m^2}\right) \bar{s}_L\gamma_{\lambda}d_L \; \bar{s}_L\gamma^{\lambda}d_L \quad . \tag{38}$$

Consequently, the contribution of near degenerate horizontal bosons to $\Delta m_{L,S}$ arising from the left-handed sector is suppressed by $(m_3^{-2} - m^{-2})$ in addition to the factor $\sin^2 2\theta$.[33] The same result holds for the contribution of the right-handed quarks. However, in the presence of both left-handed and right-handed contributions, $\Delta m_{L,S}$ will be proportional to $(m_3^{-2} - m^{-2})$ only if the mixing angles in the left-handed and right-handed sectors are equal.[34,35] This is in contrast to the suppression effect described under (b), which is valid for an arbitrary linear combination of V and A currents and which might be therefore more common.

The constraints for the branching ratios of muon-number violating K-decays implied by $\Delta m_{L,S}$ are the same as in the previous case, except that θ^2 is replaced now by $\theta^2[(m/m_3)^2 - 1]$.[36] As a consequence $(\Delta m_{L,S})_{exp}$ could allow large branching ratios even for relatively large θ. However for, say, $\theta = \theta_c$, R_{exp}^{coh} implies (with the reservations mentioned before) negligible branching ratios for $B(K_L \to \pi^0\mu e)$ and $B(K_S \to \pi^0\mu e)$, and a branching ratio for $K^{\pm} \to \pi^{\pm}\mu^{\pm}e^{\mp}$ of the order of 10^{-11} or less. (Cf. Table II.)

If we allow for CP-violation in the horizontal interactions[37] and their contribution to the $K - \overline{K}^0$ matrix element is not suppressed, then either the bosons must be much heavier ($m \geq 7 \times 10^3$ TeV) than in the CP-conserving case, or the phase (δ) responsible for CP-violation must be sufficiently small ($\delta \approx 10^{-3}$ or smaller for $m \approx 330$ TeV). In the former case, the branching ratios (1a) - (1e) would be negligible; in the latter case, CP-conserving observables such as the branching ratios would remain essentially the same as in the CP-invariant case. Alternatively, the contribution of the horizontal interactions to the $K^0 \to \overline{K}^0$ matrix element might be suppressed, either because of a cancellation of the type described earlier under case (b)[38] or because of the one discussed under (c),[39] allowing the branching ratios to be larger. They must be consistent, however, with the constraint provided by $|\varepsilon'/\varepsilon|_{exp}$.[24] The latter does not limit $B(K_L \to \mu e)$ and $B(K^{\pm} \to \pi^{\pm}\mu e)$ further and allows, with $\theta = \theta_c$, $B(K_S \to \mu e) \leq 10^{-7}$ for $\delta \geq 4.5 \times 10^{-2}$, $B(K_L \to \pi^0\mu e) \leq 10^{-5}$ for $\delta \geq 2.3 \times 10^{-2}$, and $B(K_S \to \pi^0\mu e) \leq 10^{-4}$ for $\delta \geq 3 \times 10^{-4}$.

III. OTHER POSSIBLE SOURCES OF MUON-NUMBER VIOLATION

So far we have discussed muon-number violation mediated by horizontal gauge bosons. As noted in the introduction, neutral flavor-changing gauge bosons may appear also in extended electroweak theories,[40] and even the neutral boson of the standard model might have flavor-changing couplings to possible further generations of fermions.[4] In such models neutral flavor-changing gauge bosons associated with diagonal generators will behave in a way analogous to a $U(1)_H$-type horizontal boson, while the effects of nonhermitean gauge bosons will resemble the effects of nonhermitean horizontal bosons present in nonabelian horizontal gauge models. Further possible sources of muon-number violation (apart from muon-number violation through higher order effects) is Higgs exchange and the exchange of leptoquarks.

Higgs exchange.

If the Higgs sector of the $SU(2)_L \times U(1)$ electroweak theory is extended to include more than one Higgs doublet,[41] muon-number may be violated by the Higgs-lepton couplings.[9] Muon-number may be violated also by Higgs mesons associated with gauge groups beyond $SU(2)_L \times U(1)$.

In the standard model the Higgs mesons couples to scalar fermion densities. If, however, more than one Higgs doublet exists, pseudoscalar couplings may also be present.

Let us consider the contribution of a hermitean Higgs mesons ϕ to $K_L \to \mu e$. The most general coupling responsible has the form

$$L = g''(a\,\bar{s}i\gamma_5 d + a^*\,\bar{d}i\gamma_5 s)\phi + g'(\ell\,\bar{\mu}e + \ell^*\,\bar{e}\mu + n\,\bar{\mu}i\gamma_5 e + n^*\,\bar{e}i\gamma_5\mu)\phi \quad (39)$$

Let $CP\phi(CP)^{-1} = -\phi$ for definiteness, and assume $b^* = b$. Then the coupling of ϕ to s,d is CP-invariant. The resulting $K_L \to \mu e$ branching ratio is given by[42]

$$B(K_L \to \mu e) \simeq (1.3 \times 10^4)(\sqrt{2}\, g'g''/Gm_h^2)^2(|\ell|^2 + |n|^2)(\mathrm{Re}a)^2 \quad , \quad (40)$$

where m_h is the mass of the Higgs meson and G is the Fermi constant.

$(\Delta m_{L,S})_{exp}$ requires[42]

$$m_h \geq (7.5 \times 10^6)g''|a| \ \mathrm{GeV} \quad , \quad (41)$$

so that we expect

$$B(K_L \to \mu e) \leq (6.5 \times 10^{-14})(g'/g'')^2(|\ell|^2 + |n|^2)/(\mathrm{Re}a)^2 \quad . \quad (42)$$

Thus, $B(K_L \to \mu e)$ would be of the order of the present experimental limit for $(g'/g'')^2(|\ell|^2 + |n|^2)/(\mathrm{Re}a)^2 \simeq 3 \times 10^{-6}$. Suppose that $g_h' = 2^{1/4}\, m_\mu \sqrt{G}$ and $g_h'' = 2^{1/4}\, m_d \sqrt{G}$. Then $g'/g'' = m_\mu/m_d \simeq 14$ (with $m_d \simeq 7.5$ MeV), and

$$B(K_L \to \mu e) \leq (1.3 \times 10^{-11})(|\ell|^2 + |n|^2)/(\mathrm{Re}a)^2 \quad (43)$$

so that for a not unreasonably large ratio $(|\ell|^2 + |n|^2)/(\mathrm{Re}a)^2$, $B(K_L \to \mu e)$ might be near to the experimental limit.[43] Even for $(|\ell|^2 + |n|^2)/(\mathrm{Re}a)^2 \simeq 1$, $B(K_L \to \mu e)$ could be larger than 10^{-11} since the ratio of the Higgs couplings may be larger than m_μ/m_d.[44] Moreover, the possible cancellation effect in the $K^o - \bar{K}^o$ matrix element, described for gauge bosons under case (b) and under case (c) in the previous section, could also be operative for Higgs mesons.[30,45] $B(K_L \to \mu e)$ mediated by such Higgs mesons could be as large as the experimental limit.[43]

Concerning the other decay modes, $K_1 \to \mu e$ and $K_2 \to \pi^0 \mu e$ are forbidden for $a^* = a$. All the decays (1a) - (1e) occur even in a CP-invariant case if nonhermitean Higgs mesons are involved. The three-body decays are sensitive to a scalar quark density. Any of the decays could have observable branching ratios, although for $K_S \to \mu e$, $K_S \to \pi^0 \mu e$, and $K_L \to \pi^0 \mu e$ it is very unlikely, because of the probable constraint from $K_L \to \mu e$ and $K^\pm \to \pi^\pm \mu e$, respectively.

Leptoquark exchange.

Muon-number could be violated also through the exchange of leptoquarks (bosons causing quark $\leftrightarrow$ lepton transitions). Leptoquark gauge bosons appear in theories which unify the strong and the flavor interactions. However, they are expected to be too heavy to cause detectable muon-number violating effects.[46] Relatively light ($M \simeq 200$ GeV) spinless leptoquarks (the leptoquark pseudogoldstone bosons) appear in extended technicolor models.[8,47] Leptoquark pseudogoldstone boson exchange leads to an effective four-fermion coupling of the form[47]

$$L_{eff} \simeq \frac{m_s m_d}{F_p^2} \frac{1}{m_p^2} \bar{s}\Gamma\mu \; \bar{e}\Gamma' d \quad , \tag{44}$$

where Γ,Γ' is a mixture of pseudoscalar and scalar couplings, m_s, m_d are the masses of the s and d quarks, and m_p is the leptoquark mass. $F_p \simeq 250$ GeV is the vacuum expectation value of the technisigma field.

L_{eff} gives rise to $K_L \to \mu e$ with a branching ratio near the present experimental limit.[47] $K^\pm \to \pi^\pm \mu e$ would occur presumably with an effective coupling of the same order of magnitude, i.e., with a branching ratio of the order of $10^{-2} B(K_L \to \mu e)$. The remaining muon-number violating K-decays would be too small to be observable. Note that muon-number violation via leptoquark exchange is not constrained significantly by $(\Delta m_{L,S})_{exp}$, since in lowest order there is no accompanying nonleptonic interaction.[48]

IV. CONCLUSIONS

There are many theoretical reasons to suspect that flavor-changing neutral interactions should exist at some level. We have considered the

branching ratios of muon-number violating decays in various theoretical schemes which imply the existence of such effects.

In horizontal models based on nonabelian gauge groups, muon-number violating K-decays conserve generation number and consequently could have appreciable rates, while other muon-number violating processes, such as $\mu \to 3e$, $\mu \to e\gamma$, and $\mu^- Z \to e^- Z$ might be negligible.[28] The branching ratios for $K_L \to \mu e$ and $K^{\pm} \to \pi^{\pm}\mu^{\pm}e^{\mp}$ could be as large as the present experimental limits.[49] Barring accidental cancellations this would require that one of the two suppression mechanisms described in the text be operative for the contributions of the horizontal bosons to the $K^o \to \bar{K}^o$ transition matrix element. Also, with either type of suppression, it seems necessary to have the mixing angle in the quark sector small (of the order of a few times 10^{-2}).

In horizontal gauge models of the U(1)-type, the chances for $K_L \to \mu e$ and $K^{\pm} \to \pi^{\pm}\mu e$ to have detectable branching ratios are less favorable. The source of the most important constraint for $K_L \to \mu e$, apart from $(\Delta m)_{L,S}$, appears to be in this case $B(\mu \to 3e)_{exp}$ and for $K^{\pm} \to \pi^{\pm}\mu e$ also R^{coh}. With small angles in the quark sector $B(K_L \to \mu e)$ could be as large as 2×10^{-11}, i.e., in the measurable range, but only for possible future machines. The possibility of $K^{\pm} \to \pi^{\pm}\mu e$ having a significant rate is much less likely. If the $U(1)_H$ interactions violate CP-invariance, none of the muon-number violating kaon decay rates are expected to be accessible.

Flavor-changing Higgs mesons may give rise to $K_L \to \mu e$ and $K^{\pm} \to \pi^{\pm}\mu e$ rates comparable to the present experimental limit. The requirement for this is, unless $\Delta m_{L,S}$ is suppressed, either small mixing angles in the quark sector or larger than "standard" ratios of Higgs couplings to leptons versus the quarks.

A $K_L \to \mu e$ rate near the existing experimental limit (and a $K^{\pm} \to \pi^{\pm}\mu e$ rate near the measurable domain) is <u>expected</u> in extended technicolor schemes.[47]

In all the schemes considered above, measurable branching ratios for $K_S \to \mu e$, $K_S \to \pi^0\mu e$, and $K_L \to \pi^0\mu e$ are unlikely, because of the constraints due to $B(K_L \to \mu e)_{exp}$ and $B(K^{\pm} \to \pi^{\pm}\mu e)_{exp}$.

Needless to say, observation of muon-number violating K-decays (or any other muon-number violating processes) would have an enormous impact on our

understanding of the fundamental interactions. In some of the possible theoretical schemes, muon-number violating K-decays might be the most sensitive probes of the existence of new interactions. Therefore new facilities with higher intensity kaon beams might perhaps turn out to be decisive for the eventual discovery of interactions beyond the standard three-generation gauge theory of the electroweak interactions. Stringent experimental upper limits on all muon-number violating processes are also of great importance since they provide constraints on the theoretical possibilities.

ACKNOWLEDGEMENTS

I am grateful to C. M. Hoffman, D. E. Nagle, S. P. Rosen, R. Slansky, and L. Wolfenstein for useful conversations. I would also like to thank J. D. Bjorken, H. Harari, and L. Wolfenstein for helpful correspondence.

source of the bound	lower bound on m (in TeV)	upper bounds for the branching ratios				
		$B(K_L \to \mu e)$	$B(K_S \to \mu e)$	$B(K^{\pm} \to \pi^{\pm}\mu e)$	$B(K_L \to \pi^0 \mu e)$	$B(K_S \to \pi^0 \mu e)$
$B(K_L \to \mu e)_{exp}$	9	2×10^{-9}		2×10^{-11}		2×10^{-13}
$B(K^{\pm} \to \pi^{\pm}\mu e)_{exp}$	2	-		7×10^{-9}		5×10^{-11}
$(\Delta m_{L,S})_{exp}$	120	6×10^{-14}		6×10^{-16}		5×10^{-18}
R^{coh}_{exp}	46	3×10^{-12}	$\simeq (9 \times 10^{-9}) \times B(K_L \to \mu e)$	3×10^{-14}	$\simeq (3 \times 10^{-3}) \times B(K_S \to \pi^0 \mu e)$	2×10^{-16}
$B(\mu \to 3e)_{exp}$	7	-		10^{-9}		2×10^{-11}
$B(K_L \to \mu\mu)_{exp}$	15	3×10^{-10}		3×10^{-12}		2×10^{-14}

TABLE I. Lower bounds for the mass of the horizontal gauge boson and the corresponding upper bounds for the branching ratios of muon-number violating kaon decays in CP-invariant $U(1)_H$-type models. We have assumed $\tilde{g} = g/2\sqrt{2}$, $\beta_V \simeq \beta_A \simeq \sigma_V \simeq \sigma_A \simeq \sin\theta_C$, $\xi_V \simeq \rho_V \simeq \rho_A \simeq \kappa_A = 1$, and $m_W = 80$ GeV. An empty box indicates that the upper bound implied is larger than the experimental upper limit.

source of the bound	lower bound on m (in TeV)	upper bounds for the branching ratios				
		$B(K_L \to \mu e)$	$B(K_S \to \mu e)$	$B(K^{\pm} \to \pi^{\pm}\mu^{\pm}e^{\mp})$	$B(K_L \to \pi^0 \mu e)$	$B(K_S \to \pi^0 \mu e)$
$B(K_L \to \mu e)_{exp}$	28	2×10^{-9}	4×10^{-12}	9×10^{-11}	9×10^{-11}	2×10^{-13}
$B(K^{\pm} \to \pi^{\pm}\mu^{\pm}e^{\mp})_{exp}$	9	-	3×10^{-10}	7×10^{-9}	7×10^{-9}	10^{-11}
$(\Delta m_{L,S})_{exp}$	170	2×10^{-12}	3×10^{-15}	6×10^{-14}	6×10^{-14}	10^{-16}
R^{coh}_{exp}	46	3×10^{-10}	5×10^{-13}	10^{-11}	10^{-11}	2×10^{-14}
$B(\mu \to 3e)_{exp}$	7	-	10^{-9}	-	3×10^{-8}	4×10^{-11}
$B(K_L \to \mu\mu)_{exp}$	15	-	4×10^{-11}	10^{-9}	10^{-9}	2×10^{-12}

TABLE II. Lower bounds for the mass of the horizontal gauge boson and the corresponding upper bounds for the branching ratios of muon-number violating kaon decays in the CP-invariant $SU(2)_H$ model described in the text, assuming $m_1 \simeq m_2$, $m_3 >> m_1, m_2$. We have assumed $\tilde{g} = g/2\sqrt{2}$; $\theta, \phi \simeq \theta_C$, $m_W = 80$ GeV. Empty boxes indicate that the upper bound implied is larger than the experimental upper limit.

REFERENCES

1. Particle Data Group, Rev. Mod. Phys. 52, (April 1980).

2. C. M. Hoffman, private communication. These expectations should be regarded only as first crude estimates. Also, they do not, of course, take into account possible new discoveries in experimental technology.

3. For example:

$$\Gamma(\mu \to e\gamma)/\Gamma(\mu \to e\nu\bar{\nu}) < 4 \times 10^{-17}$$

$$\Gamma(\mu^- + {}^{32}S \to e^- + {}^{32}S)/\Gamma(\mu^- + {}^{32}S \to \text{capture}) < 6 \times 10^{-14}$$

$$\Gamma(\mu \to 3e)/\Gamma(\mu \to e\nu\bar{\nu}) \to 3 \times 10^{-17}$$

$$\Gamma(K_L \to \mu e)/\Gamma(K_L \to \text{all}) < 5 \times 10^{-16}$$

$$\Gamma(K^+ \to \pi^+ \mu e)/\Gamma(K^+ \to \text{all}) < 6 \times 10^{-10} ,$$

to be compared with the present experimental upper bounds 1.9×10^{-10}, 7×10^{-11}, 1.9×10^{-9}, 2×10^{-9}, and 7×10^{-9}, respectively. For a review and references see, for example, Panel P-2 Report, Proceedings of the Workshop on Program Options in Intermediate-Energy Physics, Los Alamos Scientific Laboratory, Los Alamos, 1979, ed. by J. C. Allred and B. Talley, LASL Publication LA-8335-C, Vol. I, p. 21.

4. An example of such a situation is the (now ruled out) five-lepton model [G. Altarelli, N. Cabibbo, L. Maiani, and R. Petronzio, Phys. Lett. 67B, 463 (1977); D. Horn and G. Ross, Phys. Lett. 67B, 460 (1977)].

5. Reviews of horizontal symmetries and related questions include: H. Harari, "Quarks and Leptons: The Generation Puzzle," talk presented at the Einstein Centennial Symposium, Jerusalem, 1979, SLAC-PUB-2363, 1979; J. D. Bjorken, Proceedings of the "Neutrino 79" International Conference, Bergen, 1979, ed. by A. Haatuft and C. Jarlskog, Vol. 1, p. 9; P. Ramond, "The Family Group in Grand Unified Theories," invited talk at the Sanibel Symposia, 1979, California Institute of Technology Preprint CALT-68-709; R. Slansky, "Group Theory for Unified Model Building," Los Alamos National Laboratory preprint LA-UR-80-3495, to be published in Physics Reports; D. Bailin, "Prospects for Gauge Theories," University of Sussex preprint, 1980, to be published in Surveys in High Energy Physics; P. Langacker, "Grand Unified Theories and Proton Decay," SLAC-PUB-2544, June 1980, to be published in Physics Reports.

6. Another possibility is a large unifying group which incorporates both vertical and horizontal interactions. Such a group may or may not have a $G \times G_H$ subgroup. Cf. Ref. 5.

7. They might also be superheavy. For an example, see P. Ramond, Ref. 5.

8. S. Dimopoulos and L. Susskind, Nucl. Phys. B155, 237 (1979); E. Eichten and K. D. Lane, Phys. Lett. 90B, 125 (1980).

9. J. D. Bjorken and S. Weinberg, Phys. Rev. Lett. 38, 622 (1977).

10. Aspects of muon-number violating K-decays have been considered previously by R. N. Cahn and H. Harari, Preprint LBL-10823, (1980); G. L. Kane and R. Thun, Phys. Lett. 94B, 513 (1980); O. Shanker, TRIUMF Preprint TRI-PP-80-32 (1980); P. Herczeg, Proceedings of the Kaon Factory Workshop, Vancouver (August 1979), ed. by M. K. Craddock, TRIUMF Publication TRI-79-1, p. 20. For a recent review, see S. P. Rosen, Proceedings of the Workshop on Weak Interactions, Virginia Polytechnic Institute and State University (December 1980).

11. We shall give a more detailed account of the present investigation in a forthcoming paper.

12. A. Davidson, M. Koca, and K. C. Wali, Phys. Rev. Lett. 43, 92 (1979); Phys. Lett. 86B, 47 (1979); S. Barr and P. Langacker, Phys. Rev. Lett. 42, 1654 (1979); M. A. B. Bég and A. Sirlin, Phys. Rev. Lett. 38, 1113 (1977); T. Maehara and T. Yanagida, Lett. Nuovo Cim. 19, 424 (1977).

13. We shall ignore possible mixing of Y with the vertical neutral bosons.

14. E.g., P. Herczeg, Refs. 10 and 11. In Ref. 10 only a hermitean boson exchange was considered, with CP-invariant couplings. The r.h.s. of Eqs. (22) and (31) of this paper should have included a factor 1/2. Eqs. (23) - (28) and (32) - (37) have to be corrected accordingly.

15. A. Badertscher et al., Phys. Rev. Lett. 39, 1385 (1977), and University of Berne preprint (1980).

16. S. M. Korenchenko et al., JETP 43, 1 (1976).

17. A further constraint comes from the process $\mu \to e\gamma$. However, the contribution of Y to $B(\mu \to e\gamma)$ is suppressed by a factor of $\sim \alpha$ relative to $B(\mu \to 3e)$. Nevertheless, in view of the better experimental limit on $B(\mu \to e\gamma)$, the lower bound on m implied by $\mu \to e\gamma$ is comparable to (11). An estimate of the contribution of horizontal bosons to $B(\mu \to e\gamma)$ is contained in the paper of R. N. Cahn and H. Harari, Ref. 10.
Further information on horizontal models will come from processes involving also the third fermion generation.

18. To estimate the contribution of Y to $\Delta m_{L,S}$, we have used the "vacuum insertion" value for a V-A interaction of strength $\tilde{g}\beta_A$ or $\tilde{g}\beta_V$. [See, for example, R. E. Shrock and S. B. Treiman, Phys. Rev. D19, 2148 (1979)]. For R^{coh}, the calculation of O. Shanker [Phys. Rev. D20, 1608 (1979)] was used. We have ignored the contributions to $\mu^- \to e^-$ conversion arising from the Q = 2/3 sector.

19. Note that unlike the lower bounds for m, the upper limits on the branching ratios are independent of the choice for $\tilde{g}$.

20. A further constraint, independent of β_A is

$$\Gamma(K_L \to e\mu) < 2.5 \times 10^{-9}(\sigma_V^2 + \sigma_A^2)/\kappa_A^2 \quad ,$$

provided by $B(K_L \to \mu\mu)_{exp}$.

21. Note that if the upper limit on $B(\mu \to 3e)$ was lowered to 10^{-11}, as anticipated in the next generation experiments, the bound (16) would be replaced by $B(K_L \to \mu e) < 1.4 \times 10^{-12}$.

22. Note that an assignment in which the $U(1)_H$ quantum numbers for the lepton generations are larger than those of the quarks would not probably imply a larger $B(K_L \to \mu e)$ since the constraint from $B(\mu \to 3e)_{exp}$ would presumably become more severe at the same time.

23. Such type of CP-violation has also been suggested as a possible source of the observed CP-violation: A. Davidson, M. Koca, and K. C. Wali, Ref. 12; S. Barr and P. Langacker, Ref. 12; M. A. B. Bég, and A. Sirlin, Ref. 12.

24. Further constraints are provided by $|\mathrm{ImAo/ReAo}| < \sqrt{2}|\varepsilon_{exp}|$ and $|\varepsilon'/\varepsilon|_{exp} < 1/50$ [e.g., K. Kleiknecht, Ann. Rev. Nucl. Sci. 26, 1 (1976)]. Considering only the contribution of the term proportional to $\mathrm{Re}\xi_V \mathrm{Im}\beta$, one obtains

$$m \geq 8(\tilde{g}/g)|\mathrm{Re}\xi_V|^{1/2}|\mathrm{Im}\beta|^{1/2}\mathrm{TeV}$$

and

$$m \geq 60\tilde{g}/g|\mathrm{Re}\xi_V|^{1/2}|\mathrm{Im}\beta|^{1/2}\mathrm{TeV},$$

respectively. For the definitions of the CP-violating parameters in the $K^o - \bar{K}^o$ system and in $K \to 2\pi$ decays, see L. Wolfenstein in Theory and Phenomenology in Particle Physics, A. Zichichi, ed.), Academic Press, p. 218 (1969).

25. R. N. Mohapatra, J. C. Pati, and L. Wolfenstein, Phys. Rev. D11, 3319 (1975); S. Barr and A. Zee, Phys. Rev. D17, 1854 (1978); T. Maehara and T. Yanagida, Prog. Theor. Phys. 60, 822 (1978), 61, 1434 (1979); F. Wilczek and A. Zee, Phys. Rev. Lett. 42, 421 (1979); C. L. Ong, Phys. Rev. D19, 2738 (1979); J. Chakrabarti, Phys. Rev. D20, 2411 (1979). P. Ramond, Ref. 5; Y. Chikashiga, G. Gelmini, R. D. Peccei, and M. Roncadelli, Phys. Lett. 94B, 499 (1980); see also R. D. Peccei, talk at the XX International Conference on High Energy Physics, Madison, WI (1980), Max-Planx-Institut preprint MPI-PAE/PTh 28/80 and Ref. 5.

26. Muon-number violation in such a model, including K-decays, have been studied by T. Maehara and T. Yanagida, Ref. 25; R. Cahn and H. Harari, Ref. 10; O. Shanker, Ref. 10. Flavor violation in an $SU(2)_H$ model with different multiplet assignments and including the third generation was discussed by I. Montvay, preprint DESY 80/62 (1980).

27. θ, of course, need not be the Cabibbo angle. The Cabibbo angle could arise from mixing in the $Q = 2/3$ sector, or mixings in both the $Q = 2/3$ and in the $Q = -1/3$ sectors may be responsible.

28. The importance of the decays $K_L \to \mu e$ and $K^{\pm} \to \pi^{\pm}\mu^{\pm}e^{\mp}$ for testing horizontal models, being the simplest muon-number violating processes which conserve the generation number in nonabelian horizontal gauge models, was pointed out by H. Harari, Ref. 5.

29. R. N. Cahn and H. Harari, Ref. 10.

30. I am grateful to J. D. Bjorken, E. Harari, and L. Wolfenstein for bringing this suppression effect to my attention. Such a cancellation mechanism was invoked by T. D. Lee and C. N. Yang in their schizon theory [Phys. Rev. 119, 1410 (1960)], to cancel the contributions of strangeness changing neutral currents to $\Delta m_{L,S}$.

31. All our estimates correspond to a V-A interaction. In general, an arbitrary linear combination of V and A would be involved. We can consider therefore, e.g., $K_L \to \mu e$ (sensitive to an axial quark current) and $K^{\pm} \to \pi^{\pm}\mu e$ (sensitive to a vector quark current) as unrelated.

32. The ultimate largest possible values of $B(K_S \to \mu e)$, $B(K_L \to \pi^0\mu e)$, and $B(K_S \to \pi^0\mu e)$ are dictated by the lifetimes of $K_{L,S}$ and by the available experimental information on their decay modes.

33. T. Maehara and T. Yanagida, Ref. 25; R. Cahn and H. Harari, Ref. 10. This suppression mechanism in the Maehara-Yanagida model was further studied by O. Shanker (Ref. 10), who also formulated the conditions under which it would hold in $SU(n)_H$ models.

34. O. Shanker, Ref. 10. Note that for equal mixing angles in the right-handed and left-handed sectors the horizontal interactions in the Maehara-Yanagida model are pure vector interactions and $K_{L,S} \to \mu e$ are, therefore, forbidden at the tree level. In some other models, this need not, of course, be so.

35. It can be shown that under the same conditions all flavor-changing processes involving only two flavors (i.e., also $\mu \to 3e$ and $\mu \to e\gamma$) are forbidden in this model for degenerate bosons, even after generation mixing is included (R. Cahn and H. Harari, Ref. 10; O. Shanker, Ref. 10).

36. The contribution of Y_3 is of order $\sin\theta \sin\phi$ relative to the contribution of Y_1 and/or Y_2.

37. SU(2)-type horizontal gauge interactions have been also suggested as a possible source of the observed CP-violation: R. N. Mohapatra, J. C. Pati, and L. Wolfenstein, Ref. 25; T. Maehara and T. Yanagida, Ref. 25; C. L. Ong, Ref. 25; F. Wilczek and A. Zee, Ref. 25.

38. For a nonhermitean gauge boson $Y_+ = (Y_1 - iY_2)/\sqrt{2}$ with degenerate mass eigenstates, which is coupled to $\bar{s}\Gamma_\lambda d$ but not to $\bar{d}\Gamma_\lambda s$, the contribution of Y_1 and Y_2 to the imaginary part of the $K \to \bar{K}^o$ matrix element vanishes as well.

39. In the Maehara-Yanagida model the imaginary part of the $K^o \to \bar{K}^o$ matrix element is also proportional to $(m_3^{-2} - m^{-2})$ (for equal right-handed and left-handed mixings). Cf. T. Maehara and T. Yanagida, Ref. 25.

40. For an example, see N. G. Deshpande, R. C. Hwa, and P. D. Mannheim, Phys. Rev. D19, 2686 (1979).

41. The inclusion of additional Higgs particles may be necessary for various theoretical reasons. See, for example, G. L. Kane, "Could Higgs Bosons Be Found Before LEP?", talk at the Workshop on Producing New Particles, Madison (1979), University of Michigan Preprint UM HE79-37; Ling-Fong Li, "Properties of Higgs Particles," Carnegie-Mellon University Preprint C00-3066-145 (1980), to be published in the Proceedings of the 1980 Guangzou Conference on Theoretical Particle Physics; B. McWilliams and Ling-Fong Li, Ref. 42.

42. P. Herczeg, Ref. 10; B. McWilliams and Ling-Fong Li, Carnegie-Mellon University Preprint C00-3066-146 (1980).

43. In a given model, constraints from other processes will have to be respected. In general, the bounds on m_h will depend, apart from the mixing angles in the Higgs and the fermion sectors, on the number and kind of Higgs multiplets and on the strength of the coupling to various particles. Hence the various processes have to be treated as essentially unrelated.

44. See, for example, J. E. Kim and G. Segre', Phys. Lett. 78B, 75 (1978); B. McWilliams and Ling-Fong Li, Ref. 42.

45. For an example of cancellations involving three Higgs bosons, see A. B. Lahanas and C. E. Vayonakis, Phys. Rev. D19, 2158 (1979). I am grateful to L. Wolfenstein for bringing this paper to my attention.

46. For a review of leptoquark masses in various grand unified models and the corresponding $K_L \to \mu e$ branching ratios, see the talk by T. J. Goldman in these Proceedings.

47. J. Ellis, M. K. Gaillard, D. V. Nanopoulos, and P. Sikivie, Preprint TH-2938-CERN (1980); S. Dimopoulos and J. Ellis, Preprint TH-2949-CERN (1980).

48. In extended technicolor schemes there are also other sources of flavor-changing neutral interactions, e.g., the flavor-changing extended technicolor bosons or the low-mass flavor-changing color singlet pseudogoldstone bosons. These appear to lead to flavor-violation too strong to be compatible with experimental constraints such as the K_L - K_S mass difference. Mechanisms to suppress these effects that were thought of so far would leave flavor-violation via leptoquark pseudogoldstone boson exchange intact. Cf. Ref. 47.

49. R. N. Cahn and H. Harari, Ref. 10; O. Shanker, Ref. 10.

2) Neutrino oscillation experiments at a high-intensity facility are to be encouraged and can also have a strong impact on GUTs.

3) The burning question remains: Why is the muon? Or in more modern guise: What (if any) is the "horizontal" gauge symmetry, and what is the scale for violating this symmetry if it exists? A high-intensity intermediate energy facility offers one of the best opportunities available to answer these questions.

QUARK-DIAGRAM CONTRIBUTION TO $K_L \to \gamma\gamma$

Ernest Ma and A. Pramudita
Department of Physics and Astronomy
University of Hawaii at Manoa, Honolulu, Hawaii 96822

ABSTRACT

We compute the one-loop quark-diagram contribution to $K_L \to \gamma\gamma$ in the standard model, without making the usual approximation that the internal quark masses are much smaller than the W-boson mass.

In the standard electroweak gauge model,[1] the amplitude for the flavor-changing radiative process[2,3] $K_L \to \gamma\gamma$ is formally of the same order in the electroweak coupling as $K_L \to \mu^+\mu^-$,[4] but its rate is observed to be more than 10^4 times that of the latter. The numerical difference has to do with the detailed dependence of the respective amplitudes on the masses of the internal quarks which mediate the one-loop effective transitions $d\bar{s} \to \gamma\gamma$ and $d\bar{s} \to \mu^+\mu^-$. Early calculations of these processes have always been done with the following two approximations. (1) All external masses are much smaller than the W-boson mass. (2) All internal masses are much smaller than the W-boson mass. For the kaon, the first approximation is certainly justified. But if there are heavy quarks, such as the yet undiscovered t quark, which enter into the one-loop calculation, the second approximation may no longer be valid. In Ref. 4, we have computed the effective $Zd\bar{s}$ coupling, valid for arbitrary values of the internal quark mass. Now we have also obtained the analogous result for $d\bar{s} \to \gamma\gamma$.

Because of gauge invariance, the lowest-order nonzero contribution to the $d\bar{s} \to \gamma\gamma$ amplitude turns out to be a third-rank tensor in external momenta, and since there are 66 one-loop diagrams to be evaluated, the calculation is somewhat time-consuming. We will present the details elsewhere. Here we just write down the final results as applied to $K_L \to \gamma\gamma$.

Since the CP-nonconserving piece of $K_L \to \gamma\gamma$ is negligible, we simply take

$$K_L = \frac{1}{\sqrt{2}} (K^o + \bar{K}^o), \tag{1}$$

and use

$$\langle 0 | \bar{s}\gamma^\alpha\gamma_5 d | K^o \rangle = i f_K p_K{}^\alpha \tag{2}$$

in going from $d\bar{s} \to \gamma\gamma$ to $K_L \to \gamma\gamma$. The contribution of the one-particle irreducible diagrams is then defined unambiguously. As

Grand Unified Particle Physics and a High-Intensity Intermediate Energy Machine

T. Goldman

Theoretical Division
Los Alamos National Laboratory

I want to make a few brief comments on the current status of grand unified theories and the relation of such theories to a high-intensity facility such as has been discussed at this workshop.

1) What are Grand Unified Theories (GUTs)?

These are most simply described as extensions of the Low Energy Gauge Group (LEGG) which is presumed to be an accurate description of the strong, weak and electromagnetic interactions.

$$\text{LEGG} = SU(3)_{\text{color}} \blacksquare SU(2) \blacksquare U(1) \qquad (1)$$

The first two group factors describe the conversion of a quark of one "color" to another color by emission of a gluon (strong interaction) or of an up quark to a down quark, or of a charged lepton to a neutrino, by emission of a weak intermediate vector boson (weak interaction). The basic idea of GUTs is that if these conversions may be considered, then why not also: conversion of a lepton to a quark by emission of a (Y) vector boson, or of a quark into an antiquark by emission of a (X) vector boson, etc.? Phrased this way, GUTs do not seem very bold until one recalls that these last two processes violate lepton number (L) and baryon number (B) conservation, principles heretofore sacrosanct.

2) Dynamics: Group-Theory-Based Field Theory

The advantage of GUTs is that, unlike LEGG, the single unifying group defines the dynamics of a field theory, embodying this group symmetry, with a single coupling constant. With the application of the renormalization group, this relation can be employed to find the mass scale, M_U, at which the symmetry is manifest, from the parameter data in LEGG. As a bonus, the Glashow angle, θ_W, is predicted as a ratio of group Clebsch-Gordon coefficients at M_U. The renormalization group can then be used to follow the value of θ_W down to its value at experimentally accessible energy scales. Further, exchanges of the various X and Y bosons induce $\Delta B=1$ processes such as proton decay with lifetime τ_p and $\Delta B=2$ processes such as neutron-antineutron oscillation, with mixing time $\tau_{n\bar{n}}$. These times depend only on M_U and kinematic factors and so can be fairly precisely predicted. The following table shows the results of these calculations for SU(5) and three of the class of Pati-Salam theories, in terms of whether or not τ_p or $\tau_{n\bar{n}}$ are observable by current or prospective techniques.

Theory → / Observable Process	SU(5)	■[SU(2n)]⁴ n=5	n=4	n=3
$\tau_p = 10^{32\pm2}$ yr.	yes	yes	no	no
$\tau_{n\bar{n}} = 10^{7\pm2}$ sec.	no	yes	yes	no
M_U (GeV) Error ±50%	4×10^{14}	2×10^{4}	6×10^{5}	2×10^{8}
$\sin^2\theta_W$	0.21	.26	.25	.24

3) Horizontal Symmetries

You may have noticed that nothing has been mentioned yet about vector bosons which mediate transitions between the different quark families $\{(u,d,e,\nu_e);\ (c,s,\mu,\nu_\mu);\ (t,b,\tau,\nu_\tau)\}$ such as d-quark goes to s-quark plus vector boson (V). The (so-called) horizontal symmetries associated with such transitions try to answer the old question, "why is the muon?", but none of the answers proposed has so far found any experimental support.

GUTs do not help us here. Rather, the discovery of a horizontal gauge group G_H will mean

$$\text{LEGG} \rightarrow \text{LEGG} \blacksquare G_H \rightarrow \text{GUT} \qquad (2)$$

i.e., a new and larger "low" energy gauge group will have to be encompassed by the unifying theory. This is perhaps the prime area for a high-intensity facility to affect the future of theoretical efforts at grand unification. The S-channel exchange of an axially coupled V-boson as described above will produce the decay $K_L \rightarrow \mu^{\pm} e^{+}$. The present branching ratio (BR) limit of 10^{-9} implies that $M_V \gtrsim 10^2 M_W$, i.e. $M_V \gtrsim$ 10 TeV. Please note that this is already beyond the upper mass limit that could be observed directly by the largest proposed "world" high energy accelerator. More intense kaon beams at a high intensity facility would either lead to an improved lower bound on M_V or, with discovery of a nonzero effect, the first real inkling as to the nature of G_H.

4) GUT Predictions

I have just decribed what a high-intensity facility can do for GUTs. But what can GUTs do for the facility? Not too much that is positive, I'm sorry to say. Although exchange of Y bosons as described above does lead to $K_L \to \mu e$, the BR's lie in the range 10^{-50} to 10^{-17}. Even at the upper end, these effects are subject to the "background" of the Glashow-Iliopoulos-Maiani and neutrino-mass-mixing-suppressed contribution described in Peter Herczeg's talk. Effects on fermion anomalous magnetic moments are also small. Of course, these statements may be inverted to say that if any new effects do show up, they will be very important (as they were not predicted). In that sense, experiments at a high-intensity facility have the classic advantage of being null experiments.

There is, however, one class of effects which, while not precisely predicted, are strongly suggested by GUT ideas, which I will now describe.

5) Neutrino Masses and Mixings in GUTs

It has recently been understood that in GUTs, the natural fermion degrees of freedom are not Dirac fields, but chiral (Weyl) fields which come in conjugate pairs. Thus, a quark mass term appears in the Lagrangian in the matrix form:

$$(q_L, \; q_L^C) \begin{pmatrix} 0 & m_D \\ m_D & 0 \end{pmatrix} \begin{pmatrix} q_L \\ q_L^C \end{pmatrix} \tag{3}$$

where q_L^C is the charge conjugate of the left-chiral quark field q_L. In what was modern notation until recently, you were probably more used to seeing

$$q_L^C \; m_D \; q_L \quad \text{as} \quad \bar{q}_R \; m_D \; q_L, \tag{4}$$

since the first factors are equivalent.

In GUTs, charged lepton masses appear in the same fashion as do quark masses. In specific theories, these masses may even be related by Clebsch-Gordon factors which reflect an underlying horizontal symmetry. However, for neutrinos the two zero entries in Eq. (3) need not vanish: For charged fermions this vanishing is a consequence of a charge conservation, but for neutrinos one would need to invoke fermion number conservation. Like B and L above, this too is suspect. Thus the neutrino mass matrix takes the generic form

$$(\nu_L, \; \nu_L^C) \begin{pmatrix} \mu & m \\ m & M \end{pmatrix} \begin{pmatrix} \nu_L \\ \nu_L^C \end{pmatrix} \tag{5}$$

The off-diagonal elements are generally related to the quark and charged lepton mass matrices, but μ and M are new quantities. As many authors have pointed out, in GUTs it is natural for M to be on the order of the grand unification scale, M_U, or down by a few powers of the coupling constant. We also expect μ to be small or zero, since its value is related to a violation of the W and Z mass relation which Prof. Cabibbo has described in his talk. If this is true, then the mass eigenvalues are approximately

$$M \text{ and } mM^{-1}m \tag{6}$$

for ν_L^C and ν_L respectively. This is a desirable result since ν_L^C has never been seen and since the state which is almost ν_L has a (Majorana) mass <10 eV for reasonable m and M values.

If Eqs. (5) and (6) are generalized to describe the neutrinos of all three families. then m and M are 3x3 matrices, and an interesting consequence of Eq. (6) occurs: The outside factors of m suppress any mixing due to M^{-1} and so the effective mixing angles between the observed light neutrinos are essentially determined by the diagonalization of m alone. Since m is related to m_D, we conclude that, up to Clebsch-Gordon factors of specific models, the neutrino and quark mixing parameters are likely to very similar. For example

$$\theta(\nu_e \leftrightarrow \nu_\mu) \sim \theta \text{ (Cabibbo)} \qquad (7).$$

Such mixing angles are marginal for observation of neutrino oscillations at reactors but, especially if the mass differences are not too small, they are well within the capability of neutrino beams formed at a high intensity facility. While LAMPF provides adequate beams for $\nu_\mu - \nu_e$ mixing studies, a ν_τ appearance experiment (in a ν_μ beam) must await a higher intermediate-energy high-intensity machine. A ν_τ disappearance experiment would require even higher energies, and so may not be feasible.

Conclusions

1) A high-intensity facility will allow precision tests of expected effects and better searches for effects which are expected to be absent or unobservably small. Both cases can have significant impact on the search for the correct Grand Unified Theory.

2) Neutrino oscillation experiments at a high-intensity facility are to be encouraged and can also have a strong impact on GUTs.

3) The burning question remains: Why is the muon? Or in more modern guise: What (if any) is the "horizontal" gauge symmetry, and what is the scale for violating this symmetry if it exists? A high-intensity intermediate energy facility offers one of the best opportunities available to answer these questions.

QUARK-DIAGRAM CONTRIBUTION TO $K_L \to \gamma\gamma$

Ernest Ma and A. Pramudita
Department of Physics and Astronomy
University of Hawaii at Manoa, Honolulu, Hawaii 96822

ABSTRACT

We compute the one-loop quark-diagram contribution to $K_L \to \gamma\gamma$ in the standard model, without making the usual approximation that the internal quark masses are much smaller than the W-boson mass.

In the standard electroweak gauge model,[1] the amplitude for the flavor-changing radiative process[2,3] $K_L \to \gamma\gamma$ is formally of the same order in the electroweak coupling as $K_L \to \mu^+\mu^-$,[4] but its rate is observed to be more than 10^4 times that of the latter. The numerical difference has to do with the detailed dependence of the respective amplitudes on the masses of the internal quarks which mediate the one-loop effective transitions $d\bar{s} \to \gamma\gamma$ and $d\bar{s} \to \mu^+\mu^-$. Early calculations of these processes have always been done with the following two approximations. (1) All external masses are much smaller than the W-boson mass. (2) All internal masses are much smaller than the W-boson mass. For the kaon, the first approximation is certainly justified. But if there are heavy quarks, such as the yet undiscovered t quark, which enter into the one-loop calculation, the second approximation may no longer be valid. In Ref. 4, we have computed the effective $Zd\bar{s}$ coupling, valid for arbitrary values of the internal quark mass. Now we have also obtained the analogous result for $d\bar{s} \to \gamma\gamma$.

Because of gauge invariance, the lowest-order nonzero contribution to the $d\bar{s} \to \gamma\gamma$ amplitude turns out to be a third-rank tensor in external momenta, and since there are 66 one-loop diagrams to be evaluated, the calculation is somewhat time-consuming. We will present the details elsewhere. Here we just write down the final results as applied to $K_L \to \gamma\gamma$.

Since the CP-nonconserving piece of $K_L \to \gamma\gamma$ is negligible, we simply take

$$K_L = \frac{1}{\sqrt{2}} (K^o + \bar{K}^o), \tag{1}$$

and use

$$\langle 0 | \bar{s}\gamma^\alpha\gamma_5 d | K^o \rangle = i f_K p_K{}^\alpha \tag{2}$$

in going from $d\bar{s} \to \gamma\gamma$ to $K_L \to \gamma\gamma$. The contribution of the one-particle irreducible diagrams is then defined unambiguously. As

for the one-particle reducible diagrams, a model for the bound-state kinematics must also be specified. In the following, we take the simplest, but probably unjustified, approximation that in the center of mass, the relative momentum of the quarks is much smaller in magnitude than their total energy which is, of course, equal to m_K. The contribution of each internal quark j which mediates the transition $K_L \to \gamma\gamma$ is then given by

$$A_j = \frac{\alpha G_F}{\pi} i f_K \varepsilon_{\mu\nu\rho\sigma} \varepsilon_1^\mu \varepsilon_2^\nu q_1^\rho q_2^\sigma$$

$$\times \left\{ \frac{(Q+1)^2}{1-x} \left[2 + \frac{4x}{x_K} \int_0^1 \frac{dy}{y} \ln(1-y(1-y)\frac{x_K}{x}) \right] \right. \qquad (3)$$

$$\left. + Q^2 \left[\frac{1-5x-2x^2}{(1-x)^3} - \frac{6x^2 \ln x}{(1-x)^4} \right] + Q \left[\frac{3-9x}{(1-x)^2} - \frac{6x^2 \ln x}{(1-x)^3} \right] \right\},$$

where $x = m_j^2/M_W^2$, $x_K = m_K^2/M_W^2$, and $\varepsilon_{1,2}$, $q_{1,2}$ are the polarization and momentum vectors of the two photons. The charge Q refers to the d and s quarks and is, of course, equal to - 1/3.

In the limit of $x \ll 1$, the term in Eq. (3) proportional to $(Q+1)^2$ dominates, and our result reduces to that of Ref. 3. However, if x is comparable to one, then the other terms are more important. The contribution of the t quark to $K_L \to \gamma\gamma$ can now be studied as a function of its mass and possible information on its coupling to d and s quarks be extracted. The numerical results will be reported elsewhere.

This work was supported in part by the U. S. Department of Energy under Contract DE-AC03-76ER00511.

REFERENCES

1. S. Weinberg, Phys. Rev. Lett. 19, 1264 (1967); A. Salam, in Elementary Particle Theory (Nobel Symposium No. 8), ed. by N. Svartholm (Almqvist and Wiksell, Stockholm, 1968), p. 367; S. L. Glashow, Nucl. Phys. 22, 579 (1961); A. Salam and J. C. Ward, Phys. Lett. 13, 1684 (1964); S. L. Glashow, J. Iliopoulos, and L. Maiani, Phys. Rev. D 2, 1285 (1970).
2. E. Ma, Phys. Rev. D 9, 3103 (1974).
3. M. K. Gaillard and B. W. Lee, Phys. Rev. D 10, 897 (1974).
4. E. Ma and A. Pramudita, Phys. Rev. D 22, 214 (1980); and references therein.

PRELIMINARY REPORT ON A NEW PION BETA DECAY EXPERIMENT

by

V. L. Highland, W. K. McFarlane, L. B. Auerbach,
F. C. Gaille, E. Jastrembski, N. Haik
Temple University

and

R. J. Macek, G. E. Hogan, R. E. Morgado, R. D. Werbeck,
J. C. Pratt, C. M. Hoffman, F. Cverna, J. D. Bowman, M. D. Cooper
Los Alamos National Laboratory

The conserved vector current hypothesis (CVC), a cornerstone of the unified theory of electromagnetic and weak interactions, provides a precise prediction for the branching ratio of the pion beta decay reaction $\pi^+ \rightarrow \pi^o e^+ \nu$. The predicted ratio is 1.045×10^{-8} with an uncertainty of 0.5% due to errors in the pion masses and an additional 1% uncertainty due to the electromagnetic corrections. The most precise existing experiment is that of Depommier et al.[1] who found a branching ratio of $1.00 \, ^{+\,0.08}_{-\,0.10} \times 10^{-8}$.

This experimental result is consistent with the theory within the errors, but it is clearly very desirable to improve the experimental precision so that it approaches that of the theory. We have just completed taking data on a new pion beta decay experiment. Here we present a preliminary report on the experiment to indicate the extent and quality of the data obtained.

In contrast to the previous experiments done with stopping pions, this one observes decays in flight of a 400-MeV π^+ beam in the P^3 East Channel at LAMPF. The massive π^o from the π^+ beta decay has essentially the same momentum as the π^+, and we detect the two energetic γ rays from the π^o decay. It is necessary to use a very intense beam of 2×10^8 π^+/s.

In order to avoid background from pion charge exchange, the decays take place in a vacuum tank at 2×10^{-7} torr. There is an intense flux of secondary μ's from decay of the π's. The beam is collimated and the detectors located so that they cannot see these μ's. The last collimator is toroidally magnetized iron in order to reduce μ scattering out of the collimator. This magnetization of the collimator allowed us to run at a beam rate three times more intense than would otherwise have been tolerable. In order to monitor this intense beam we

used ion chambers and $\pi \rightarrow \mu\nu$ detectors downstream of the experiment.

The γ rays were detected by the Pb-glass counters of the LAMPF π^0 spectrometer, using XY scintillation hodoscopes for position definition. The time and energy calibrations of the detectors were frequently checked by swinging a CH_2 target inside the vacuum tank into the beam and producing π^0's by charge exchange. As a final calibration, the entire tank was filled with H_2 gas and the beam changed to π^-.

In Fig. 1 is given the spectrum of the sum of the two γ-ray energies after selecting on prompt timing of each γ with respect to the beam RF and making some low energy cuts in each of the counters. There is a clean well-defined peak with the expected resolution. To verify the π-beta identification one can look at the transverse momentum and coplanarity. These variables show distinct peaks as expected for beta decay. These variables provide additional potential cuts, but it will not be necessary to make any but very mild cuts to further clean up the event selection.

The events shown in Fig. 1 therefore represent very nearly our final sample. That is, we will have about 1100 pion beta decay events. To produce a branching ratio we have to accurately determine the incident pion flux, the detection efficiency, and various corrections. We believe these numbers can all be determined to 1 or 2%. We therefore expect soon to have a significant improvement on the experimental determination of the pion beta decay branching ratio, although still not with a precision that equals that of the theory.

REFERENCE

1. P. Depommier, J. Duclos, J. Heintze, K. Kleinknecht, H. Rieseberg, and V. Soergel, Nucl. Phys. B4, 189 (1968).

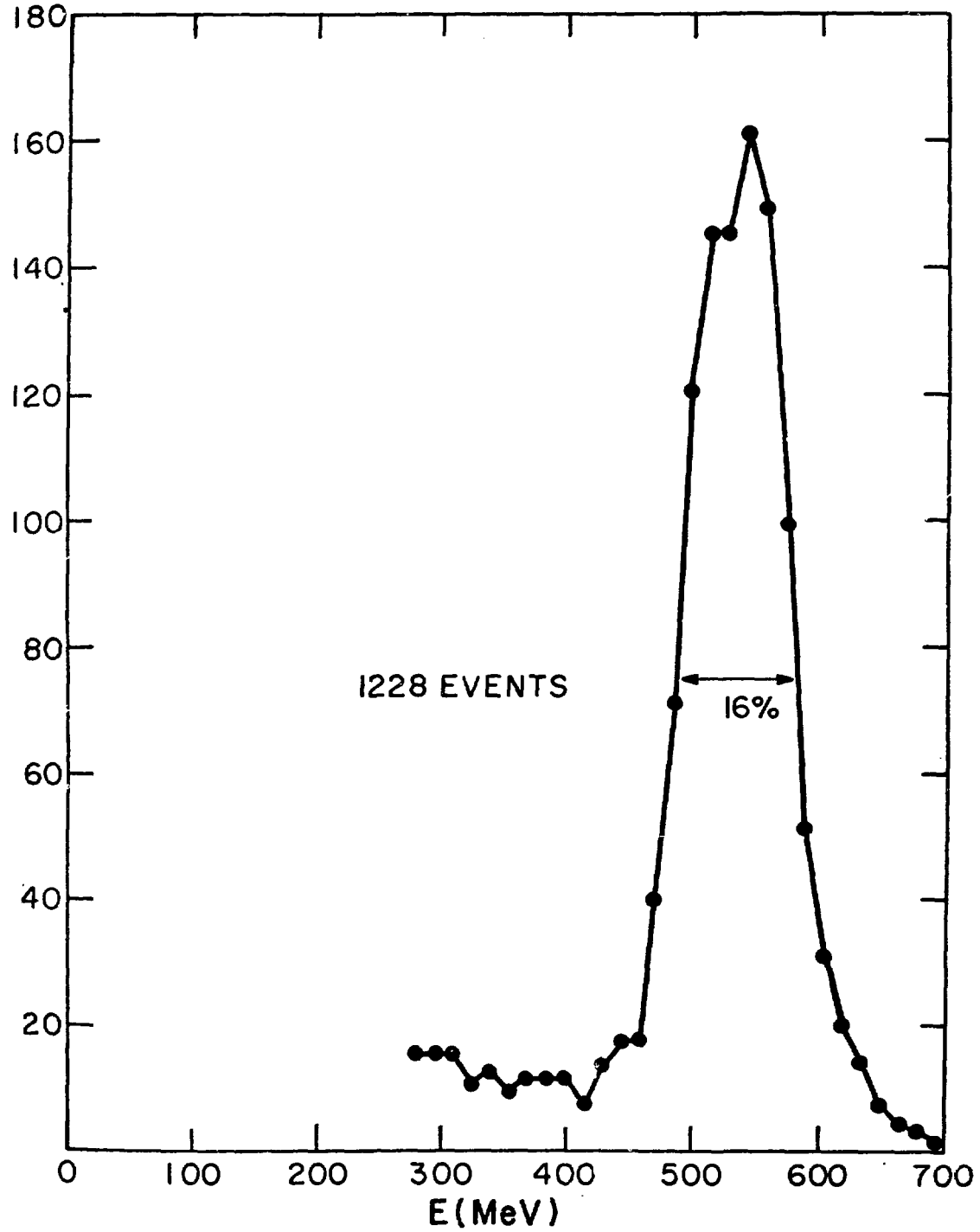

Fig. 1. π_β energy spectrum $E_{\gamma_1} + E_{\gamma_2}$.

NEUTRINO OSCILLATIONS*

by

Alfred K. Mann
Department of Physics, University of Pennsylvania†
Philadelphia, PA 19104

ABSTRACT

A status report on neutrino oscillations is presented. Reasons are given for the increasing interest in neutrino oscillations, and the theory is reviewed with illustrative examples. A summary of types of neutrino oscillation experiments and of data available at the moment is given. Some representative proposed neutrino oscillation experiments are discussed with emphasis on experiments at LAMPF and the BNL AGS.

This is an attempt to give a brief, elementary overview of the subject of neutrino oscillations. The outline of the talk contains six major sections: I. History of and reasons for interest in neutrino oscillations, II. Phenomenological theory, including examples, III. Summary of types of neutrino oscillation experiments and of data now available, IV. Some proposed neutrino oscillation experiments, V. Possibilities for neutrino oscillation experiments at the Brookhaven National Laboratory AGS, and VI. Summary and conclusions.

To supplement the consideration underlying this workshop, i.e., the physics that might profitably be studied with a very intense source of K-mesons (kaon factory), it is useful to point in addition to the possibilities for carrying out experiments of considerable interest with a very intense source of energetic neutrinos (neutrino factory), which might be combined with the kaon factory. This is a second, albeit indirect and subsidiary, purpose of my talk.

I. INTRODUCTION TO NEUTRINO OSCILLATIONS

The origin of the subject lies in a suggestion by Pontecorvo[1] which remarked on a possible generalization of neutral kaon oscillations in vacuum that might

---

*Talk given at Los Alamos Scientific Laboratory Workshop for Nuclear and Particle Physics, January 5-8, 1981.

†Research supported in part by Department of Energy, Contract DE-AC02-76-ERO-3071.

lead to vacuum oscillations of neutrino type. In the kaon system, one has $K^0(S = +1) \leftrightarrow \bar{K}^0(S = -1)$, and hence $|\Delta S| = 2$, where S is the strangeness quantum number, while in the neutrino system, one might have, e.g., $\nu_\mu(L_e = 0, L_\mu = +1) \leftrightarrow \nu_e(L_e = +1, L_\mu = 0)$, and hence $|\Delta L_e| + |\Delta L_\mu| = 2$, where L_e and L_μ are the electron and muon lepton quantum numbers, respectively. It was also noted by Pontecorvo that CP-violation, previously observed in the oscillating neutral kaon system, might be manifested in an oscillating neutrino system.

Shortly after the solar neutrino experiment of Davis[2] began to take data, it was noted by Gribov and Pontecorvo[3] that neutrino oscillations might be a possible explanation for a decrease in the solar neutrino flux to be expected at the earth, and in line with this suggestion, Bahcall and Frautschi[4] commented on the need to average the oscillation probability over the solar neutrino energy spectrum. Other possible explanations for a possible decrease of the solar neutrino flux were given by Bahcall, Cabibbo and Yahil[5] who discussed the implications of a finite neutrino lifetime leading to $\nu_e \rightarrow \nu_\mu + \phi$, with ϕ a long-lived boson, and by Wolfenstein[6] who has considered neutrino oscillations in matter resulting from a forward scattering amplitude with off-diagonal components dependent on neutrino type.

There are a number of reasons for the quickening interest in neutrino oscillations. (i) It is a possible means of probing properties of neutrinos, such as mass, and of improving our knowledge of the weak interaction hamiltonian, e.g., testing the validity of separate lepton number conservation. These being, as we shall see, the necessary conditions for neutrino oscillations to occur. (ii) It has significant implications for astrophysics apart from the solar neutrino question. As remarked dramatically by Cowsik and McClelland[7] in connection with binding of the Coma cluster, if neutrinos have a small mass (5-50 eV), then "neutrinos would dominate the gravitational dynamics of the universe." They would provide sufficient total mass in the universe to effect closure. (iii) In many attempts to formulate grand unified theories of the weak, electromagnetic and strong forces, baryon and lepton number non-conservation follow naturally, and there is room for neutrinos with nonzero mass. Further, under certain assumptions of quark-lepton symmetry, e.g., by Kobayashi and Maskawa,[8] the mixing parameters of quarks and leptons are the same, and CP-violation would occur naturally in neutrino oscillations. (iv) The direct, but as yet unconfirmed, measurement of a nonzero mass of $\bar{\nu}_e$ by Lubimov et al.[9] is still another stimulus to search for neutrino oscillations.

II. THEORY OF NEUTRINO OSCILLATIONS IN VACUUM

In general, a quantum mechanical system described by a hamiltonian H with states $|a\rangle$ and $|b\rangle$, and with $\langle a|H|a\rangle = \langle b|H|b\rangle$, will oscillate between a and b with frequency ω. The probability of finding the system in state a at time t if it began in state a at time zero is

$$P(a,t|a,o) = |\langle a|e^{-iHt}|a\rangle|^2 = \frac{1}{2}(1 + \cos \omega t) = \cos^2(\omega t/2) ,$$

while the probability of finding the system in state b at time t is

$$P(b,t|a,o) = |\langle b|e^{-iHt}|a\rangle|^2 = 1 - P(a,t|a,o) = \frac{1}{2}(1 - \cos \omega t) = \sin^2(\omega t/2)$$

with

$$\omega = 2\langle b|H|a\rangle = 2\langle b|H|a\rangle^* .$$

Hence, for example,

$$P(b,t = \frac{\pi}{\omega}|a,o) = 1$$

and

$$P(a,t = \frac{\pi}{\omega}|a,o) = 0 .$$

Such oscillations will take place unless expressly forbidden.

More specific to neutrino oscillations, one defines the quantity

$$\Delta^2_{kj} = m^2_{\nu k} - m^2_{\nu j} , \quad k, j = 1, 2...$$

where $m_{\nu k}$ and $m_{\nu j}$ are masses of the eigenstate neutrinos $|\nu_k\rangle$ and $|\nu_j\rangle$, which are linear combinations of the observed neutrino states $|\nu_e\rangle$, $|\nu_\mu\rangle$, $|\nu_\tau\rangle$,.... Thus

$$|\nu_j\rangle = \sum_\zeta |\nu_\zeta\rangle\langle\nu_\zeta|\nu_j\rangle$$

where the Greek letter subscript denotes e, μ, τ,..., and

$$E_j = \langle\nu_j|H^{(0)} + H^{(1)}|\nu_j\rangle$$

or

$$E_j = \sum_\zeta |\langle\nu_\zeta|\nu_j\rangle|^2 \left[p_\nu + \langle\nu_\zeta|H^{(1)}|\nu_\zeta\rangle\right] + \sum_{\zeta\,\eta}{}' \langle\nu_\zeta|\nu_j\rangle^*\langle\nu_\eta|\nu_j\rangle\langle\nu_\zeta|H^{(1)}|\nu_\eta\rangle$$

so that

$$E_k - E_j = \frac{\Delta_{kj}^2}{2E_\nu}$$

and the wavelength of the oscillations is

$$\lambda_{kj}\ (\text{meters}) = \frac{2.5\ E_\nu\ (\text{MeV})}{\Delta_{kj}^2\ (\text{eV}^2)}$$

We see that $E_k - E_j \to 0$ if $\Delta_{kj}^2 \to 0$, or, more usefully, if $\langle\nu_\zeta|H^{(1)}|\nu_\zeta\rangle \to 0$ and $\langle\nu_\zeta|H^{(1)}|\nu_\eta\rangle \to 0$. Hence at least one of the ν_ζ must have nonzero mass and also the matrix element connecting ν_ζ with ν_η must be nonzero (violation of separate lepton number conservation) if oscillations are to take place.

Although the existence of ν_τ has not yet been demonstrated, it is useful to consider some examples of neutrino oscillations involving ν_e, ν_μ and ν_τ, because they reflect the complexity that is likely to be present if neutrino oscillations do in fact occur. These examples illustrate arbitrary choices of $\langle\nu_\zeta|H^{(1)}|\nu_\eta\rangle$.

(i) Choose (as in Ref. 10)

$$m_{\nu_e} = m_{\nu_\mu} = m_{\nu_\tau} \equiv m$$

$$m_{\eta\zeta} \equiv 2\mathrm{Re}\langle\nu_\zeta|H^{(1)}|\nu_\eta\rangle \rightarrow m_{\mu e} = \sqrt{2}\, m_{\tau\mu} \equiv m' \quad , \quad m_{e\tau} = 0$$

therefore

$$m_{\nu_1} = m - \frac{1}{2} m' \quad , \quad m_{\nu_2} = m \quad , \quad m_{\nu_3} = m + \frac{1}{2} m'$$

and

$$|\nu_e\rangle = \frac{1}{\sqrt{3}} (|\nu_1\rangle + |\nu_2\rangle + |\nu_3\rangle)$$

$$|\nu_\mu\rangle = \frac{1}{\sqrt{2}} (-|\nu_1\rangle + |\nu_3\rangle)$$

$$|\nu_\tau\rangle = \frac{1}{\sqrt{6}} (|\nu_1\rangle - 2|\nu_2\rangle + |\nu_3\rangle) \quad .$$

Hence, averaging over E_ν,

$$\langle P(\nu_e \rightarrow \nu_e)\rangle = \frac{1}{3} \quad ; \quad \langle P(\nu_\mu \rightarrow \nu_e)\rangle = \langle P(\nu_e \rightarrow \nu_\mu)\rangle = \frac{1}{3}$$

$$\langle P(\nu_\mu \rightarrow \nu_\mu)\rangle = \frac{1}{2} \quad ; \quad \langle P(\nu_\tau \rightarrow \nu_e)\rangle = \langle P(\nu_e \rightarrow \nu_\tau)\rangle = \frac{1}{3}$$

$$\langle P(\nu_\tau \rightarrow \nu_\tau)\rangle = \frac{1}{2} \quad ; \quad \langle P(\nu_\tau \rightarrow \nu_\mu)\rangle = \langle P(\nu_\mu \rightarrow \nu_\tau)\rangle = \frac{1}{6} \quad .$$

We see that <P> depends on the number of ν-types, but not symmetrically.

(ii) Another particularly interesting choice suggested independently by Cabibbo, Nussinov and Wolfenstein[11] illustrates the effect of CP-violation on neutrino oscillations. Choose

$$m_{\nu_1} = M_1 \quad , \quad m_{\nu_2} = M_2 - \delta \quad , \quad m_{\nu_3} = M_3 + \delta$$

where δ is a CP-violating parameter, then

$$|\nu_e\rangle = \frac{1}{\sqrt{3}} (|\nu_1\rangle + |\nu_2\rangle + |\nu_3\rangle)$$

$$|\nu_\mu\rangle = \frac{1}{\sqrt{3}} (|\nu_1\rangle + e^{-i\alpha}|\nu_2\rangle + e^{-2i\alpha}|\nu_3\rangle)$$

$$|\nu_\tau\rangle = \frac{1}{\sqrt{3}} (|\nu_1\rangle + e^{i\alpha}|\nu_2\rangle + e^{2i\alpha}|\nu_3\rangle)$$

with

$$\alpha = 2\pi/3$$

and

$$P(\nu_\eta \to \nu_\eta) = \frac{1}{3}\left\{1 + \frac{2}{3}\left[\cos\frac{2\pi\ell}{\lambda_{21}} + \cos\frac{2\pi\ell}{\lambda_{31}} + \cos\frac{2\pi\ell}{\lambda_{32}}\right]\right\}$$

$$\left.\begin{aligned} P(\nu_\mu \to \nu_e) &= \\ P(\nu_\tau \to \nu_\mu) &= \\ P(\nu_e \to \nu_\tau) &= \end{aligned}\right\} \quad \frac{1}{3}\left\{1 - \frac{1}{3}\left[\cos\frac{2\pi\ell}{\lambda_{21}} + \cos\frac{2\pi\ell}{\lambda_{31}} + \cos\frac{2\pi\ell}{\lambda_{32}}\right] + \frac{1}{\sqrt{3}}\left[\sin\frac{2\pi\ell}{\lambda_{21}} - \sin\frac{2\pi\ell}{\lambda_{31}} + \sin\frac{2\pi\ell}{\lambda_{32}}\right]\right\}$$

$$P(\nu_e \to \nu_\mu) = P(\nu_\mu \to \nu_\tau) = P(\nu_\tau \to \nu_e) =$$
$$\frac{1}{3}\left\{1 - \frac{1}{3}\left[\cos\frac{2\pi\ell}{\lambda_{21}} + \cos\frac{2\pi\ell}{\lambda_{31}} + \cos\frac{2\pi\ell}{\lambda_{32}}\right] - \frac{1}{\sqrt{3}}\left[\sin\frac{2\pi\ell}{\lambda_{21}} - \sin\frac{2\pi\ell}{\lambda_{31}} + \sin\frac{2\pi\ell}{\lambda_{32}}\right]\right\}$$

Observe that the probability for all types of oscillations averages to $\frac{1}{3}$, i.e., is maximal since only three neutrino types are considered, and that

$$P(\nu_\zeta \to \nu_\eta) \neq P(\nu_\eta \to \nu_\zeta) \quad .$$

(iii) For completeness, let us suppose there exists a right-handed leptonic charged current coupling. Then oscillations of the kind $\nu \leftrightarrow \bar{\nu}$ are possible (see, for example, Ref. 12). Note that these involve violation of total lepton number and of total fermion number, and not of L_e, L_μ separately as in $\nu_\eta \to \nu_\zeta$.

Look at the case of two neutrinos, $|\nu_e>$, $|\bar{\nu}_e>$, $|\nu_\mu>$, $|\bar{\nu}_\mu>$ for which

$$P(\bar{\nu}_e \to \bar{\nu}_e) = \left(\cos\frac{\Delta_{21}^2\ell}{4E}\right)^2$$

and

$$P(\nu_e \to \bar{\nu}_e) \cong \frac{4\varepsilon^2}{(1+\varepsilon^2)^2}\left(\sin\frac{\Delta_{21}^2\ell}{4E}\right)^2$$

where ε is the amplitude of the right-handed coupling, and

$$\frac{4\varepsilon^2}{(1+\varepsilon^2)^2} \leq 0.04$$

from measurements of the longitudinal polarization of e^- in beta-decay. Note that $P(\nu_e \to \bar{\nu}_e)$ differs from, say, $P(\nu_e \to \nu_\mu)$ by a factor proportional to the strength of the right-handed coupling.

In summary, the several models of possible oscillations given above exhibit clearly the two necessary conditions for neutrino oscillations to occur: neutrino mass, and the non-conservation of separate lepton number. In addition, the potential richness of the physics that might become available for study if oscillations are found is also indicated. Thus, neutrino oscillations, if they exist, might lead to the following: (i) a direct determination of the number of "communicating" neutrino types; (ii) an opportunity to study CP-violation in a system other than the neutral kaon system, providing the interaction responsible for neutrino oscillations is CP-violating; (iii) the observation (in $\nu_\eta \leftrightarrow \bar{\nu}_\eta$) of the non-conservation of total lepton and total fermion numbers; and (iv) the observation of a weak, leptonic, right-handed charged current. It is easy to see why interest in the subject of neutrino oscillations has steadily increased since the subject was first opened.

III. SUMMARY OF EXPERIMENT TYPES AND AVAILABLE DATA

Neutrino oscillation experiments have been and are being done using most known neutrino sources. From Section II we observe that the arguments of the trigonometric functions in the expressions for the various oscillation probabilities are $2\pi\ell/\lambda_{kj} = 2\pi\ell\Delta^2_{kj}/2.5\ E_\nu$. For this reason it is useful to take E_ν/ℓ (or its reciprocal) and Δ^2_{kj} as figures of merit with which to compare different experiments.

Experiments that are possible with the four more-or-less directly available neutrino sources are briefly indicated in Table I. The values given for E_ν/ℓ and Δ^2 are representative, not definitive. The experiments that have so far been carried out with these sources are also shown. The values given under Δ^2 correspond to maximal mixing in an analysis involving only two neutrinos; since analyses of the data are continuing, some of these values will probably change with time. An example of a more elaborate (3-neutrino type) analysis of the results from Davis et al., Reines et al., and deep mine neutrino data is given in Fig. 1, which is taken from a paper by Barger et al.[20] This solution is primarily of heuristic value, since other interpretations of the data of each experiment are equally, if not more, probable.

The oscillation data obtained at higher neutrino energy set upper limits on Δ^2 for $(\nu_\mu \to \nu_e)$ and $(\bar{\nu}_\mu \to \bar{\nu}_e)$ of about 1 eV^2, and on Δ^2 for $(\nu_\mu \to \nu_\tau)$ of 2.5 eV^2. The results of the two reactor experiments (Refs. 13 and 14) appear not to be

TABLE I

SUMMARY OF EXPERIMENT TYPES

Source	$\frac{E_\nu}{(MeV)}$	$\frac{\ell}{(m)}$	$\frac{E_\nu/\ell}{(MeV/m)}$	$\frac{\Delta^2}{(eV^2)}$	Type
SUN	0.2-10	10^{11}	4×10^{-11}	10^{-12}	$(\nu_e \to \nu_e)$ abs meas; model
Davis[2]	^8B(0-14)		$\frac{1}{3} \approx \frac{(\nu_e + {}^{37}Cl \to e^- + {}^{37}Ar)\ expt}{standard\ solar\ model}$		
REACTOR	3-10	10^1-10^2	0.25	0.1	$(\bar{\nu}_e \to \bar{\nu}_e)$; ℓ_1,ℓ_2
					$(\bar{\nu}_e \to \bar{\nu}_\eta)$; WNC/WCC
Reines[13]			0.5	$0.7<\Delta^2<1.0$	WNC/WCC
Boehm[14]			0.5	<0.12	$\bar{\nu}_e$ spectrum; model
Davis[15]			0.3	$\frac{\varepsilon^2}{4}\Delta^4<10^{-4}$	$(\bar{\nu}_e \to \nu_e)$
MESON FACTORY	100-250	10^1-3×10^2	2.0	0.1	$(\nu_e \to \nu_e)$; ℓ_1,ℓ_2
					$(\nu_\mu \to \nu_e)$; $(\bar{\nu}\to\bar{\nu})$
Willis[16]			4.0	<0.9	$(\bar{\nu}_\mu \to \bar{\nu}_e)$
HI-E ACCEL.	10^2-10^4	10^2-10^4	1-10	0.1	as in M.F. + $(\nu_\mu \to \nu_\tau)$, $(\nu_e \to \nu_\tau)$
Blietschau[17]			21	$\lesssim$1.0	$(\nu_\mu \to \nu_e)$
Cnops[18]			10	$\lesssim$1.0	$(\nu_\mu \to \nu_e)$
				$\lesssim$2.5	$(\nu_\mu \to \nu_\tau)$

Other: Deep mine ν_μ flux[19]

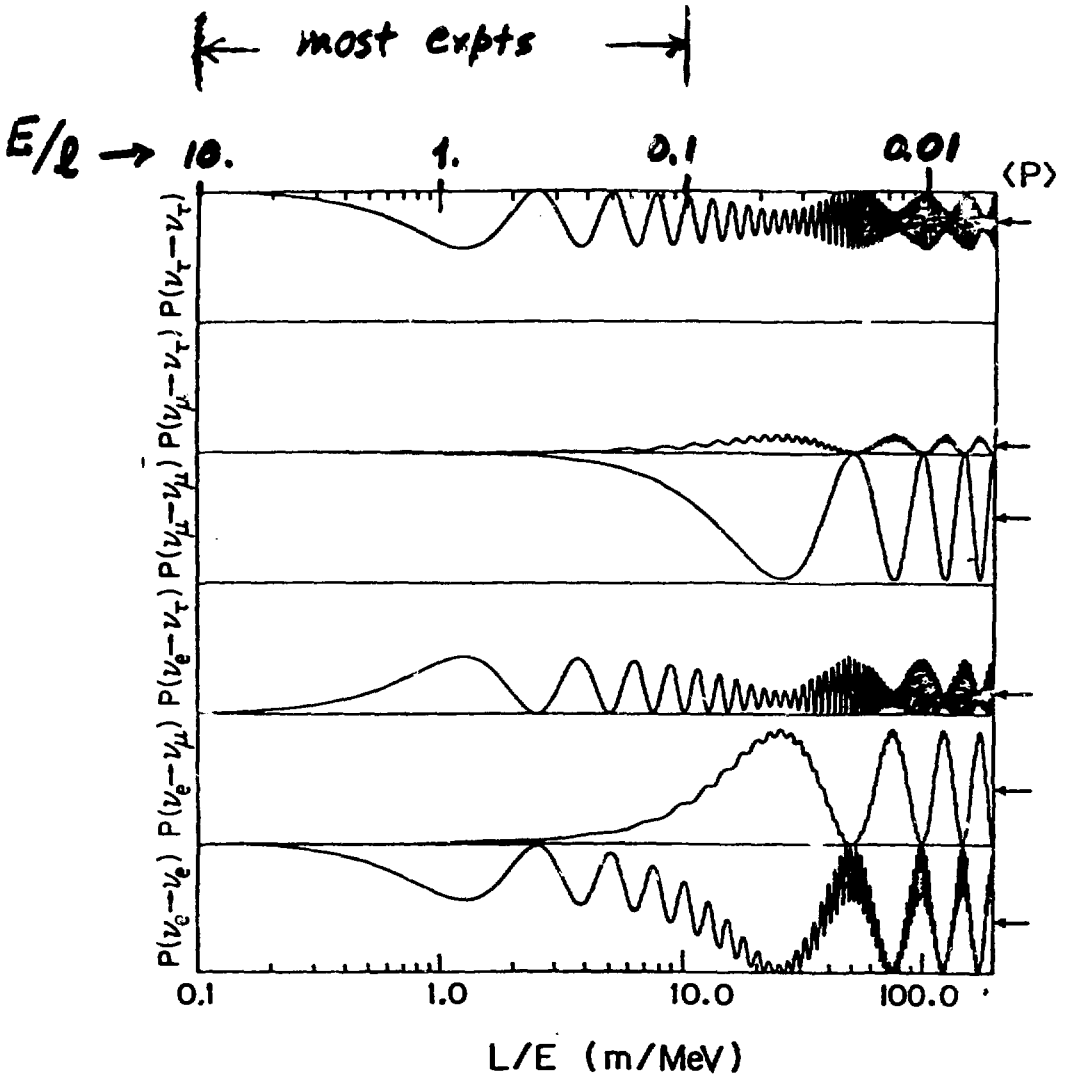

Fig. 3

Barger (ref 20)

$$P(\bar{\nu}_e \to \bar{\nu}_e) = 1 - 0.44 \sin^2(1.27\, L/E)$$

$$\Rightarrow \Delta^2_{31} \approx 1\ eV^2 \quad \text{(from ref 13 data)}$$

$$\Delta^2_{21} \approx 0.05\ eV \quad \text{(from ref 2, ref 19 data)}$$

Fig. 1. Subasymptotic neutrino oscillations for all channels based on solution A in Ref. 20. Arrows on the right-hand side denote asymptotic mean values.

consistent, but these are difficult experiments for the analysis of which the properties of the reactor antineutrino spectrum are necessary, and which are in process of taking additional data. More recent results from these experiments will be presented by other speakers at this workshop. Consequently, it is still too early to reach any firm conclusion. A similar statement is applicable to the data from the solar neutrino experiment which now represents a real signal, but any conclusion relating to neutrino oscillations depends on comparison of the data with a standard solar model prediction that is far from completely convincing.

IV. SOME PROPOSED NEUTRINO OSCILLATION EXPERIMENTS

There is a need for more, and improved, neutrino oscillation experiments, and a number of these are planned or about to begin. Table II lists some representative proposed experiments in a format similar to that of Table I. For the purpose of this workshop I have emphasized proposals using moderate energy (100-1000 MeV) neutrinos. The main content of Table II is that experiments with limits on Δ^2 down to about 0.1 eV^2 appear to be feasible and are likely to be done in the next few years. As Table I and II indicate, however, none of the terrestrial experiments can compete with the solar neutrino experiment using ^{71}Ga as a detector. This experiment, if it can be carried out successfully, will observe neutrinos from the primary burning reaction $p + p \rightarrow d + e^+ + \nu_e$, which is much better understood than the reaction giving rise to ^8B, from which have come the solar neutrinos thus far detected. Comparison of Ga-detector data with the expected neutrino flux from $p + p \rightarrow d + e^+ + \nu_e$ is likely to prove more convincing than the present solar neutrino analysis.

V. POSSIBILITIES OF NEUTRINO OSCILLATION EXPERIMENTS AT BNL

In view of the construction--now almost complete--of a massive neutrino detector at BNL, it is, perhaps, of particular interest to this workshop (as the organizers have suggested) to learn in more detail of the possibilities for neutrino oscillation experiments with that detector.

One such possibility is to study the E_ν-dependence of the ratio $\sigma(\nu_\mu + p \rightarrow \nu_\mu + p)/\sigma(\nu_\mu + n \rightarrow \mu^- + p)$ in the region between 0.5 and 5 GeV. Since these data will be taken in the normal course of the experiment, which is intended to study electroweak interactions generally, we have not attempted yet to specify how useful they will be. A rough estimate indicates that the survival of ν_μ can be

TABLE II

REPRESENTATIVE PROPOSED NEUTRINO OSCILLATION EXPERIMENTS

Source	Proponent	E_ν/ℓ (MeV/m)	Δ^2 (eV^2)	Type
SUN	Davis (BNL,Penn,MPI)	4×10^{-11}	$<10^{-12}$	$\nu_e+{}^{71}Ga\rightarrow{}^{71}Ge+e^-$ (chem; 40 tons→ 1 capt/day; $p+p\rightarrow d+e^-+\nu_e$)
	Pomansky, USSR			
REACTOR	as before		$\lesssim0.05$	ℓ_1, ℓ_2
MESON FACTORY	Chen (Irvine,LASL)	150/9	$\lesssim0.25$	$(\bar\nu_\mu\rightarrow\bar\nu_e)$
	Dombeck (LASL,Md)	150/(40-280)	$\lesssim0.05$	$(\nu_\mu\rightarrow\nu_e)$;PSR '85
			$\lesssim0.24$	$(\nu_\mu\rightarrow\nu_\mu)$ liq scint+PDT; 50tns
	Ling (OSU,ANL,LSU,CIT)	40/(20-250)	$\lesssim0.1$	$(\bar\nu_\mu\rightarrow\bar\nu_e)$; $(\nu_e\rightarrow\nu_e)$
			$\lesssim0.2$	$(\nu_\mu\rightarrow\nu_\mu)$ D_2O+PDT; 5 tns at ℓ_1 + 15 tns at ℓ_2
	Phillips, Minh (Rice,UH,LASL)	40/(10-100)	0.03-0.05	$(\bar\nu_\mu\rightarrow\bar\nu_e)$; liq scint; 15 tns
HI-E ACCEL.	White (AGS) (BNL,Brown,KEK Osaka,Penn,Tokyo)	3-10	$\lesssim1.0$	$(\nu_\mu\rightarrow\nu_\eta)$;$E_p$=28 GeV
				$(\nu_e\rightarrow\nu_e)$;muon storage ring
		1	$\lesssim0.2$	$(\nu_\mu\rightarrow\nu_e)$;$E_p$=0.8 GeV
	FNAL, SPS		0.1-1.0	Bm dumps; B.C.: VLD (Jura Mts); $I_{Booster}=10\ I_{mr}$ PS→ISR→SPS ν-expt

determined with a sensitivity in Δ^2 less than 1.0 eV^2. Another possibility is to make use of the roughly 1.5% ν_e content of BNL ν_μ beam to study ν_e survival through the E_ν-dependence of the ratio $\sigma(\nu_e + n \to e^- + p)/\sigma(\nu_\mu + n \to \mu^- + p)$ in conjunction with the measurement of the ratio of weak neutral current to weak charged current mentioned above. This will also be done in normal running of the experiment.

Still another possiblity for a ν_e survival experiment is to construct a muon storage ring at BNL (where there are several large aperture, high field magnets available for this purpose). A target for the extracted 28 GeV proton beam of the AGS may be located at an edge of the magnetic field region in which will be trapped pions and muons until they decay. This method will yield, e.g., ν_μ from π^+ decay and ν_e and $\bar{\nu}_\mu$ from μ^+ decay at approximately equal rates which are quite substantial. It might be noted that preliminary estimates concerning this source of ν_e (and $\bar{\nu}_e$) suggest that it is likely to be superior to a K_L^o-beam as a ν_e source in intensity, purity and cost. This suggestion for a muon storage ring was made by P. Grannis and M. Marx, who are continuing intensive study of it.

One possibility for a particularly sensitive search for neutrino oscillations using the detector at BNL involves lowering the energy of the proton beam extracted from the AGS which, in turn, significantly lowers the average incident neutrino energy. I would like to be more specific about this experiment than about the others, in part because it is very similar to experiments that might be done at LAMPF. First, however, it is useful to describe briefly the nature of the neutrino detector at BNL.

It is the work of a collaboration of physicists from BNL, Brown, KEK, Osaka, Pennsylvania, Stony Brook and Tokyo.[21] It is directed primarily toward the study of neutrino interactions at what are now relatively low neutrino energies, with emphasis on the elastic scattering processes $\nu_\mu(\bar{\nu}_\mu) + e^- \to \nu_\mu(\bar{\nu}_\mu) + e^-$ and $\nu_\mu(\bar{\nu}_\mu) + p \to \nu_\mu(\bar{\nu}_\mu) + p$. The overall layout of the detector is shown in Fig. 2 which includes the on-line computer configuration. The properties of the boxes labeled "unit" in Fig. 2 are listed in Table III, as are values of interest for the entire detector. The design of the liquid scintillator calorimeter cells and their support structure, and the "airplane wing" structure of the proportional drift tubes lead to a detector with a minimum of dead space, a radiation length of 90 cm, and the capability of sampling track position, energy deposition per unit length and range. In addition, provision is made for timing measurements to identify muon decays.

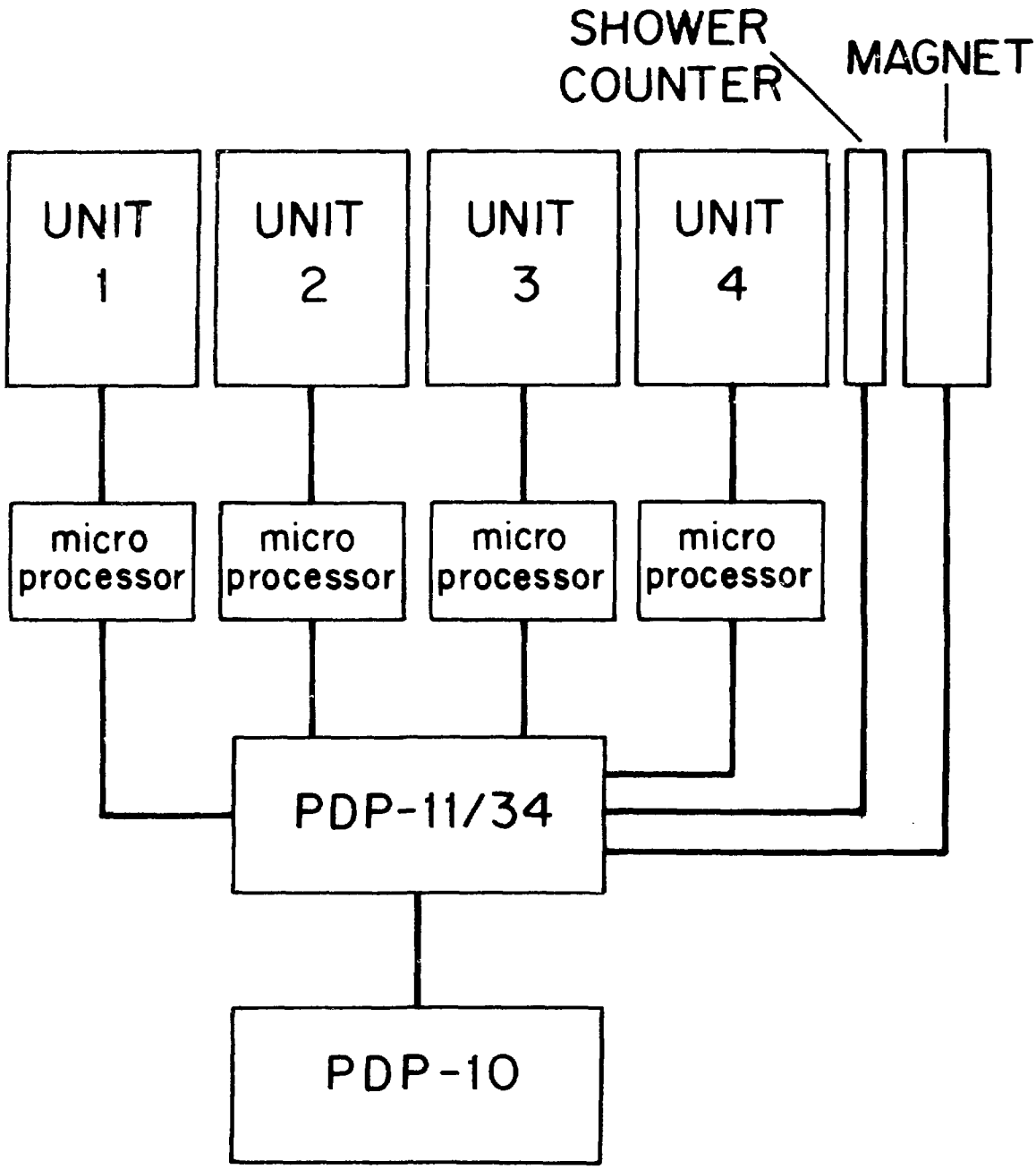

Fig. 2. Layout of the BNL-Brown-KEK-Osaka-Pennsylvania-Stony Brook-Tokyo neutrino detector.

TABLE III

PROPERTIES OF THE
BNL-BROWN-KEK-OSAKA-PENNSYLVANIA-STONY BROOK-TOKYO
NEUTRINO DETECTOR

Single Unit

32 Liquid scintillator slabs

Active area/slab	4.22 m x 4.09 m
Thickness/slab	7.9 cm
No. cells/slab	16
Cell size	4.1 m x $\begin{matrix}7.70\text{ cm (empty)}\\8.46\text{ cm (full)}\end{matrix}$ (along beam) x 25 cm
Wt. (liq. & acrylic)/slab	1.35 metric tons
Total wt. (liq. & acrylic)	43 metric tons
Total PM	1024

31 PDT x-y (double) planes

Active area/plane	4.1 m x 4.1 m
Thickness/plane	7.9 cm
No. cells/slab	54 x 2
Cell size	4.1 m x 3.75 cm (along beam) x 7.50 cm
Skin thickness	0.5 mm x 4
Total cells	3348

Totals for Experiment

Wt. (liq. & acrylic)	172 metric tons
PM (S2212/A)	4096
PDT cells	13392
Vol	4 m x 4 m x 23 m

The response of a 14-ft.-long acrylic calorimeter cell as a function of position along the cell is shown in Fig. 3 and compared with that of teflon-coated cells used previously in neutrino experiments at BNL and Fermilab. In separate tests carried out with e, μ, π and p, the calorimeter energy resolution was determined to be $0.12/\sqrt{E(GeV)}$ for e, and $(0.08\text{-}0.12)/\sqrt{E(GeV)}$ for μ, π and p.

The measured response of a PDT cell as a function of distance from the central wire is shown in Fig. 4 which exhibits a very high track efficiency over almost the entire cell area. The observed pulse height response of a PDT to different particle types at various momenta is shown in Fig. 5 and compared with the expected energy deposition. Finally, the measured angular resolution for electrons of a sub-unit of PDT cells and liquid scintillator modules is given in Fig. 6, where it is compared with the kinematic limit for the process $\nu_\mu + e^- \rightarrow \nu_\mu + e^-$ appropriate to the BNL neutrino spectrum. Monte Carlo studies of neutrino-induced events using these response functions show clear discrimination of electrons, muons and protons in most instances, and clearly delineate the final states of most neutrino interactions.

We turn now to a description of the neutrino oscillation experiment $\nu_\mu \rightarrow \nu_e$ that might be done with this detector using low ($\langle E_\nu \rangle \approx 160$ MeV) neutrinos. Much of the design of this experiment was done by R. Galik. The calculated neutrino spectrum obtained from 800 MeV protons and magnetic focusing of the secondary pions is shown in Fig. 7, and the corresponding quasi-elastic cross sections ($\nu_\ell + n \rightarrow \ell^- + p$) are shown in Fig. 8. At these low neutrino energies the electron-muon mass difference has a large effect on the final state kinetic energy of the quasi-elastic reactions as indicated in Fig. 9. Also the contributions of other reactions that might simulate $\nu_e + n \rightarrow e^- + p$ are significantly reduced. These effects are summarized in Table IV which shows that the only process which has a substantial survival rate is $\nu_e + n \rightarrow e^- + p$. The next largest category of surviving events is from $\nu_\mu + n \rightarrow \mu^- + p$; possible confusion of these with the $e^- + p$ final state provide the primary background in the experiment which searches for a possible increase in the number of ν_e relative to the very small number of ν_e, primarily from muon decay, expected in the incident ν_μ beam. Various possible results of an experiment of 6 weeks duration are indicated schematically in Table V. Here f is the corrected observed ratio $N(\nu_e + n \rightarrow e^- + p)/N(\nu_\mu + n \rightarrow \mu^- + p)$, and $N_B = .02\ N_\mu$ is the total estimated background due to ν_e in the incident beam and misidentified $\mu^- + p$ final states. One sees that this experiment seems capable of reaching a 90% confidence limit on Δ^2 of about 0.2 eV^2.

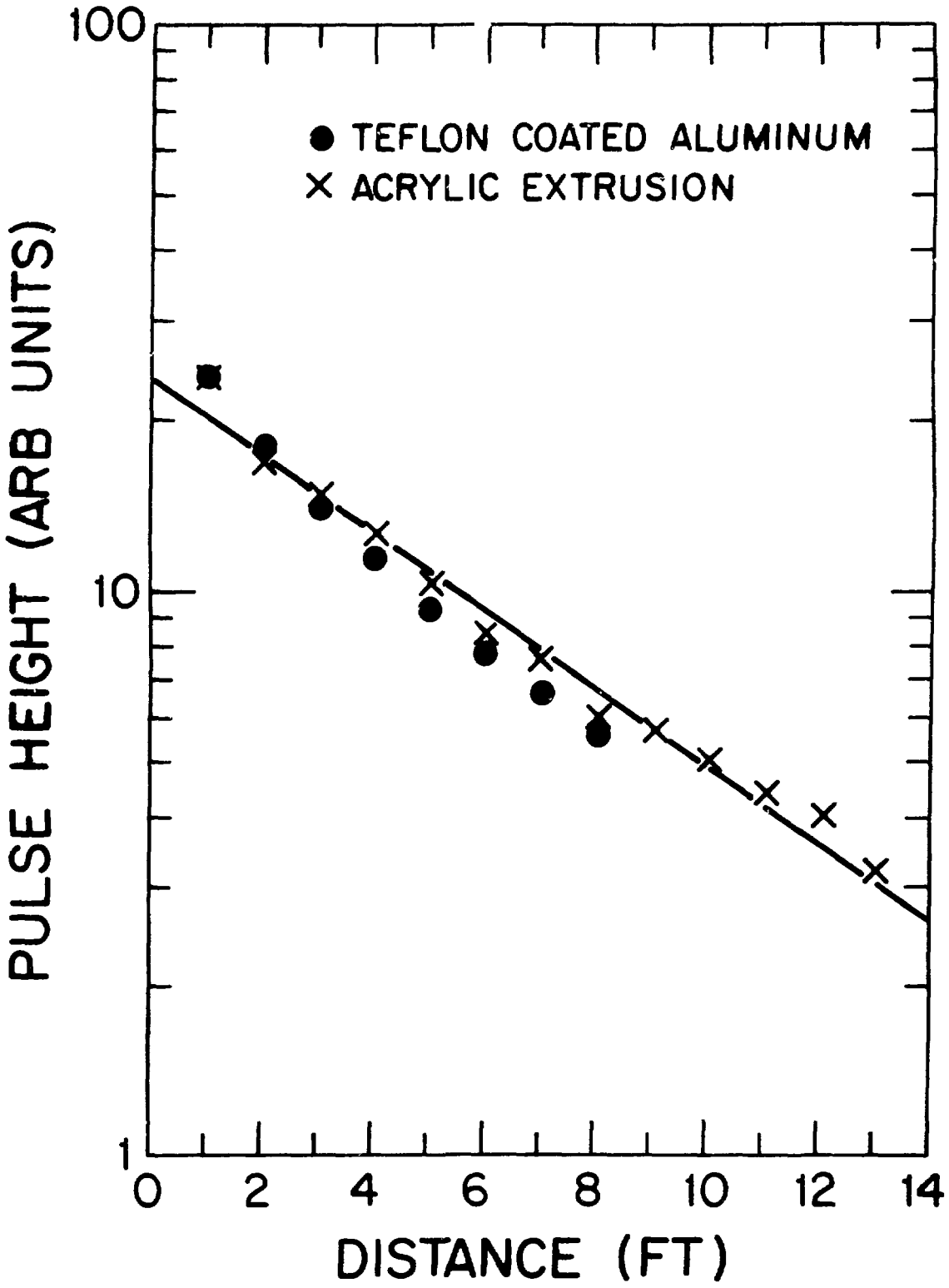

Fig. 3. Response of two types of calorimeter cells as a function of position along the cell.

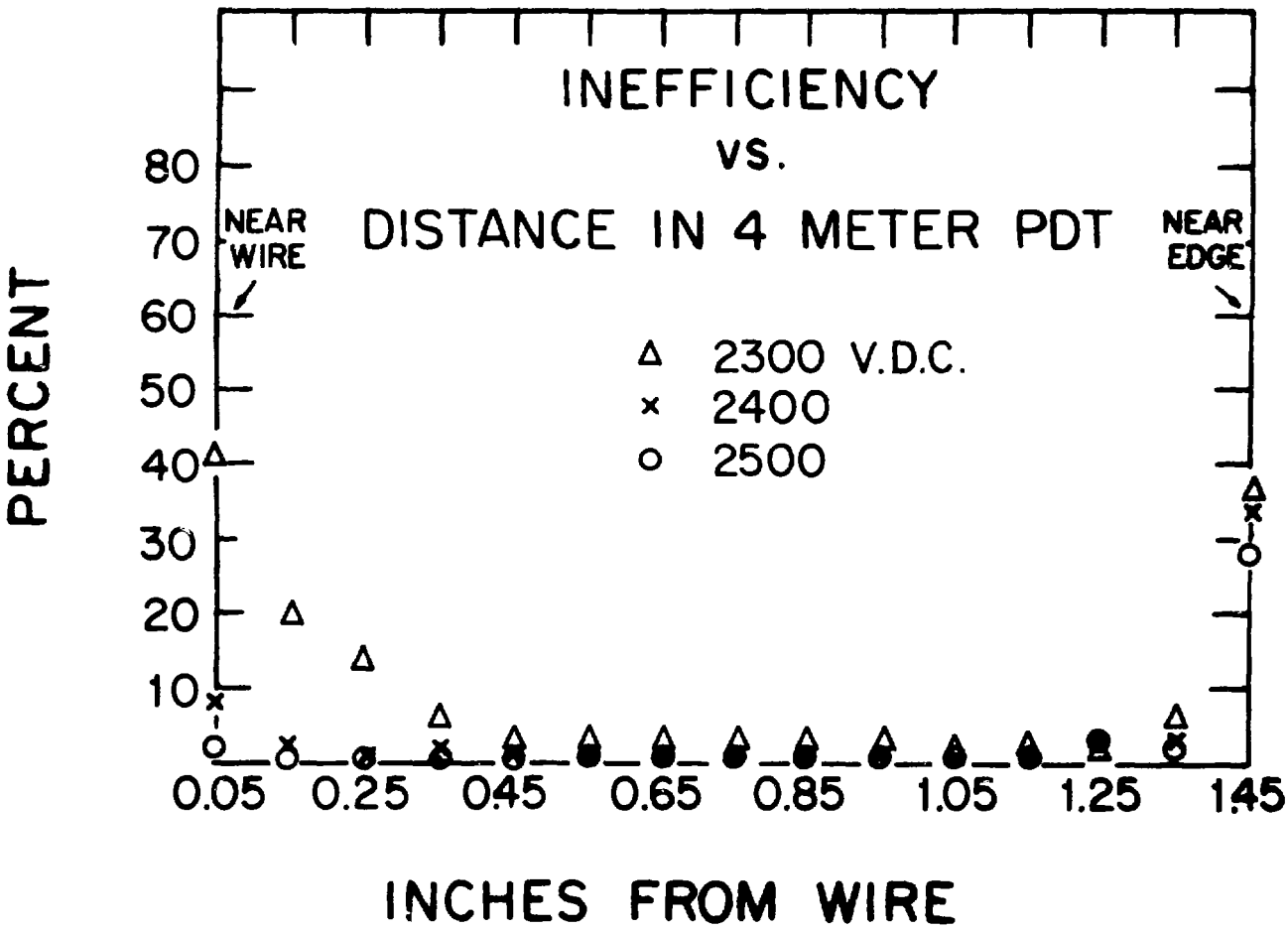

Fig. 4. Response of a PDT cell as a function of distance from central wire for various voltages.

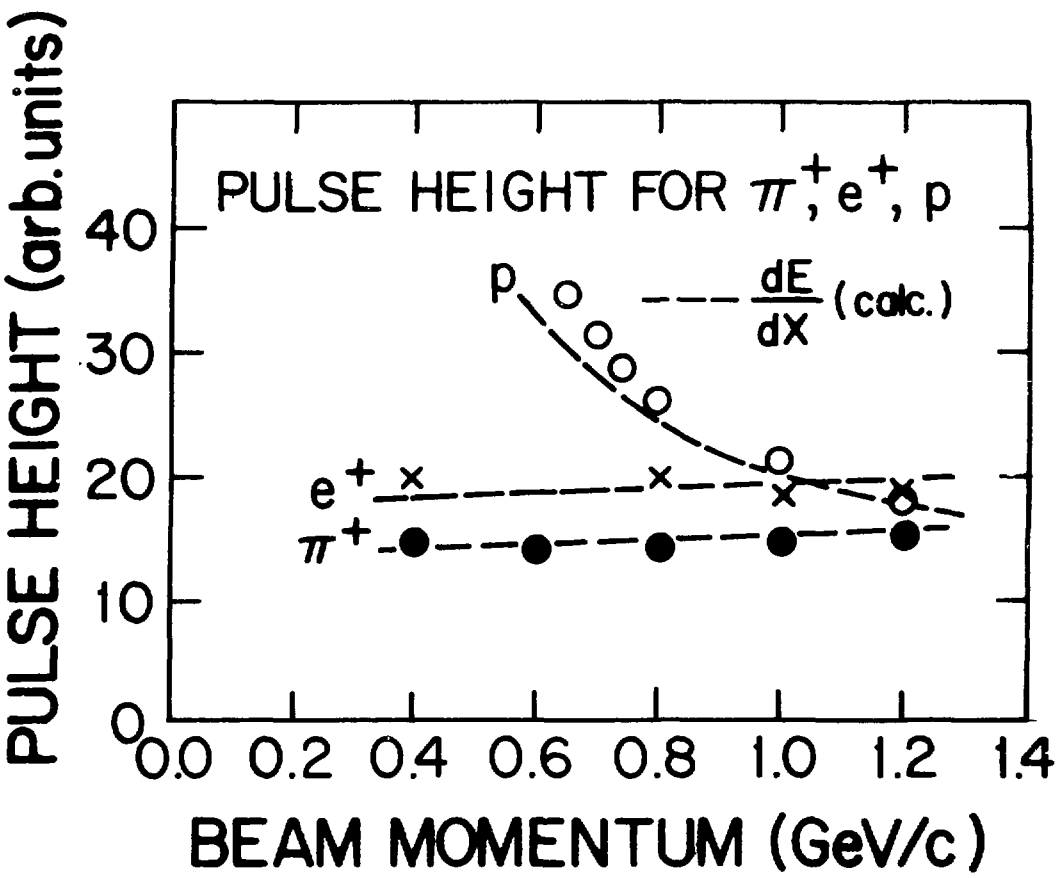

Fig. 5. Pulse height for various particle types as a function of momentum.

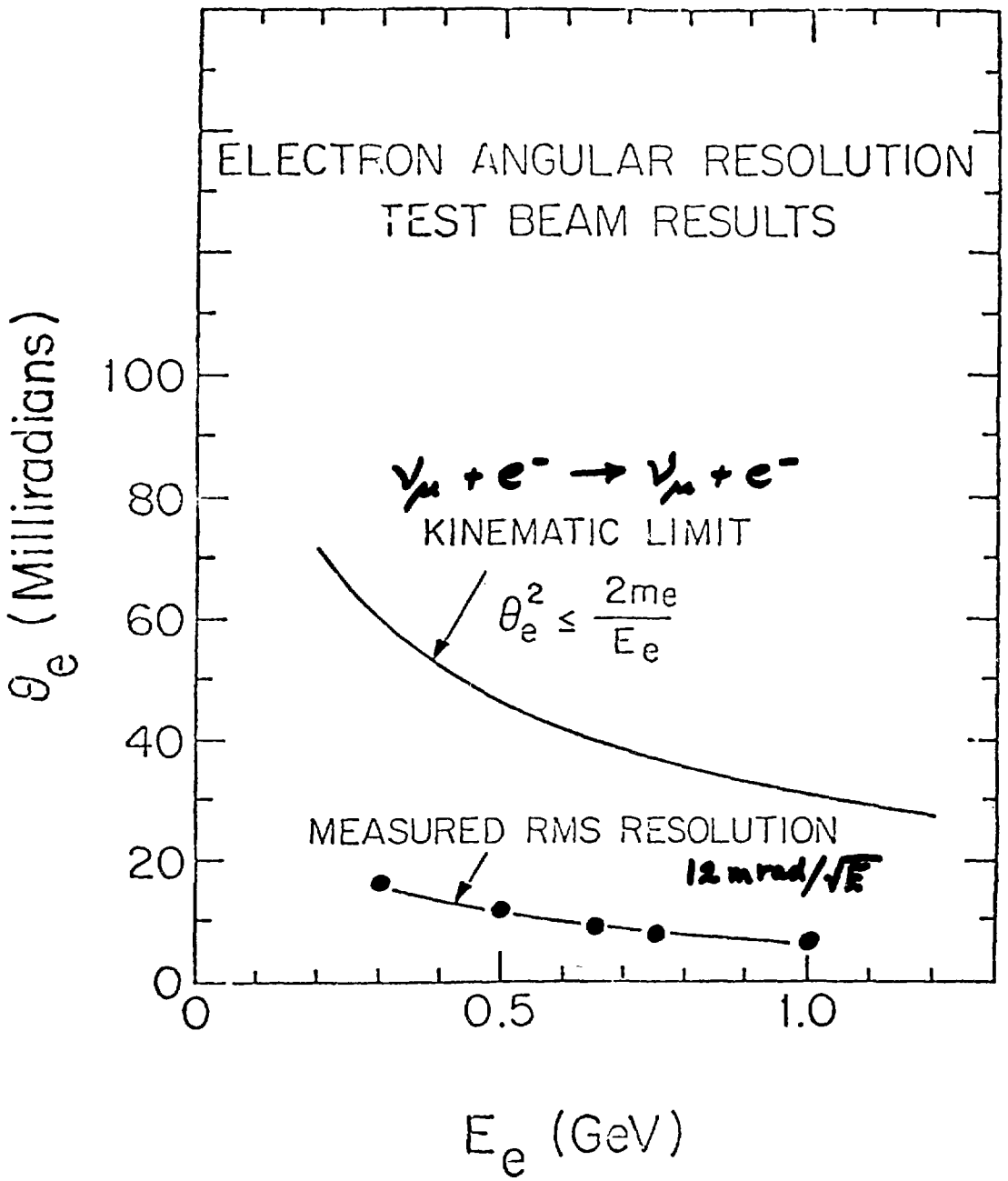

Fig. 6. Measured angular resolution as a function of electron energy.

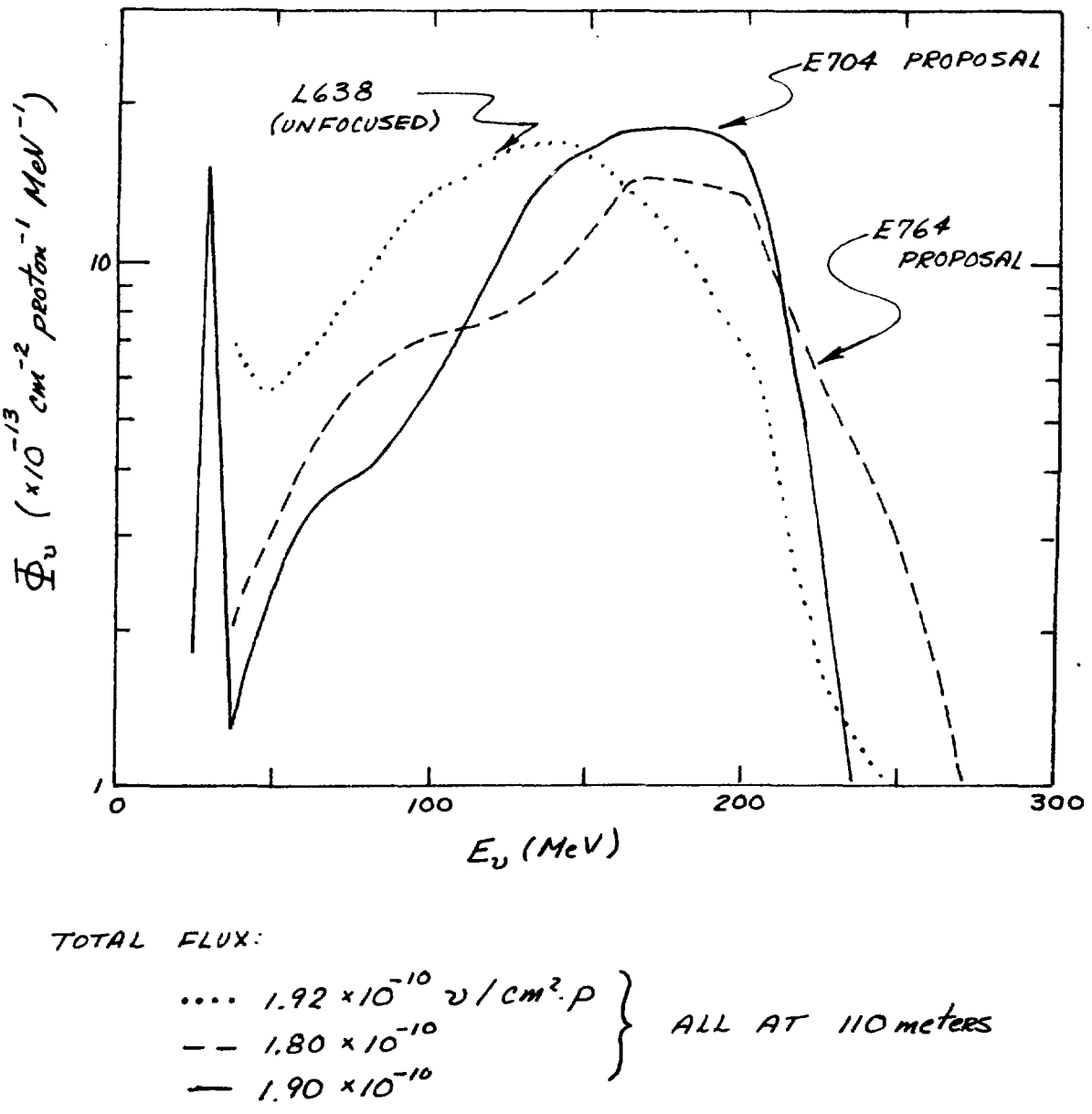

Fig. 7. Three calculations of the neutrino flux into a detector 110 meters downstream from a carbon target struck with 1.46 GeV/c protons. The L-638 curve is from a LAMPF proposal, while the E-704 and E-764 curves are from BNL proposals.

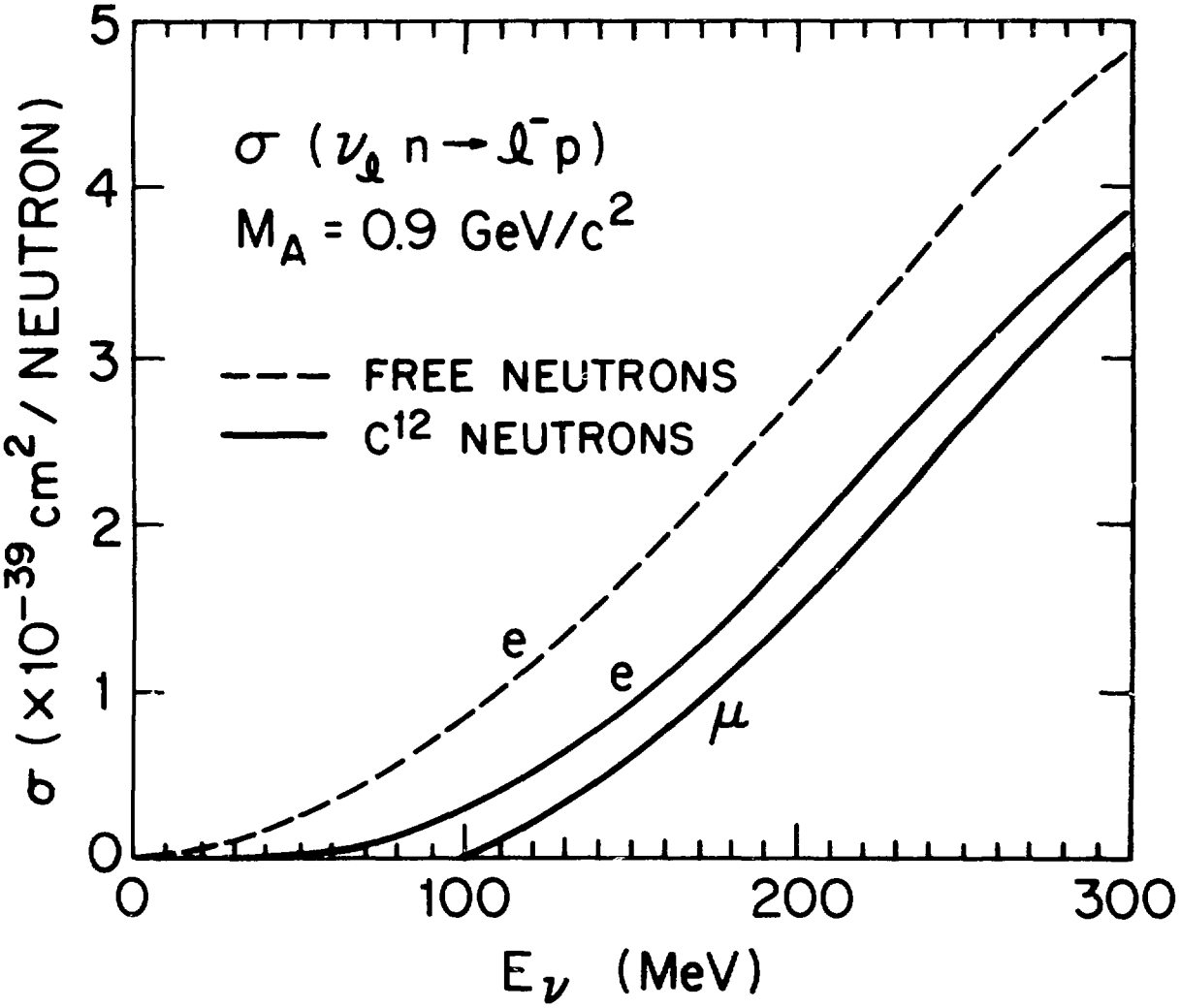

Fig. 8. The quasi-elastic cross sections of ν_e on free neutrons and of ν_e, ν_μ on neutrons bound in carbon.

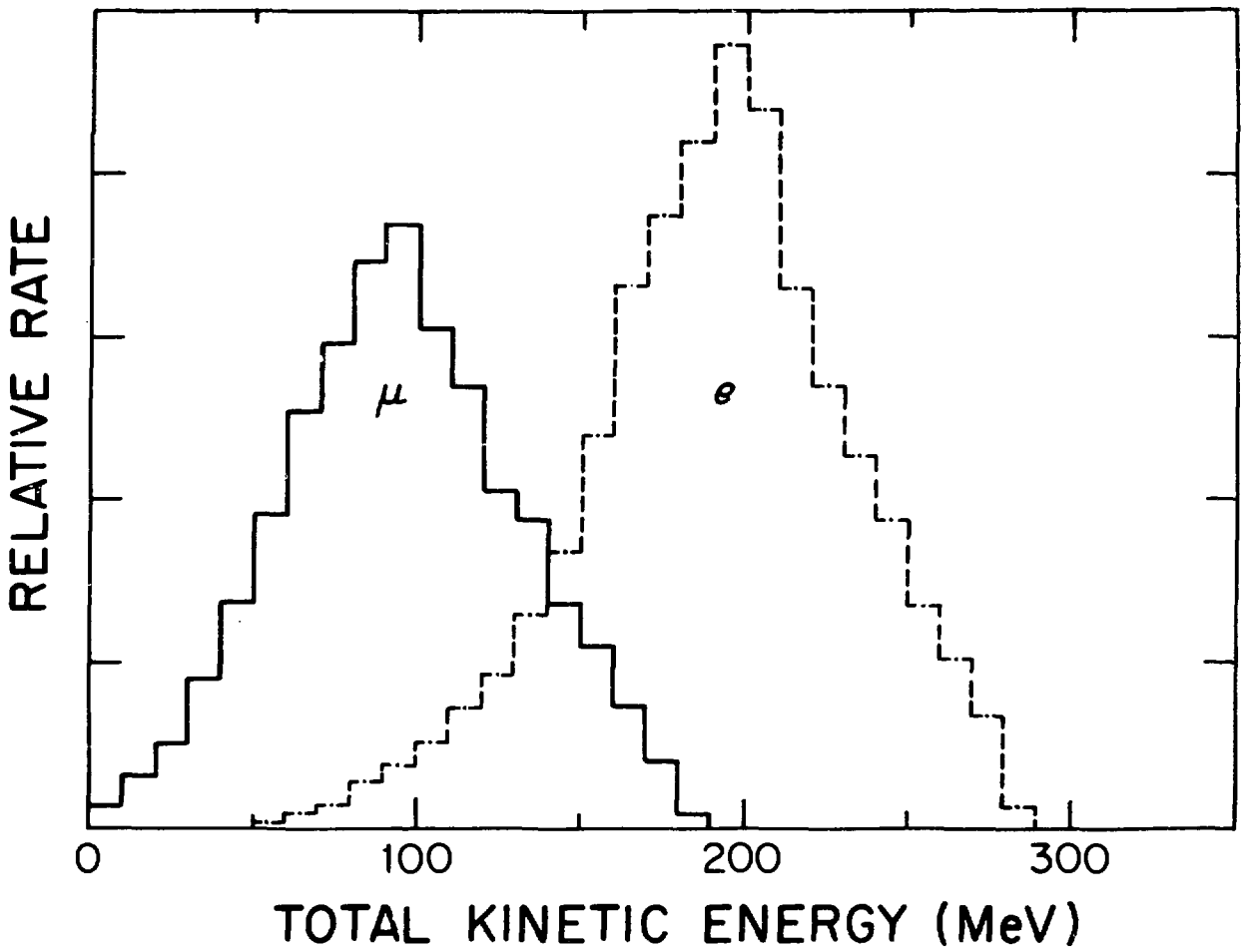

Fig. 9. Distributions of total final state kinetic energies for quasi-elastic events. The visible energy will be ~95% of what is plotted for muons and ~90% for electrons.

TABLE IV

RELATIVE SURVIVAL OF VARIOUS REACTIONS
AFTER APPLYING VARIOUS EVENT CRITERIA

Reaction	Energy (1)	Decay (2)	Clusters (3)	dE/ex (4)	Shower (5)	S Total	$\langle\sigma\rangle^*$	$\langle\sigma\rangle^* S$
$\nu_\mu n \rightarrow \mu^- p$	.13	.30	--	.25	.90	.009	0.87	.008
$\nu p \rightarrow \nu p$	.01	--	--	.40	--	.004	.16	.001
$\nu n \rightarrow \nu n$	.01	--	.40	--	--	.004	.16	.001
$\nu n \rightarrow \nu \pi^- p$	.05	.90	.90[+]	.90	--	.036	.01	.000
$\nu n \rightarrow \nu \pi^0 n$	.70	--	.28	.50	--	.098	.01	.001
$\nu p \rightarrow \nu p \pi^0$	.70	--	.28	.50	--	.098	.01	.001
$\nu p \rightarrow \nu \pi^+ n$	.05	.30	.75	.90	--	.011	.01	.000
$\nu_e n \rightarrow e^- p$	.87	--	.97	.90	.92	.699	1.18	.825

*x 10^{-39} cm^2/nucleon

[+]from nuclear "stars"

TABLE V

PREDICTED RESULTS FROM 6 WEEKS' DATA ACCUMULATION

f	N_μ $\#\nu_\mu n \to \mu^- p$	N_e $\#\nu_e n \to e^- p$	N_B other e^-	$\frac{N_{eB} \pm \sqrt{N_{eB}}}{N_B}$	ℓ/λ	λ (m)	Δ^2 (eV^2)
.005	70.6	0.3	1.4	1.2±0.9	.022	5000	0.08
.010	70.3	0.7	1.4	1.5±1.0	.032	3437	0.11
.020	69.6	1.4	1.4	2.0±1.2	.045	2444	0.16
.040	68.1	2.7	1.4	3.0±1.4	.064	1719	0.22
.075	65.7	5.1	1.3	4.9±1.9	.088	1246	0.30
.100	63.9	6.8	1.3	6.2±2.2	.102	1078	0.35
.150	60.3	10.2	1.2	9.5±2.8	.127	868	0.44
.200	56.8	13.6	1.1	13.4±3.5	.147	748	0.52
.300	49.7	20.4	1.0	21.4±4.6	.185	594	0.65
.400	42.6	27.2	0.9	31.2±6.2	.218	504	0.77

$N_{eB} = N_e + N_B$

*background from muon decay and misidentifications

VI. SUMMARY AND CONCLUSIONS

1. From the experiments planned and in progress it appears that neutrino oscillations might be observed in the next few years in definitive experiments using terrestrial sources, providing $\Delta^2_{kj} \gtrsim (0.1\text{-}0.2)eV^2$ and $\sin^2 2\theta_{kj} \gtrsim$ several times $\sin^2\theta_c$, where θ_{kj} is the mixing angle between ν_k and ν_j, and θ_c is the usual Cabibbo angle.

2. If item 1 above is realized, there would be great value in a neutrino factory which would

   (a) test for the total number of neutrino types (flavors)

   (b) test for CP-violation in neutrino oscillations

   (c) test for right-handed weak leptonic coupling.

3. If item 1 above is not realized, the search for neutrino oscillations will be more or less limited to experiments using extra-terrestrial neutrino sources, e.g., solar neutrinos.

4. If the yield of solar neutrinos from $p + p \rightarrow d + e^+ + \nu_e$ or $p + e + p \rightarrow d + \nu_e$, when measured, agrees with the expected yield (which appears to be subject to only minor uncertainty), we will be forced to conclude that neutrino oscillations probably do not occur. Conversely, if solar experiment and theory show significant disagreement, the possibilities again become open ended.

REFERENCES

1. B. Pontecorvo, Zh. Eksp. Teor. Fiz. 53, 1717 (1967) [Sov. Phys.-JETP 26, 984 (1968)] ; ZhETF Pis. Red. 13, 281 (1971). See also Pontecorvo's early papers: Zh. Eksp. Teor. Fiz. 33, 549 (1957); 34, 247 (1958). See also Z. Maki, M. Nakagawa, and S. Sakata, Prog. Theor. Phys. 28, 870 (1962).

2. R. Davis, Jr., J. C. Evans, and B. T. Cleveland, Proceeding of Neutrino '77, edited by E. C. Fowler (Purdue University Press, 1978).

3. V. Gribov and B. Pontecorvo, Phys. Lett. 28B, 495 (1969).

4. J. N. Bahcall and S. Frautschi, Phys. Lett. 29B, 623 (1969).

5. J. N. Bahcall, N. Cabibbo, and A. Yahil, Phys. Rev. Lett. 28, 316 (1972). See also S. Pakvasa and K. Tennakone, Phys. Rev. Lett. 27, 757 (1971); 28, 1415 (1972); Lett. Nuovo Cimento 6, 675 (1973); S. Eliezer and A. R. Swift, Nucl. Phys. B105, 45 (1976); S. Eliezer and D. A. Ross, Phys. Rev. D 10, 3088 (1974); M. Nakagawa et al., Prog. Theor. Phys. 30, 727 (1963).

6. L. Wolfenstein, Phys. Rev. D 17, 2369 (1978).

7. R. Cowsik and J. McClelland, Astrophys. J. 180, 7 (1973).

8. M. Kobayashi and T. Maskawa, Prog. Theor. Phys. 49, 652 (1973).

9. V. A. Lubimov et al., Phys. Lett. 94B, 266 (1980).

10. A. K. Mann and H. Primakoff, Phys. Rev. D 15, 655 (1977).

11. S. Nussinov, Phys. Lett. 63B, 201 (1976); L. Wolfenstein, Phys. Rev. D 18, 958 (1978); M. Cabibbo, Phys. Lett. 72B, 333 (1978).

12. J. N. Bahcall and H. Primakoff, Phys. Rev. D 18, 3463 (1978).

13. F. Reines et al., Phys. Rev. Lett. 45, 1307 (1980).

14. H. Kwon, talk at Neutrino Mass Mini-Conference, Telemark, Wisconsin, October 1980 (V. Barger and D. Cline, organizers); F. Boehm et al., CIT Preprint 5P-80-115, October 1980.

15. R. Davis, Jr., Phys. Rev. 97, 766 (1955).

16. R. Burman et al., Phys. Rev. Lett. 44, 522 (1980), and Errata, Phys. Rev. Lett. 45, 1370 (1980).

17. J. Blietschau et al., Nucl Phys. B133, 205 (1978).

18. A. M. Cnops et al., Phys. Rev. Lett. 40, 144 (1978).

19. M. R. Krishnaswamy et al., Proc. Phys. Soc. Lond. A323, 489 (1971); L. V. Volkova and G. T. Zatsepin, Sov. J. Nucl. Phys. 14, 117 (1972); M. F. Crouch et al., Phys. Rev. D 18, 2239 (1978).

20. V. Barger, K. Whisnant, and R. J. N. Phillips, Phys. Rev. D 22, 1636 (1980).

21. BNL: L. Ahrens, S. Aronson, P. Connolly, R. Gibbard, M. Murtagh, S. Murtagh, S. Terada, A. Thorndike, P. Wanderer, H. White. Brown: D. Cutts, R. Dulude, B. Hughlock, R. Lanou, J. Massimo, Y. Suzuki. KEK: S. Kabe. Osaka: Y. Nagashima. Pennsylvania: K. Abe, K. Amako, E. Beier, D. Doughty, R. Galik, A. K. Mann, M. Newcomer, R. Van Berg, H. H. Williams, T. York. Stony Brook: M. Marx. Tokyo: T. Miyachi.

Grenoble Neutrino Experiment

by

Alan Hahn
Caltech and ILL

ABSTRACT

The electron-antineutrino spectrum has been measured at a 8.76 m position from the "point-like" core of the ILL ^{235}U fission-reactor, using the reaction $\bar{\nu}_e + p \rightarrow e^+ + n$. Positrons and neutrons were detected in coincidence by means of a low-background liquid scintillator and ^3He detector system. The observed neutron correlated positron spectrum is consistent with an experimentally derived spectrum assuming no neutrino oscillations. Upper limits for the oscillation parameter are presented.

I. INTRODUCTION

The possibility for the occurrence of neutrino oscillations and the related question of neutrino rest masses has been of great concern in recent years[1,2]. We report here on a neutrino experiment which initiated in 1976 at the research reactor of the Institut Laue-Langevin (ILL). The goal of our study is to measure with good accuracy the energy spectrum of electron-anti-neutrinos ($\bar{\nu}_e$) emitted following the fission of ^{235}U in order to search for neutrino oscillations of the type $\bar{\nu}_e \rightarrow$ anything. The present experiment measures the energy dependence of the antineutrino yield at a fixed distance d = 8.76 m. The possible existence of neutrino oscillations is of particular interest in connection with the solar neutrino puzzle[1], cosmological considerations[3], and the fundamental structure of leptonic currents[1,2].

Neutrino oscillations of the weak interaction eigenstates ($\nu_e, \nu_\alpha, \ldots$) may occur if these "physical" neutrinos are superpositions of the mass eigenstates

(ν_1, ν_2,...). If we confine our discussion to the case of a two-neutrino system (which might well approximate the general case), the superposition can be written as

$$\begin{pmatrix} \nu_e \\ \nu_\alpha \end{pmatrix} = \begin{pmatrix} \cos\theta & \sin\theta \\ -\sin\theta & \cos\theta \end{pmatrix} \begin{pmatrix} \nu_1 \\ \nu_2 \end{pmatrix} \tag{1}$$

where θ is a mixing parameter. This desciption[1,2] allows for flavor oscillations ($\nu_\alpha = \nu_\mu, \nu_\tau, \ldots$) as well as for particle-antiparticle oscillations ($\bar{\nu}_\alpha = \bar{\nu}_{eL}, \ldots$) where L stands for lefthanded). The time development of the system in Eq. (1) is given by

$$|\nu_e(t)|^2 = |\nu_e(0)|^2 \left(1 - \frac{\sin^2(2\theta)}{2} (1 - \cos (E_2 - E_1)t)\right)$$

where E_i is the energy of the neutrino ν_i. For momenta $p >> m_i$ (m_i being the mass) $E_2 - E_1 \simeq (m_2^2 - m_1^2)/(2p)$.

The oscillation length Λ (in meters) is related to the neutrino kinetic energy E_ν(in MeV) and to the mass squared difference $\Delta^2 = |m_1^2 - m_1^2|$ in $(eV)^2$ by

$$\Lambda = 2.48\ E_\nu/\Delta^2. \tag{2}$$

The oscillations are thus characterized by the parameters Δ^2 and $\sin^2(2\theta)$. The counting rate Y in a $\bar{\nu}$-detector at a distance d from an antineutrino source (reactor core) is (using the same units) given by

$$Y(E_{\bar{\nu}}, \Delta^2 d) = \varepsilon\ N(E_{\bar{\nu}})\ \sigma(E_{\bar{\nu}}) \left(1 - \frac{\sin^2(2\theta)}{2} (1 - \cos (2.53\Delta^2 d/E_{\bar{\nu}})\right) \tag{3}$$

where $N(E_{\bar{\nu}})$ is the reactor produced $\bar{\nu}$ spectrum and ε is the detection efficiency. The cross section $\sigma(E_{\bar{\nu}})$ with $E_{\bar{\nu}}$ in MeV) of the detector reaction is given by[4]

$$\sigma(E_{\bar{\nu}}) = (9.13 \pm 0.11)\ (E_{\bar{\nu}} - 1.293)\ \sqrt{(E_{\bar{\nu}} - 1.293)^2 - (0.511)^2}\ 10^{-44}\ \text{cm}^2. \tag{4}$$

Here a neutron lifetime of $\tau_n = (926 \pm 11)$ s[5] has been used.

As can be seen from Eq. (2), reactor experiments ($E_{\bar{\nu}} < 10$ MeV, $d < 100$ m) are suitable to study mass squared differences in the range of $0.01 < \Delta^2 < 5$ $(eV)^2$ for sufficiently large mixing angles. Previous published limits for the parameter Δ^2 in the channel $\nu_\mu \leftrightarrow \nu_e$ (assuming full mixing) are in the vicinity of $\Delta^2 \leq 1$ $(eV)^2$ (90% c.l.)[6,8]. However, experiments at CERN and Serpukhov which explored different channels might be interpreted as suggesting non-vanishing values of Δ^2 and large mixing angles[2,9,10]. Recently, Reines *et al.*[11] have reported evidence for non-zero oscillation parameters, in a study of the reactions $\bar{\nu}_e + d \rightarrow \bar{\nu}_e + p + n$ and $\bar{\nu}_e + d \rightarrow e^+ + n + n$.

An outline of the work reported here has been published in Ref. 12.

II. METHOD AND APPARATUS

The ILL reactor (57 MW; 93% ^{235}U) has been chosen as the antineutrino source, because the small size of its core (40 x 80 cm) makes it suitable for the study of very small oscillation lengths. A neutrino flux of 0.98×10^{12} cm^{-2} s^{-1} is available at our detector position. The inverse beta decay $\bar{\nu}_e + p \rightarrow e^+ + n$, which has a threshold energy of 1.8 MeV, is used as the detection reaction . The central detector consists of 30 lucite cells filled with a total of 377 l of proton-rich liquid scintillator (NE 235 C^+; $\rho = 0.861$ g cm^{-3} ; H/C = 1.71) arranged in five vertical planes. Four ^3He wire chambers at atmospheric pressure are sandwiched between the scintillation counters, as shown in Fig. 1. The scintillator cells serve as proton target, positron detector and neutron moderator. The dimensions of the target cells were chosen to optimize neutron moderation, light collection and minimize neutron absorption. The central detector is surrounded by a liquid scintillator veto and various shieldings, as depicted in Fig. 1. Efficient discrimination against proton recoil pulses initiated in the target cells by fast neutrons of cosmic-ray origin is achieved by means of pulse shape discrimination. A typical rejection rate of 98% is obtained (with only 2% loss of the positron signal). The energy resolution of the target cell is 18% FWHM at 1 MeV. Absolute energy calibration was done with the 4.44 MeV gamma ray from $^{12}C^X$ emitted by an Am(Be) source. The advantage of the ^3He neutron counters is the high neutron efficiency and

the low gamma background. The background rate in each ^{3}He counter from natural activities is about 0.75 counts/min in our energy window. The neutron detection efficiency was measured by using a calibrated Sb(Be) source which emits neutrons of about 20 keV, closely approximating the actual neutron spectrum. The source could be moved to different positions within the detector volume. The total efficiency was found to be $(19.5 \pm 1.7)\%$ for e^+ -neutron coincidence events falling into a 200 μs time window. This rather long time window is necessary to allow for an efficient migration of the moderated neutrons to the ^{3}He detectors (80.1% acceptance). Gain stability checks and adjustments are performed every three days, employing an external Am(Be) source. This procedure insured counting rate stabilities of our detector system to within 1% over the entire measurement period. The tagged signals from veto coutners and target cells are sored in a buffered and continuously cycling multichannel ADC. An accepted ^{3}He signal (in the proper energy window) causes the ADC to transfer into a PDP 11 the energy, time and tagword of several preceeding target-cell events. Various software cuts can be applied to the stored data. Signal rates are typically 216 counts/s for the 30 target cells, 0.4 counts/s for the four ^{3}He counters and 257 counts/s for the six veto counters. These rates, corrected for the true correlated neutrino events, remained unchanged to within better than 1% for reactor on and off, demonstrating the effectiveness of our shielding arrangement. The principal background source above 2.5 MeV is of cosmic-ray origin, in spite of about 2.5 m of concrete overhead shielding. Detailed information on the detector system can be found in Ref. 4 and 14.

III. RESULTS AND DISCUSSION

Measurements were taken during seven reactor-on cycles interspersed with background runs during six reactor-off periods. The difference spectrun, which represents the effect caused by the reactor neutrinos, is shown at the top of the Fig. 2. The signal to background ratio is better than 1:1 above $E_{e^+} = 2$ MeV. A total number of 4890 ± 180 neutrino-induced events with $E_{e^+} > 1$ MeV has been observed, with an average counting rate of (1.58 ± 0.06)/h.

Calculations of neutrino spectra from fission products have been published by Davis *et al.* (DV)[15] and by Avignone and Greenwood (AG)[16].

Recently, a measurement of the beta decay spectrum following ^{235}U fission was made at the ILL using the BILL electron magnetic spectrometer.[17] The results agreed to within 5% with the calculated beta spectrum of Ref. 15. However, in order to avoid relying upon any calculated neutrino spectrum, a direct transformation of the experimental beta spectrum into the neutrino spectrum was attempted. Empirically, it was found that to better than 1%, the experimental spectrum could be approximated by 25 individual allowed beta decays, i.e.

$$N_\beta^{Fiss}(E) \approx \sum_{1=i}^{25} N_\beta\ (E, E_0^i)$$

with the allowed beta shape being

$$N_\beta(E, E_0^i) = kpE(E_0^i - E)^2\ F(Z,E)$$

where k is the absolute normalization, p and E the momentum and energy of the electron, and F(Z,E) the usual Fermi Coulomb function. The fission neutrino spectrum follows by simply replacing E by $E_0 - E_\nu$, E_0 being the end point energy.

The sensitivity of this transformation to Z (through F(Z,E)) was explored in the following manner. The neutrino spectra from Z = 36 and Z = 55 (the peaks of the fission product yields) were averaged into one spectrum, in order to qualitatively take into account the fact that heavy nuclei generally have lower Q values. Then a neutrino spectrum was generated with the average value , Z = 46. Comparison showed that the two differed by less than 2%. Finally as a check of the method itself, the calculated beta spectrum of Ref. 14 was transformed and compared to the calculated "exact" neutrino spectrum of the same reference. Again any differences were less than 2%. To be conservative, a 4% error due to the conversion method was assumed. Therefore, the total error including absolute normalization in the energy range of 2 to 7.5 MeV of 6.5% (90% C.L.) was adopted.

Using the BILL derived neutrino spectrum, our experiment gives an

integrated yield (for $E_{e^+} > 1$ MeV) of

$$\frac{Y_{exp}}{Y_{BILL}} = 0.955 \pm \begin{matrix} 0.035 \text{ (statistical error)} \\ 0.115 \text{ (systematic error + theoretical uncertainty)} \end{matrix}$$

This ratio is consistent with one. A more detailed comparison between our experimental points and the theoretical predictions for different oscillation parameters is presented at the bottom half of Fig. 2. The points represent the ratios of the measured to the theoretical yields for zero oscillation, corrected for finite energy resolution and core and detector size. The error bars are statistical errors only. The drawn lines give the theoretical curves for different sets of oscillation parameters. An estimated maximum uncertainty is explicitly shown in the figure for the case of zero oscillation (dashed curves).

Figure 3 shows the upper limits for the parameters Δ^2 and $\sin^2(2\theta)$ obtained from a χ^2 test to our experimental data as well as the results from Ref. 11. Curves for 90% and 68% confidence level are shown. A limit of $\Delta^2 = 0.15$ (eV) (90% c.l.) is obtained from our experiment if one assumes maximum mixing. For smaller mixing angles the upper limit for Δ^2 increases correspondingly. For example, the parameters $\Delta^2 = 2.4$ $(eV)^2$ and $\sin^2(2\theta) = 0.3$ shown in Fig. 2 are consistent with our data. For very large values of Δ^2, owing to the finite energy resolution, one averages over the oscillation periods and our results then give only information on $\sin^2(2\theta)$. We obtain for Δ^2_∞, $\sin^2(2\theta) < 0.32$ (90% c.l). The experimental limits reported in Ref. 6-8 are consistent with our results, however one should keep in mind that these experiments sample different oscillation channels. The large mixing ratios implied by the results of Ref. 11 (see caption to Fig. 3) are inconsistent with our results at the 90% confidence level.

A continuation of the present measurements employing improved detectors and taking data at different distances is expected to eliminate the uncertainties stemming from the uncertainties in the neutrino spectrum and absolute

detector efficiency. A detailed account of the present experiment will be published[14].

ACKNOWLEDGEMENTS

This work has been carried out in collaboration with F. Boehm, H. E. Henrikson, J.-L. Vuilleumier, H. Kwon (CalTech), J.-F. Cavaignac, D. H. Koang, B. Vignon (ISN, Grenoble), F. v. Feilitzsch and R. Mössbauer (TU München).

REFERENCES

1. S. M. Bilenky and B. Pontecorvo, Physics Reports 41, 226 (1978), H. Fritzsch, Fundamental Physics with Neutrons and Neutrinos, ed. T. v. Egidy, Inst. Physics, Bristol and London (1978), p. 117; P. Minkowski, Ibid, p. 144.

2. A. De Rujula *et al.* Report TH-2788 CERN (1979).

3. D. Schramm and G. Steigen, Phys. Lett. 87B, 141 (1979).

4. H. Kwon, Thesis, California Institute of Technology, Pasadena (1980).

5. C. J. Christensen *et al.*, Phys. Rev. D5, 1628 (1972); J. Byrne *et al.*, Phys. Lett. 92B, 274 (1980).

6. J. Blietschau *et al.*, Nucl. Phys. B133, 205 (1978).

7. S. E. Willis *et al.*, Phys. Rev. Lett. 44, 522 (1980); P. Nemethy *et al.*, Neutrino 80, Erice (1980), to be published.

8. J. K. Bienlein *et al.*, Phys. Lett. 13, 80 (1964).

9. F. Boehm, Rapporteur talk, Neutrino 80, Erice (1980), to be published.

10. F. Dydak, Rapporteur talk, Neutrino 80, Erice (1980), to be published.

11. F. Reines, H. W. Sobel and E. Pasierb, Phys. Rev. Lett. 5, 1307 (1980).

    E. Pasierb, contributed paper, Nuclear and Particle Physics at Energies Below 31 GeV, Los Alamos, New Mexico, Jan. 1981.

12. Caltech-ILL-ISN Grenoble-TU Munchen collaboration, F. Boehm *et al.*, Phys. Lett. 97B, 310 (1980).

13. F. A. Nezrick and F. Reines, Phys. Rev. 142, 852 (1966).

14. Caltech-ILL-ISN Grenoble-TU Munchen collaboration, Phys. Rev., to be published.

15. B. R. Davis *et al.*, Phys. Rev. C19, 2259 (1979).

16. F. T. Avignone and Z. D. Greenwood, Phys. Rev. C22, 594 (1980).

17. K. Schreckenback *et al.*, Phys. Lett., to be published.

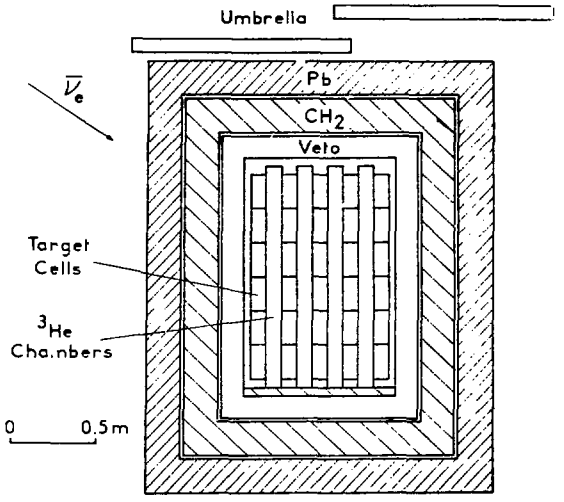

Fig. 1
Experimental arrangement.

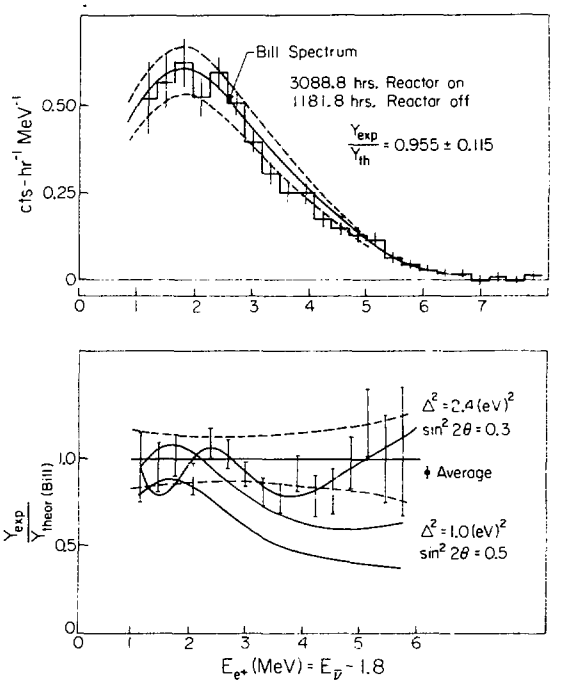

Fig. 2
Experimental results. The upper figure shows the neutrino produced positron spectrum. The dashed curves are the systematic errors (90% C.L.). The lower figure is the experimental positron spectrum normalized to the expected spectrum. The envelope labeled $\Delta^2 = 1.0(eV)^2$ corresponds to the solution of Ref. 11.

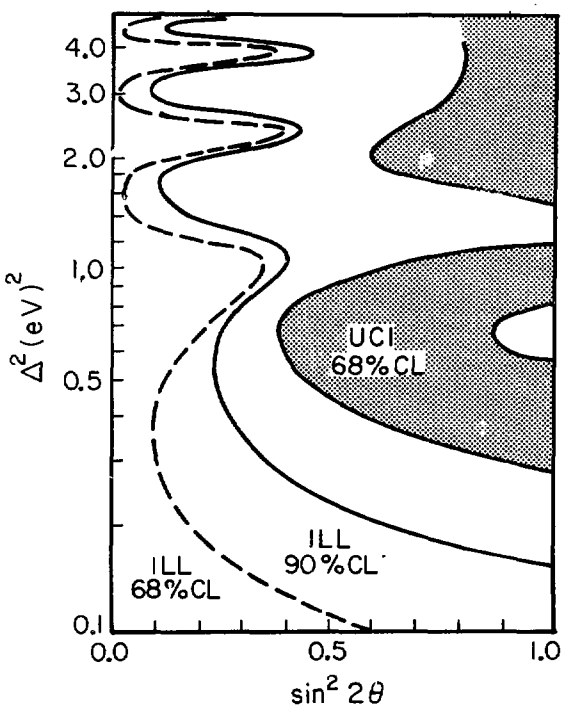

Fig. 3
Limits for Δ^2 and $\sin^2 2\theta$ from this experiment. The allowed region is to the left of the ILL curves.

STATUS OF U. C. IRVINE NEUTRINO OSCILLATION DETECTOR[†]

by

E.L. Pasierb[*] H.S. Gurr,[††] W.R. Kropp, M. Mandelkern,
S.Y. Nakamura,[†††] L. Price, F. Reines, H.W. Sobel

Presented by Elaine Pasierb
Department of Physics
University of California
Irvine, California 92717

ABSTRACT

Updated theoretical calculations of the reactions $\bar{\nu}_e + d \rightarrow n + p + \bar{\nu}_e$ and $\bar{\nu}_e + d \rightarrow n + n + e^+$ have increased the value of the "ratio of ratios", R, from values ranging between 0.38 and 0.40 to .41 and .43. A moveable neutrino oscillation detector is nearing completion and should be installed at a 2000 MW fission reactor at the Savannah River Plant this summer. The positron energy spectrum will be measured at distances ranging from 13 to 50 meters from the center of the reactor core.

I. THE DEUTERON EXPERIMENT

This past year we have reported[1] on neutrino instability based on the results of an experiment to measure the charged current (ccd) and neutral current (ncd) cross sections of $\bar{\nu}_e$ on deuterium. The reactions are:

$$\bar{\nu}_e + d \rightarrow n + n + e^+ \quad \text{(ccd)}$$

$$\bar{\nu}_e + d \rightarrow n + p + \bar{\nu}_e \quad \text{(ncd)}$$

This experiment was conducted at a 2000 MW fission reactor at the Savannah River Plant, at a distance of 11.2 meters from the center of the reactor core.

We realized that this experiment could be used as a neutrino oscillation test. The ncd reaction is independent of neutrino type, while the ccd reaction will only occur for incident $\bar{\nu}_e$'s. In the paper by Reines, Sobel and Pasierb[2] we defined a quantity

$$R = \frac{\left(\frac{ccd}{ncd}\right)_{experiment}}{\left(\frac{ccd}{ncd}\right)_{predicted}} \quad . \tag{1}$$

The denominator is independent of the reactor neutrino absolute normalization, and insensitive to the precise shape of the reactor neutrino spectrum. For stable neutrinos R is expected to be unity. A value of R below unity could signal the instability of $\bar{\nu}_e$.

The experimental ratio i.e. the numerator in (1) has been found to be 0.167 ± 0.093. As previously reported[2] the denominator has been evaluated using two different models for the fission $\bar{\nu}_e$ spectrum, that of Avignone and Greenwood[3] (AG) and that of Davis et al,[3] (DVMS). These models yield 0.44, and 0.42 respectively for the denominator in (1). In this way we obtained the two values $R_{AG} = 0.38 \pm 0.21$ and $R_{DVMS} = 0.40 \pm 0.22$.

We have updated these values of R using new calculations of the theoretical cross section which incorporate different n-n and n-p ^1S_o scattering length values (as reported by W. R. Gibbs and G. J. Stephenson, Jr.), as well as effective range corrections previously taken into account.[4] Based on calculations by A. Soni and D. Silverman[5] ($a_s^{nn} = -18.5$ fm, and $a_s^{np} = -23.7$ fm, and $r_s^{nn} = 2.8$ fm and $r_s^{np} = 2.73$ fm.) we now find the values

$$R_{AG} = 0.41 \pm 0.23$$

$$R_{DVMS} = 0.43 \pm 0.24$$

which is a (2.4 - 2.6) standard deviation departure from unity. These represent an 8.5% increase over the previous values.

If we attribute this departure from unity to neutrino oscillations as described by Nakagawa, Okonogi, Sakata, and Toyoda and by Pontecorvo,[6] and for illustrative purposes assume a simple two neutrino case, then from the value of R we find a relationship between $\Delta = m_1^2 - m_2^2$, and $\sin^2 2\theta$ (where θ is the mixing angle). The allowed regions of Δ and $\sin^2 2\theta$ are shown in Figure 1 for $R = 0.41 \pm 0.23$.

The ideal approach to look for neutrino oscillations is to measure the $\bar{\nu}_e$ spectrum versus distance from the reactor with the same detector. Any deviation of the flux from a $1/r^2$ (r is the distance from the reactor) behavior would indicate that the electron antineutrino is not stable.

To this end we have designed a mobile detector to look for neutrino oscillations. This detector which has been under construction the past $4\frac{1}{2}$ years is nearing completion, and it will be used at the same 2000 MW reactor where the deuteron experiment was performed.

II. MOBILE NEUTRINO OSCILLATION DETECTOR

The detector shown in Figure 2 consists of an inner "target" detector, surrounded by a "blanket" detector which in turn is surrounded by 2" of lead shielding. An anticoincidence system completely surrounds the system and all is mounted on a moveable cart. The components will weigh ~ 12 tons.

The inner detector is filled with 270 liters of xylene based, gadolinium-loaded liquid scintillator, viewed by twenty-one EMI-9870 hemispherical phototubes. This will enable us to measure the positron energy spectrum from the inverse beta reaction $\bar{\nu}_e + p \rightarrow n + e^+$. The system will trigger on a prompt pulse from the positron and its annihilation gamma rays with a delayed coincidence from the neutron capture on gadolinium. To discriminate against neutron background mocking a real event we will use pulse shape discrimination in the inner detector.

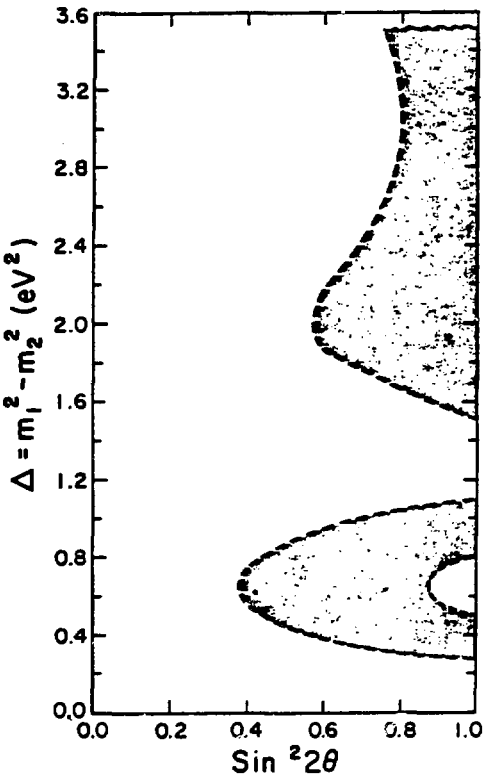

Fig. 1.
Allowed regions of Δ and $\sin^2 2\theta$ for R = 0.41 ± 0.23.

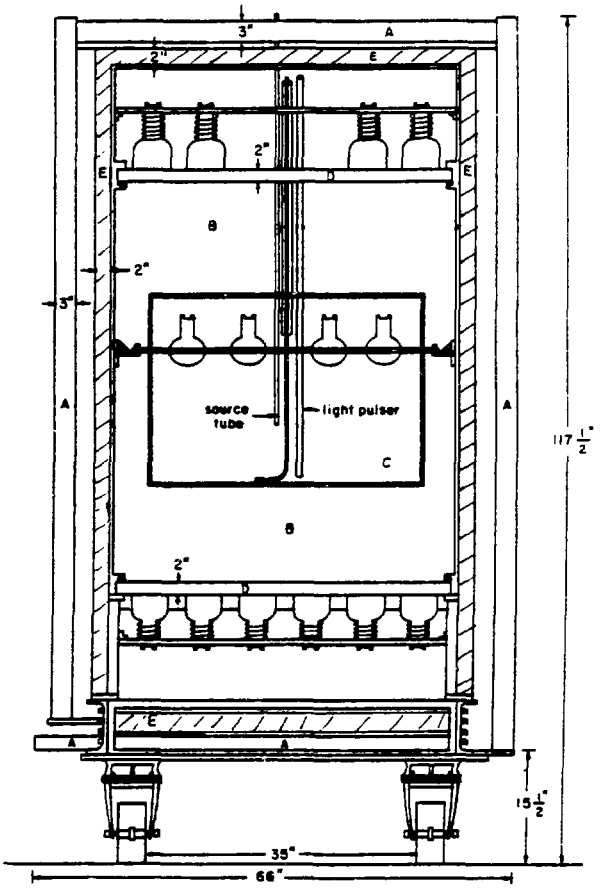

Fig. 2.
Neutrino oscillation detector. A = Anticoincidence system. B = "Blanket" detector. C = "Inner" detector, gd. loaded scintillator. D = Lucite window. E = Lead.

The blanket detector consists of 1250 liters of liquid scintillator ($CH_{1.8}$). This detector will be viewed through lucite windows by 30, 5" photomultiplier tubes on both the top and the bottom.

The anticoincidence system will consist of 3" of plastic scintillator (PVT)* and will completely surround the 2" of lead shielding.

Reactor associated background measurements were taken at distances ranging from 13 to 50 meters from the center of the reactor. γ-ray energy spectra were measured using a 2" sodium-iodide crystal in a variety of shielding configurations incorporating lead, cadmium, wax, and borated polyethylene. At the further positions there was no measurable reactor associated background. Taking the closest point, 13 meters, and using the worst case spectra we infer the γ-ray flux above 3 MeV to be less than $27/in^2$-sec-ster; that above 5 MeV less than $12/in^2$-sec-ster.

We find as a result of the above background measurements that using a 50 μsec trigger window an additional 6" thick lead shield outside our anticoincidence is required to reduce the maximum background from accidental coincidences to a reasonable rate (< 100/day). We are presently designing such a lead shield to surround the entire detector system described above.

We expect to detect inverse beta decay events at rates of around 300/day at 15 meters, 100/day at 25 meters and 25/day at 50 meters, for $3.2<E_{e+}<8.2$ MeV with detection efficiency $\simeq$ 50%.

The detector will be installed 40 feet below ground, and the building overhead gives an attenuation factor of about 5 in the charged cosmic ray flux. This shielding along with our lead shields will reduce the cosmic ray background in our detector to a negligible rate.

---

*We are thankful to LASL for the loan of a portion of this scintillator.

A Monte Carlo program will simulate all particle interactions in the detector and enable us to assess detection efficiencies for real events. A series of programs to control the on-line data collection and storage, data retrieval, and automatic system calibration are also being written.

We plan to have the inner and blanket detectors operational in the next few months and to have a fully operational detector in our construction facility at the University of California, Irvine soon thereafter. We will then ship the detector system to the Savannah River Plant and will begin data taking during the summer.

A determination of $\Delta(eV)^2$ is dependent on the background which will be measured. Assuming maximal mixing of two neutrino base states, ($\sin^2 2\theta = 1$) and a background estimate of 200/day with 20% statistics, then at 50 meters the experiment will be sensitive to $\Delta < 0.04\ (eV)^2$. This represents ~ 45 days of data accumulation assuming the reactor is on three times more often than off.

ACKNOWLEDGMENTS

We wish to acknowledge discussions with D. Silverman, A. Soni, and G.J. Stephenson. We are grateful to the Savannah River Plant of the E.I. Dupont de Nemours Company where these measurements were made.

REFERENCES

†Work supported in part by the United States Department of Energy.

††University of South Carolina, Aiken, South Carolina.

†††S.Y. Nakamura, deceased.

1. H. W. Sobel, F. Reines, E. Pasierb, Proceedings of the XXth International Conference on High Energy Physics, Madison, Wisconsin, 6-80 (to be published), UCI-10P19-145.

2. F. Reines, H. W. Sobel, E. Pasierb, Phys. Rev. Lett. 45, 1307 (1980).

3. F. T. Avignone, III, and Z. D. Greenwood, Phys. Rev. C22, 594 (1980); B. R. Davis, P. Vogel, F. M. Mann, and R. E. Schenter, Phys. Rev. C19, 2259 (1979).

4. W. R. Gibbs and G. J. Stephenson, Jr., LA-UR/953, Los Alamos report, submitted to Phys. Rev. D; also see Arnon Dar, Technion-PH-80-40 (1980), and D. Silverman and A. Soni, UCLA-80-TEP/25, October 1980, submitted to Phys. Rev. Lett.

5. A. Soni and D. Silverman (UCLA/UCI), private communication.

6. M. Nakagawa, H. Okonogi, S. Sakata, and A. Toyoda, Prog. Theor. Phys. 30, 727 (1963); B. Pontecorvo, Zh. Eksp. Teor. Fiz. 53, 1717 (1967) [Sov. Phys. JETP 26, 984 (1968)]; V. Gribov and B. Pontecorvo, Phys. Lett. 28B, 493 (1969).

AN EXPERIMENT TO INVESTIGATE $\bar{\nu}_\mu \rightarrow \bar{\nu}_e$ OSCILLATIONS AT LOS ALAMOS MESON PHYSICS FACILITY*

by

H.W. Kruse and J. W. Toevs**
Los Alamos National Laboratory

ABSTRACT

An experiment, being planned at LAMPF, aims to investigate a possible neutrino oscillation channel, $\bar{\nu}_\mu \rightarrow \bar{\nu}_e$. If $\bar{\nu}_\mu$, produced in the LAMPF beam stop, oscillate to $\bar{\nu}_e$, then interactions $\bar{\nu}_e + p \rightarrow e^+ + n$, may be detected.

A large volume liquid scintillator (4470 liter) emplaced at 33 m from the beam stop, detects e^+ and n, after moderation in the hydrogenous liquid and capture in Gd, loaded into the scintillator.

Our anticipated signal rate is currently estimated at 1.67 $(\delta m^2)^2$/day assuming full amplitude oscillation. The corresponding counting rate, assuming all $\bar{\nu}_\mu$ have oscillated to $\bar{\nu}_e$ at the detector is 1.5/day. Cosmic rates are estimated at 0.033/day. Correlated backgrounds from the beam stop are calculated to be small in comparison to cosmic events, except for reactions of ν_e in Pb. These reactions may be reduced with an Fe shield within the detector.

With the above rate, a limit on the sensitivity of our experiment for the value of δm^2 is estimated at 0.12 eV^2 with 70 days of counting.

Detector features, estimated background rates, and sensitivity values are discussed.

---

*Work performed under the auspices of US DOE.

**Visiting scientist from Hope College, Holland, Michigan.

I. INTRODUCTION

The high, current interest in neutrino oscillation experiments is derived from the intense desire to demonstrate a nonzero neutrino mass. Experimental determination of upper limits on the oscillation coefficients provides important tests of unified theories.[1] We are currently fielding an experiment to investigate one possible oscillation mode, $\bar{\nu}_\mu \rightarrow \bar{\nu}_e$ with improved sensitivity over previous results.[2] In the two-state oscillation problem, the probability of a $\bar{\nu}_e$, given a $\bar{\nu}_\mu$ by a weak decay, at a distance X, is

$$P(\bar{\nu}_\mu \rightarrow \bar{\nu}_e) = [a]^2 \sin^2(1.27 \frac{\delta m^2 X}{E_\nu}) \qquad (1)$$

where the neutrino energy, E_ν, is in MeV, X is in meters, and δm^2 is in eV^2. The quantity $\delta m^2 = m_2^2 - m_1^2$, where m_1 and m_2 are the masses of neutrino mass eigenstates in oscillation.

At Los Alamos Meson Physics Facility (LAMPF) $\bar{\nu}_\mu$ are generated from the decay of μ^+ in the beam stop. If these $\bar{\nu}_\mu$ oscillate to $\bar{\nu}_e$, they may be detected in our detector by the inverse β decay reaction,

$$\bar{\nu}_e + p \rightarrow e^+ + n \quad . \qquad (2)$$

For small values of the function argument in Eq. (1), the sensitivity is nearly independent of detector distance; the signal varies inversely with X^2 but the probability in Eq. (1) increases directly as X^2. For our anticipated neutrino energy range of 20 to 53 MeV, the argument is sufficiently small for values of X up to ~ 70 m, provided a null result is obtained with a corresponding upper bound of ~ 0.1 eV^2 for δm^2. Consequently, we have chosen a value for our detector distance of 33 m, primarily influenced by convenience of logistics and adequacy of shielding from the beam stop. If, however, a positive signal is observed at the value of the limit for δm^2 previously determined,[2] 0.9 eV^2, then our signal will be reduced by a factor of 1.2 at 53 MeV and a factor of 3.9 at the threshold of 20 MeV.

In order to compare various proposed experiments, it is useful to compute a sensitivity to δm^2 based on a presumed null result, as will be described. If a positive result should be observed, then a huge incentive will have been generated for relocating the detector at other positions, thereby seeking confirmation of the oscillation phenomenon.

II. DETECTION EFFICIENCY

The detector features and characteristics have been described in detail elsewhere.[3] A central volume (4470 liter) of xylene-based liquid scintillator contains 2.2×10^{29} free proton targets. A bank of 20 cm-dia photomultipliers (EMI D340 B) views the scintillator and converts the positron energy deposition into an electrical signal. The neutron generated in reaction (2) moderates in the scintillator until captured in Gd, which is dissolved in the scintillator. Upon capture, gamma rays are produced with 8 MeV total energy. These two events, occurring within the moderation time of ~ 30 μs, constitute a signature for reaction (2).

Calculated detection efficiencies for various factors have been described[3] for the configuration illustrated in Fig. 1. Currently, these values are estimated as follows: dead time factor, 0.98, assuming 25 μs gate time on the anticoincidence events; positron detection efficiency, 0.77, assuming 20 MeV threshold; neutron capture probability, 0.8, assuming 0.5% Gd loading, and capture within a gate time of 27 μs; neutron capture gamma detection efficiency, 0.77, assuming 4 MeV threshold. A total detection efficiency of 0.46 is thus anticipated although actual operating conditions and measured values for efficiencies may alter this value.

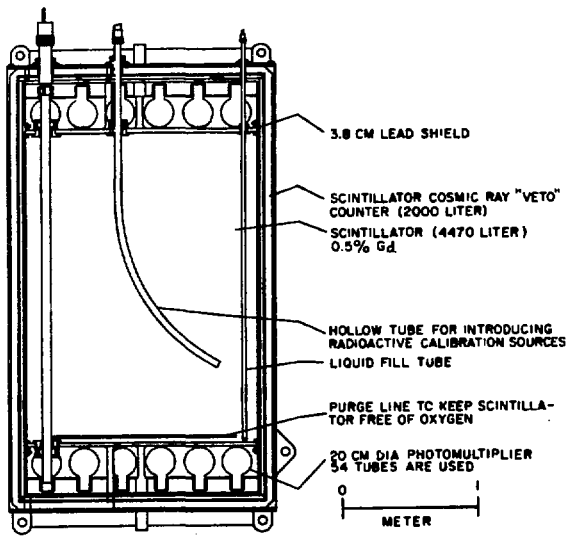

Fig. 1. Neutrino Detector Assembly

III. SIGNAL RATES

We expect 3×10^{7} $\bar{\nu}_{\mu}$ s^{-1} cm^{-2} at 8 m from the beam dump with 750 μa primary proton beam current. At 33 m, we then anticipate 1.8×10^{6} s^{-1} cm^{-2} or 1.5×10^{11} cm^{-2} LA day^{-1} (the LA day is 1/16 of normal day due to LAMPF duty factor).

Our anticipated counting rate, R, is given by

$$R = N_0 \int_0^{52.8} N(E)\,\sigma(E) Np\, V\, P(E)\, F\, dE \qquad (3)$$

$$N_0 = 1.5\times10^{11}\ cm^{-2}\ day^{-1}$$

$$N(E) = 2\,\varepsilon^2(3-2\,\varepsilon)/52.8;\ \varepsilon = E/52.8$$

$$\sigma(E) = (3.465\times10^{-3}\,E_{\bar{\nu}}^{2} + 0.1755\,E_{\bar{\nu}} - 1.870)\times 10^{-41}\ cm^{2}$$

Np is the number of protons/cm^3, 4.9×10^{22} cm^{-3}

V is the detector volume, 4.47×10^{6} cm^{3}

P is from Eq. (1)

F is the detection efficiency, 0.46

E is the neutrino energy in MeV

The resulting value for R is $1.47[a]^2 day^{-1}$ for $P(E) = [a]^2$. Retaining the dependence on energy in P(E), in the integral, the value for R is $1.67\times(\delta m^2)^2[a]^2$ LA day^{-1}.

IV. BACKGROUND ESTIMATES

Cosmic backgrounds may best be determined by actual measurements with our detector in position. At this time we can only estimate various components and attempt to identify those that are important.

A. Accidental Cosmic Coincidence Rate

We have estimated single counting rates anticipated within the energy window of (20-60) MeV for e^+ and (4 to 9) MeV for neutrons. Assuming a 27 μs gate time, the accidental rate is .011 LA day^{-1}.

B. Beam Associated Rates

Concrete and tuff shielding between the beam stop and our detector is about 7 m equivalent Fe. Consequently we estimate negligible accidental coincidence rates from the beam stop.

High-energy neutrons from the beam stop region may give energy deposition from proton recoil and subsequent capture, giving rise to a correlated background. Such events will be discriminated against with PSD (pulse shape discrimination) technique. The resultant rate is expected to be ~ .001/LA day.

Another beam-associated rate results from the interactions[4] $\nu_e + Pb \rightarrow Bi + n + e^-$. This reaction has a negative Q value of 18.5 MeV and therefore a maximum electron energy of 34.5 MeV. We anticipate this rate to be ~ 0.06/LA day for events in the energy range 20-34.5 MeV.

C. Correlated Cosmic Background Rates

There are several possible mechanisms for producing correlated events [those that have a two-pulse signature like the one corresponding to reaction (1)]. We believe there are three areas of major concern.

1. High-energy neutrons give energy from recoil protons and subsequent capture. Attempts to compute such rates are in progress. The sand and Pb above the detector comprise 2.4 m Fe equivalent and rejection of 500/1 by PSD is assumed. If necessary, additional Fe shielding may be installed. A correlated rate of .005/LA day has been estimated.

2. Undetected muons may enter the detector and subsequently decay. Even with charged cosmic rejection of 10^6 supplied by the two veto counters, ~ .02/LA day events may be expected. Only 4% of the decay electrons, however, would appear in the (4-9) MeV window, so our estimated correlated rate is .001 LA day^{-1}.

3. Direct reactions of muons outside the detector give high-energy neutron-gamma pairs that may simulate a neutrino event. We expect that many of these events are associated with other charged reaction products, somewhere in the cascade, which might be detected in our double veto counter. Two layers of Pb (total 7.6 cm) provide additional shielding for these gammas as well as for muon bremsstrahlung. A rate of ~ .015/LA day is estimated but we are uncertain of this value.

The total estimated background may be tabulated as follows:

	Counts/LA Day
Accidental cosmic coincidence	.011
Beam-associated accidental coincidence	.000
Beam-associated coincidence	.001
Cosmic neutron	.005
Undetected cosmic muon	.001
Muons outside detector	.015
Total	.033/LA Day

V. SENSITIVITY TO NEUTRINO OSCILLATION

The signal is 1.67 $(\delta m^2)^2$ $[a]^2$ LA day^{-1}. For full amplitude oscillation with δm^2 = 0.1 eV^2, the counting rate is .0167 LA day^{-1}.

In the absence of a net positive signal, a limit results due to the background uncertainty, $\sqrt{BD}$, during the beam-on time, where B is the background rate, .033/LA day, and D is the number of days counting. A limit of 0.1 eV^2 may then be set in D days if

$$\sqrt{.033\ D} = .0167\ D$$

$$D = 118 \text{ days} .$$

This limit is based on the estimates referred to and is qualified by our ability to achieve 10^6 charged cosmic rejection efficiency, pulse shape discrimination rejection efficiency of 500, and cosmic correlated background rates as low as estimated.

We also have ignored the effect of ν_e reactions in Pb, believing that these can be effectively reduced with an Fe shield located inside the detector, between the scintillator and Pb shield. In the absence of such a shield, the sensitivity would be based upon signals occurring above the 34.5 MeV maximum e^- energy from these reactions. This eliminates about 15 percent of the signal events; the time required to achieve a given sensitivity is increased ~ 15 percent.

In the absence of the Fe shield, the estimated counting time to achieve a limit on δm^2 of 0.1 eV^2, thus becomes 136 days. The corresponding time to achieve a sensitivity limit of 0.12 eV^2 is 70 days.

Observation of reaction (4) events occur at a rate several times the estimated background, in the e^- energy range of 20 to 34.5 MeV. Such a recognizable signal may be quite welcome if reaction (2) is not observed.

ACKNOWLEDGEMENTS

We are grateful for discussions regarding cosmic background rates with H.H. Chen, T.J. Bowles, and R.L. Burman.

REFERENCES

1. H. Georgi and D. Nanopoulos, Nuclear Physics Bulletin 155, 52 (1979).
   T. Goldman, Los Alamos Science, to be published (1981).
   S.M. Bilenky and B. Pontecorvo, Physics Reports (Section C of Physics Letters) 41, No. 4 (1978) 225-261.

2. S.E. Willis, V.W. Hughes, P. Nemethy, R.L. Burman, D.R.F. Cochran, J.S. Frank, R.P. Redwine, J. Duelos, H. Kaspar, C.K. Hargrove, and U. Moser, Phy. Rev. Lett. 44, 522 (1980).
   P. Nemethy, et. al, submitted to Phys. Rev. D.

3. H.W. Kruse, R. Loncoski, and J.M. Mack, "Antineutrino Detector for $\bar{\nu}$ Oscillation Studies at Fission Weapon Tests and at LAMPF," submitted to 1980 Nuclear Science Symposium, IEEE.

4. J.W. Toevs and H.W. Kruse, this conference.

Competition from the ν_e $^{208}Pb \rightarrow {}^{208}Bi\ e^-$ Reaction in a Search for $\bar{\nu}_\mu \rightarrow \bar{\nu}_e$ Oscillation*

by

J.W. Toevs** and H.W. Kruse
Los Alamos National Laboratory

ABSTRACT

Inverse beta-decay reactions produced by electron neutrinos may compete with muon neutrino reactions in experiments utilizing the neutrino flux from a beam stop. The cross section and angular distribution for one such reaction, ν_e $^{208}Pb \rightarrow {}^{208}Bi\ e^-$, have been calculated, using the results of an investigation of $^{208}Pb\ (p,n)\ ^{208}Bi$ at low momentum transfer. The implications of this reaction on an experiment to study neutrino oscillation are discussed.

I. INTRODUCTION

Inverse beta-decay reactions may be induced by electron neutrinos on various materials in a detector. As ν_e are produced along with $\bar{\nu}_\mu$ from μ^+ decay in a beam stop, these reactions, of the form $\nu_e\ X \rightarrow e^-\ Y$, can compete with the reaction $\bar{\nu}_e\ p \rightarrow e^+\ n$. The latter reaction is being used in a search for the oscillation $\bar{\nu}_\mu \rightarrow \bar{\nu}_e$ in an experiment in preparation at LAMPF.[1] Background reactions in which Y is left sufficiently excited to decay by neutron emission are especially important to this experiment because the positron and neutron from $\bar{\nu}_e\ p \rightarrow e^+\ n$ are detected in delayed

---

*Work performed under the auspices of US DOE.

**Visiting scientist from Hope College, Holland, Michigan.

coincidence to discriminate against cosmic-ray events. This experiment involves an 11-ton cylindrical lead shield inside the cosmic-ray veto counters, so the reactions $\nu_e\ ^{206,207,208}Pb \rightarrow e^-\ ^{206,207,208}Bi$ are of particular interest.

To estimate the rate from such reactions, one must have values for the Fermi and Gamov-Teller matrix elements for the reactions in question. Published ft values from normal beta decay are inadequate because they include only F and GT strength from low-lying nuclear levels, often seriously underestimating the strength available from other nuclear states accessible at the neutrino energies involved--up to 53 MeV. Useful matrix elements for inverse beta decay can be extracted from (p,n) reaction cross sections at 0 degrees, as pointed out by Goodman, et al.[2] This is possible because, like beta decay, the (p,n) reaction at small forward angles is a charge exhange reaction involving low momentum transfer.

The Gamov-Teller matrix element for a nucleus may be estimated by counting the unpaired neutrons. For ^{208}Pb, $|GT|^2 = 3(N-Z) = 142$. The cross section for $^{208}Pb\ (p,n)\ ^{208}Bi$ has been measured by Horen, Goodman, and coworkers,[3] who found that about 1/2 of the estimated Gamov-Teller strength is contained in or near a single strong resonance at 15.6 MeV above the ground state in ^{208}Bi, well above the 7.1 MeV neutron separation energy for this nucleus. Furthermore, the entire Fermi strength, estimated as $|F|^2 = (N-Z)$, is thought to be contained in the isobaric analog state at 15.1 MeV in ^{208}Bi.

II. ESTIMATE OF CROSS SECTION

With values for the matrix elements in hand, the cross section for $\nu_e\ ^{208}Pb \rightarrow e^-\ ^{208}Bi$ can be calculated, using the known ν_e spectrum from μ^+ decay at rest, and including the effects of kinematics and weak magnetism. O'Connell[4] has obtained the following cross section for $\nu_e\ n \rightarrow e^-\ p$:

$$\frac{d\sigma_{\nu n}}{d\Omega_e} = \frac{G^2\ kE}{4\pi^2}\left\{2\left(1-\frac{\omega^2}{q^2}\right)\cos^2\frac{\theta}{2} + 4\left[F_A^2+\left(\frac{q\mu_\nu}{2M_p}\right)^2\right]\left(\frac{1}{2}+\frac{1}{2}\sin^2\frac{\theta}{2}\right) - 8\,F_A\left(\frac{q\mu_\nu}{2M_p}\right)\sin\frac{\theta}{2}\right\} \qquad (1)$$

where $G = 10^{-5}/M_p^2$, $F_A = -1.24$

M_p = proton mass

$\vec{k}$ = electron momentum

E = electron energy

$\vec{q} = \vec{\nu} - \vec{k}$, the momentum transfer

$\vec{\nu}$ = neutrino momentum

$\omega = \nu - E$, the energy transfer

$\cos\theta = \vec{k} \cdot \vec{\nu}$

$\hbar = c = 1$

and $\mu_\nu = \mu_p - \mu_n = 4.71$, the nuclear vector magnetic moment.

The Q value for $\nu_e\ ^{208}Pb \rightarrow e^-\ ^{208}Bi$ is -2.9 MeV, giving $\omega = 18.5$ MeV for production of ^{208}Bi in the 15.6 MeV Gamov-Teller state, and $\omega = 18$ MeV for production in the isobaric analog state. The value 18.5 was used for this estimate. The results of Horen, et al. were interpreted to mean that all 44 unpaired neutrons participate in Fermi transitions for this reaction, and one half of the unpaired neutrons participate in Gamov-Teller transitions. Therefore, the cross section for $\nu_e\ ^{208}Pb \rightarrow e^-\ ^{208}Bi$ was estimated by multiplying the F_A^2 and F_A terms in Eq. (1) by 1/2, evaluating $d\sigma/d\Omega$, and multiplying the result by 44. The angular distribution appears in Fig. 1. This was integrated over solid angle to obtain the cross section as a function of energy. The term containing weak magnetism and kinematic effects was linear with energy to within 1% to $E_\nu = 53$ MeV. The cross section may therefore be expressed as

$$\sigma(E_\nu) = 7.4 \times 10^{-43} (E_\nu - 18.5)^2 (2.20 + 0.041\ E_\nu)\ \text{cm}^2/\text{MeV}$$

for E_ν above the 18.5 MeV threshold.

The energy spectrum for electron neutrinos from stopped μ^+ decay is given by

$$\frac{dN}{dE_\nu} = \frac{12E_\nu^2(E_\nu - 53)}{(53)^4}$$

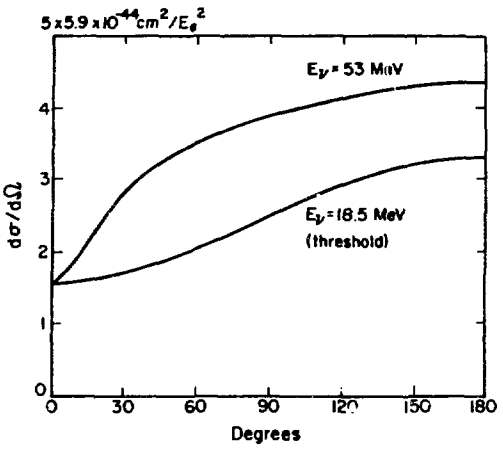

Fig. 1. Electron angular distribution at threshold and at the maximum neutrino energy.

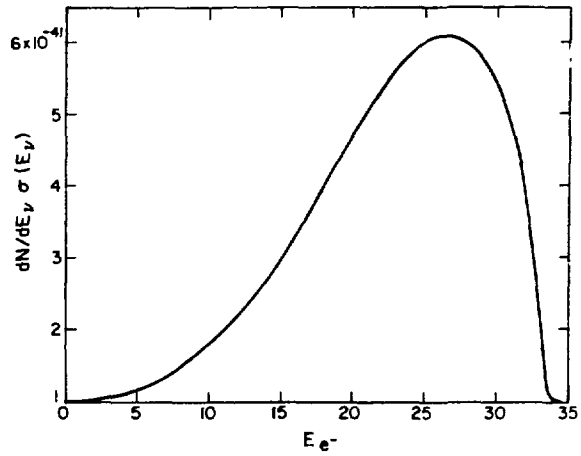

Fig. 2. Product of the ν_e energy spectrum and the cross section, in terms of the energy of the outgoing electron.

Multiplying this by $\sigma(E_\nu)$ and integrating yields the total cross section for ν_e $^{208}Pb \rightarrow e^-$ ^{208}Bi from stopped muons,

$$\sigma = 8.3 \times 10^{-40} \text{ cm}^2 \quad .$$

This is 57 times the cross section calculated by Donelly[5] for ν_e $^{12}C \rightarrow$ $^{13}Ne^-$, 1.46×10^{-41} cm^2. The electron spectrum is shown in Fig. 2.

III. RATE IN DETECTOR

Although ^{208}Pb comprises only 52% of natural lead, it has been the experience of Goodman and coworkers[6] that in heavy nuclei, the Gamov-Teller strength is always concentrated in a single, large resonance, and that the location of the resonance changes quite slowly with Z and N. Therefore, it was assumed for this calculation that all Pb participated as ^{208}Pb in contributing detected events. In the various bismuth isotopes produced by this reaction, the neutron separation energies are well below the excitation of the strong Gamov-Teller resonance. Neutron emission should therefore strongly dominate the de-excitation of the residual bismuth nuclei.

Thus, this reaction would produce events in the detector with almost the same signature as $\bar{\nu}_e\ p \rightarrow n\ e^+$.

The production rate for the reaction in 11 tons of Pb (3×10^{28} atoms), for a ν_e flux of $1.5 \times 10^{11}/cm^2$ LA day, is 3.7 events/day, where the LA day includes a factor of 16 for the LAMPF duty cycle. This flux assumes 750 μa of primary proton beam. The count rate in the detector will be smaller than the production rate because of several factors. First, since both the neutron and the electron must be counted in the detector, scattering of either or both particles out of the detector reduces the count rate by a factor of 4 (25%). With a 20-MeV threshold on the electron signal, 70% of the electrons will be counted. A Monte Carlo calculation indicates that, due to energy loss in the Pb, only 23% of the primary electrons will deposit greater than 20 MeV in the detector. Finally, the combined detection efficiency for neutrons and electrons is 46%. The product of these factors reduces the count rate to 0.06 counts/day, about 3/2 times our anticipated background rate. However, the maximum electron energy from the reaction is about 35 MeV. Raising the threshold on the signal reaction ($\bar{\nu}_e\ p \rightarrow n\ e^+$) to 35 MeV reduces the signal rate by only 15%, so the ν_e Pb reaction should not seriously hamper the measurement of $\bar{\nu}_e$.

On the other hand, the rate of ν_e Pb could be enhanced by adding thin lead sheet to the active volume of the detector. Internal, thin sheets would not be subject to the same factors of 25% and 23% from geometry and loss of e^- energy as in the thick cylindrical shell. Thus, $\nu_e\ ^{208}Pb$ could be used at least to monitor neutrino production and possibly to study ν_e disappearance, should the detector be relocated at a different distance from the beam stop.

ACKNOWLEDGEMENTS

The authors wish to express their appreciation to G.J. Stephenson and T.J. Goldman for helpful discussion of theoretical aspects of this problem, to C.A. Goulding for providing the ^{208}Pb (p,n) ^{208}Bi cross section data, and to J.M. Mack for performing the Monte Carlo calculation.

REFERENCES

1. H.W. Kruse and J.W. Toevs, "An Experiment to Investigate $\bar{\nu}_\mu \rightarrow \bar{\nu}_e$ Oscillations at LAMPF," this conference.

2. C.D. Goodman, Workshop on Nuclear Structure, LASL report LA-8303-C, pages 176-188.
C.D. Goodman, et al., Phys. Rev. Lett. 44 (1980) 1755.

3. D.J. Horen, C.D. Goodman, et al., ISU Cyclotron Report, 1980, pages 44-46.

4. J.S. O'Connell, LASL report LA-5175-MS.

5. T.W. Donnelly, Phys. Lett. 43B (1973) 93.

6. C.D. Goodman, private communication.

Nuclear and Particle
Physics Meeting,
Los Alamos, New Mexico
January, 1981

Phenomenological Analysis of Reactor Data for Neutrino Oscillations* +—

by

D. Silverman

Department of Physics

University of California, Irvine, CA 92717

and

A. Soni

Department of Physics

University of California, Los Angeles, CA 90024

ABSTRACT. Reactor data from experiments performed at different distances is analyzed. We find that no distance independent reactor $\bar{\nu}_e$ spectrum, irrespective of its shape, can account for all the data with a CL $\gtrsim$ .0028. Oscillation with 3(2)ν's yield fits to all the 4 experiments with CL $\simeq$ .06 (.03) and to the two high statistics experiments with CL $\gtrsim$ .31 (.18)

---

*This work is supported in part by the National Science Foundation under Grants Nos. PHY 78-21502 and PHY 79-10262

+—Presented by A. Soni

In this talk I will present a phenomenological analysis[1,2] of data from reactor experiments performed at different distances. The work was done in collaboration with Dennis Silverman from University of California, Irvine.

An ideal experiment to search for $\bar{\nu}_e$ oscillations of $\delta m^2 \sim lev^2$ consists of measurements of the positron energy spectrum via the inverse beta (IB) reaction

$$\bar{\nu}_e + p \rightarrow n + e^+ \tag{1}$$

as a function of distance from a reactor source. Such measurements can be used to deduce the $\bar{\nu}_e$ spectrum monitored as a function of distance. The $\bar{\nu}_e$ spectrum at a distance ℓ from a reactor source is given by

$$n_\ell(E_\nu) = n_o(E_\nu) \times p(E_\nu, \ell) \tag{2}$$

where $n_o(E_\nu)$ is the reactor $\bar{\nu}_e$ spectrum and $p(E_\nu, \ell)$ is the survival probability of neutrino of energy E_ν at distance ℓ. Thus from measured spectra at two different distances one has

$$\frac{n_{\ell 1}(E_\nu)}{n_{\ell 2}(E_\nu)} = \frac{p(E_\nu, \ell 1)\, \cancel{n_o(E_\nu)}}{p(E_\nu, \ell 2)\, \cancel{n_o(E_\nu)}} \tag{3}$$

Departure of the ratio $n_{\ell 1}/n_{\ell 2}$ from unity would signal neutrino oscillation and substitution of the theoretical expressions for the survival probability on the right and the measured data on the left can lead to a solution for the oscillation parameters without any knowledge of the reactor $\bar{\nu}_e$ spectrum.[3]

No such oscillation experiment is currently available.[4] We will therefore try to learn what we can about $\bar{\nu}_e$ oscillations from reactor experiments performed at different distances, data from which has recently become available. Our main motivations are:

(1) to introduce a framework for analysis of reactor experiments with no theoretically calculated reactor $\bar{\nu}_e$ spectra.

(2) to find sensitive test(s) for searching for oscillations in such experiments.

(3) to solve for the most favorable oscillation parameters.

(4) to suggest most favorable distances for detecting $\bar{\nu}_e$ oscillations in such experiments.

So far as the overall conclusions reached about existence or non existence of $\bar{\nu}_e$ oscillations are concerned they will necessarily be limited by the accuracy of the input experimental data.

There are four experiments initiated by reactor $\bar{\nu}_e$ that are being used in our analysis. Three of these are IB experiments performed at 6.5m[5], 8.7m[6] and 11.2m[7] from reactor sources. The 6.5m experiment was the first experiment of its kind and had only 500 events whereas the 8.7m and the 11.2m experiments, data from which became available only in the past 6 months, had each about 4000 and 7000 events. The positron energy spectrum measured in the three experiments is recorded in the form of a histogram with 16, 24 and 9 data points respectively. In addition to these 49 data points the systematic efficiency of each experiment (10%, 8%, and 13.8% respectively) are used as additional data points in our analysis.

Besides these three IB experiments we also include the deuteron experiment[8] of Reines, Sobel and Pasierb in our analysis. However this experiment measures only the total rates for 1 neutron and 2 neutron events via:

$$\bar{\nu}_e + d \rightarrow n + p + \nu \qquad (4)$$

$$\bar{\nu}_e + d \rightarrow n + n + e^+ \qquad (5)$$

The measured rates (165 ± 25)/day for neutral current and (28 ± 12)/day for change current reaction on deuteron are being used as two data points in our work.

Framework for Analysis Without Using Theoretically Calculated Reactor $\bar{\nu}_e$ Spectra.

In our analysis instead of using any one of the theoretically calculated spectra,[9] which are different by as much as 25% to 50% and therefore cannot be reliably used for ruling in favor of or against oscillations, we shall solve for the spectra that are compatible with the data separately under the oscillation and the no oscillation hypothesis. To that end we assume that the reactor $\bar{\nu}_e$ spectrum, $n_o(E_\nu)$, can be parameterized in the general form:

$$\ell n n_o(E_\nu) = \sum_{j=0}^{N} A_j (E_j/\text{MeV})^j \qquad (6)$$

Chi-squared minimization is then used to extract A_j and N from the data sets.[10] If $\bar{\nu}_e$'s did not oscillate then the data taken at different distances should be accountable by using a no oscillating spectrum of the general form given in (6). On the other hand, if $\bar{\nu}_e$'s do oscillate then the $\bar{\nu}_e$ spectrum at a dist ℓ can be obtained by using (6) in (2).

Main Results of the Analysis

Table I presents a summary of such a general analysis of data taken at different distances. The no oscillation hypothesis is not supported with or without the 6.5m experiment. The maximum attainable confidence level (CL) for the no oscillation solution to all the 4 experiments is $\simeq$ .003. Taking only the 8.7m and the 11.2m IB experiments[11] the maximum CL for the no oscillation solution is found to be $\simeq$ .03. In comparison the 3(2)ν oscillation fits to all the 4 experiments have CL .06 (.03) and we find that these joint oscillation fits are in very good agreement with the two high statistics (8.7m and 11.2m) experiments i.e., most of the chi-squared in those fits originates from the 6.5m experiment

To understand better why the no oscillation hypothesis is being excluded and the oscillation hypothesis is being favored we proceed as follows. Using the

parameteriz. ion (6) we solve the $\bar{\nu}_e$ spectrum $n(E_\nu, L)$ "seen" at the distance of each IB experiment. The solutions for $A_0, A_1 \ldots A_5$ are :

$$6.5m \Rightarrow 2.18,\ -.951,\ .0061,\ 0,\ 0,\ 0; \qquad \chi^2/d_f = 14.3/13$$

$$8.7m \Rightarrow 1.57,\ -.506,\ -.0583,\ 0,\ 0,\ 0; \qquad \chi^2/d_f = 16.5/21$$

$$11.2m \quad 0,\ -.846,\ -.5322,\ .08208,\ -.005517,\ 0, \qquad \chi^2/d_f = 6.2/5$$

The resulting spectra shown in Fig.1 exhibit an interesting trend. For $E_\nu \gtrsim 6$ MeV the 6.5m spectrum is the highest and the 11.2m one is the lowest with the 8.7m lying between those two. For $E_\nu \lesssim 6$ MeV that ordering is reversed. To analyze this trend we divide the overlapping energy range of the three experiments into two halves and integrate each of these spectra for the intervals $4.0 < E_\nu < 8.5$ MeV and $6.2 < E_\nu < 8.5$ MeV. To remove the normalization uncertainties we take the ratio R_ν (expt) of those two integrals for each experiment. We find (see Fig. 2) that R_ν (expt) = $7.9 \pm .9$, 14.3 ± 1.2 and 21.7 ± 1.0 respectively for the 6.5m, 8.7m and the 11.2m experiments. These numbers, taken in pairs, differ from each other by about 4 to 9 standard deviations.

Finally, from the e^+ histograms measured in the three IB experiments we extract the numbers N_{e1} and N_{e2} of e^+ observed in the intervals $(2.2 \lesssim E_e \lesssim 6.7)$ MeV and $(4.4 \lesssim E_e \lesssim 6.7)$ MeV. We find, once again, that the ratio R_e (expt) of those two numbers (see Fig. 3) equals $\sim 2.7 \pm .5$, $5.6 \pm .6$, and $8.20 \pm .35$ respectively for the IB experiments performed at 6.5m, 8.7m and 11.2m. Again, these numbers differ by ~3 to ~8 standard deviations.

Oscillation Solutions to Reactor Data

Table I which presents a summary of our "multibin analysis" and Fig. 2, and Fig. 3 which show the observed distance dependence from the reactor experiments via our "two bin" analysis lead us to the same conclusion: that either some of the experiments being used as input are incorrect or neutrinos oscillate.

Fig. 4 shows our "effective' 2 ν solutions, altogether three of them, to data from all the reactor experiments. The range of δm^2, $\sin^2 2\theta$ shown correspond to 90% CL obtained by disregarding the 6.5m experiment. The central values of these fits have CL from 0.2 to 0.5 for all the data from the remaining 3 experiments and correspond to the best fits including the 6.5m experiment as well.

Fig. 5 compares our joint solutions to the reactor data with the allowed regions of the ILL group of Boehm et.al and UCI group of Reines, Sobel and Pasierb. The ILL group's allowed region (to the left of their contours) is obtained by using only their own data namely their IB experiment[6] at 8.7m and using DVMS[9] theoretically calculated spectrum. The UCI allowed region (to the right of their contours) reported by RSP is based on analysis of the ratio (ccd/ncd) from their deuteron experiment[8] using the DVMS theoretically calculated spectrum.[9] Our solutions are to all the reactor data and uses no theoretically calculated spectrum.

Consistency Check

As a consistency check we compare in Fig 6 our reactor $\bar{\nu}_e$ spectrum deduced in conjunction with the oscillation hypothesis with that of DVMS allowed band. The reader should note that the reactor $\bar{\nu}_e$ spectrum and the oscillation parameters solved for are coupled to some extent, thus, a change in the latter modifies the former even though the input data set is the same.[12] This can be seen by a comparison of Fig 6 & Fig 7.

Summary

A phenomenological analysis of data from the existing reactor experiments is presented without the use of any theoretically calculated spectra. Our multibin analysis shows that data from all the 4 reactor experiments or for that matter

even the data from the two high statistics (IB) experiments performed at 8.7 and 11.2m do not support the no oscillation hypothesis. Through our two bin analysis we exhibit the essential source of the distance dependence in the three inverse beta experiments. The ratio

$$R_\nu = \frac{\#\text{ of } \bar{\nu}_e \text{ "seen" with } (4.0 < E_\nu < 8.5) \text{ MeV}}{\#\text{ of } \bar{\nu}_e \text{ "seen" with } (6.2 < E_\nu < 8.5) \text{ MeV}}$$

is different between pairs of experiments by $\gtrsim$ 3 standard deviations. We are therefore led to the conclusion that either some of the experiments are incorrect or neutrinos oscillate.

Assuming neutrino oscillations we find three "effective" 2 ν species joint solutions to the reactor experiments. These have the values $\delta m^2 \sim 0.85$, ~ 2.2, ~ 3.7 eV^2 and $\sin^2 2\theta \sim .2$ to 1 for each.

We thank Terry Goldman and Peter Rosen for discussions. We are extremely grateful to Fred Reines, Hank Sobel and Elaine Pasierb for numerous helpful conversations and for their continued interest and encouragement.

References and Footnotes

1. D. Silverman and A. Soni, Phys. Rev. Lett. 46, 467(1981)
2. A detailed article is currently in preparation and will be submitted for publication.
3. Independently emphasised by P. Rosen (private communication).
4. Oscillation experiments to measure reaction 1 as a function of distance are underway by Reines et al and by Boehm et al. A Georgia Tech ($\bar{\nu}_e + p \rightarrow n + e^+$) experiment of Lang et al., was recently installed at the Savannah River Plant.
5. F. Nezrick and F. Reines, Phys. Rev. 142, 852 (1966).
6. F. Boehm et al., CALT-63-350 (1980).
7. F. Reines, H S. Gurr, and H. W. Sobel. See H. Sobel, Neutrino'80, Erice (80).
8. F. Reines, H. W. Sobel and E. Pasierb, Phys. Rev. Lett. 45, 1307 (80).
9. F. T. Avignone and Z. D. Greenwood, Phys. Rev. C22, 594 (1980); B. R. Davis et al., Phys. Rev. C19, 2259 (1979); S. A. Fayans et al., J. Phys. G: Nucl. Phys. 5, 209 (1979)
10. This method was independently thought of by W. Gibbs, T. Goldman and G. Stephenson (private communication).
11. The reactor $\bar{\nu}_e$ spectra at the Savannah River Plant (Ref.7 and 8) ($.88U^{235}$, $.04U^{238}$, $.08Pu^{239}$ fissions) are estimated to differ from those at the reactor used in Ref.5 (only U^{235} fissions) by no more than 2.4% for 1MeV < E_ν < 7MeV using the calculations of Ref.8.
12. The reactor $\bar{\nu}_e$ spectra deduced under the oscillation hypothesis in conjunction with the other (δm^2, $\sin^2 2\theta$) solutions are found to be in good agreement with the DVMS band. See Ref.2 for details.

Table: Comparison of Confidence Levels for Hypotheses

No.	Input Data	Hypothesis	$\chi^2_{(CL)}/d_f$
1.	8.7m + 11.2m (only overlapping data points)	No oscillations	31.5/18 (.025)
2.	Data from all 4 Reactor Experiments, i.e. 6.5m, 8.7m, 11.2m + ncd + ccd	No oscillations	76.8/46 (.0028)
3.	Same as #2	Oscillations	57/42 (.061)
4.	8.7m + 11.2m + ncd + ccd i.e. disregard 6.5m experiment	Oscillations (same solution as for #3)	<28/25 (>.31)
5.	Same as #1	Oscillations (same solution as for #3)	<18.5/14 (>.18)

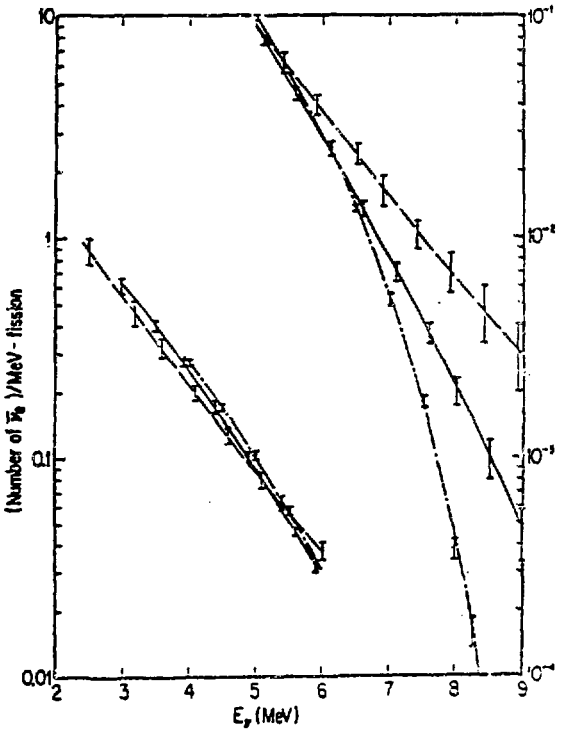

Fig. 1. The $\bar{\nu}_e$ spectra fitted to produce the e^+ spectra observed at 6.5m (dash), 8.7m (solid), and 11.2m (dash-dot). The vertical scale on the left is for E_ν < 6 MeV, and the one on the right is for E_ν > 5 MeV.

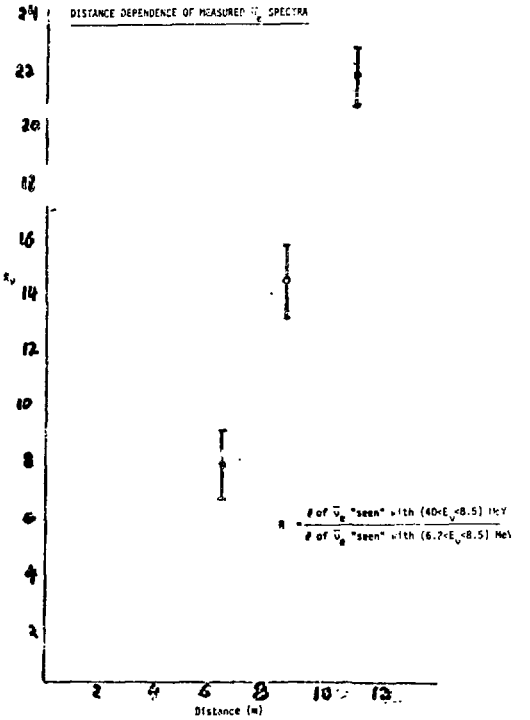

Fig. 2. Shown as a function of distance are the values of R_ν deduced from individual fits given in Fig. 1.

Fig. 3. Shown as a function of distance are the measured values of R_e deduced directly from the observed e^+ histograms.

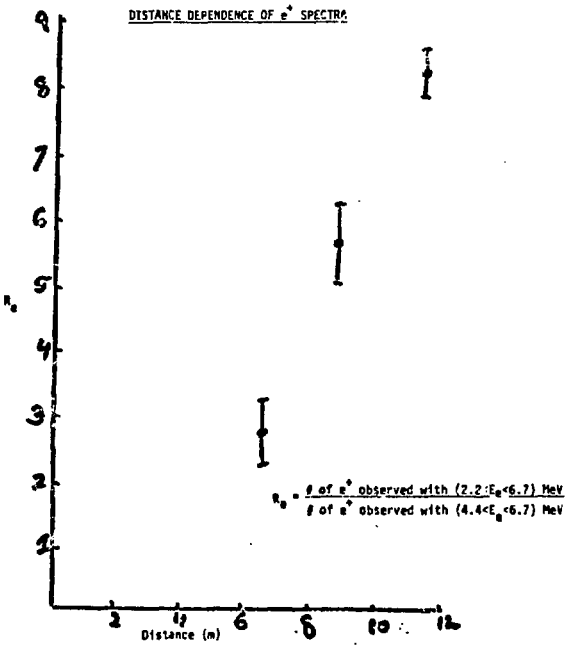

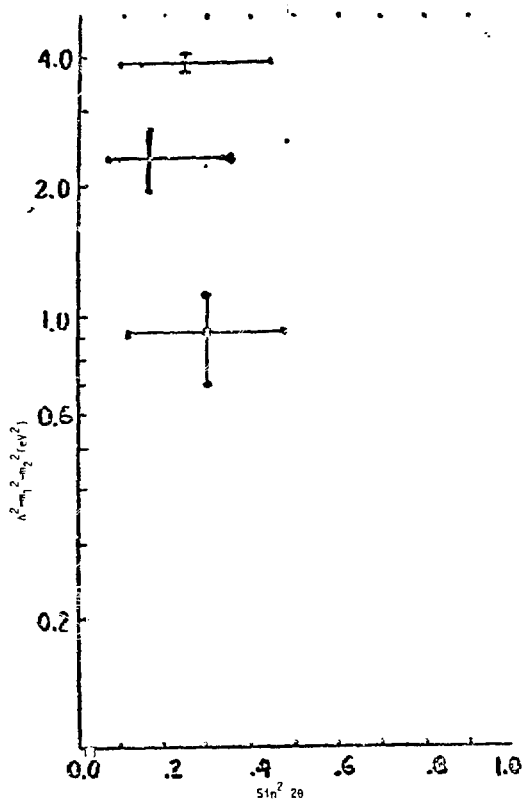

Fig. 4. The values of the oscillation parameters for the "effective" 2ν solutions to the reactor data resulting from our analysis. The range of δm^2, $\sin^2 2\theta$ indicated corresponds to 90% CL obtained by disregarding the 6.5m experiment.

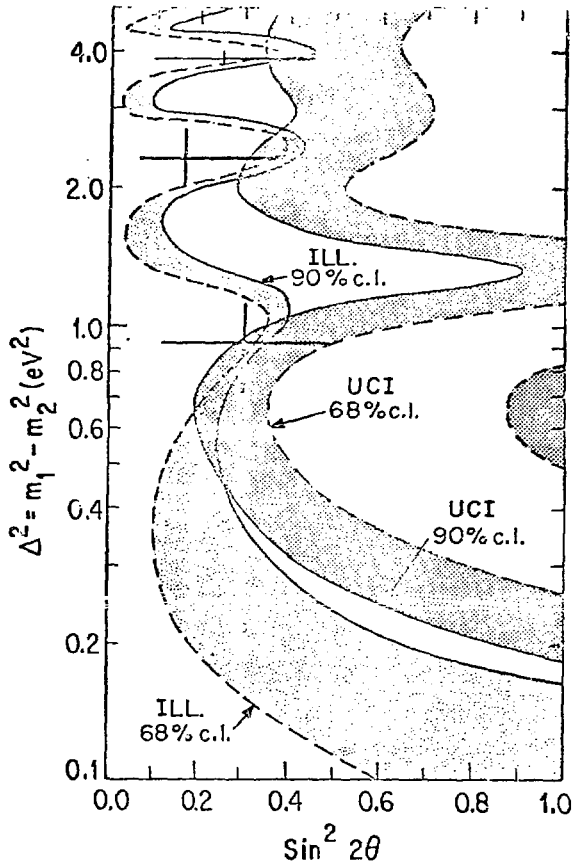

Fig. 5. Our oscillation solutions are compared with the allowed regions of Boehm et al. (to the left of contours on the left) and by Reines et al. (to the right of the contours on the right.

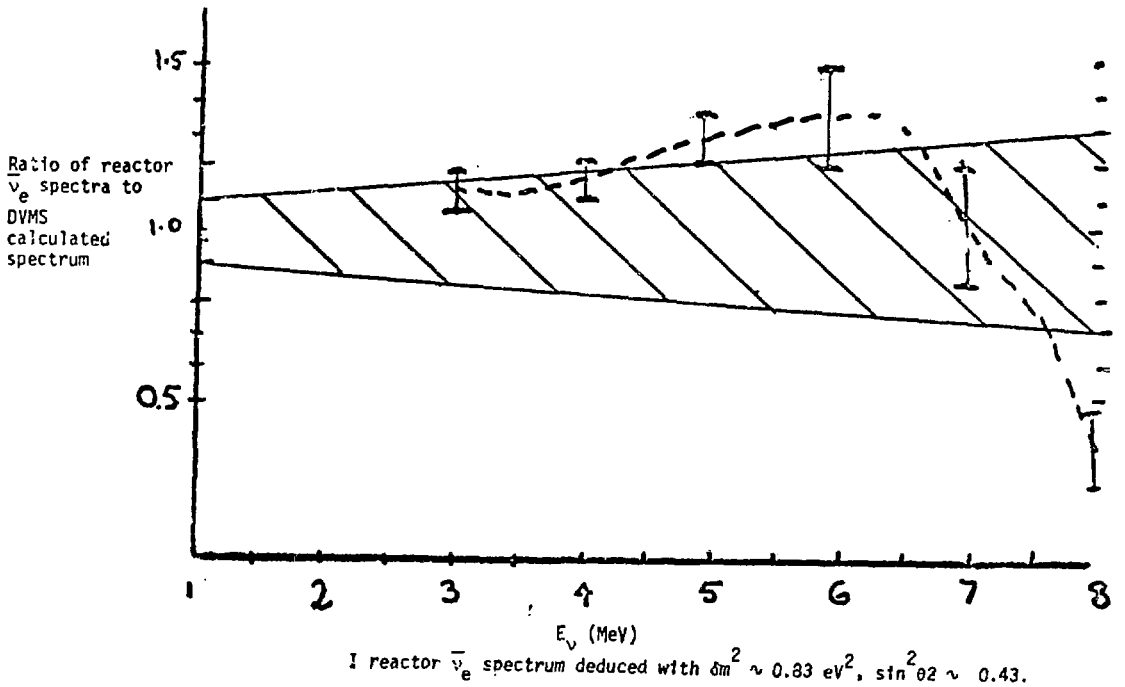

Fig. 6. The reactor $\bar{\nu}_e$ spectrum deduced in conjunction with the oscillation hypothesis. Shown is the ratio of the spectrum obtained with one of our oscillation solution (having $\delta m^2 = 0.83\ eV^2$, $\sin^2 2\theta = 0.43$) to all reactor data divided by the DVMS spectrum (Ref. 9). The DVMS allowed band for such a ratio is shown.

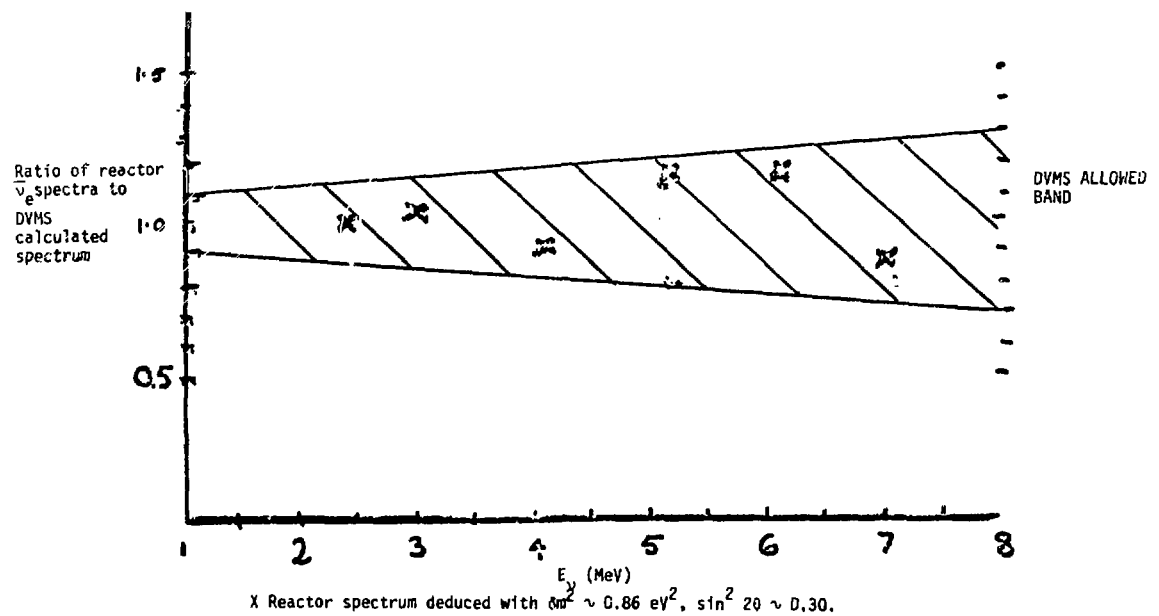

Fig. 7. Illustrates the coupling between the parameters of the reactor $\bar{\nu}_e$ spectrum with the oscillation parameters. The spectrum and the oscillation parameters of Fig. 6 change to the one in Fig. 7.

πN, $\bar{K}N$, and KN Phenomenology

by

R.L. Kelly
Lawrence Berkeley Laboratory
University of California
Berkeley, CA 94720

ABSTRACT

The current status of experimental and phenomenological knowledge of the spectrum of N, Δ, Y^*, and possible Z^* resonances is reviewed. The review concentrates on formation experiments, partial wave analyses, and quark models of baryon resonances. Particular emphasis is given to areas in which there are promising opportunities for future research.

Knowledge of baryon resonances has increased significantly in recent years. For the N, Δ, Λ, and Σ resonances most of this progress has been achieved through large formation experiments, with both hydrogen and polarized targets, and through partial wave analysis. Recent results have consisted primarily of determinations of new and more accurate parameters for known resonances. There have also been a number of weak resonance candidates which have been confirmed (and many that have not!), and a few serious new resonance candidates have been discovered. Concurrently, quark models of increasing sophistication have been formulated and compared with the resonance spectrum and properties. We can look forward to increasing refinement of these models as they are subjected to further experimental constraints.

The well established baryon resonances are summarized in Table I. I will give a general review of the S=0 and S=-1 sectors, as well as possible S=+1 Z^*'s, as observed in πN, $\bar{K}N$, and KN formation experiments. I will emphasize those areas in which there appear to be promising avenues for future research.

This is a very broad area of phenomenology and I will only be able to give a comprehensible overall picture at the expense of omitting many interesting details.

πN scattering experiments in the last decade, particularly at Rutherford Laboratory, have amassed a tremendous amount of precise data on cross sections and polarizations. The elastic processes are now quite well known up to 2.0 - 2.5 GeV/c with the exception of spin-rotation parameters (for which there exist no data) and $\pi^- p$ elastic polarization. This is illustrated in Fig. 1 which shows "amalgamated" data[1] at 1437 MeV/c. The comparative lack of precision in $\pi^- p$ elastic polarization is typical of the situation in the entire resonance region. This is the main reason why the I=3/2 Δ resonances are generally better determined that the I=1/2 N^* resonances in partial wave analyses. Measurements of $\pi^- p \to \pi^o n$ charge exchange data are also shown in Fig. 1. These come primarily from the experiment of Brown et al.[2] which dominates all previous charge exchange measurements. Two-body inelastic scattering has been measured in the ηn, $K\Lambda$, and $K\Sigma$ channels. The $\pi^- p \to K^o \Lambda$ polarization data of Saxon et al.[3] are shown in Fig. 2. The $\pi\pi N$ final state has been observed in a series of large bubble chamber exposures. The latest extensive results are on $\pi^+ p \to \pi^+ \pi^+ n$ by an Imperial College group.[4] The $\pi\pi N$ work has been primarily confined to energies below 1700 MeV.

The two largest πN elastic partial analyses are those of CMU-LBL[1] and Karlsrühe-Helsinki[5] (KH). Both make extensive use of analyticity in parametrizing and fitting resonance region data. The CMU-LBL results are confined to momenta below 2.5 GeV/c, while KH extend their analysis up to 10 GeV/c. In the region above 2 GeV/c Hendry[6] has carried out an analysis specifically aimed at finding the most prominent peripheral high-spin resonances. A number of two-body inelastic partial wave analyses have been done for the channels mentioned above, and isobar model analyses have fit the $\pi N \to \pi\pi N$ data.

Several interesting results have emerged from these analyses in the region of the first excited multiplet of the $SU(6) \otimes O(3)$ quark model, the $[70,1^-]$. Argand plots of the J=1/2 and J=3/2 $\pi N \to \pi N$ partial waves with non-strange resonances in this multiplet are shown in Fig. 4. All elastic analyses are consistent with significant splitting of the D_{33} and S_{31} Δ's in this multiplet as shown in Fig. 3. The Particle Data Group[7] range for the D_{33} mass includes estimates from photoproduction analyses which are probably less accurate.

Generation of this splitting in theoretical models[8] requires novel dynamical features such as three-body spin-orbit forces and/or mixing with higher lying multiplets. Analyses of the ηn, $K\Lambda$, and $K\Sigma$ channels have determined many couplings which provide useful constraints on the SU(6) composition of N and Λ resonances. In the $[70,1^-]$, for example, Saxon et al.[3] have found that of the three N^*'s with masses around 1700 MeV the D_{15} and D_{13} essentially decouple from $K^O\Lambda$, while the S_{11} has a branching ratio of about 8%. Since $K^O\Lambda$ can only couple to quark spin S=1/2 through single quark transitions this confirms the usual mixing scheme in which the D_{15} is pure S=3/2, the D_{13} has only a very small S=1/2 component, and the S_{11} is a mixture with an appreciable amount of S=1/2. Perhaps the most interesting result of the $\pi\pi N$ analyses in this region is the observation of a narrow, positive parity P_{31} state at 1525 MeV which, if it survives, will be very hard to accomodate in SU(6)$\otimes$O(3) without assigning it to some sort of multi-quark state. The evidence for this resonance in the Imperial College analysis[4] is shown in Fig. 5; a similar effect was seen in the Saclay isobar analysis,[9] but it has never been observed in a two-body final state.

The 7 predicted N's and Δ's in the $[70,1^-]$ are by now all observed, well-established resonances. As one moves into the higher multiplets this happy situation quickly changes. At the next level of the harmonic oscillator spectrum there are 5 SU(6)$\otimes$O(3) multiplets, the $[56,0^+]^*$, $[56,2^+]$, $[70,0^+]$, $[70,2^+]$, and $[20,1^+]$. The $[20,1^+]$ has an antisymmetric flavor-spin wave function, and its non-strange members cannot decay to πN via single quark transitions. There is no obvious reason, however, why the 19 non-strange members of the remaining multiplets should not be observed. The CMU-LBL and KH analyses confirm the results of previous analyses that in fact only about half of these states couple to πN. No more than 10 states can be assigned to the 19 available slots. Nine of these are included in Table I; the tenth is a possible third P_{33} resonance at $\sim$1900 MeV. The missing states could all be assigned to the $[70,0^+]$ and $[70,2^+]$, and this has contributed to the notion that even 70's and odd 56's are absent from the physical spectrum. (Or nearly absent; there is at least one positive-parity N^*, the $F_{17}(1990)$, that can be rather unambiguously assigned to the $[70,2^+]$.) Recent work of Isgur and Karl[10] and Koniuk and Isgur[11] indicates a solution to this problem. Isgur and Karl calculate baryon wave functions and masses in a specific broken-SU(6) model with spin-spin interactions arising from single gluon exchange. At the N=2 level they find extensive mixing among the

SU(6) multiplets, so much mixing that even qualitative assignments of resonances to a single multiplet are in many cases not possible. Koniuk and Isgur calculate meson and radiative decay amplitudes using the wave functions of Isgur and Karl and using simple vertices for meson and photon emission by quarks. Considering the simplicity of the model, and the small number of adjustable parameters involved, the overall agreement with experiment is reasonably good. In particular, the observed decoupling pattern of the N=2 N's and Δ's is reproduced, as shown in Fig. 6.

The KH and Hendry analyses have found numerous new candidates for high-spin resonances with masses $\gtrsim$2500 MeV. These resonances are important for understanding the behavior of leading Regge trajectories where deviations from the usual linear behavior in M^2 may begin to appear due to centrifugal barrier effects. The agreement between the older KH and Hendry results was not particularly good; in no more than 4 cases could the resonance claims of the two analyses above 2500 MeV reasonably be said to coincide -- $I_{111}(2600)$, $K_{113}(2700)$, $I_{313}(2750)$, and $K_{315}(2950)$. This situation appears to have improved in the more recent results, however the experimental situation is now confused by conflicting results from a Columbia-ANL-Minnesota experiment[12] which finds evidence for high mass narrow resonances above 2 GeV/c and a CERN-College de France-Ecole Polytechnique experiment[13] which finds no evidence for these effects.

For more details on N and Δ resonances see Refs. 14 and 15.

Until recently nearly all knowledge of the Y^* spectrum came from bubble-chamber measurements of the two-body reactions $\bar{K}N \to \bar{K}N$, $\bar{K}N \to \pi\Sigma$, $\bar{K}N \to \pi\Lambda$ and from Y^* production experiments in bubble chambers. With the advent of improved K^- beams more precise counter measurements are now possible; examples of measurements made at BNL are shown in Figs. 7 and 8. $K^-p \to \bar{K}^0n$ angular distributions measured by LBL-Mt. Holyoke[16] are shown in Fig. 7. K^-p elastic polarization data measured by Yale-BNL-Kyoto[17] are shown in Fig. 8. Another important recent development is the measurement and analysis of quasi-2-body final states such as $\omega(780)\Lambda$, $\pi^0\Lambda(1520)$, $\pi\Sigma(1385)$, $\bar{K}^*(890)N$, and $\bar{K}\Delta(1232)$. An extensive study in this area has been carried out by the Rutherford-Imperial College collaboration[18] (RL-IC). Two of the most important areas in which there are still no data at all are $K^-n \to K^-n$ and $K^-p \to \bar{K}^0n$ polarization. As in πN scattering, there are also no measurements of spin rotation parameters in any channel.

The most ambitious analyses of two-body $\bar{K}N$ scattering include data on all three types of final state -- $\bar{K}N$, $\pi\Sigma$, and $\pi\Lambda$ -- and analyse these channels simultaneously over a wide energy range. The only recent analyses of this type are those of UCL[19] and RL-IC.[20,21] The UCL analysis covers the energy range 1540-2020 MeV, and RL-IC covers 1480-2170 MeV. Both analyses impose the consistency constraints required by multi-channel unitarity on their partial wave amplitudes. In the UCL analysis this is done directly using a K-matrix parametrization. In the RL-IC analysis each channel is initially treated separately and the constraints are subsequently imposed on the amplitudes in an iterative manner. There are also many smaller parital wave analyses involving fewer channels and/or narrower energy ranges. The most extensive recent $\bar{K}N \to \bar{K}N$ analysis is that of LBL-Mt. Holyoke-CERN.[22] The D_{15} amplitudes from these analyses are compared in Fig. 9. This wave contains the $\Sigma(1765)$ which is one of the most prominent and unabmiguous Y^* resonances; other waves are not so pretty.

In the Y^*'s we run into missing states already at the $[70,1^-]$ level. $SU(6)\otimes O(3)$ predicts single D_{15} and D_{05} resonances at this level, and 3 resonances in each of the D_{13}, S_{11}, D_{03}, ahd S_{01} partial waves. As seen in Table I a $3/2^-$ Λ, a $3/2^-$ Σ, and two $1/2^-$ Σ's are missing (or are at least not yet convincingly established). The number of missing states increases rapidly with mass; there are only 5 well established Y^*'s at the N=2 level. Koniuk and Isgur claim that their decoupling mechanism can also be used here to explain the apparent absence of many Y^*'s. However, their model neglects spin-orbit coupling and this is a more dubious approximation for the Y^*'s than for the N's and Δ's. The most obvious evidence for spin-orbit forces in the Y^*'s is the 115 MeV splitting between the $1/2^-$ $\Lambda(1405)$ and the $3/2^-$ $\Lambda(1520)$. Within the framework of one-gluon-exchange models there exists a natural mechanism for suppressing simple $\underline{L}\cdot\underline{S}$-type spin-orbit interactions in the non-strange baryons while retaining it in the Y^*'s.[23] The question of 3-body spin-orbit interactions and the S_{31}-D_{33} Δ splitting also remains open. In addition to a better treatment of spin-orbit interactions it will be necessary to confront calculations of quasi-2-body resonance decays with data and probably to allow for more general mixing schemes[8] before one can claim to have a successful phenomenological model of baryons.

See Ref. 21 for a thorough review of the Y^* spectrum.

Turning now to the question of Z^*'s (exotic S=+1 baryon resonances), Table II gives a summary of recent and current KN scattering experiments as of late 1978.[24] I have not updated this table because there has been little change in the last two years. The only new data that have appeared are those of the Queen Mary-Rutherford collaboration[25] (QM-RL). They have measured K^+n elastic and charge exchange polarization at 5 momenta between 851 and 1351 MeV/c. The elastic data are shown in Fig. 10 where they are compared with predictions from the KN partial wave analyses of Martin[26] and solutions A,C, and D of Bologna-Glasgow-Rome-Trieste[27] (BGRT). The new measurements clearly favor Martin's results.

Already in 1978 there was a need for a new combined I=0 and I=1 KN partial wave analysis. The analyses of Martin and BGRT were done before any of the data in Table II became available. A new analysis has now been done by QM-RL[25] including the newer data and they find no evidence for Z^* resonances. The most likely candidates in the past have been the broad inelastic loops observed in the P_{13} and P_{01} waves, but the QM-RL analysis fails to find resonance-type energy dependence in either of these structures. This is in agreement with most previous analyses, but in disagreement with the I=1 analysis of the VPI-Maryland[28] (VM) group. The VM analysis found evidence for a P_{13} Z^* at 1800 MeV. The discrepancy may be connected with the lack of K^+p elastic polarization data below 650 MeV/c. Because of the absence of this constraint any KN analysis has some arbitrariness in the threshold behavior of its I=1 P-waves. Another possible Z^* test could be made by measuring the elastic spin rotation parameters. Fig. 11 compares the predictions of CMU-LBL-ANL[29] (who have a non-resonant solution similar to that of QM-RL) and VM for the Wolfenstein spin rotation angle. There are large differences, particularly in the backward direction.

Although the situation remains somewhat controversial, the current evidence favors the view that Z^*'s do not exist.

REFERENCES

1. R.L. Kelly and R.E. Cutkosky, Phys. Rev. D 20, 2782 (1979).
   R.E. Cutkosky et al., Phys. Rev. D 20, 2804 (1979).
   R.E. Cutkosky et al., Phys. Rev. D 20, 2839 (1979).

2. R.M. Brown et al., Nucl. Phys. B117, 12 (1976).
   R.M. Brown et al., Nucl. Phys. B137, 542 (1978).

3. D.H. Saxon et al., Nucl. Phys. B162, 522 (1980).

4. K.W.J. Barnham et al., Nucl. Phys. B168, 243 (1980).

5. G. Höhler et al., Handbook of Pion-Nucleon Scattering (Fachinformationszentrum Energie, Physik, Mathematik, Karlsruhe, 1979), Physik Daten Vol. 12-1.
R. Koch, TKP 80/12, Karlsruhe, 1980.
R. Koch, Proc. IVth Intl. Conf. on Baryon Resonances (Univ. of Toronto, July 1980), in press.

6. A.W. Hendry, Phys. Rev. Lett. 41, 222 (1978).
A.W. Hendry, Proc. IVth Intl. Conf. on Baryon Resonances (Univ. of Toronto, July 1980), in press.
A.W. Hendry, Indiana University preprint, 1980.

7. Particle Data Group, Rev. Mod. Phys. 52, No. 2, Part II (1980).

8. C.P. Forsyth and R.E. Cutkosky, COO-3066-161, Carnegie-Mellon, 1980.

9. R.S. Longacre and J. Dolbeau, Nucl. Phys. B122, 493 (1977).

10. N. Isgur and G. Karl, Phys. Rev. D 18, 4187 (1978).
N. Isgur and G. Karl, Phys. Rev. D 19, 2653 (1979).
N. Isgur and G. Karl, Phys. Rev. D 20, 1191 (1979).

11. R. Koniuk and N. Isgur, Phys. Rev. D 21, 1868 (1980).
R. Koniuk, Proc. IVth Intl. Conf. on Baryon Resonances (Univ. of Toronto, July 1980), in press.

12. K.A. Jenkins et al., Phys. Rev. D 21, 2445 (1980).

13. P. Baillon et al., Phys. Lett. 94B, 533 (1980).
E. Basselet et al., Phys. Lett. 94B, 541 (1980).

14. R.L. Kelly, Proc. IVth Intl. Conf. on Baryon Resonances (Univ. of Toronto, July 1980), in press.

15. P.J. Litchfield, Proc. IVth Intl. Conf. on Baryon Resonances (Univ. of Toronto, July 1980), in press.

16. M. Alston-Garnjost et al., Phys. Rev. D 17, 2226 (1978).

17. R.D. Ehrlich et al., Phys. Lett. 71B, 455 (1977).

18. W. Cameron et al., Nucl. Phys. B131, 399 (1977).
W. Cameron et al., Nucl. Phys. B132, 189 (1978).
W. Cameron et al., Nucl. Phys. B146, 327 (1978).

19. B.R. Martin et al., Nucl. Phys. B126, 266 (1977).
B.R. Martin et al., Nucl. Phys. B126, 285 (1977).
B.R. Martin et al., Nucl. Phys. B127, 349 (1977).

20. G.P. Gopal et al., Nucl. Phys. B119, 362 (1977).

21. G.P. Gopal, Proc. IVth Intl. Conf. on Baryon Resonances (Univ. of Toronto, July 1980), in press.

22. M. Alston-Garnjost et al., Phys. Rev. D 18, 182 (1978).

23. L.J. Reinders, J. Phys. G 4, 1241 (1978).
L.J. Reinders, Proc. IVth Intl. Conf. on Baryon Resonances (Univ. of Toronto, July 1980), in press.

24. R.L. Kelly, Proc. of the Meeting on Exotic Resonances, Hiroshima, 1978.

25. T.P. Shah, Proc. IVth Intl. Conf. on Baryon Resonances (Univ. of Toronto, July 1980), in press.
D.V. Bugg, priv. comm., 1980.

26. B.R. Martin, Nucl. Phys. B94, 413 (1975).

27. G. Giacomelli et al., Nucl. Phys. B71, 138 (1974).

28. R.A. Arndt et al., Phys. Rev. D 18, 3278 (1978).

29. R.E. Cutkosky et al., Nucl. Phys. B102, 139 (1976).

Table I. Established baryons and baryon resonances. Approximate masses in MeV are followed by J^P where known. Level assignments in the non-relativistic harmonic-oscillator quark model are given in the first column; these are rather unambiguous for N=0 and N=1 (the $[56,0^+]$ and $[70,1^-]$ SU(6) supermultiplets for non-charmed baryons) but may be unreliable for higher N.

Level	N $S=0, I=\frac{1}{2}$	Δ $S=0, I=\frac{3}{2}$	Λ $S=-1, I=0$	Σ $S=-1, I=1$	Ξ $S=-2, I=\frac{1}{2}$	Ω $S=-3, I=0$	Λ_c Charm $S=I=0$
0	939 $\frac{1}{2}^+$	1232 $\frac{3}{2}^+$	1116 $\frac{1}{2}^+$	1193 $\frac{1}{2}^+$ 1385 $\frac{3}{2}^+$	1318 $\frac{1}{2}^+$ 1533 $\frac{3}{2}^+$	1672 $\frac{3}{2}^+$	2273 $\frac{1}{2}^+$
1	1540 $\frac{1}{2}^-$ 1650 $\frac{1}{2}^-$ 1520 $\frac{3}{2}^-$ 1700 $\frac{3}{2}^-$ 1675 $\frac{5}{2}^-$	1625 $\frac{1}{2}^-$ 1685 $\frac{3}{2}^-$	1405 $\frac{1}{2}^-$ 1670 $\frac{1}{2}^-$ 1780 $\frac{3}{2}^-$ 1520 $\frac{3}{2}^-$ 1690 $\frac{3}{2}^-$ 1820 $\frac{5}{2}^-$	1775 $\frac{1}{2}^-$ 1675 $\frac{3}{2}^-$ 1925 $\frac{3}{2}^-$ 1775 $\frac{5}{2}^-$	1825 $\frac{3}{2}$		
2	1440 $\frac{1}{2}^+$ 1710 $\frac{1}{2}^+$ 1745 $\frac{3}{2}^+$ 1680 $\frac{5}{2}^+$ 2000 $\frac{7}{2}^+$	1900 $\frac{1}{2}^+$ 1700 $\frac{3}{2}^+$ 1910 $\frac{5}{2}^+$ 1930 $\frac{7}{2}^+$	1880 $\frac{3}{2}^+$ 1820 $\frac{5}{2}^+$ 2110 $\frac{5}{2}^+$	1635 $\frac{1}{2}^+$ 1915 $\frac{5}{2}^+$	2025 (levels unknown)		
>2	2150 $\frac{7}{2}^-$ 2200 $\frac{9}{2}^-$ 2225 $\frac{9}{2}^+$ 2640 $\frac{11}{2}^-$ 3030	1915 $\frac{5}{2}^-$ 2200 – 2415 $\frac{11}{2}^+$ 2850 + 3270	2100 $\frac{7}{2}^-$ 2380 $\frac{9}{2}^+$ 2585	2250 2455 2620			

Table II. Recent KN scattering experiments below 3 GeV/c. References cited in column 4 are given in Ref. 24.

Measurement	Momenta (MeV/c)	Group	Status
$K^+n \to K^+n$ DCS $K^+n \to K^0p$ DCS $K^+d \to K^+d$ DCS	252,342,470,587	Maryland-IIT	Published[4]
$K^0p \to K^+n$ DCS	550-1000	CMU-Iowa-ANL	Published[5]
$K^0p \to K^+n$ DCS	600-1500	Manchester-Daresbury	Published[6]
$K^+n \to K^0p$ DCS	700,800,900	BNL	Published[7]
$K^+n \to K^0p$ DCS	2200,2450,2700	IC-Westfield	Published[8]
$K^+n \to K^+n$ POL	700-900	BNL-Case-Western	Expt.641, BNL. Completed running 12/77.[9]
$K^+n \to K^+n$ POL $K^+n \to K^0p$ POL	660-1360	Queen Mary-Rutherford	Expt.138, RL. Completed running 4/78.[10]
$K^+n \to K^+n$ POL $K^+n \to K^0p$ POL	1300,1600,1900	KEK-Saga-Tokyo-Tsukuba-Hiroshima	Expt.34, KEK. Approved 2/76.[9]
$K^+p \to K^+p$ POL $K^+p \to K^+p$ DCS	650,700,845,940	Yale-BNL	Expt.524,BNL. Running and POL analysis completed.[11]
$K^+p \to K^+p$ 180° DCS	500-1000	LBL-Mt.Holyoke-BNL	Expt.691, BNL. In progress.[12]
$K^+p \to K^+p$ Re f(0°)	1209,1798,2608	CERN-Caen	Published[13]
$K^+p \to K^0\Delta^{++}$ DCS&DME $K^+N \to K^*N$ DCS&DME	890-1520	Bolgona-Glasgow-Rome-Trieste	Published[14]

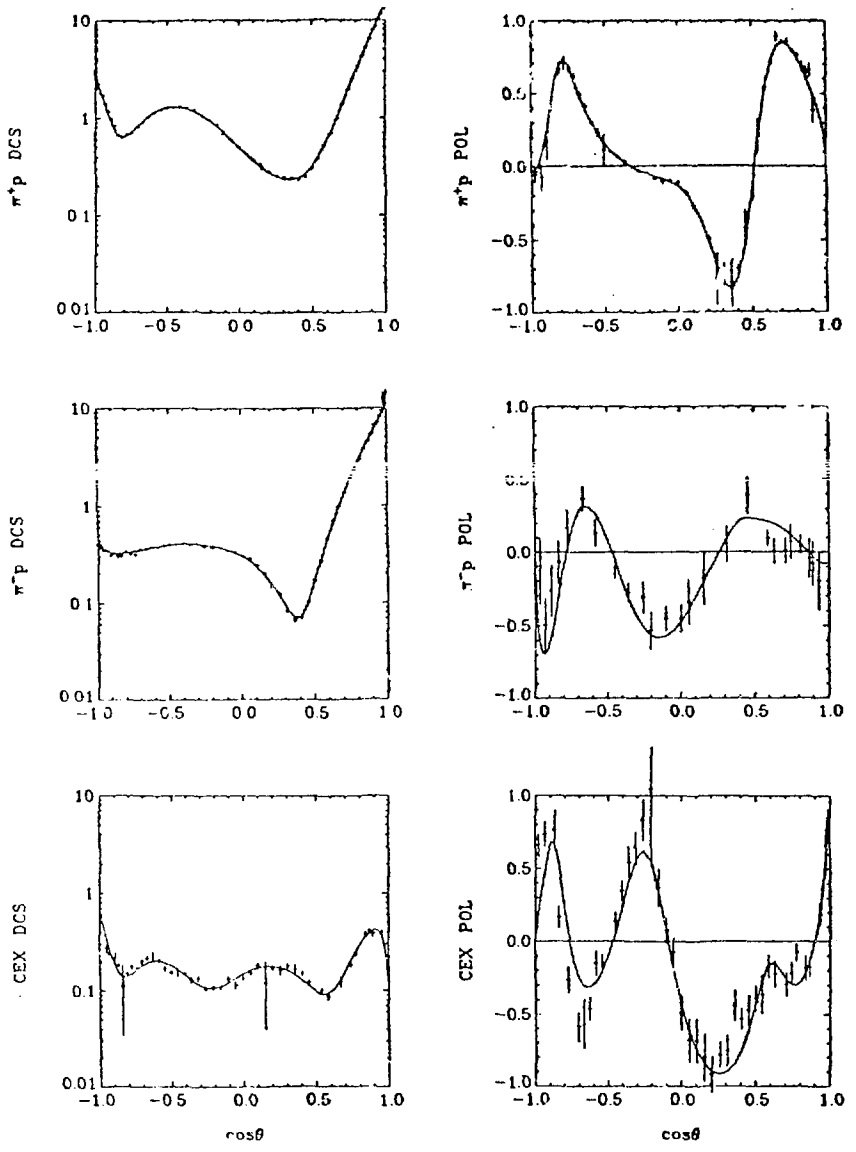

Fig. 1. Amalgamated πN→πN scattering data at 1437 MeV/c. DCS units are mb/sr. The curves are from the partial wave analysis of Ref. 1.

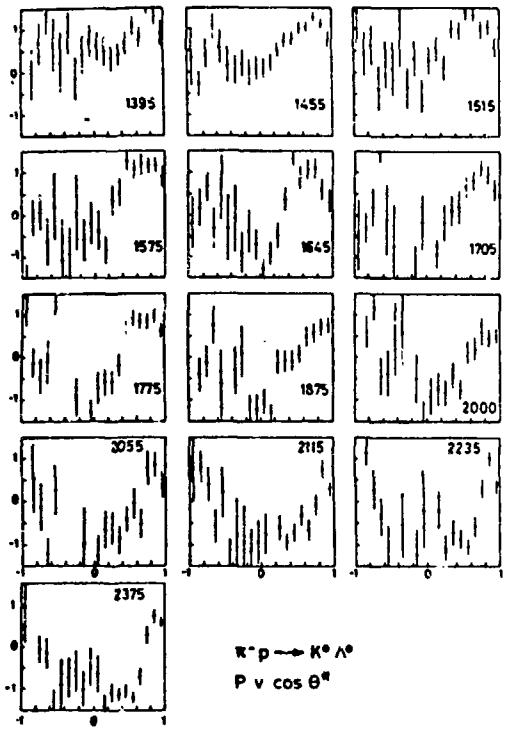

Fig. 2. The polarization data of Saxon et al. plotted against cm scattering angle for 13 incident beam momenta.

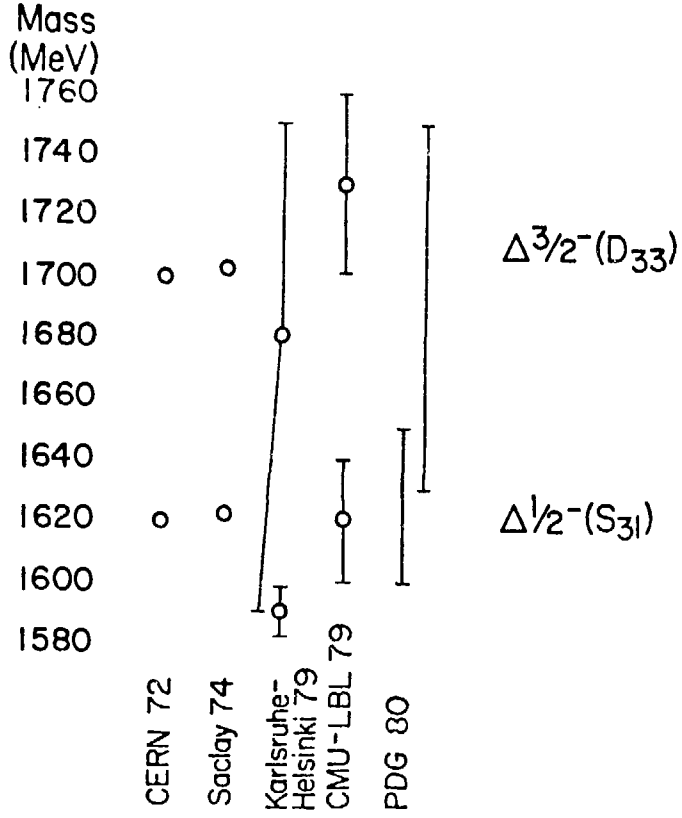

Fig. 3. D_{33}-S_{31} mass splitting in the [70,1⁻].

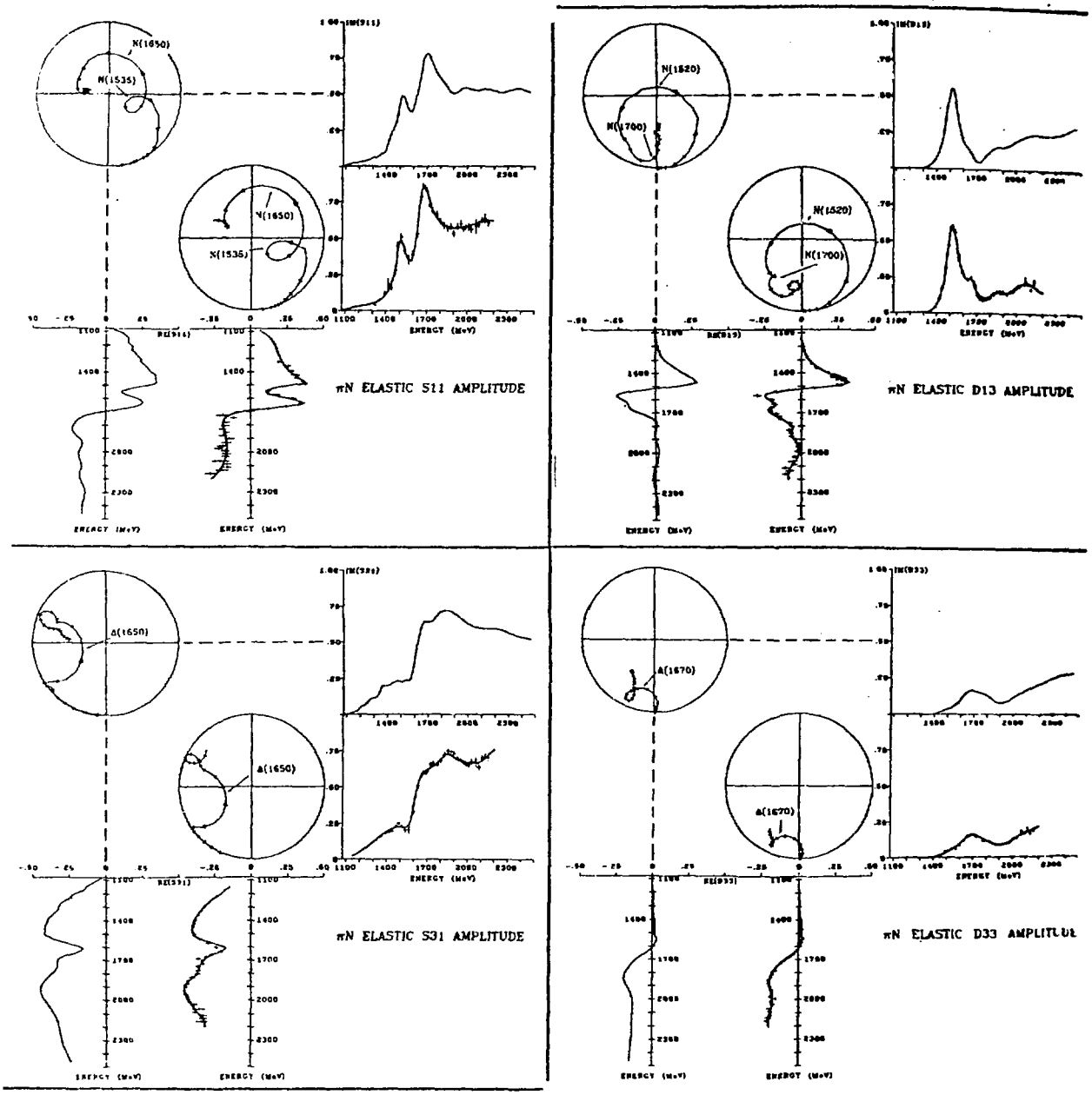

Fig. 4. $\pi N \to \pi N$ partial wave amplitudes containing the $[70,1^-]$ N and Δ resonances. The energy dependence of each amplitude is displayed by plotting its real and imaginary parts vs. energy, in alignment with the corresponding Argand plot. In addition, arrows are plotted on the Argand plots with bases positioned at integer multiples of 50 MeV and a base-to-tip length of 5 MeV. All the energy axes run from elastic threshold to 2500 MeV. The established resonances in these waves are indicated on the Argand plots. The results of two different analyses are shown; the energy axes for the two analyses are aligned for ease of comparison. The lower Argand plot for each wave is from CMU-LBL (results of energy-independent fitting are shown as data points; the curves show an energy-dependent fit). The upper plot for each wave is from KH.

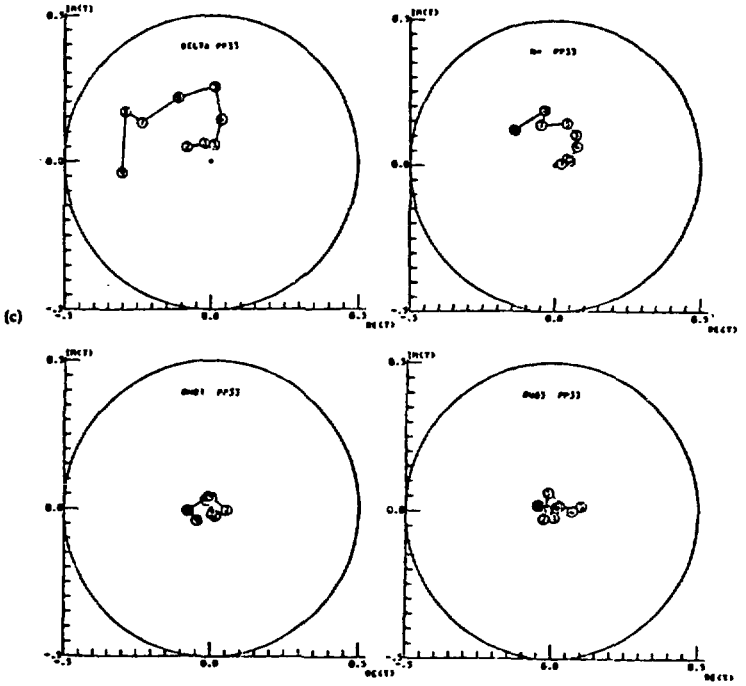

Fig. 5. Argand plots for the P_{31} partial waves of Barnham et al., in the $\pi\Delta$, $\pi N^*(1470)$, and ρN (S=1/2 and 3/2) final states. Points 1 to 9 denote the following energies (in MeV): 1-1439, 2-1495, 3-1526, 4-1551, 5-1577, 6-1612, 7-1640, 8-1668, 9-1693.

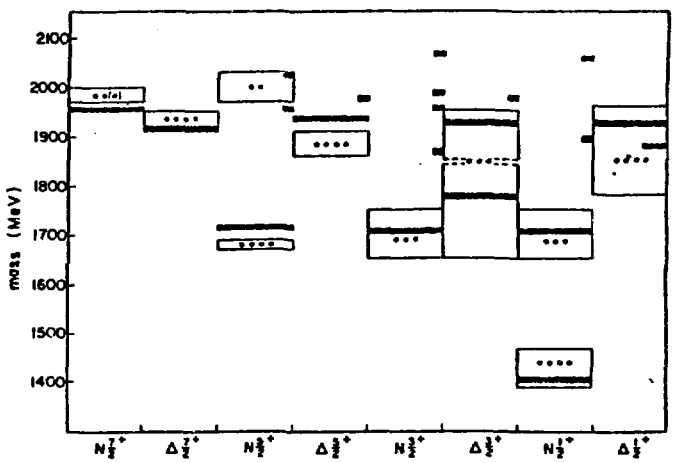

Fig. 6. The decoupling pattern of positive parity non-strange resonances found by Koniuk and Isgur. The known mass ranges of established 3- and 4-star resonances are indicated by open boxes. Predicted resonances are denoted by bars whose length indicate their predicted visibility relative to the strongest resonance in the partial wave.

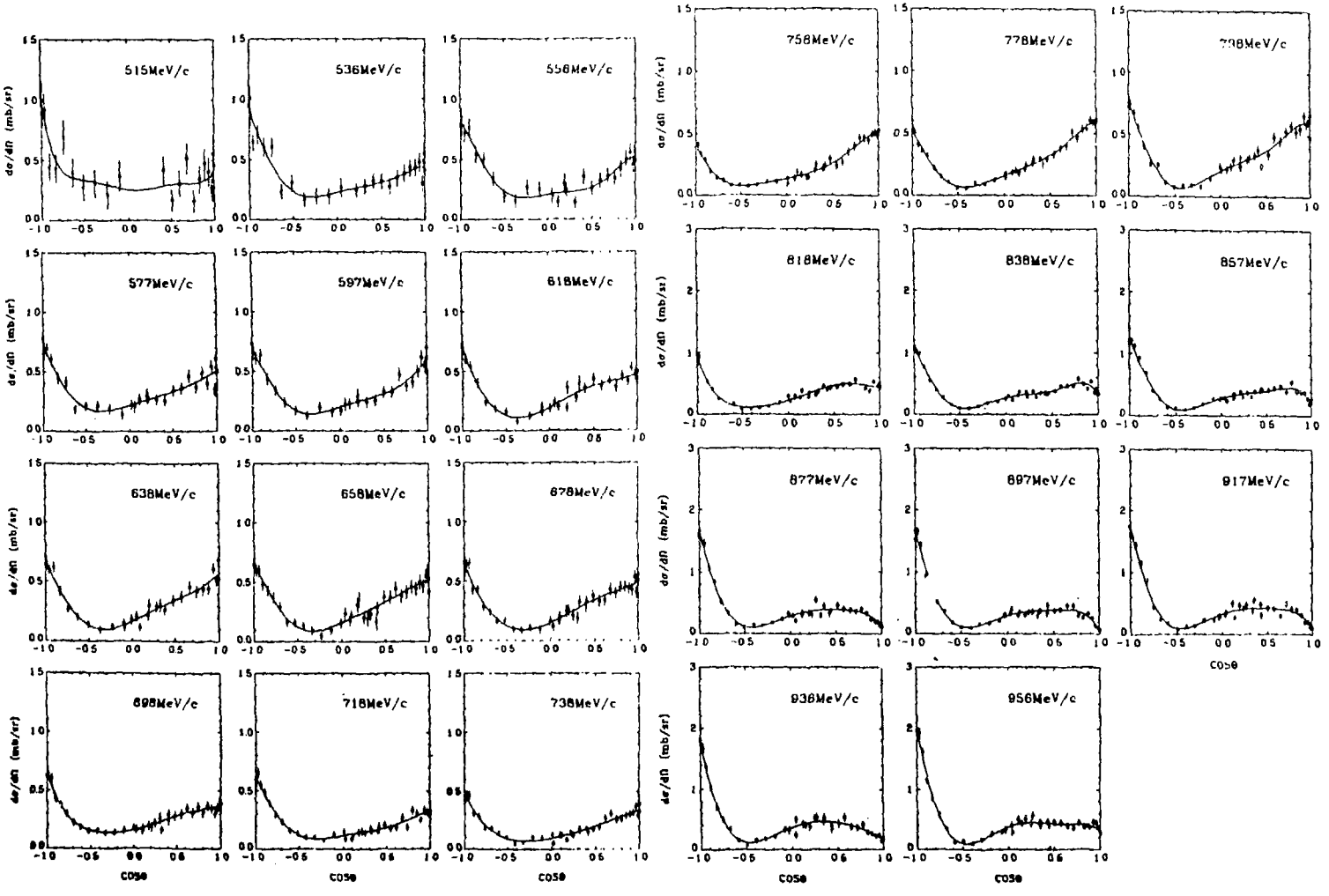

Fig. 7. Angular distributions for $K^- p \to \bar{K}^0 n$ measured by LBL-Mt. Holyoke.[16] The curves are Legendre fits.

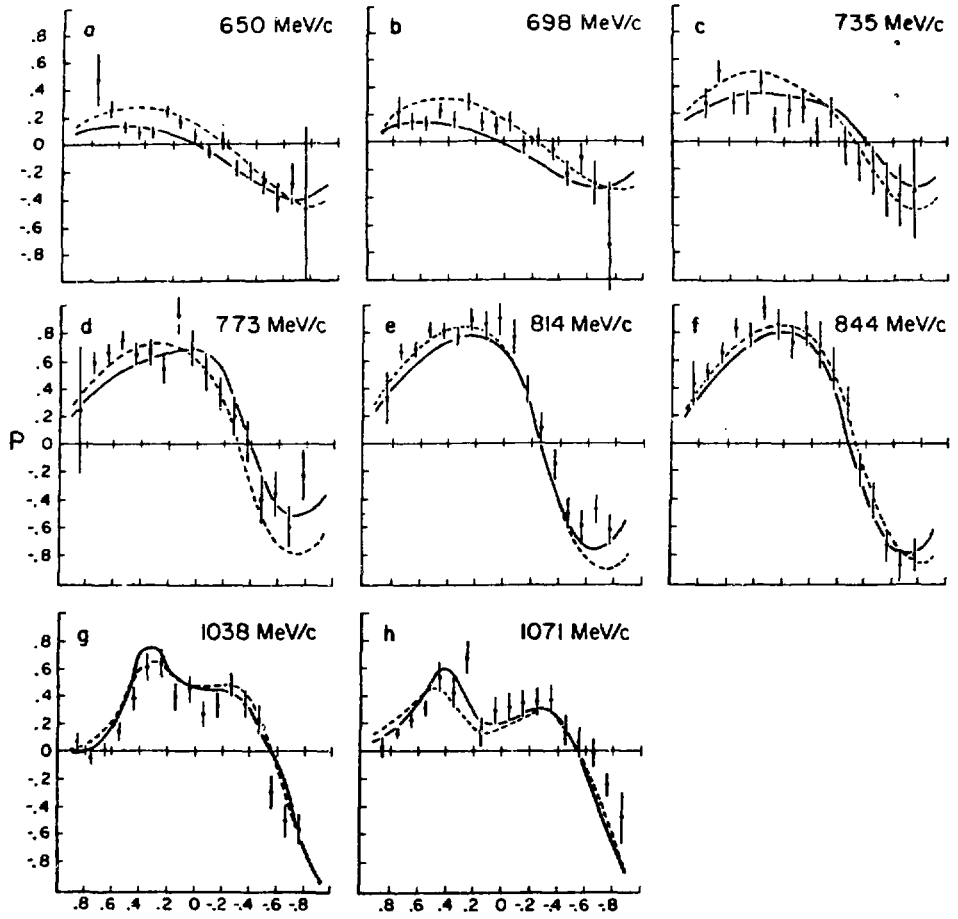

Fig. 8. Polarization parameter for $K^- p \to K^- p$ measured by Yale-BNL-Kyoto.[17] The solid and dashed curves are from an early version of Ref. 22 and from Ref. 20, respectively.

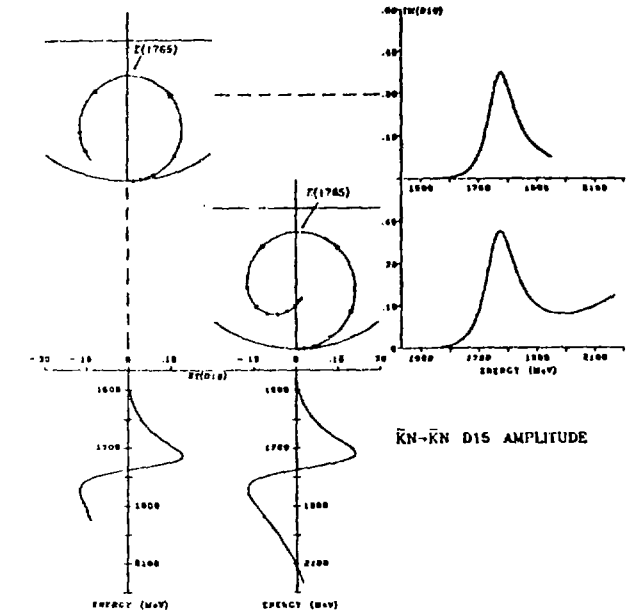

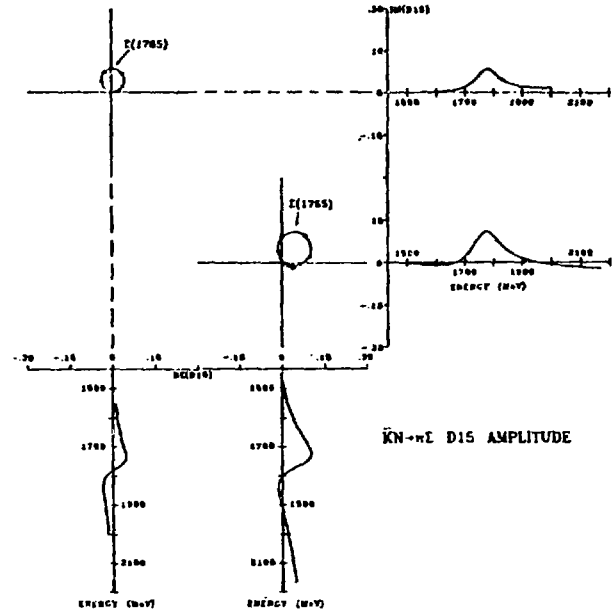

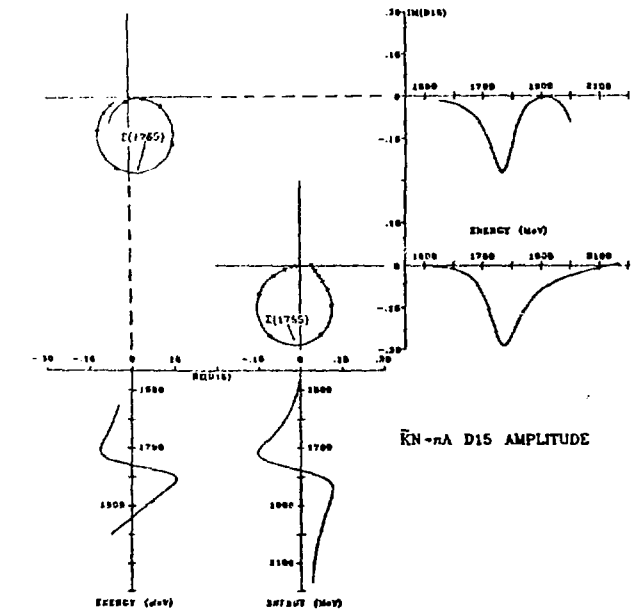

Fig. 9. Amplitudes for $\bar{K}N$ scattering in the D_{15} partial wave. The energy dependence of each amplitude is displayed by plotting its real and imaginary parts versus energy, in alignment with the corresponding Argand plot. In addition, arrows with bases positioned at integral multiples of 50 MeV and a base-to-tip length of 5 MeV are plotted on the Argand plots, and the only established resonance in this wave, the $\Sigma(1765)$, is indicated. The results of two different analyses are shown for each channel; the energy axes all run from elastic threshold to 2200 MeV and are aligned for ease of comparison. The lower plot for each channel is from Ref. 20. The upper plot is from Ref. 22 for the elastic channel and from Ref. 19 for the inelastic channels.

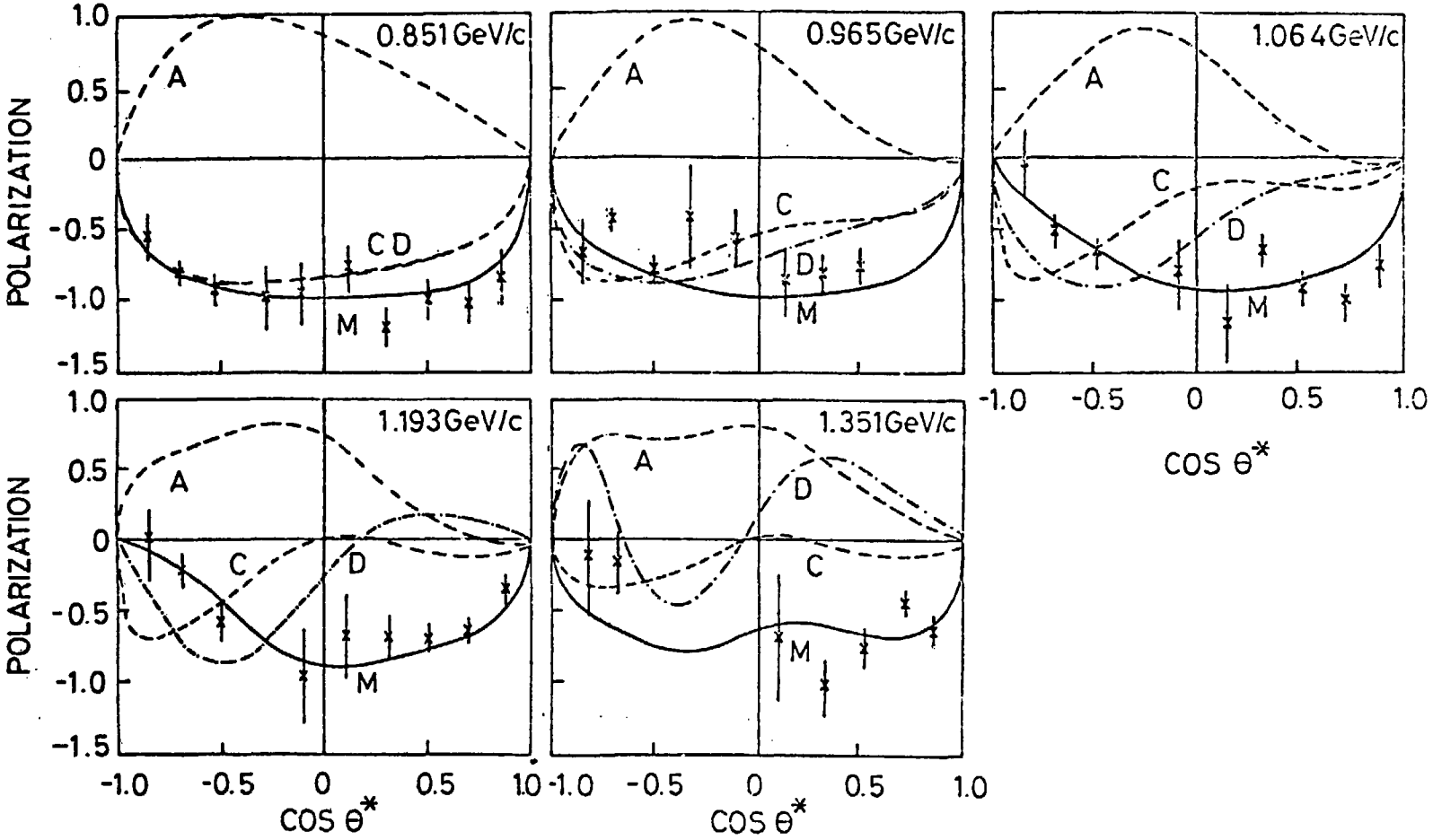

Fig. 10. K^+n elastic polarization measurements of QM-RL. The solid and broken curves are from the fits of Martin and BGRT, respectively.

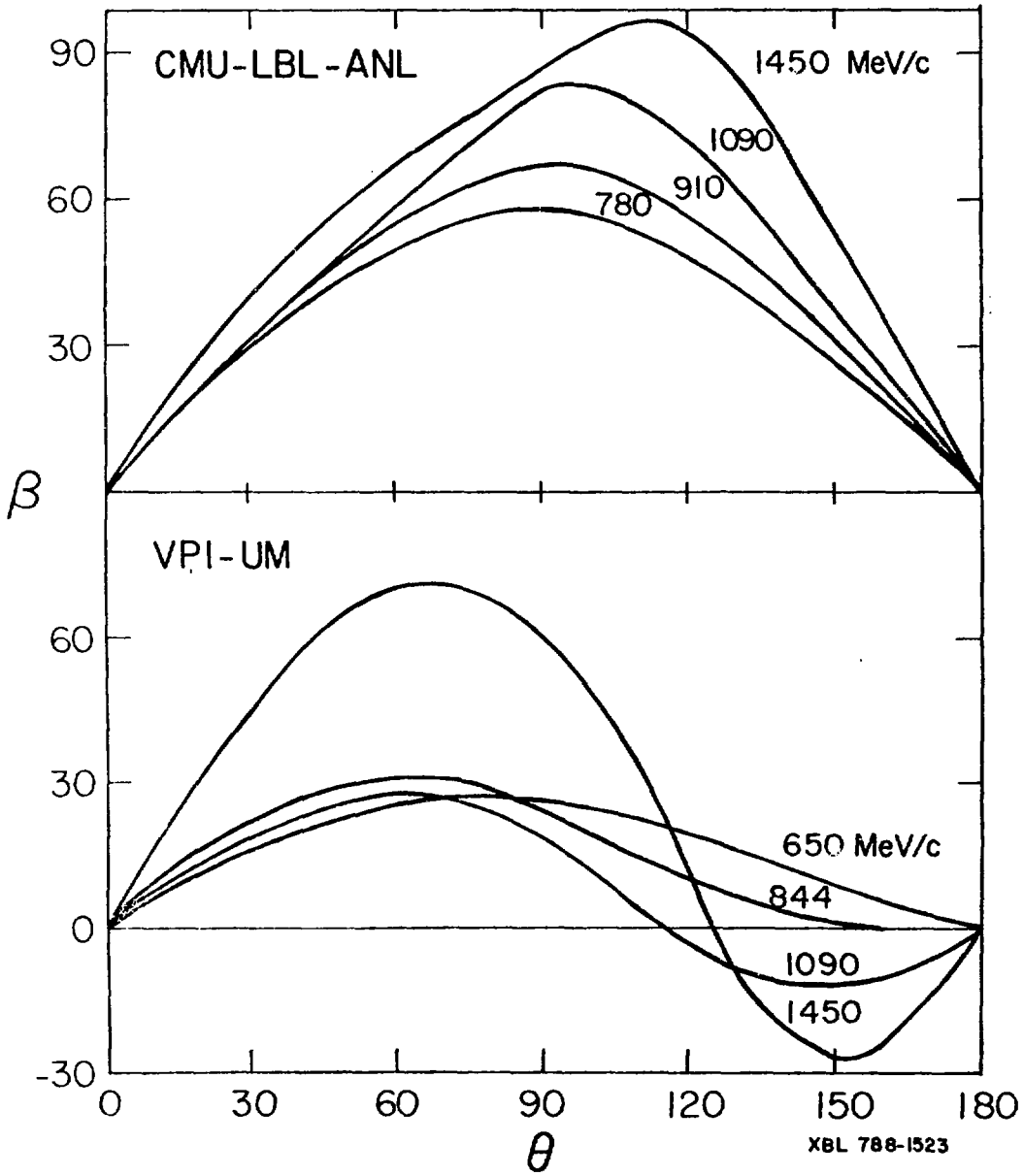

Fig. 11. Comparison of the spin-rotation angle predictions of Ref. 29 (upper plot) and Ref. 28 (lower plot).

COO-3066-163
December 1980

ODD-PARITY BARYONS: PROGRESS AND PROBLEMS

R. E. Cutkosky
Carnegie-Mellon University, Pittsburgh, PA 15213

Abstract

The odd-parity baryons have provided a graveyard for many cherished ideas about hadrons. The simple quark shell model, with QCD-inspired phenomenological perturbations, is the only model able to describe the states with even partial qualitative success. There are also important unexplained residual dynamical effects. Resonance decays can be accounted for, provided the usual spectator model is abandoned. Better experimental data could help to sort out the many remaining puzzles.

At the Baryon 80 conference, Hey[1] called attention to the "Isgur-Karl catastrophe" - the catastrophe being that Isgur, Karl, and others had seemingly explained everything about baryons in terms of a very simple model.[2] In other words, the physics of baryon resonances seemed to be a closed field and no longer presented any interesting problems for theorists. Furthermore, if that were true, there would be no reason to try to obtain any new experimental data.

To see if this catastrophe might be staved off, Forsyth and I decided to look more closely at the odd-parity N/Δ resonances, including all with masses below 2.0 GeV, not just the ones from 1.5 to 1.75 GeV. (See Fig. 1).[3] There are precedents for thinking that the odd-parity baryons might provide some surprises. Bootstrap models did reasonably well with the lowest even parity baryons, but failed to anticipate the explosion of excited states. The spherical bag model gives a reasonable account of the ground state, but as shown by DeGrand and Jaffe,[4] it describes the odd-parity baryons rather badly. Dual resonance models give many excited states, on linear trajectories, but there is no reasonable extension to baryons. Only the most naive model of all, the simple quark shell model (QSM) has been able to provide a useful scheme for classifying the states, as well as a satisfactory starting point for putting in QCD-inspired perturbations.[2]

As shown in Fig. 1, Forsyth and I managed to fit the masses reasonably well within the QSM/QCD framework. However, mixing between the $(70,1^-)$ and

Conference on "Nuclear and Particle Physics at Energies up to 31 GeV"

$(56,1^-)$ turned out to be very strong. The hyperfine force parameters are somewhat different than suggested by one-gluon exchange, and residual dynamical effects are also important.

We tested three different models for meson emission: 1) the "standard model", using single-quark transition operators, which is quite unsatisfactory; 2) the Koniuk-Isgur modification[2] in which certain structure-dependent factors are replaced by extra parameters; 3) our proposed modification in which the structure-dependent factors are retained but the emission from a given quark is allowed to depend on the state of the "spectator" quarks[3] (see Fig. 2). Figure 3 shows our fits to the elastic width of the lowest state in several partial waves. Model 3 gives a more satisfactory representation of the data, although admittedly using more parameters. We have at least succeeded in presenting a quite different alternative model to be tested against further data. Unfortunately, the necessary data are rather sparse.

Could this energy region be holding still further surprises? This is not at all unlikely, because the data for $0.5 \lesssim P_{Lab} \lesssim 1.0$ GeV/c is not very good. (The π^-p polarization data are also weak above 1.0 GeV/c). In fact, the widths quoted for the S_{11} resonances in different analyses differ appreciably, for complicated reasons. Figure 4 shows the partial wave energy dependence given by two recent analyses.[5] In the two sets of curves, the $S_{11}(1650)$ is noticeably different, but the $S_{11}(1540)$ looks rather similar. In the CMU/LBL analysis, however, the resonance parameters for $S_{11}(1540)$ depended strongly on how the background was parametrized and over how big an energy region one tried to fit. In any case, the energy dependence was hard to fit, suggesting possible problems with the data. Thus, to pin down the S_{11} resonances better may require quite a bit more work.

The S_{11} partial wave is generally strongly correlated with the P_{11}, also shown in Fig. 4. In both analyses the $P_{11}(1470)$ has a peculiar shape; in particular, there is a funny bump at 1600 MeV. I have thought of four possible explanations for the bump, not mutually exclusive:

1) Both analyses were misled by bad data.

2) Both analyses were misled by having assumed isospin symmetry.

3) The wriggle is a real effect, and arises from a structure-dependent factor in the matrix element for meson emission by the $P_{11}(1470)$.

4) There is another P_{11} resonance near 1600 MeV.

We are probably not able to distinguish among these possibilities without new experimental data. In the meantime, theorists have been consciously or unconsciously choosing among them when they discussed models, and as a result such discussions have a somewhat provisional nature. It seems that theorists usually assume that possibility #1 is correct, so they ought to be pushing for new experiments.

In summary, the QSM/QCD as pioneered by Isgur and Karl remains qualitatively successful, although interband mixing is much more important than they realized. Spectator models of resonance decay give a poor description

of elastic widths. A problem hindering future work is that a lot of theoretical speculation has been erected on an experimental data base which turns out to be rather flimsy in certain spots, as one sees when one probes beneath the surface.

References

1. A. J. G. Hey, Baryon 80 Proceedings (in press).
2. N. Isgur and G. Karl, Phys. Rev. D 20, 1191 (1979); R. Koniuk and N. Isgur, Phys. Rev. D 21, 1868 (1980). Other references are given in these papers.
3. C. P. Forsyth and R. E. Cutkosky, CMU preprint COO-3066-161 (Dec. 1980).
4. T. A. DeGrand and R. L. Jaffe, Ann. Phys. 100, 425 (1976).
5. Particle Data Group, Rev. Mod. Phys. 52, S177 (1980); G. Höhler et al., Handbook of π-N Scattering, Physik Daten Vol. 12-1 (Karlsruhe, 1979); R. E. Cutkosky et al., Phys. Rev. D 20, 2839 (1979).

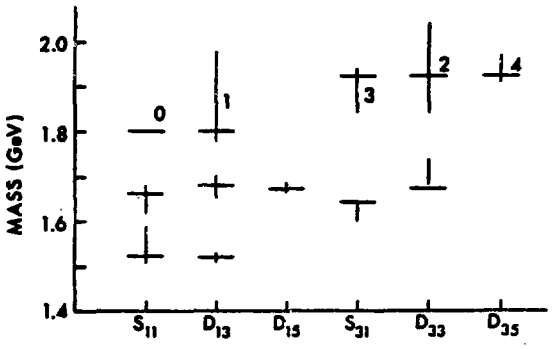

Fig. 1. Odd parity N/Δ resonances. The vertical bars show the experimental mass, with errors; the horizontal lines show a fit. The numbers for the $(56,1^-)$ states are the number of "stars."

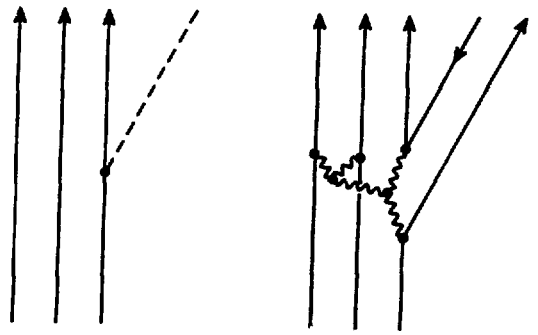

Fig. 2. Resonance decay contributions with (left) single-quark transition operators and (right) spectator-dependent effects.

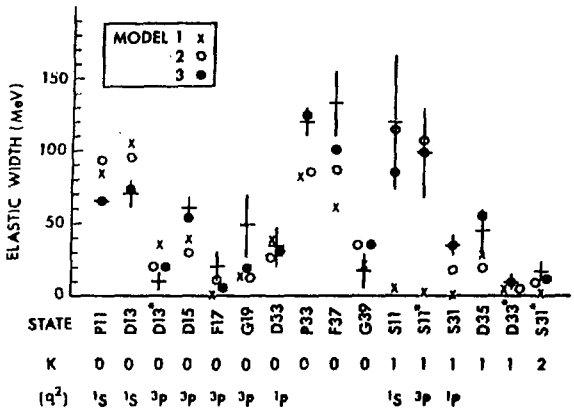

Fig. 3. Elastic widths of the lowest state in several partial waves, as fit in models 1-3. K denotes the degree of a structure-dependent polynomial factor, if mixing is ignored. The main (q^2) spectator configuration, in addition to ^3S, is also listed.

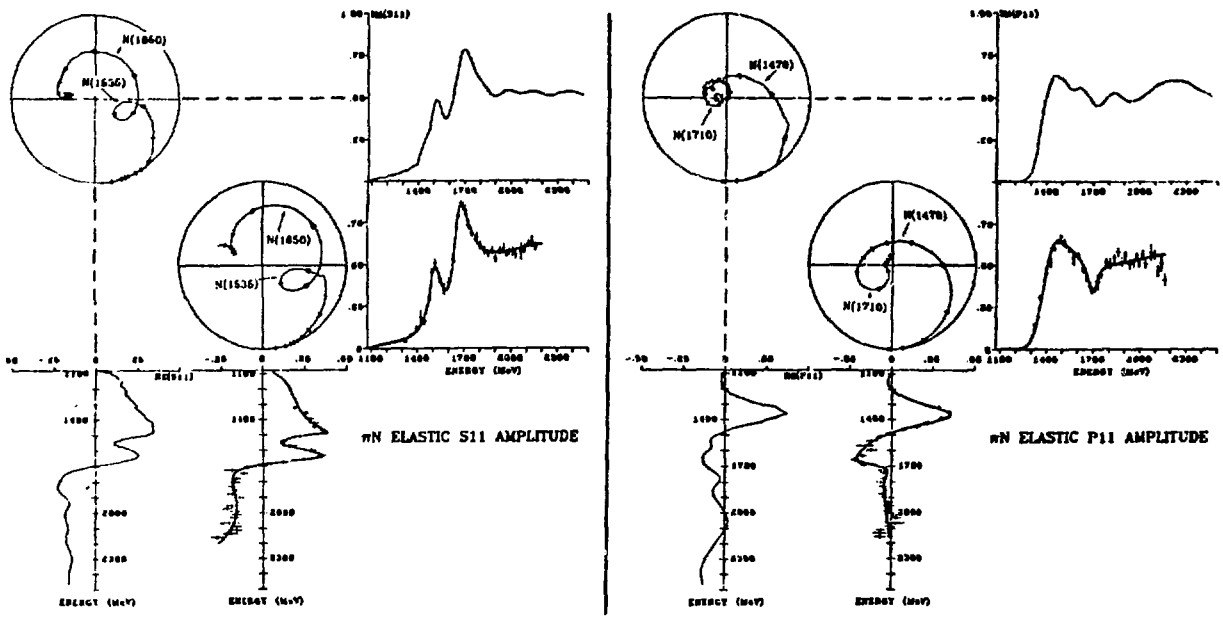

Fig. 4. S_{11} and P_{11} partial waves from the Helsinki-Karlsruhe and CMU-LBL analyses.

MESON-NUCLEAR INTERACTIONS AT MEDIUM ENERGIES

by

R. A. Eisenstein*
Carnegie-Mellon University, Pittsburgh, PA 15213

ABSTRACT

A brief review of selected directions in medium energy physics is given. Special attention is paid to the propagation of hadrons in the nuclear medium which results in a modification of the free properties of the probe hadron and the nucleus. Such modifications are germane to our understanding of both particles and nuclei. Examples are given involving pion and kaon scattering, absorption and production from nuclei. Some of what has been learned is summarized and some of the hopes for the future are outlined.

I. Introduction

A principal reason for studying strong interaction physics is to understand how a many-body system governed by such interactions can be constructed from the basic two-body amplitude. Today it is clear that essentially the same problem is faced by workers in low-energy nuclear physics who seek to understand nuclei in terms of nucleon and meson constituents, and by high energy physicists who wish to build the hadrons and mesons from quarks and gluons.

Medium energy physics is a fruitful meeting ground of these two previously disparate areas. A principal motivation for studying this field is to be able to learn new information about both particles and nuclei. On the particle side, a considerable amount has already been learned. Static properties (mass, magnetic moment) of several particles have been determined using "exotic atom" techniques. Such work has also led to some information regarding near-threshold strong interactions of few-body systems, which could not be obtained in any other way. In addition, many people are now engaged in fundamental tests of the electroweak interaction using intense medium energy accelerators. Finally, it will be shown below that new experimental and theoretical work holds promise for learning about the modification of particle properties (and interactions) under dynamical conditions.

In the case of nuclei, a fundamental issue concerns the role of mesonic degrees of freedom in determining nuclear dynamics. The utilization of mesons

as nuclear probes will hopefully make clearer certain aspects of the interactions between nucleons in nuclei. Mesonic interactions with nuclei in some cases also provide new means of probing the nucleus, exploiting for example isospin selectivity, meson absorption, or "strangeness". Lastly, there is excitement over new possibilities involving, for example, states of matter never seen before, such as pion condensation. Several of these aspects will be discussed below. It is clear from the outset that a complete understanding of meson-nuclear processes will involve incorporation of meson degrees of freedom, true absorption phenomena, relativity and non-local interactions. Many of the ideas discussed are treated in more detail in refs. [1-4].

II. Basic Considerations

Much qualitative understanding can be achieved by examining the basic properties of the two-body interactions of pions and kaons with nuclei. Figure 1 shows the principal quantum numbers of these mesons in the pseudoscalar meson octet. The pions form an isospin triplet with strangeness zero; the isospin invariance properties of the pion play a very important role in its use as a probe of nuclear structure, as will be seen below. The π^+ and π^- are antiparticles, as are the K^+ and K^-; in the latter case, however, the $K^{\pm}N$ amplitudes are *not* related by isospin invariance. The presence of non-zero strangeness in the kaon-nucleon system has important consequences for the formation and decay of resonances in that system.

The situation as seen in the quark model is shown in fig. 2. The pions and the K^- may interact with nucleons to form other baryon states or resonances

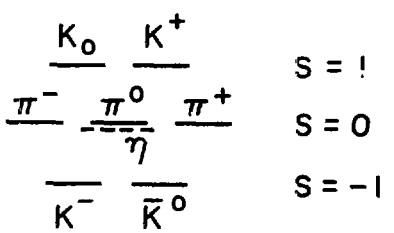

Fig. 1
The pseudoscalar meson octet.

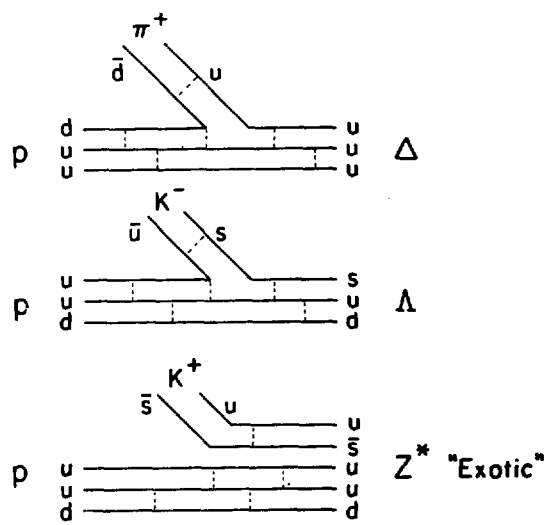

Fig. 2
Diagrams showing Δ and Λ formation in π^+p and K^-p interactions. A resonance in K^+p scattering requires formation of a 5 quark object.

(3-quark objects) via u- or d-quark annihilation; the K^+N interaction, however has no such channels available to it, and requires the formation of a 5-quark object to obtain a resonant structure. Such "exotic" 5-quark objects are not known in nature. The elementary total cross sections for $\pi^{\pm}N$ and $K^{\pm}N$ interactions (figs. 3-5) reflect these ideas. The K^-N cross sections show a rich spectrum of fairly narrow resonances (compared to the πN (3,3) resonance), while the K^+p cross section shows only monotonic increases over the momentum range of interest. The I=1 values of the cross section for K^- are roughly three times larger than those of K^+ and both are much smaller than the value for πN scattering at the peak of the (3,3) resonance. Figs. 3 and 4 also show the positions of several of the prominant resonances in the πN and K^-N systems.

A good qualitative idea[8] of what to expect when these particles interact with nuclei is given by fig. 6, which shows the mean free path λ $(1/\sigma_{tot}\rho)$ for several particles interacting with nuclear matter at average nuclear densities ($\sim$0.17 nucleons/F^3). Of special interest are the manifestations of resonances in the πN and K^-N systems, the dramatic effect of annihilation in the $\bar{p}N$ system, and the resulting very long mean free path for K^+ due to the weakness of the

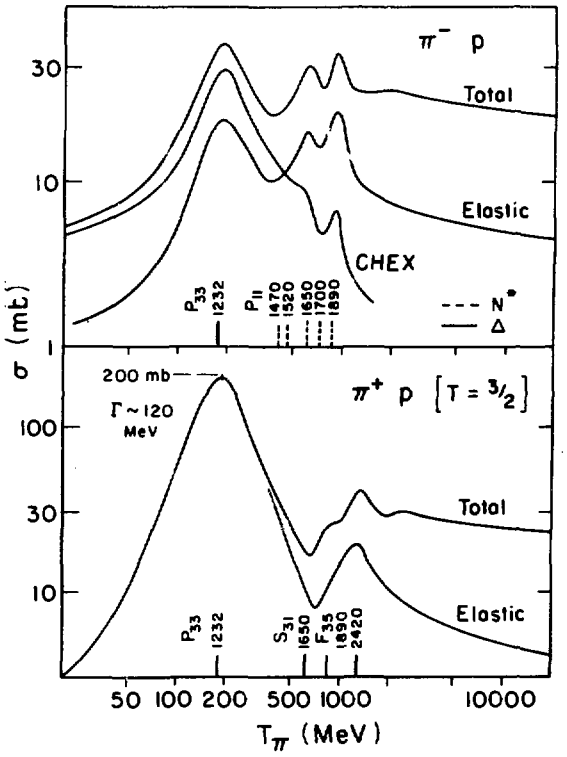

Fig. 3
Cross sections for π-proton scattering. The solid (T=3/2) and dashed (T=1/2) lines show the positions of some known resonances. The principal regions in which π-nucleus experiments have been done are KE $\sim$ 50 MeV, $\sim$ 180 MeV and $\sim$ 672 MeV.

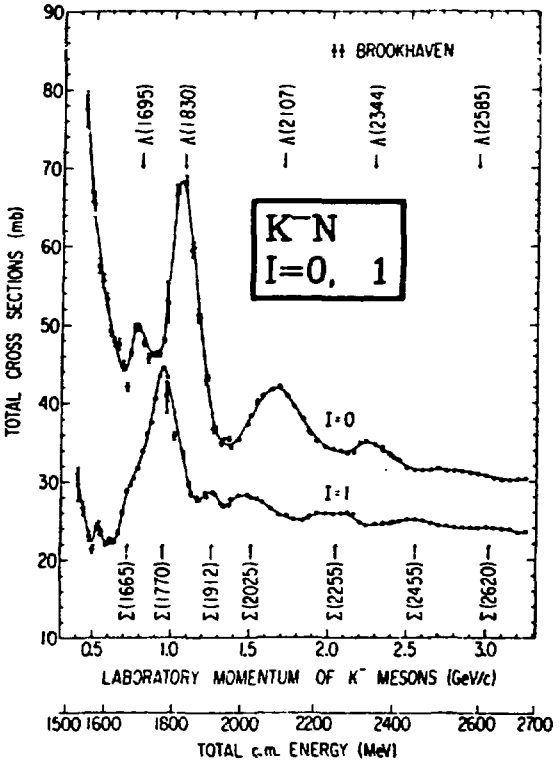

Fig. 4
The K^--nucleon total cross-sections.[5] Note the narrow width and small strength of the resonances compared to the $\Delta(3,3)$.

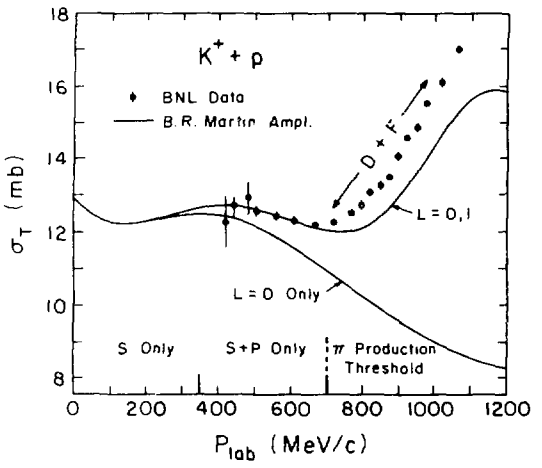

Fig. 5
The K^+-p total cross section data[6] compared to a calculation by B. R. Martin.[7] Taken from ref. [9].

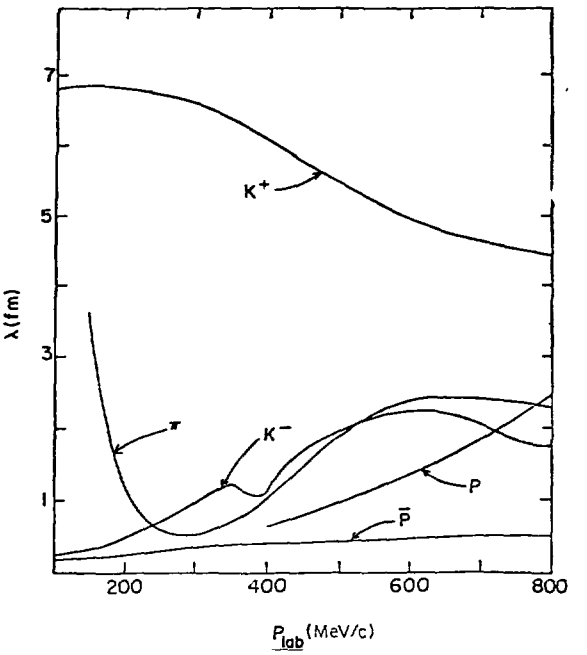

Fig. 6
The mean free path in nuclear matter as a function of lab momentum for various projectiles. Taken from ref. [8].

K^+N interaction. Such a long mean free path can be found also in π scattering at energies below 50 MeV, but there one has the additional complication of true π absorption to contend with. The simple, weak nature of the K^+ nucleus interaction has led to hopes that for this probe the multiple scattering series will converge rapidly. One would then have a good understanding of a strong interaction probe that is sensitive to the entire nuclear volume and matter distribution. Use of the K^+ as a neutron distribution probe would still be difficult, however, because over a significant energy range the I=1 amplitude is significantly larger than the I=0, and very precise experiments would be necessary.

III. Theoretical Approaches

Much effort has been made to provide a theoretical understanding of the data which is emerging from the meson factories. This is especially true of scattering data, as it presents the simplest test of our ideas.

At best one would like to construct a meson-nucleus field theory which builds the meson-nucleus interaction in a dynamically consistent way from the two-body problem. One would thus build in from the beginning such things as relativity and true absorption. This very ambitious project has been attacked by many authors[11-16] but because of its extremely complicated nature has not been solved. Nonetheless, some encouraging progress has been made in studies of the πd→pp reaction[14] and in understanding some of the dynamical questions

involved with the πN range. Due to its fundamental nature, work in these areas will certainly continue.

A considerably more tractable approach, which lends itself to simple calculations in first order, has been to presume that potential scattering generated by a multiple scattering theory is an adequate description of these processes. The resulting optical potential is exact if carried to all orders, but this can be done only in restricted circumstances.[17,18] Most authors[1,17-25] have calculated such potentials to at most second order, including various kinematic and nuclear medium effects. For pions the effect of true absorption has been introduced in an *ad hoc* manner, and important effects due to nuclear recoil have been neglected. In first order, such potentials all have the form

$$V(\vec{k},\vec{k}') \sim \int d^3p \, \langle \vec{k}\,\vec{p}\,|t|\vec{k}'\vec{p}-\vec{q}\rangle \, F(\vec{q}-\vec{p},\vec{p}) \tag{1}$$

where <t> is the fully off shell t-matrix for scattering from a bound nucleon, and F is a nuclear structure function. The above form has been used extensively by Liu and Shakin[23] and by Landau and Thomas,[24] wherein the effects due to nucleon binding, Fermi motion and off-shell behavior have been esimated using various models.

By approximating the above expression with a factorized form one obtains the simple "tρ" optical potential, the most common variation of which is the Kisslinger form:

$$V(\vec{k},\vec{k}') = At\rho(\vec{q}) \sim A(b_0 + b_1 \, \vec{k}\cdot\vec{k}')\rho(\vec{q}) \ . \tag{2}$$

Here $\rho(q)$ is the Fourier transform of the ground state nuclear density and $t_{\pi N}$ is the on-shell two-body t-matrix. This potential suffers from several difficulties which arose originally because of the desire to use these potentials in coordinate space. The principal problems are the zero range of the interaction, its off-shell behavior, and the omission of d-wave and higher ℓ-value amplitudes in the two-body t-matrix. Nonetheless, coordinate space codes using the Kisslinger potential for analysis of elastic π and K data[26,27] are in widespread use. "Effective" values of b_0 and b_1 for a wide range of nuclei and energies have been generated.

Many of the shortcomings mentioned above for the "tρ" potential can be cured by working in momentum space. This was first elucidated by Landau, Phatak and Tabakin,[21] who wrote a more general form for the two-body t-matrix:

$$\langle \vec{k}|t|\vec{k}'\rangle = \sum t_\ell^{IJ} \frac{g_\ell(\kappa)g_\ell(\kappa')}{g_\ell(\kappa_0)^2} \, P_\ell(\cos\theta) . \tag{3}$$

In this form t_ℓ represents the on-shell two-body information and g_ℓ the off-shell form factors. The resulting optical potential can then be inserted

into a relativistic Lippmann-Schwinger momentum space calculation (PIPIT, ref. 28) to generate elastic cross sections. Some results will be shown below.

As an indication of the influence of nuclear effects on the basic two body physics, Rosenthal and Tabakin[29] examined the role of Fermi motion in determining the propagation of K^-N resonances in nuclei. To do this they averaged the two-body t-matrix over the nucleon momentum distribution in the nucleus, which was constructed from momentum space harmonic oscillator wavefunctions. The results are shown in fig. 7, where Kisslinger parameters b_0 and b_1 with and without Fermi averaging are plotted. It is disappointing that the presence of the two body resonances is so greatly muted by the averaging procedure. It appears that it will be difficult to learn about some aspects of resonance propagation due to momentum smearing.

Let us now turn our attention to another way of describing meson-nuclear interactions, one which focusses directly on the formation of resonant structures as the principal feature of the interaction.[30-36] This model stipulates that the incoming meson interacts with a single nucleon, forming a baryon-hole state which acts as the "doorway" to all other states. The baryon thus formed, and which propagates through the nuclear medium, may have properties which are quite different from those in free space because of its interaction with the medium. This will be examined in more detail below.

These ideas find an extremely natural expression in the projection operator formalism of Feshbach.[30] "Doorway" ideas were first applied to pion scattering by Kisslinger and Wang[31] and extensively studied by groups at MIT and SIN,[32,33] Erlangen,[34] and Regensburg.[35] They have also recently been applied to kaon scattering by Kisslinger.[37] In all models of this type, the meson-nuclear Hilbert space is broken up into three segments (see fig. 8). These correspond to (1) the entrance channel and any other states which are to be treated explicitly, labelled P; (2) the possible doorway states, labelled D; and (3) the remaining states, labelled Q, which account for reaction processes. In the usual formulation all states Q much be reached by passing through D; D may also decay back to P thus allowing for elastic scattering. However, in cases where true absorption may take place, some direct coupling between P and Q should be allowed.[31] Fig. 8 also shows schematically the formation of the Δ-h state in pion scattering and indicates the dependence of the process on the $\pi N\Delta$ coupling constant and the Δ propagator $G_{\Delta h}$. Thus, the theory allows very naturally for the formation, propagation and decay of the resonance and the influence of the nuclear medium. It also allows one to include nucleon recoil and non-localities in the interaction, which are known to be present.

As one might expect, such a theory works best in the cases when strong resonances are present. If the absorption takes place in the surface region of the nucleus rather than the entire nuclear volume, rather few baryon-hole states will be available. The resulting matrix can be diagonalized to provide wavefunctions for the system, as is the case for nuclear shell model calculations. Even so, such calculations can be very cumbersome and have been limited to light nuclei.[32-35] However, the Green function techniques now in use by the Seattle group[36] promise to make possible calculations in much heavier systems.

One of the most interesting aspects of the doorway theory is that it allows one to extract from it the *average properties* of the propagating baryon, and therefore to gain some insight into the modification of these

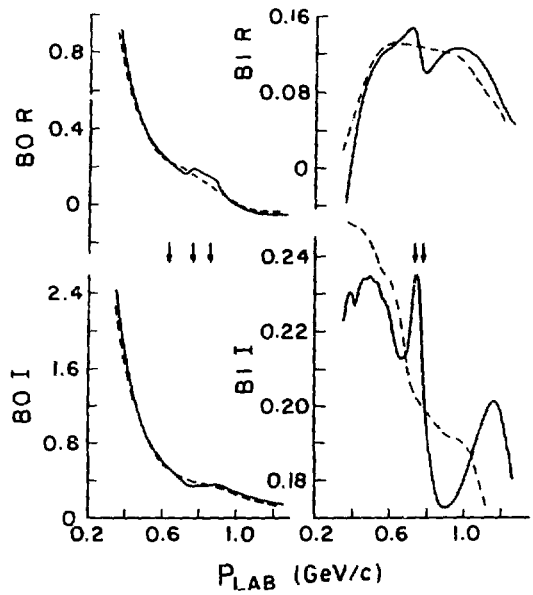

Fig. 7
The effect of Fermi averaging (dashed curves) on the Kisslinger parameters b_0 and b_1. The solid curves are the unaveraged values. See ref. [29].

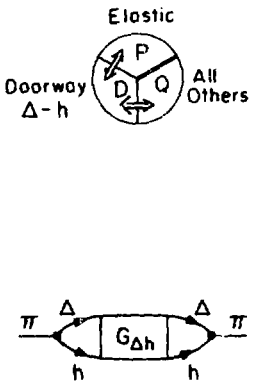

Fig. 8
(Upper) Pie diagram showing the division of π-nucleus Hilbert space into entrance states (P), doorway states (D) and reaction states (Q). (Lower) Diagram showing formation of the Δ-hole state and its dependence on $g_{\pi N\Delta}$, the Δ propagator and the nuclear medium (hole state).

properties by the nuclear medium. Such information is simply not available from any other source. This can be seen, in a simpler rendition of doorway theory, in the construction of the optical potential for pion-nucleus scattering:

$$V_{OPT} = V_{NR} + \frac{E - M_\Delta + i\Gamma_\Delta/2}{E - M_\Delta - \Delta E + i\beta\Gamma_\Delta/2} \langle t\rangle \rho_\Delta(k,k',\lambda) \ . \qquad (4)$$

Here V_{NR} is the non-resonant part of the potential, M_Δ and Γ_Δ are the mass and decay width of the free Δ, $\langle t\rangle$ is the on-shell t-matrix for scattering of a free Δ, and ρ_Δ is a nuclear structure function with non-locality parameter λ.[37] The parameters ΔE and β are of special interest, as they relate to the properties of the Δ in the nucleus. They are, respectively, the nuclear binding energy and ratio of bound to free width. Tabulations of these quantities are just now becoming available for some resonances, as shown below:[37]

Table I

	ΔE	β	Source
Δ(1232)	10 MeV	1.1	π^- elastic
Λ(1405)	19 MeV	1.3	K^- atoms
Λ(1520)	10 MeV	1.3	K^- bubble chamber

It is of considerable interest that these resonances are apparently *less bound* in nuclei than they are as free objects. In addition, their decay widths are *enhanced* when so bound, and not restricted as one might expect due to Pauli blocking or some other mechanism. Of course the exact mechanisms producing these effects are complicated and the final result is no doubt the result of a careful cancellation between competing processes. More data of this kind could help greatly in understanding the properties of these resonances in nuclear matter.

One can also describe the interaction of these particles with nuclei in terms of an effective optical potential of the form

$$V_{OPT}(r) = (V + iW)\rho(r) + V_{SO}\,\vec{\sigma}\cdot\vec{\ell}\; m_\pi^{-2}\; r^{-1}\; \rho'(r) \quad . \tag{5}$$

Parameters for this potential have been tabulated by Kisslinger.[38]

Table II

	-V(MeV)	W(MeV)	V_{SO}(MeV)	Refs.
Δ(1232)	50 ± 5	-5 ± 5	20	33,36
Λ	32	--	2 ± 1	39
N	54 - 0.32E + 0.4Z/$A^{1/3}$	0(E < 12.3) 0.22E - 2.7(E > 12.3)	20	40

We note that the Δ is apparently subject to a potential of roughly the same parameters as the nucleon. Of particular interest is the spin-orbit strength; evidence for the importance of this term can be found in the work of Horikawa, Thies and Lenz[33], shown in fig. 9. There "doorway" calculations with and without the spin-orbit contribution are shown, compared to the data of Jansen et al.[41] Inclusion of the spin-orbit term makes dramatic improvements in the results both well below and well above the (3,3) resonance.

Let us turn now to an examination of some recent results for kaon scattering at 800 MeV/c, obtained by Marlow et al.[42] at Brookhaven. Figs. 10 and 11 show the data for elastic $K^\pm$ scattering from ^{12}C compared to momentum space calculations made by Rosenthal and Tabakin.[43] The theory makes use of the best available amplitudes for K^+N[7] and K^-N[44] in the "tρ" optical potential, with an interaction range of 0.25 F. All partial waves germane to the calculation are included. Agreement is seen to be reasonably good; based on better congruence at forward angles, one might claim more success for the K^+ case, as one would naively predict ahead of time. Fig. 12 shows the data[42]

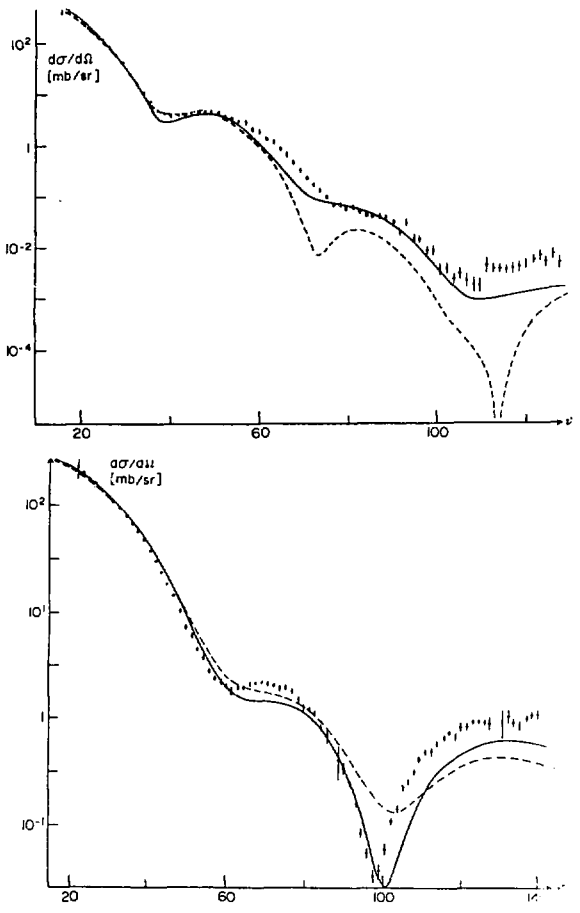

Fig. 9
Data of Jansen et al.[41] compared to doorway Δ-h calculations of Horikawa, Thies and Lenz.[33] Note importance of Δ-nucleus spin-orbit potential.

for K^+ - ^{40}Ca compared to a coordinate space calculation using a Kisslinger potential. The agreement is quite good; the K^- - ^{40}Ca case (not shown) is slightly worse. All the calculations mentioned here have used ground state densities taken from electron scattering.

The inelastic results[42] shown in fig. 12 for ^{12}C are compared to standard DWIA calculations using as the transition form factor the derivative of the ground state density. The deformation parameter β_2 was taken to be 0.56 as measured with other probes. Incoming waves were distorted with an optical potential constructed using either the Martin[7] or the Gopal[45] amplitudes in a Kisslinger form. The very poor agreement with the data in the K^+ case is due to the transition form factor; Sakamoto et al.[46] have shown that use of a form factor that fits electron scattering removes most of the disagreement. Thus, as has been pointed out often in the past, several probes are yielding consistent information about the nuclear states involved. Kaon data for the 3^- transition (9.64 MeV) in ^{12}C are also available;[42] one draws similar conclusions from that analysis as well.

Fig. 13 shows BNL data[42] for elastic scattering of π^- projectiles from ^{12}C and ^{40}Ca compared to momentum space calculations using PIPIT.[28] Data for π^+ scattering on the same targets is being analyzed now. Here the basic amplitudes were constructed from the CERN theory phase shift set[47] including partial waves through ℓ=3. Electron scattering ground state densities were used and a πN range of 0.25 F, although variation of the latter had little effect. This is not surprising, since the scattering at these energies (∿ 670 MeV) is dominated by the considerations of geometric optics. Thus the impulse "tρ" approximation ought to be reliable, and the agreement with the data indicates that this is generally so. However, the disagreement at forward angles is not understood at present. If the interaction mechanism really is under control, then experiments stressing nuclear structure might be quite fruitful in this energy region. (See the contribution of Arch Theissen to this Conference.)

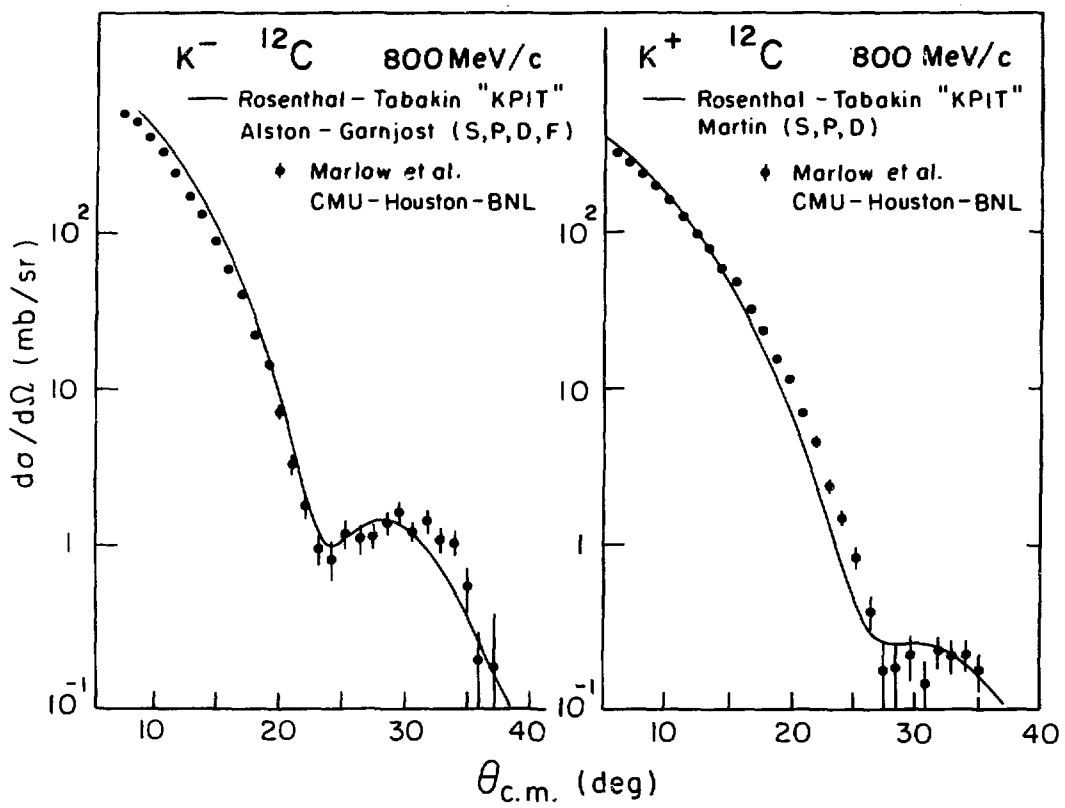

Fig. 10
$K^{\pm}$ - ^{12}C data of Marlow et al.[42] compared to calculations of Rosenthal and Tabakin.

IV. Nuclear Structure Information from Meson Scattering

One of the principal justifications for construction of the meson factories was the isospin structure of the πN interaction, particularly in the region of the (3,3) resonance. There, the I=3/2 amplitude is much larger than the I=1/2 case; this leads to expectations for large differences between π^- and π^+ elastic scattering from neutron-rich nuclei. If the optical potential could be unambiguously connected to the nuclear matter distribution, then an excellent means would exist for probing the neutron component.

Although such a firm connection does not yet exist,[48] several authors[49-55] have tried to explain the observed experimental differences (figs. 14-16)in terms of the matter distributions. Such explanations are appealing if not entirely convincing. Fig. 14 shows results obtained by Jansen et al.[41] at 162 MeV for scattering of $\pi^{\pm}$ from ^{16}O and ^{18}O. The π^- data clearly show the influence of the two extra neutrons in ^{18}O; further, if one can link the positions of diffraction minima to nuclear size, then the neutron distribution in ^{18}O has a larger spatial extent than in ^{16}O. How much larger is the key question.

An interesting study of this question in larger nuclei has been made by Olmer et al.[49] at 162 MeV; their results for ^{208}Pb are shown in fig. 15 compared

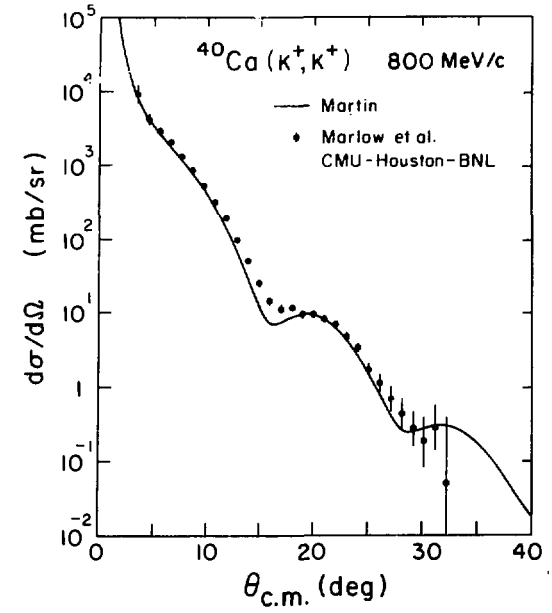

Fig. 11
K^+ - ^{40}Ca data of Marlow et al.[42] compared to coordinate space calculations using Martin[7] amplitudes.

to calculations using their modified version of PIPIT.[28] After adjustments[49] for nucleon size, nucleon binding and the Coulomb shift of the incoming π energy, good agreement with the data is achieved. However, the resulting radius difference for protons and neutrons is not the same as obtained with proton scattering[56] or predicted by DDHF calculations.[57]

Some very interesting information on this question has been discovered[53-55,58] in an unexpected energy region. In fig. 16, data[53] for the ratios of π^+ - ^{12}C to π^+ - ^{11}B at 48 MeV, and for[54] π^- - ^{18}O to π^- - ^{16}O, are shown. In each case, the data are compared to a wide spectrum of theoretical calculations, all of which agree among themselves on common values for the difference in neighboring proton or neutron distribution radii. The

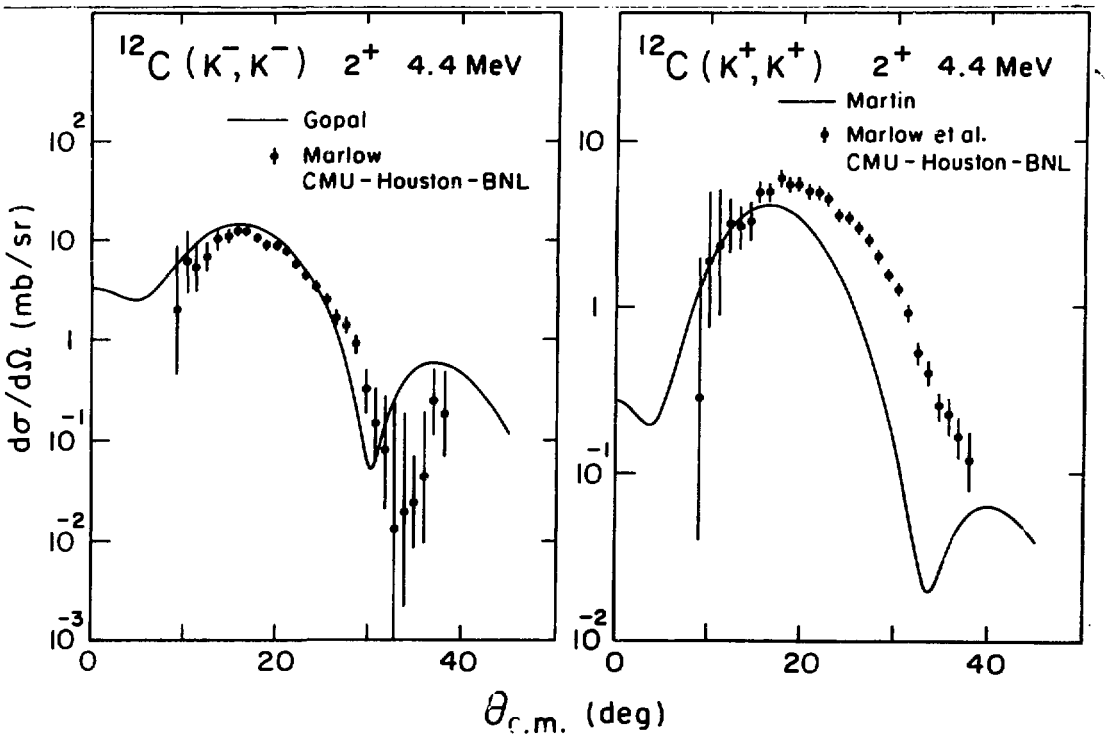

Fig. 12
$K^\pm$ - ^{12}C inelastic scattering data[42] for the 2^+ state at 4.44 MeV.

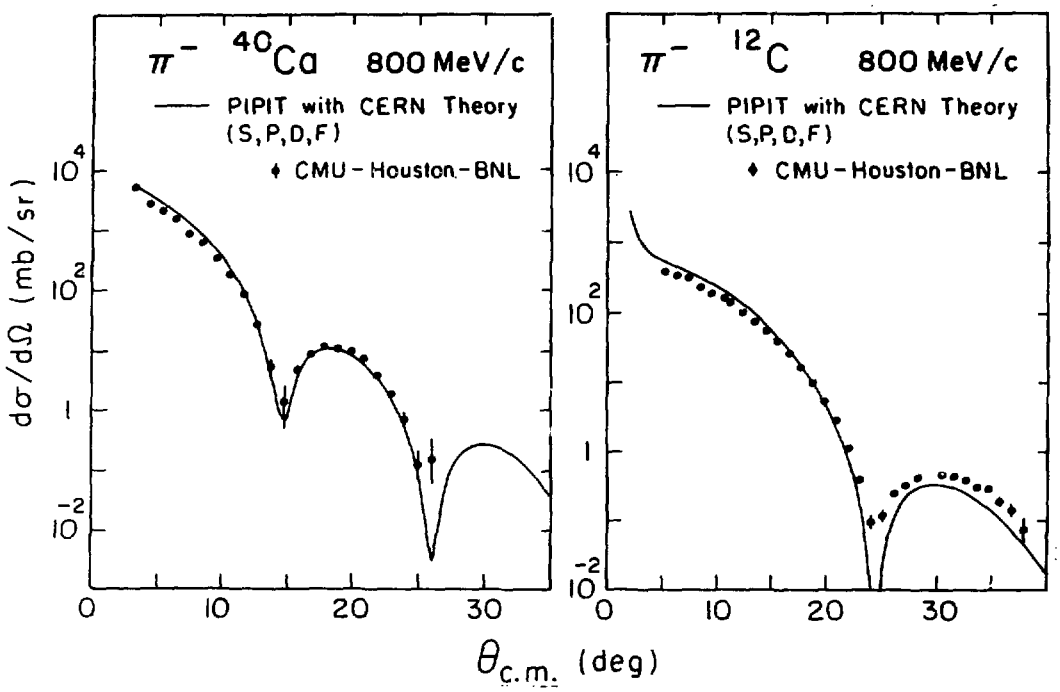

Fig. 13
π^- elastic data[42] for scattering from ^{12}C and ^{40}Ca at 800 MeV/c lab momentum.

attractive (and surprising) feature of this work is that although the πN interaction is weaker, the ratio of T=3/2 to T=1/2 amplitudes is three times larger than at resonance! Thus, it may be that low energy π scattering will become an excellent tool for exploring ground state matter distributions in nuclei.

What of the situation for inelastic scattering? As usual, the problem divides itself into two parts: (1) reaction mechanism, and (2) nuclear structure. For question (1), it appears that the interaction can be well accounted for in terms of the usual DWIA prescriptions.[59,60] Fig. 17 shows the data of Olmer, et al.[49] compared to DWIA calculations of Lee and Chakravarti.[61] The transition densities and rates used are in good agreement with other experiments and the data are seen to be well described. At the energy used in this experiment the cross section will arise almost entirely from the nuclear surface region, due both to the surface peaking of the π absorption and the transition density. Therefore, a better test of the *pion wavefunction* away from the surface region might well be at lower energies.[62]

Question (2) concerns the question of spectroscopy with pions. Again because of the isospin structure of the πN interaction, differences between π^+ and π^- scattering should arise when exciting states of mixed isospin or transitions which involve promoting only neutrons or protons. The work of Morris et al.[63] is an example of the former case in an I=0 nucleus. In studying $\pi^\pm$ inelastic scattering from ^{12}C at 162 MeV, these workers discovered two 4^- states [19.25 MeV (T=0) and 19.65 MeV (T=1)] which show differing sensitivity to π^+ or π^- (see fig. 18). The difference spectrum for the yield curves shows

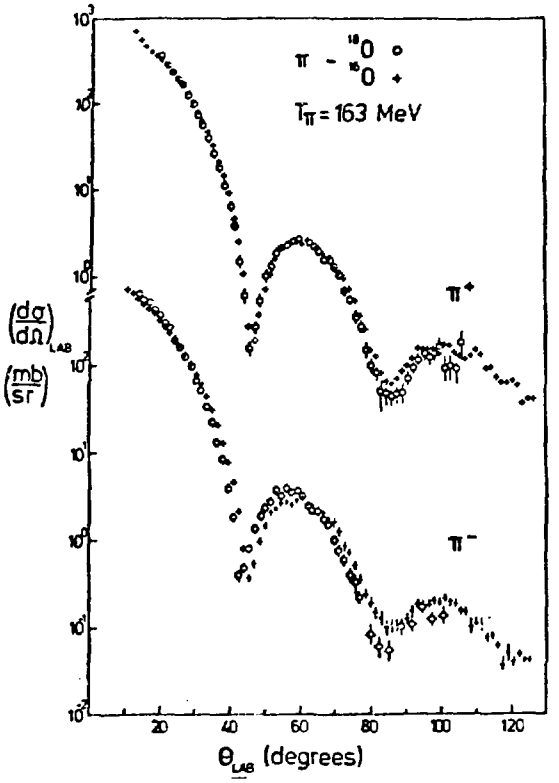

Fig. 14
$\pi^{\pm}$ elastic data[41] for scattering from ^{16}O and ^{18}O. The π^- data show clear sensitivity to the size difference between the two nuclei.

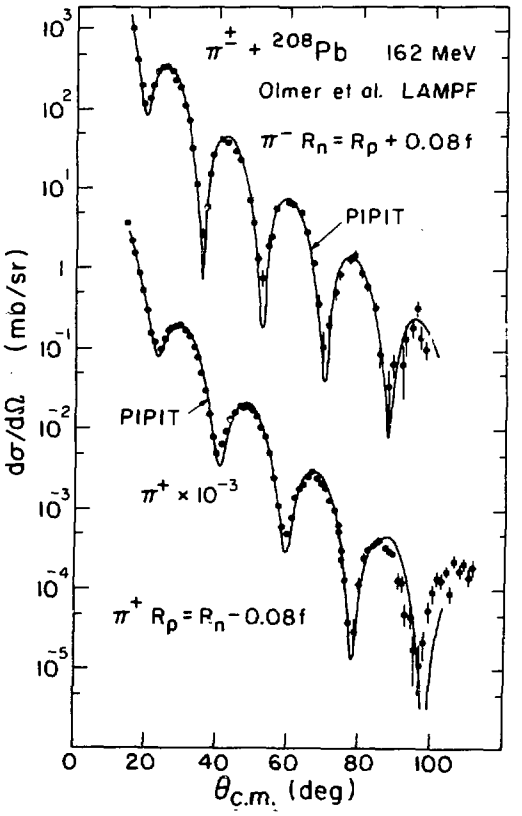

Fig. 15
$\pi^{\pm}$ - ^{208}Pb elastic data[49] compared to PIPIT[28] calculations with corrections for binding energy, Coulomb shifts and nucleon size.

the strong effects which arise due to the isospin mixing of the two 4^- states. This is due to the large non-diagonal Coulomb matrix element connecting them. Shell model calculations can generate about the same mixing strength as is seen experimentally in this, and other[64] cases.

As a last example, consider the work of Dehnhard et al.[65] which involved scattering of π^+ and π^- from ^{13}C. The results are shown in fig. 19. Of special interest is the excitation, by π^- only, of the pure neutron state at 9.5 MeV. This state is most likely to be a stretched $d_{5/2} - p_{3/2}^{-1}$ configuration since the angular distribution corresponds to an M4. The very clear signature of this state indicates the efficiency of pion scattering for determining the detailed structure of certain nuclear states.

V. Absorption and Photoproduction

A principal feature distinguishing meson from nucleon reactions is the possibility of meson absorption and production. This process is of interest

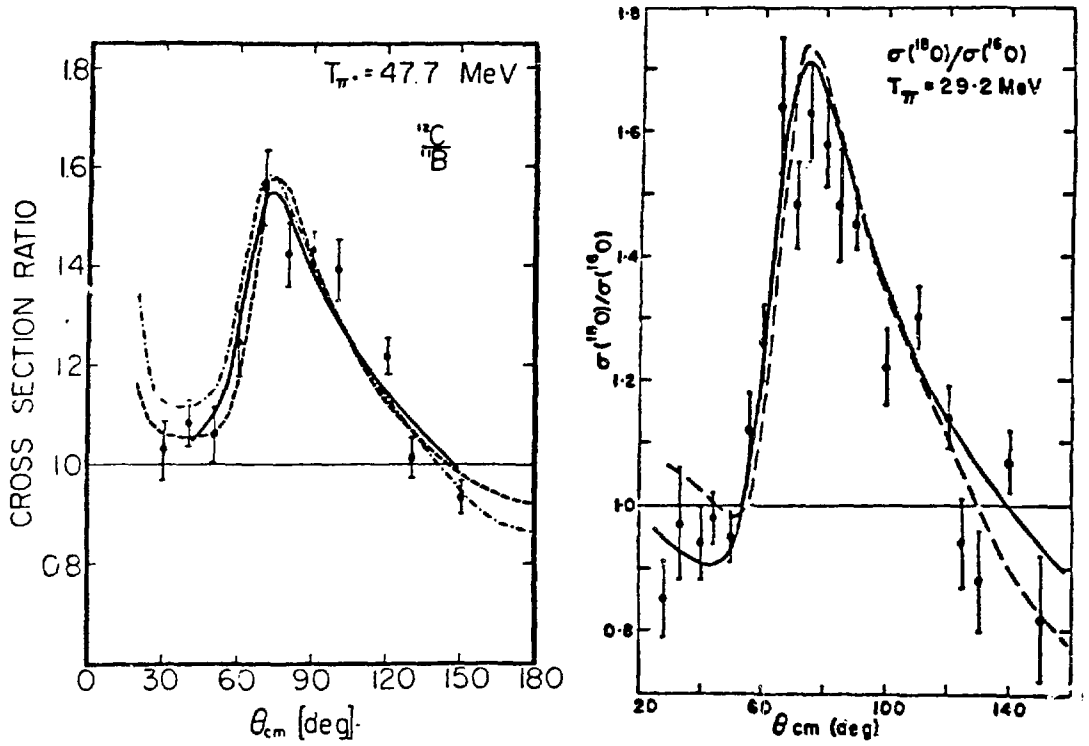

Fig. 16
Results for the elastic ratios of π^+ scattering from ^{12}C and ^{11}B (curve (a), ref. [53]) and π^- scattering from ^{18}O and ^{16}O (curve (b), ref. [54]).

to nuclear physics because of the large energy and momentum transfers available, which potentially allow examination of nuclear wavefunctions in a region for which no information exists at present.

The current status of the (π,p) and (p,π) reactions has been reviewed recently by Fearing[66] and by Miller and Measday.[67] Quite a lot of data exist for low and moderate π energies, on a wide range of nuclei, taken at Uppsala, Saclay, IUCF, LAMPF and TRIUMF. These include data taken with polarized protons from TRIUMF. (See ref. 68.)

Much of the effort to describe the (π^+,p) data and its inverse has focussed on the "pionic stripping" model shown diagrammatically in fig. 20. However, because of the many uncertainties in the model and the large number of adjustable parameters, the systematics of the data have not been successfully described. The model is limited in a fundamental way since a two-nucleon absorption mechanism is *required* to describe the (π^-,p) data, and also, apparently, the observed polarization asymmetries. These are quite large and appear to be a universal feature independent of nucleus. This suggests that perhaps a $\pi d \rightarrow pp$ mechanism is a primary feature of the overall reaction.

Although some features of a two-nucleon mechanism are included in the ONM via incoming and outgoing distortions, it is desirable to make certain features of it explicit in the calculation. The principal one of these is the rescattering mechanism shown in fig. 20, which is known to be important at all

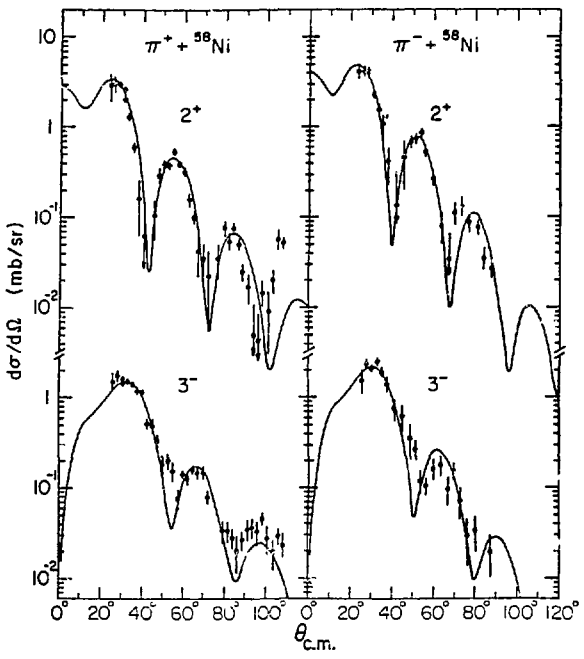

Fig. 17
$\pi^{\pm}$ - ^{58}Ni scattering[49] from the first 2^+ and 3^- states. Solid curves are the results of DWIA momentum space calculations.[61]

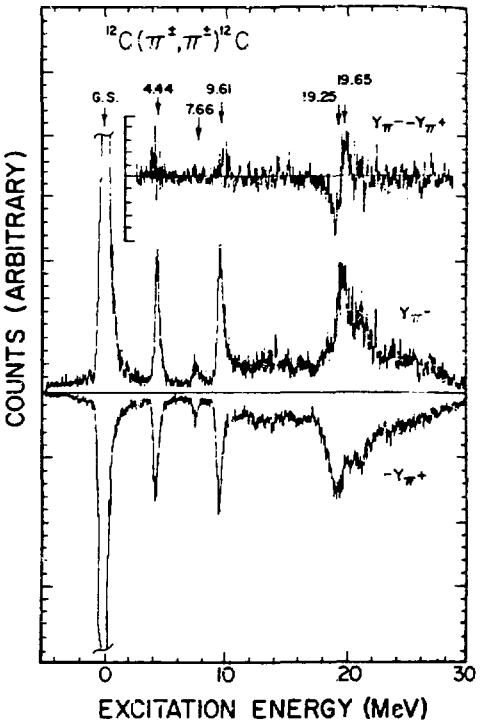

Fig. 18
$\pi^{\pm}$ - ^{12}C inelastic spectra at 162 MeV from ref. [63].

energies at which experiments have been done. Another advantage of the model over the ONM is that momentum sharing is available, and no single nucleon is required to absorb all of it. The incoming and outgoing distortions are made without including the presence of the (3,3) channel and are shown as dashed ovals in the figure. Since doorway theory provides in a natural way for isobar formation in the incoming channel, it is well suited to describing this interaction, including also the possibility for non-resonant processes to occur. Calculations stressing these ideas are being done by Keister and Kisslinger.[68]

As a final topic, the photoproduction of pions is considered. Excellent reviews of the subject can be found in the work of Singham and Tabakin[70] and the compendium edited by Stoler.[71]

One of the most attractive features of this work is the crisp combination of what is well known with what is not so well known. This can be seen in the construction of the production amplitude

$$T(\gamma,\pi) \sim \langle J_i M_i ; \gamma(\vec{k}) | H_{BL} | J_f M_f ; \pi(\vec{q}) \rangle \ . \qquad (6)$$

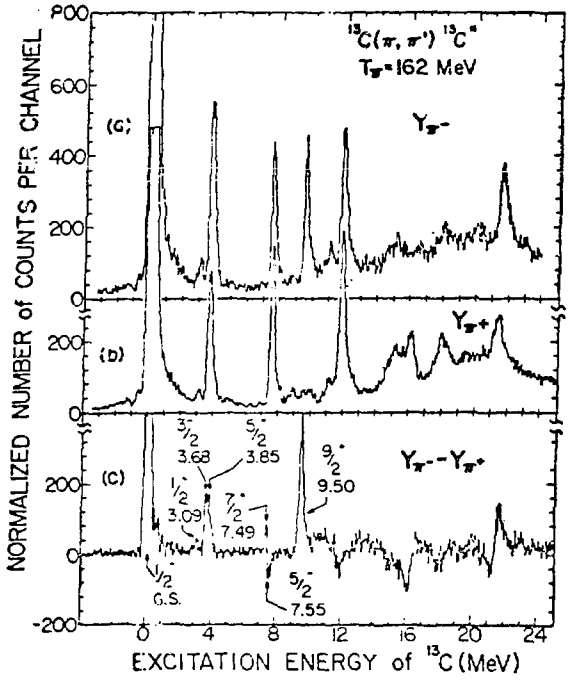

Fig. 19
$\pi^{\pm}$ - ^{13}C inelastic spectra at 162 MeV from ref. [63].

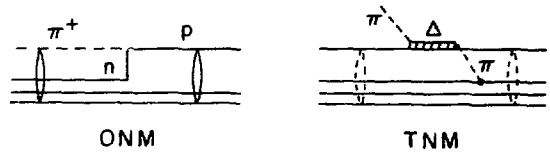

Fig. 20
Diagrams showing the basic (π,p) one- and two-nucleon mechanisms. The incoming and outgoing distortions used are described in the text.

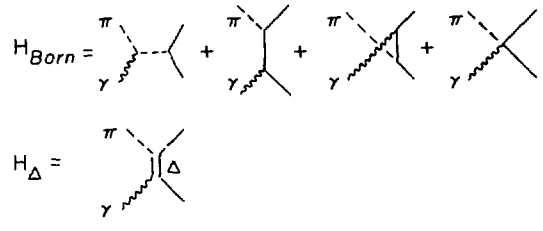

Fig. 21
Diagrams included in the Blomqvist-Laget[72] π photoproduction operator.

In this expression, the initial wavefunctions and the production operator are "well known", while the final nuclear state and the π wavefunction are not so well known. Thus, a good method exists for learning about the latter.

A central feature of the calculation is the Blomqvist-Laget[72] photoproduction operator H_{BL} goes over to the usual Kroll-Ruderman term, $G_1 \vec{\sigma} \cdot \vec{\epsilon}$. Use of the full BL operator with appropriate pion distortions has given good agreement with the data (see refs. 70, 71, 73).

A very interesting application of these ideas to the inverse (π,γ) process has been made by Reynaud and Tabakin[74] in their study of ^{15}N(π,γ)^{15}O. For pions incident at 50 MeV, there turns out to be a destructive interference between the leading Kroll-Ruderman term and the pion pole term shown in fig. 21. Results with π distorted waves but only these two terms are shown on the right of fig. 22; the interference effect is very large. The left side of the figure shows that when all BL terms are included with π distortions the effect is still dramatic but somewhat mitigated. The interest in these calculations is that should pion condensate precursor phenomena be present, the role of the pion pole term would dramatically increase and alter substantially the predicted cross section. This could conceivably be a firm signature of these processes and as such would open the door to the study of a new phase of nuclear matter. That would be a fitting way to dedicate a new (31 GeV?) meson physics facility!

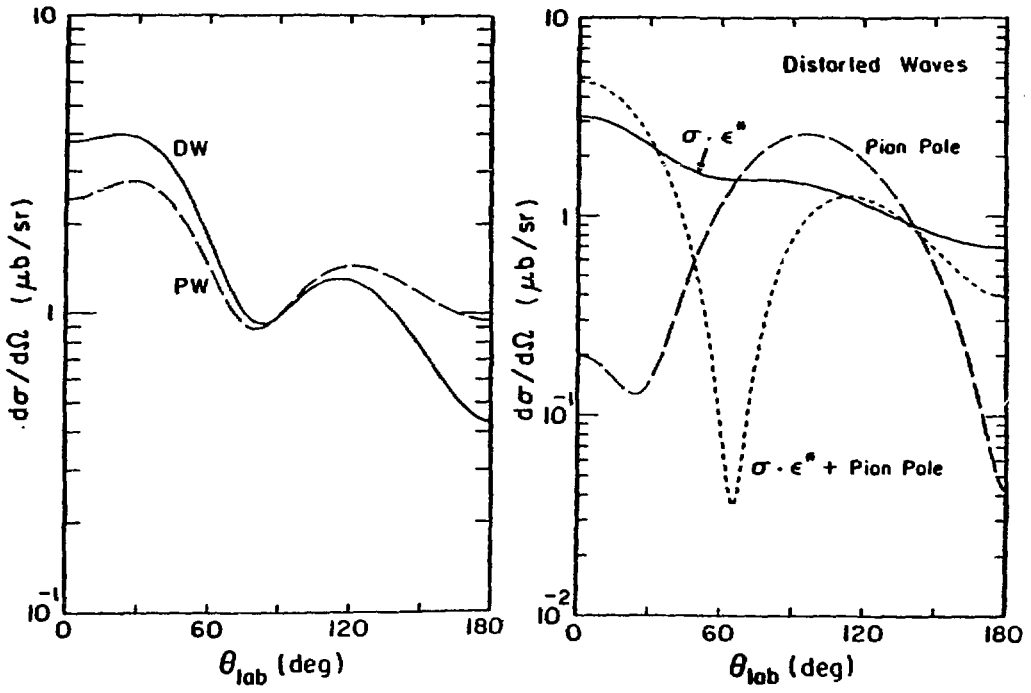

Fig. 22
Calculations of Reynaud and Tabakin[74] for $^{15}N(\pi,\gamma)^{15}O$ at 50 MeV pion energy. See text.

VI. Conclusions

The study of meson-nucleus interactions is in its infancy. Nonetheless, the examples described above show that the field holds rich promise and much diversity. In particular, we are beginning to learn in some detail how it is that mesons interact and propagate in nuclei, and how their properties (and those of the hadronic resonances formed) are modified in nuclear matter. In the cases studied so far, these particles are apparently less bound and have enhanced decay widths compared to their free values. More systematic information is necessary before firm conclusions can be drawn about this very interesting question.

In the course of this work, better dynamical theories have been developed to understand better the basic interactions. In this regard, doorway ideas are beginning to display fully their "comparative advantages" over more traditional calculations. This is especially true now that better computational techniques are available.

Studies with mesons are beginning to fulfill their promise as probes of nuclear structure and spectroscopy. Pion experiments have shown great sensitivity to both neutron and proton distributions in nuclei, both for ground- and

excited states. It is very interesting that this sensitivity is not as large at (3,3) resonance energies as it is at 40 MeV! However, since the connection between matter density and optical potential is not entirely clear, there is still some reservation regarding use of this probe as a measure of density information.

Finally, the current situation in pion absorption and photoproduction was noted briefly. In the former case a large body of cross section and polarization data exists, which is ill described by current one-nucleon absorption models. Since it is known that pion rescattering plays an important (perhaps dominant) role in this process, there is much interest in the development of two-nucleon mechanisms. Although these calculations are difficult, the work is in progress.

A major attraction of photoproduction is that it allows one to focus on pion dynamics in a situation that is better understood than usual. With the insertion of the Blomqvist-Laget photoproduction operator into a detailed nuclear structure calculation, good agreement with data is found in many cases. A tantalizing hope for the future is that careful photoproduction studies will become useful tests for the precursors of pion condensation.

VII. Acknowledgements

I would like to thank Peter Barnes, Leonard Kisslinger and Frank Tabakin for much time spent discussing the above subject. I would also like to thank Bob Chopnak, Maria Markwell and Francis Megahan for crucial assistance in the preparation of this paper.

REFERENCES

* Work supported in part by USDOE grant DE-AC02-76ERO 3244.A006.

1. J. M. Eisenberg and D. S. Koltun, *Theory of Meson Interactions with Nuclei*, John Wiley (1980).

2. J. Hufner, Phys. Repts. 21 (1975) 1.

3. F. Lenz, "Aspects of the π-Nucleus Interaction," SIN 2/77-100 320-430.

4. G. E. Brown, B. K. Jennings and V. I. Rostokin, Phys. Repts. 50C (1979) 227.

5. N. Barash-Schmidt, et al., Rev. Mod. Phys. 52 (1980).

6. A. S. Carroll et al., BNL Report No. 17915 (1973).

7. B. R. Martin, Nuc. Phys. B94 (1975) 413.

8. C. B. Dover and G. E. Walker, Phys. Rev. C19 (1979) 1393.

9. C. B. Dover and P. J. Moffa, Phys. Rev. C16 (1977) 1087.

10. S. R. Cotanch, *Proceedings of the Kaon Factory Workshop*, Vancouver, 1979 (TRIUMF Pub. 79-1).

11. M. Betz and T.-S. H. Lee, Phys. Rev. C23 (1981) 375.

12. L. Heller, in *Meson-Nuclear Physics-1976*, AIP Conference Proceedings No. 33, American Institute of Physics.

13. M. K. Banerjee and J. B. Cammarata, Phys. Rev. D19 (1979) 145.

14. G. A. Miller, in *Meson-Nuclear Physics-1979*, AIP Conference Proceedings No. 54, American Inst. of Physics.

15. J. V. Noble, Nuc. Phys. A329 (1979) 354.

16. C. B. Dover and R. H. Lemmer, Phys. Rev. C7 (1973) 2312.

17. L. Foldy and J. Walecka, Ann. Phys. 54 (1969) 447.

18. W. R. Gibbs, A. T. Hess and W. Kaufman, Phys. Rev. C13 (1976) 1982.

19. L. S. Kisslinger, Phys. Rev. 98 (1955) 761.

20. M. M. Sternheim and E. H. Auerbach, Phys. Rev. Lett. 25 (1970) 1500.

21. R. Landau, S. Phatak, and F. Tabakin, Ann. Phys. 78 (1973) 299.

22. K. Stricker, H. McManus, J. A. Carr, Phys. Rev. C19 (1979) 929.

23. L. C. Liu and C. M. Shakin, Phys. Rev. C16 (1977) 1963.

24. R. H. Landau and A. W. Thomas, Nuc. Phys. A302 (1978) 461.

25. N. DiGiacomo, A. Rosenthal, E. Rost and D. Sparrow, Phys. Letts. 66B (1977) 421.

26. R. A. Eisenstein and G. A. Miller, Comp. Phys. Commun. 8 (1974) 130.

27. M. D. Cooper and R. A. Eisenstein, "FITPI," Los Alamos Report LA-5929-MS (unpublished).

28. R. A. Eisenstein and F. Tabakin, Comp. Phys. Commun. 12 (1976) 237.

29. A. S. Rosenthal and F. Tabakin, Phys. Rev. C12 (1980) 711.

30. H. Feshbach, A. Kerman, and R. Lemmer, Ann. Phys. 41 (1967) 230.

31. L. S. Kisslinger and W. L. Wang, Ann. Phys. 99 (1976) 374.

32. M. Hirata, J. H. Koch, F. Lenz and E. J. Moniz, Ann. Phys. 120 (1979) 205.

33. Y. Horikawa, M. Thies and F. Lenz, MIT Preprint CTP #844.

34. K. Klingenbeck, M. Dillig and M. Huber, Phys. Rev. Lett. 41 (1978) 387.

35. E. Oset and W. Weise, Nuc. Phys. A329 (1979) 365.

36. R. A. Freedman, G. A. Miller and E. Henley, Univ. Washington Preprint RLO-1388-842.

37. L. S. Kisslinger, Phys. Rev. 22 (1980) 1202.

38. L. S. Kisslinger, Proceedings of the 15th Annual Los Alamos User's Group Meeting, to be published.

39. A. Bouyssy, Phys. Lett. 84B (1979) 41.

40. F. Becchetti and G. Greenlees, Phys. Rev. 182 (1969) 1190.

41. J. Jansen, J. Zichy, J. P. Albanese, J. Arvieux, J. Bolger, E. Boschitz, C. Ingram, and L. Pflug, Phys. Lett. 77B (1978) 359.

42. D. Marlow, P. Barnes, N. Colella, S. Dytman, R. Eisenstein, F. Takeutchi, W. Wharton, S. Bart, R. Hackenberg, D. Hancock, E. Hungerford, B. Mayes, L, Pinsky, T. Williams, R. Chrien, H. Palevsky, R. Sutter, in progress.

43. A. S. Rosenthal and F. Tabakin, private communication. See also ref. 29.

44. M. Alston-Garnjost, R. Kenney, D. Pollard, R. Ross, R. Tripp and H. Nicholson, Phys. Rev. D17 (1978) 2226.

45. G. Gopal, R. Ross, A. Van Horn, A. McPherson, E. Clayton, T. Bacon and I. Butterworth, Nuc. Phys. B119 (1977) 362.

46. Y. Sakamoto, Y. Hatsuda and F. M. Toyama, Kyoto (Preprint).

47. "πN Partial Wave Amplitudes," Lawrence Radiation Lab UCRL-20030 πN.

48. M. M. Sternheim and K.-B. Yoo, Phys. Rev. Letts. 41 (1978) 1781.

49. C. Olmer, D. Geesaman, B. Zeidman, S. Chakravarti, T.-S. H. Lee, R. Boudrie, R. Siemssen, J. Amann, C. Morris, H. Thiessen, G. Burleson, M. Devereux, R. Segel, and W. Swenson, Phys. Rev. C21 (1980) 254.

50. J.-F. Germond and C. Wilkin, Nuc. Phys. A237 (1975) 477.

51. H. A. Bethe and M. Johnson, Comments. Nuc. Part. Phys. 8 (1978) 75.

52. J.-F. Germond and M. Johnson, Phys. Rev. C22 (1980) 1622.

53. B. M. Barnett, et al., U. Colorado preprint.

54. R. R. Johnson, B. Bassalleck, K. Erdman, B. Gyles, T. Marks, T. Masterson, D. R. Gill, and C. Sabev, Phys. Lett. 78B (1978) 560.

55. S. A. Dytman, J. F. Amann, P. D. Barnes, J. N. Craig, K. G. R. Doss, R. A. Eisenstein, J. D. Sherman, W. R. Wharton, G. R. Burleson, S. L. Verbeck, R. J. Peterson and H. A. Theissen, Phys. Rev. C18 (1978) 2316.

56. G. W. Hoffman, in "Nuclear Structure with Intermediate Energy Probes," Los Alamos Pub. LA-8303-C, page 99.

57. J. W. Negele and D. Vautherin, Phys. Rev. C5 (1972) 1472.

58. A. W. Thomas, Intl. Conf. on Nuc. Phys., Berkeley (TRIUMF preprint TRI-PP-80-22).

59. R. A. Eisenstein and G. A. Miller, Comp. Phys. Commun. 11 (1976) 95.

60. T.-S. H. Lee and F. Tabakin, Nuc. Phys. A226 (1974) 253.

61. S. Chakravarti and T.-S. H. Lee, unpublished.

62. S. A. Dytman, et al. (see ref. 55), Phys. Rev. C19 (1979) 971.

63. C. L. Morris, J. Piffaretti, H. A. Thiessen, W. Cottingame, W. Braithwaite, R. Joseph, I. Moore, D. Holtkamp, C. Harvey, S. Greene, C. Moore, R. Boudrie, and R. Peterson, Phys. Lett. 86B (1979) 31.

64. D. B. Holtkamp, W. Braithwaite, W. Cottingame, S. Greene, R. Joseph, C. Moore, C. Morris, J. Piffaretti, E. Siciliano, H. Thiessen, and D. Denhard, Phys. Rev. Lett. 45 (1980) 420.

65. D. Dehnhard, S. Tripp, M. Franey, G. Kyle, C. Morris, R. Boudrie, J. Piffaretti, and H. Thiessen, Phys. Rev. Lett. 43 (1979) 1091.

66. H. Fearing, Prog. in Particle and Nuc. Phys. (to be published).

67. D. F. Measday and G. A. Miller, Univ. Washington Preprint RLO-1388-772.

68. R. D. Bent, in ref. 56, page 208.

69. B. D. Keister and L. S. Kisslinger (private communication).

70. M. Singham and F. Tabakin, Ann. Phys. (to be published).

71. P. Stoler, *Photopion Nuclear Physics*, Plenum, (N.Y.).

72. I. Blomqvist and J. Laget, Nuc. Phys. A280 (1977) 405.

73. P. Bosted, K. Blomqvist, A. Bernstein, S. Dytman and R. Miskimen, Phys. Rev. Lett. 45 (1980) 1544.

74. W. Reynaud and F. Tabakin, University of Pittsburgh Preprint (1980).

I=1 DIBARYONS - THEORETICAL

by

W. M. Kloet
Department of Physics and Astronomy, Rutgers University
New Brunswick, New Jersey 08903, U.S.A.

ABSTRACT

New data analyses predict resonance poles close to the NΔ branchcut. Model calculations show $^3F_3$ and $^1D_2$ phase parameters in qualitative agreement with the data, but cannot make definitive statements about resonances yet. They show, however, that counterclockwise loops in Argand diagrams are not always resonances.

I. INTRODUCTION

Initial evidence in favor of I=1 dibaryon resonances was based on measurements of $\Delta\sigma_l$ (Fig. 1), $\Delta\sigma_T$ (Fig. 2), and C_{LL} (Fig. 3).[1] The observed structure was interpreted as due to $^1D_2(2140)$, $^3F_3(2260)$, and possibly $^1G_4(2430)$ resonances.[1-3]

Hoshizaki's phaseshift analysis,[4] including the above data, shows rapid variations in particular in the $^1D_2$ and $^3F_3$ phases (see Fig. 4). A Breit-Wigner parametrization gives mass M = 2.17 GeV, a width Γ = 50-100 MeV (Γ_{el}/Γ = 0.1) for $^1D_2$ and M = 2.22 GeV, Γ = 100-250 MeV (Γ_{el}/Γ = 0.2-0.4) for $^3F_3$.

Arndt and VerWest[5] do an energy-dependent phase shift analysis up to 850 MeV (see Fig. 5). They find a much smoother energy behavior but also find counterclockwise looping in the argand diagrams of $^1D_2$ and $^3F_3$.

Grein and Kroll[6] use dispersion relations to construct the three forward helicity amplitudes. Defining $\sigma_{tot} = 4\pi/p_L$ Im F_1, $\Delta\sigma_T = -4\pi/p_L$ Im F_2, $\Delta\sigma_L = 4\pi/p_L$ Im F_3, dispersion gives the real parts of F_1, F_2, and F_3. Input for this method consists of the pp total cross sections and some assumptions about Im $F_i(\omega)$ for $\omega<0$. The Argand diagrams for F_2 and F_3 show a looping behavior. Again a Breit Wigner parametrization leads to a $^3F_3$ resonance at 2.37 GeV with Γ = 250 MeV and a pin singlet (possibly $^1G_4$) at 2.39 GeV with Γ = 100 MeV.

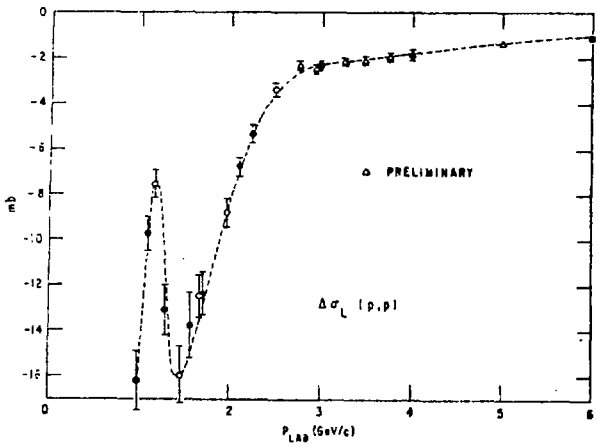

Fig. 1. Proton-proton total cross section difference $\Delta\sigma_L$(pp), Ref. 1.

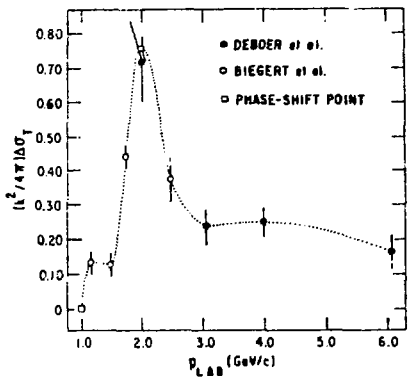

Fig. 2. Proton-proton total cross section difference $\Delta\sigma_T$(pp), Ref. 1, expressed as $(k^2/4\pi)\Delta\sigma_T$.

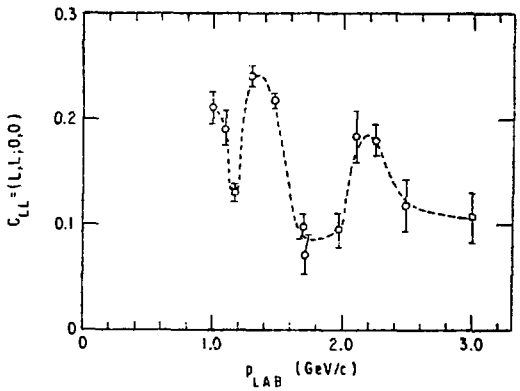

Fig. 3. C_{LL} at $\theta_{cm} = 90^0$ for proton-proton scattering, Ref. 1.

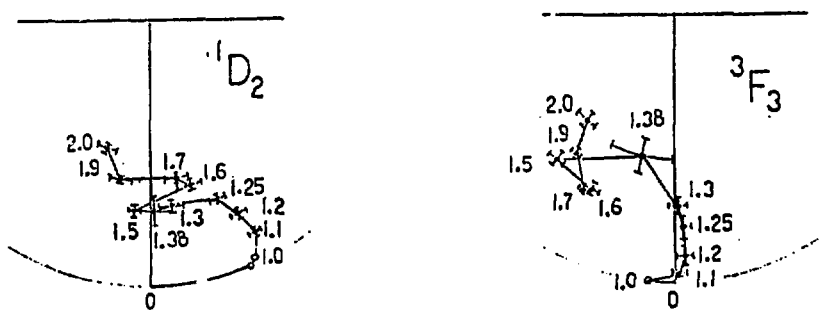

Fig. 4. Argand diagrams for $^1D_2$ and $^3F_3$ pp partial waves for Hoshizaki's phaseshift analysis, Ref. 4. Numbers are laboratory momenta in GeV/c.

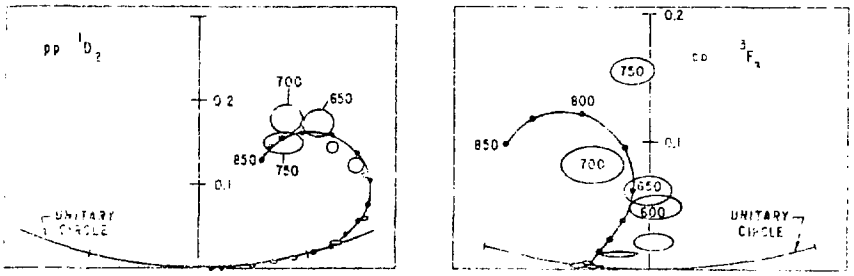

Fig. 5. Argand diagrams for $^1D_2$ and $^3F_3$ pp partial waves for Arndt and VerWest's phaseshift analysis (Ref. 5). Numbers are laboratory energies in MeV. Curves are results of energy dependent analysis.

Bugg[7] noticed a discrepancy in the predictions for Re F_3 by Grein and Kroll based on the Argonne $\Delta\sigma_L$ data and the phaseshift analysis of 264-516 MeV TRIUMF data. A Recent TRIUMF measurement of $\Delta\sigma_L$ indeed has shown that differences of 1-1.5 mbarn exist between Argonne-$\Delta\sigma_L$ and TRIUMF-$\Delta\sigma_L$. For Bugg this has resolved the discrepancy but it may indicate that earlier phaseshift analyses,[4,5,8] which could accommodate the Argonne data, have too much freedom in them.

II. ANALYSIS

Apart from some discrepancies in the earlier data and further new results to come from the measurements at Los Alamos, a basic problem remains how to interpret the phase shifts in terms of dibaryon resonances. Analytic continuation of the scattering amplitude away from the real axis by a Breit-Wigner parametrization is too crude since it ignores the cut-structure of the complex energy plane. Two recent attempts to overcome this problem will be discussed.

Edwards and Thomas[9] use a K-matrix parametrization for a two-channel problem. One channel is NN, the second channel contains NNπ and NΔ. For this case there are three cuts in the energy plane. The K-matrix is related to the (2*2) T-matrix by $T = K\,(1-CK)^{-1}$. C is the Chew-Mandelstam function. It is completely determined by the particle masses and the total energy. K is assumed to be a meromorphic function of the energy. It is parametrized by $K_{ij} = a_{ij} + b_{ij}\,s + c_{ij}\,s^2$. The actual input available is one element of the T-matrix, T_{11}, for real values of s, which has to be fitted by the nine parameters a_{ij}, b_{ij}, c_{ij}. The poles in T are then found from the zeros in (1-CK).

For $^1D_2$ one pole is found, located on the second sheet of the NN cut, the second sheet of the NNπ cut, and the first sheet of the NΔ cut. Using four

different fits to the $^1D_2$ phase shifts of Hoshizaki[4] and Arndt et al.[5] the pole positions are respectively M_R = 2.17 - 0.062i, 2.14 - 0.054i, 2.14 - 0.106i, and 2.14 - 0.054i GeV. One should note that all poles (except for the third case) are very close to the NΔ branch point that occurs at 2.149 - 0.050i GeV.

In a similar analysis Arndt[10] reports finding a $^1D_2$ pole at M_R = 2.165 - 0.056i and a $^3F_3$ pole at M_R = 2.186 - 0.072i GeV.

A comparison with Breit-Wigner parametrizations shows agreement for $^1D_2$ but a very different $^3F_3$. The Breit-Wigner fit is certainly more suspect because it ignores the cut structure. It assumes an interpretation as in Fig. 6a, where the pole is directly below the location on the real axis where a peak in the cross section is observed. The K-matrix analysis for $^3F_3$ gives the interpretation as in Fig. 6b, where a second sheet pole below the branch point has to detour around the ℓ = 1 angular momentum barrier in order to make its influence felt on the real axis.

A further analysis using the K-matrix could be improved if data for T_{12} (NN→NNπ) become available.

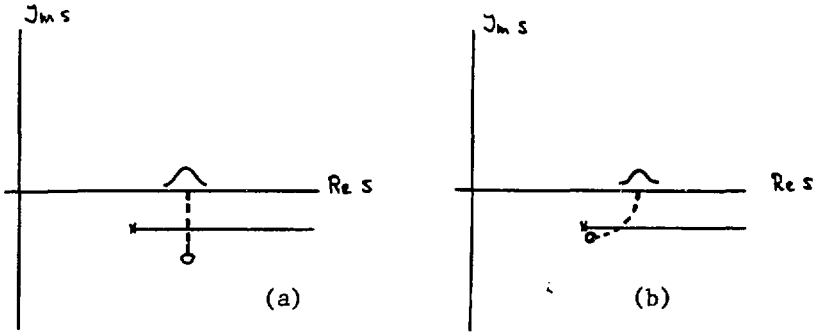

Fig. 6. Location of resonance pole in complex s-plane for Breit Wigner fit (a) and for the K-matrix method (b).

III. MODEL PREDICTIONS

Several calculations of spin-dependent cross sections have appeared in the literature.[2,11-16] In this report, however, we restrict ourselves to explicit predictions for the $^3F_3$ and $^1D_2$ partial wave phase parameters.

Araki, Koike, and Ueda[17] present results for a Faddeev calculation of the NNπ system. The πN subsystem interacts via P_{11} and P_{33}, and the NN subsystem interacts via $^3P_2$. The $^3P_2$ component of the NN interaction is chosen because, in

the $J^{\pi} = 3^{-}$ NNπ system, it is the only strongly attractive NN force. Results for $^3F_3$ are shown in Fig. 7. Both the 3-channel and the full 9-channel calculation show resonating behavior for the phase shift δ and the inelasticity parameter η. The data points are Hoshizaki's phase shifts.[4]

Silbar and I have followed a different approach.[18] We first solved the Faddeev NNπ problem where the πN subsystem interacts via P_{11} and P_{33}. This model can be viewed as an extension of a two-nucleon one-pion-exchange model. The extension includes non-static pion exchange, intermediate NN and NΔ states with self-energy pion bubbles. Both features are related by unitarity. The model at this point contains effectively the long range NN-force due to pion exchange as well as part of the medium range force due to the NΔ intermediate states. Subsequently the short range part of the NN interaction was introduced by static heavy-boson-exchange, whose parameters are fitted to the low-energy phase shifts for $\ell>1$. The results for $^1D_2$ and $^3F_3$ are shown in Fig. 8. Curve A is the result without heavy bosons. Curves B, C, and D are results for three different fits of the heavy boson parameters.

In Fig. 9a the Argand diagrams are shown for the cases A-D and compared with the phase shift analysis of Hoshizaki[4] and Arndt et al.[5] It shows that conventional models, without additional dibaryon resonances, can give qualitative agreement with the $^1D_2$ and $^3F_3$ phase shifts found by Arndt et al. It is very unlikely that sharp energy variations as found by Hoshizaki (see 800-MeV region in $^3F_3$) can be accommodated by models as described above.

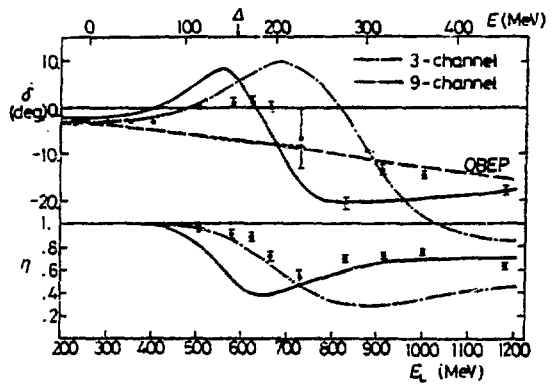

Fig. 7. $^3F_3$ phaseshifts and inelasticity of Ref. 17. Solid curve is the full 9-channel calculation. Data points are from Ref. 4.

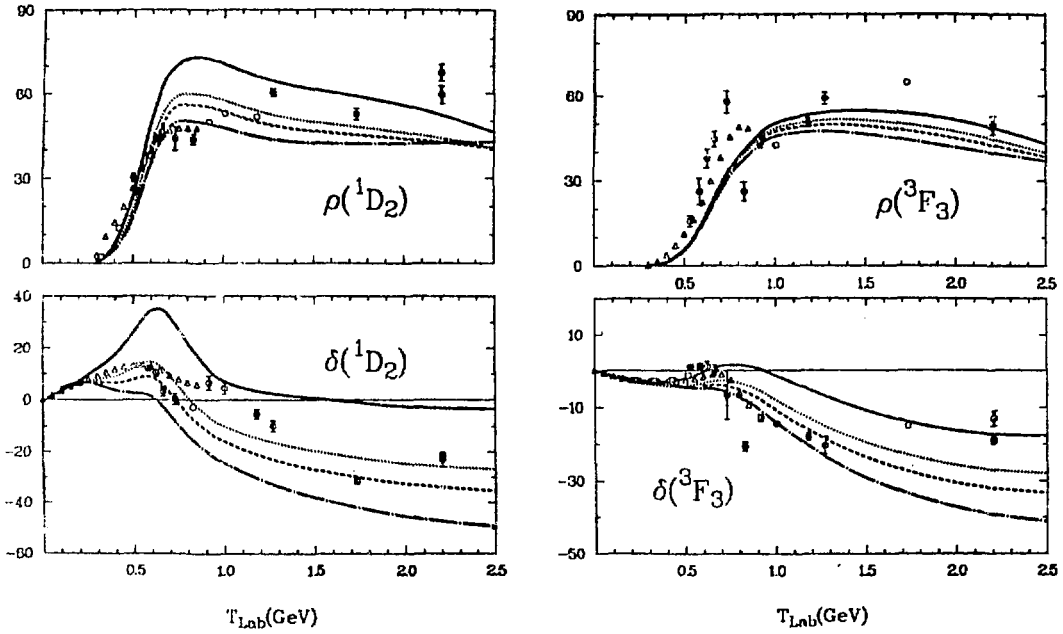

8a

$^1D_2$ phase parameters of Ref. 18.

8b

$^3F_3$ phase parameters of Ref 18.

Fig. 8. Solid curves (A) are without heavy boson exchange. Dotted (B), dashed (C), and dash-dotted (D) curves represent three different fits of heavy boson parameters.

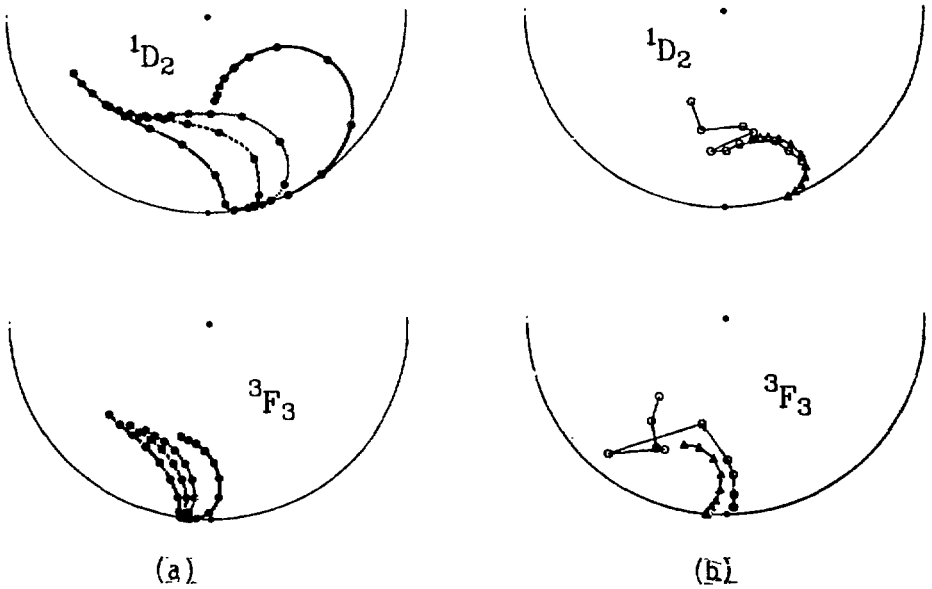

Fig. 9. Argand plots for $^1D_2$ and $^3F_3$. Curves in (a) are as in Fig. 8a. In (b) circles are from Hoshizaki (Ref. 4), triangles are from Arndt and VerWest (Ref. 5).

IV. MODEL INTERPRETATIONS

The presence of a counterclockwise loop in the Argand plot is a necessary but not a sufficient condition for the existence of a resonance, that is, a nearby pole in the second sheet. In fact, it can be shown[19] directly that the loops A and B in Fig. 9a correspond to scattering amplitudes that have no resonance poles. This can be seen by studying the multiple scattering series of the $^3F_3$ and $^1D_2$ amplitudes. In case A and B this series converges. Terms in the series are subsequently the Born term, single box diagrams, double box diagrams, etc., and we know the analytic structure of each of the separate terms. One concludes that the $^3F_3$ and $^1D_2$ scattering amplitudes have no nearby pole in the complex energy plane, because each amplitude is given by a finite sum of diagrams and none of these diagrams has a resonance pole. The same conclusion can be drawn for the $^3F_3$ amplitude of Araki, Koike and Ueda.[17] Their multiple scattering series is also convergent, although much less so than in case A, discussed above. The difference can be understood because of the added $^3P_2$ attraction.

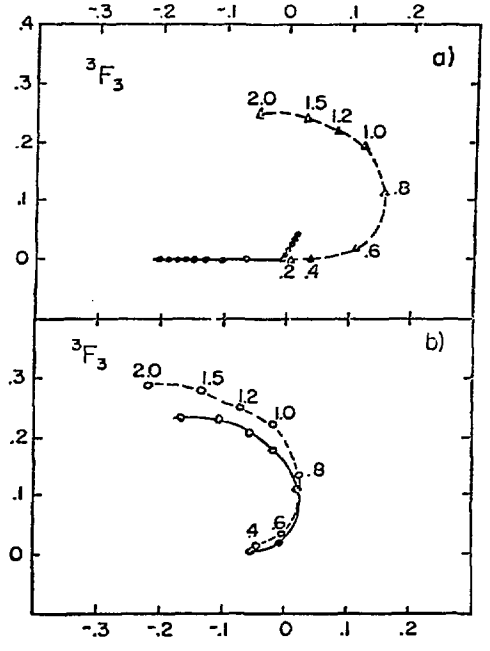

Fig. 10. $^3F_3$ contributions to Argand from Born (solid), NN-box (dots), and NΔ-box (dashed) in Fig. 10a. b) Total $^3F_3$ Argand amplitude (solid) and sum of 3 contributions of (a) dashed. T_{Lab} (GeV).

In fit D for the $^3F_3$ and fits C and D for the $^1D_2$ the multiple scattering series becomes divergent. In Ref. 19 it was argued that this still would not lead to a nearby pole because the reason for the divergence is a net additional repulsion that moves the poles even further away. In a simple model calculation we have found that this may not always be the case, if the attractive part of the heavy boson contribution is large. Therefore the pole structure of amplitudes in general can best be studied by performing the model calculation for complex energies.

It would also be very interesting to test the method of K-matrix analysis, used by Edwards and Thomas and Arndt with this type of model calculation.

The origin of the looping behavior in the Argand diagram for non-resonant

amplitudes like case A of $^3F_3$ lies in the NΔ box diagram. This diagram by itself shows a looping behavior and it dominates the total amplitude (see Fig. 10). Box diagrams were studied by a number of people.[20] They give rise to so-called pseudo-resonance behavior due to a square root singularity in s. In the model of Ref. 18 the NΔ-box and its iterates are responsible for the looping behavior of J=L partial waves. It causes peaking in these partial wave cross sections at increasing energies corresponding to the relative angular momentum of the NΔ intermediate state. In the J≠L amplitudes the effect of the NΔ-box is washed out by the NN-tensor box.

As long as the NΔ-box dominates the partial wave amplitude (such as in the high J=L waves) the T-matrix has no nearby pole. When the multiple scattering series becomes less convergent (or divergent) poles can sometimes move closer to the real axis and could be interpreted as resonances.

V. CONCLUSIONS

Speaking of dibaryon resonances one can mean two things. First it may mean a tightly "bound" two-baryon system that can only be understood in terms of a six-quark picture. As yet there is no compelling need for such an object if Arndt et al.'s energy-dependent phase shift analysis persists. However, if Hoshizaki's energy-independent phase shift analysis is confirmed, this first type of resonance may be the only explanation.

Secondly, a dibaryon resonance may mean a resonance that can be understood from conventional NN forces and the coupling to the inelastic NNπ channel. The K-matrix analysis of Refs. 9 and 10 may point in this direction because of the strong association of the poles with the NΔ branch cut.

Theoretical models should still be further improved to give better fits to the data, before they can be used to make more definitive statements about resonances.

REFERENCES

1. I. P. Auer, et al, Phys. Lett. 67B 113 (1977); Phys. Lett. 70B, 475 (1977); Phys. Rev. Lett. 41, 354 (1978); Phys. Rev. Lett. 41, 1436 (1978); I. P. Auer, High Energy Physics and Nuclear Structure, ed. D. F. Measday, et al., 193 (1979).

2. G. L. Kane, G. H. Thomas, Phys. Rev. D13, 2944 (1976).

3. K. Hidaka, et al, Phys. Lett. 70B, 479 (1977).

4. H. Hoshizaki, Prog. Theor. Phys. 60, 1796 (1978); 61, 129 (1979).

5. R. A. Arndt, B. VerWest, Polarization Symposium, Santa Fe (1980), and private communication.

6. W. Grein, P. Kroll, Nucl. Phys. B137, 173 (1978).

7. D. V. Bugg, J. Phys. G5, 1349 (1979), and talk at Lausanne (Sept. 1980); D. V. Bugg, et al, Phys. Rev. C21, 1004 (1980).

8. J. Bystricki, C. Lechanoine, F. Lehar, CEN Saclay DPhPE 79-01.

9. B. J. Edwards, G. H. Thomas, Phys. Rev. D22, 2772 (1980).

10. R. A. Arndt, Polarization Symposium, Santa Fe (1980), and private communication.

11. D. W. Joynson, J. Phys. G2, 65 (1976).

12. G. N. Epstein, D. O. Riska, AIP Conf. Proceedings 41, 542 (1977).

13. M. Arik, P. G. Williams, Nucl. Phys. B136, 425 (1978).

14. A. M. Green, J. A. Niskanen, M. E. Sainio, J. Phys. G4, 1055 (1978).

15. A. M. Green, M. E. Sainio, J. Phys. G5, 503 (1979).

16. W. M. Kloet, R. R. Silbar, preprint RU-80-239.

17. T. Ueda, Phys. Lett. 74B, 123 (1978), 79B, 487 (1978); M. Araki, Y. Koike, T. Ueda, Prog. Theor. Phys. 63, 335 (1980), and private communication.

18. W. M. Kloet, R. R. Silbar, Nucl. Phys. A338, 281,317 (1980); Phys. Ref. Lett. 45, 970 (1980).

19. W. M. Kloet, J. A. Tjon, R. R. Silbar, to be published in Phys. Lett. B.

20. M. M. Hoenig, A. S. Rinat, Phys. Rev. C10, 2102 (1974); B.L.G. Bakker, I. M. Narodetsky, Tu. A. Simonov, Lett. Nuovo, Cim. 19, 265 (1977); Yu. A. Simonov, M. van der Velde, J. Phys. G5, 493 (1979); I. M. Narodetsky, Yu. A. Simonov, Yad. Fiz. 28, 1356 (1978); Yu. A. Simonov, M. van der Velde, Phys. Lett. 76B, 277 (1978).

EXPERIMENTAL EVIDENCE FOR DIBARYONS*

by

Harold Spinka
Argonne National Laboratory

ABSTRACT

This talk will attempt to summarize some of the experimental evidence dealing with dibaryon resonances. Specific suggestions for future measurements will be made.

Several years ago it was commonly believed that resonances of two baryons, and in particular diproton resonances, did not exist. Since that time there has been a large number of nucleon-nucleon spin parameters measured at Gatchina, LAMPF, SIN, TRIUMF and the Argonne ZGS. Evidence for the existence of dibaryons was found in spin-dependent pp total cross section data from the ZGS, combined with previous polarization and differential cross section results. Both the measurements and the interpretation were challenged and the experiments were repeated. I would like to try to summarize the experimental situation as it stands today and to make comments about the existence of dibaryons from an experimenter's point of view. Professor Kloet will discuss dibaryons from a theoretician's view.

1. EVIDENCE FOR S=0, I=1 NN DIBARYONS

A. Total Cross Sections

Figures 1 and 2 give the three experimental total cross sections for the pp system:

$$\sigma^{Tot} = 1/2[\sigma^{Tot}(\uparrow\downarrow) + \sigma^{Tot}(\uparrow\downarrow)]$$

$$= 1/2[\sigma^{Tot}(\uparrow\uparrow) + \sigma^{Tot}(\uparrow\uparrow)]$$

$$\Delta\sigma_T = \sigma^{Tot}(\uparrow\uparrow) - \sigma^{Tot}(\uparrow\uparrow)$$

$$\Delta\sigma_L = \sigma^{Tot}(\uparrow\downarrow) - \sigma^{Tot}(\uparrow\downarrow)$$

* Work supported by the U.S. Department of Energy.

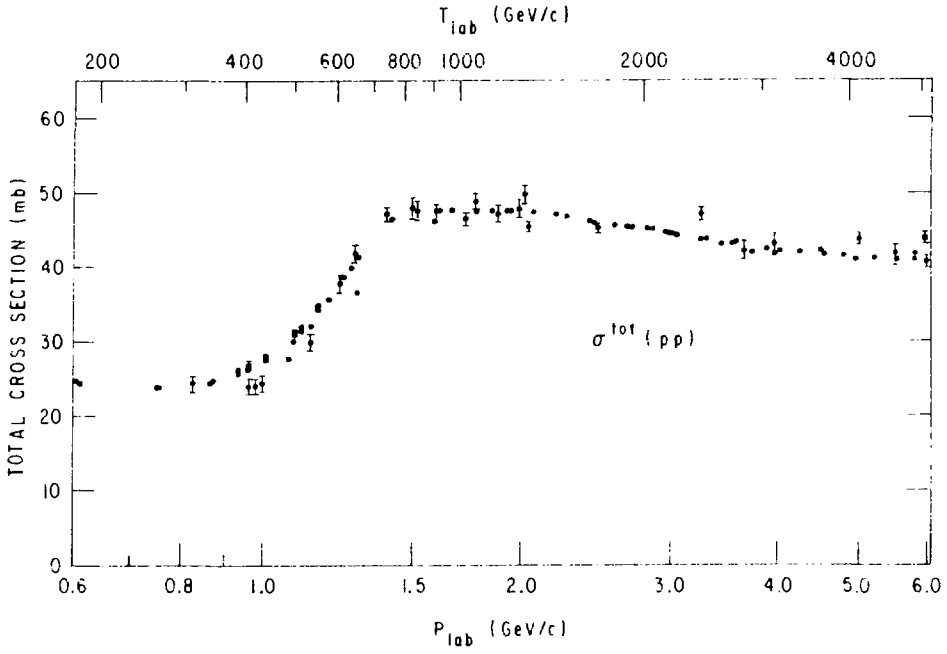

Fig. 1
Experimental measurements of the spin-averaged pp total cross section from Refs. 1 and 2. For clarity, results with errors larger than ± 1.5 mb were excluded.

where σ^{Tot} is the spin-averaged total cross section, previously measured at many accelerators.[1,2] The quantity $\Delta\sigma_T$ is the difference in total cross sections for beam and target transversely polarized. It has been measured by the University of Michigan[3,4] and the Rice University[5-7] groups at the ZGS, by the BASQUE group at TRIUMF,[8,9] and by the Rice group at LAMPF.[10] The quantity $\Delta\sigma_L$ is the difference in total cross sections for beam and target longitudinally polarized (the arrows denote the spin directions in the laboratory frame). It has been measured in a series of experiments by the ANL polarized target group at the ZGS[11-16] and at LAMPF[17], by the BASQUE group at TRIUMF,[9] and by the University of Geneva group at SIN.[18]

The following comments apply to these data:

1. The spin-averaged pp total cross section should be measured to better accuracy and with finer energy steps,[19] especially at the meson factories. At this time there does not seem to be evidence for narrow dibaryon states (except the deuteron). However, there are several energy regions where a narrow resonance may have escaped detection in σ^{Tot}. The search for narrow states is

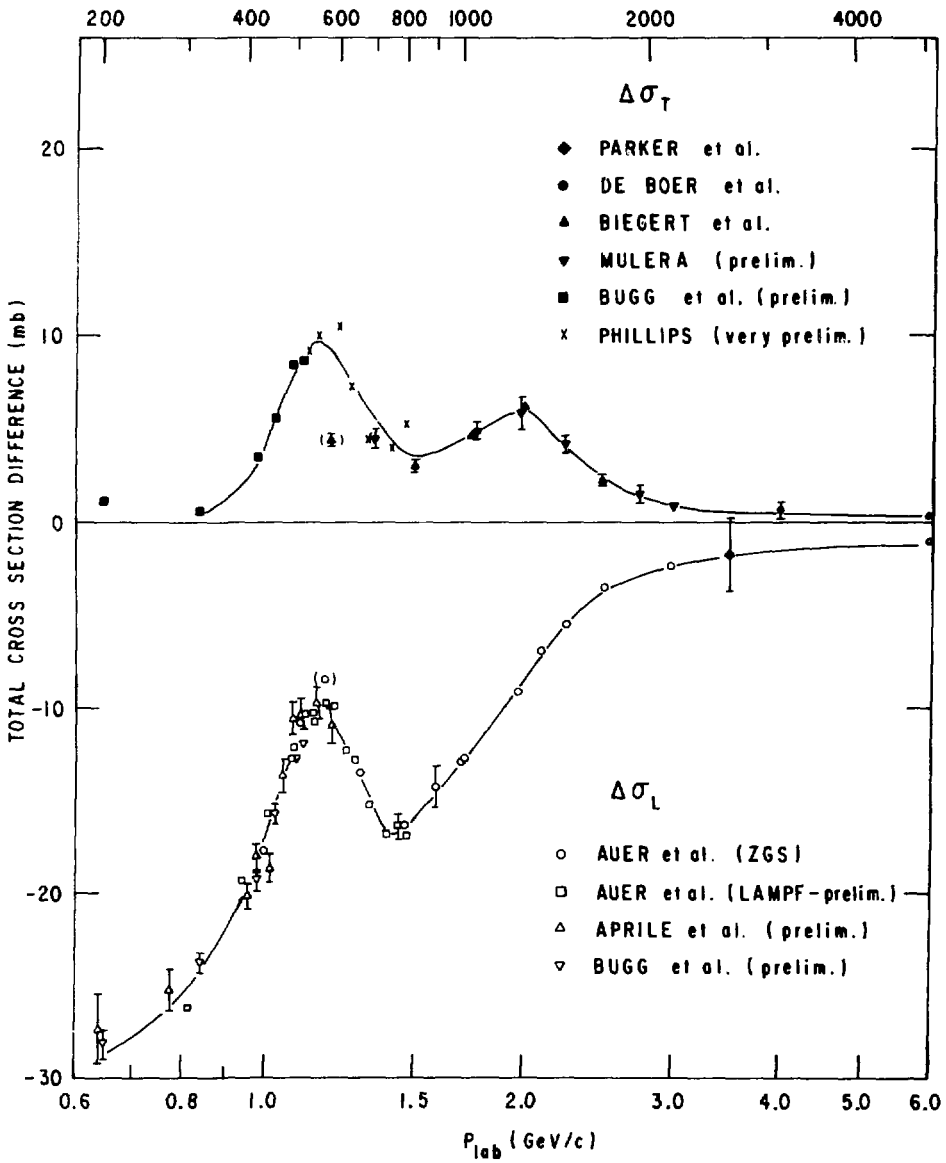

Fig. 2

Experimental values of the pp total cross section differences $\Delta\sigma_T$ and $\Delta\sigma_L$. The lines shown are to guide the eye. The $\Delta\sigma_T$ results are from Refs. 3-6, 9, and 10. Errors on the very preliminary LAMPF points have not been accurately computed, but are roughly ± 1 mb. The $\Delta\sigma_L$ results are from Refs. 9, 14, 17, and 18. The old ZGS data near 1.2 GeV/c are suspect because of beam depolarization.

more properly done with σ^{Tot}, than with the more difficult $\Delta\sigma_L$ or $\Delta\sigma_T$ measurements.

2. The TRIUMF results on $\Delta\sigma_T$ and $\Delta\sigma_L$ appear to be larger in magnitude that the data from the other laboratories, indicating a possible systematic error somewhere. These discrepancies need to be resolved, since the interpretation of the data in terms of dibaryons is significantly affected by these results. Since many of the results are preliminary, the discrepancies may change in the final data. Systematic effects in the beam and target polarizations may account for all of the discrepancies as well.

3. The good agreement of the SIN, LAMPF and ZGS $\Delta\sigma_L$ results is quite encouraging. Three different polarized beams, polarized targets, detectors, and sets of problems were involved. Also, the experimental groups were almost completely different (there was relatively little overlap of people from ANL on the LAMPF and the early ZGS experiments). In all fairness, the $\Delta\sigma_T$ measurements are more difficult than $\Delta\sigma_L$ in my opinion. The magnetic field from the polarized target deflects the beam and the outgoing particles, leading to alignment problems at the target and the detectors.[8] (These problems could be reduced by remeasuring $\Delta\sigma_T$ with a frozen spin target and lowered magnetic field.) There are also non-zero asymmetries for the scattering of transversely polarized protons on unpolarized nuclei in the target, whereas such asymmetries correspond to parity violation in the case of a longitudinally polarized beam.

4. The three total cross sections are linearly related to elastic scattering amplitudes by the optical theorem. Elastic scattering spin observables and cross sections for specific channels are bilinear in the amplitudes, except for elastic scattering at small angles in the Coulomb-nuclear interference region, where the Coulomb amplitude is known.

5. Spin-singlet partial waves make positive contributions of equal magnitude to both $\Delta\sigma_T$ and $\Delta\sigma_L$. Certain spin-triplet partial waves ($^3P_1$, $^3F_3$, $^3H_5$, ...) make a negative contribution to $\Delta\sigma_L$ and do not contribute at all to $\Delta\sigma_T$. It is possible to isolate the spin-singlet terms by taking an appropriate combination of σ^{Tot}, $\Delta\sigma_T$ and $\Delta\sigma_L$ (for example, see Grein and Kroll[20]).

6. Using various bits of evidence, it is possible to show that the peaks in $\Delta\sigma_T$ and $\Delta\sigma_L$ near 550 MeV are largely caused by the $^1D_2$ partial wave, and the deep dip in $\Delta\sigma_L$ near 750 MeV is largely from the $^3F_3$ partial wave. Various phase shift analyses[21,22] indicate that both these waves have resonance-like behavior. The partial wave(s) responsible for the peak in $\Delta\sigma_T$ at 2 GeV/c is (are) uncertain at this time, but the $^1G_4$ wave has been suggested.

B. $\Delta\sigma_L$ and $\Delta\sigma_T$ for Specific Reactions

Figure 3 presents some data on other spin-averaged total cross sections in the pp system (see also Ref. 23).[1] In addition, recent SIN data[24-26] permit the

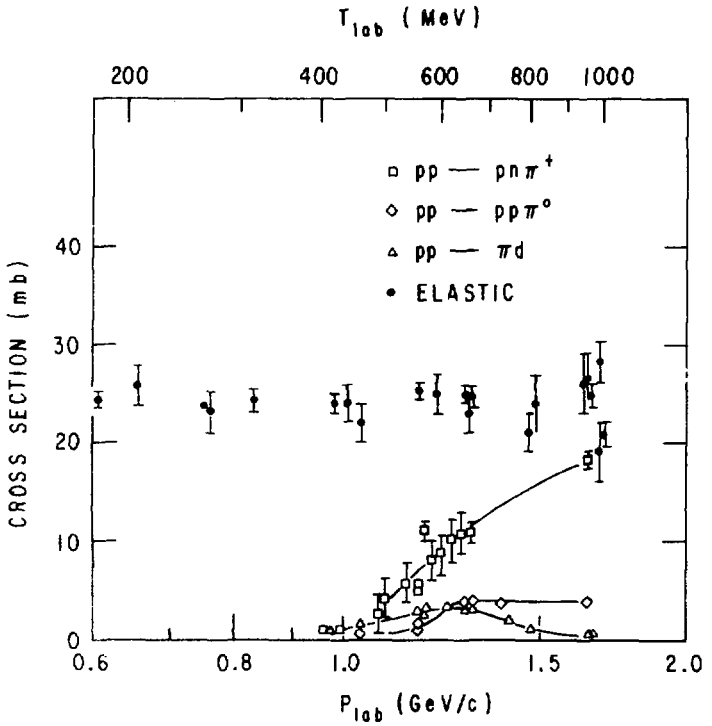

Fig. 3

Experimental pp elastic and reaction cross sections from Ref. 1. Additional data are shown in Fig. 15.

calculation of

$$\Delta\sigma_T(\text{elastic}) = -\int (C_{NN} + C_{SS}) \cdot (d\sigma/d\Omega)\, d\Omega$$

$$\Delta\sigma_L(\text{elastic}) = -2\int C_{LL}\, (d\sigma/d\Omega)\, d\Omega$$

where the spin directions $\vec{N}$ (transverse to the plane of scattering), $\vec{L}$ (longitudinal), and $\vec{S} = \vec{L} \times \vec{N}$ are defined in Fig. 4. The quantities C_{LL}, C_{NN}, C_{SS} are asymmetries in elastic scattering with beam and target polarized.

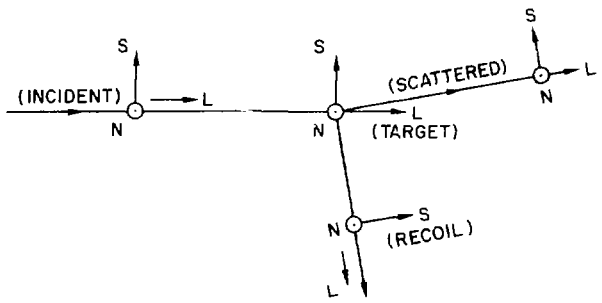

N: NORMAL TO THE SCATTERING PLANE
L: LONGITUDINAL DIRECTION
S = N x L IN THE SCATTERING PLANE

Fig. 4

Definition of the three spin directions N, S, and L.

(Note, in various other notations $C_{NN} = A_{NN} = A_{yy} = A_{oonn} = (N,N;0,0)$, and $C_{LL} = A_{LL} = A_{zz} = A_{ookk} = (L,L;0,0)$, etc.) For example:

$$C_{NN} = \frac{d\sigma/d\Omega\ (\uparrow\uparrow) - d\sigma/d\Omega\ (\uparrow\downarrow)}{d\sigma/d\Omega\ (\uparrow\uparrow) + d\sigma/d\Omega\ (\uparrow\downarrow)} \ .$$

Similar relations also hold for the reactions $pp \to \pi d$, $pp \to NN\pi$, etc. Data from the Geneva group are shown in Fig. 5.[24-26] At $T_{lab} = 579$ MeV, they obtain

$$\Delta\sigma_T(\text{elastic}) = -0.4 \pm 0.7 \text{ mb}$$
$$\Delta\sigma_T(pp \to \pi d) = +3.9 \pm 0.3 \text{ mb}$$
$$\Delta\sigma_L(\text{elastic}) = -15.4 \pm 0.4 \text{ mb}$$
$$\Delta\sigma_L(pp \to \pi d) = +2.7 \pm 0.2 \text{ mb}$$

Since the cross sections for the other inelastic reactions, such as $pp \to NN\pi\pi$, are negligible below $P_{lab} = 1.5$ GeV/c or $T_{lab} = 800$ MeV, then[27]

$$\Delta\sigma_L(pp \to NN\pi) = \Delta\sigma_L - \Delta\sigma_L(\text{elastic}) - \Delta\sigma_L(pp \to \pi d)$$
$$\simeq +1.4 \pm 1.0 \text{ mb at } 578 \text{ MeV}.$$

Likewise, using the value of $\Delta\sigma_T$ near 580 MeV from LAMPF,[10]

$$\Delta\sigma_T(pp \to NN\pi) \simeq +6.5 \pm 1.5 \text{ mb at } 578 \text{ MeV}.$$

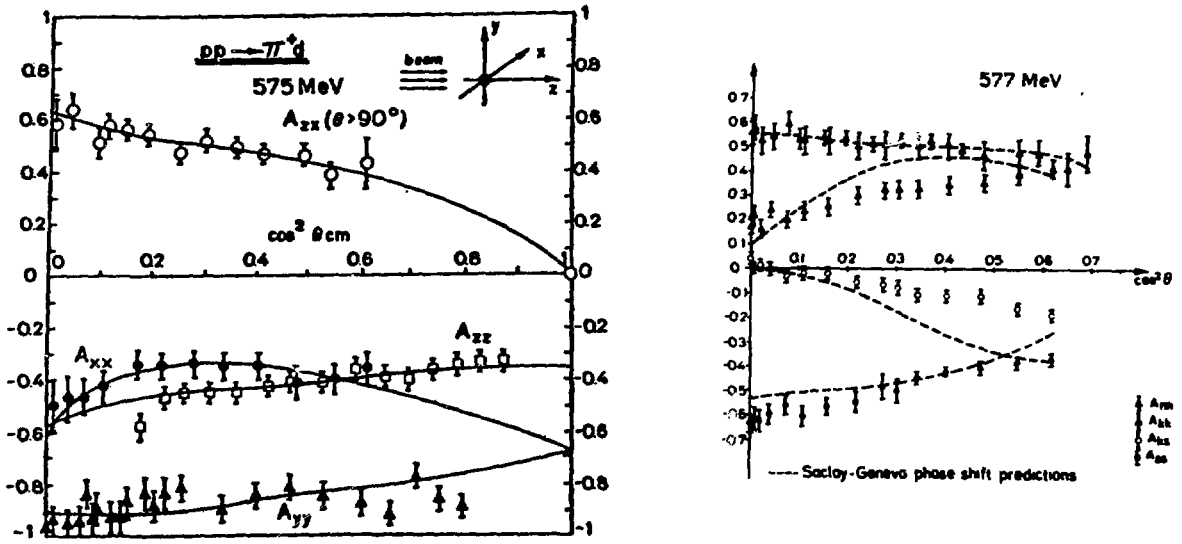

Fig. 5

Experimental measurements of C_{NN} (or A_{nn} or A_{yy}), C_{LL} (or A_{kk} or A_{zz}) and C_{SS} (or A_{ss} or A_{xx}) for pp elastic and pp → πd near 580 MeV from SIN (Ref. 27). These values were used to compute the elastic and πd contributions to $\Delta\sigma_T$ and $\Delta\sigma_L$ as described in the text.

Thus, it appears that $\Delta\sigma_T$ is mainly inelastic and $\Delta\sigma_L$ is mainly elastic near 600 MeV. Also, the contributions to $\Delta\sigma_T$ from the πd and NNπ channels are comparable. Such results are important for a complete understanding of the NN system in the medium energy range. All present diproton candidates couple strongly to inelastic channels, yet the experimental data base for pp → NNπ contains far fewer spin observables than elastic scattering. The question of the existence of dibaryon resonances may not be resolved to everyone's satisfaction until much more is known about the inelastic reactions (see Section II B).

The lack of sufficient inelastic data has led to considerable controversy in the interpretation of the $\Delta\sigma_L$ and $\Delta\sigma_T$ results. For example, in 1978 Bugg[28] stated that "either current prejudices about the mechanism of the inelastic channels or Argonne values of $\Delta\sigma_L$ must be wrong". The new TRIUMF $\Delta\sigma_T$ measurements[8] indicate the first alternative may be true. Combining $\Delta\sigma_T$ with various estimates of $\Delta\sigma_T$(elastic), whose values are generally close to or below zero between 150 and 600 MeV, leads to the statement that there is little spin-triplet inelasticity in this energy range.[8] This is at variance with the inelasticities of Bugg[28] and of Green and Sainio.[29] (On the other hand, the $\Delta\sigma_T$(pp) data from TRIUMF presented

at Lausanne[9] are somewhat smaller than those in Ref. 8. Therefore the disagreement may be reduced.) Bugg's second alternative is probably ruled out by the fairly good agreement of the new SIN and LAMPF results with the old ZGS data, although the disagreement with TRIUMF is of concern.

It should be noted that some theoretical predictions have had notable success. Bystricky and Lehar[30] predicted structure in $\Delta\sigma_L$ close to the ANL measurements before the data were taken. Mandelstam's[31] model of pion production, updated by Hollas,[32] is also consistent with the data on the three pp total cross sections. The coupled channel calculations of Kloet and Silbar[33-34] seem to reproduce the structure in $\Delta\sigma_T(pp \to NN\pi)$ and $\Delta\sigma_L(pp \to NN\pi)$, at least up to 500 MeV. Green and Sainio,[29] Arik and Williams[35] and Berger et al.[36] agree with $\Delta\sigma_L$(inelastic) in the same energy range.

Above 500-600 MeV, the experimental situation is less clear since there are no measured values for $\Delta\sigma_L$(elastic), $\Delta\sigma_T(pp \to \pi d)$, etc. Data were collected at the ZGS on C_{LL} from $\theta_{c.m.}$ = 20-90° (P_{lab} = 1.18, 1.35, 1.48, 1.71, 1.97, 2.22, 2.47 GeV/c), but the analysis is not yet complete. Furthermore, the predictions differ above 600 MeV. In particular, Hollas[32], Berger et al.[36], and Arik and Williams[35] would get a change in sign for $\Delta\sigma_L$(inelastic), whereas Kloet and Silbar[33-34] do not.

Future measurements should include C_{NN}, C_{SS} and C_{LL} at all angles and a number of energies above 600 MeV, for both pp elastic and $pp \to \pi d$. These data will be useful for phase shift analyses, as well as for calculation of $\Delta\sigma_T$ and $\Delta\sigma_L$ in specific channels. As pointed out by Edgington,[8] and Arik and Williams,[35] it is important for the elastic measurements to go to small angles, where the cross section is high, in order to obtain accurate values of $\Delta\sigma_T$(elastic) or $\Delta\sigma_L$(elastic). The inelastic contributions would be directly determined from these data for comparison with theory.

C. Elastic Scattering Parameters

There are considerable data on the energy dependence of various elastic scattering parameters in addition to the total cross section results. For example, the polarization P = (N,0;0,0) = (0,N;0,0,) has been measured at fixed laboratory angle or fixed 4-momentum transfer t over a wide energy range. Similarly, at $\theta_{c.m.}$ = 90°, C_{NN}, C_{LL} and $D_{NN} = K_{NN}$ = (N,0;0,N) = (0,N;0,N) have also been measured. These are shown in Fig. 6. For a complete understanding of the energy dependence of these, and other spin parameters, detailed phase shift

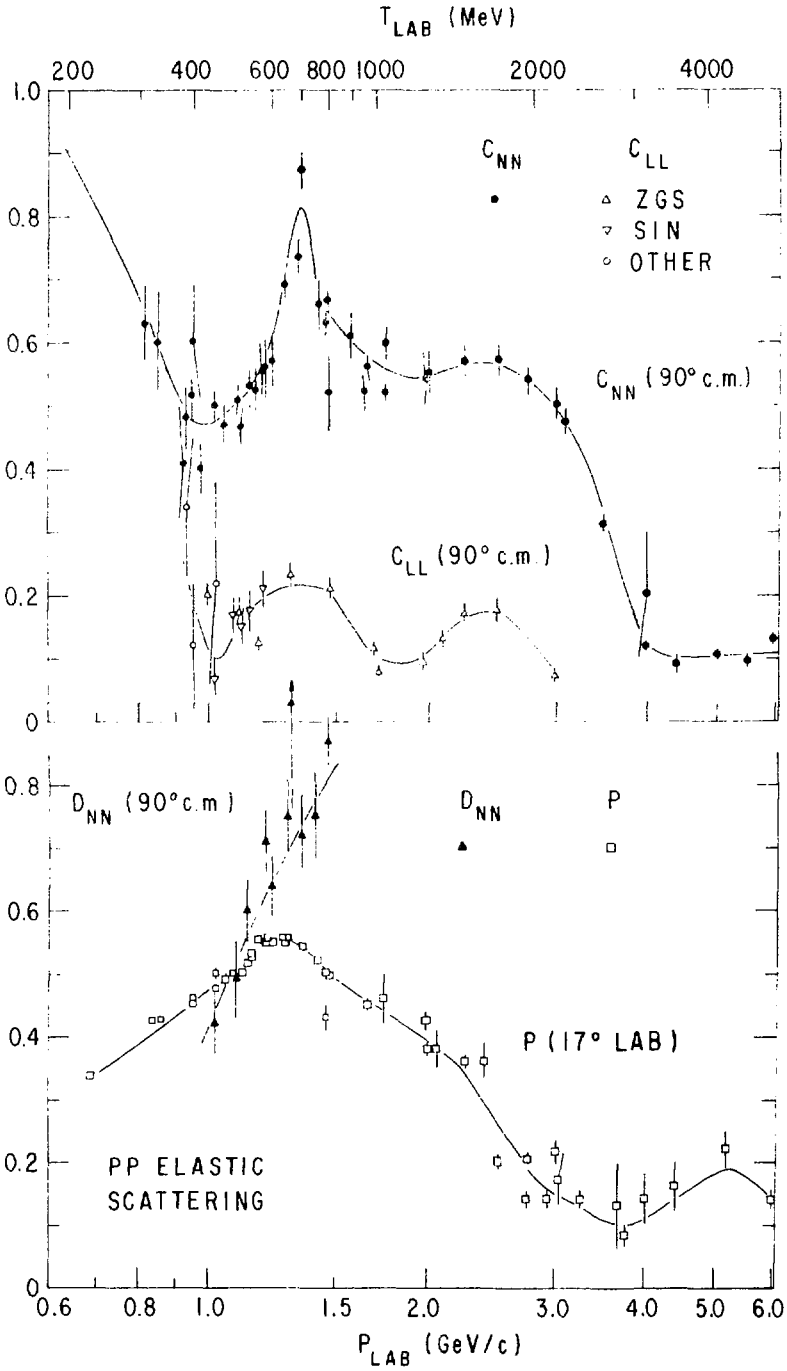

Fig. 6

Measurements of pp elastic scattering observables as a function of beam momentum. The $C_{NN}(90°)$ data are from Refs. 37-49, $C_{LL}(90°)$ from Refs. 25, 37, 38, 50, $D_{NN}(90°)$ from Refs. 53, 54 and the polarization values are from Refs. 42, 48, 49, 55-61. Additional polarization data are discussed in Ref. 62. The lines shown are to guide the eye.

analyses are required. However, some of the first indications about the quantum numbers of the partial wave responsible for the structure in $\Delta\sigma_L$ came from a Legendre coefficient analysis[13] of the differential cross section and polarization data as a function of angle and energy.

Some information can also be obtained from the spin parameters mentioned above. For example, it should be noted that the following spin parameters have no contributions from spin-singlet partial waves:

$$D_{NN}\ (d\sigma/d\Omega) \quad \text{at } \theta_{c.m.} = 90°$$

and

$$P \quad (d\sigma/d\Omega) \quad \text{at all angles.}$$

In addition, there are pp amplitudes ϕ_s (spin-singlet contributions only) and ϕ_t, ϕ_T (spin-triplet contributions only) at $\theta_{c.m.} = 90°$, where the following relations are valid:

$$d\sigma/d\Omega = |\phi_s|^2 + |\phi_t|^2 + |\phi_T|^2$$

$$C_{NN}\ (d\sigma/d\Omega) = -|\phi_s|^2 + |\phi_t|^2 + |\phi_T|^2$$

$$C_{LL}\ (d\sigma/d\Omega) = -|\phi_s|^2 - |\phi_t|^2 + |\phi_T|^2$$

$$D_{NN}\ (d\sigma/d\Omega) = 2\ \mathrm{Re}\ \phi_t \phi_T^* .$$

In terms of helicity amplitudes

$$\phi_s = {}^{i}\!/_{2}\,(\phi_1 - \phi_2)$$

$$\phi_t = {}^{1}\!/_{2}\,(\phi_1 + \phi_2)$$

$$\phi_T = \phi_3 = -\phi_4 .$$

In particular, the magnitude of each of the amplitudes at 90° can be determined from these relationships, as well as one relative phase. Certain spin-triplet partial waves ($^3P_1$, $^3F_3$, $^3H_5$,...) contribute only to ϕ_T (and $\Delta\sigma_L$).

The C_{NN} data[37-49] exhibit considerable structure in this energy range. At low energies, pp scattering is dominated by the $^1S_0$ parial wave; so $C_{NN} \approx -1$. As the energy is increased, the $^3P_1$ and $^1D_2$ partial waves begin to contribute. There is a cancellation of the spin-singlet partial waves $^1S_0$ and $^1D_2$ in ϕ_s at $\theta_{c.m.} = 90°$ and $T_{lab} \approx 140$ MeV; consequently $C_{NN} \approx +1$.[40] At still higher energies, there seems to be another peak in C_{NN} near 700 MeV, close to the energy corresponding to the minimum value in $\Delta\sigma_L$ and the proposed $^3F_3$ dibaryon resonance. Finally C_{NN} drops to a value of roughly 0.1. Near the top energies of the former ZGS, a striking rise occurs. This high energy behavior is not understood at this time.

The C_{LL} results[25,37,38,50] also show structure in this energy range. The value of $C_{LL}(90°)$ was obtained from the $C_{KP} = (0,0;S,S)$ measurements of Refs. 37,38 using the relations[51]

$$C_{NN} - C_{LL} - C_{SS} = 1 \qquad \theta_{c.m.} = 90°$$

$$C_{LL} = C_{KP} + \tfrac{1}{2}(C_{NN} - 1) \; .$$

The agreement of the ZGS[50] and the SIN results[25] is quite good except at the lowest energies. Hess[27] has pointed out that a slight shift in the energy of the lowest ZGS point would give agreement with phase shift predictions and the SIN data. Such a shift is probably consistent with knowledge of the absolute beam momentum at the ZGS. (The ZGS data were collected simultaneously with the $\Delta\sigma_L$ measurements. This procedure was also followed at LAMPF, but the analysis is not yet complete. Some of the C_{NN} data from the Rice group were almost simultaneous with the $\Delta\sigma_T$ measurements; a different beam intensity was used.) The C_{LL} results had a significant impact on Arndt's phase shifts. The behavior of $C_{LL}(90°)$ as a function of energy was explained by Hidaka[52] on the basis of interference between a $^3F_3$ Breit Wigner resonance and background partial waves from Hoshizaki's phase shift analysis.

The D_{NN} results[53,54] rise smoothly over the LAMPF energy range, and the polarization data[42,48,49,55-61] exhibit a maximum near the minimum value in $\Delta\sigma_L$ as well. There are considerable data at the lower energies (see Ref. 62 for a review). These two spin parameters exhibit less structure than C_{NN} or C_{LL} since $P \cdot (d\sigma/d\Omega)$ and $D_{NN} \cdot (d\sigma/d\Omega)$ contain no spin-singlet contributions. Therefore, structure in the $^1D_2$ partial wave, which contributes to the peaks in $\Delta\sigma_L$ and $\Delta\sigma_T$ near 550 MeV, would be absent.

Additional measurements of $C_{NN}(90°)$, $C_{LL}(90°)$, and especially $D_{NN}(90°)$ above LAMPF energies would probably be useful in understanding the structure in $\Delta\sigma_T$ near 2 GeV/c and would also be beneficial to high energy phase shift analyses. Such measurements are likely to be more sensitive to dibaryons than total cross sections, such as $\Delta\sigma_T$, at higher energies.

Elastic scattering results at small angles, in the Coulomb-nuclear interference region, are also important. The three pp total cross sections σ^{Tot}, $\Delta\sigma_T$ and $\Delta\sigma_L$ have been used with dispersion relation calculations[20] to obtain the amplitudes at $\theta = 0°$. In turn, these amplitudes are used as inputs to phase shift analyses. Dispersion relation results have been tested for the spin-averaged case. For example, the data on the small angle pp differential cross sections from the LAMPF HRS[63] at T_{lab} = 800 MeV (Fig. 7) agree with Grein and Kroll's predictions.[20] Bugg[9,28] has suggested that there are inconsistencies even at TRIUMF energies between dispersion relation predictions based on the ZGS $\Delta\sigma_L$ data, and the other two amplitudes at $\theta = 0°$ from phase shift solutions excluding $\Delta\sigma_L$. These other amplitudes have been tested experimentally at SIN energies,[64] but it is not clear whether the results were of sufficient precision

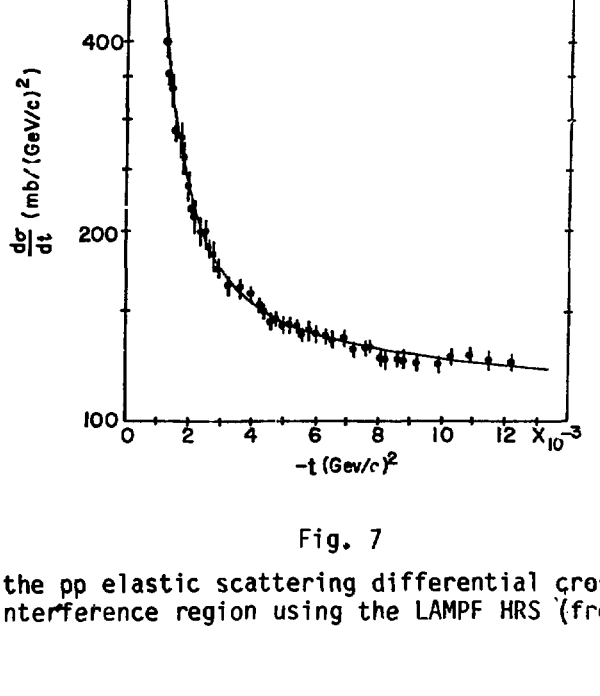

Fig. 7

A measurement of the pp elastic scattering differential cross section in the Coulomb-nuclear interference region using the LAMPF HRS (from Ref. 63).

to test Bugg's assertion. A high quality direct measurement of some spin parameters in the Coulomb-nuclear interference region at two energies would be quite beneficial. These measurements should be chosen to be sensitive to the amplitudes associated with $\Delta\sigma_L$ and/or $\Delta\sigma_T$.[65]

With the completion of pp elastic scattering measurements at 650 and 800 MeV in the next year at LAMPF, it would probably be useful to reevaluate the phase shift solutions. There have been a huge number of new results below 800 MeV in the last two years, and there are enough data at a few energies to even perform model independent amplitude determinations.[27] If resonance-like behavior persists in the $^1D_2$ and $^3F_3$ partial waves, then presumably additional elastic scattering measurements will not be of great value below 800 MeV in understanding dibaryons. Above this energy, many elastic measurements are needed to understand the amplitudes near 2.0 GeV/c, where structure appears in $\Delta\sigma_T$.

D. Other Reactions

The conjectured $^1D_2$ and $^3F_3$ dibaryon resonances would have large inelasticity. Therefore, the effects of these resonances should be observable in the inelastic channels $pp \rightarrow pn\pi^+$, $pp\pi^\circ$, and perhaps πd as well. Many cross section and polarization data exist for the latter channel,[66] and the Geneva group[24,26] has measured several other spin parameters at SIN (see Fig. 5). This reaction is easy to study experimentally with a polarized target since it has a two body final state. Thus, reactions on hydrogen can be separated from those on nuclei in the polarized target using coplanarity and scattering angle correlations. Additional measurements may be necessary in the $pp \rightarrow \pi d$ channel to unambiguously interpret the present data, if the pp elastic case is used as a guide. In particular, it would be useful to measure some spin parameters above SIN energies, perhaps at LAMPF, since the understanding of the $^1D_2$ partial wave behavior (pp elastic scattering) may be greatly influenced by these data. Recent theoretical studies of this reaction include those of Niskanen,[67] Chai and Riska,[68], Maxwell et al.,[59] and Kamo and Watari.[70] The first three do not include dibaryons, whereas the last claims dibaryons are needed to explain the data.

The study of the $pp \rightarrow NN\pi$ reaction is quite important for resolving the question of the existence of the $^1D_2$ and $^3F_3$ dibaryon resonances. However, it is experimentally very difficult to perform measurements of this reaction with a polarized target, since it has a three body final state and since very large solid angles are required to detect both charged particles (both need to be

momentum analyzed). The polarization of this reaction has been studied at TRIUMF[71,72] and at the ZGS[73] by the ANL Effective Mass Spectrometer (EMS) group using a polarized beam incident on a liquid hydrogen target. The Rice group has made a number of recent measurements of this reaction at LAMPF,[10,74,75] and also at the ZGS in collaboration with the ANL EMS group. The LAMPF data were taken with two relatively small acceptance arms in the horizontal plane, one of which included momentum determination (see Fig. 8). The ZGS data utilized a large acceptance magnetic spectrometer, with cylindrical wire chambers surrounding the liquid hydrogen target (see Fig. 9). In some sense these two approaches are complimentary - one involves less hardware and software effort, but the other produces more information. For example, for the pp → NΔ → NNπ reaction, measuring the decay of the Δ over all angles (not just in the horizontal plane), provides the ability to measure additional, independent spin parameters. These more complicated measurements are clearly "second generation experiments"

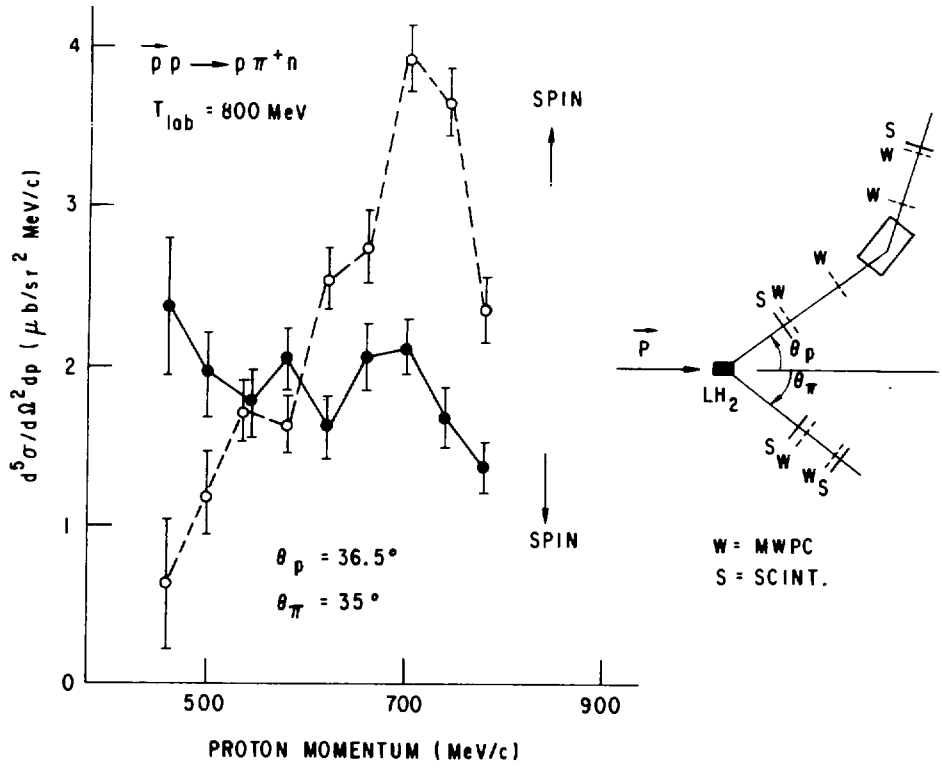

Fig. 8

A sample of data taken by the Rice group on the reaction pp → pn π^+ with a polarized beam on a liquid hydrogen target. A schematic of the experimental apparatus is also shown. These results are from Ref. 10, and the lines are to guide the eye.

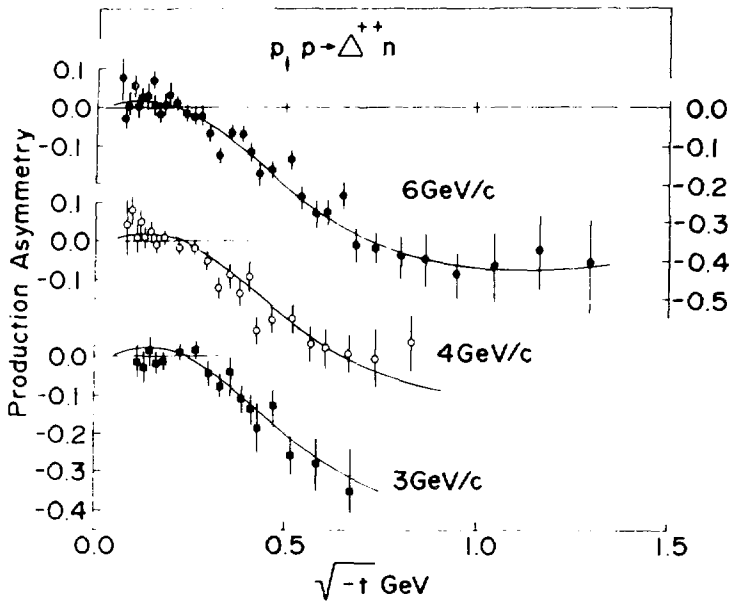

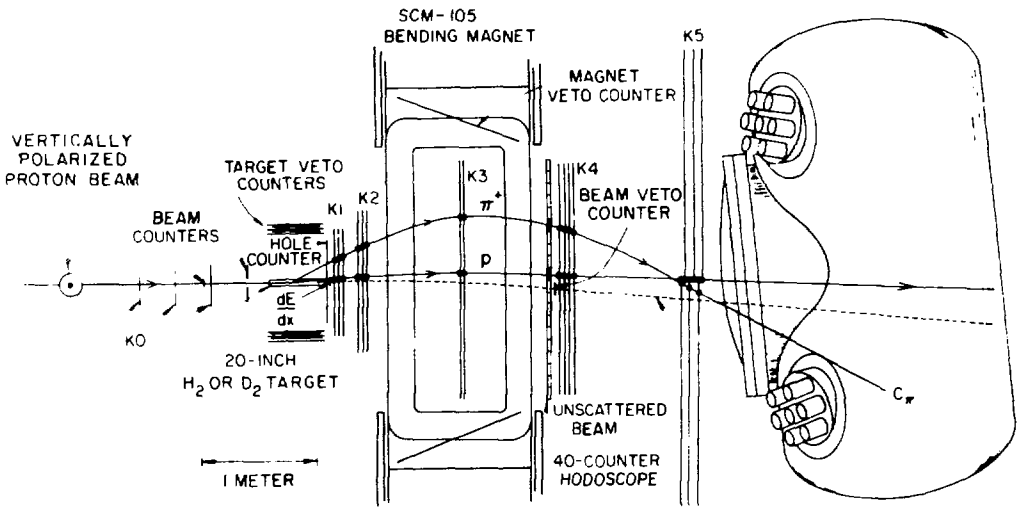

Fig. 9

Measurements of the reaction $\vec{p}\vec{p} \to \Delta^{++}n$ taken with the ANL Effective Mass Spectrometer and a schematic of the experimental apparatus (from Ref. 73). A large amount of information about this reaction was gathered by observing the decay of the Δ^{++} over all angles. This was made possible by the large acceptance of the spectrometer.

at the meson factories. Perhaps the results from the ZGS experiment at 1.2, 1.5, 1.75 and 2.0 GeV/c will demonstrate that a very large acceptance spectrometer with a polarized target is needed for the future. On the other hand, the use of a liquid hydrogen target with a polarized beam and with measurements of the spin of the outgoing protons (with a carbon polarimeter) may be the better approach. In any case, it seems clear that some theoretical guidance would be beneficial to the experimenters for which spin measurements are the most important, given present and future hardware constraints.

There are two recent π^+ + d elastic scattering experiments performed at SIN which see structure that could be caused by dibaryon resonances. In the first, Frascaria et al.[76] measured the differential cross section at θ_π = 180° for π^+p and π^+d at 7 energies between 130 and 280 MeV. They observed structure at 240-260 MeV, which is located in the vicinity of the possible $^3F_3$ resonance (see Fig. 10). Data from other groups[77-79] are also shown for comparison. The source of this structure is unclear; they claim either pion absorption or dibaryon resonance formation can produce an enhancement in the backward elastic cross section.

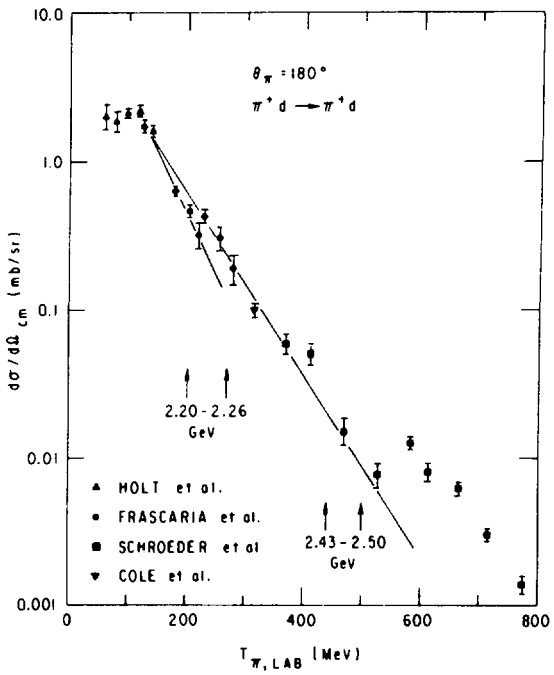

Fig. 10

Differential cross section for backward π^+d elastic scattering. The measurements are from Refs. 76-79. The structure near T_π = 250 MeV may be due to the possible $^3F_3$ dibaryon resonance seen in pp elastic scattering and the pp total cross sections. The lines are to guide the eye.

The second SIN experiment, Bolger et al.,[80] measured the asymmetry in π^+d elastic scattering with a vector polarized deuteron target at two energies. Their results are consistent with Faddeev calculations without dibaryons at T_π = 142 MeV (see Fig. 11). However, the theory fails at the higher energy (note that T_π = 142 MeV is near the $^1D_2$ "resonance" and T_π = 256 MeV is near the $^3F_3$ "resonance" in pp elastic scattering). The data indicate a strong contribution from a higher partial wave interfering with the calculated background, and these results provide good evidence for the presence of one or more dibaryon resonances in π^+d elastic scattering. Measurements at additional energies are planned.

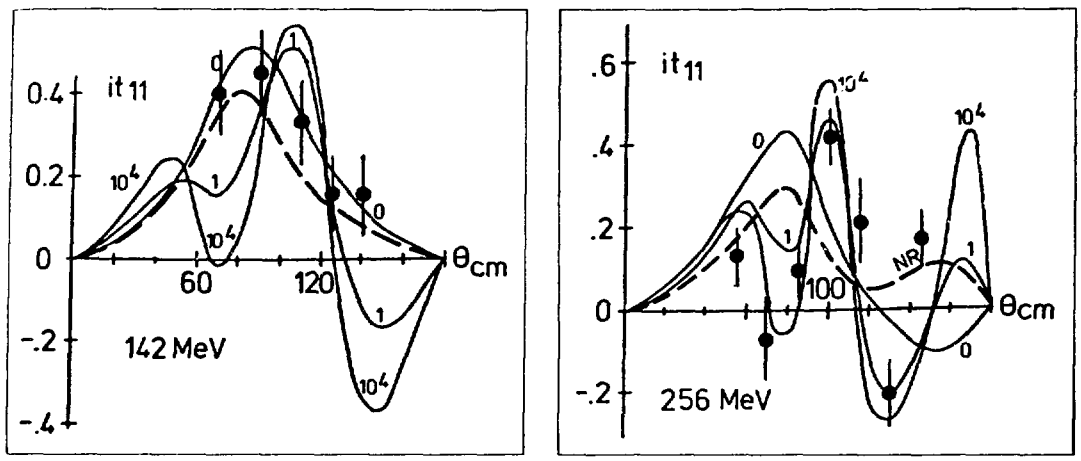

Fig. 11

Measurements of π^+d elastic scattering with a vector polarized deuterium target from Ref. 80. The curves are predictions of Kubodera et al. (Ref. 81) made before the measurements. The dashed curve is the nonresonant prediction and the solid curves include the effects of dibaryons. The 142 MeV results are near the expected $^1D_2$ dibaryon resonance and the 256 MeV results are near the $^3F_3$ resonance in pp scattering.

Calculations of πd elastic scattering have been performed by Kubodera et al.[81], by Kanai et al.[82], and by Simonov and Van der Velde.[83] The results of Kubodera (predicted before the measurements) were used to compare to the data of Bolger et al.[80] They concluded that the backward cross sections, as well as the vector and tensor polarizations, are sensitive to dibaryon resonances. Kanai et al. used Glauber amplitudes as the background and concluded dibaryon resonances are needed to fit the measured cross sections. Simonov and Van der Velde

concluded that πd elastic scattering has little contribution from dibaryon resonances, but instead that threshold effects (pseudoresonance) are the cause of structure observed in the forward and backward cross sections. It is not clear how model independent all these conclusions are. Additional measurements would be required to test other predictions. However, it may be more profitable to do a phase shift analysis including pp and πd channels (and perhaps $NN\pi$ as well) in order to choose the most important measurements for the future in the inelastic channels.

II. STRUCTURE IN THE I=0 NN SYSTEM

A. Total Cross Sections

There is considerably less data in the I=0 NN system than in I=1. The shape of the I=0 spin-averaged total cross section, as well as the pp and Nd total cross sections, is again rather smooth. Measurements of σ^{Tot} by several experimental groups[2,84-89] are plotted in Figs. 12-14. It is clear that systematic errors are nonnegligible. Threshold effects are not expected to cause structure near 1.5 GeV/c in the I=0 system because neither πd nor $N\Delta$ can contribute to I=0. Note also that the rise in σ^{Tot} (I=0) occurs at a somewhat higher energy than the pp case.

Preliminary results of $\Delta\sigma_L$(pd) are given in Fig. 12. These data are relatively smooth and featureless compared to the pp data. Statistical errors are shown; systematic errors are roughly ± 15%, primarily from uncertainty in the target polarization. During these measurements, $\Delta\sigma_L$(pp) data were collected simultaneously, and the results agree within statistics with earlier ZGS measurements shown in Fig. 2.

In order to extract the I=0 total cross section difference $\Delta\sigma_L$(I=0), a number of theoretical inputs were required. In the simplest approximation

$$\Delta\sigma_L(pd) \approx \Delta\sigma_L(pp) + \Delta\sigma_L(pn)$$
$$\Delta\sigma_L(I=0) = 2\Delta\sigma_L(pn) - \Delta\sigma_L(pp).$$

However, there are deviations from these simple relations because the neutron can be shadowed by the proton when the incident particle strikes the deuteron, and also because the neutron is moving inside the deuteron (Fermi-motion).

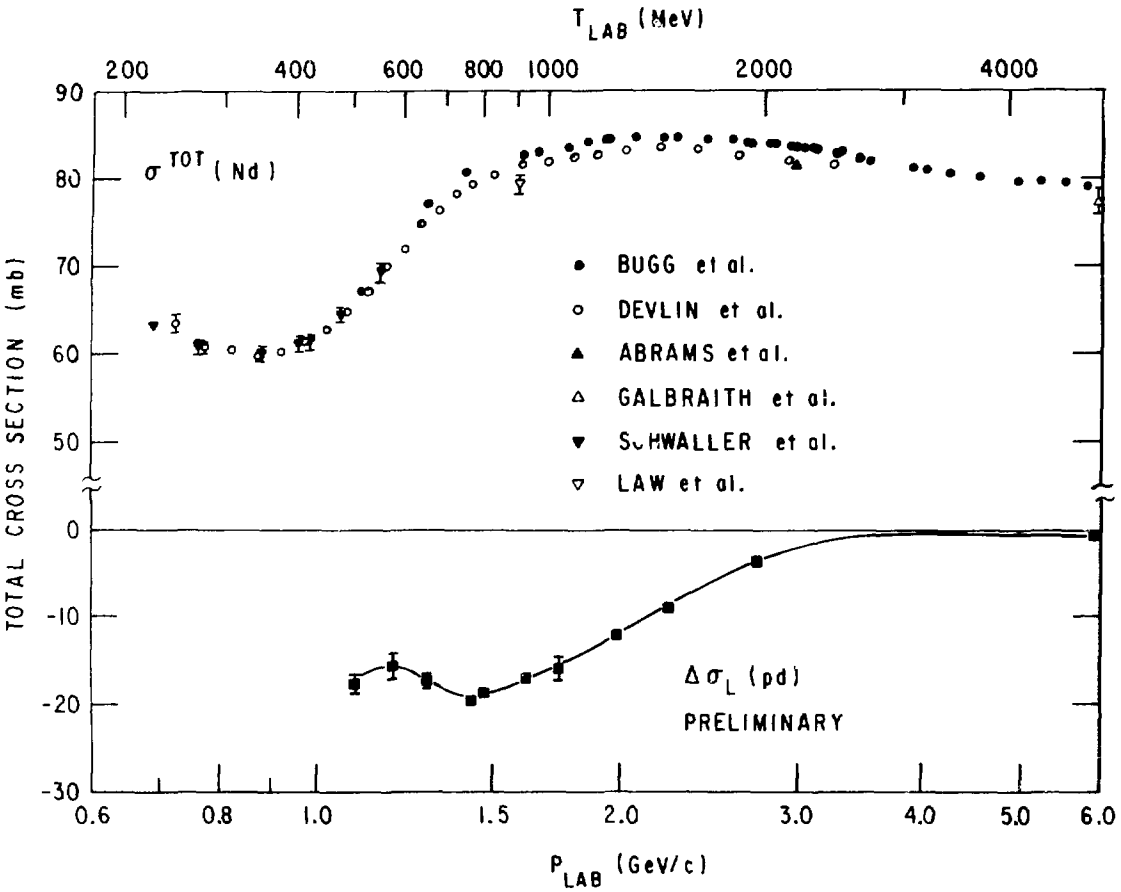

Fig. 12

Experimental measurements of Nd total cross sections. The values of σ^{Tot} are from Refs. 2, 84-88. The $\Delta\sigma_L$(pd) data were taken at the ZGS by the ANL polarized target group. The line is to guide the eye.

C. Sorensen[90] and G. Alberi et al.[91] derived formulae relating $\Delta\sigma_L$(pn) to various quantities within the framework of Glauber theory. These quantities include $\Delta\sigma_L$(pd), $\Delta\sigma_L$(pp), σ^{Tot}(pn), σ^{Tot}(pp), and the real parts of the forward pp and pn amplitudes. These real parts were obtained from dispersion relations,[92] which were also used to make Coulomb-nuclear interference corrections. Simple corrections were applied to the data for the D-state part of the deuteron wave function (which causes a reduction in the effective neutron polarization). Finally, in order to account for Fermi-motion effects, the $\Delta\sigma_L$(pp) values were averaged for the momentum distribution of the proton inside the deuteron. The results for

$\Delta\sigma_L$(pn) are shown in Fig. 13. They are smeared by the Fermi-motion of the neutron inside the deuteron. Statistical errors coming from the $\Delta\sigma_L$(pd) measurement are shown. However, it is not known what systematic error should be assigned to the theoretical corrections mentioned above.

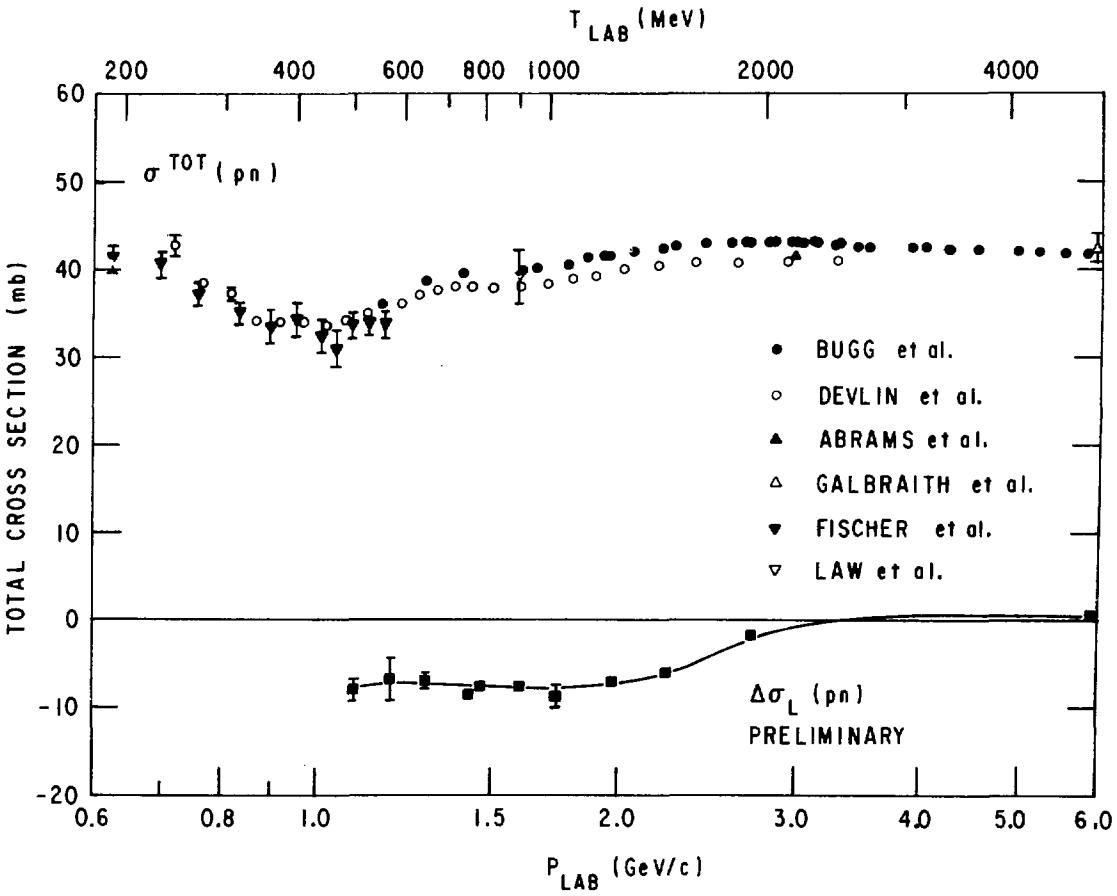

Fig. 13

Experimental measurements of σ^{Tot}(pn) from Refs. 84-89 and of $\Delta\sigma_L$(pn) extracted from $\Delta\sigma_L$(pd) as described in the text. Note the lack of structure between 1.0 and 2.0 GeV/c. The line is to guide the eye.

Finally, the $\Delta\sigma_L$(I=0) results are shown in Fig. 14 (again smeared by Fermi-motion effects). From Figs. 12 and 13 it can be seen that $\Delta\sigma_L$(pd) and $\Delta\sigma_L$(np) are relatively smooth. Therefore, the peak in $\Delta\sigma_L$(I=0) near 1.5 GeV/c arises from the subtraction of the smeared $\Delta\sigma_L$(pp). Fermi-motion effects cannot smear

$\Delta\sigma_L$(pp) sufficiently to make the peak in $\Delta\sigma_L$(I=0) disappear, because the averaging is typically ± 100 MeV/c in P_{lab}. As mentioned previously, this striking peak in $\Delta\sigma_L$(I=0) cannot be caused by the πd or NΔ channels, since they cannot contribute to I=0.

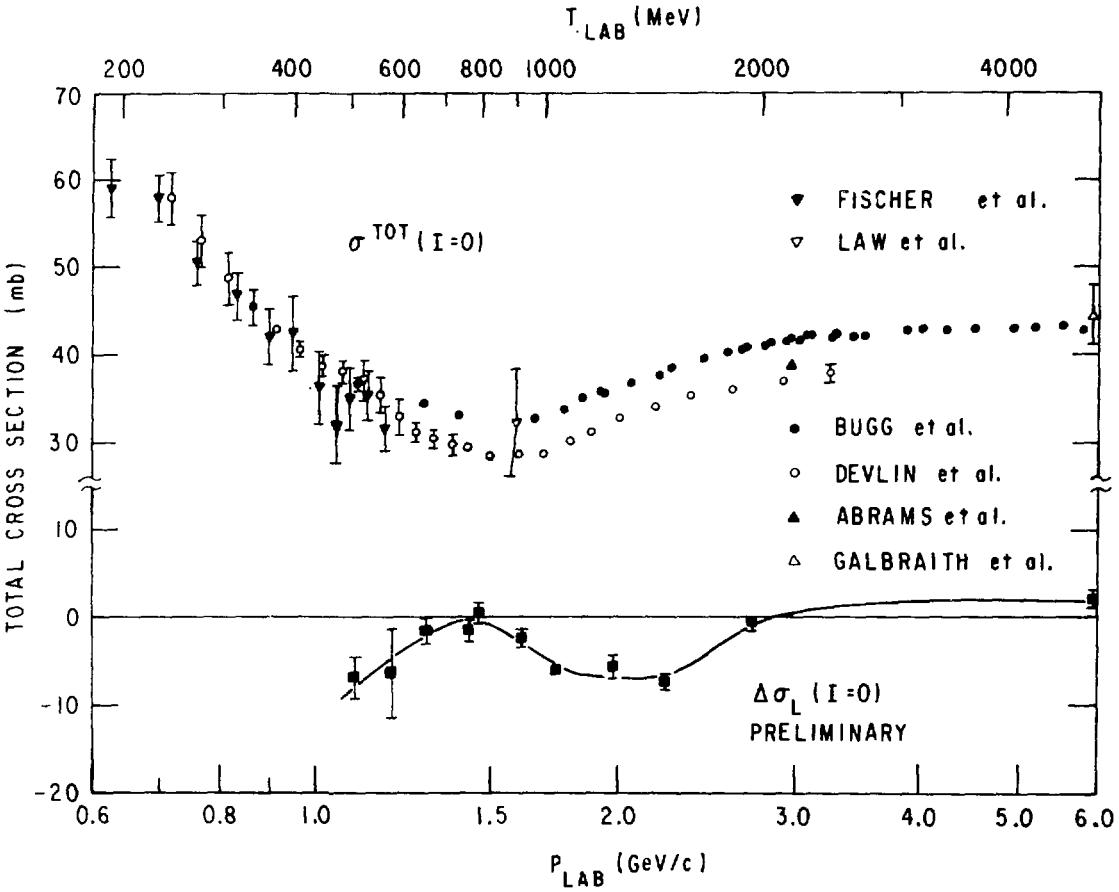

Fig. 14

Total I=0 NN cross sections. The spin-averaged cross sections are from Refs. 84-89; note the systematic errors are significant. The values of $\Delta\sigma_L$(I=0) were derived from $\Delta\sigma_L$(pp) as described in the text. The line shown is to guide the eye.

It is of interest to determine what partial wave or waves are responsible for the observed structure. A peak in $\Delta\sigma_L$(I=0) could be caused by spin-singlet waves, such as $^1P_1$ and/or $^1F_3$, or by coupled spin-triplet waves, such as $^3S_1$, $^3D_1$, $^3D_3$, $^3G_3$, etc. A Legendre coefficient analysis, similar to the one performed in the pp case,[13] is not possible at this time because polarization data for I=0 are sparse and often do not cover wide angular ranges. Such an analysis

would be quite useful if a spin-triplet wave was responsible for the structure. On the other hand, contributions from spin-singlet waves are isolated in the quantity

$$\sigma^{Tot} + \Delta\sigma_T + \tfrac{1}{2}\,\Delta\sigma_L .$$

Data on $\Delta\sigma_T$(pd) were taken by the Rice group at the ZGS, but the results have not been published yet and they would be subject to a similar set of corrections as $\Delta\sigma_L$(I=0).

There have been two analyses[93-95] of the structure in $\Delta\sigma_L$(I=0) indicating different partial waves are responsible. Kroll et al.[93,94] have used dispersion relations to derive all 6 NN amplitudes at $\theta = 0°$. The experimental inputs include: A) I=1 total cross sections σ^{Tot}, $\Delta\sigma_T$, $\Delta\sigma_L$, B) I=0 total cross sections σ^{Tot}, $\Delta\sigma_L$, and C) the forward differential cross section for pn charge exchange (CEX). There was apparently no conflict of the CEX and $\Delta\sigma_L$(I=0) data, as reported earlier,[96] once corrections for the real parts of the pp and pn amplitudes were included in the determination of $\Delta\sigma_L$(pn) from $\Delta\sigma_L$(pd). Kroll was able to predict $\Delta\sigma_T$(I=0) and concludes that one or more of the coupled spin-triplet partial waves (odd J, even parity) such as $^3S_1$, $^3D_1$, $^3D_3$, $^3G_3$, are responsible for the observed $\Delta\sigma_L$(I=0) structure. On the other hand, Hoshizaki[95] has fit NN data and finds resonance-like behavior in the $^1F_3$ (spin-singlet) partial wave. Therefore, neither experiment nor theory provides a unique solution for the partial wave or waves responsible for the structure in $\Delta\sigma_L$(I=0). Many more pn elastic scattering results are needed, especially above TRIUMF energies.

The procedure for obtaining $\Delta\sigma_L$(I=0) from $\Delta\sigma_L$(pd) can be criticized because of the large amount of theoretical input required. In particular, Glauber theory has not been tested experimentally for total cross sections involving spin. In addition, Glauber theory may not work very well for total cross sections which exhibit significant structure. For example, the observed values of σ^{Tot} (πd) are not reproduced exactly by Glauber theory and the πp and πn cross sections[97] in the resonance region. Therefore, it would be beneficial to directly measure $\Delta\sigma_L$(pn) with a polarized neutron beam incident on a polarized proton target at a few energies near 1.5 GeV/c. Experimental values of $\Delta\sigma_T$(pd) and $\Delta\sigma_T$(I=0) would be very useful as well. In addition, measurements of various elastic scattering spin parameters will be quite important to better understand the behavior of the

I=0 phase shifts. Although it appears there is significant structure in $\Delta\sigma_L(I=0)$, the interpretation will remain unclear until additional data are available in the I=0 system.

B. Other Reactions

Kroll[94] has also calculated reaction cross sections for NN → NNπ assuming a background estimated from the Deck model and an I=0 (M = 2250 MeV) resonance plus the I=1, $^3F_3$ (2240 MeV) resonance. His results are compared with measurements in Fig. 15. It appears that the effects of dibaryons should be clearly observable, but the experimental data need to be improved, particularly above TRIUMF or SIN energies.

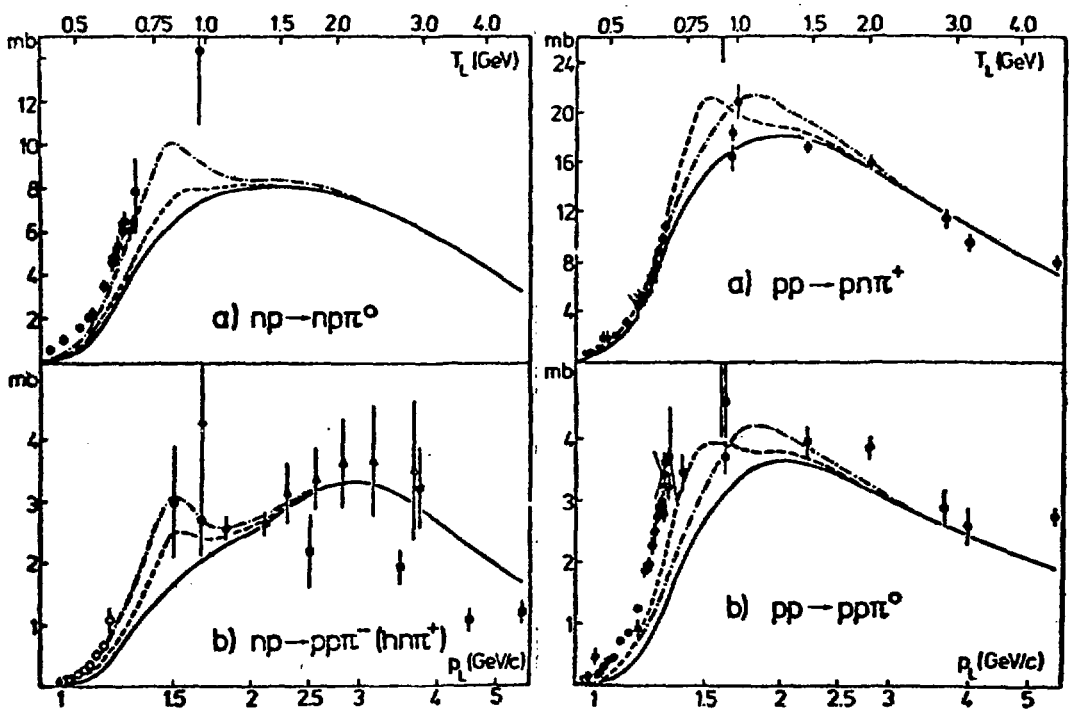

Fig. 15

Experimental measurements of cross sections for NN → NNπ. The solid curves are predictions of the Deck model without dibaryon resonances, and the dashed curves include dibaryons. The figure was taken from Ref. 94.

In a series of experiments, Kamae et al.[98-102] have made measurements of the proton polarization in the reaction $\gamma + d \to \vec{p} + n$ between E_γ = 350 and 700 MeV.

A partial wave analysis was performed using differential cross section data and their polarization results. They assumed the amplitudes consist of a calculable nonresonant part and a dibaryon part. The nonresonant contribution was estimated by the nucleon-exchange Born amplitude and the one-pion reabsorption amplitude; it does not seem to be able to describe the experimental results. A fit to the data with one resonance also gives poor results. However, with two resonances ($I=0$, $J^P = 3^+$, $M = 2360$ MeV and $I=1$, $J^P = 3^-$, $M = 2260$ MeV, $^3F_3$ partial wave in NN scattering) the fit is substantially improved; see Fig. 16. Calculations which promise to fit the data without the assumption of dibaryons are in progress.[103]

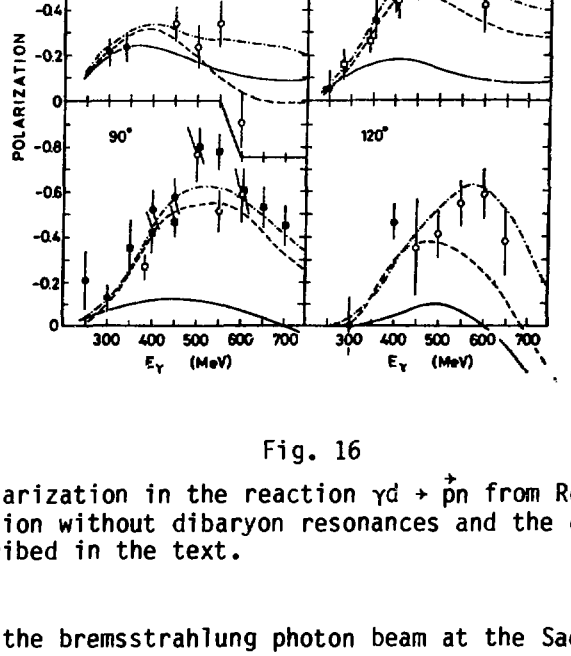

Fig. 16

Measurements of polarization in the reaction $\gamma d \to \vec{p}n$ from Ref. 101. The solid line is the prediction without dibaryon resonances and the dashed curves include dibaryons, as described in the text.

A group using the bremsstrahlung photon beam at the Saclay Linac (Argan et al.[104]) has performed a number of experiments also suggesting the existence of a dibaryon resonance of mass near 2230 MeV and a width of about 40 MeV. They found an anomaly in the counting rate as a function of E_γ for the reaction $d(\gamma, p\pi^-)$ X compared to the predictions of the first order quasi-free model. They also measured the yield of the inclusive reaction $\gamma + d \to p + X$ at fixed proton angle and momentum as a function of the bremsstrahlung endpoint energy (incident electron

energy). An excess yield was noted at energies somewhat above the kinematical limit for pion production. Argan et al.[104] claim the cross section cannot be explained by rescattering contributions, but can be explained by a dibaryon resonance with the parameters mentioned above.

Although the evidence for dibaryons from these inelastic channels is quite interesting, it does not seem conclusive. At this time, theory must be relied on to compute the nonresonant background. Deviations from theory provide the evidence for dibaryons in these cases. It would be beneficial for additional spin parameters to be measured in the reactions $\gamma + d \to p + n$ and $\gamma + d \to p + X$; however many parameters would probably be needed for an unambiguous conclusion (if the pp elastic scattering situation is used as a guide). Some of these measurements would be quite difficult, just as in the $NN \to NN\pi$ case. On the other hand, these existing data strengthen the evidence for the pp $^3F_3$ dibaryon resonance. They also suggest a possible I=0 resonance, and more work is certainly needed to establish its existence, perhaps using different reactions.

III. EVIDENCE FOR S = -1, 2 DIBARYONS

The search for dibaryons with strangeness S = -1 or -2 has generally been the domain of bubble chamber experiments. Therefore, the sample of events is usually quite small (less than 1000 over the full mass range covered), and statistical fluctuations have led to spurious claims of resonance-like structure at times.

One feature that has been seen by a number of different experiments is a peak in the $\Lambda^0 p$ mass spectrum near 2130 MeV from the reactions[105-113]

$$K^- d \to \Lambda^0 p\, \pi^-$$
$$\to \Lambda^0 p\, \pi^-\pi^0$$
$$\to \Lambda^0 p\, \pi^+\pi^-\pi^-$$

and also[114-117]

$$K^-\, {}^4He \to \Lambda^0 p\, \pi^- d$$
$$nC \to \Lambda^0 p\, X\ .$$

The 2130 MeV peak is quite close to the threshold for Σ^+n and it may correspond to a Λ^0p dibaryon resonance or a threshold cusp in Λ^0p elastic scattering (see Fig. 17).

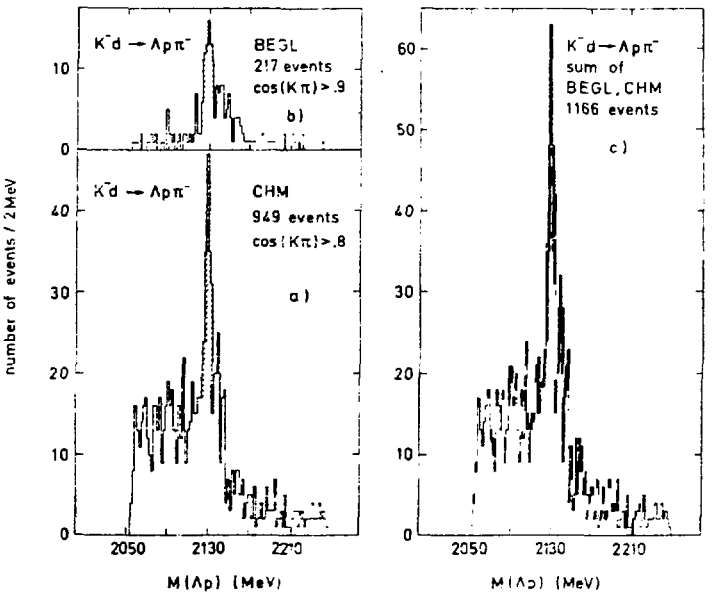

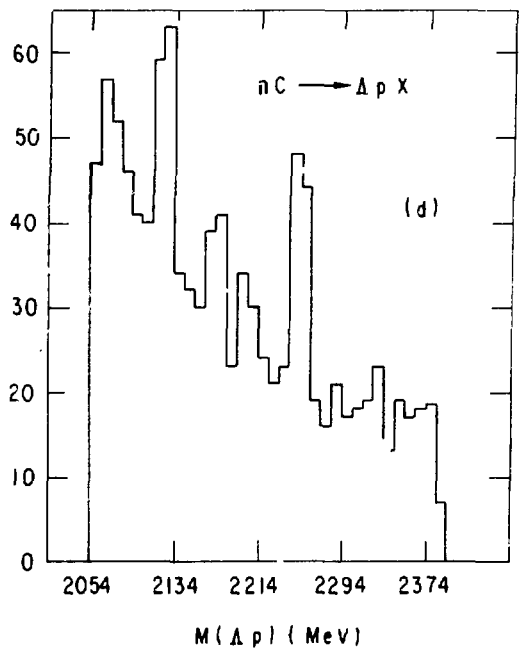

Fig. 17

Observation of possible dibaryons in the Λ^0p mass spectrum from Refs. 112 and 116. The 2130 MeV peak is very close to the Σ^+n threshold.

Another peak is seen near 2250 MeV in neutron interactions in a heavy liquid bubble chamber,[115,116] which is not close to any known threshold. There is some evidence for this peak in other experiments,[113,118] but the statistics are quite small. The $\Lambda^0 p$ effective cross section for elastic scattering[119,120] is fairly smooth, but Shahbazian[121] suggests that the elastic data are not inconsistent with resonances corresponding to both the 2130 and 2250 MeV $\Lambda^0 p$ mass peaks. If these peaks are resonances, they would probably have the quantum numbers B=2, S=-1, I=$\frac{1}{2}$ and spins larger that 0.[121]

Recent evidence for a B=2, S=-1, I=3/2 bound state of ΣN has been found by Ströbele et al.[122] in the reaction

$$K^- d \to \pi^+ X^- \to \pi^- nn$$

where events of the type

$$K^- d \to \pi^+ \Sigma^- n$$

$$\to \pi^+ \Sigma^- n \pi^0$$

were rejected. The observed peak in the missing mass distribution for $K^- d \to \pi^+ + MM$ occurred close to the Σn threshold, but the selection criteria was claimed to exclude masses above threshold. It is not clear whether this peak is a dibaryon at this time.

There are several suggestions of peaks in the $\Lambda^0\Lambda^0$ and $\Xi^- p$ mass spectra[115,116,123-125] for the B=2, S=-2 case. These experiments were performed in heavy liquid bubble chambers and the interpretation was complicated by two step processes (for example, a Λ^0 is formed by a $K^- N$ interaction on one nucleon in a nucleus, and the Λ^0 then scatters off a different nucleon in the same nucleus). However, the peaks were not substantiated in other experiments and the statistics were always very small in these unusual final states.

There was also a counter experiment (Carroll et a.[126]) performed to search for a dibaryon below the $\Lambda\Lambda$ threshold which was predicted by Jaffe[127] using the MIT bag model. Previous experiments could only place very crude limits on the cross section for such a dibaryon. Carroll et al. searched for such a resonance using the $pp \to K^+K^+ X$ reaction, but they found no evidence of it to the 100 nb level.

This field of study could greatly benefit from measurements with at least one or two orders of magnitude more counts. High intensity K^- beams and counter experiments or hybrid experiments with one of the new high resolution bubble chambers would be quite important. These would make a large impact on the study of dibaryons with strangeness, as well as on ΛN, ΣN, ΞN elastic and inelastic reactions.

IV. CONCLUSIONS

Although there are a number of good dibaryon candidates, none of them seem to be acceptable to nearly everyone. Many are close to thresholds, which clouds their status. Others suffer from a lack of sufficient spin parameter data for a precise interpretation, and some are seen in only one experiment with poor statistics The list of good candidates includes three from the I=1 NN system ($^1D_2$, $^3F_3$ and $^1G_4$(^) partial waves near 1.2, 1.5 and 2.0 GeV/c respectively), two from the I=0 NN system (the Kamae et al. resonance candidate and the bump in $\Delta\sigma_L(I=0)$), and several with strangeness S=-1 (2130 and 2250 MeV in Λ°p and the ΣN bound state). A summary of recommendations for further study of these dibaryon candidates is given in the Appendix. Additional measurements may change the status of these candidates, or may, as in the pp case, still leave the interpretation somewhat uncertain.

The case for the $^3F_3$ pp dibaryon seems particularly strong. There are many spin parameters measured in the pp case. This state shows up as a bump in a total cross section ($\sigma^{Tot}(\ddagger)$). It corresponds to a counterclockwise loop in Argand diagrams from dispersion relation calculations and from phase shift analyses. It can explain the energy dependence of $d\sigma/d\Omega$ ($\theta\pi$ = 180°) and the vector polarization at $T\pi$ = 256 MeV in πd elastic scattering. It is needed to explain the γd → pn results of Kamae et al., and it can explain the observations of Argan et al. At this time, it seems that the simplest explanation to account for these obervations is that there is a diproton resonance of mass ~ 2250 MeV, with large inelasticity and quantum numbers $J^P = 3^-$, I=1, S=0 and B=2.

ACKNOWLEDGEMENTS

I wish to gratefully acknowledge many useful discussions with my experimental colleagues at Argonne, LASL and New Mexico State University, especially I. P. Auer and A. Yokosawa, and with E. Berger, C. Sorensen and G. Thomas (Argonne). I would also like to thank B. Bonner, D. Bugg, R. Hess, and G. Phillips for experimental details concerning their measurements and for permission to use their preliminary results. Finally, I wish to thank the many, many others with whom I have discussed the experimental evidence for dibaryons for their insights.

REFERENCES

1. E. Bracci et al., "Compilation of Cross Sections III" CERN/HERA 73-1, (1973).

2. P. Schwaller et al., Nucl. Phys. A316, 317 (1979).

3. E. F. Parker et al., Phys. Rev. Lett. 31, 783 (1973).

4. W. deBoer et al., Phys. Rev. Lett. 34, 558 (1975).

5. Ed. K. Biegert et al., Phys. Lett. 73B, 235 (1978).

6. T. A. Mulera, High Energy Physics with Polarized Beams and Polarized Targets, Argonne, American Institute of Physics Proceedings, Vol. 51, 428 (1979).

7. J. D. Lesikar et al., Bull. Am. Phys. Soc., 25, 562 (1980).

8. J. A. Edgington, Fifth International Symposium on Polarization Phenomena in Nuclear Physics, Santa Fe, New Mexico, (1980).

9. D. V. Bugg et al., 1980 International Symposium on High-Energy Physics with Polarized Beams and Polarized Targets, Lausanne, Switzerland.

10. G. Phillips, private communication and very preliminary.

11. I. P. Auer et al., Phys. Lett. 67B, 113 (1977).

12. I. P. Auer et al., Phys. Lett. 70B, 475 (1977).

13. K. Hidaka et al., Phys. Lett. 70B, 479 (1977).

14. I. P. Auer et al., Phys. Rev. Lett. 41, 354 (1978).

15. E. Colton et al., Nucl. Instrum & Methods 151, 85 (1978).

16. I. P. Auer, Nucl. Phys. A335, 193 (1980).

17. I. P. Auer, G. Burleson, W. Cottingame, W. R. Ditzler, S. Greene, D. Hill, E. Hoffman, K. Imai, J. Jarmer, K. H. and M. McNaughton, H. Spinka, R. Stanek, S. Stewart, K. Toshioka, D. Underwood, R. Wagner, A. Yokosawa from Argonne, LAMPF and New Mexico State University - preliminary.

18. E. Aprile et al., 1980 International Symposium on High-Energy Physics with Polarized Beams and Polarized Targets, Lausanne, Switzerland.

19. T. H. Fields and A. Yokosawa, Phys. Rev. D21, 1432 (1980).

20. W. Grein and P. Kroll, Nucl. Phys., B137, 173 (1978).

21. N. Hoshizaki, Prog. Theor. Phys., 60, 1796 (1978); 61, 129 (1979).

22. R. A. Arndt, Fifth International Symposium on Polarization Phenomena in Nuclear Physics, Santa Fe, New Mexico (1980).

23. F. Lehar, T. Siemiarczuk, P. Winternitz, J. Bystricky, Saclay preprint D Ph P E 79-28, (1979).

24. E. Aprile et al., Nucl. Phys. A335, 245 (1980).

25. E. Aprile et al., Eighth International Conference on High Energy Physics and Nuclear Structure, Vancouver, Canada (1979) - C_{LL} at 445, 494, 514, 536, 577 MeV (see also Ref. 96).

26. E. Aprile et al., Fifth International Symposium on Polarization Phenomena in Nuclear Physics, Santa Fe, New Mexico, (1980).

27. R. Hess, 1980 International Symposium on High-Energy Physics with Polarized Beams and Polarized Targets, Lausanne, Switzerland.

28. D. V. Bugg, High Energy Physics with Polarized Beams and Polarized Targets, Argonne, American Institute of Physics Proceedings, Vol. 51, 362 (1979).

29. A. M. Green and M. E. Sainio, J. Phys., G5, 503 (1979).

30. J. Bystricky and F. Lehar, Fourth International Symposium of Polarization Phenomena in Nuclear Reactions, Zurich, 1975.

31. S. Mandelstam, Proc. Phys. Soc. London, A244, 491 (1958).

32. C. L. Hollas, Phys. Rev. Lett. 44, 1186 (1980).

33. W. M. Kloet and R. R. Silbar, Nucl. Phys. A338, 281 (1980); A338, 317 (1980); Nucl. Phys. A., to be published.

34. W. M. Kloet et al., Phys. Rev. Lett. 39, 1643 (1977).

35. M. Arik and P. G. Williams, Nucl. Phys. B136, 425 (1978).

36. E. L. Berger, P. Pirila, G. H. Thomas, Argonne preprint ANL-HEP-PR-75-72 (unpublished).

37. J. V. Allaby et al., Proc. Phys. Soc. London 77, 234 (1961) - C_{NN}, C_{KP} at T_{lab} = 382 MeV.

38. E. Engels et al., Phys. Rev. 129, 1858 (1963) - C_{NN}, C_{KP} at T_{lab} = 400, 450 MeV.

39. G. Coignet et al., Nuo. Cim. 43A, 708 (1966) - C_{NN} at T_{lab} = 575 MeV.

40. A. Beretvas, Phys. Rev. 171, 1392 (1968) - C_{NN} at T_{lab} = 305, 330, 386, 415 MeV.

41. N. S. Borisov et al., High Energy Physics with Polarized Beams and Targets, Argonne, American Institute of Physics Proceedings, Vol 35, 59 (1976) - C_{NN} at T_{lab} = 610 MeV.

42. D. Miller et al., Phys. Rev. D16, 2016 (1977) - C_{NN}, P at P_{lab} = 2, 3, 4 GeV/c

43. A. Lin et al., Phys. Lett. 74B, 273 (1978) - C_{NN} at P_{lab} = 1.75, 2.5, 3.1, 3.5, 4.0, 4.4, 5.0, 5.5 GeV/c.

44. H. Willard et al., High Energy Physics with Polarized Beams and Polarized Targets, Argonne, American Institute of Physics Proceedings, Vol. 51. 420 (1979) - C_{NN} at T_{lab} = 643, 796, MeV.

45. M. McNaughton et al., to be published in Phys. Rev. C, Feb, (1981) - C_{NN} at T_{lab} = 796 MeV.

46. D. G. Crabb et al., Phys. Rev. Lett. 43, 983 (1979) - C_{NN} at P_{lab} = 6.0 GeV/c.

47. N. S. Borisov et al., Leningrad, Nuclear Physics Institute preprint # 581 (1980) - C_{NN} at T_{lab} = 690, 760, 804, 892, 950 MeV.

48. D. A. Bell et al. Phys. Lett. 94B, 310 (1980) - C_{NN} at P_{lab} = 1.10, 1.34, 1.45, 1.65, 1.75, 2.00, 2.25, 2.75 GeV/c and P at P_{lab} = 1.45, 1.65, 2.00, 2.25, 2.75 GeV/c.

49. D. Besset et al., Nucl. Phys. A345, 435 (1980) - C_{NN}, P at T_{lab} = 396, 446, 470, 515, 537, 557, 578 MeV.

50. I. P. Auer et al., Phys. Rev. Lett. 41, 1436 (1978) - C_{LL} at P_{lab} = 1.00, 1.10, 1.17, 1.30, 1.47, 1.69, 1.71, 1.97, 2.10, 2.25, 2.49, 3.00 GeV/c.

51. P. Catillon et al, Nucl. Phys. B2, 93 (1967).

52. K. Hidaka, Argonne preprint ANL-HEP-CP-78-15, (1978).

53. Iu.P. Kumekin et al., Sov. Phys. JETP, 8, 977 (1959) - D_{NN} at T_{lab} = 660 MeV.

54. B. E. Bonner, private communication and talk at the LAMPF Users Grops Meeting, October, 1980 - D_{NN} at T_{lab} = 450, 500, 530, 580, 600, 650, 700, 750, 800 MeV.

55. H. A. Neal and M. J. Longo, Phys. Rev. 161, 1374 (1967) - P at T_{lab} = 1.03, 1.32, 1.63, 2.24, 2.84 GeV.

56. J. H. Parry et al., Phys. Rev. D8, 45 (1973) - P at P_{lab} = 2.50, 2.75, 2.93, 3.25, 3.75, 4.40 GeV/c.

57. G. W. Abshire et al., Phys. Rev. Lett. 32, 1261 (1974) - P at P_{lab} = 5.15 GeV/c.

58. R. C. Fernow et al., Phys. Lett. 52B, 243 (1974) - P at P_{lab} = 6.00 GeV/c.

59. P. R. Bevington et al., Phys. Rev. Lett. 41, 384 (1978) - P at T_{lab} = 643, 787, 796 MeV.

60. L. G. Greeniaus et al., Nucl. Phys. A322, 308 (1979) - P at T_{lab} = 225, 327, 520 MeV.

61. M. McNaughton, private communication - P at T_{lab} = 318, 398, 447, 496, 530, 547, 581, 597, 630, 647, 699, 750, 800 MeV.

62. M. McNaughton, Fifth International Symposium on Polarization Phenomena in Nuclear Physics, Santa Fe, New Mexico (1980).

63. A. Wriekat et al., Phys. Lett. 97B, 33 (1980).

64. D. Besset et al., Phys. Rev. D21, 580 (1980).

65. N. H. Buttimore et al., Phys. Rev. D18, 694 (1978).

66. Ch. Weddigen, Nucl. Phys. A312, 330 (1978).

67. J. A. Niskanen, Nucl. Phys. A298, 417 (1978).

68. J. Chai and D. O. Riska, Nucl. Phys. A338, 349 (1980).

69. O. V. Maxwell et al., Nucl. Phys. A348, 388 (1980); A348, 429 (1980).

70. H. Kamo and W. Watari, Prog. Theor. Phys. 62, 569L (1979); 62, 843L (1979); 62, 1035 (1979).

71. G. Jones, Second International Conference on Nucleon-Nucleon Interactions, Vancouver, Canada, American Institute of Physics Proceedings, Vol. 41, 292 (1978).

72. P. Walden et al., Phys. Lett. 81B, 156 (1979).

73. R. Diebold, A. B. Wicklund et al., High Energy Physics with Polarized Beams and Targets, Argonne, American Institute of Physics Proceedings, Vol. 35, p. 92 and 198 (1976); D. S. Ayres et al., Orbis Scientiae: Deeper Pathways in High Energy Physics, Proceedings of the 1977 Coral Gables Conference, p. 109 (1977).

74. J. Hudomalj - Gabitzsch et al., Phys. Rev. C18, 2666 (1978).

75. J. H. Hoftiezer et al., Phys. Lett. 88B, 73 (1979).

76. R. Frascaria et al., Phys. Lett. 91B, 345 (1980).

77. L. S. Schroeder et al., Phys. Rev. Lett. 27, 1813 (1971).

78. R. H. Cole et al., Phys. Rev. C17, 681 (1978).

79. R. J. Holt et al., Phys. Rev. Lett. 43, 1229 (1979).

80. J. Bolger et al., 1980 International Symposium on High Energy Physics with Polarized Beams and Polarized Targets,Lausanne, Switzerland, and CERN Courier, 20, 399 (1980).

81. K. Kubodera et al., J. Phys. G6, 171 (1980).

82. K. Kanai et al., Prog. Theor. Phys. 62, 153 (1979).

83. Yu. A. Simonov and M. Van der Velde, J. Phys. G5, 493 (1979).

84. M. E. Law et al., Nucl. Phys. 9, 600 (1959).

85. W. Galbraith et al., Phys. Rev. 138, B913 (1965).

86. D. V. Bugg et al., Phys. Rev. 146, 980 (1966).

87. R. J. Abrams et al., Phys. Rev. D1, 2477 (1970); see also K. F. Riley, Phys. Rev. D1, 2481 (1970).

88. T. J. Devlin et al., Phys. Rev. D8, 136 (1973).

89. Th. Fischer et al., Eighth International Conference on High Energy Physics and Nuclear Structure, Vancouver, Canada (1979); see R. Vinh Mau, Nucl. Phys. A335, 211 (1980).

90. C. Sorensen, Phys. Rev. D19, 1444 (1979).

91. G. Alberi et al., Phys. Rev. D20, 2437 (1979).

92. W. Grein and P. Kroll, Nucl. Phys. B157, 529 (1979).

93. W. Grein et al., Phys. Lett. 96B, 176 (1980).

94. P. Kroll, 1980 International Symposium on High Energy Physics with Polarized Beams and Polarized Targets, Lausanne, Switzerland.

95. K. Hashimoto, Y. Higuchi and N. Hoshizaki, Kyoto University preprints NEAP-21,24,25 (1980).

96. D. V. Bugg, Nucl Phys. A335, 171 (1980).

97. G. Faldt and T. E. O. Ericson, Nucl. Phys. B8, 1 (1968).

98. T. Kamae et al., Phys. Rev. Lett. 38, 468 (1977).

99. T. Kamae et al., Nucl. Phys. B139, 394 (1978).

100. T. Kamae and T. Fujita, Phys. Rev. Lett. 38, 471 (1977).

101. H. Ikeda et al., Phys. Rev. Lett. 42, 1321 (1979).

102. K. Ogawa et al., Nucl. Phys. A340, 451 (1980).

103. L. S. Kisslinger, private communication and talk at the LAMPF User's Meeting, 1980.

104. P. E. Argan et al., Phys. Rev. Lett. 46, 96 (1981).

105. O. I. Dahl et al., Phys. Rev. Lett. 6, 142 (1961).

106. D. Cline et al., Phys. Rev. Lett. 20, 1452 (1968).

107. G. Alexander et al., Phys. Rev. Lett. 22, 483 (1969).

108. T. H. Tan, Phys. Rev. Lett. 23, 395 (1969).

109. D. Eastwood et al., Phys. Rev. D3, 2603 (1971).

110. W. H. Sims et al., Phys. Rev. D3, 1162 (1971).

111. A. V. Sodhi and D. P. Goyal, Nucl. Phys. B97, 403 (1975).

112. O. Braun et al., Nucl. Phys. B124, 45 (1977).

113. D. P. Goyal and A. V. Sodhi, Phys. Rev. D18, 948 (1978).

114. K. Bunnell et al., Phys. Rev. D2, 98 (1970).

115. B. A. Shahbazian and A. A. Timonina, Nucl. Phys. B53, 19 (1973).

116. B. A. Shahbazian et al., Lett. Nuo.Cim. 6, 63 (1973).

117. R. Roosen et al., Nuo. Cim. 49A, 217 (1979).

118. V. F. Vishnevskii et al., Sov. Phys. JETP Lett. 5, 252 (1967).

119. J. Kadyk et al., Nucl. Phys. B27, 13 (1971).

120. J. M. Hauptman et al., Nucl. Phys. B125, 29 (1977).

121. B. A. Shahbazian et al., XIX International Conference on High Energy Physics, Tokyo (1978).

122. H. Ströbele et al., submitted to Phys. Lett. B.

123. P. Belliere et al., Phys. Lett. 39B, 671 (1972).

124. G. Wilquet et al., Phys. Lett. 57B, 97 (1975).

125. D. P. Goyal et al., Phys. Rev. D21, 607 (1980).

126. A. S. Carroll et al., Phys. Rev. Lett. 41, 777 (1978).

127. R. L. Jaffe, Phys. Rev. Lett. 38, 195 (1977); 38, 617 (1977).

APPENDIX

SUMMARY OF RECOMMENDATIONS

The following recommendations are listed according to the section of this paper where they appear. The order does not necessarily signify importance or priority.

IA) Measure $\sigma^{Tot}(pp)$ in fine steps to search for narrow dibaryon states at the meson facilities.

IB) Determine $\Delta\sigma_T(pp \to NN\pi)$ and $\Delta\sigma_L(pp \to NN\pi)$ at a number of energies above 600 MeV. This involves measurements of C_{NN}, C_{SS} and C_{LL} at all angles for $pp \to pp$, and $pp \to \pi d$. Small angle data are important.

IC) # 1. Measure spin parameters in the Coulomb-nuclear interference region to test the dispersion relation predictions for the real part of the amplitudes associated with $\Delta\sigma_T$ and $\Delta\sigma_L$.

2. Finish the scheduled and approved pp elastic scattering measurements up to 800 MeV. Then see if more measurements are needed on the basis of phase shift analyses.

3. Many elastic scattering measurements are needed around 2 GeV/c (near the structure in $\Delta\sigma_T$). For example, $D_{NN}(90°)$ and $C_{SS}(\theta)$ would be useful.

ID) # 1. Additional measurements are needed in the inelastic channels $pp \to \pi d$ and $pp \to NN\pi$, and in the πd elastic channel.

2. Theoretical guidance would be helpful for which measurements to perform in the $pp \to NN\pi$ reaction. Hardware constraints need to be considered. Plans should be initiated for second generation measurements at the meson factories.

3. A phase shift analysis for the combined channels $pp \to pp$, $pp \to \pi d$ and $\pi d \to \pi d$ is probably appropriate.

IIA) # 1. Measure $\Delta\sigma_L(np)$ at a few energies to test the theory used to extract $\Delta\sigma_L(np)$ from $\Delta\sigma_L(pd)$. The primary goal is to obtain $\Delta\sigma_L$ (I=0).

2. Measure $\Delta\sigma_T$ (I=0).

IIB) #1. Better data are needed for the <u>spin averaged</u> total reaction cross sections σ^{Tot} $(pp \to NN\pi)$ and $\sigma^{Tot}(np \to NN\pi)$ above TRIUMF or SIN energies.

#2. Many np elastic scattering parameters are needed above TRIUMF energies.

#3. More experimental and theoretical study is needed on the possible I=0 dibaryon observed in $\gamma d \to \vec{p}n$.

III) The statistics for the S=-1 and -2 dibaryon candidates need to be increased by at least one to two orders of magnitude. High intensity kaon beams will probably be necessary for these studies.

In addition to the above recommendations, I would like to add the following one on the basis of my experience at the ZGS and LAMPF:

At any new medium energy proton accelerator, provision should be made to accelerate <u>both</u> polarized protons and polarized deuterons.

EVIDENCE AGAINST CLUSTERS IN ^{12}C NUCLEI AND AGAINST THE $^1D_2$ 2140 DIBARYON RESONANCE

by

R J Ellis, H J Ziock, K O H Ziock, Y Tzeng
Physics Dept., University of Virginia, Charlottesville, VA 22901.

J Bolger, E Boschitz
Kernforschungszentrum und Universitat Karlsruhe, IEKP, P O Box 3640
D-7500 Karlsruhe, Germany.

J Arvieux
Institut des Sciences Nucléaires, Université de Grenoble, BP 257,
F-38044 Grenoble-Cedex, France.

R Corfu, J Piffaretti
Institute de Physique, Université de Neuchâtel, CH-2000 Neuchâtel,
Switzerland.

L-C Liu, E R Siciliano
LAMPF, Los Alamos, New Mexico 87545

ABSTRACT

We have made coincidence measurements of the reaction $^{12}C(\pi^+,\pi^+d)^{10}B$ using a high resolution double-arm spectrometer system. We present angle and momentum distributions for incident energies in the range 160 to 200 MeV. We have made fits to these distributions using a plane wave impulse approximation (PWIA) overlap shell model and using a plane wave two-step knock-out reaction model. We find the data is fitted best by the PWIA model with a χ^2/DF of 1.7, assuming systematic errors of 15%. The cluster, which forms the deuteron in this model, arises naturally from the overlap of the standard proton and neutron P-state shell model wave functions. With the proviso that distortions are not included in these calculations, we find no evidence for clustering within the ^{12}C nucleus, other than that which is predicted by the shell model. We have also extracted the π-d elastic differential cross-section as a function of the π-d invariant mass. It shows a peak near 2125 MeV with a width of about 50 MeV FWHM, which

could be associated with the supposed $^1D_2$ $B^2(2140)$ dibaryon resonance. Our calculations show that this is probably a manifestation of the (3,3) resonance, and so we find no evidence to support the $B^2(2140)$.

The quasi elastic knock-out of deuterons by high energy protons was first observed by Azhgirei et al (1). This and similar observations have led to the development of the cluster model, which presumes that multi-nucleon systems already exist as "clusters" inside the nucleus (1,2). There has been considerable discussion on how to reconcile the coexistence of the "cluster" properties of nuclei with their well established single particle and collective properties (3).

During the course of studying the reactions $^{12}C(\pi^{\pm},\pi^{\pm}p)^{11}B$, with two high resolution spectrometers in coincidence (4), we have obtained data on the reactions $^{12}C(\pi^{\pm},\pi^{\pm}d)^{10}B$ (5). We find evidence suggestive of quasi elastic πd scattering (5). And we obtain the suprising result that negative pions knock out deuterons from ^{12}C at about the same rate as protons (5). The apparatus is described in reference 6. The data was taken at SIN.

In order to investigate the reaction mechanism(s) for deuteron knock out, we have obtained angle and momentum distributions for the reaction $^{12}C(\pi^{+},\pi^{+}d)^{10}B$. We have made theoretical calculations to fit the data, which are based on a naïve cluster model and on the shell model.

There has recently been interest in the possible existence of dibaryon resonances (7). Since these suspected resonances in the pp channel have large inelasticities, there must be considerable coupling into the πd and πnp channels. This, together with the apparent evidence for quasi elastic πd scattering and the high deuteron knock out rate, both mentioned above, persuaded us to analyse our data in search of a πd resonance.

Figures 1, 2 and 3 show the angular distributions of the scattered pion for incident pion kinetic energies of 160, 180 and 200 MeV respectively. (Angles are given in the laboratory frame throughout.) The scattered proton angle was 30° for all the data presented here. The triple differential cross-section is averaged over the large momentum bite of 60.6 MeV/c of the pion spectrometer. The central momentum was 169.5 MeV/c and pions were accepted in the range 143 to 203.6 MeV/c. Each event was weighted to allow for the variation of the spectrometer acceptance with momentum. The cross-sections have been corrected for the actual number of incident pions, for the attenuation due to nuclear interactions, for pion decay, for muons counted as pions and for wire chamber inefficiences.

Figure 4 shows the cross-section versus the scattered pion momentum at an incident pion energy of 200 MeV and a scattered pion angle of 117.5°. The error bars show the statistical errors. The momentum distribution in figure 4 is based on three overlapping

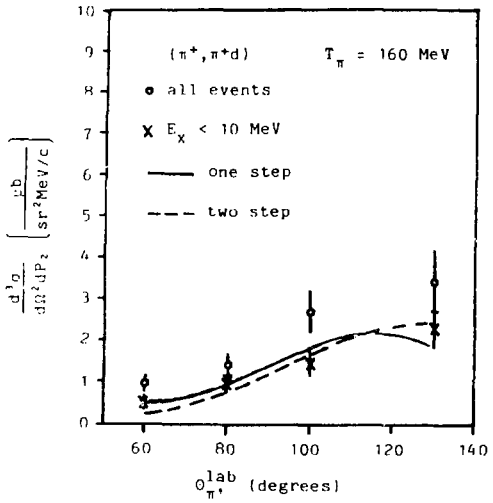

Fig. 1.
Angular distribution at 160 MeV.

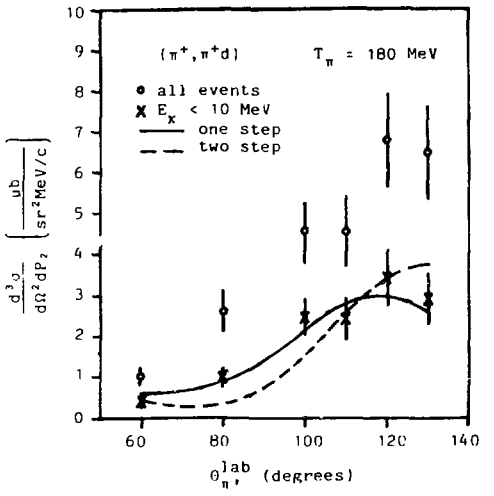

Fig. 2.
Angular distribution at 180 MeV.

runs with different spectrometer magnetic field settings. By examining the higher statistics proton data it was possible to check that the spectrometer acceptance function was correct and to estimate systematic errors to be about 15%.

By measuring the energies of the incident and outgoing pions and the deuteron it is possible to reconstruct the mass and momentum of the recoiling ^{10}B nucleus (5), with a resolution, in this particular case, of about 1.5 MeV. The open circles in these

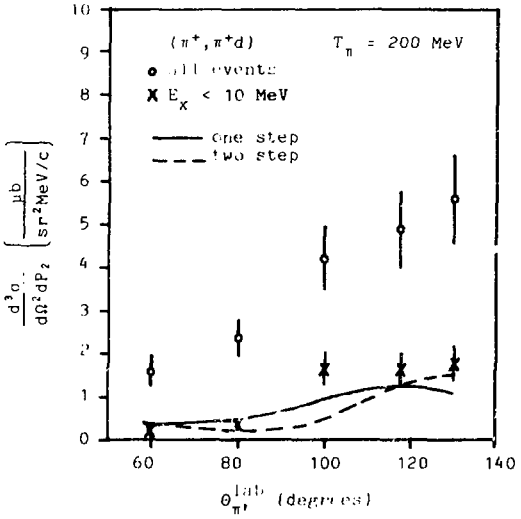

Fig. 3.
Angular distribution at 200 MeV.

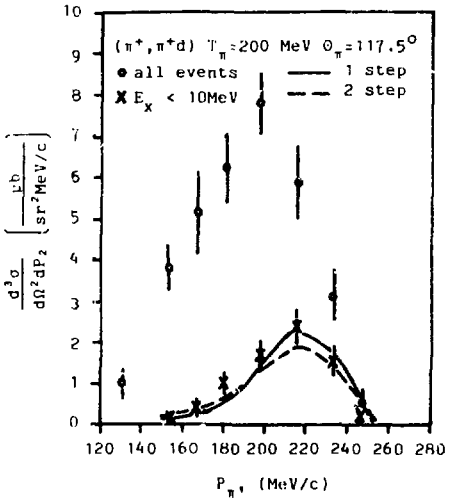

Fig. 4.
Momentum distribution at 117.5°.

four figures show the cross-sections obtained from all the data. The crosses show the cross section for the events with a ^{10}B excitation energy less than 10 MeV. That is to say, the particle stable states of ^{10}B, which are suspected to correspond to the quasi elastic events because they involve only P-shell nucleons and presumably do not involve a significant final state interaction. Our data shows a peak in the region of the ground state and first few excited states, which is one of the pieces of evidence suggesting quasi elastic scattering. We find this suprising considering that the deuteron is weakly bound ($\sim$2.2 MeV) and that they are knocked out with about 40 to 80 MeV kinetic energy in this experiment. Another fact that makes the whole process seem all the more curious is that a free deuteron has an rms radius about equal to that of a ^{12}C nucleus and yet it appears to be undergoing a relatively point-like interaction. This objection can, in part, be explained if the screening nucleons can also couple to the screened nucleon in a quasi deuteron state.

The first step in modelling this data was to assume that there were quasi-free deuteron clusters inside the nucleus and to construct a simple PWIA model as in figure 5a. Since the radial momentum distribution of the clusters was unknown we tried S, P and D-state harmonic oscillator wave functions and linear combinations of these. As a result we got a very good fit to the momentum distribution in figure 4 for the lowexcitation energy data, which is most sensitive to the choice of the radial momentum distribution, provided that we assumed that the quasi-free deuterons were in the S-state. However this seemed, intuitively, implausible because the two nucleons had to be in the P-state because the excitation energy was less than 10 MeV. (The fit was very similar to the solid curve shown in figure 4 and is not shown for the sake of clarity.)

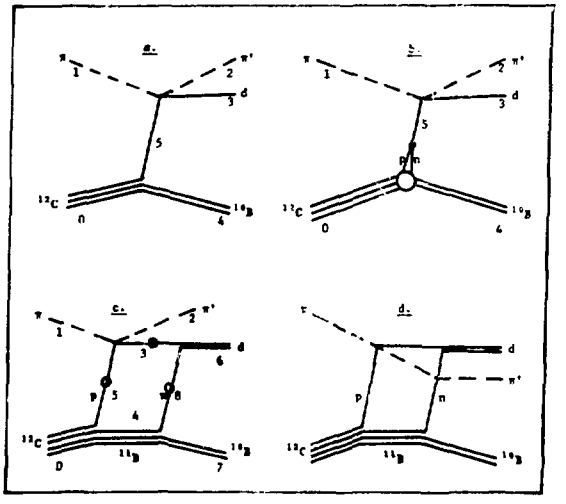

Fig. 5.
Various Feynmann graphs discussed in the text.

Doubting the implication of this result, namely that there are S-state quasi-free deuterons in ^{12}C, we constructed a PWIA overlap shell model based on the graph in figure 5b and a plane wave two-step model based on the graph in figure 5c.

The overlap shell model is fully compatible with the standard shell model. It evolved from a calculation for the reaction $^{6}Li(p,pd)^{4}He$ (8). We first note that the ^{12}C nucleus and the deuteron both have zero isospin and so we are only concerned with the isospin zero states of ^{10}B. We then rewrite the wave function for the N P-shell nucleons in the target nucleus in terms of a core nucleus (^{10}B) with N-2 nucleons and a "cluster" formed by the overlap of the wave function of two P-shell nucleons. We then use the Brody-Moshinsky transformation to transform the 2-particle overlap function into an internal wave function for the cluster and a wave function for the cluster relative to the ^{10}B core. The coefficients of fractional parentage (9) are included so that the calculation can be done for several final states of ^{10}B. The P-shell neutron and proton have the quatum numbers $n_1 = n_2 = 0$ and $l_1 = l_2 = 1$. The "cluster" is required to have the quantum numbers of the deuteron, namely $l = 0$ and $S = 1$. We then require energy conservation in the Brody-Moshinsky bracket (10). As a result the cluster can only have the angular momentum states of $L = 0$ and $L = 2$ with respect to the core. Since ^{12}C has zero spin and the cluster has a spin of unity, this model predicts that only the $J = 1$ and $J = 3$ states of ^{10}B will be seen in this reaction. Unfortunately our resolution and statistics are just not quite good enough to test this prediction. (As this model appears to fit the data well, it is of interest to try to test this prediction by repeating the experiment with better resolution and higher statistics.) For $L = 0$ the internal wave function has $n = 1$ and the relative wave function $N = 0$ or $n = 0$ and $N = 1$. For $L = 2$, $n = N = 0$. The overlap function is then inserted into a PWIA calculation. The internal wave function of the cluster is made to overlap the deuteron wave function and the πd interaction at the upper vertex in figure 5b is assumed to be given by the amplitude for πd elastic scattering. The deuteron wave function was taken to have the form $\phi_d(r) = 0$, $r < r_c$; $= (N/\sqrt{4\pi})(\exp(-\alpha(r-r_c)) - \exp(-\beta(r-r_c)))/r$, $r \geq r_c$, where $\alpha = .232$ fm^{-1}, $\beta = 3.05$ fm^{-1}, $r_c = 0.4$ fm, and $N^2 = 2\alpha\beta(\alpha+\beta)/(\alpha-\beta)^2$. Harmonic oscillator wave functions were used for the neutron and proton since they can be readily transformed by the Brody-Mishinsky transformation. The oscillator paramter was taken to be 1.69 fm, which corresponds to the experimental rms radius for ^{12}C of 2.47 fm. The nucleon cores were not allowed to overlap inside the cluster by multiplying the internal harmonic oscillator wave function by a correllation function $f(r) = 0$, $r < r_c$; $= (1-\exp(-\gamma(r/r_c-1)))$, $r \geq r_c$, where $r_c = 0.4$ fm and $\gamma = 2.0$.[c] Then the cross-section is given by:

$$\frac{d^3\sigma}{d\Omega^2 dp} = F\,J\,\frac{\left.\frac{d\sigma}{d\Omega}\right|_{el}^{\pi d}}{8\pi^4 |\rho_d(Q')|^2}\,G(k) \qquad (1)$$

where:

- F is a normalization factor required because it is a plane wave calculation. The method of calculation of F is discussed below.
- J is the Jacobian from the cm system to the lab system.
- $d\sigma/d\Omega$ is the πd elastic differential cross-section.
- $\rho_d(Q') = \int \exp(i\bar{Q}'.\bar{r})|\phi_d(r)|^2$
- $\bar{Q}' = |\bar{k}'_\pi - \bar{k}'_\pi,|/2$
- $\bar{k}'_\pi$ is the momentum of the incident pion in free πd elastic scattering which corresponds to the same value for s as is found at the upper vertex in figure 5b. Likewise $\bar{k}'_\pi$, is the momentum of the scattered pion in free πd scattering which corresponds to the same t as at the upper vertex in figure 5b.
- G(k) is the nuclear vertex function, where k is the momentum of the cluster with respect to the core, which is equal in magnitude to the ^{10}B recoil momentum. It is given by:

$$G(k) = \left(\frac{b^3}{a^3}\right) e^{-b^2k^2/2} \sum_{\alpha,\beta}^{N_\alpha N_\beta} \{(i_0(Q))^2\left[\frac{3}{2}C_1^{0\alpha} - C_1^{0\alpha}(b^2k^2) + \left(\frac{C_1^{0\alpha}}{6} + \frac{(C_1^{2\alpha}+C_3^{2\beta})}{15}\right) b^4k^4\right] + (i_1(Q))^2\frac{3}{2}C_1^{0\alpha} + i_0(Q)i_1(Q)C_1^{0\alpha}(3-b^2k^2)\} \quad (2)$$

where:

- $b = \sqrt{(A/(A-2))}\, a$, where a = 1.69 fm and A = 12.
- $i_0(Q) = \int_{r_c}^{\infty} j_0(Qr)r^2\phi_d(r)f(r)e^{-r^2/4a^2}$ (3)
- $i_1(Q) = \int_{r_c}^{\infty} j_0(Qr)r^2\phi_d(r)f(r)(1 - (r^2/4a^2))e^{-r^2/4a^2}$ (4)
- $\bar{Q} = |\bar{k}_\pi - \bar{k}_\pi,|/2$, where $\bar{k}_\pi$ and $\bar{k}_\pi$, are the incident and scattered pion momentum respectively in the $(\pi,\pi d)$ data.
- C_J^{Li} is the coefficient of fractional parentage for the ith state of J,L. We took the first three excited states for both J = 1 and J = 3, ie $N_\alpha = N_\beta = 3$.

Despite the apparent complexity of equation 2 it is important to note that it is a polynomial in k^2 damped by a Gaussian. The constant term is the strongest because the Gaussian damping is relatively strong and consequently this function is very similar in shape to a S-state radial momentum distribution. Hence it is not surprising that our simple cluster model fitted the data with an S-state wave function since that is almost exactly what the shell model predicts. In fact it is not easy to distinguish between the two models by comparing fits to the momentum distribution because they give such similar predictions. Probably the clearest prediction of the overlap shell model is that only J = 1

and $J = 3$ final states are allowed, as mentioned above. Given that we cannot test this prediction we are still inclined to reject the naïve cluster model, provided the overlap shell model fits the data, since the shell model has much greater standing in nuclear physics.

The πd elastic scattering differential cross-section was obtained by linearly interpolating the recent SIN data (11). This interpolation was done for the effective incident pion energy and centre of mass scattering angle which give the same s and t in free πd scattering as that found at the upper vertex in figure 5b.

The integrations were done using Simpson's rule. The cross-section was calculated in 1 MeV/c steps of the scattered pion momentum over the full 60.6 MeV/c range and then averaged. The cross-section was calculated at each measured data point with F set equal to one. The value of F chosen for each spectrum was that which minimized the chi-square for that spectrum. The theoretical cross-sections were then recalculated with these values of F. The resulting fits are shown by the solid curves in figures 1 to 4. They reproduce the main features of both the angle and momentum distributions quite successfully. They yield a chi-square of 1.7 per degree of freedom for the four distributions.

This result has no free parameters in it, except for the scaling factor F and possibly γ, which is only allowed to be in the range 0.75 to 2.0 (8), because all the parameters in the model have either been determined experimentally or by fitting the shell model to other nuclear data. We have tried varying the parameters α, β, γ, r_c and a and found that the fit did not improve over that for the values given above. The optimum value for γ is 2.0. We have also summed over fewer final states (ie $N_{\alpha,\beta} < 3$) and also cut the data at an excitation energy of 6 MeV and repeated the fits. In no case was there any significant improvement.

Note that the standard shell model correlation function f(r) was used, the primary function of which is to supress the wave functions in the region of the hard core of the nucleon to prevent the nucleon hard cores from overlapping. Therefore the model fits the data without any abnormal clustering, other than that which occurs naturally in the shell model.

At the time that we started doing these shell model calculations the πd elastic scattering cross-section was not very well known (12). As a result the fits were not very satisfactory, particularly at backwards angles. We were therefore curious to know what elastic cross-sections gave the best fits. For the reasons given above, we were also interested to search for dibaryon resonances and so we decided to calculate the πd elastic differential cross-section as a function of the πd invariant mass from the $(\pi,\pi d)$ data. This was done by solving equation (1) for the πd elastic cross-section and rebinning the data in $M_{\pi d}$, as described in reference (6). The result is shown in figure 6. Since then the new SIN data has become available and the relevant points have been plotted in figure 6 and they agree well with our data. The data shows a peak at 2125 MeV with a width of about 50 MeV. We were interested to know whether this might be associated with the supposed $^1D_2$ $B^2(2140)$ dibaryon resonance. (Note that the peak we see is only 15 MeV from the 2140 whereas it

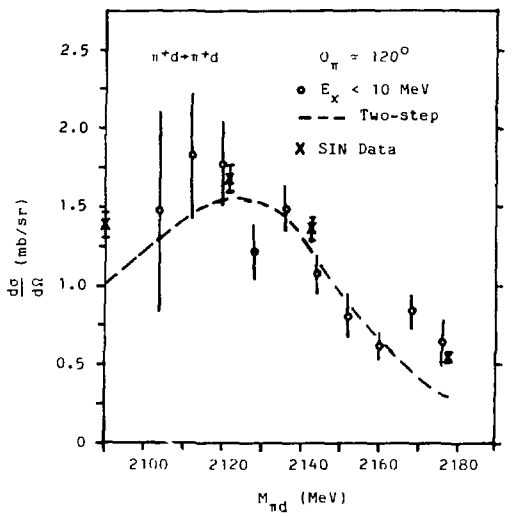

Fig. 6.
The πd invariant mass distribution.

is about 50 MeV from the NΔ mass. Hence our interest in it being a $B^2(2140)$ effect rather than an NΔ effect.)

The two-step calculation we have done throws light on this. It is based on the graph in figure 5c. The idea behind the calculation is that the pion would strike, say, a proton, quasi-elastically and the proton would then pickup a neutron as it left the nucleus, to emerge as a deuteron.

We assume that all the external particles are on the mass shell and that the recoilling ^{10}B is in the ground state (J = 3). It was also assumed that the ^{11}B was in the ground state (J = 3/2). Particles 3,5 and 8 were allowed to be off the mass-shell as discussed below. Distortions were not included in the calculation. The calculation was done at the amplitude level in the $\pi^{12}C$ cm system. It was assumed that particles 3 and 5 were a proton, since the π^+p cross-section is so much larger than that for π^+n. The π^+p spin-flip and non-flip amplitudes were calculated in a program due to Professor G Burleson (13). The proton and neutron are both in the P-shell. We assume that the deuteron is in the S-state so that the D-state and the interference terms are ignored. The cross section is given by:

$$\frac{d^3\sigma}{d\Omega^2 dp} = F' \sum_{M_7=-3}^{3} \sum_{\nu_8,\nu_3=-\frac{1}{2}}^{\frac{1}{2}} \left| J \int d\vec{p}_3^{\,*} X \sum_{M_4,M_8=-3/2}^{3/2} \sum_{m_5,m_8=-1}^{1} \sum_{\nu_5=-\frac{1}{2}}^{\frac{1}{2}} \Phi \right|^2 \quad (5)$$

where:

. F' is a scaling factor because it is a plane wave calculation.

. The numbered subscripts refer to the particle of that number in figure 5c.

. J is the Jacobian to transform to the lab system.

. The asterisk superscript refers to the $\pi^{12}C$ cm system.

$$X = \left(\frac{M_{23}}{2\pi^2 M_3}\right)\left(\frac{E_2' E_3'}{E_1' E_5'}\right)^{\frac{1}{2}}\left(\frac{E_8^*}{4E_1^* E_2^* M_n}\right)^{\frac{1}{2}} \tag{6}$$

$$\Phi = \langle 1\tfrac{1}{2} m_5 \nu_5 | \tfrac{3}{2} - M_4 \rangle \Psi_{1m_5}(\bar{Q}_I) \langle 1\tfrac{1}{2} m_8 \nu_8 | \tfrac{3}{2} M_8 \rangle \langle \tfrac{3}{2} 3 M_8 M_7 | \tfrac{3}{2} M_4 \rangle \Psi_{1m_8}(\bar{Q}_{II})$$
$$\times \phi^*_{0,0}(|\bar{Q}_{III}|) f_{\nu_3,\nu_5} \tag{7}$$

. The prime superscripts refer to the πp cm system.

. The proton and neutron (subscript 5 and 8) wave functions are taken to be standard shell model harmonic oscillator wave functions.

$$\bar{Q}_I = -\bar{P}_4^* - \left(\frac{A-1}{A}\right)\bar{P}_1^* \tag{8}$$

$$\bar{Q}_{II} = -\bar{P}_7^* + \left(\frac{A-2}{A-1}\right)\bar{P}_4^* \tag{9}$$

$$\bar{Q}_{III} = \tfrac{1}{2}\bar{P}_6^* - \bar{P}_3^* \tag{10}$$

. $\phi^*_{0,0}$ is the deuteron wave function. We used the non-relativistic part of the F Gross wave function, which is paramatrized by Laguerre polynomials (14).

. f_{ν_3,ν_5} is the πp scattering amplitude.

The kinematics of the graph in figure 5c can only be solved if the mass of particle 3 is known. The initial calculations were done with it equal to the free proton mass. We found that the cross-section increased nearly an order of magnitude if this mass was increased about 20 MeV. If it was increased another 20 MeV the cross-section dropped back to where it had been, indicating a maximum at around 20 MeV in excess. The intuitive explanation for this is that the neutron, particle 8, is about 20 MeV below the free neutron mass because it is in the potential well of the ^{11}B nucleus. Therefore the deuteron mass will be about 20 MeV too low unless either the momentum transfer between the neutron and proton is very large, which is unlikely, or the proton, particle 3, is about 20 MeV above the mass shell. Since the latter is more likely we made the following simple model:

1. The kinematics for the external particles were solved as in figure 5a. This allows the off-shell mass m_d, of the exchanged deuteron to be calculated.
2. We assume that the amount by which the deuteron is off the mass shell is split evenly between the proton and the neutron.

We define $\Delta M = (m_d - m_{d'})/2$. (11)

3. We then define $m_3 = m_p + \Delta M$ (12)

This then defines m_3 so that $m_3 + m_8 \simeq m_d$. Now that m_3 is defined we can solve the kinematics in two stages and determine m_5 and m_8, which is why we specify the approximate equality only in the previous sentence.

The integration over $\cos\theta_3^*$ was done using 16 point Gaussian quadrature The resulting fits are shown by the dashed lines in figures 1 to 4. The overall chi-square is 2.7 per degree of freedom. The calculation does not fit the angular distributions as well as the overlap shell model calculation. The most plausible explanation for this is that this calculation omits the double scattering term in the deuteron. It is well known that the single scattering term gives a diffraction minimum around 80° to 90°, which is where the two-step model is significantly below the data. It is our belief that this model would give essentially the same fit as the overlap shell model if the double scattering term, as shown in figure 5d, would be included. Care would have to be taken to exclude double counting effects and the calculation would be quite complicated. We note that the overlap shell model calculation, figure 5b, includes the double scattering term because the free πd cross-section is used.

We have used the two-step model to calculate the πd differential cross-section as a function of the πd invariant mass by modifying the program to calculate the cross-section for various incident pion energies. The ^{10}B recoil momentum was arbitrarily fixed at 100 MeV/c, in order to eliminate nuclear effects from the calculation, atleast to first order. The curve obtained is shown by the broken line in figure 6. It fits the data very well with a chi-square of 1.3 per degree of freedom. (Note that the position of this peak is a function of m_3. It just so happens that by using the simple model above the theory matches the experiment.) We therefore conclude that this peak is most likely due to the (3,3) resonance in the single scattering contribution to the reaction. It is therefore not necessary to invoke the $B^2(2140)$ dibaryon resonance to explain this data.

To summarize: we do not need to invoke clusters to explain the data and the standard shell model fits it adequately, given the proviso that distortions have not been included; we find that a simple two-step model does not fit the data as well as the overlap shell model, presumably because the πd double scattering term is excluded; however we find that the two step model does fit the peak in the πd invariant mass spectrum and conclude that this peak is probably an NΔ effect in the single scattering term.

REFERENCES

1. L S Azhgirei et al., Zh. Eksp. Teor. Fiz. 33, 1185 (1957) (Sov. Phys. JETP 6, 911 (1958)).
2. D I Blokhintsev. Zh. Eksp. Teor. Fiz. 33, 1295(1957) (Sov. Phys. JETP 6, 995 (1958))
K Wildermuth and Y C Tang, "A Unified theory of the nucleus",

(Vieweg, Braunschweig, 1977).
3. V V Balashov, AIP Conf. Proc. No. 47 (Winnipeg, Canada, 1978).
4. H J Ziock et al., Phys. Rev Lett. 43, 1919(1979).
5. R J Ellis et al., Phys. Letts. 88B, 253 (1979).
6. R J Ellis et al., Proc. of the Workshop on Nuclear Structure with Intermediate Energy Probes, Los Alamos, NM January, 1980.
6. H J Ziock, Thesis, "Department of Physics, University of Virginia, 1980.
H J Ziock et al. To be submitted to Phys. Rev. C.
7. K Kubodera et al., J. Phys. G: Nucl. Phys. 6, 171(1980).
N Hoshizaki, Prog. of Th. Phys. 61, 129(1979).
8. Y Sakamoto, Phys. Rev. 134, B1211(1964).
9. S Cohen and D Kurath, NP A141, 145(1970).
10. T Brody and M Moshinsky,"Tables of Transformation Brackets for Nuclear and Shell Model Calculations", Gordon and Breach (1967)
11. K Gabathuler et al., SIN preprint, PR 80-011.
12. A M Sach et al., Phys. Rev. 109, 1733(1958).
K G Rogers & L M Lederman, Phys. Rev. 105, 247(1957).
E G Pewitt et al., Phys. Rev. 131, 1826(1963).
J H Norem, Nuc. Phys. B33, 512(1971).
13. This program is based on a parametrization of the πN phase shifts due to G Rowe et al., Triumf preprint, TRI-PP-78-1(1978)
14. W Buck and F Gross, Phys. Letts. 63B, 286(1976).

RELATION BETWEEN $d\sigma(p + d \to {}^3He + \gamma)$ AND $d\sigma(p + d \to {}^3He + \pi^0)$ AT INTERMEDIATE ENERGY BASED ON ISOBAR DOMINANCE

by

B.M.K. Nefkens, W. J. Briscoe, D. H. Fitzgerald and B. H. Silverman
University of California, Los Angeles, California

The reaction mechanism responsible for the reactions $p + d \to {}^3He + \gamma$ and $p + d \to {}^3He + \pi^0$ are quite likely rather similar. We speculate that they involve the excitation of an intermediate state isobar, analogous to pion production in NN interactions. The leading candidate for the isobar at our incident beam energies is the P_{33} (1232) πN resonance. Thus we write

$$p + d \to [P_{33} + X] \to [(N\pi) + X] \to {}^3He + \pi^0, \qquad (1a)$$

$$p + d \to [P_{33} + X] \to [(N\gamma) + X] \to {}^3He + \gamma. \qquad (1b)$$

If indeed both reactions proceed mainly via the P_{33} intermediate state the angular distribution of the differential cross section ratio:

$$R(\theta) = d\sigma(p\,d \to {}^3He\,\pi^0) \,/\, d\sigma(p\,d \to {}^3He\,\gamma), \qquad (2)$$

must be similar to the angular distribution of the P_{33} pionic and radiative decay ratio

$$r(\zeta) = d\sigma(P_{33} \to N\pi^0) \,/\, d\sigma(P_{33} \to N\gamma), \qquad (3)$$

where θ in Eq 2 is the π^0 angle in the p d center of mass system and ζ in Eq 3 is the π^0 angle in the πN center of mass system. Around the peak of the P_{33} resonance the ratio $r(\zeta)$ can be written as

$$r(\zeta) = \left(\frac{1}{A}\right)(1 + 3\cos^2\zeta) \,/\, (2 + 3\sin^2\zeta). \qquad (4)$$

A is a scaling factor which is of the order 1-3 times α. Experimentally the ratio $r(\zeta)$ can be studied as the ratio of the reactions :

$$\rho = d\sigma(\pi^- p \to \pi^0 n) \,/\, d\sigma(\pi^- p \to \gamma n) . \qquad (5)$$

For incident beam energies of interest here it is found that ρ does not change appreciably with energy and that $\rho \simeq r(\zeta)$ with $A \simeq \alpha$. Eq. 4 shows that $r(\zeta)$ has a characteristic shape: it is symmetric around $\zeta = 90^0$ and increases a factor of 10 between $\zeta = 90^0$ and 0^0 or 180^0.

We will make the comparison between R and r in the laboratory system as it shows more clearly the effect of the angle transformation which removes the symmetry around $\zeta = 90^0$. Using the kinematics for p-π elastic scattering we have transformed $r(\zeta)$ to $r(\theta_\ell)$, where θ_ℓ is the lab angle of the scattered pion. Fig. 1 shows $r(\theta_\ell)$ scaled to fit the data. Also shown are the experiment values for R at $T_p = 450$ MeV. These R's are based on the new UCLA p d $\to$ ^{3}He γ results and data on the inverse reaction obtained by Heusch et al.[1], and on p d $\to$ ^{3}He π^0 results by Carroll et al.[2] and Crewe et al.[3]. Furthermore, we made use of the p d $\to$ ^{3}H π^+ data by Dollhopf et al.[4] and Auld et al.[5] and the n d $\to$ ^{3}He π^- data by Franz et al.[6] since they are simply isospin related to p d $\to$ ^{3}He π^0. There is good agreement between the experimental values for R and our simple calculation thereby providing support for the hypothesis of P_{33} resonance formation in radiative pion capture at our beam energy.

A similar agreement between R and r holds at $T_p = 550$ MeV. Instead of making another version of Fig. 1 we used our calculated ratio r to predict the cross section for p d $\to$ ^{3}He γ. We used the pion production data of Dollhopf et al.[4], Carroll et al.[2], Aslanides et al.[7], Harting et al.[8], N. Booth[9], and Franz et al.[6]. The parameter, A, of Eq. 4 was adjusted to fit the data. Our prediction is shown in Fig. 2 together with our p d $\to$ ^{3}He γ data and the results of the inverse reaction of Heusch et al.[1]; the agreement is good.

Fearing [10] has recently calculated $d\sigma$(p d $\to$ ^{3}He γ) using a modification of his earlier p d $\to$ ^{3}H π^+ calculation, based on a distorted wave impulse approximation.

The physical picture is that of a triangle diagram in which the incoming proton interacts with the neutron from the target ^{3}He: p + n → d + γ, and the intermediate state deuteron picks up the leftover proton to form ^{3}He. Thus in Fearing's model the p d → ^{3}He γ cross section is given by the n p → d γ cross section, a form factor and some kinematic quantities. To the extent that the reaction n p → d γ is dominated by the P_{33} resonance we see that the Fearing calculation also has some P_{33} dominance, but in a much less straightforward way than our simple model. The prediction of the Fearing model is compared to our data at T_p = 550 MeV in Fig. 2. Even if one were to adjust the scale, the agreement is not spectacular.

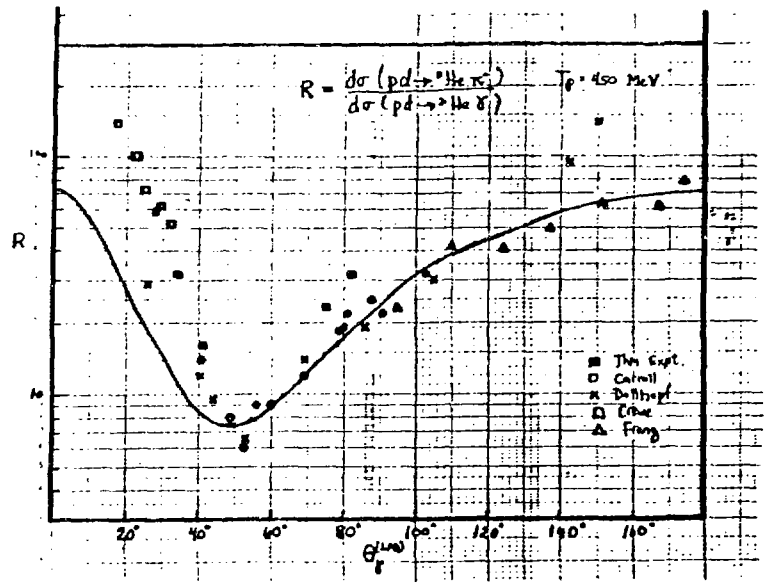

Fig. 1. Ratio R, defined in the text, as a function of θ_γ. The solid line is our theoretical calculation adjusted to fit the data at back angles.

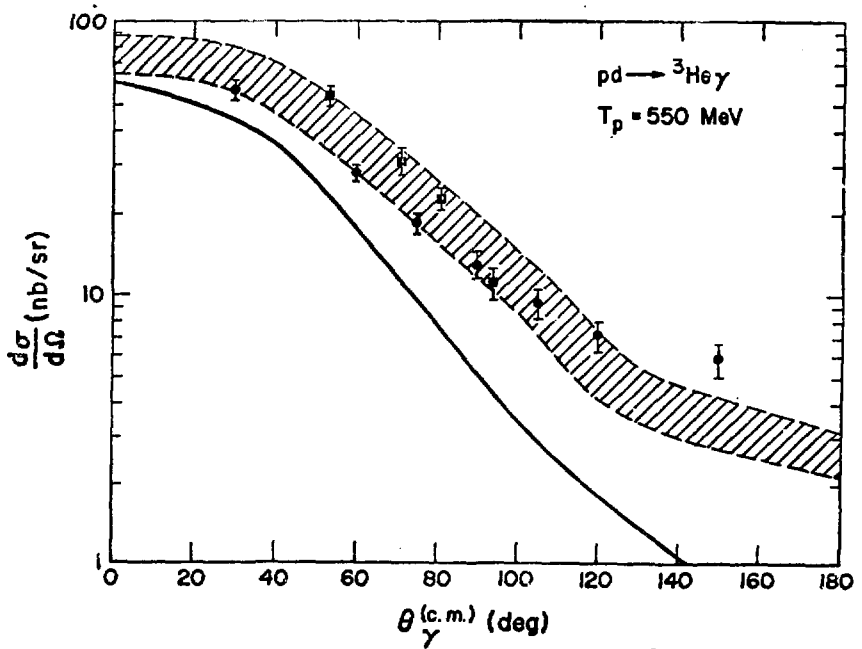

Fig. 2. Differential cross section for p+d→^{3}He γ at T_p = 550 MeV. The solid squares are our data points. The open circles are the Cal. Tech. results on γ+^{3}He→p+d with the appropriate detailed balance factor. The cross hatched band is our theoretical prediction, the solid line is the theoretical prediction by Fearing.

ANTIPROTON-NUCLEON EXPERIMENTS

by

R. D. Tripp
Lawrence Berkeley Laboratory

ABSTRACT

Recent investigations of antinucleon-nucleon interactions are in direct conflict with earlier experiments concerning the existence of narrow structures in the $\bar{p}$ N system. We here review the current status of formation experiments, summarize and comment upon production experiments, and point out deficiencies in the data.

I. INTRODUCTION

During the mid-1970's interest in narrow states of the antinucleon-nucleon system grew dramatically. It was kindled by experimental indications for narrow resonances, followed by intense theoretical interest in the subject. A number of theoretical conjectures were put forth to account for the scanty and sometimes conflicting evidence. Whether called a potential model, quark model, or topological bootstrap model, these various notions became known as baryonium, which can loosely be described as a narrow boson state decaying predominantly into $\bar{N}N$ whenever energetically possible. For a time, experiment and theory acted coherently, encouraging the belief that a whole new spectroscopy would soon be uncovered. However, during the past two years many experiments have been performed which are in direct conflict with the earlier results. In this talk I shall emphasize recent formation experiments whereby a systematic study of the energy dependence of antinucleon-nucleon cross sections is made. Production experiments - those in which the antinucleon-nucleon system appears as a part of a multibody final state - will also be summarized and commented upon.

II. FORMATION EXPERIMENT

A. $P_{\bar{p}} < 1$ GeV/c (Region of S(1936) and 2020)

Because of its prominent appearance in four measurements of the total or annihilation cross section,[1,4] the S meson has always been regarded as the best established of all narrow $\bar{N}N$ states, and thus as the cornerstone for the notion of baryonium. Table 1 shows this evidence as of two years ago, along with the original production experiment[5] of 1966 from which the S derives its name. Inspection of this table reveals substantial inconsistencies among the four formation experiments concerning the mass, height and width of the resonance, although all experiments claimed to be observing the same phenomenon. Table 2 shows the situation as it exists today. Here are listed, in two groups, the various formation experiments: i) before the last $\bar{N}N$ conference in Barr in 1978 and, ii) those performed or in progress since then. Whereas at Barr experiments were overwhelmingly in favour of the S, the more recent results find little or no evidence for structure in this mass region. In this table, I have tried to estimate in a consistent way the rms mass resolution of each experiment, along with its statistical precision. The next section will cover the five new total and annihilation cross section experiments as well as new $\bar{p}p$ backward elastic and charge exchange work and a measurement of the 5 pion annihilation cross section.

1. LBL-BNL-MT Holyoke Experiments

Let me first discuss the recently published total and annihilation cross section experiment of Hamilton et al. in which I was a participant.[6] This was done in the old LESBI beam of the BNL AGS. To remind you of directly comparable previous experiments, Fig. 1 shows the $\bar{p}p$ and $\bar{p}d$ total cross section results of Carroll et al[1] and Fig. 2 the $\bar{p}p$ annihilation cross sections as measured by Bruckner et al.[3] In both experiments, a narrow and prominent structure appears in the vicinity of 500 MeV/c corresponding to the S meson mass. Figure 3 schematically compares our apparatus with that of Carroll et al. Experimental details can be found in the two papers. Suffice it to say that both are classic transmission experiments whereby the total cross section is obtained by extrapolation of the cross sections measured by a series of counters of diminishing size to one subtending zero solid angle. Figure 4 illustrates this extrapolation procedure at one of our momenta (480 MeV/c). The most significant difference between

the two experiments was that our target and transmission counters were approximately four times thinner. The first greatly improved the mass resolution for narrow resonance searches, while together they permitted us to descend considerably lower in momentum before antiprotons stopping in the transmission counters began to seriously impair the proper functioning of the apparatus. The charged annihilation cross section was measured simultaneously by a scintillator box surrounding the target but open at both ends. This arrangement also recorded wide angle elastic scatters as well as neutral processes converted in the target or surrounding materials and therefore the cross sections we recorded were about 15% higher than other measurements. Our results for the total and annihilation cross sections as a functior of momentum appear in Fig. 5a. Although we find no evidence for the narrow structure seen by other experiments, there is a hint of a broad and gentle enhancement in the region of 500 MeV/c. It appears in both cross sections and is evident in all three systematic passes made through this mass region in the process of collecting the data. The solid lines show our best fit to the data assuming a Breit-Wigner resonance added incoherently to simple nonresonant backgrounds containing two parameters for the total cross section and four parameters for the annihilation cross section. The dashed line on the total cross section plot is what was expected from the results of Carroll et al.; disagreement is clearly unavoidable. Figures 5b and 5c show our two measured cross sections after subtracting the non-resonant background. The dashed line in 5c is the expectation for the narrow enhancement in the annihilation cross section derived from the resonance parameters found by Bruckner et al. If for some reason our mass resolution were much poorer than it is believed to be, our results could be reconciled with those of Bruckner et al. However, there are only two contributions to the resolution: the length of the target (8 cm) and the momentum spread of the beam. Both contribute about equally at 500 MeV/c. The beam was deliberately arranged to have a narrow momentum bite and a range curve confirms that the momentum spread of the beam was as expected from Monte Carlo studies of the acceptance. Thus there is no doubt that our rms mass resolution is ± 1.5 MeV at the mass of the S and therefore contributes a negligible amount to our measured width. Deuterium cross sections were also measured and are exhibited in Fig. 6. There is no indication here for the broad structure found in $\bar{p}p$. Table 3 lists the resonance parameters obtained in our best fits for hydrogen and deuterium. Apart from deuterium corrections, an I=0 resonance should appear the same size in hydrogen as in deuterium, whereas an

I = 1 resonance should be three times larger in deuterium. For a resonance of the width observed in hydrogen, internal momentum smearing and Glauber shadowing should diminish the height of the observed bump by a factor of two. Thus our results in deuterium appear to exclude I = 1 structure and are barely consistent with I = 0 (two standard deviations low in σ_T ($\bar{p}d$)).

Although we express no uncertainty concerning the absence of narrow structure in the S region of a magnitude claimed by previous experimenters, our evidence for a broad resonance must be qualified. It should be stressed that the rapidly falling background is changing seven times faster than the resonance in the region where the resonant cross section is varying most rapidly! How this background is parametrized will clearly influence the resonance parameters as well as the strength of evidence for its existence. Indeed there is no reason for the total cross section background to fall precisely as A + B/p (where p is the $\bar{p}$ laboratory momentum) when there are many rising and falling partial waves contributing to the cross section. In Fig. 7 we display the total cross section times laboratory momentum plotted as a function of momentum (thereby linearizing the plot) along with best fits with and without a resonance. The χ^2, although never really good, shows a marked improvement of 53 with the introduction of three additional resonance parameters. There are indications from other experiments to be mentioned next, of changes in the vicinity of 500 MeV/c not necessarily associated with a resonance. Accordingly, if we ask for the best fit of σ_T for not one but two straight lines (see Fig. 8), an improvement in χ^2 of 10 occurs with two additional parameters, the break falling near 500 MeV/c. The improvement is thus much less marked than with the introduction of a resonance. We therefore feel that the most plausible, but by no means unique, conclusion to be drawn from our data is that there is a broad resonance in I = 0 in the S region coupled predominantly to the annihilation channels since the elasticity $x = 1 - (\Delta\sigma_A/\Delta\sigma_T)$ is found by us to be $x = 0.2\ ^{+0.3}_{-0.2}$.

Now let me turn briefly to discuss two other experiments done by us at BNL. The results of two charge exchange experiments $\bar{p}p \to \bar{n}n$ appear in Fig. 9, the open circles being that of Alston-Garnjost et al. in 1975[7] (done with poor energy resolution) while the full circles are recent results of Hamilton et al.[8] No evidence is found in either for a narrow S(1936). Being however a different experiment one can always invoke ad hoc reasons for the non-appearance of the S in this particular channel - for example two isospin degerate resonances. The broad structure we have observed in the total cross section would, given its small

elasticity, appear here under the simplest assumption as only a 1/4 mb enhancement. This would be impossible to see with our statistical uncertainty.

Our other recent work investigated the $\bar{p}p$ differential cross section at 180 degrees.[9] This experiment was prompted by the earlier bubble chamber measurements of Cline et al.[10] and d'Andlau et al.[11] who claimed evidence for abundant structure in the vicinity of 500 MeV/c. The upper part of Fig. 10 shows these earlier data while the lower figure presents our counter results. The general form of our data are consistent with those of d'Andlau but with no evidence for narrow structure. The large and very broad enhancement centered (by sheer coincidence) near 500 MeV/c can be adequately accounted for as being due to the passage of the second diffraction maximum through 180° as the incident momentum changes. The broken curves are representative theoretical calculations[12,13] describing this phenomenon. Although we see no evidence for narrow structure at 500 MeV/c we certainly cannot exclude the possibility of a broader enhancement sitting squarely on top of the diffraction peak as might arise from our observed structure in the total cross section.

In none of the three experiments described above do we find an enhancement in the 2020 MeV mass region (805 MeV/c) where a production experiment[14] has found evidence for a resonance.

2. College de France - Pisa $\sigma(\bar{p}p \to \pi^+\pi^-\pi^+\pi^-\pi^0)$

An 81 cm bubble chamber experiment of some years ago has recently published[15] evidence for a very broad enhancement in the five pion annihilation cross section, shown in Fig. 11. This is the largest of the many $\bar{p}p$ annihilation channels, amounting to more than 20% of the total annihilation cross section. Adding a resonance incoherently to a two parameter non-resonant background, they find an enhancement of 5.5 ± 1.5 mb at M = 1949 ± 10 MeV with a width Γ = 80 ± 20 MeV. The $\omega^0\rho^0$ appears prominently in this enhancement,[16] thus specifying the effect as I = 1. Because of its isospin as well as its larger width, it cannot be identified with the previously discussed enhancement seen by Hamilton et al. Given the difficulty of observing the latter, due to its large width and small height, it would be even harder to identify this broader structure in the total cross section.

3. Tokyo-Hiroshima Measurement of the $\bar{p}p$ Total Cross Section

The results of the KEK experiment of Kamae et al., on the $\bar{p}p$ total cross section have recently appeared in print.[17] The experiment is of the transmission type and utilizes both wire chambers and counters. They present two

measurements of the total cross section, one obtained by an extrapolation from a laboratory scattering angle of 5° (with Coulomb corrections) and the other an unextrapolated measurement of all events where a $\bar{p}$ was scattered out of a counter subtending a substantial solid angle of 160 msr. The latter is understandably 10-20% lower but is statistically somewhat better due to a smaller empty target subtraction. Why the statistical fuctuations in one cross section do not appear in the other is puzzling since most of the events contributing to the extrapolated cross section were also scattered out of the transmission counter used to measure the unextrapolated cross section.

In Fig. 12 these two cross sections are displayed and compared with two earlier experiments. In neither do they see evidence for narrow structure of the magnitude suggested by the experiments of Carroll et al. or Chaloupka et al., although they cannot with their limited statistical accuracy exclude the smaller structure claimed by Bruckner et al. Their experiment appears to have some normalization difficulty since the absolute value of their extrapolated total cross sections are about 10 mb lower than those measured by the Carroll, Chaloupka and Hamilton experiments.

4. Temple-Irvine-New Mexico Measurement of the $\bar{p}p$ Annihilation Cross Section

A paper by Jastrzembski et al. presented at the Bressanone $\bar{N}N$ Conference[18] describes an experiment done to measure the $\bar{p}p$ charged annihilation cross section in the region of the S meson. The experiment took place in the new LESB II beam at BNL and utilized a one meter long target. Pion detectors consisting of multiwire proportional chambers and scintillation counters detected charged particles emerging from the target over about 10% of the full solid angle. Elastically scattered events were eliminated by time of flight. The vertex position was located by wire chambers to a precision of 2.5 cm, thereby permitting a good energy resolution despite the long target which had the advantage of yielding relatively good statistical precision in a short running time.

Their results appear in Fig. 13. Only the relative annihilation cross section as a function of momentum is presented due to absolute uncertainties associated with their long target method and their small solid angle acceptance. No narrow structure of the form suggested by earlier experiments is evident in the data near the S meson mass. A fit to a featureless $A + B/p + C/p^2$ cross section yields a good fit in spite of the apparent discontinuity near 500 MeV/c. A fit

using the resonance parameters of Bruckner et al. (but with the mass allowed to vary) gives a much higher χ^2.

5. BNL-DOE-Michigan State-Syracuse $\bar{p}p$ Annihilation Cross Section

A second measurement of the $\bar{p}p$ charged annihilation cross section by Lowenstein et al., was presented at the Bressanone Conference.[18] Similar in conception to the previously described experiment, it utilized the momentum recombined branch of the LESB II beam at BNL. A shorter 50 cm target necessitated seven different incident momenta to cover the region of the S meson. Drift chambers located the annihilation vertex for improved energy resolution. The overlapping data from the seven momentum settings were merged into one plot of the charged annihilation cross section shown in preliminary form in Fig. 14. Again, only a relative cross section is measured, their results being normalized to other measurements at 500 MeV/c. No statistically significant evidence for an enhancement is seen in their data over the region from 440 to 570 MeV/c, and a reasonable fit can be obtained to the form A + B/p for the annihilation cross section. The background-subtracted cross section appears at the top of the figure where about a 4 standard deviation dip very near the S mass of approximately the same size and width as the enhancement of Bruckner et al. can be seen. It is interesting to speculate about the ensuing turmoil into which the field would have been thrown if this presumably statistical structure had been positive rather than negative.

6. Frascati-Padova-Rome-Trieste Measurement of $\bar{p}p$ Total and Partial Cross Sections

The latest formation experiment results concerning the S meson are those of the 2 meter bubble chamber presented at Bressanone[18] in preliminary form by Marcello Cresti. The experiment is very similar to that of Chaloupka et al.,[2] in fact with many of the same participants. The important differences are that it was carried to somewhat higher momentum (620 rather than 550 MeV/c) and utilized a new, better defined, antiproton beam. The earlier experiment had evidence for an 11 mb bump, coming mainly from the elastic channel but the new data do not confirm this structure. A major problem in the first experiment arose from the fact that since the measurements extended only to 550 meV/c, they were required to utilized some data points of Carroll et al. at higher momentum in order to better constrain the fit. Since there was a small

systematic difference in normalization between the two experiments, this yielded an exaggerated structure not nearly as apparent in their data alone. In Fig. 15 the new total cross section data are shown plotted as a function of momentum. In this plot of $p\sigma_T$ a straight line adequately describes the measurements apart from the highest momentum point of each of the two runs where losses are believed to set in. Their data also appear consistent with a break in the slope near 500 MeV/c.

B. $p_{\bar{p}} > 1$ GeV/c (T(2190) and U(2350) Regions)

Above 1 GeV/c $\bar{p}$ formation experiments become much easier to do because $\bar{p}$ beams of high intensity are readily available. It has long been known[19] and confirmed[20] that there are broad structures between 1 and 2 GeV/c in the total cross sections, both in hydrogen and deuterium. These are displayed in Fig. 16. Here again, as in the S region, the rapidly falling background is varying considerably faster than the resonant structure. Effects attributable to these structures have also been seen in the elastic[21] and charge exchange[22] cross sections and even more clearly in the two body annihilation channels $\pi^+\pi^-$[23] and $\pi^o\pi^o$.[24] The energy dependence of the angular distributions in these annihilation channels are very striking and indicate that there is more going on than meets the eye when one inspects only the total cross sections of Fig. 16. In fact, one of the latest phenomenological analyses of the combined $\pi^+\pi^-$ and $\pi^o\pi^o$ angular distributions[25] require resonances in nearly all partial waves that contribute to the two pion final state! All of these new sub-structures appear to be broad (> 100 MeV), as befitting exothermic processes at high energy. However, it should be pointed out that these higher energy experiments have all been done with relatively poor energy resolution so that narrow resonances, say less than 5 MeV, would probably have escaped detection. It would perhaps be worthwhile to reinvestigate this region with improved resolution, as has recently been done for the πp system.[26]

III. RECENT PRODUCTION EXPERIMENTS

Given the many degrees freedom involved in the choice of beam particles, momenta, final states, and various cuts in the data, this review must of necessity be a very superficial and impressionistic view of the subject of production experiments. These experiments are summarized in Table 4 which makes no pretense of being a complete list but should contain most of the important ones that have reported effects at masses below 2500 MeV. This table is biased in the sense that no attempt is made to compile an exhaustive list of negative results and their degree of significance. Nevertheless the latter clearly dominate those experiments reporting positive effects. References appear in the table when not noted below.

A. Bound States

Three peaks in the gamma ray spectrum obtained from stopped $\bar{p}$ in hydrogen have been reported in a CERN experiment[27] using a Sodium Iodide detector. Their background-subtracted spectrum in Fig. 17 shows line widths consistent with their experimental resolution (~ 20 MeV). A repetition of the experiment with comparable statistics by the same group is said to confirm the 1646 and 1684 states. A larger NaI detector, essentially 1/12 of a crystal ball, built by the same group, will soon be yielding data with much improved resolution and counting rate. An experiment is also in progress at BNL to detect these gamma rays using a high resolution pair spectrometer, while another BNL experiment has already reported negative results from apparatus which measured the momentum spectrum of nucleons emitted from $\bar{p}$ capture in deuterium.

B. S(1936)

Two production experiments from CERN have within the past year reported evidence for a narrow S meson of marginal statistical significance. The ACCMOR group has repeated their own experiment at higher energy. With improved statistics, rumor has it that they see no effect at this time.

C. The 2020 and 2200 States

The statistically strongest production evidence for states interpreted as baryonium has come from an Ω spectrometer experiment.[14] The evidence is displayed in Fig. 18. This triggered a series of similar experiments, done mainly at BNL, that have recently reported negative results with comparable or higher

sensitivity, thereby casting serious doubt on their reality. The only glimmer of hope at the Bressanone Conference came from a group using the SLAC hybrid facility who showed a striking $\bar{p}n$ enhancement at 2020. It however appeared only in their 6 GeV/c and not in the 9 GeV/c data, leaving them in a quandary as to its significance.

D. Strange Baryonium

The notion of baryonium applies as well to strange particles. Weak indications for such a state at 2460 MeV decaying into $\overline{\Lambda}\Delta^{++}(1236)$ and $\overline{\Sigma}^{+}(1385)$ p have not been supported by more recent studies with comparable or better statistics. Other channels have also been investigated with no evidence for structure.

IV. CONCLUSIONS AND OUTLOOK

Concerning formation experiments, five recent measurements of the total and/or annihilation cross section [17,18] are unanimously in conflict with earlier strong evidence for narrow structure in the S(1936) region near a $\bar{p}$ momentum of 500 MeV/c. What went wrong with the previous experiments? The first good formation evidence for the S meson, that of Carroll et al.[1] suffered at these low momenta from the use of too long a target and an excessive number of thick transmission counters. As a result, the "transmitted" antiportons stopped in their transmission counters in the 430-520 MeV/c region precisely where they observed their enhancement and, quite likely gave rise to a spurious effect. This personal opinion, I should say, is not shared by the experimenters who still stand by their data. The experiment of Chaloupka et al.[2] has been repeated under similar but better conditions, by many of the same participants of the original experiment, and the source of their earlier effect seems to be understood. The bubble chamber evidence of Sakamoto et al.,[4] statistically never very strong (3.7σ) can be attributed to a fluctaution. This leaves the experiment of Bruckner et al.[3] as the only remaining contender in support of narrow structure. I know of no explanation for what may have generated their effect, which, taken by itself, remains statistically and experimentally quite convincing.

Most of the recent negative experiments contain "statistical" wiggles or glitches in the 500 MeV/c region, though none are compatible with previous evidence for narrow enhancements in essentially identical processes. Only the LBL-BNL-Mt Holyoke measurements of the total and annihilation cross sections[6] show evidence for anything resembling a resonance. Their smaller and much broader structure is made apparent only after the whole momentum region from 350 to 1050 MeV/c is fitted to a simple background parametrization. In the presence of this rapidly falling background of uncertain nature, it is impossible to present a convincing argument for the resonant origin of the effect which is seen only in the $\bar{p}p$ and not in the $\bar{p}d$ cross sections. There is no incompatibility of this broad and gentle structure with the absence of evidence in the other four recent measurements. The experiment of Kamae et al. lacks the statistical precision while the other three covered only a very limited momentum region from 400 to 600 MeV/c.

The Heidelberg-Saclay group has run again at the CERN PS and should be producing results soon. The new experiment differs considerably from their former incarnation as Bruckner et al., and they expect to measure both the total and annihilation cross sections with high statistical precision and good energy resolution. A new BNL experiment has been proposed by Sakitt et al and they are presently setting up. The KEK experiment[17] is, I believe, continuing to take data. All other experiments are dismanteled or are pursuing other questions.

The long range future for formation experiments clearly lies in the direction of LEAR, the low energy antiproton ring at CERN. Intensities in excess of 10^6 $\bar{p}$/sec are expected from the facility. As envisioned, when fully developed, it will permit investigation of $\bar{p}$ reactions all the way from 0.1 to 2 GeV/c. The richness of available reactions may allow us someday to understand the $\bar{N}N$ system better than we now understand NN. It should be remarked that none of the present generation of formation experiments has an energy resolution better than 1 MeV. Thus if states of baryonium with a width comparable to, for example, J/ψ (< 100 KeV) were to exist, they would have escaped detection. The higher resolution obtainable from LEAR will clearly improve on our present limits. Alternatively, if some unusual decay mode of a very narrow state were to exist, it could be seen even with present resolution.

As for production experiments, many have been undertaken in order to investigate earlier evidence for narrow states. These have nearly all produced negative results. A number of these experiments have analyzed only a sample of their data, so that further results can be expected soon. Although future for narrow resonances does not look promising, let me point out that very high statistics production experiments occasionally reveal surprising results. For example, Fig. 19 shows recent evidence[28] for quite a different object, a strange baryon of narrow width decaying into a final state full of strangeness ($\Sigma|S|=3$). Perhaps some heretofore uninvestigated meson decay may likewise offer a surprise.

Let me close by indulging in some speculation, supported only by historical precedent, about the ultimate outcome of studies of the $\bar{N}N$ system. Based on analogy with other two body interactions amoung what we once naively regarded as elementary particles, I think that there is good reason to suppose that when we dig deeply enough in our analysis of the $\bar{N}N$ system, it will yield perhaps as many resonances as the πN or $\bar{K}N$ systems. Here, as we know, what at first

appeared to be simple bumps in the total cross section, well described by Breit-Wigner resonant forms, when more detailed studies of angular distributions and polarizations were performed, usually turned out to harbor whole nests of resonances. For those who may object that we are dealing here with quark structures that are too different to draw a plausible analogy, let me remind you that the same evolution appears to be taking place in the T and U regions of the $\bar{N}N$ system. A superficial analysis of only the total cross section gave evidence for several broad resonances,[19] while detailed examination of the reactions $\bar{p}p \to \pi^+\pi^-$ and $\pi^0\pi^0$ have uncovered structures requiring resonances in nearly all partial waves that can contribute to the two pion final state![25] Even the NN system, so well studies over the past decades, is revealing unexpected activity when pure spin states are explored.[29] In no case are any of these resonances anomalously narrow, their various widths being understood in terms of centrifugal barrier effects and, for the πN and $\bar{K}N$ systems, couplings derived from the quark model. Thus, the nearly featureless $\bar{p}N$ total and annihilation cross sections may well contain a large number of resonant states, probably all of normal widths. Although the exciting narrow structures we were hoping for may not be in the cards, what superficially looks rather like a desert may yet provide a lot of interest for future users of LEAR.

REFERENCES

1. A. S. Carroll et al., Phys. Rev. Lett. 32, 247 (1974).
2. V. Chaloupka et al., Phys. Lett. 61B, 487 (1976).
3. W. Bruckner et al, Phys. Lett. 67B, 222 (1977)
4. S. Sakamoto et al, Nucl. Phys. B158, 410 (1979).
5. G. Chikovani et., Phys. Lett. 22, 233 (1966).
6. R. P. Hamilton et al., Phys. Rev. Lett. 44, 1182 (1980).
7. M. Alston-Garnjost et al., Phys. Rev. Lett. 35, 1685 (1975).
8. R. P. Hamilton et al., Phys. Rev. Lett. 44, 1179 (1980).
9. M. Alston-Garnjost et al., Phys. Rev. Lett. 43, 1901 (1979).
10. D. Cline et al., Phys. Rev. Lett. 21, 1268 (1968).
11. Ch. D'Andlau et al., Phys. Lett. 58B, 223 (1975).
12. C. B. Dover and J. M. Richard, private communication.
13. O. D. Dalkarov and F. Myhrer, Nuovo Cimento 40A, 152 (1977).
14. P. Benkheiri et al., Phys. Lett. 68B, 483 (1977).
15. Ch. Defoix et al., Nucl. Phys. B162, 12 (1980).
16. P. Espigat et al., Nucl. Phys. B162, 41 (1980).
17. T. Kamae et al., Phys. Rev. Lett. 44, 1439 (1980).
18. Proceedings of the 5th European Symposium on Nucleon-Antinucleon Interactions, Padova 1980 (M. Cresti, editor).
19. R. J. Abrams et al., Phys. Rev. D1, 1917 (1970).
20. J. Alspector et al., Phys. Rev. Lett. 30, 511 (1973).
21. M. Coupland et al., Phys. Lett. 71B, 460 (1977).
22. D. Cutts et al., Phys. Rev. D17, 16 (1978).
23. A. Carter et al., Phys. Lett. 67B, 117 (1977).
24. A. S. Dulude et al., Phys. Lett. 79B, 335 (1978).
25. M. R. Pennington, paper appearing in reference 18.

26. P. Baillon et al., Phys. Lett. 94B, 533 and 541 (1980).

27. P. Pavlopoulos et al., Phys. Lett. 72B, 415 (1978).

28. J. Amirzadeh et al., Phys. Lett. 89B, 125 (1979).

29. K. Hidaka et al., Phys. Lett. 70B, 479 (1977).

FIGURE CAPTIONS

Fig. 1. Total cross sections of $\bar{p}p$ and $\bar{p}d$ as measured by Carroll et al.[1] The observed structure, appearing about equally in both cross sections, indicated a preference for I = 1.

Fig. 2. The measured $\bar{p}p$ cross sections of Bruckner et al.[3] A narrow enhancement was observed in the charged annihilation and in the elastic cross sections. The inset shows the background subtracted annihilation cross section.

Fig. 3. Comparison of the apparatus of Carroll et al.[1] with that of Hamilton et al.[6] Both experiments maintained their transmission counters at fixed momentum transfer by repositioning them for each incident momentum. The veto box surrounding the latter experiment permitted the extrapolation of purely elastic scattering to 0° as well as a measurement of the charged annihilation cross section.

Fig. 4. Illustration of the extrapolation done at one momentum (480 MeV/c) in Ref. 6. The three outermost counters were used for the extrapolation of the form $\sigma(t) = \sigma(o) + [d\sigma/dt]_o (1 - \frac{bt}{2})t$ which yielded both the total cross section $\sigma(o)$ and the forward scattering amplitude $[d\sigma/dt]_o$. The forward slope b, obtained from other experiments done at higher momentum transfer, was parametrized as $b = (3 + \frac{1}{p})^2$.

Fig. 5. (a) The $\bar{p}p$ total and "charged annihilation" cross sections measured by Hamilton et al.[6] The solid curved are best fits to the data using an incoherent superposition of a resonance with a simple background parametrization. The dashed line represents the data of Carroll et al.[1] The "charged annihilation" cross section is uncorrected for large angle elastic scattering and converted neutral interactions. (b) and (c) The background subtracted total and "charged annihilation" cross sections along with the best fits (see Table 3 for resonance parameters). The dashed line represents the fit to the data of Bruckner et al.[3]

Fig. 6. The $\bar{p}d$ total and "charged annihilation" cross sections measured by Hamilton et al.[6] along with the best fits. See Table 3 for the resulting resonance parameters.

Fig. 7. The total cross sections of Ref. 6 multiplied by lab momentum and plotted vs lab momentum, with a resonance ($\chi^2 = 104$) and without a resonance ($\chi^2 = 157$).

Fig. 8. The total cross sections of Ref. 6 multiplied by lab momentum and plotted vs lab momentum. Here is shown the best fit with two straight lines, with without a resonance ($\chi^2 = 147$).

Fig. 9. The charge exchange cross section $\bar{p}p \to \bar{n}n$ as measured in Ref. 7 (open circles) and Ref. 8 (full circles) plotted as function of lab momentum.

Fig. 10. (a) Earlier bubble chamber measurements of $\bar{p}p$ backward elastic scattering ($\cos\theta_{cm} \leq -0.8$) of Refs. 10 and 11. (b) Recent measurements of Alston-Garnjost et al.[9] for $\bar{p}p$ backward elastic scattering ($< \cos\theta_{cm} > = 0.994$). Broken curves are theoretical predictions of Refs. 12 and 13.

Fig. 11. The cross section for $\bar{p}p \to \pi^+\pi^+\bar{\pi}^-\bar{\pi}^0$ as measured by Defoix et al.[15]

Fig. 12. The $\bar{p}p$ total cross sections measured by Kamae at al.[17] Full circles are the extrapolated $\bar{p}p$ total cross sections while the open circles are the unextrapolated cross sections as measured by a counter subtending a solid angle of 160 msr.

Fig. 13. The $\bar{p}p$ annihilation cross sections measured by Jastrzembski et al.[18] The solid line is a three parameter non-resonant fit ($\chi^2/DF = 1.06$), while the dashed line has a resonance of fixed width (4 MeV) and height (6.5 mb) with a resulting $\chi^2/DF = 1.56$).

Fig. 14. The $\bar{p}p$ annihilation cross sections measured by Lowenstein et al.[18] The solid line is a two parameter fit without a resonance. The upper plot shows the data after background is subtracted.

Fig. 15. The preliminary $\bar{p}p$ total cross sections measured in the 2-meter bubble chamber by Cresti et al.[18] multiplied by lab momentum and plotted vs lab momentum. The full circles are obtained from a run with the beam momentum set at 673 MeV/c and the crosses are from a run at 710 MeV/c.

Fig. 16. Total cross section measurements of Abrams et al.[19] made in the T and U regions at higher momenta. The upper figure are measurements taken in hydrogen and the lower in deuterium.

Fig. 17. Background-subtracted γ-ray spectrum from an investigation[27] of the reaction $\bar{p}_S p \to \gamma$ MM. The first peak presumably comes from $\pi_S^- p \to \gamma n$ while the others correspond to missing masses of 1684, 1646 and 1395 MeV.

Fig. 18. $\bar{p}p$ invariant mass from the reaction $\pi^- p \to p_f \pi^- (\bar{p}p)$ showing peaks in the mass spectrum at 2020 and 2200 MeV.

Fig. 19. Mass spectrum of R^+ in the reaction $K^- p \to \pi^- R^+$ where R^+ decays into 5 or 6 body final states with 2 or more strange particles.

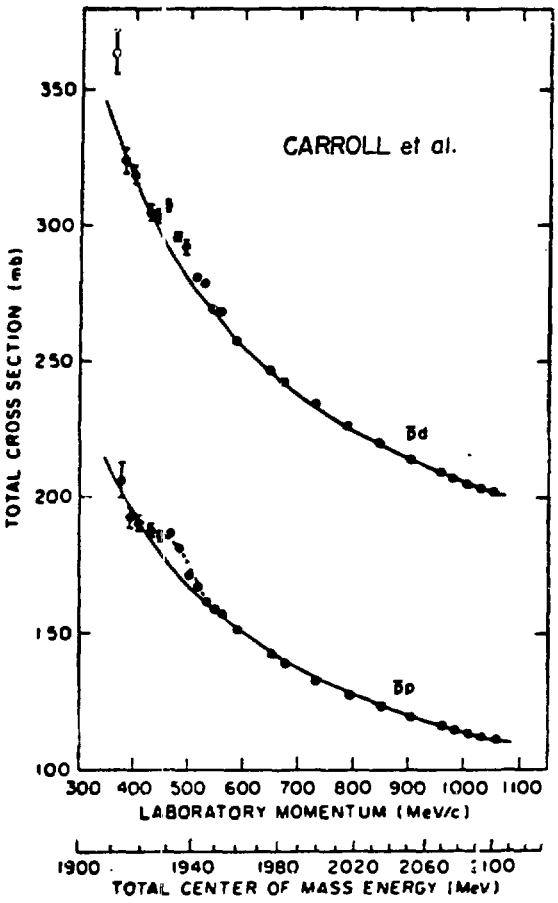

Fig. 1.

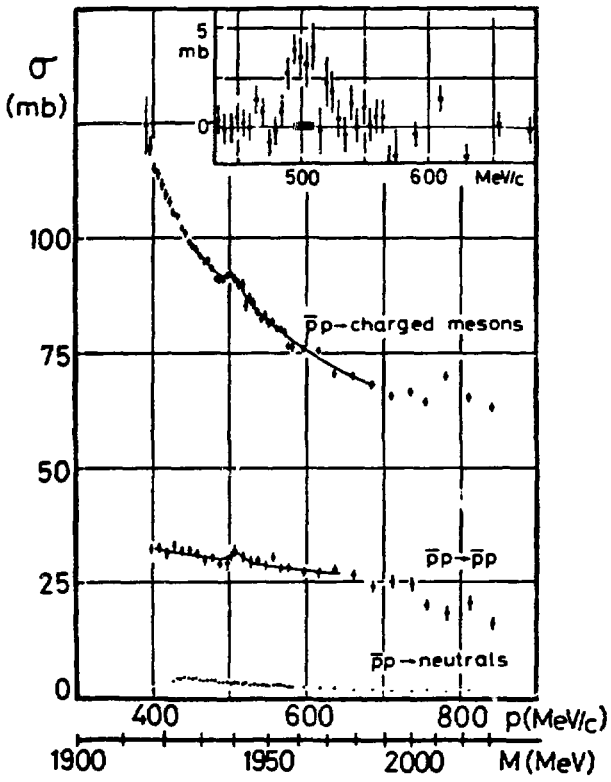

Fig. 2.

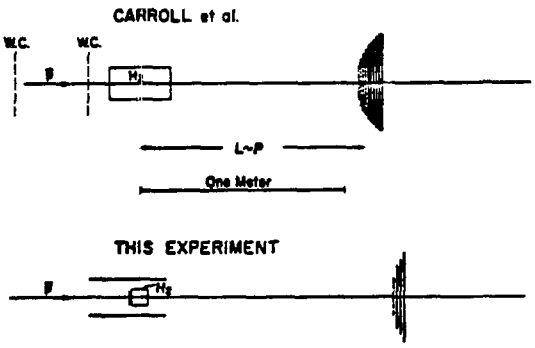

Fig. 3

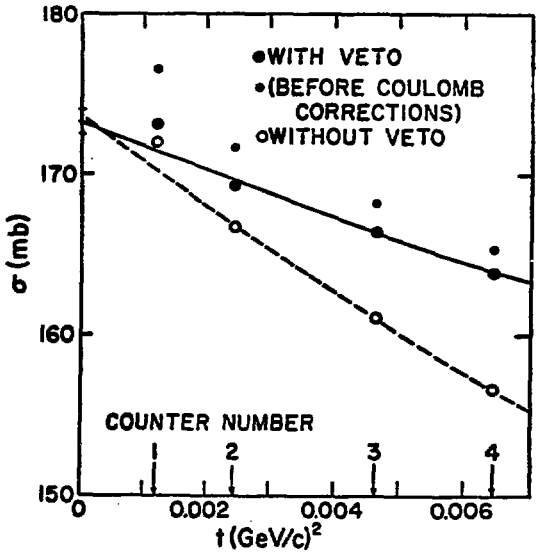

Fig. 4

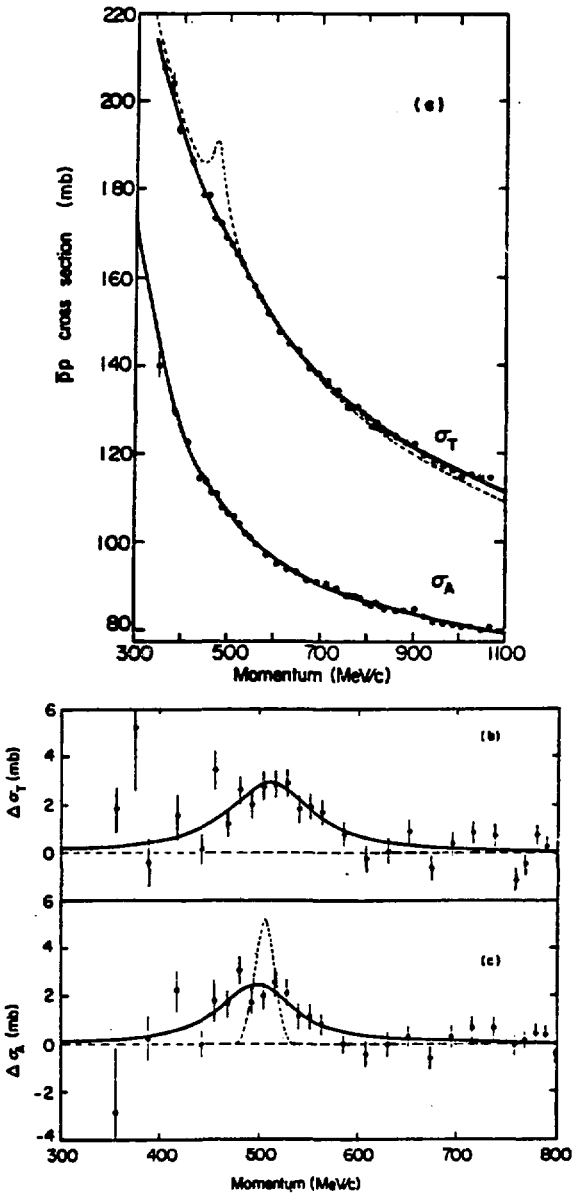
(a)
$\bar{p}p$ cross section (mb)
σ_T
σ_A
Momentum (MeV/c)
(b)
$\Delta\sigma_T$ (mb)
(c)
$\Delta\sigma_L$ (mb)
Momentum (MeV/c)

Fig. 5.

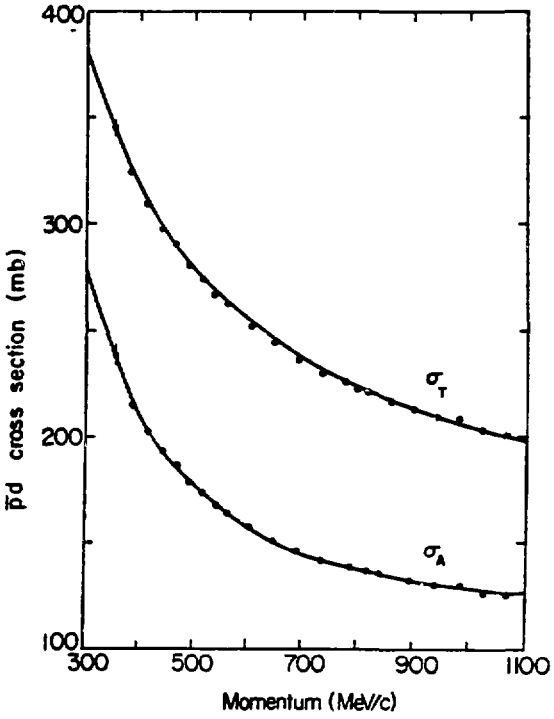
$\bar{p}d$ cross section (mb)
σ_T
σ_A
Momentum (MeV/c)

Fig. 6.

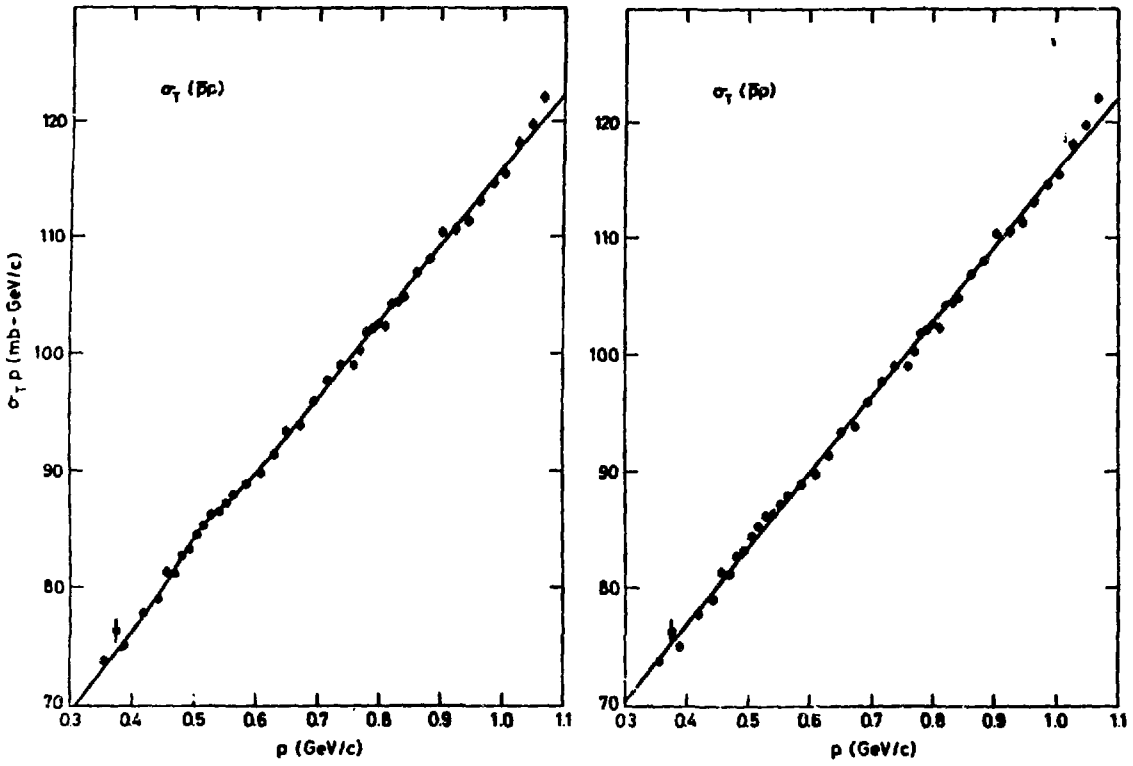
σ_T ($\bar{p}p$)
σ_T ($\bar{p}p$)
$\sigma_T p$ (mb - GeV/c)
p (GeV/c)
p (GeV/c)
120
110
100
90
80
70
0.3
0.4
0.5
0.6
0.7
0.8
0.9
1.0
1.1

Fig. 7.

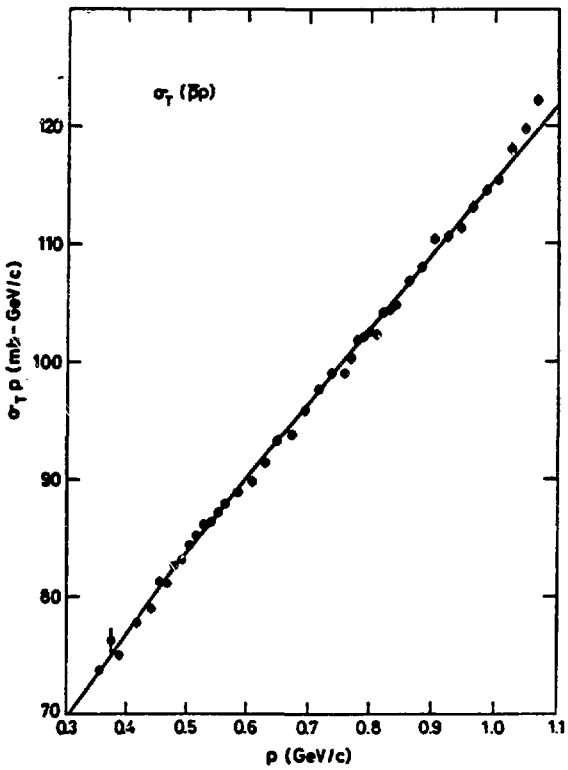
σ_T ($\bar{p}p$)
$\sigma_T p$ (mb - GeV/c)
p (GeV/c)

Fig. 8.

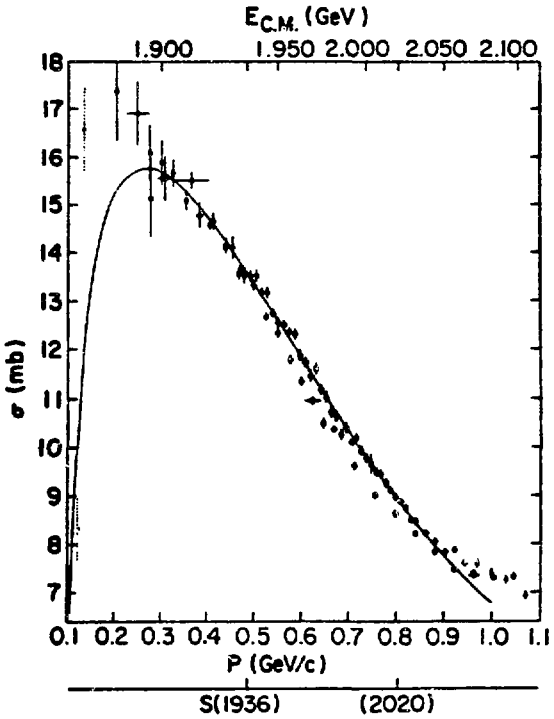
$E_{C.M.}$ (GeV)
σ (mb)
P (GeV/c)
S(1936)
(2020)

Fig. 9.

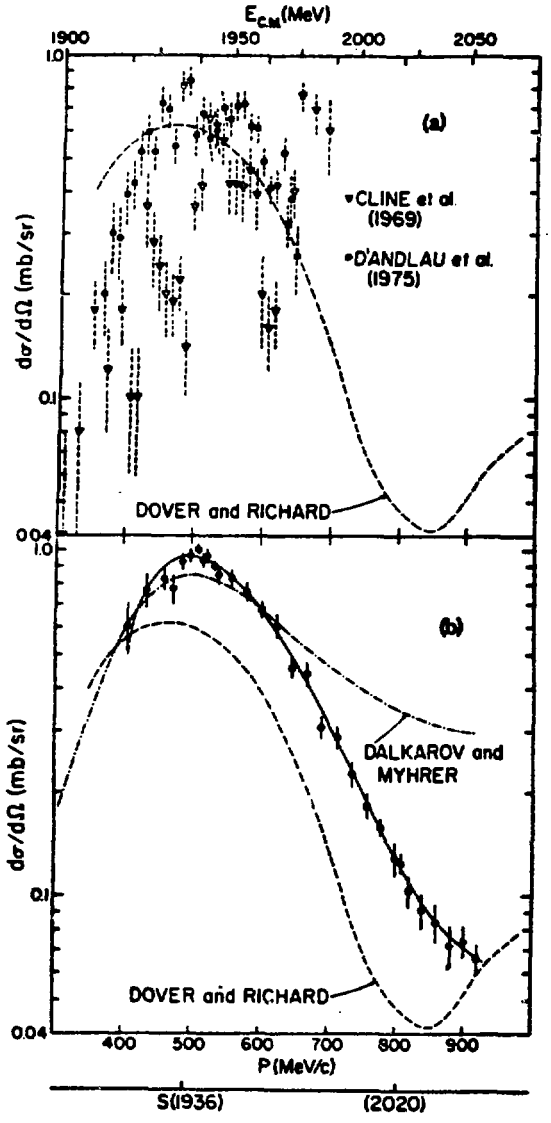

Fig. 10.

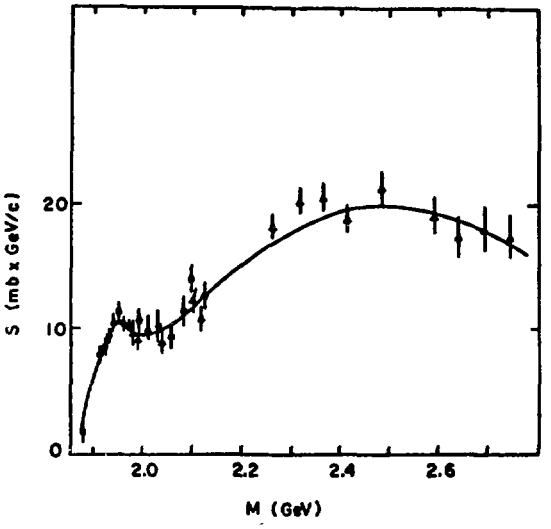

Fig. 11.

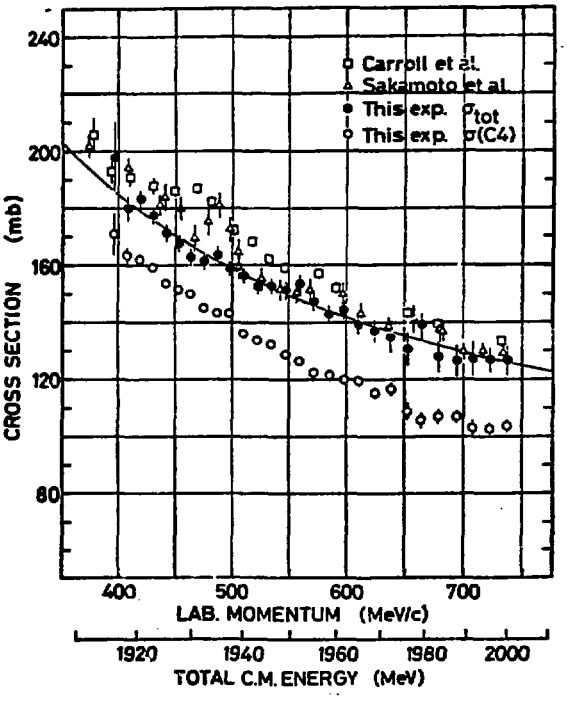

Fig. 12.

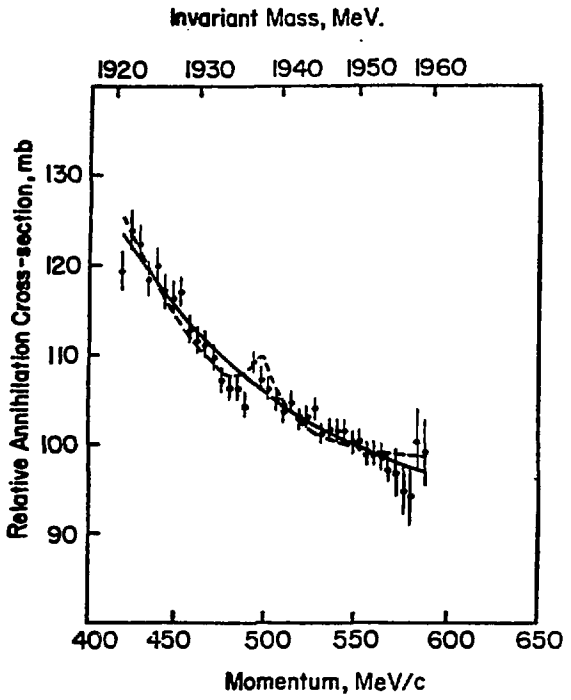
Invariant Mass, MeV.
1920
1930
1940
1950
1960
Relative Annihilation Cross-section, mb
130
120
110
100
90
400
450
500
550
600
650
Momentum, MeV/c

Fig. 13.

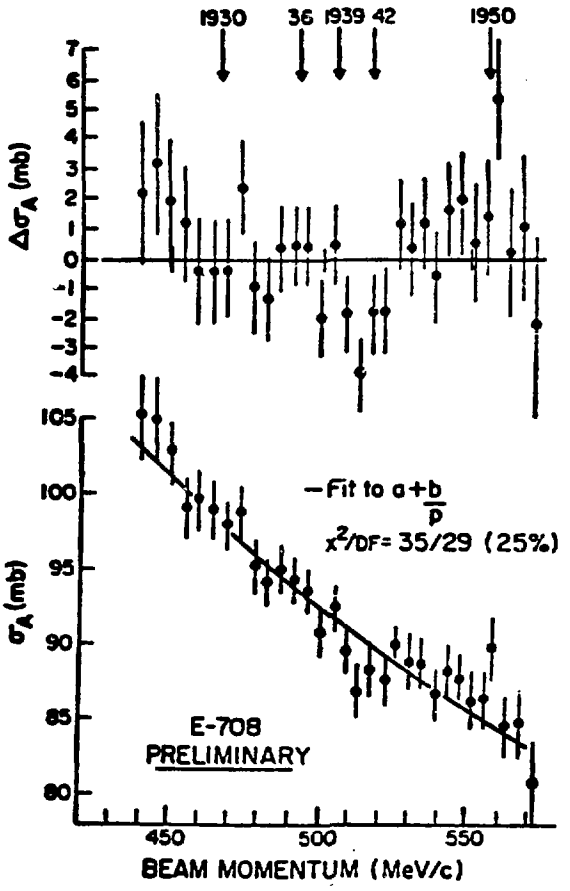
1930
36
1939
42
1950
$\Delta\sigma_A$ (mb)
σ_A (mb)
—Fit to $a+\frac{b}{p}$
$x^2/DF = 35/29$ (25%)
E-708
PRELIMINARY
BEAM MOMENTUM (MeV/c)

Fig. 14.

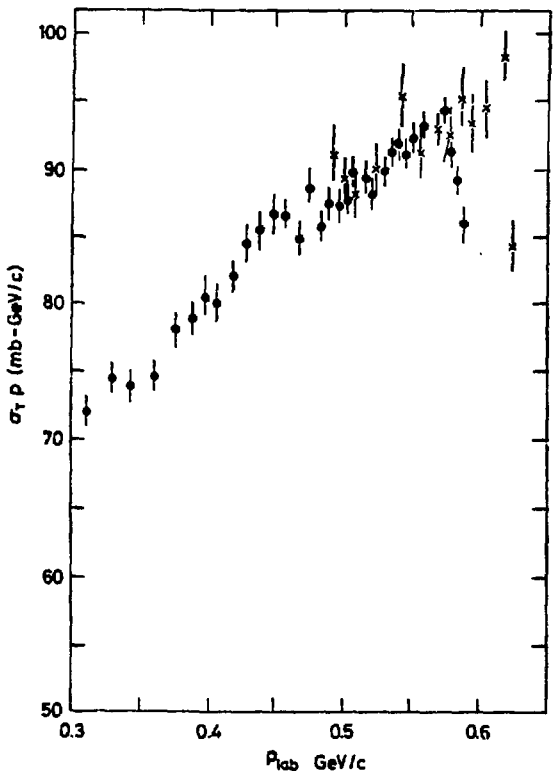

Fig. 15

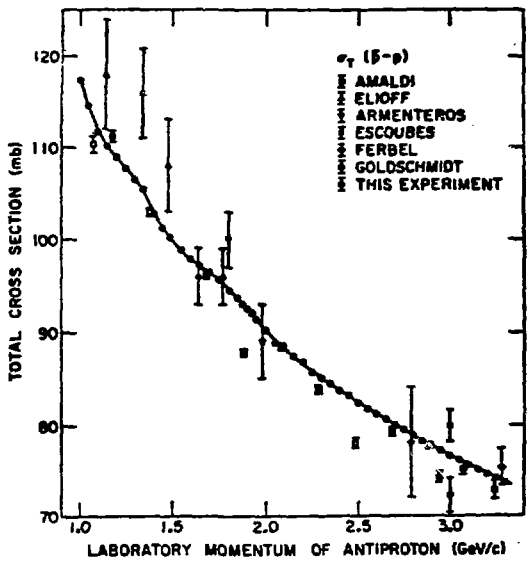

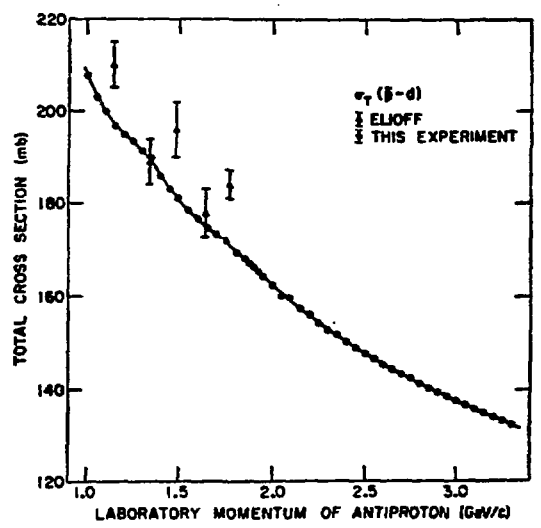

Fig. 16.

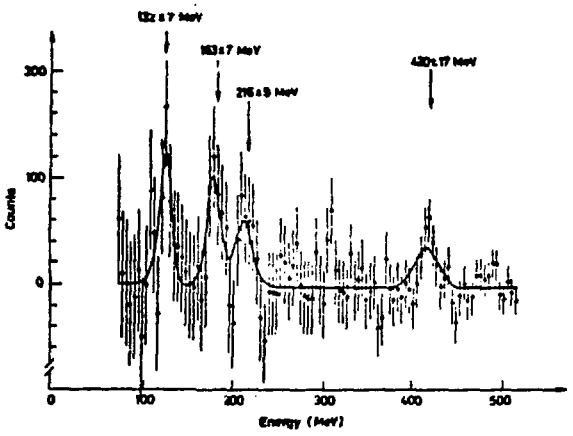

Fig. 17

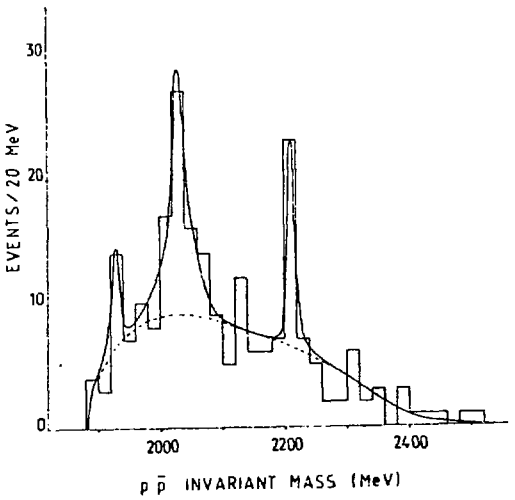
EVENTS / 20 MeV
30
20
10
0
2000
2200
2400
p p̄ INVARIANT MASS (MeV)

Fig. 18.

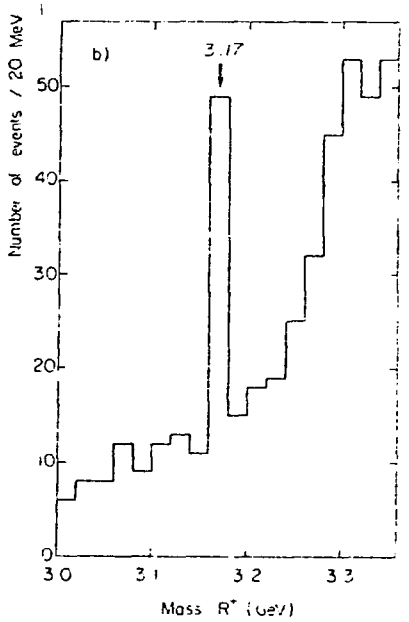
b)
3.17
Number of events / 20 MeV
50
40
30
20
10
0
3.0
3.1
3.2
3.3
Mass R* (GeV)

Fig. 19.

TABLE I

S MESON PARAMETERS

EXPERIMENT	M(MeV)	Γ(MeV)	$\Delta\sigma_T$(mb)	$\Delta\sigma_{EL}$(mb)
CHICOVANI (1966)	1929±4	≤35		
CARROLL (1974)	1932±2	9^{+4}_{-3}	18^{-3}_{+6}	
CHALOUPKA (1976)	1936±1	$8.8^{+4.3}_{-3.2}$	10.6±2.4	7.0±1.4
BRUCKNER (1977)	1939±3	≤ 4	9±2	4±2
SAKAMOTO (1978)	1936±1	2.8±1.4	14.5±3.9	

TABLE II

FORMATION EXPERIMENTS IN THE S-MESON REGION

Resonance	Experiment (Ref)	Type	RMS, Energy Resol. (MeV)	Precision mb/10MeV/c
I. PRE-BARR (1978)				
yes	CARROLL [1]	CTR	± 4.3	± 2.5
yes	CHALOUPKA [2]	BC $\sigma_T, \sigma_A \cdots$	1.5	2.2
yes	BRUCKNER [3]	CTR σ_A, σ_{EL}	1.0	0.7
yes	SAKAMOTO [4]	BC σ_T	1.5	4.3
yes	CLINE [11]	BC $\bar{p}p180^o$	1.5	0.1 (mb/sr)
yes	D'ANDLAU [12]	BC $\bar{p}p180^o$	1.5	0.1 (mb/sr)
no	ALSTON-GARNJOST [8]	CTR $\bar{p}p \to \bar{n}n$	5.5	0.2
II. 1979-1980				
no	ALSTON-GARNJOST [10]	CTR $\bar{p}p$ 180^o	3.0	0.04 (mb/sr)
no	HAMILTON [9]	CTR $\bar{p}p \to \bar{n}n$	1.5	0.14
yes (broad)	DEFOIX [16]	BC $\bar{p}p \to 5\pi$	1.5	1.4
possible (broad)	HAMILTON [6]	CTR σ_T, σ_A	1.5	0.6
no	KAMAE [18]	CTR σ_T	1.5	2.7
no	JASTRZEMBSKI [19]	CTR σ_A	1.5	0.9
no	LOWENSTEIN [20]	CTR σ_A	2.0	0.9
no	CRESTI [21]	BC $\sigma_T, \sigma_A \cdots$	1.5	1.8
	HEIDELBERG-SACLAY in analysis	CTR σ_T, σ_A		
	BNL scheduled	CTR σ_T		

TABLE III

BEST FIT RESONANCE PARAMETERS OF REF. 6

	$\sigma_T(\bar{p}p)$	$\sigma_A(\bar{p}p)$	$\sigma_T(\bar{p}d)$ [a]	$\sigma_A(\bar{p}d)$ [a]
Mass (P_R) MeV/c	510±6	497±9	[505]	[505]
MeV	1940±1	1937±2		
Width (Γ) MeV/c	101±28	90±42	[142]	[142]
MeV	23±6	21±10		
Height (Δ) mb	3.0±0.7	2.5±0.8	-0.4±0.9	1.9±1.7

(a) The mass and width (broadened by internal momentum) have been fixed in deuterium.

TABLE IV

RECENT PRODUCTION EXPERIMENTS

Resonance		Experiment	Reaction	P (GeV/c)
Bound States				
1395,1646,1684	NaI	PL 72B,415(1978	$\bar{p}_s p \to \gamma(\bar{p}p)$	0
(in progress)	Xtal Ball	Bressanone (Prelim.)	" "	0
No (1650-1930)	Spect.	PRL 44,853 (1980)	$\bar{p}d \to N\ (\bar{p}N)$	.4
S(1936)				
Yes (4σ)	ACCMOR	PL 90B,475(1980)	$pp \to (\bar{p}p)+X$	93
No	ACCMOR	rumor	" "	>100
Yes (4.5σ)	Ω	PL 93B,517(1980)	$\gamma p \to p(\bar{p}p)$	44-70
No	Spect.	Bressanone(Prelim.)	$\pi^- p \to X^+(MM)^-$	1.3
2020 **2200**				
Yes(7.6σ) Yes(6.5σ)	Ω	PL 68B,483(1977)	$\pi^- p \to p_f \pi^- (\bar{p}n)$	9, 12
No No	Ω	PL 81B,380(1979)	$\pi^- p \to p_f (\bar{p}n)$	9, 12
Yes(3σ) Yes(2σ)	Cornell	PRL 42,1593(1979)	$ep \to ep(\bar{p}p)$	11.5
No No	MPS	PRL 44,909(1980)	$\pi^+ p \to \Delta^{++}_f (\bar{p}p)$	9.8
No No	DA Spect.	PRL 44,1572(1980)	$\pi^- p \to \bar{p}p+X^0$	8.1
No No	EMS	PRL 45,316(1980)	$pp \to pp(\bar{p}p)$	11.75
No No	MPS	PRL 45, 1990 (1980)	$\pi^+ p \to \Delta^{++}(\bar{p}p)_f$	9.8
No No	DA Spect.	PRL 44,1572(1980)	$\pi^- p \to \bar{p}p+X^0$	8.1
No No	EMS	PRL 45,316(1980)	$pp \to pp(\bar{p}p)$	11.75
No No	MPS	PRL 45,1611(1980)	$\pi^- p \to p_f \pi^- (\bar{p}p)$	16
No No	Ω,Ω'	Bressanone(Prelim.)	$\bar{p}p \to \bar{p}p+X^0$	12
Yes (5σ) } No	SLAC HF	Bressanone(Prelim.)	$\bar{p}p \to (\bar{p}n)\pi^+\pi^-\pi^-$	6 { 9
($\bar{Y}$N)				
Yes $\bar{\Lambda}p\pi^+(2460)$ (4σ)	Ω	PL 77B,447(1978)	$K^+ p \to \bar{\Lambda}p\pi^+ n$	12
No $p\pi^+(2460)$	Ω	Bressanone(Prelim.)	$K^+ p \to \bar{\Lambda}p\pi^+ n$	13
No $(\bar{\Lambda}N)$	Ω	Bressanone(Prelim.)	$K^+ p \to \bar{\Lambda}pN\pi$	13
No$(\bar{p}p)/(\bar{Y}^*p)$	Ω	Bressanone(Prelim.)	$K^+ p \to K^+ \bar{p}pp$	13

RESEARCH PROGRAM AT LEAR

by

P. DALPIAZ

Istituto di Fisica-Università di Ferrara-Italy
Istituto Nazionale Fisica Nucleare-Torino-Italy

ABSTRACT

The CERN LEAR Program is outlined. The approved experiments are described, together with the possible future developments in the same field.

I. INTRODUCTION

In recent years considerable interest has been focused at CERN[1] on experimental possibilities offered by the antiproton proton interactions to answer some of the fundamental questions of the present day physics.

The poor quality of present low-energy antiprotons beams severly limits the possibility of obtainig physics information from antiproton-proton annihilation.

The idea to add to the antiproton accumulator[2] (AA) built at CERN, a facility for experiments with low energy antiprotons[3] has received an enthusiastic support of the CERN physicist community.

The advent in about two year from now of the LEAR (low-energy antiproton ring) project[4], a small synchrotron to accelerate and decelerate antiprotons, at CERN gives at this laboratory the possibility to study carefully the antiproton-proton annihilation and give anwers mainly to the following physics subjects:

a) Deailed study of hadronic $\bar{p}$-p annihilation and definitive answer to the existence of narrow or large baryonium states.
b) First experiments with antineutrons beams.
c) Detailed study of the atomic transition $\bar{p}p$, $\bar{p}$-nuclei.
d) Exploratory experiments in antiproton interactions with nuclei.
e) Precise measurement of the fundamental properties of the antinucleons.

f) Measurements of the electromagnetic form factors of the proton in the time like region and related arguments.

II. LEAR PROJECT.

The part of the LEAR project[5] approved by CERN is the extracted beam operation. This option should give 10^6 $\bar{p}$/sec in the momentum range of 300 MeV/c to 2000 MeV/c, with 100% duty cycle and without contamination. The electron cooling application should extend the momentum range to 100 MeV/c.

Fig.1. shows the LEAR project located in the PS south hall with the six experimental areas where 2 experiments can run simultaneously.

Other options are discussed[5] but not yet approved:

i) Jet target[6] crossing the antiproton circulating beam:

a) A H_2 molecular jet of 10^{-9}-10^{-11} g/cm^2, while giving a very good definition of the interaction energy ($\Delta p/p < 10^{-4}$ with electron cooling) permits at the same time a very efficient use of the available antiprotons. It is important to use in conjunction the electron cooling to compensate the beam blow up due to multiple Coulomb scattering; in this case, internal jet targets will yield a maximum luminosity for a given beam. A maximum intensity antineutron beam can be obtained from a jet target[7] installed in the center of a magnet sector of LEAR[5].

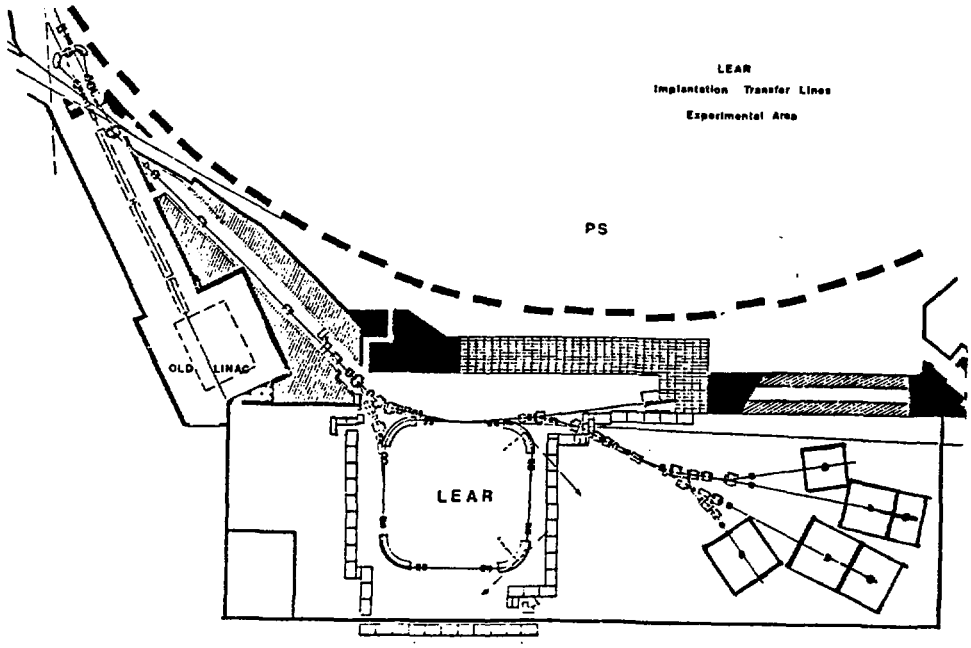

Fig. 1. LEAR lay out

b) An H atomic polarized jet of $\sim 10^{-12}$ g/cm^2, to perform very clean polarization experiments[8].

ii) Co-rotating beams of antiprotons and H^-.

To perform experiments with protonium ($\bar{p}p$ at rest) in absence of the Stark effect it was proposed[9,10] to store in LEAR co-rotating beams of antiprotons and H^-. Beams of neutral states of ($\bar{p}p$) formed in flight would come out of the straight sections.

This technique can profit of the Doppler shift of the forward emitted X-rays by $\bar{p}p$ atoms in flight.

Tuning the Doppler shift by varing the storage energy in LEAR, the energy of the X-ray can be measured by differential absorption with the precision of the internal beams of LEAR ($< 10^{-4} - 10^{-5}$ with electron cooling).

iii) LEAR mini collider of $\bar{p}$ and p.

To study of charmonium family spectroscopy with a resolution < 1 MeV also for $J^P = 1^-$ particles it was proposed [3,11,12] to use LEAR as a minicollider of $\bar{p}p$ in the range of $2.8 < E_{cm} < 4.6$ GeV.

Out of official papers other possibilities were discussed such as:

iv) Minicollider of $\bar{p}$ and p to reach $E_{cm} = 12$ GeV.

To study the T family spectroscopy [11,12] and related arguments.

v) Low energy parallel beams of $\bar{p}$ and p or d.

To study the annihilation and the elastic and total cross section of $\bar{p}$ and p or d, it was proposed to use two rings with common straight sections where the beams circulate at different momenta.[13,10,14].

With this technique it is possible to obtain very small Δp between the two beams.

III. LEAR PHYSICS PROGRAM

In this chapter the experiments approved by the PSCC of CERN are presented together with a discussion of the further possible developments.

A. Elastic and total cross section of $\bar{p}p$ and hadronic annihilation of $\bar{p}p$[15].

The succession of contrastant experiment on the search of baryonium states shows clearly the limits on the present possibilities of antiproton low energy experimentation.

The importance of the exsistence of exotic states like baryonium was pointed out by several anthors[16] from two points of view: the nuclear bounds and the quark color.

The experimentation with LEAR gives the opportunity to clarify this problem and give a definitive answer in the search of narrow or large baryonium states and in any case to cover our lack of informations on the interactions of antiproton at low energy.

Several experiments are approved in this field:

i) Elastic and total cross section $\bar{p}p$.

- The ABGOST collaboration[17] proposes a measurement of σ_{tot} and $\sigma(\bar{p}p \to \text{neutrals})$ with good mass resolution (±0.4 MeV/c over the S region) and high statistics (±0.25%) and small steps of momentum (∿ 10 MeV/c) down to 200 MeV/c. The objective of this measurement is to look for narrow states. If any such narrow state is located, subsequent measurements of the two-body channels would be concentrated on this mass range in an attempt to determine the quantum numbers.

- The Heidelberg experiment[18] proposes the measurement of $\bar{p}p$ cross sections (integrated and differential elastic, charge exchange and annihilation cross sections) at very low momenta (150 MeV/c < $\bar{p}$ < 500 MeV/c). The measurement of the spin averaged real and imaginary scattering lengths as well as the forward scattering amplitudes will be derived.

The elastic cross sections are measured by a multiwire proportional chamber and a scintillator hodoscope placed in a scattering chamber under vacuum. The charge exchange cross section is measured by a ring of 18 calorimeter modules covering a solid angle of 1.5 sr. The annihilation cross section will be determined by a calorimeter box surrounding the target. To cope with low $\bar{p}$ momenta a liquid hydrogen target of 2 mm thickness will be developed.

Measurement with better resolution can be obtained with the jet target option[6]. To perform measurements at momentum lower than 100 MeV/c the low energy paralel beams option [13,10] is needed.

ii) Hadronic annihilation at rest.

The ASTERIX experiment[19] proposes the study of the $\bar{p}p$ strong interactions at rest with a detection system of large acceptance that provides simultaneous information on both the initial atomic and final annihilation state. X-ray transitions to the 1S, 2P and 3D atomic levels of protonium ($\bar{p}p$ atom) will be detected by the original XDC[20] counter ($\Omega/4\pi \sim 90\%$) which surrounds a H_2 gas target at normal pressure. Charged $\bar{p}p$ annihilation products will be detected inside an upgraded version of the Orsay DM1 solenoidal magnetic spectrometer[21] ($\Omega/4\pi \sim 50\%$, $\Delta p/p \sim \pm 2.5\% \frac{p(\text{MeV/c})}{500}$ supplemented by position-sensitive gamma detection in the end caps ($\Omega/4\pi \sim 50\%$). The detector can be triggered on preselected initial and/or final state configurations.

The objectives of the experiment ordered according to increasing complexity and statistics are: $\bar{p}p$ annihilation dynamics (comparison of branching ratios of annihilations in P-and S-wave), and exotic and nonexotic meson spectroscopy, in particular, search for narrow states (for instance, neutral and charged quasinuclear $\bar{N}N$ bound states, $qq\bar{q}\bar{q}$ baryonium states).

This experiment is very sensitive in the search of baryonium states with a mass < 2 m_p with charged final states.

This kind of studies can be continued with the co-rotating $\bar{p}$ and H^- beam

due to the absence of Stark effect, the P-wave should increase, and consequently the possibility of baryonium state formation under threshold [10,14].

iii) Polarization experiments.

The ABGOST collaboration[17] has also proposed an experiment to study the spin effect in the $\bar{p}p$ annihilation, mainly with the aim of exploring the possibility of the existence of large width baryonium states. In fact they propose to measure the $d\sigma/d\Omega$ and P (polarization) in

$$\bar{p}p \to \pi^+\pi^- \qquad (1)$$
$$\bar{p}p \to K^+K^- \qquad (2)$$
$$\bar{p}p \to \bar{p}p \qquad (3)$$

in the momentum range 300-2000 MeV/c at about 15 different momenta using a conventional polarized target. In reactions (1) and (2) the complete angular range 0-180° will be covered. Reaction (3) will be studied over the angular range where p and $\bar{p}$ have sufficient range to escape from the target. Statistics will be > 10^4 per momentum for reaction (2), and correspondingly higher for other channels. With the same set-up, two subsidiary measurements are possible. Firstly, at those energies and angles where the proton from reaction (3) has sufficient energy, a measurement of its polarization can be made parasitically to determine the Wolfenstein parameter $D \equiv I(0,n;0,n)$. Secondly, if carbon has significant analysing power for antiprotons, the parameter $D_t \equiv I(0,n;n,0)$ will also be obtained. An important preliminary in deciding whether polarized $\bar{p}$ beams can be made by scattering from carbon, and also in devising a polarimeter for $\bar{p}$ polarization, is a measurement of the polarization of $\bar{p}$ scattered at small angles from C. This also can be done with existing equipment. The same small-angle set-up can be used to measure at a few energies the real part of the elastic scattering amplitude at $|t|=0$.

This is a particulary complete experiment and should give some definitive answer in the baryonium states physics.

iv) Annihilation in neutral channels.

These channels are at present very poorly investigated. The Heidelberg experiments[18] will measure the charge exchange and the ASTERIX collaboration[19] can measure the gamma-rays with not a very good resolution.

Three specific experiments are proposed in this field[22], but they are still under discussion.

B. Experiment with antineutron beam.

The experiment proposed by a group of Padova[23] is a test experiment to measure the $\bar{p}p \to \bar{n}n$ forward cross section in order to study the $\bar{n}$ production around 0° and establish an absolute monitoring of flux and momentum of $\bar{n}$'s. This study is intended to be preliminary to the construction of the $\bar{n}$ monochromatic beam.

The physics is complementary with the baryonium search in $\bar{p}p$ interactions. The $\bar{n}n$ channel has never been studied and the $\bar{n}p$ should be the same as $\bar{p}n$ but without the deuterium complications.

C. Atomic transitions.

The ASTERIX experiment[19] intends to perform the protonium spectroscopy: search for X-ray transition to the 1S ground state and measurement of the shift ΔE and the width Γ of the single $^1S_0$ and triplet $^3S_1$ sublevels, yields of M,L, and K transitions, with the large solid angle central detector exploiting the X ray drift chamber technique[20] using H_2 an D_2 gas targets where the absorption of X-rays in not strong.

Three specific experiments are approved in this field:

i) The experiment of a British-Dutch collaboration[24] proposes to search for the K X-ray series from $\bar{p}p$ ($\bar{p}d$) atoms and to measure their shift and width relative Q.E.D. predictions.

The $\bar{p}$ will be stopped in 1 atmosphere of H_2 (D_2) gas in a large aluminium flask whose 1 mm thick wall eliminates externally produced low energy X-rays. The Si (Li) X-ray detector with 300 mm^2 area and 250eV resolution FWHM at 5.9 keV, penetrates the vacuum to come very close to a large beryllium window. High purity metals are used for flask, window and detector and-housing to eliminate background lines in the energy region of interest. Previous $\bar{p}p$ X-ray experiments show a large continuum background attributed to small angle Compton scattering of high-energy γ-rays in the detector. The γ-rays come from the hydrogen and from nearby material. In the present experiment Compton suppression using NaI or Pb glass detectors will be provided. The flask will be surrounded by a 4π scintillation counter hodoscope. This will better define stopped $\bar{p}$ and help to distinguish between singlet and triplet K X-rays where only the spin singlet $^1S_0$ state can annihilate into neutral pions.

ii) The experiment of the Karlsruhe grupe[25] propose to measure the energies and intensities of the $n \to 1$ (Lyman) and $n \to 2$ (Balmer) transitions with high accuracy in both $\bar{p}H$ and $\bar{p}D$, from which the strong interaction effects of the 1s-and 2p-level can be extracted. These observables may be related to the antiproton-proton and antiproton-neutron scattering lenght.

Since in these targets collisional Stark effect occurs, the antiprotons are stopped in extreme thin gaseous targets (pressure as low as 10 Torr), where no Stark effect occurs and the 2 - 1 transition is favoured. In order to use antiprotons with high efficiency despite of the low target density, they will be trapped at a momentum of 150 MeV/c in a magnetic field of cyclotron characteristics. The antiprotons are decelerated by their energy loss in the target gas. The focussing properties of the magnetic field serve to compensate the multiple scattering and will end up with a concentrated stopping distribution at the center. Due to the long orbiting time, background from the modera-

tion is entirely separated in time from the atomic cascade. The energies of the X-rays will be measured by Si (Li)-detectors in a double guardring reject configuration. Thus, background in the used energy range below 10 keV can be reduced.

iii) The BKSST collaboration[26] propose to study the X-ray spectra of antiprotonic atoms and the gamma spectra of residual nuclei after the antiproton absorption. They intend to begin with measurements on selected isotopically pure targets.

Strong interaction effects, the antiproton absorption and the atomic cascade are analyzed through the measurement of energies, lineshapes, relative and absolute intensities of all observable lines. The expirements are continued to determine strong interaction effects in resolved fine structure levels and in different isotopes of the same element.

The experimental apparatus to being with is a standard set up for the detection of X-ray from exotic atoms (Ge and Si(Li) detectors), and all the components are existing already.

The X-ray from $\bar{p}p$ can have a new experimental development with the option of $\bar{p}$, H^- co-rotating beams.

D. Interaction with nuclei.

Two exploratory experiments are approved.

i) An experiment on heavy hypernuclei of CERN-IKO-Uppsala collaboration[27]. The aim of this experiment is to produce heavy hypernuclei by $\bar{p}N$ annihilations and to measure their lifetimes. Kaons emitted in this decay process of antiprotonic atoms could possibly interact with the residual nucleus and undergo a strangeness exchange reaction: $K + N \rightarrow \Lambda + \pi$. The Λ-hyperon will then be attached to the nucleus with a certain probability forming a hypernucleus. Estimates give a probability of about 4×10^{-6} per antiprotonic atom. The lifetime for a heavy hypernucleus is expected to be of the order of 10^{-10} s. A signature of its decay would be delayed fission. For the detection of delayed fission, the "recoil-distance method"[28] is to be used. This method is suitable for lifetimes in the expected region. The fission fragments will be detected by position-sensitive counters in combination with track detectors.

ii) The Italian-Dubna collaboration[29].Proposes an exploratory experiment with antiprotons on nuclear physics.

This experiment intend to perform a systematic study of the interaction between low energy antiprotons and the H, ^2H, ^3He, Ne, ^{40}Ar - nuclei, using a self shunted streamer chamber in a magnetic field to be exposed to the $\bar{p}$ beam of LEAR. The properties of the self shunted streamer chamber, which makes possible the use of filling gas (hydrogen or helium or mixture He-Ar at a pressure of 1 atm) as a target, permit to carry out experiments also in the low energy region ($p_{\bar{p}} < 600$ MeV/c), where there are very few and fragmentary data. The

experimental apparatus is suitable for a large program of experiments, where it is necessary to see the vertex of the interaction, to measure the range of very low energy particles, to estimate the ionization, to detect interactions with many secondary particles and to deduce their angular correlations. The aim of the experiments is to measure the elastic and inelastic interaction cross section and the annihilation of antiprotons both in flight and at rest, together with the identification of the various channels and of the energy of the charged particles emitted.

E. Fundamental properties of antinucleons.

With LEAR the antinucleons porperties can be measured several orders of magnitude better than before[30].

Several proposals where presented during the preparatory workshop of LEAR for the different measurement with several original techniques[31].

An interesting letter of intent to the PSCC was presented by an Orsay group[32] who intends to measure with a precision of 10^{-9} the mass difference between $\bar{p}$ and H^- using a mass spectrometer on line. From LEAR a beam of $\bar{p}$ and H^- is expected.

F. $\bar{N}N$ annihilation into charged leptons.

This field can profit completely of the high proton intensity of LEAR and can have very interesting developments.

i) Proton electromagnetic form factors.

Our knowledge of the electromagnetic structure of hadrons is still extremely limited, both theoretically and experimentally. The available data on their electromagnetic form factors (EMFF) are very incomplete. Amongst the pseudoscalar mesons, the pion form factor, which is the simplest from the theoretical point of view, is in a relatively good shape; data exist on both space-like and time-like regions and the relation of all the data via analyticity begins to be possible; in particular, the reaction $e^+e^- \to \pi^+\pi^-$ has been well studied [33] in the low-q^2 region, where the cross-section, dominated by the ρ pole, is rather high.

In the case of the proton EMFF, many precise measurements [34] in the space-like region have been performed years ago at SLAC, Orsay, Saclay, Bonn and DESY laboratories, via ep elastic scattering. Recent improvements at low energy[35] have given rise to an accurate value of the electromagnetic r.m.s. radius of the proton $(r_p)^{\frac{1}{2}} = 0.84 \pm 0.02$ fm. Nothing comparable exists in the time-like region, where the EMFF are measured via the reaction $\bar{p}p \rightleftarrows e^+e^-$. The intensity of present $\bar{p}$ beams and the luminosity of the e^+e^- colliding beams give typical rates for these experiments of the order of 1 event per day, which have severely limited the statistics of the seven existing measurements[36]: two upper limits from CERN and BNL former experiments, one point measured at

ADONE in 1971, two points at rest and near rest measured at CERN in 1975, and finally four points measured at DCI in 1978.

The situation is worse for the neutron EMFF; in all cases but one, the available information is obtained from experiments using a deuteron target and after a theoretical analysis. No data at all exist in the time-like region.

The advent of LEAR high-intensity antiproton beams should drastically improve the situation of the proton EMFF, since they will allow precise determination of $|GE|$ and $|GM|$ in the time-like region, which is the most important region to determine the function $F(q^2)$ describing the EMFF. In the phase representation, the EMFF are the boundary values of the analytic function $F(q^2)$ in the complex q^2 plane with a cut along the real axis from $-4m_\pi^2$ to $-\infty$[37]; $F(q^2)$ is real in the space-like region and above $-4m_\pi^2$, and it is complex below $-4m_\pi^2$ and in particular in the time-like region. The determination of $F(q^2)$ in the region of the cut will determine its value over the whole contour. This is what makes accurate data in the time-like region particularly important.

The hadron EMFF are generally interpreted in terms of the Vector Dominance Model (VDM)[38]. In the proton case, the time-like EMFF are sensitive to the heavy vector mesons which are coupled to the $\bar{p}p$ system. The existing data on $|GE|$ indicate a rather high value of the proton EMFF in the time-like region incompatible with the simple dipole model. A VD model using several isovector and isoscalar vector mesons (ρ,ρ',ω,ϕ, ...) is needed to fit the data in both space-like and time-like regions[39]. Parameters of the fit are the masses and the coupling constants of the mesons to the bare nucleon. The results are not satistactory suggesting the existance of other unknown vector mesons. In any case, the few data with large uncertainties in the time-like region give little constraint to the fits. Accurate data in the time-like region should allow the determination of the parameters of these fits and discrimination between various models. Also angular distributions will provide the values of $|GE|$ and $|GM|$ separately[40].

Furthemore, theoretical considerations suggest a particular sensitivity of the e^+e^- channel to the presence of $\bar{p}p$ bound states near threshold[41]. In particular, angular distributions at $\bar{p}$ momenta below 500 MeV/c should show a large excess of events in the 90° c.m. region if such states exist.

ii) Vector mesons.

A clarification of the vector meson spectrum between the ϕ and J/ψ is still needed, in spite of the large amount of work done in the last few years with e^+e^- colliding beams[42] and in photoproduction experiments[43]. In particular, the existence of the ρ' (1250) meson is still an open question. Important information on the various decay channels of vector mesons above 1.3 GeV are expected from the improved apparatus of DCI[44]; however, normalization problems and low luminosity will still be present.

One experiments proposed by an Italian-French collaboration[45] was approved by the PSCC.

The aim of this experiment is to measure with precision the electromagnetic form factors of the proton in the time-like region via the reaction:

$$\bar{p}p \rightarrow e^+e^- \qquad (4)$$

with antiprotons of momenta between 0 and 2 GeV/c. Up to $\sim$ 800 MeV/c, a continuous energy scan in $\sim$ 2 MeV ($\sqrt{s}$) bins will be performed. The form factors |GE| and |GM| will be determined separately since large statistics can be collected with LEAR antiproton beams, so that angular distributions can be obtained at many momenta.

In addition, e^+e^- pairs produced via the reaction:

$$\bar{p}p \rightarrow V^\circ + \text{neutrals}, \quad V^\circ \rightarrow e^+e^- \qquad (5)$$

where the antiprotons are at rest, will be detected allowing the vector meson mass spectrum between $\sim$ 1 GeV and $\sim$ 1.7 GeV to be obtained with high statistics and in one run.

The proposed apparatus consists of a central detector, surrounded by a gas Cerenkov counter, wire chambers, hodoscopes, and an electromagnetic calorimeter. The central detector consists of several layers of proportional chambers around a liquid-hydrogen target in the vertical field of a C-magnet. A V° mass resolution of the order of 2% is expected. The Cerenkov counter together with the calorimeter will provide an efficient detection for e^+e^- pairs with a rejection power against hadron pairs of at least 10^{10} (10^8 at the trigger level).

The e^+e^- rates, using an intensity of 10^6 $\bar{p}$ per second of the LEAR extracted beam, and assuming a $\sim$ 100% duty cycle, should vary between 5000 events per day at rest and 10 events per day at 2 GeV/c.

iii) Charmonium Spectroscopy.

The charmonium family lies at $2.8 < E_{cm} < 4.6$ GeV. Obviously this energy range is not reachable with the $\bar{p}$ beam extracted from LEAR, but can be reached with the option of using LEAR as a $\bar{p}p$ collider[5].

In spite of the extensive and beatiful work performed in the charmonium spectroscopy with e^+e^- colliding beams, several problems are still unsolved. The limits in the study of charmonium states with the e^+e^- colliding are related to the fact at low energies the process with two-photon echange is strongly depressed. So for experiments, it is realistic to tune the e^+e^- colliding beams only on vector mesons ($J^P = 1^-$). The search for the other states is done tuning the colliding beams on the ψ' and sudying the decay of that particle. The limitation comes from the rates of decay in some particular channel including the non-vector meson, and from the fact that the resolution for these states is not ±1 MeV as for vector mesons but ±(50-100) MeV typical of spectrometers. For this reason some problems are still unsolved:

a) the χ state width. This measurement can give information on the gluon spin. In fact, it is expected from QCD that χ_0 ($1\,^3P_0$) and χ_2 ($1\,^3P_2$) decay into two gluons and the state χ_1 ($1\,^3P_1$) into three gluons. The ratio $R = \Gamma_h(\chi_0)/\Gamma_h(\chi_2)$ is very sensitive to the gluon spin;
b) confirmation of the existence of η_c (2976): The η_c was believed to be di-

scovered at DORIS with DASP at 2800 MeV. Recently, the experiment with a crystal ball at SPEAR[46] demonstrated that at these energies no state exist, but showed some evidence (5σ) for a structure at 2976 MeV. It is evident that such measurements need confirmation by other experiments;

c) measurement of the η_c width: Several models give precise predictions[47];

d) search for η'_c and $^1P_1$ states: No experimental evidence for such states yet exists;

e) search for D charmonium states: $^1D_2(2^{-+})$, $^3D_2(2^{--})$ and $^3D_3(3^{--})$. The predictions for the masses are very near the $D\bar{D}$ threshold. The decay into $D\bar{D}$ is forbidden by parity conservation. So the expected width should be narrow.

With $\bar{p}p$ annihilation, all the states, independently of J^P, can directly be reached. The hadronic background is very high with respect to the one expected with e^+e^- colliding beams. Looking at the vector mesons, but choosing well-signed channels like

$$\bar{p}p \to J/\psi\ (\psi') \qquad (6)$$
$$\qquad\quad |_{\to e^+e^-}$$

or

$$\bar{p}p \to \chi \to \gamma + J/\psi \qquad (7)$$
$$\qquad\qquad\quad |_{\to e^+e^-}$$

or

$$\bar{p}p \to \eta_c \to \gamma\gamma \qquad (8)$$

we can overcome the background, and in this way we have direct access also to the non-vector meson states of the charmonium family with the energy resolution of the proton-antiproton beams[48]. Using LEAR as a $\bar{p}p$ collider and applying the electron cooling, we can reach resolutions down to 50 KeV.

In Table I is a summary of the cross-sections of production of the states on the peak of the resonance σ_R ($\bar{p}p \to s$) and of the cross-sections for the observed channel σ_R ($\bar{p}p \to$ obs.ch.).

The cross section for the J/ψ and ψ' calculated on the basis of the data on the process $e^+e^- \to J/\psi\ (\psi') \to \bar{p}p$ measured in e^+e^- colliding beams, so we have no doubt about these previsions. For the χ states, the σ_R was calculated interpolating the data on J/ψ and ψ': these results are pessimistic with respect to the previsions of several models. For the σ_R ($\bar{p}p \to$ obs.ch.) we use the known branching ratios. For the states η_c, η'_c and $^1P_1$ we use the previsions of Cahn and Suzuki[49].

The rates/day, calculated on the hypothesis of a luminosity of 10^{30} cm^{-2} s^{-1}, are very encouraging; also the value of R = signal/background wich could vary from 10^{-6} - 10^{-8} is tolerable.

iv) LEAR $\bar{p}p$ collider luminosity.

The possibility of using LEAR as a $\bar{p}p$ collider was considered as an option in the LEAR design study[45]. For such an option, head-on collisions with

TABELLA I

J^{PC}	STATE	MASS MeV	Γ exp. MeV	Γ Pred. MeV	$\sigma_R(\bar{p}p \to s)$ μb	OBSERVED CHANNEL	$\sigma_R(\bar{p}p \to obs.\ ch.)$ μb	events day $L=10^{30}$ c^{-2} s^{-3}	Signal Backgr.	STATE
0^{-+}	$1\ ^1S_0(\eta_c)$	2976	<50	6.5	3	$\bar{p}p \to \eta_c \to \gamma\gamma$	1.5	130	2.5×10^{-8}	η_c
1^{--}	$1\ ^3S_1(J/\psi)$	3098	.069	-	3	$\bar{p}p \to J/\psi \to e^+e^-\ (\mu^+\mu^-)$	210.	18000	3×10^{-6}	J/ψ
0^{++}	$1\ ^3P_0(\chi_0)$	3413	<25	15	1.6	$\bar{p}p \to \chi$	3.5	300	6×10^{-8}	χ_0
1^{++}	$1\ ^3P_1(\chi_1)$	3510	<10	1.4	1.3	$\chi \to J/\psi + \gamma$	21.	1800	3×10^{-7}	χ_1
2^{++}	$1\ ^3P_2(\chi_2)$	3554	<14	4	1.0	$J/\psi \to e^+e^-\ (\mu^+\mu^-)$	11.	930	2×10^{-7}	χ_2
0^{-+}	$2\ ^1S_0(\eta'_c)$	?	-	5	1.8	$\bar{p}p \to \eta'_c \to \gamma\gamma$	0.9	70	1.5×10^{-8}	η'_c
1^{+-}	$1\ ^1P_1(^1P)$	?	-	3	5.4	$\bar{p}p \to {}^1P \to \eta_c\ \gamma \to \gamma\gamma\gamma$	0.8	65	1.4×10^{-8}	^1P
1^{--}	$2\ ^3S_1(\psi')$	3684	.228	-	0.2	$\bar{p}p \to \psi' \to e^+e^-$	1.8	150	3×10^{-8}	ψ'
2^{+-}	$1\ ^1D_2(^1D)$	?	-	narr.	?	$\eta_c\ \gamma$, $\psi\gamma$, $\gamma\gamma$	?	?	?	^1D
1^{--}	$1\ ^3D_1(\psi'')$	3772	26	-	?	$\bar{p}p \to \psi'' \to e^+e^-$	?	?	?	ψ''
2^{--}	$1\ ^3D_2(D_2)$	?	-	narr.	?	$\eta_c\gamma$, $\psi\gamma$, $\gamma\gamma$	?	?	?	D_2
3^{--}	$1\ ^3D_3(D_3)$	?	-	narr.	?	$D\bar{D}^*$	?	?	?	D_3

an interaction region of 5 m were considered because with an RF amplitude of ΔV = 54 kV we can obtain a bunch lenght of 5 m. An upper limit of the luminosity was calculated using the Amman-Ritson limit:

$$L = \frac{N \cdot f_{rev} \cdot \Delta\nu \cdot \gamma}{(1+\beta^{-2}) \cdot r_p \cdot \beta_v}$$

where: $N = 6 \times 10^{11}$ $\bar{p}$ (the maximum accumulable in one day);
$\Delta\nu = 0.005$ (the conventional beam-beam tune shift for $\bar{p}p$);
$\beta_v = 5$ m (β value at the intersection region choses equal to the bunch length).

In these conditions we can have a luminosity of

$L = 0.6 \times 10^{29}$ $cm^{-2}s^{-1}$ at 1 GeV/c
$L = 1.4 \times 10^{29}$ $cm^{-2}s^{-1}$ at 2 GeV/c

This solution is a little marginal for the physics program proposed. We must find other solutions to improve the luminosity and decrease the interaction region length.

In fact, a further bunch length compression can be obtained with a system of RF, composed of not only the first harmonic, as is proposed in the design study, but also of the second harmonic, as is proposed by M. Conte[50]. With this system it is possible to obtain a bunch lenght of 1 m. In these conditions, with a low β section, a β_v = 1 m can be considered and we gain a factor of 5 in the luminosity figures. In these conditions, the whole scheme for the LEAR $\bar{p}p$ collider becomes more satistactory.

An interesting proposal to keep cold by electron cooling at all energies of LEAR, antiproton and proton beams precooled at low energy, has been recently advanced[51]. In fact, the electron beams from a Cockroft-Walton can give 10A with 5 cm diameter up to 4 MeV of electrons with $< 10^{-6}$ mrad emittance and with $\Delta p/p \simeq 10^{-4}$. The authors calculate beam decay constants of 11 sec and 34 sec for 1 GeV/c protons (0.54 MeV electrons) and 2 GeV/c protons (1.1 MeV electrons), respectively.

From the constant decay time of the beam we can obtain the corresponding beam-beam tune shift[52]. We obtain $\Delta\nu = 0.035$ at 1 GeV and correspondingly a gain in luminosity of a factor or 7.

We can conclude that is is possible to have, for the LEAR $\bar{p}p$ collider, a luminosity of 10^{30} cm^{-2} s^{-1} with a bunch length usable in an experiment.

Another possible solution is with coasting beams. In fact, with such a solution it is possible to keep the luminosity, but the bunch density is lower than in the case of head-on collisions. It could be a solution to have the best possible $\Delta p/p$ for both beams and consequently the best energy resolution.

v) Future developments.

In analogy with charmonium it is possible to study the spectroscopy of bottonium with $\bar{p}p$ annihilation with analogous reactions (6,7,8).

The T was discovered at Fermilab with ± 300 MeV of resolution and was confirmed by DORIS with a resolution of ± 10 MeV. At present, it is being studied with CESR with a resolution of ± 6 MeV.

It is difficult, in any case, to perform a study of the χ_T states similar to the study which was performed for the χ_{charm} states with e^+e^- colliding beams. The reason are mainly the lower production of T' with respect to the ψ' and the resolution one order of magnitude worse, which increases the background with respect to the signal.

With $\bar{p}p$ annihilation, a resolution of two orders of magnitude better than in e^+e^- colliding beams is possible in principle, and the direct access to the χ_T states can help a lot in this search.

At present not sufficient information is available to calculate the rates of production of χ_T states form $\bar{p}p$ annihilation. They should be two orders of magnitude lower than those of the χ_{charm} states.

To perform this search we need a $\bar{p}p$ collider that can reach 6 GeV/c in each beam and has a luminosity of 10^{31} cm^{-2} s^{-1}.

In the same range as the T family lies the Higgs boson according to the mass predictions for this particle done by S. Coleman and E. Weinberg[53]. In fact, they generate the symmetry-breaking through radiative corrections and on the hypothesis of $m_f \ll m_W$ and $\sin^2\theta_W \sim 0.2$ give $m_{H^\circ} = 10.4$ GeV.

The coupling with a scalar boson with $\bar{p}p$ is done by two gluons and should be one or two orders of magnitude lower than for T states.

Searching for processes like

$$\bar{p}p \to H^\circ \to \tau^+\tau^- \quad \begin{cases} \to e^- \nu\bar{\nu} \ (\mu^-\nu\bar{\nu}) \\ \to e^+ \nu\bar{\nu} \ (\mu^+\nu\nu) \end{cases}$$

with the prevision[54] of (25 to 50)% for the $\Gamma(H^\circ \to \tau^+\tau^-)/\Gamma(H^\circ \to \text{total})$ and looking for e^+e^-, $\mu^+\mu^-$ or $\mu^\pm e^\mp$ pairs, it is possible to hope to make a contribution to solving this importan problem.

IV. CONCLUSION.

The programme presented is very extensive. One can certainly expect new important developments after the first results. In any case it seems difficult that LEAR at CERN can perform all the physics programme in a resonable time table.

REFERENCES

1) C.Rubbia, P. McIntyre and D. Cline, Proc. Int. Neutrino Conference, Aachen, 1976 (EDS. M.Faissner, H.Rethler and P.Zernas) (Wieweg und Sohn, Braunschweig, 1977) p. 683.

2) Design study of a $\bar{p}p$ colliding beam facility CERN/PS/AA 78-3.

3) P.Dalpiaz. Electromagnetic annihilation in Low Energy $\bar{p}p$ colliding beams- CERN - $\bar{p}p$ Note 06 - (March 1977) $\bar{p}p$ first study week - CERN
- U.Gastaldi, K.Killian, O.Möhl. Deceleration of antiprotons for physics experiments at low intensity. Proceedings 10 th. International Conference on High Energy Accel., Serpukov 1977.
- P.Dalpiaz, U.Gastaldi, K.Kilian and M.A. Scheegans. Low energy antiproton experiments with an "Antiproton factory" at CERN. Memorandum to the Chairman of the workshop on medium energy physics, Held in Sept 1977 at CERN (14-June 1977).
-Chairman Report, CERN Workshop on medium energy physics, R. Klapish, PS-CDI 177-50 (1977) and B. Povh CERN-PS-CDI-77-49 (1977).
- A.Astbury, P.Dalpiaz, U.Gastaldi, K.Kilian; E.Lorhmann, B.Povh and M.A. Schneegans, Possible Experiments with Antiprotons at low and Intermediate Energies. Memorandum to PSCC dated 6 th Febr. 1978.
- Proc. Joint CERN-KfK Workshop on Physics with cooled low energetic antiprotons- Karlsruhe, 1979 KfK Report 2836 (ed. by H.Poth).

4) W.Hardt, L.Hoffmann, P.Lefevre, D.Möhl, G.Plass and D.Simon. Conceptual study of a facility for low energy antiproton experiments, PS/DL Note 79-1 and KfK 2836 pg.1

5) Design study of a facility for experiments with low energy antiprotons (LEAR) CERN/PS/DL 80-7.

6) K.Kilian. Comment concerning internal gas targets in LEAR. CERN/PSCC/80-8.

7) C.Voci. Antineutron beam at LEAR, CERN $\bar{p}$ LEAR-Note 20 and KfK 2836 pg.125 and Proc. 5th. Europ.Symp. on Nucleon-Antinucleon Interactions (Ed.Cleup-Padova 1980) pag.703.

8) P.Dalpiaz and K.Kilian. Polarization with LEAR, CERN $\bar{p}$ LEAR- Note 31.

9) U.Gastaldi. Protonium Spectroscopy in flight CERN/PSCC 79-67 and References given therin.

10) U.Gastandi. $\bar{p}p$ experiments at very low energy using cooled antiprotons. Proc. 4th. Europ. Antiproton Conf., Barr-Strasburg 1978 (Editions du CNRS, Paris Ed. By A.Friedman) pg. 607 vol. II.

11) P.Dalpiaz, P.F.Dalpiaz, L.Tecchio and M.A.Schneegans. Proc. 4th. Europ. Antiproton Conf. Barr.Strasbourg 1978. (Editions du CNRS, Paris, Ed. By A. Friedman) pag. 689 vol. II.

12) P.Dalpiaz. Charged lepton pairs and rare neutral channels from $\bar{p}$-p annihilation. Proc. 5th. European Symp. Nucleon-Antinucleon interactions (Ed.CLEUP-Padova, 1980) pag.711.

13) T.E.Kalogeropoulos. Intersecting storage rings for studing interactions at very low energy. CRISP 72-11, Isabelle Project 1972.

14) U.Gastaldi. Proc. 1st. Intern.School of Physics of Exotic Atoms, Erice,1977 (Ed. G.Fiorentini and Torelli, Servizio Documentazione dei L.N.Frascati - Rome 1977) pg. 205.

15) M.A.Schneegans. $\bar{N}N$ annihilation al LEAR. KfK 2836 - Karlsruhe 1979 pag.93.

16) See for Example.
- I.S.Shapiro, Phys.Report 35C , (1978) 129
- A.M.Badalyan, M.I.Polikarpov, Ju.A.Simonov, Phys.Lett. 76B (1978)277
- Chang Hong Ho and A.Hogaasen, Nucl.Phys. B136 (1978) 401.

17) J.Bailey et al. Amsterdam-Bedford-Geneva - QMC -Surrey-Trieste Collaboration $\bar{p}p$ Total Cross-Sections and Spin Effects in $\bar{p}p \to K^+K^-$, $\pi^+\pi^-$, $\bar{p}p$ above 200 MeV/c - CERN/PSCC/80-77

18) K.Braune et al. Measurement of $\bar{p}p$ cross section at low $\bar{p}$ momenta. CERN/PSCC/80-86.

19) R.Armenteros et al. (CERN-Mainz-Munich-Orsay(LAL)-TRIUMF-Zurich Collaboration). A study of $\bar{p}p$ interactions at rest in a H_2 gas target at LEAR CERN/PSCC/80-102

20) U.Gastaldi, Nucl. Inst. and Meth. 157 (1978) 441.

21) A.Cordier et al., Nucl.Instr. and Meth. 133 (1976) 237.

22) L.B.Averbach et al. U.C.Irwine, Michigan state, New Mexico - Temple Collaboration. Study of $\bar{p}p$ and $\bar{p}d$ interaction at LEAR - CERN/PSCC/80-93

- L.Adiels et al. (Basel, Karlsruhe, Stockholm,Strasburg,Tessaloniki collaboration) Search for Baryonium states below threshold at LEAR. CERN/PSCC/80-97
- Athen-Democritos-MVSU-Syracuse-Tecnical Univ. Coll. Measurment of charge and γ production CERN/PSCC/80-108

23) D.Bisello, F.Gasparini, S.Limentani, A.Meneguzzo, P.Sartori and C.Voci. Study Antineutron production at LEAR. CERN/PSCC/80-91.

24) J.D.Davies et al. Birmingham-Amsterdam-Rutherford-William & Mary Coll. Precision survey of X-rays from $\bar{p}p$ ($\bar{p}d$) atoms using the initial LEAR beam CERN/PSCC/80-82

25) P.Blum et al. Measurement of the Antiprotonic Lyman- and Balmer X-Rays of $\bar{p}H$ and $\bar{p}D$ atoms at very low target pressures. CERN/PSCC/80-100

26) L. Adiels et al. Basel-Karlsruhe-Stockholm-Strasbourg-Thessaloniki Coll. Study of X-ray and gamma-ray spectra from antiprotonic atoms at the slowly extracted antiproton beam of LEAR. CERN/PSCC/80-104

27) T.Johansson et al. CERN-IKO-Uppsala Collaboration. A search for heavy Hypernuclei at LEAR. CERN/PSCC/80-75

28) U.Metag et al. Nucl.Instr. and Meth. 114 (1974) 445.

29) F.Balestra et al. Dubna-Frascati-Padova-Pavia-Torino Collaboration. Study of the interaction of low energy antiprotons and antineutrons with ^{2}H, ^{3}H ^{4}He, Ne, ^{40}Ar. Nuclei using a streamer chamber in a magnetic field. CERN/PSCC/80-79

30) H.Poth. Fundamental Properties of antinucleons. KfK 2836 (1979) pg.129

31) H.Poth. Phys. Lett. 77B, 321 (1978)
G.Torelli, $\bar{p}$ LEAR Note 16 (1979)
U.Gastaldi Ref. 10
C.Voci $\bar{p}$ LEAR Note 20 (1979)
H.Poth, $\bar{p}$ LEAR Note 15 and 51 (1979)

32) C.Thibault, R.Klapish, G.Audi, M.Epherre, M.De Saint Simon and T.Touchard. CERN/PSCC.80-7

33) See, for example, A.Quenzer et al. Phys.Lett. 76B, 512 (1978)

34) C.H.Berger et al., Phys.Lett. 142, 922 (1966)
C.H.Berger et al. Phys.Lett. 28B, 276 (1968)
L.E.Price et al. Phys.Rev. D 4, 45 (1971)
W.Bartel et al. Phys.Lett. 25B, 236 (1967)
W.Bartel et al. Phys.Lett. 33B, 245 (1970)

35) F.Borkowski et al. Nucl. Phys. A222, 269 (1974)

36) M.Conversi et al. Nuovo Cimento 40, 690 (1965)
D.L.Hartill et al. Phys.Rev. 184, 1415 (1969)
M.Castellano et al. Nuovo Cimento 14, 1 (1973)
G.Bassompierre et al. Phys.Lett. 64B, 475 (1976)
G.Bassompierre et al. Phys.Lett. 68B, 477 (1977)
B.Delcourt et al. Phys.Lett. 86B, 395 (1979)

37) See, for example, M.Gourdin, Phys.Reports 11, 29 (1974)

38) See, for example:
T.Massam and A.Zichichi, Nuovo Cimento, 43, 1137 (1966)
S.Blatnik and N.Zovko, Acta Phys. Austriaca, 39, 62 (L974)

39) G.Bassompierre et al. Phys. Lett. 68B (1977)

40) See, for example, A.Zichichi, S.Berman,N.Cabibbo and R.Gatto, Nuovo Cimento 24, 170 (1962).

41) See, for example, M. van der Velde, Quasinuclear resonances and annihilation in nucleon-antinucleon scatterign, Academisch Proefschrift, Amsterdam. University, Amsterdam, 1980

42) See, for example:
C.Bacci et al. Phys.Lett. 38B, 551 (1972)
B.Bartel et al. Phys.Rev. D 6, 2374 (1972)
M.Conversi, Phys.Lett. 52B, 493 (1974)

- V.Alles-Borelli et al. Nuovo Cimento 30A, 136 (1975)
- G.Cosme et al. Phys.Lett. 63B, 349 (1976)
- A.Corater et al. Phys.Lett. 81B, 389 (1979)
- G.Cosme et al. Nucl.Phys. B152, 215 (1979)
- J.E.Augustin, Proc. EPS Conf. on Hish-Energy Physics, Geneva, 1979 (CERN Geneva, 1979) p.282
- B.Delcourt et al. Orsay report LAL 79/21 (1979), Proc. 9th Int.Symposium on Lepton and Photon Interactions at High Energies, Batavia, 1979 (Fermilab, Batavia, 1980) p.499
- C.Bacci et al. Frascati report LNF-80/25 (P) (1980)
- J.C.Bizot et al. Proc.EPS Int.Conf.on High-Energy Physics, Geneva, 1979 (CERN Geneva, 1979) p.362
- R.Baldini Celio, Proc.EPS Int.Conf.on High Energy Physics, Geneva, 1979 (CERN, Geneva, 1979) p.350

43) See for example:
- Particle data Group, Phys.Lett. 75B, 1 (1978)
- M.S.Atiya et al. Phys.Rev. Lett.43, 1691 (1979)
- F.Richard, Proc. 9th Int.Symposium on Lepton and Photon Interactions at High Energies, Batavia, 1979 (Fermilab, Batavia, 1980) p.469
- D.Aston et al. preprint CERN-EP/80-85 (1980), submitted to Phys.Lett. B.
- D.P.Barber et al., preprint Daresbury DL/P289E (1980), submitted to Nucl. Phys. B).

44) J.E.Augustin et al., Orsay report LAL 78/52 (1978)

45) L.P.de Brion et al. (Annecy,Saclay,Padova,Torino Collaboration). Precision measurements of the proton electromagnetic form factors in the time-like region and vector meson spectroscopy. CERN/PSCC/80-96

46) E.D.Bloom (Cristall Ball Coll.) Proc. 1979 Intern. Symp. on Lepton and Photon Interactions at High Energy. Ed. T.B.Kirk and H.Abarbanel, Batavia USA (1979) pg.92

47) See, for example, R.Barbieri, M.Caffo, R.Gatto and E.Remiddi, Strong QCD corrections to p-wave quarkonium decays, UGVA-OPT 1980/06-247

48) P.Dalpiaz, Electromagnetic annihilation in low energy $\bar{p}p$ colliding beams, CERN $\bar{p}p$ Note 6 (1977)
- P.Dalpiaz, P.F.Dalpiaz, L.Tecchio and M.Schneegans, Proc. of the IV European Antiproton Conference, Barr-Strasbourg, 1978, ed. A.Fridman,CNRS, Paris, 1979
- P.Dalpiaz, KfK 2836 (Karlsruhe 1979) ed. H.Poth, p.111
- P.Dalpiaz, Proc. 5th European Symposium on Nucleon Antinucleon Interactions (Ed. CLEUP-Padova 1980) pg. 711

49) R.N.Cahn and M.Suzuki, Production of charmonium states by resonant $p\bar{p}$ annihilation, LBL Int.Note 10505 (1980)

50) M.Conte, Head-on collisions in LEAR, CERN $\bar{p}$ LEAR Note 46 (1979)

51) U.Bizzarri, M.Conte and L.Tecchio, Wide energy range electron cooling at LEAR. Proc. 5th European Symposium on Nucleon Antinucleon Interactions (Ed.CLEUP-Padova 1980) pag.19.

52) B.Zotter, Experimental investigations of the beam-beam limit of proton beams. Proc. of the 10th Int.Conf. on High Energy Accelerators, Protvino (July 1977), vol.2, p.23

53) S.Coleman and E.Weinberg, Phys.Rev. D7 (1973) 1888
- E.Weinberg, Phys.Rev. D7 (1973) 2887

54) J.Ellis et al. CERN TH. 2634 (1979)

SEARCHING FOR STRUCTURE IN NUCLEON-ANTINUCLEON INTERACTIONS NEAR THRESHOLD

by

W. K. McFarlane
Temple University
Philadelphia, PA 19122

INTRODUCTION

The purpose of this paper is to help make the case for a new machine being an antiproton factory as well as a kaon factory. The energy of such a high-intensity accelerator should be near 30 GeV, rather than the 15 GeV which would be adequate for the production of kaons as the most massive particle.

Primarily, we wish to point out that there are regions of nucleon-antinucleon interactions which have not been carefully explored and which may contain interesting phenomena despite existing negative experiments. The enormous variety of proposals for the LEAR facility at CERN, as described at this meeting[1] make it obvious that a great deal of interesting physics can be done with antiprotons, so that perhaps this small contribution is not necessary. Nevertheless, to counterbalance the negative results presented by Tripp,[2] we describe below two areas of interest to us.

ANTIPROTON-DEUTERON ANNIHILATIONS

The reaction $\bar{p} + d \rightarrow N + X$ when N is a proton (p) or neutron (n) provides a way of exploring the spectrum of states formed from an antinucleon and a nucleon. The system X will annihilate into multipion states or decay into a $B\bar{B}$ pair. The advantage of this reaction, as pointed out by Kalogeropoulos,[2] is that states can be formed over a wide range of mass and angular momentum and detected via a missing mass technique by looking at the spectator or recoil nucleon.

In bubble chamber experiments detecting the recoil proton[3,4] indications for several bound states or resonances were found. However, a high-statistics experiment performed by us,[5] looking at recoil nucleons of both kinds (n and p), found no evidence of structure at the level of 0.3% of the interactions. Despite this negative result, we feel that improvements in detection efficiency and the level of background could lead to several orders of magnitude improvement in mass

resolution and sensitivity. Efficiency would be greatly improved by using large solid angle detectors and identification of all products of the reaction, particularly the neutral products. Additional information (e.g., through polarization of the initial particles) would also be helpful. A major problem with the experiment of Ref. 5 was the substantial neutron background from the production target; a way must be found to eliminate this, either through very long beam lines or by storage of the antiprotons for use independently of the production process. Therefore, although this experiment was more sensitive than previous ones (and uniquely sensitive to production of $\bar{p}p$ states below threshold through detection of neutron recoils) improvements can clearly be envisaged for experiments at a future accelerator.

It should also be noted that substantial theoretical effort has been devoted to the study of the $\bar{N}N$ system near threshold using potential models,[6] quark models,[7] and the topological structure of the scattering amplitudes.[8] These models did succeed in predicting the possibility of narrow $\bar{N}N$ states and therefore the search should not be given up too easily.

PROTON-ANTIPROTON ANNIHILATIONS ABOVE THRESHOLD

The S(1936) meson has had a long history, finally apparently disappearing (see the review by Tripp, Ref. 2), despite a number of definite "sightings." There is the possibility raised by Kelly and Phillips[9] that this is not a simple Breit-Wigner resonance added incoherently to a background of other processes, but in fact interferes with the other processes. For example, the annihilation cross section of antiprotons on protons at momentum p might be of the form

$$\sigma_A = A + B/p + \frac{C + D\varepsilon}{1 + \varepsilon^2} \qquad (1)$$

where the background is parameterized at $(A + B/p)$, and ε is $2(p - p_0)/\Gamma$ where p_0 is the central momentum of the effect and Γ the width.

Jastrzembski et al.[10] have recently performed a high-statistics measurement of the $\bar{p}p$ annihilation cross-section between 400 and 600 MeV/c antiproton momentum (i.e., around the S region). Using a 1-m-long liquid hydrogen target they were able to scan this region with a fixed beam momentum using the interaction point and the path length in the target to obtain the momentum at interaction. Thus the systematic problems of combining runs at different beam momenta were avoided. Since the incident momentum of each interacting antiproton was

individually measured, the momentum of each event was known very well relative to the others. This method is uniquely suited to searching for small, narrow structures in a rapidly varying cross section.

The analysis previously presented (Ref. 10) was in terms of a simple Breit-Wigner resonance and showed that the fit with such a resonance was significantly worse than that obtained with a simple background (quadratic in 1/p), i.e., $\chi^2 = 1.56$ per degree of freedom for a resonance with parameters suggested by previous experiments as opposed to $\chi^2 = 1.06$ per degree of freedom. However, if the data (see Fig. 1) is fitted with the form suggested by Eq. (1), (with a simpler background, linear in 1/p) an improved fit is found ($\chi^2 = 0.9$ per degree of freedom) with the parameters $p_o = 490$ MeV/c, $\Gamma = 13.4$ MeV/c, C = -0.76 mb, D = 2.05 mb.

The particular values found for the parameters are not important, nor is the functional form used. What is relevant is that an improved fit is obtained with a more complex behavior than the simple form normally used; moreover, most other measurements of the annihilation cross section are consistent with this bahavior (see Ref. 2 for a review of previous experiments). Each experiment covered different angular ranges for the annihilation products, and some included elastic scattering as part of the cross section, thus the size of any effect may vary. Note also that typical total errors are of the order of one percent at the level of 2 MeV in mass resolution. It is possible that the elusiveness of the "S" is due to complexity in its angular distribution, and to its not being a simple Breit-Wigner resonance. More careful measurements of the annihilation process are needed with improved mass resolution and complete identification of the initial and final states.

CONCLUSION

We feel that there is a great deal of physics to be done with antiprotons in the energy range which would be accessible to a 30 GeV accelerator, even in areas (such as those described above) which have already been explored to some extent.

REFERENCES

1. Dalpiaz, this meeting.

2. R. D. Tripp, Proc. of the 5th European Symp. on Nucleon-Antinucleon Interactions, Bressanone, Italy, 1980, and this meeting.

3. T. E. Kalogeropoulos and G. S. Tzanakos, Phys. Rev. Lett. 34, 1047 (1975).

4. L. Gray et al., Phys. Rev. Lett. 26, 1491 (1971).

5. C. Amsler et al., Phys. Rev. Lett., 44, 853 (1980).

6. W. W. Buck et al., BNL Rpt. No. 23315; and I. S. Shapiro, Phys. Rep. C35, 129 (1978).

7. Chan Hong-Mo and H. Hogaasen, Nucl. Phys. B136, 401 (1978); R. Jaffe, Phys. Rev. D17, 1444 (1977) and 15, 267 (1977).

8. G. C. Rossi and G. Veneziano, Nucl. Phys. B123, 507 (1977); G. F. Chew and C. Rozenzweig, Phys. Rev. C41, 263 (1978).

9. R. L. Kelly and R.J.N. Phillips, Rutherford Laboratory Report RL-76-053-T.159 or LBL Report, LBL-4879 (1976).

10. E. A. Jastrzembski et al., Proc. of the 5th European Symp. on Nucleon-Antinucleon Interactions, Bressanone, Italy, 1980.

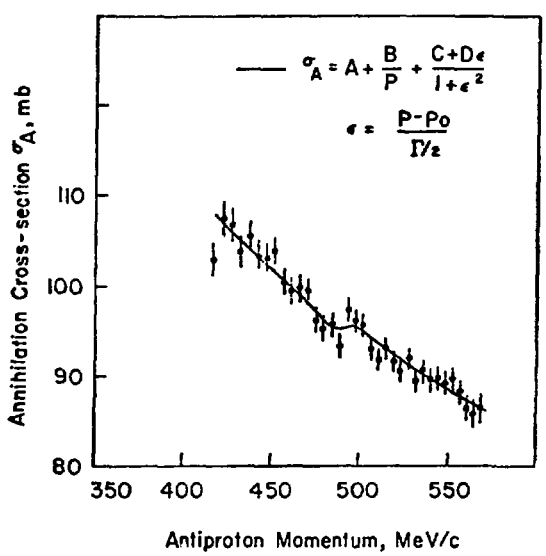

Fig. 1. The variation of the proton-antiproton annihilation cross section σ_A as a function of momentum (Ref. 10), compared with the functional form of Eq. (1); the fitted value of parameters are given in the text.

Note that the absolute scale for the cross sections is obtained from other measurements in this energy range; this experiment gives only the relative cross sections.

IMPLICATIONS OF QCD FOR SOFT HADRONIC AND NUCLEAR PROCESSES

by

Rudolph C. Hwa

Institute of Theoretical Science and Department of Physics

University of Oregon, Eugene, Oregon 97403

ABSTRACT

Physical implications of QCD for strong forces in soft processes are discussed. Topics include long-range force, Van der Waals force, nuclear force, hadron and quark structures. In the absence of a reliable calculational scheme phenomenological models have been built that incorporate QCD ideas as far as possible. In the framework of those models calculations have been made that provide an understanding of the soft processes in terms of quarks and gluons. We review recent work on nuclear potential, form factors at low Q^2, pion decay constant, inclusive distribution at low p_T, and radiation length of fast quark in nuclear matter.

I. INTRODUCTION

It should not be presumed from the title of this talk that either the organizers of this workshop or this speaker regard QCD as having been developed to the point of being able to describe soft hadronic processes let alone nuclear physics. If one does not demand mathematical precision but ask for only physical implications in so far as possible at this stage, then it is not only relevant but of great interest to this workshop to have a discussion on this topic.

The subject matter of this talk can best be described by first stating what will not be covered. We shall not discuss hard processes which involve momentum transfers with $Q^2 > 10\ \text{GeV}^2$. For such processes one can use perturbative QCD with a fair degree of confidence. However, lowest-order calculations did not yield any sensible results without considerable phenomenological adjustments;[1] moreover, on purely theoretical grounds higher-order corrections have been found to be important.[2] On the other extreme we shall also not discuss the confinement problem which requires non-perturbative methods in QCD. The solution of that problem remains elusive so far. Despite (or perhaps because of) the lack of spectacular success in either problem, considerable efforts have been devoted to perturbative and non-perturbative calculations in QCD, since at least the problems are amenable to precise formulations from first principles and exact consequences of well-posed questions can be investigated.

But what about the rest of strong interaction physics? What about soft processes that involve small to zero momentum transfers? For them neither perturbative nor non-perturbative methods would work. Surely, QCD as a basic theory should have some implications for the dominant hadronic reactions at any energy. Are there ways to extract those implications in the absence of any precise calculational scheme? Can the experimental data be used to shed light on the manner in which QCD manifests itself in soft processes? These are some of the questions that will be addressed in this talk. Our general aim will be to interpret all aspects of the strong forces in terms of the interactions among hadronic constituents.

Specifically, we shall examine various types of strong forces. Classified according to their ranges using R ~ 1fm as a reference, they are:

(a) Long-range force: $r/R >>> 1$

(b) Van der Waals force: $r/R >> 1$

(c) Nuclear force: $r/R \gtrsim 1$

(d) Hadron structure: $r/R \gtrsim 0.2$

(e) Quark structure: $r/R << 1$

The last topic sounds either wildly speculative or at best inappropriate for this talk. However, as we shall see, one cannot give a satisfactory description of the hadron structure without an adequate understanding of what the hadronic constituents and their own structures are. It is analogous to the problem of understanding nuclear forces, especially in connections with scattering.

Since the scope of material to be covered here is broad, I shall only be able to summarize the essential ideas in each topic without any details. This is also not intended to be an exhaustive review, so only key references will be given to serve as leads to other references.

II. LONG-RANGE FORCE

Whereas what is long-range to one may be short-range to another, to consider $r >>> R$ is surely long enough for every one. The criterion is really that r be large enough such that hadrons may be regarded as point particles. We raise the question about strong forces of such range because gluons in QCD are, like photons, massless. An immediate response is that the exchange of a gluon by hadrons is forbidden because of color, so there can be no "Coulomb" force between hadrons. Indeed, a gluon being a color octet cannot couple to a singlet hadron for reasons similar to why a photon cannot couple to a point neutron. But what about exchanging two gluons? Two gluons can form a color singlet which is no longer forbidden from being exchanged between hadrons, and can lead to a long-range force that is strong.

To see why this is not possible, it is only necessary to recognize that if a hadron is point-like we may ignore the spatial part of the wave function of the quarks and consider only ε_{ijk} for a nucleon and δ_{ij} for a meson as far as the color indices of the quarks are concerned. When we sum over the coupling of a gluon to each of the quarks in a hadron, the identities

$$\varepsilon_{i'jk}\lambda^a_{i'i} + \varepsilon_{ij'k}\lambda^a_{j'j} + \varepsilon_{ijk'}\lambda^a_{k'k} = 0 \qquad (1)$$

$$\delta_{i'j}\lambda^a_{i'i} + \delta_{ij'}\lambda^a_{j'j} = 0 \tag{2}$$

guarantee that the net coupling to the hadron vanishes,[3] where $\lambda^a_{i',i}$, a=1,...8, are the SU(3) matrices. Note that the argument does not even refer to multigluons explicitly. The hadronic virtual state (ijk) after emitting or absorbing the gluon must necessarily be in an octet state. At some later stage that virtual state must return to a singlet state via the exchange of another gluon. Nevertheless, so long as r is large enough such that the internal structure of the hadron may be neglected, (1) and (2) apply at the initial and final states. Thus we have the reassuring result that strong interaction is not long-ranged despite the massless gluons in QCD.

III. VAN DER WAALS FORCE

The Van der Waals force is usually also considered to be long ranged, but compared to a Coulomb-like potential, c/r, which is independent of a reference scale, the Van der Waals potential

$$V(r) = \frac{\lambda}{r}\left(\frac{r_o}{r}\right)^{N-1} \tag{3}$$

depends on a scale r_o, and is considerably shorter in range. Nevertheless, the inverse power, r^{-N}, refers to the large r behavior of the potential. If r_o is chosen to be around R (i.e. ~1 fm), present experimental data cannot rule out a Van der Waals force with $N \geq 6$.[4] Clearly, the value of N depends on r_o which in turn is related to whether the missing-mass spectrum extends to zero, a question that deserves more careful experimental study.

Theoretically, if Van der Waals force exists in strong interaction, it would have to arise from multigluon exchange. Now, gluons leaving a confined hadron system and being absorbed by another many units of r_o away would seem to be in conflict with the precepts of confinement. One way to implement confinement is to assume that the scattering amplitude vanishes when an external gluon line is on mass shell. In examining the possibility of Van der Waals force in the context of QCD, Feinberg and Sucher[4] have studied the implication of two-gluon exchange between hadrons and assume the behavior

$$M_{irr}(k_1, k_2) \sim (k_1^2 k_2^2)^a \hat{M}_{irr}(k_1,k_2) \tag{4}$$

$$M(k_1,k_2) \sim (k_1^2 k_2^2)^b \hat{M}(k_1,k_2) \tag{5}$$

as k_1^2 and $k_2^2 \to 0$, where $M(k_1, k_2)$ is the amplitude with two external gluons having momenta k_1 and k_2, and $M_{irr}(k_1,k_2)$ is the two-gluon irreducible part of the same. $\hat{M}(k_1,k_2)$ and $M_{irr}(k_1, k_2)$ are regular and non-vanishing at $k_1^2 = k_2^2 = 0$. The exponents a and b are non-integers and positive. For large r behavior it is necessary to study at least the behavior of

$$F_2(t) = \int M(k_1,k_2) D_g(k_1^2) D_g(k_2^2) M_{irr}(k_1,k_2) \delta(Q-k_1-k_2) d^4k_1\, d^4k_2 \tag{6}$$

near t=0 where $t=Q^2$. The gluon propagator has the general form

$$D_g(k^2) = d_g(k^2)/k^2 \tag{7}$$

where $d_g(k^2)$ is allowed the general behavior

$$d_g(k^2) \sim (k^2)^c, \quad k^2 \to 0 \tag{8}$$

It should be noted that Van der Waals force can exist even if c=1. The analytic property of $F_2(t)$ at t=0 depends on the $t \to 0$ behavior of

$$(\hat{M}\hat{M})_{\text{averaged over angles}} \sim t^p, \quad (t \to 0) \tag{9}$$

In QED one has a=b=c=0, and p=2. In QCD these parameters are unknown. However, Feinberg and Sucher have shown that Van der Waals potential follows if a and b are non zero, and that N in (3) is

$$N = 4(a+b+c) + 2p+3 \tag{10}$$

If p=2 as in QED, then one obtains N > 7, which is just beyond what can be ruled out by experiment (unless $r_o \gg R$).

Note that the SU(3) color symmetry plays no explicit role in this investigation unlike the consideration in the previous section. Effects of confinement are introduced by hand through the parameters a,b,c and p, and increase the power N relative to that in QED. Theoretical analysis so far can only offer a measure of safety for QCD in that it does not predict an undetected force. But it would surely be exciting if there is an experimental clarification of the nature of the Van der Waals force, if it exists. Imagine the effect on studies of confinement if such a force with N=8 or 10 were discovered. Here is an area of experimental investigation having important consequences but requiring no large accelerators. A careful determination of the energy levels of hadronic atoms (meson-nucleus or $\bar{p}$-nucleus) may be a way to learn about such forces.

IV. HADRONIC FORCE

Going down in range, this ought to be the point to discuss nuclear forces, that is, forces between nucleons due to one pion, two pions, ω, . . . exchanges, etc. In the framework of the subject matter of this talk, one should ask whether such forces can be deduced from QCD. That is obviously too difficult a question to tackle at this stage. A more modest one would be: can the nucleon-nucleon potential be derived from some quark potential inspired by QCD? To answer that it is necessary to review the status of quark potential which constitutes a non-relativistic description of the hadronic force. The discussion of nuclear force is therefore postponed to the next section.

The range of interest here is $r \gtrsim 0.2R$. It corresponds roughly to Q < 1 GeV. The scale of cut-off chosen here is intended to guarantee that the internal structure of quarks themselves is not resolved. Thus in this and the following sections we may regard the (constituent) quarks as point-like objects.

In the absence of a satisfactory solution to the confinement problem, there have been constructed various phenomenological models, such as the MIT bag model[5] or non-relativistic potential model.[6] A number of speakers have already discussed various aspects of these models at this workshop, so I need only selectively record here what is useful for our purpose. At large separations r between quarks the confining potential has been assumed to rise

either linearly or quadratically, i.e.

$$V^{conf} \sim \beta_1 r \quad \text{or} \quad \beta_2 r^2 \quad \text{at large } r \tag{11}$$

At short distance one may take QCD to imply a Coulomb-type potential due to one-gluon exchange

$$V^{1ge} \sim \alpha/r \tag{12}$$

The color matrix for one-gluon exchange is obvious, but what is it for V^{conf}? Presumably, confinement is due to a many-gluon effect. (Thinking about it in a perturbative sense is dangerous.) Representing the effect by a potential between two quarks, one would expect singlet and octet exchanges to be equally likely, i.e.

$$V_{ij} = U_{ij} + \Sigma_a \lambda_i^a \lambda_j^a W_{ij} \tag{13}$$

where U_{ij} is the singlet potential and W_{ij} the octet potential. There is no a priori reason to believe that U_{ij} and W_{ij} should be very different in magnitudes. However, if U_{ij} exists, it not only can act between two quarks within the same hadron, but can also "leak" out and act between quarks belonging to two nearby hadrons. It can then be argued that there must exist either strong attraction or repulsion between those hadrons,[4] which are unobserved. Thus it is by phenomenology, not QCD, that we would write

$$V_{ij} = \Sigma_a \lambda_i^a \lambda_j^a (V_{ij}^{conf} + V_{ij}^{1ge}) \tag{14}$$

For a specific form of V_{ij}^{1ge} the Fermi-Breit interaction has been chosen by deRújula, Georgi, Glashow[7] and later by Isgur and Karl[8] without the spin-orbit term. It is (for equal quark mass)

$$V_{ij}^{1ge} = \alpha_S \{ \frac{1}{r} - \frac{1}{2m^2 r} [\hat{r}\cdot(\hat{r}\cdot\vec{p}_i)\vec{p}_j] - \pi\delta^3(\vec{r}) \frac{1}{m^2}(1+\frac{8}{3}\vec{s}_i\cdot\vec{s}_j)$$

$$- \frac{1}{2r^3 m^2} [\vec{r} \times \vec{p}_i \cdot \vec{s}_i - \vec{r} \times \vec{p}_j \cdot \vec{s}_j + 2\vec{r} \times \vec{p}_i \cdot \vec{s}_j - 2\vec{r} \times \vec{p}_j \cdot \vec{s}_i$$

$$-2\vec{s}_i\cdot\vec{s}_j + \frac{6}{r^2}(\vec{s}_i\cdot\vec{r})(\vec{s}_j\cdot\vec{r})] \} \tag{15}$$

This potential has been used successfully to describe the level splittings of SU(6) multiplets for a variety of hadronic states. In fact, it has precipitated the so-called "Isgur-Karl catastrophe"[9] in that very little is left to be done in baryon spectroscopy.

It is then natural to ask: if the potential (14) between quarks is really good, can it be used to infer the nuclear force between nucleons?

V. NUCLEAR FORCE

To derive nuclear force from quark potential is not a new problem. What I wish to report here is a piece of work by Morley, Pursey, Williams[10] which

has recently come to my attention. They have not finished writing up their work yet, so I have no details to give. But the claim sounds sufficiently impressive that it seems appropriate to outline what they purport to have done.

They consider a six-quark non-relativistic system having the Hamiltonian

$$H = \sum_{i=1}^{6} T_i + \sum_{i<j} V_{ij} \tag{16}$$

where $T_i = -(2m)^{-1}\nabla_i^2$ and V_{ij} is given by (14) and (15) with V_{ij}^{conf} being either linear or harmonic as in [11] (11). Considering two subsystems A and B each consisting of three quarks, they rewrite (16) as

$$H = T_A + T_B + T_{AB} + V_A + V_B + V_{AB} \tag{17}$$

in obvious notation. The Schrodinger equation $H\Psi=E\Psi$ is then to be solved by variational method using the Heitler-London ansatz for Ψ

$$\Psi = \frac{N}{10}\sum_{k=0}^{9} (-1)^{g_k} g_k \psi(r)\phi_A\phi_B |\text{spin, isospin, color}\rangle \tag{18}$$

where ϕ_A and ϕ_B are the spatial nucleon wave functions in terms of the quark coordinates which are to be reordered in the sum in accordance to the transposition operator

$$\{g_k\} = \{e, 14, 15, 16, 24, 25, 26, 34, 35, 36\}$$

$\psi(r)$ is an unknown wave function in terms of the relative separation between the center of A and B.

The solution of the problem is that $\psi(r)$ turns out to satisfy a non-local dinucleon Schrödinger equation

$$\int d^3r' [T(\vec{r},\vec{r}')+U(\vec{r},\vec{r}')]\psi(\vec{r}') = \lambda\psi(\vec{r}) \tag{19}$$

The non-local potential $U(\vec{r},\vec{r}')$ has many terms all of which have the feature that they correspond to the interchange of two quarks between A and B. Thus nuclear force arises from constituent interchange and not from gluon exchange which is excluded by color consideration. So far the result is not surprising and has been anticipated qualitatively by others.[11]

What is intriguing, however, is that the authors of Ref. 10 go on to claim that the phenomenological meson theory can be inferred from their result. By expanding the non-local potential up to p^2 terms they obtain an approximate local potential

$$V(r)_{local} = V_1(r) + V_2(r)\,\vec{L}\cdot\vec{S} + V_3(r)L^{\vec{}2} + V_4(r)\vec{p}^2$$

$$+V_5(r)\,\vec{r}\vec{r}:\vec{p}\vec{p} + V_6(r)S_{12}(\hat{r}) \tag{20}$$

Each of these terms can be identified with a corresponding part of the N-N potential. V_6S_{12} acts as the attractive π exchange potential, V_1 is the attractive central term like σ exchange, $V_2\vec{L}\cdot\vec{S}$ is the repulsive spin-orbit ω exchange, and $V_4p^2+V_5\vec{r}\vec{r}:\vec{p}\vec{p}$ represents the repulsive hard core. The spin structure of the various terms is not unexpected but what would be impressive is that $V_i(r)$ have the correct phenomenological forms. They are supposed to be known analytically in terms of hypergeometric functions. It is hard to believe that precise correspondence with each term in the meson theory can be

established, since surely the model cannot predict the masses of the mesons, especially the pion. What is possible is that (20) taken as a whole may reproduce the local nuceon-nucleon potential as determined phenomenologically in the meson-exchange theory, and that both descriptions are only approximations of the non-local quark exchange potential.

The picture that emerges is that the nucleons are held together in a nucleus by a covalent bonding mechanism in much the same way that hydrogen atoms are held together in a hydrogen molecule. It would be of interest to see how this picture can arise from a bag model consideration. Evidently progress is being made in learning about long-distance forces from short-distance potential rooted in QCD. It may be that the quark-exchange mechanism is more important than the exact confinement mechanism. At the same time the mystery about the short-range hard-core potential between nucleons is beginning to be resolved in the more appropriate language of quark-quark interaction, as it should be.

VI. QUARK STRUCTURE

We have given the quark potential in Sec. IV and stated its success in explaining hadron levels and its implication for nuclear forces. Do we then have a reliable description of the structure of hadrons? If so, what are the proton and pion internal wave functions? If they are known, then one should be able to calculate many measurable quantities which are manifestations of hadron structures, such as form factors, structure functions, decay constants, etc. But before such a description can be given, it is necessary first to clarify what one means by hadron wave function in terms of its constituents. What are the constituents? Are they the quarks discussed in the preceding two sections? Or, are they the quarks probed by deep inelastic scattering? Obviously, the wave function depends on what constituents one refers to. Hence, just as it was necessary to discuss the quark potential first before the nuclear potential, the subject of hadron structure must follow a discussion of the quark structure. These reversals are natural if QCD is the basis for the formation of one's physical picture of the hadronic system even if first-principle calculations cannot yet be made.

In the bound-state problem we regard the proton as consisting of three quarks and the pion a quark-antiquark pair. These are the constituent quarks. On the other hand, in deep inelastic scattering a hadron is regarded as having valence quarks, sea quarks, and gluons (collectively called partons). In fact, even at Q^2 between 1 and 3 GeV^2 the gluons carry nearly half the nucleon momentum. How can this picture of the hadron reconcile with that of the bound-state problem? It must first be recognized that the quarks probed in deep inelastic scattering are current quarks, since they are coupled to electromagnetic or weak currents. Evidently, constituent quarks are different from current quarks. The failure to recognize this difference has led to much confusion and many mistakes in the literature. Let me give a few examples.

1. Since the total cross section for πp collision is about 2/3 that of pp, in the additive quark model one regards the constituent quarks as having independent q-q cross section, so that $\sigma_{qp} \sim 1/3\ \sigma_{pp}$. Such quarks should therefore <u>not</u> be given a momentum distribution $q(x) \propto (1-x)^3$, which is the large-x behavior of current quarks.

2. In the bag model one is dealing with constituent quarks. But in estimating the bag size it would be wrong to draw on the primordial quark transverse momentum (0.6-0.8 GeV) inferred from large-p_T reactions as a

phenomenological input. The estimated bag size (~0.3fm) comes out too small because in a hard process it is the current quarks that are involved.

3. Recent experiments in deep inelastic leptoproduction on nucleons give data on the hadrons produced in the target fragmentation region. It is incorrect to interpret those hadrons as products of "diquark" fragmentation because the quark knocked out by the virtual photon (or W) is a current quark, not a constituent quark, so what remains in the hadron is not a diquark, meaning two remaining constituent quarks.

Many other examples of the confusion can be found in the literature once one is aware of the difference.

The way to unify the two manifestations of the hadron constituents is to regard the constituent quark as a dressed quark in QCD. In a bound-state problem the gluons and sea-quark pairs are virtual. Because the relevant value of Q^2 is low, the resolution is too poor to discern the internal structure of the dressed quark. Thus without loss of any accuracy the constituent quark may be regarded as point-like and structureless, as far as the static properties of the hadrons are concerned. In a hard scattering problem, on the other hand, the value of Q^2 is high so the internal structure of the constituent quark can be resolved. Moreover, the virtual partons are momentarily free, so a constituent quark may be more usefully viewed as a cluster of partons carrying the quantum numbers of the valence quark. It should be stated here that the cluster picture of the constituent quark is far more appropriate when one considers hadron-hadron collisions in which the virtual partons can readily be excited and be on mass shell before hadronization. Moreover, the parton distribution in a cluster would not be left unchanged during the course of the collision process, so the concept of a constituent quark behaving as an unalterable unit is unrealistic.

To avoid the confusion and the awkwardness of distinguishing two types of quarks, we shall hereafter use the term quark only in reference to the current quark, whose field appears in the basic Lagrangian of QCD. For the other we shall call it valon to signify valence quark cluster (in a scattering problem) or a constituent quark (in a bound-state problem).[12] Note that in this terminology the title of this section is made inappropriate and misleading, but it serves to identify the subject.

QCD has not been developed to the point where we can get guidance on how to proceed from here. From the phenomenological success of the three-valon model in describing the static properties of baryons, and from the theoretical success of the renormalization group analysis in QCD in describing the scaling-violation behavior of the nucleon's structure functions at high Q^2, one can construct a sensible model relating quarks and valons in a hadron. The ideas to be described below have been around for a few years,[13,14] although in detail there are variations in how they are implemented. The deep inelastic scattering data that recently became available allow the model to acquire a more quantitative status.[15] I give here an outline of how I have been describing the subject, and refer to it as the valon model.

In the valon model the quark distribution in a hadron h, denoted by q_i^h, is expressed as a convolution of a valon distribution in h, V_j^h, with a quark distribution in the valon, p_i^j, i.e.

$$q_i^h(x,\vec{r},Q^2) = \sum_j \int \frac{dx'}{x'} d\vec{r}' \, V_j^h(x',\vec{r}') \, p_i^j\left(\frac{x}{x'}, \vec{r}-\vec{r}', Q^2\right) \qquad (21)$$

where x denotes momentum fraction and $\vec{r}$ transverse position. Implicit in (21) is an assumption of impulse approximation in that the valons in h contribute

independently to the quark distribution. p_i^j describes the valon structure; its dependence on Q^2 at high Q^2 is calculable in perturbative QCD. V_j^h summarizes the confinement complication; it can be determined theoretically only upon the solution of the confinement problem, or some phenomenological approximation of that problem. The main significance of (21) is the separation of two aspects of the problem concerning hadron structure: the binding of the valons in a hadron (long-distance behavior) and the structure of the valons themselves (short-distance behavior). This is consistent with the nature of the solution of the renormalization group equation.[12] Note that the valon distribution $V_j^h(x,\vec{r})$ has no explicit Q^2 dependence, although implicitly it is defined at some low Q_o^2 relevant to the bound-state problem. Correspondingly, $p_i^j(z,\vec{\rho},Q^2)$ has an implicit dependence on Q_o^2. When $Q^2=Q_o^2$, the valon structure cannot be resolved and p_i^j becomes trivial, i.e. $\delta(z-1)\delta(\vec{\rho})$. It is a failure of QCD to provide a reliable calculational scheme for p_i^j when Q^2 is less than an order of magnitude larger than Q_o^2.

VII. HADRON WAVE FUNCTIONS

It is clear from the discussion in the preceding section that the wave functions of hadrons will be described in terms of the valons; in fact, for valon j the absolute square of its wave function in h is just $V_j^h(x,\vec{r})$. This is, however, not the only way to describe a hadron. Brodsky et al[16] prefers to use the Fock space which has an infinite number of sectors involving different numbers of quarks, antiquarks, and gluons. A complete description in that representation is, of course, at present impossible. What they do then is to go to certain kinematical regions (such as $x\to 1$ or large Q^2) and discuss the wave functions in selected sectors that are dominant. The wave function that we seek in the valon representation is for all x and $\vec{r}$ and is independent of the value of Q^2 of the probe.

Before proceeding to the determination of $V_j^h(x,\vec{r})$, let us first separate its longitudinal and transverse behaviors, beginning with the definition of the *longitudinal momentum distribution*

$$G_j^h(x) = \int d\vec{r} V_j^h(x,\vec{r}) \tag{22}$$

Then by assuming factorization in the variables x and $\vec{y}$ where $\vec{y}$ is the transverse coordinate of a valon (with momentum fraction x) relative to the center of the other valons in h, i.e. $\vec{r}=(1-x)\vec{y}$,[17] we have

$$V_j^h(x,\vec{r}) = (1-x)^{-2} G_j^h(x) H_j^h(\vec{y}) \tag{23}$$

The $\vec{y}$ distribution is normalized by

$$\int d\vec{y} H_j^h(\vec{y}) = 1 \tag{24}$$

Without adopting any phenomenological confinement model, V_j^h can only be determined by direct analysis of appropriate data on the basis of (21). The result is probably more reliable than that of any model calculation. Since the concept of valon serves as a bridge between the bound-state problem and the deep inelastic scattering problem, the valon distribution can therefore be approached from either side of the bridge. We summarize below the results obtained from the two approaches.

A. Structure Function[12,15]

From the deep inelastic scattering side the structure function is related to the valon distribution by

$$F^h(x,Q^2) = \sum_j \int dx' \; G_j^h(x') \; F^j \; (x/x', \; Q^2) \tag{25}$$

where F^h and F^j are the structure functions of hadron h and valon j. When Q^2 is large, F^j is calculable in leading log approximation. From the experimental data for F^h, we can extract G_j^h using (25). The result for proton is[15]

$$G_U^p(x) = 8.0 \; x^{0.65}(1-x)^2 \tag{26a}$$

$$G_D^p(x) = 6.0 \; x^{0.35}(1-x)^{2.3} \tag{26b}$$

Because only leading log approximation has been used for F^j, (26) should be regarded as effective distributions, which may differ from the actual distributions at Q_o, but which is nevertheless useful for the calculation of quark and gluon distributions at any high Q^2 by adhering to the leading log approximation.

B. Form Factor[18]

From the bound-state side of the bridge we can determine V_j^h by considering the charge form factors $F_h(Q^2)$ at low Q^2. The precise relationship between F_h and the quark distribution q_i^h at any Q^2 is

$$F_h(Q^2) = \sum_i e_i \int dx d\vec{r} \, e^{i\vec{Q}\cdot\vec{r}} \; q_i^h(x,\vec{r},Q^2) \tag{27}$$

In view of (21) and the convolution theorem, we have

$$F_h(Q^2) = K_h(Q^2) \; F_v(Q^2) \tag{28}$$

where K_h and F_v are Fourier transforms of V_j^h and p_i^j, respectively, with the appropriate placing of the valon charge e_j such that $F_v(0) = 1$ and $K_h(0) = \sum_j e_j = e_h$. $F_v(Q^2)$ is independent of flavor and color because the valons have universal structure due to QCD virtual processes. In terms of the valon transverse momentum distribution

$$\tilde{H}_j^h(\vec{k}) = \int d\vec{y} \; e^{i\vec{k}\cdot\vec{y}} \; H_j^h(\vec{y}) \tag{29}$$

K_h can be expressed explicitly as

$$K_h(Q^2) = \sum_j e_j \int_o^1 dx G_j^h(x) \tilde{H}_j^h(\vec{k})\big|_{\vec{k}=(1-x)\vec{Q}} \tag{30}$$

Assuming that the valon structure cannot be resolved at low Q^2, we make the reasonable approximation that $F_v(Q^2) \approx 1$ for $Q^2 < 1$ GeV^2. Then the low-Q^2 data on F_h for h=π,p,n together with the application of (30) permit us to extract the following distributions:[18]

$$G_v^\pi(x) = 1.8 \; [x(1-x)]^{0.3} \tag{31}$$

$$\tilde{H}_v^\pi(k^2) = \exp\left(-\beta^\pi k^2\right), \quad \beta^\pi = 6 \text{ GeV}^{-2} \tag{32}$$

and $$G_U^p(x) = 10.8\, x^{0.9}(1-x)^2 \tag{33a}$$

$$G_D^p(x) = 4.6\, x^{0.1}\,(1-x)^{2.8} \tag{33b}$$

$$\tilde{H}_j^p(k^2) = \exp(-\beta_j^p k^2)$$

$$\beta_U^p = 6.1\ \text{GeV}^{-2}, \quad \beta_D^p = 3.0\ \text{GeV}^{-2} \tag{34}$$

The solid lines in Fig. 1 show K_h as calculated from (30)-(34). The deviation of K_h from the data on F_h for $Q^2 > 1\ \text{GeV}^2$ are to be accounted for by F_v.

We note that (33) differs somewhat from (26). This is to be expected because no leading log approximation is used in the determination of (33), which therefore is a truer representation of the valon distribution. However, (33) cannot be used to determine quark and gluon distributions at high Q^2 because there is no reliable evolution function that connects (33) at low Q_o^2 to high Q^2. The difference between (26) and (33) is a reflection of the fact that the bridge mentioned above is not complete. The stumbling block is, of course, our inadequate knowledge about p_i^j at intermediate values of Q^2 where non-leading order and higher-twist terms are important. Despite this apparently insurmountable difficulty, the mismatch between (26) and (33) is actually not too bad. For accuracy in applications of the hadron wave function, (26) should be the basis for high-Q^2 predictions using leading log approximation, while (33) should be used for low-Q^2 problems.

VIII. HADRON FORM FACTORS

An interesting consequence of (28) is the cancellation of F_v in the ratio of F_h's for different hadrons, e.g.

$$\frac{F_\pi(Q^2)}{F_p(Q^2)} = \frac{K_\pi(Q^2)}{K_p(Q^2)} \tag{35}$$

The right hand side can be calculated in accordance to (30) for all Q^2 although the inputs are the valon distributions (31)-(34) with no Q^2 dependence. Instead of comparing our result directly with the left-hand side of (35) owing to the difficulty of taking the ratio of experimental data, we approximate F_p by the dipole formula

$$F_p^D = \left(1+\frac{Q^2}{0.71}\right)^{-2} \tag{36}$$

which is shown by the dotted curve in Fig. 1. We then compare $(K_\pi/K_p)F_p^D$, shown by the dashed curve in Fig. 1, with the data on F_π. The good agreement confirms that F_h differs from K_h by a common factor F_v for $h=\pi$ and p. This result gives support not only to the valon model but also to the reliability of the valon distributions determined. The form factor for kaon has unfortunately not yet been measured to even moderate values of Q^2.

To determine F_h completely it is necessary to calculate F_v, which in turn depends on p_i^j, in particular, on the transverse momentum distribution of a quark in a valon. The latter has been investigated in perturbative QCD at

high Q^2,[19] and the implication on $F_v(Q^2)$ is that it behaves as $(Q^2)^{-0.6}$ for $Q^2 \gg 1\,GeV^2$.[20] For $Q^2 < 1\,GeV^2$ we have imposed the requirement that $F_v \approx 1$. A smooth joining of the large- and small-Q^2 behaviors (with an adjustable parameter) results in a useful formula for $F_v(Q^2)$ for all Q^2. Applying it to (28) leads to a determination of the proton form factor which fits the data to such an accuracy over the whole measured range ($0.1 < Q^2 < 20\ GeV^2$) that even the wiggling deviation from the dipole formula can be well reproduced.[20]

IX. SPATIAL PROPERTIES OF HADRONS AND VALONS

From the transverse momentum distributions of the valons we can learn about the spatial properties of the hadrons. Although our predicted values of charge radii for proton, neutron and pion are not bad,[20] we feel that they can be improved by further consideration of the local behavior at $Q^2=0$, which has not been taken into account in our investigation of the global behavior $0.1 < Q^2 < 1\,GeV^2$. Nevertheless, we can extract some qualitative features from (34). From the Gaussion approximation of the k^2 dependence, we have

$$\beta_j^h = \langle k_T^2 \rangle_{j/h}^{-1} \propto \langle r^2 \rangle_{j/h} \tag{37}$$

Thus (34) implies the following relationship for the mean square radii of the U and D valons in proton:

$$\langle r^2 \rangle_{U/p} \sim 2 \langle r^2 \rangle_{D/p} \tag{38}$$

It means that the U valons are mainly on the periphery of the proton while D is more toward the center. If one were to picture the three valons in a linear array, then it would spell *UDU* for proton and DUD for neutron. The latter configuration is precisely what is obtained to explain the neutron charge radius when the spin and statistics considerations are taken into account for the valons.[21]

From the discussions in the preceding section it is clear that we are dealing with a hierarchy of sizes: hadron, valon, parton. The hadron size is characterized by β_v^h (valon in hadron) while the valon size is characterized by β_q^v (quark in valon). Obviously, the former determines a transverse scale in soft processes, while the latter in hard processes. This explains why there are two transverse scales observed in experiments. It is known that in multiparticle production at "high" energies (E>15 GeV) the average transverse momentum of produced pions is about 350 MeV. But in massive lepton-pair production ($M_{\mu\mu} > 4$ GeV) the transverse momentum of the pair can be understood phenomenologically only if a primordial parton distribution with $\langle k_T \rangle \sim 800$ MeV is assumed.[22] The latter corresponds to $\beta_q^v = 1.23\ GeV^{-2}$. Comparing this with (32) reveals that $\beta_q^v / \beta_v^h \sim 1/5$. Thus the mean square radius of a valon is about five times smaller than that of a hadron. The implication is that the constituent quarks are far from being point-like and that the hadrons are not very "spacious" (like the atoms) nor very "crowded" (like the nuclei).

X. PION DECAY CONSTANT

Knowing the pion wave function as given in (31) and (32) should allow us to calculate the pion decay constant f_π, which is related to the wave function

at the origin. Since f_π is a property of the (PCAC) pion as a Goldstone boson, its connection with the pion as a bound-state of two constituent quarks has been somewhat problematical in the past.[24] Recently, progress is being made in elucidating this problem in the context of the bag model[25] as well as in various schemes of breaking chiral symmetry.[26,27] We approach it in yet another way.[18]

The definition of f_π is

$$\langle 0|A^i_\mu(0)|\pi^j(P)\rangle = \delta_{ij} iP_\mu f_\pi \tag{39}$$

where $f_\pi = 93$ MeV experimentally. A^i_μ is the axial-vector current defined in terms of the (current) quark fields. Thus it is possible to relate f_π to the quark distribution q^π_i by[18]

$$f_\pi = \left(\frac{3}{\pi}\right)^{\frac{1}{2}} \int_0^1 dx(1-x)[q^\pi_i(x,\vec{0})]^{\frac{1}{2}} \tag{40}$$

What we know from (31) and (32) is, however, the valon distribution V^π_j:

$$V^\pi_j(x,\vec{0}) = [2\pi(1-x)]^{-2} G^\pi_j(x) \int d^2k \tilde{H}^\pi_j(k^2) \tag{41}$$

The difference between q^π_i and V^π_i is minor for the present problem because $Q^2 = m^2_\pi$. Nevertheless, it accounts for the difference between quarks and valons. The result is[18]

$$f_\pi = \frac{\sqrt{3}}{2\pi}(\beta^\pi_v + \beta^v_q)^{-\frac{1}{2}} \tag{42}$$

In previous sections we have found $\beta^\pi_v = 6$ GeV^{-2} and $\beta^v_q = 1.2$ GeV^{-2}. It therefore follows that

$$f_\pi = 102 \text{ MeV} \tag{43}$$

which is only 10% greater than the experimental number. We believe that this is quantitatively the best number obtained among the various approaches and is theoretically most direct.

Note that what sets the scale is the pion radius, corrected by effects of the valon size. The masses of the quarks and valons do not enter since we work in the light-cone variables. Yet they enter in a crucial way in other approaches.[25-28] The connections among these approaches remain to be established. Because it is the meson radius that is important in our approach, our estimate for f_K/f_π is roughly 1.1 to 1.2, just as what the experimental value appears to be.

The color factor $\sqrt{3}$ and the valon-size factor β^v_q would not have entered (42) if it were not for QCD. Hence, the accuracy of the numerical result in (43) could not have been achieved without QCD as the basis for our analysis.

XI. SOFT HADRONIC PROCESSES

We now turn to multiparticle production at low p_T in hadron-hadron collisions. This is one area where intense beam at E<31 GeV can contribute significantly to the study of hadron structure. One who is familiar with hard processes, such as large-p_T reactions, may be surprised by the suggestion that

soft processes can equally well be used to probe hadron structure. But the fact is that inclusive distribution of produced pions in the fragmentation region has been obtained with less phenomenological adjustments than that in the large-p_T region,[23] and with more success.[29]

To understand soft processes at the constituent level it is important to be clear about what constituents one should be considering. A large number of theorists adhere to the view that a constituent quark behaves as an integral unit in the collision process and that it either gets scattered by another constituent quark in the other hadron or goes through the interaction region unscattered, causing a color-elongated configuration which results in multiparticle production.[30-32] Some aspects of this view could perhaps be valid to describe inclusive cross section in the central region,[33] since there has been a large body of theoretical work done on the dual topological unitarization (DTU) scheme with successes that cannot be ignored.[34] The extention to fragmentation region is, however, on less firm ground. In any case, it seems that DTU ought to be an output in a QCD-based theory or model rather than a crucial input along with words about color separation.

My view is that the concept of a constituent quark is useful only in dealing with static problems of hadrons or for keeping track of quantum numbers (not momenta) of constituents in dual diagrams. In scattering problems there is no evidence that they remain as integral units during the course of collision. This is where the concept of valons as clusters of partons is more appropriate. Each valon has a primitive distribution of parton momenta which can be determined from electroproduction at low Q^2. Recall that even at Q^2=1-3 GeV^2 nearly half the momentum of a nucleon is carried by the uncharged gluons. In a collision at high energy these partons do not require more than a few hundred MeV in excitation energy to be put on mass shelland they can propagate and interact independently as free partons for a long time (in a frame where these partons are moving fast) before hadronization at the final stage takes place. Since partons with different momenta interact differently with the target (especially if the target is a large nucleus, a subject to be discussed in the next section), the parton momentum distribution changes as it goes through the interaction region. For this reason valons cannot maintain their identities upon collision, unlike the static problem in a bag. Stated differently, in a time-dependent problem such as inclusive reactions it is difficult to describe accurately the development of a constituent quark as soon as the confining bags are broken, since even the definition of a constituent quark is in question.

For hadron-hadron collision at high energy our approach is the following.[35] Each valon has a primitive distribution of partons before collision. In the c.m. frame of the incident particles the fast partons are regarded as being on mass shell and propagate as free quarks and gluons whose interaction with other partons will be estimated in the next section. The changes on the longitudinal momenta of the fast partons are not significant, so they are neglected. As the partons propagate beyond the original interaction region, they gradually dress themselves up by virtual processes and become valons. Time dilation prolongs the time scale of this dressing process for the fast partons. Each such valon has the same momentum as the original bare parton before dressing begins. Pairs of those valons with appropriate quantum numbers can then recombine to form produced pions in the fragmentation region.[36] Various steps in this process involve phenomenological inputs that can independently be determined. But putting these steps together involves no adjustable parameters, so predictions on the inclusive distributions can be calculated.

The result agrees well with experiment, as shown in Fig. 2.

The recombination model has been applied with success to various proton induced reactions,[37] meson induced reactions,[38] baryon production,[39] two-particle correlation,[40] and polarization of produced hyperons.[41] It also plays an important role in the hadronization part of an approach that estimates the large-x behavior at low p_T using counting rules[42] on more explicit QCD diagrams.[43] As a description of hadronization the recombination mechanism is equally applicable to the final stage of a quark or gluon fragmentation process, which is more amenable to QCD calculations.[44]

Recently, there has been some interest in applying the recombination model to the production of mesons in the cumulative region of nuclear fragmentation.[45] The aim is to learn about the quark distribution in a nucleus in the rare configuration where some of the quarks carry a large fraction of the momentum of the whole nucleus. It is my view that soft rather than hard processes can yeild more useful information.

Phenomenology on hard processes such as large-p_T reactions has by now lost most of its initial euphoric expectations partly because lowest-order QCD diagrams have been found not to be dominant,[2] but more probably because there are too many components in the processes that are unknown. For example, the primordial k_T distribution of the partons directly affects the inclusive cross section of produced pions at large p_T. This defect is absent at low p_T. Moreover, whereas hard scattering is damped in ways that are difficult to calculate at present energies ($E \gtrsim 300$ GeV) if the lowest order result is inadequate soft scattering of quarks is not damped even at intermediate energies ($10 < E < 30$ GeV). In the next section we shall examine quantitatively how weak the damping is if the observer does not demand large angle scattering. If the longitudinal momentum of a fast parton is insignificantly damped, soft hadronic processes should be far more suitable for providing information on the parton distributions in the initial hadrons than hard processes. Besides, such experiments are considerably less expensive. High precision experiments in the beam and target fragmentation regions are therefore strongly urged.

XII. RADIATION LENGTH OF FAST QUARK IN NUCLEAR MATTER

Intensive investigations of multiparticle production in hadron-hadron collisions more than ten years ago have yielded many general features, among which two very basic ones are factorization and short-range correlation. Factorization means that particles produced in the beam fragmentation region is independent of the target, and vice-versa. Short-range correlation means that produced particles that are well separated in rapidity ($\Delta y > 2$) are not correlated. These features have become such basic guiding principles that models have been built mainly on the basis of them, such as: multiperipheral model, Mueller-Regge model, Feynman's fluid model, and the parton model.

Suppose we take factorization to be exactly true. Interpreted at the constituent level it means that the fast quarks in a beam particle that finally become a part of a detected particle are unimpeded by the target particle. If so, then it would remain to be true even with nuclei as target. That would mean that a fast quark can penetrate nuclear matter with infinite radiation length. Can that really be true? If not, can one give a quantitative estimate of the radiation length?

To find answers to these questions one, of course, does not demand that there be a quark beam and a quark detector. Hadron beam and hadron detector are sufficient since fast quarks in the beam hadron penetrate a nuclear target

almost as free "particles", for otherwise factorization would be far from true and its myth would not have survived so long. Moreover, it has long been recognized[46] that most of the hadronization occurs far outside the nuclear target so there can be no cascading, which is unobserved.[47] Now, if the radiation length L is finite, albeit large, then the pion distribution in the beam fragmentation region should depend on the nucleon number A of the target nucleus. Since the valon model provides a calculational scheme for the determination of inclusive distributions of produced hadrons, the effect of nuclear attenuation on the parton momenta can be built into the scheme, thereby providing a way to relate L to the A dependence.

Experimentally, it has been found that the inclusive cross section for $p+A\to\pi+X$ can be (imperfectly) expressed in the form[48]

$$x\frac{d\sigma}{dx} = \left(x\frac{d\sigma}{dx}\right)_o A^{\alpha(x)} \tag{44}$$

where

$$\alpha(x) = \alpha_o + \alpha' x \tag{45}$$

The empirical value for $\alpha(x)$, average over x, is less than 2/3, and an explanation for it has been advanced by Dar and Takagi[49] on the basis of "quark attennation and recombination." From the data on $\alpha(x)$ compiled in Ref. 49, one can obtain the best parametrization in terms of

$$\alpha_o = 0.62, \quad \alpha' = -0.17 \tag{46}$$

which is also compatible with the data in Ref. 48. The fact that α' is nonzero and negative proves that factorization is not strictly correct and that a fast quark has finite radiation length due to strong interaction with nuclear matter. To translate the value of α' into a value for L would be very interesting, since we would have for the first time a quantitative statement about the validity of factorization and of the conjecture that quarks in the fragmentation region are undisturbed by the collision process.

To do that,[50] we propose a parton evolution equation in the variable N, the number of nucleons that a parton traverses, i.e.

$$\frac{d}{dN} q(x,N) = \int \frac{dy}{y} q(y,N)A(x/y) \tag{47}$$

where A(x) is the attenuation function of parton momentum as it traverses one nucleon. Number conservation requires

$$\int_o^1 A(x)dx = 0 \tag{48}$$

because the probability that a parton has momentum fraction x after emerging from a nucleon is

$$P(x) = \delta(x-1) + A(x) \tag{49}$$

Since QCD cannot be used to determine A(x) for these soft processes, we can

only assume a form for A(x) which contains the essence of bremsstrahlung of massless bosons

$$A(x) = \frac{k}{(1-x)_+} \tag{50}$$

where k is a constant to be determined, and

$$\frac{1}{(1-x)_+} = \frac{1}{1-x} - \delta(x-1)\int_0^1 \frac{dx}{1-x} \tag{51}$$

Evidently, k gives an estimate of the degree of radiation loss, as a parton passes through a nucleon.

On the basis of (47) and (50) the N dependence of $q(x,N)$ can be calculated. The result is used in the valon-recombination model[35] for hA inclusive reaction, with N set to be $A^{1/3}$. Not surprisingly, the A dependence is exponentiated in the form (for moments of x)

$$\exp[kA^{1/3}(\text{moments})] \tag{52}$$

whereas (44) implies (before moments are taken)

$$\exp[\alpha' \times \ell n\, A] \tag{53}$$

Fortunately, $A^{1/3}$ is very nearly ℓnA for $5<A<200$, so a relationship between α' and k can be determined. The final result is[50]

$$k = 0.02 \tag{54}$$

We have not distinguished quarks from gluons, so (54) represents an average value for all partons.

From (50) we obtain the average momentum fraction of a parton as it emerges from a nucleon

$$\langle x \rangle = 1-k = 0.98 \tag{55}$$

Using t to denote the average thickness of a nucleon, we may define the radiation length L in the incremental form

$$\frac{t}{L} = 1 - \langle x \rangle = k \tag{56}$$

Consequently, we obtain

$$L = t/k \approx 50 \text{ fm} \tag{57}$$

where we have taken $t \approx 1$ fm as a reasonable rough approximation. Whether or not 50 fm is surprising depends upon one's preconceived notion about strong interactions. Here we have obtained an estimate that is based on experimental data.

The implication of (55) is that in hadron-hadron collision factorization is correct to an accuracy of about 2%, which is certainly good enough. It is therefore eminently reasonably in the recombination model to regard the fast

quarks to go through the interaction region unimpeded. Note that the same cannot be said about the valons which include wee partons at very small momenta. Slow partons interact strongly with the target and are responsible for the copious production of particles in the central region. A valon therefore changes its profile as it propagates through the interaction region. The meaning of a constituent quark in scattering problems is therefore not clear.

XIII. CONCLUSION

A great deal of information has been extracted from soft hadronic and nuclear processes that provides insight into the structure of hadrons and the nature of interactions among the constituents. It is not clear how much we have learned are inevitable consequences of QCD, yet without QCD we do not even have the framework either to extract the information or to describe the properties. What is clear, however, is that the results of the phenomenological investigations in the large number of problems discussed here add up to a collective picture which is not only self-consistent but provides a description of what QCD is likely to imply at the constituent level, if QCD is indeed the basis for what we observe. Since the possibility of being able to do a precise QCD calculation on soft processes is nowhere within sight, it may be necessary to be content with the kind of analysis briefly outlined here. This position becomes all the more respectable when it is clear that QCD offers no more precision on observable predictions in hard processes. If one subscribes to the dictum that a theory is useless unless it predicates observable consequences, which in the case of QCD implies not leaving out the hadrons, then there is a need for a theory of hadron physics as nuclear theory has described nuclear physics. Indeed, evidences are gathering that point to their parallelism: the hierarchy of substructures is being repeated in similar ways at yet another level. For this reason there is a lot that particle and nuclear physicists can learn from one another.

ACKNOWLEDGMENT

I am grateful to the organizers of this workshop for their invitation to me to speak and for their hospitality. This work was supported in part by U.S. Department of Energy under contract EY-76-S-06-2230.

REFERENCES

1. R.D. Field, Proc. of the 19th International Conference on High Energy Physics, Tokyo (1978), p. 743; R.C. Hwa, Proc. of the 1980 Guangzhou Conference on Theoretical Particle Physics, Science Press, Beijing (1980), p. 228.

2. C.H. Llewellyn Smith, Proc. of 20th International Conference on High Energy Physics, Madison (1980), to be published.

3. J.F. Gunion and D.E. Soper, Phys. Rev. D15, 2617 (1977).

4. G. Feinberg and J. Sucher, Phys. Rev. D20, 1717 (1979).

5. A. Chodos et al., Phys. Rev. D9, 3471 (1974); T. de Grand et al., Phys. Rev. D12, 2060 (1974).

6. See, for example, C. Quigg, Proc. of the 1979 International Symposium on Lepton and Photon Interactions at High Energies, Fermilab (1979), p. 239.

7. A. De Rújula, H. Georgi, and S.L. Glashow, Phys. Rev. D12, 147 (1975).

8. N. Isgur and G. Karl, Phys. Rev. D18 4187 (1978), D19, 2653 (1979).

9. A.J.G. Hey, Proc. of the 1980 Baryon Conference, Toronto (1980); See however, R. Cutkosky's talk in this workshop.

10. P.D. Morley, D. Pursey, and S. Williams (unpublished). Thanks are due to Dr. Morley for communicating to me their results prior to publication.

11. See, for example, talks by A. Kerman and R. Blankenbecler in this workshop.

12. R.C. Hwa, Phys. Rev D22, 759 (1980).

13. G. Altarelli, N. Cabibbo, L. Maiani and R. Petronzio, Nucl. Phys. B69, 531 (1974); N. Cabibbo and R. Petronzio, Nucl. Phys. B137, 395 (1978).

14. V.V. Anisovich, Ya. M. Shabelsky and V.M. Shekhter, Nucl. Phys. B133, 447 (1978).

15. R.C. Hwa and M.S. Zahir, Phys. Rev. D23, (1981), (OITS-139).

16. G.P. Lepage and S.J. Brodsky, Phys. Lett. 87B, 359 (1979); Phys. Rev. Lett. 43, 545 (1979); Phys. Rev. D22, 2157 (1980); S.J. Brodsky, T. Huang, and G.P. Lepage, SLAC-PUB-2540 (1980).

17. D.E. Soper, Phys. Rev. D15, 1141 (1977).

18. R.C. Hwa and C.S. Lam, OITS-158 (1980).

19. J.C. Collins and D.E. Soper, OITS-155 (1980).

20. R.C. Hwa and C.S. Lam (unpublished).

21. R. Carlitz, S.D. Ellis, and R. Savit, Phys. Lett. 64B, 85 (1977); N. Isgur, G. Karl, and D.W.L. Sprung, RL-80-053 (1980).

22. R.D. Field in Ref. 1.

23. M. Jacob, Proc. of EPS International Conference on High-Energy Physics, Geneva (CERN, 1979), p. 473.

24. See, for example, the reviews by R.L. Jaffe, Acta Physica Austriaca, Suppl. 22, 269 (1980), and M.D. Scadron, Arizona preprint (to be published in Reports on Progress in Physics).

25. J. Donoghue and K. Johnson, Phys. Rev. D21, 1975 (1980).

26. H. Pagels and S. Stokar, Phys. Rev. D20, 2947 (1979).

27. J.M. Cornwall, Phys. Rev. D22, 1452 (1980).

28. R. Tarrach, Z. Physik C2, 221 (1979).

29. For a recent review see R.C. Hwa, Proc. of the 11th International Symposium on Multiparticle Dynamics, Bruges, 1980, edited by E. De Wolf and F. Verbeure (Univ. Instelling, Antwerpen 1980), p. 101.

30. B. Anderson, G. Gustavson, and C. Peterson, Phys. Lett. 69B, 231; 71B, 227 (1977).

31. A. Capella, U. Sukhatme, and J. Tran Thanh Van, Z. Physik C3, 329 (1980).

32. G. Cohen-Tannoudji et al, Phys. Rev. D17, 2930 (1978); ibid. D19, 3398 (1979); ibid. D21, 2689 (1980); R. Peschanski, Bruges Symposium, loc. cit., p. 117.

33. A. Capella, U. Sukhatme, C.I. Tan, and J. Tran Thanh Van, Phys. Lett. 81B, 68 (1979).

34. G. Veneziano, Nucl. Phys. B117, 519 (1976); H.M. Chan et al., Nucl. Phys. B86, 479 (1975); B92, 13 (1975).

35. R.C. Hwa, Phys. Rev. D22, 1593 (1980).

36. K.P. Das and R.C. Hwa, Phys. Lett. 68B, 549 (1977).

37. D.W. Duke and F.E. Taylor, Phys. Rev. D17, 1788 (1978).

38. W. Aitkenhead et al., Phys. Rev. Lett. 45, 157 (1980).

39. E. Takasugi and X. Tata (to be published); E. Takasugi, Bruges Symposium, loc. cit., p. 141.

40. E. Takasugi and X. Tata, Phys. Rev. D21, 1838 (1980); E. Takasugi, Bruges Symposium, loc. cit., p. 141.

41. T.A. De Grand and H.I. Miettinen (to be published).

42. R. Blankenbecler and S.J. Brodsky, Phys. Rev. D10, 2973 (1974); J.F. Gunion, ibid. D10, 242 (1974); G.R. Farrar, Nucl. Phys. B77, 429 (1974).

43. R. Blankenbecler, S.J. Brodsky, and J.F. Gunion, Phys. Rev. D12, 3469 (1975); J.F. Gunion, Phys. Lett. 88B, 150 (1979); see also J.F. Gunion, Bruges Symposium, loc. cit., p. 767.

44. V. Chang and R.C. Hwa, Phys. Rev. Lett. 44, 439 (1980); OITS-138, Phys. Rev. (to be published); L. Jones et al., (to be published); V. Chang, G. Eilam and R.C. Hwa, OITS-156 (to be published).

45. G. Berlad, A. Dar, and G. Eilam, Phys. Lett. 93B, 86 (1980).

46. K. Gottfried, Phys. Rev. Lett. 32, 957 (1974).

47. See, for example, a review by W. Busza, Proc. of the 12th Rencontre de Moriond, edited by J. Tran Thanh Van (1977), vol. II, p. 129.

48. C. Halliwell (to be published); D.S. Barton, Bruges Symposium, loc. cit., p. 211.

49. A. Dar and F. Takagi, Phys. Rev. Lett. 44, 768 (1980).

50. R.C. Hwa (unpublished).

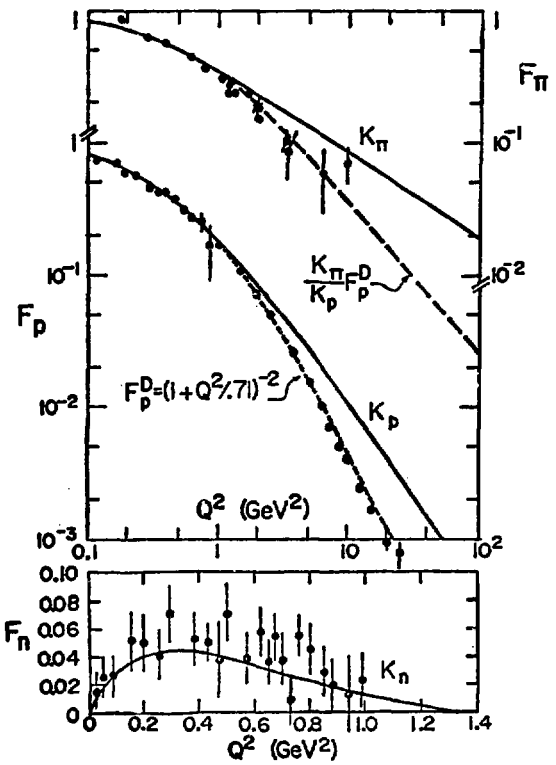

Fig. 1. Form factors of π, p, n.

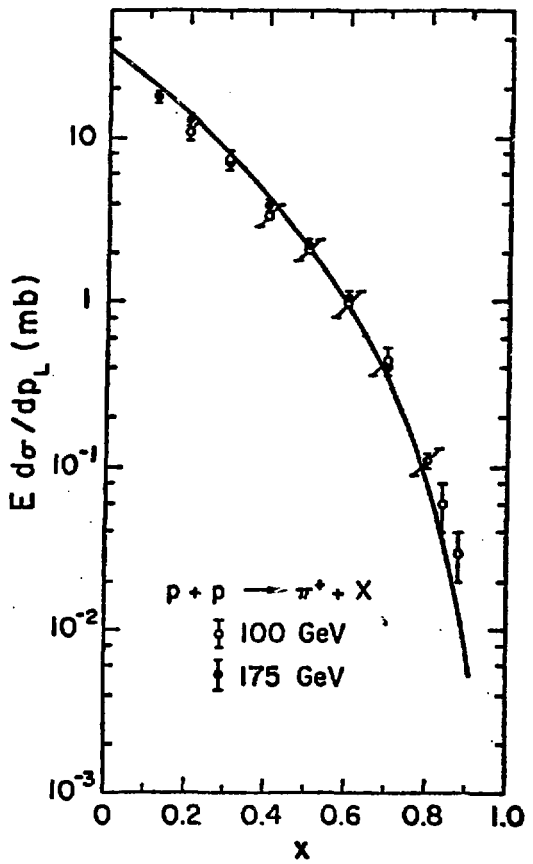

Fig. 2. Comparison of theoretical prediction with data on inclusive cross sections $p+p\to\pi^{\pm}+X$.

QUARK BAGS

by

Arthur K. Kerman
Massachusetts Institute of Technology
Cambridge, Massachusetts

What I was planning to do in this short talk was to give some very general comments (therefore you won't be able to ask specific questions like the one Herb Anderson was just asking), on what I see as the impact on nuclear physics of the last ten years' developments in the picture of the nucleon and the hadron. On the other hand there may also be some nuclear physics lessons--lessons we've learned by trying to deal with the multi-fermion system over a long period--and I will discuss what those lessons might be for the problem at hand, hadron physphysics up to 31 GeV. After that I will discuss a number of implications of quarks for low energy physics. There are a lot of different kinds of comments you can make in those two general areas.

Let me try to organize by starting with the general statements that Vernon Hughes was making toward the end of his talk. There are many different models for the hadrons, but I think everyone agrees by now that some form of QCD, which is unique, underlies them all. The nucleon has three quarks, those quarks have roughly the same masses, and they extend over the nucleus or over the nucleon. As Vernon was pointing out, when you try old fashioned pictures of the nucleon (like a point proton with pions around it), you don't get any of the right answers. I think everyone agrees on that. At MIT we have been discussing and beating on what gets called the MIT bag model, and I will talk from that point of view. However, I think many of the points that one can make are more general, and not based on the specific details of the bag model. In fact, those details are, I think, still changing and specific parameterizations are going to continue to change.

Let me start with the classic nuclear physics problem of the nucleon-nucleon interaction. From the beginning of the bag model discussions it was clear that that kind of picture of the nucleon had to have some strong implications on the issue of nucleon-nucleon scattering. This is certainly true at very high

energies, where the QCD discussions apply. But it is also true at low energies in the regime, where we try to unravel what the nuclear forces are for purposes of studying nuclei. The basic change, it seems to me, is the statement that we are going to take seriously the composite nature of the nucleon. In the old days we tried to do everything with some form of field theory. We were going to have exchanges of this and that with point interactions, and everything was going to get described in that way. In a way this really is a revolution, because the way we are going to look at the nucleon-nucleon interaction for some purposes is completely an opposite viewpoint from that. We look at this six (or more) quark system as a many body system, rather than focusing on the nucleon-nucleon channel. And that leads one who has been in nuclear physics to think about it in a different way.

The analogy which people have pursued--I would like to bring it up here and then discuss it later in context of specific nuclear physics questions--is very close to a nuclear physics problem which is familiar and has been treated over a long period of time--the problem of ^{8}Be. The nucleus in ^{8}Be has eight nucleons, not six, but it does like to decay into two alpha particles which are each clusters of four nucleons. The fact is that there is a wide range of energy before you get anything else, since it costs at least 20 MeV or more to get a nucleon out of the alpha particles. So the physics of ^{8}Be is my model for the physics of the nucleon-nucleon interactions. In that situation what you try to do is to deal with the eight nucleons on an equal footing by describing the system by some kind of collective variable, rather than the variables of the individual nucleons, to describe the fact that the system decays into two alpha particles. That doesn't mean that one doesn't deal in detail with the independent particle variables (nucleon variables) in that case. One does, and we've got all kinds of lore about how to do that. You get a deformed system with eight nucleons in it where you have localized nucleon orbitals. You see that that looks a little bit like two alpha particles, and you end up understanding why it is that ^{8}Be has a narrow resonance at 96 keV and doesn't have a bound state.

It seems to me that the only right way to think about the nucleon-nucleon interaction in these times is in that kind of language. The bag model gave us the entree to do that. That is, we didn't have a specific enough picture before that to try to carry that out. The job has not yet been done. It is six or seven or eight years already that this has been going on, that people have been thinking about it, trying various approaches.

Again learning from nuclear physics, a thing like the R matrix has recently come into the discussion. That is, Jaffe and Low brought in what they called the P matrix, which somebody was referring to yesterday. The notion there is to try to do the physics of the many-quark system in the same way that you try to do the physics of a large nuclear system. This approach discusses the dynamics of what goes on in the internal region without reference to what the channels are (to how the system decays), and then focusing on the channels afterwards, as secondary kind of degree of freedom or process to discuss. That has been successful in the situation of the nuclear case and therefore I don't see why it shouldn't be successful in discussing hadron interactions.

In the case of the nucleon-nucleon interaction, if I follow that analogy and if I believe something like the MIT bag model, there are quarks which have zero (or small) rest mass, moving nearly relativistically inside of a slowly changing volume. I am talking about an adiabatic approximation. So the appropriate collective variable here is the shape of the system. When it comes apart and I've got two nucleons, I can think about a potential, but when it's close together I've got to think about all of the degrees of freedom.

One very important conclusion I can draw from this without doing any calculations is the following, which again comes back to the ^{8}Be discussion. We have learned there that if we want to describe that in terms of a potential, that the potential is not local. That is, if we want to talk about a degree of freedom--say, the degree of freedom which becomes the distance between the alpha particles at the large distances and in some way represents the shape of the system at small distances--that the problem is essentially non-local in that degree of freedom. The reason for that is easily seen in the case of the nuclear problem. Different shapes of the system, with different single particle wave functions, have finite overlaps. That is, you can't break the Hilbert space into orthogonal sub-spaces in a simple way, when you are trying to deal with the internal dynamics that way. And so a scheme has been invented called generator coordinates, where you take for your trial wave function linear combinations of these different states which are not orthogonal. You then have to deal with the fact that they are not orthogonal. Basically, what that leads you to it this essential non-locality. So the first lesson, it seems to me, that one learns from bag pictures of the nucleon-nucleon interaction--and therefore of any hadronic interaction--is that one really should treat it as totally non-local.

On what scale? The bag radius for the nucleon in the bag model is about one fermi; there is still plenty of discussion about whether it is less or more than that, but that is the order of magnitude. In a big bag with six quarks that's supposed to represent what's going on in the deuteron when the nucleons are close together. Since the quarks move at the velocity of light, we have to expect that signals are transmitted across the bag from one side to the other. So if we are trying to define the interaction in terms of a potential, the range of the non-locality is going to be the size of the bag. And that implies that the nucleon-nucleon interaction is non-local with a range of the order of a fermi. Now, in specific detail, it may turn out to be as small as 0.5 fm, but certainly not 0.1 fm.

It seems to me that's something that we have to pay attention to; people have used non-local potentials for nucleon-nucleon interactions in the past but they didn't have this kind of justification. In fact, they didn't have this kind of specific model on which to try to build and to try to calculate further. That's one general lesson.

One problem with the present-day bag models is that the surface of the bag is very sharply defined. It is difficult to deal with the physics of how the surface of a single large thing breaks up and becomes two things. Also, how it can be that virtually some of the time there is a pion there? The pion has a low mass and that leads to the long range exchange force, the exponential one-pion-exchange force. Exactly how that dynamics works itself out is the challenging problem. There is a matching problem between the physics at long distances, where you can talk about a local potential and maybe even an exponential falloff associated with one pion exchange, and the internal region, where you must speak about a non-local potential. This matching problem is physics. The general statement is that we are not going to understand that physics from an experimental or theoretical point of view without covering the range of energies that deals with the dynamics that are going on inside. In other words, 0 to 300 MeV, which was the traditional range for nucleon-nucleon interactions, ain't gonna do it! We can find a million different potentials that will fit that data as long as we are below pion threshold, and we've learned from the nuclear problem that we can't use the nucleus as the further tool to pin that down. What we've got to do is go to higher energy and look at what is produced in the reactions. That is, we must ask what channels open up, and we must try to deal with the physics of those opening channels.

Now various simplifications can be brought to bear on this, such as saying that every process goes through two-body channels first. This, incidentally, is the simplification that has been introduced in nuclear physics from the beginning. Note that very few nuclear reactions--even if they are very complicated and many particles come out--are known to go except through two-body processes. One produces resonances, which then decay, and the daughters then produce more resonances which then decay, and so on. It appears that all of hadron physics happens the same way, and it seems to me that it is not accidental. In both cases we are dealing with the physics of a many-fermion system with relatively strong interactions (but not very strong interactions), and it is a general property in such systems that you can deal with them in that way. That is the second general insight we learn from nuclear physics.

A third insight applies to the hadron question. What about the spectrum of the mesons, for example? There is a long history in nuclear physics of the compound nucleus, doorway states, giant resonances, etc., all in a many-fermion system. We can apply the same notions to hadrons. If we want to talk about the mesons, we can talk about "compound mesons." We've got a bag with a quark and an anti-quark for the lowest kind of meson. Then we have two quarks and two anti-quarks in a bag and, further, excited states of that system. We should be able to talk about the level density of that system the same way we talk about the level density of the nuclear system. In fact, in the nuclear system we talk about particles and holes, but the "holes" here are the anti-quarks and the counting is identical. You have therefore, to expect that you are going to get some form of exponential growth in the level density, because you have a fermi gas inside of a finite volume in both cases. Of course, the well-known picture of Hagedorn and others (and also the Regge picture) also involve the limiting temperature, together with an exponential level density. But now we've got a perfectly natural explanation for these facts in a dynamical picture. We could, in fact, try to do more calculations in this direction. If you estimate the level density of bosons in the neighborhood of 3 or 4 GeV, or of a nucleon (spin 1/2 system) up at a similar excitation, the level density, because of the exponential, gets to be 1 or 10 per MeV or something like that. There is no reason why many of the properties that occur in the compound nucleus at 10 MeV shouldn't also appear in the hadronic systems, namely, that there should be a large level density of resonances that are some way going to be visible.

The way we have seen the existence of the large level density of states in the nuclear system is by looking first at low energy, seeing the specific levels, and counting them. That's already been done for hadrons. Then, secondly, by looking at higher energies and seeing the effects of the large level density on cross sections. The particular effect that really showed the presence of those levels directly (although there was plenty of indirect proof earlier) was the business of Ericson fluctuations. If there is a very large level density of states in the system--think about it just like a nucleus--then there simply have to be Erickson fluctuations. That is, that if I start with a very specific channel with the spins lined up and then look at a final channel with the spins lined up (so that I don't average things out), then the presence of the large number of degrees of freedom in that system has got to produce fluctuations in that cross section. Those fluctuations have been seen in the specific experiments that were done in nuclei, and they proved once and for all that there was a large density of levels there. You don't have to see the individual resonances. In fact, you can't, in the situation where there are so many of them that they are overlapping and they produce those fluctuations. The characteristic width of the fluctuations tells you something about the nature of the states that are being produced and their presence tells you that you have all that internal dynamics going on.

I think there have been intensive efforts to look for Ericson fluctuations at CERN and other places, but in my view every one of those efforts has been inconclusive because they haven't really focused on the issue of refining the channel. Polarization comes in because you've got to have as few amplitudes in your cross section as possible, preferably one. Any fluctuation effects that occur are going to get obviously averaged out if your cross section, the thing that you measure, is the sum of the squares of many different amplitudes. In principal, you can always choose a reaction to measure which has only one amplitude if you have polarized targets, etc. I think that's the thing that's been missing in the attempts to now find Ericson fluctuations in hadronic systems.

Apart from Ericson fluctuations, or just a proof that the degrees of freedom are there in a specific way, there is of course the indirect way of proceeding. In the case of the nucleus we knew that there was a compound nucleus contribution to the various cross sections because we just calculated it directly. We could see that it affected the angular distributions and other things, and, to my knowledge, I don't think anyone has done anything like that in hadron physics in the

range 1 to 5 GeV. One could try it. The Regge analysis and all of the dispersion relations and so on are, in some funny way, orthogonal to any attempts to think along these lines, and they dominated the field for a long time. I think the opening up of the complex models of the nucleon is going to allow us to think along these lines a little more than we have.

The other thing which is characteristic of the nuclear systems, when they are in the presence of a very large level density, is the surprising--it was surprising for a while--emergence of structure in the cross sections anyway, even after you have averaged over the fluctuations. That is, there are things like the giant resonances--the single-particle giant resonances and the giant dipole resonances--and all the things that have been being discovered ever since. In fact, the history of nuclear physics for the last 30 years is a continual discovery of more of that structure. Analog resonances were discovered 15 years ago, and that was a surprise. That turned out to be the effect of a symmetry to produce narrower things than you expected; not as narrow as a compound nucleus state, however, and that's the point I want to make here. The kind of structures we see in nuclei, because it is a many-fermion system, are simple multi-particle, multi-hole states in the background of states of many particles and many holes. The reason we see them is that our probes have particularly strong matrix elements to produce them. For example, the photon likes to flip the spin, and in the case of a nucleus the photon also likes to separate the neutrons and the protons. Thus, since our probes have specific properties and since the forces are related to those probes, it has turned out that simple modes of excitation are not damped into the complex mess so totally that they disappear. In fact, they are visible as what we call intermediate structure doorway states and show up as energy dependences in cross sections.

It seems to me that in hadron physics we are going to find those things more easily than we are going to find the fluctuations. But to understand them completely we need to recognize that when something like that happens, it is an average property of a system that comes from averaging the energy. And, for example, to remember that the total width of the system is not equal to the sum of all the partial widths into the channels that are open. We have devised the whole discussion for when you have such an averaged resonance property of the system. You can still think of a Breit-Wigner form with partial widths, but there is a new partial width in that Breit-Wigner form which corresponds to the damping of that simple mode into the more complicated modes of the system. It seems to

me that we ought to be thinking and looking for things like that in the strong interaction physics of mesons and nucleons in this intermediate regime where the level density is very high.

So that's sort of the kind of nuclear physics lesson I would like to urge on you. People ought to be thinking a little more along those lines if they are going to go into this domain and try to understand the structure of the hadrons in an excitation region where you do get all the degrees of freedom of colored quarks of various flavors coming into play.

That is one side of the coin. There are other things one can say, but I don't have time. Also I should say I am only talking; there are very few specific calculations along these lines. That doesn't mean that the ideas are right or wrong. They look to me as though they've got to be right, but we are not going to know until we get quite a bit more specific.

A subject which I would like to turn to now which is the opposite side of the coin. There is this picture of the nucleon as a complicated object with three quarks to start with but all possible quark anti-quark excitations in it. This picture of the nucleon can be extended so that the three quarks carry equal amounts of momentum on the average, etc. What does it tell us about nuclear physics, in particular, about low energy nuclear physics? Does it tell us anything interesting? Is there some handle we can get on those things in our discussions of low lying excitations of an actual nucleus? I don't know for sure, but I have some suggestions which I want to present.

If you start thinking from the point of view of the quark picture (which we have been doing for a long time now), you begin to worry about the whole nuclear picture. After all, the picture that was built up was that of an independent nucleon moving through nuclear matter, affected by the Pauli principle with two-body nucleon-nucleon correlations changing the energy significantly but not dominating it. That is, basically, a free particle system, a free fermi gas, and it explains almost everything about the low-lying states of nuclei in the zeroeth approximation. It explains the deformed nuclei in the rotational spectra in a natural combination of the independent particle picture and the collective variables describing the shape of the whole system. It explains a good fraction of what we know and it had predictive power in the past in terms of specifics--specific levels in nuclei, etc. There is no way we are going to throw all tnat success away, no matter who comes along and tells us about this internal structure of the nucleon.

But I do want to ask the question if we are in trouble if you take the MIT bag literally. This model says that the bag is one fermi in radius with three quarks running around inside a mean square radius of 0.8 or whatever. You begin to wonder because in the nucleus the nucleons are an average of two fermis apart. If the radius of the bags is one fermi, then the bags are touching in nuclei. So from the point of view of the bag model the nucleus is a liquid. (This is not a new idea.) What's new is, in some way, the nucleus is literally a liquid, i.e., it is a liquid of "atoms" of nucleons. And the nucleons have structure just like ordinary atoms have. It is a strict analogy. Maybe that's why the liquid drop model works so well.

Well, the success of the liquid drop model is not the issue. The question is, can the two models co-exist? Is it possible to talk about nucleons that are that large and still talk about the independent particle model of the nucleus and have it behave a little bit like a liquid drop? I think the answer to that is, yes, it is possible. It is a matter of dealing with a many-quark system, including in a correct way--nobody knows how to do this--the correlations among triplets of quarks which form the nucleon, and then learning how to deal with the motion of the nucleons as though they then were nearly independent entities. That doesn't seem to me an impossible situation intellectually. It also doesn't seem impossible that the independent nucleon picture would work because, even though the bags are nearly touching if I take the bag model literally, the main charge density is inside that one fermi. Thus they are only about half the time touching, and even when they do touch, that is taken care of by saying there is some force which keeps them intact. Between all of those things we might get ourselves down to a 90% description of the nucleus. We certainly should never expect to be able to calculate things better than that.

In view of all this, it is probably no surprise whatsoever that we have never been able to calculate the binding energy of nuclear matter from nuclear forces. Historically, we do the best we can to fit the low energy data, and then we get the wrong answer in nuclear matter no matter how hard we try. It doesn't seem to me that that is any longer an accident. The error we end up making, in fact, is of the order of 10 or 20% of the potential energy, and we can't expect to do any kind of calculations in this framework that would be that accurate.

The quark picture also means something for a lot of our other discussions. I said the word "van der Waals" before. Of course, one key point about the bag model is confinement. In that picture of absolute confinement there is no

van der Waals interaction between nucleons. The only long tail that's left is the one-pion-exchange tail that comes from the virtual production of a colorless pion between the two nucleons. There is no r^{-7} force (or something like that) that comes from the mutual polarization of the two systems through the gluons, because the gluons can't get out of the bag when they are not touching. And it seems to me that that is an aspect of nuclear physics that could be pushed a little harder. We were discussing that here the other day. It comes up all the time. What is our limit on the van der Waal's force between two nucleons? Come to think about it, I don't really know. I know it's not large, or we would have been in trouble in some of those nucleon-nucleon discussions long ago. Exactly how small do we know it is? Maybe someone will have something to say about that. In a way that is a side issue, but I think it is an important thing to remember, because it has to do with some of the properties of quark matter which I want to get to later.

Another thing I can think of that the quark picture tells us we ought to pay attention to in our nuclear discussions has to do with the way probes interact with the nucleus--protons or pions or whatever--and that's the following. We've thought traditionally that we should think about the charges on the nucleons and their form factors and then when that doesn't work (since we expect it won't be 100% accurate), we should start talking about exchange currents of π mesons and so on. Now it seems to me that, especially with respect to the photons but also for other things, the quark picture should change our thinking on that radically. The notion that there is one-pion-exchange going on inside the nuclear matter when the nucleons are touching seems to me too difficult to tolerate. In any case, if there is even a little bit of that, it must be cut off by a large radius (i.e., by a small momentum). None of the estimates of exchange effects with photon interactions have ever done that. When you do it, you get basically no effect. It seems to me that the right physics to be discussing is the physics of the six quarks as they come close together. And the right way to organize that discussion is to talk about the electromagnetic current of the whole system.

What carries the electric current in the nucleus? It is the quarks, as we heard. It is not the gluons, and all there is left is quarks. If there is a pion it is a quark anti-quark pair, so it is only the quarks that carry the charge. Therefore, we should focus on that. Now, since we haven't got a picture which takes care of the three-quark correlations and makes one unified model out of the nuclear chromodynamics, we have to make a separation of our interactions. The

traditional, and I think the only way we are going to do it in the long run is to separate things, writing down interactions in terms of nucleon operators. In other words, there is a one-nucleon current, for which we can measure the form factor and all of that. There ought to be a two-nucleon current and a three-nucleon current, etc. A hierarchy of that kind, which may not be absolutely unique, I think is nevertheless necessary, because all of our information about nuclear physics comes on the basis of that kind of picture, i.e., the one-nucleon modes, the two-nucleon modes, etc. We are forced to discuss the currents in that language.

And if we do that, it isn't that hard to see that, if the bag models are correct, the two-nucleon current is an extended thing, just like the one-nucleon current is an extended thing. We know that there is a form factor for the nucleon and it has a radius and so on. Also, we now know that the neutron form factor didn't work because there is no heavy center inside, but three quarks moving around uniformly. What we now also know, I claim, is that in the nucleus there are two-nucleon currents and maybe more. In fact, the size of the two-nucleon currents is going to be larger, not smaller than the nucleon itself. There is no way to pack the six quarks into a smaller bag than one nucleon--it's a bigger bag and so, as the two nucleons come close together, the current has to change. It has to reflect the degrees of freedom of the quarks inside, and one can wirte down charge form factors for such a system very simply.

No one to my knowledge has as yet done anything like that or tried to find the consequences of that in nuclear physics. There are indeed consequences in nuclear physics. There is lots of information about the low-lying spectra of nuclei. There are lots of states that are known to be very small in one-particle, one-hole excitation sense but which are known to be predominantly two-particle, two-hole excitations (in nucleon language). Those can only be excited by a current that gets hold of two nucleons, and it seems to me that that search for the two-nucleon form factor, if you want to call it that, separating it from the one-nucleon form factors, would be a useful way of coming to grips with the consequences of the quark picture in low energy nuclear physics. It ought to be pursued.

That same thing therefore holds also for pion-nucleus interactions. We know that when pions get absorbed, they get absorbed on pairs. They don't get absorbed on single nucleons, and so there is another ideal situation. The pion is a quark anti-quark pair. How does that manage to disappear into a six-quark system when

the six quarks are close together? Because that is where it happens in the nucleus, it doesn't happen when the six quarks are far apart. So the discussion of the dynamics of that system of six quarks plus, now, an extra quark anti-quark is a relevant consideration in the presence of the nuclear matter.

You notice that what one has done there is to separate the physics into an intensive vs. an extensive part. That is, the operator we are talking about is kind of an intensive property of the nuclear matter. What goes on in the neighborhood of two nucleons when other things are all around the outside knowing that we can then discuss spectral properties of the whole system? That, it seems to me is the big consequence of the quark bag model for lower energy nuclear physics. It may very well be relevant for LAMPF and for pion interactions, and probably also for kaon interactions with nuclei.

The third subject I wanted to bring up is a much more speculative and more general kind of question. I've talked so far about the low-lying structure of hadrons up to 30 GeV, if you want, and the consequences of the bag model on low-lying structure of nuclei. What about high energy? In what context do nuclei come into the high energy discussion? Well, we all know there has been plenty of discussion and work on the subject of what happens when 300 or 400 GeV protons go through nuclei. People have looked at the dependence on A of high $P_\perp$. There are all kinds of models, and it comes out peculiarly. Again, it seems to me that an attempt just to think in terms of the quarks and the bags may be more useful than at first sight one would imagine.

In pp collisions at high energies, as I see it, the quarks pass right through. The bag doesn't have any interaction with itself--they also just come through. One gluon is exchanged, and that causes triplets of three quarks to be colored. They then have to pull out lines of glue and from then on what stuff happens? The cross section you know is not geometrical. The nucleon-nucleon cross section is not πR^2, but smaller--it's half or a third of πR^2. What that means is that the interaction is not very strong. That's what I meant earlier, that one-gluon-exchange is probably not crazy; it's just a first order statement for determining the total cross section. Francis Low made that remark quite a few years ago already.

What are the consequences of that notion in nucleon-nucleus collisions? Why not think of it the same way? Three quarks go through a region of nuclear matter. Now the distance is so much longer, if I think of uranium, that the probability that there will be a gluon exchange is bigger than one. There will be several

gluon exchanges, which means that the three quarks that come out the other side are not necessarily, for example, a color octet, as in the nn collision. They may be in some color multiplet of much higher dimension. What does that mean for the leading particle that comes out in the nucleon-nucleus collision? What is the branching ratio between deltas and nucleons? Even in pp collisions, in fact, I don't think that's been studied very carefully. It requires more exclusive data.

The last thing I want to bring up is what happens--just go one step further--in uranium-uranium collisions. We are talking about multi-GeV heavy ion colliding beams at high energies such as in the Venus project at Berkeley. (We have been talking about it for quite a while, in fact.) In the context of the Bevalac, what's different between that process and a proton collision with a nucleus? Well now you've got, if you take a head-on collision of uranium on uranium, an area that's 10 fermis across or more, of quarks which are very correlated. But now they are coming through this other region at 200 GeV per nucleon or whatever we can get, and there is no reason why they shouldn't go right through also.

And why there shouldn't be gluon exchanges occurring across that whole system? What that opens up, to my mind, is the possibility that we produce in such a situation a quite different regime of color-ordering than there is in the ordinary nuclear system. There is the possibility of some long range QCD effect in the transverse direction, which could express itself in that system in a way that cannot be expressed in the nucleon-nucleon system. The latter is only one fermi across, so no matter what energy you go to, all you've got is one fermi in the transverse direction. With uranium on uranium you've got 15, and I'll quit at that point with the suggestion that we ought to be thinking about those things. It may turn out that the heavy ion high-energy collisions are the best laboratory for quark plasma physics that we are going to get.

This paper was transcribed from tape by L. J. Shreffler and minimally edited by R. R. Silbar.

QUARK STRUCTURE OF NUCLEI*

by

R. Blankenbecler

Stanford Linear Accelerator Center

Stanford University, Stanford, California 94305

ABSTRACT

A brief review is given of selected topics involved in the relativistic quark structure of nuclei such as the infinite momentum variables, scaling variables, counting rules, forward-backward variables, thermodynamic-like limit, QCD effects, higher quark bags, confinement, and many unanswered questions.

The study of nuclei and of their intersections (as well as the nucleon-nucleon interaction) has historically proceeded from the large distance and global properties to smaller distances as the energy of accelerators has increased. In the large distance regime nucleons can be considered point-like and there is no particle production. In the intermediate regime, the finite nucleon size is important but particle production effects are small. In the small distance regime, nucleons are "large", particle production is important and the internal degrees of freedom of the nucleons and mesons (the quarks) are fully excited.

Theoretically, one would like to start from a theory of quarks and their interactions, compute the properties of their bound states, i.e., nucleons and mesons, and then predict the properties of bound states of these bound states (nuclei). This is obviously a tall order and it may be some time before this program can be carried out in quantitative terms. In the roughest qualitative terms, it does seem to work, or at least tie together quite different phenomena.

In this regard it may be of some benefit to develop models that are valid in the regimes listed above and which continue correctly and bridge the gaps between these regimes. Ironically, it may prove to be more difficult to develop suitable models if nature is too smooth than if there are sharp delineations between these regimes.

I will try to organize this talk into three overlapping topics: kinematics, descriptive-parametrizations, and finally dynamics. However, of course, the

* Work supported by the Department of Energy, contract DE-AC03-76SF00515.

dynamical model (and we will be particularly interested in QCD here) and its associated calculational scheme will suggest convenient parametrizations and useful kinematic variables. This will also lead to problems in that any acceptable fundamental theory will be relativistically invariant and will lead to a relativistic description of bound states.

How can one treat this problem so that the connection to the nonrelativistic problem, where one has developed considerable insight and phenomenology, is obvious and can be used? I shall attempt to demonstrate that the use of the infinite momentum frame, or rather the infinite momentum variables, provides this close connection. In listening to some earlier talks and questions at this conference, it is clear that there is considerable misunderstanding about the meaning and uses of the infinite momentum frame. Excuse me for spending an extraordinary amount of time on this point, but if you take anything from this talk, please remember the clear physics of this choice of variables.

Our notation will be simple: A will denote a particle's name, A_μ its four-momentum, and A its mass. Confusion is therefore impossible! In the finite momentum frame, the general four-vector A_μ is written as:

$$A_\mu = (A_o;\ A_T,\ A_z) \quad ,$$

$$A_\mu = \left(yP + \frac{1}{4yP}\left(A^2 + A_T^2\right);\ A_T,\ yP - \frac{1}{4yP}\left(A^2 + A_T^2\right)\right) \quad , \tag{1}$$

where P is a parameter

$$A_\mu A_\mu = A^2 \quad ,$$

$$y = (A_o + A_z)/2P \quad , \tag{2}$$

and $d^4A = dA_o\, d^3A = d^2A_T\, dA^2\, dy/2|y|$.

The variable y is the misnamed momentum fraction. The infinite momentum frame can be achieved by taking the limit $P \to \infty$ but this is unnecessary since all relevant quantities will, in fact, be independent of the parameter P. The rest frame is achieved by choosing P so that A_z vanishes and by setting $A_T = 0$.

There are, at least, three general approaches to the problem of the relativistic description of bound states.[1] The first is an explicitly four-dimensional approach using Feynman rules which leads to the familiar Bethe-Salpeter type of equation. The second is the time ordered approach using old-fashioned noncovariant perturbation theory which actually is an integral over the fourth component P_o of some relative four-momentum in the first approach leaving $\vec{p}$ as the variable. The third is the "infinite momentum frame" approach which uses the parametrization illustrated for A_μ and an integration over dp^2 which leaves $\vec{p}_T$ and y as the three variables. The last two approaches can be made to yield similar final results but I prefer the latter because of its simplicity (one does not have to worry about all possible time orderings, for example). In addition, and contrary to what one would expect, the (P_T, y) variables yield a result that is very close to that from the nonrelativistic Schrodinger equation.

To illustrate this point consider the vertex function for $B \to C + b$, where first b and then C is off-shell (this vertices could be used in the computations

the processes shown in Fig. 1, for example). We will choose our frame by writing B_μ in the form of Eq. (1) with $y = 1$, and $B_T = 0$. For C on shell, we choose $y = x, C_T$ and then compute the off-shell quantity b from momentum conservation. The relevant propagator for the equal mass case, $b^2 = C^2$, is

$$\left(b^2 - b_\mu b_\mu\right)^{-1} = \left[\frac{\left(C_T^2 + C^2\right)}{x(1-x)} - B^2\right]^{-1}$$

For the case of C off-shell, choose b_μ of the form of Eq. (1) with $y = 1 - x$, $b_T = -C_T$, and then

$$\left(C^2 - C_\mu C_\mu\right)^{-1} = \left[\frac{\left(C_T^2 + C^2\right)}{(1-x)} - B^2\right]^{-1} \quad .$$

These denominators differ only by a factor of x. To show that the first is closely related to the familiar Schrodinger energy denominator $H_o - E \cong -E + \vec{k}^2/m$, simply write $B = 2C + E$, $x = \frac{1}{2}(1 + k_z/C)$, and one finds

$$b^2 - b_\mu b_\mu = 4C\left[-EC + k_T^2 + k_z^2\right] \quad ,$$

as expected in the nonrelativistic limit.

After a short calculation, one finds that it is possible to introduce probability functions for finding particle C in state B with momentum fraction x and transverse momentum C_T by [2]

$$G_{C/B}\left(x, C_T\right) = \frac{1}{2(2\pi)^3}\,\frac{x}{1-x}\,\left|\psi\left(x, C_T\right)\right|^2 \quad , \tag{3}$$

where ψ is a truncated Bethe-Salpeter amplitude. One needs a detailed dynamical model to be able to compute ψ for all x and C_T but it will be shown that the $x \to 1$ and the $C_T \to \infty$ behaviors are a simple function of the short-range nature of the force between the constituents. The inclusive distribution of detected particle C will in general be of the form [2]

$$\frac{d\sigma}{dC_T dx} \propto G\left(x, C_T\right) + \ldots \quad .$$

Let us now examine "scaling", the search for scaling variables, their uses, and a few cautions. There are many scaling variables that have been found to be useful. A few of them are discussed in Ref. 3. Here, I would just like to briefly discuss one that follows from our previous discussion of the infinite-momentum frame variables. For an excellent review of certain applications of this approach, I refer you to the articles by Chemtob.[4]

If absorption and final state interactions can be neglected (or rather, if they do not drastically change the longitudinal momentum distribution — they certainly will spread the transverse momentum distribution) then the inclusive

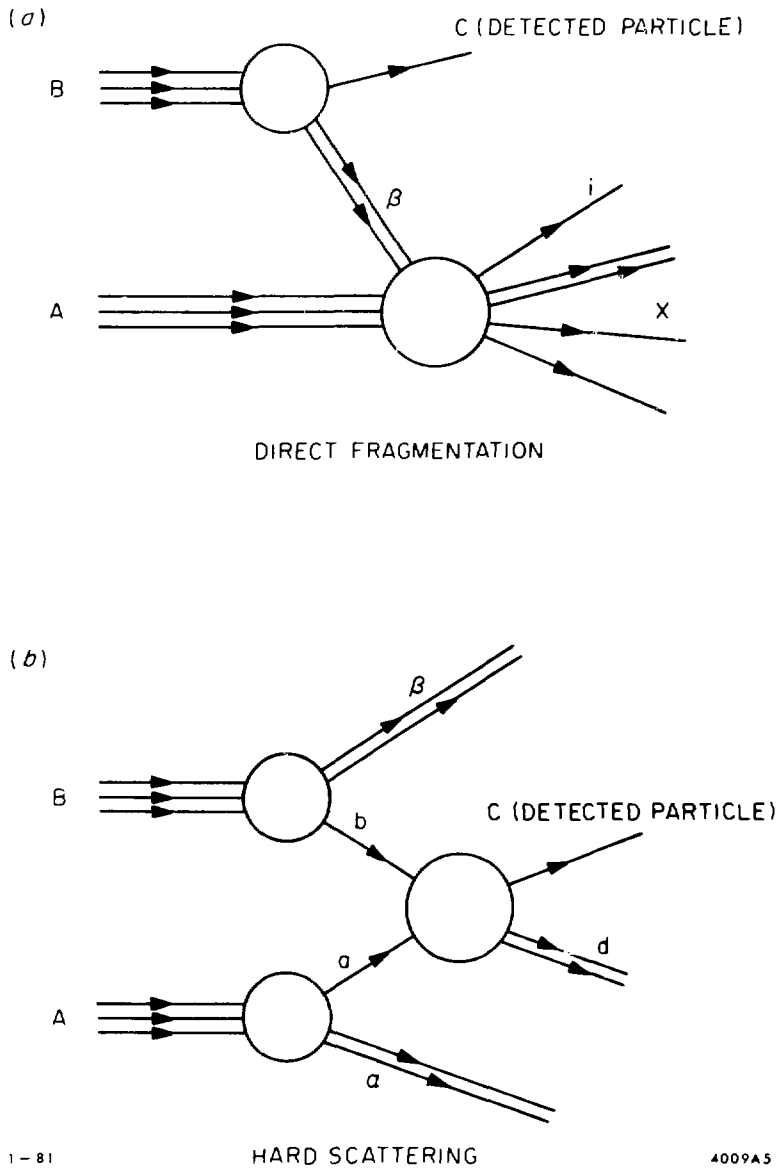

1-81

4009A5

Fig. 1

distribution (see Fig. 1) will be proportional to $G_{C/B}(x,C_T)$ in B-fragmentation region. Clearly x is predicted to ge a scaling variable[5,6] where

$$x = \frac{C_o + C_z}{B_o + B_z} = x_L x_{max}(W) \quad , \tag{4}$$

where

$$x_L = \frac{C_o + C_z}{(C_o + C_z)_{max}} \quad ,$$
$$x_{max} = \frac{(C_o + C_z)_{max}}{B_o + B_z} \quad . \tag{5}$$

Now x_{max} depends only on the center-of-mass energy W and the minimum "missing mass", M, of the reaction $A+B \to C+X$, and x_L clearly must be between 0 and 1. It is easy to see that as $W \to \infty$, $x_{max} \to 1$. For finite energies (W includes the rest masses) one finds the approximate results for the forward and backward directions (the exact expressions are not very transparent):

$$x_{max}(\theta \sim 0^o) \simeq (W^2 - M^2)/(W^2 - A^2) \quad ,$$
$$x_{max}(\theta \sim 180^o) \simeq (W^2 - M^2)/(W^2 - B^2) \quad . \tag{6}$$

Hence at moderate energies, for a light beam particle B incident on a heavy target a, one finds

$$x_{max}(0^o) = \frac{W^2 - B^2}{W^2 - A^2} \; x_{max}(180^o) \gg x_{max}(180^o) \quad . \tag{7}$$

Thus kinematics tells us that x_L scaling may look very different in the forward and backward direction. Note that x_L is not the Feynman scaling variable $x_F = |C_z| / |C_z|_{max}$, but approaches it for large C_z ($>> C$).

Let us now briefly look at an example of a "counting rule". The object here is to relate the behavior of $G(x,C_T)$ for $x \to 1$ or for $C_T \to \infty$ to some simple property of the nucleon-nucleon force at short distances.[5,7] Note that for $x \to 1$, all the other particles in the bound state must be stopped (the sum of all the x's must be 1). It is intuitively clear that the "softer" the N-N force, the faster G must vanish in these limits. For the probability of pulling a nucleon or a bound state C out of the state B, one finds

$$G_{C/B} \sim (1 - x)^g$$
$$\sim (C_T^2)^{-g+1} \tag{8}$$

where $g = 2T(B - C) - 1$, and T depends on the nucleon-nucleon force. For example, if nucleons interacted point-like with the exchange of vector gluons, then $T = 1$. If the N-N force were due to exchange of rho's and omega's with monopole form factors, then $T = 3$. Likewise, $T = 3$ if the quark degrees of freedom are fully excited. In general, however, T must be considered to be a parameter that effectively describes the N-N force in a certain regime. Rough fits to the data yield $T \sim 3\text{-}4$.

If there is very strong momentum clustering in the nucleus,[8] then one will find that $(B - C)$ is replaced by the $(\bar{B} - C)$, where $\bar{B}$ is the number of nucleons in the average cluster and the G function vanish at $x = \bar{B}/B$ rather than at $x = 1$ (if one gives the clusters some fermi momentum then this point is averaged over).

When one extracts the parameter g from data by fitting the inclusive momentum distribution it is very important to use the correct variable x rather than x_L. The factor of $x_{max}(W)$ can have a large effect on the value of g, especially when comparing the beam and target fragmentation region.

Note that we are not claiming that x is the "best" scaling variable. Indeed, it is not, since clearly there will exist arbitrarily chosen scaling functions that fit the data better than any arising from a given theory (which necessarily will yield correction and extra nonscaling terms), even the correct theory!

One's first reaction to a formula such as Eq. (7) is that it probably is nonsense for nuclei, especially for large atomic number. However, this is not necessarily the case. Consider the variable x in the limit $B \to \infty$, then $(C_+ \equiv C_o + C_z)$

$$x = C_+ / \left(B_o + B_z\right) \sim C_+ / BM \quad , \tag{9}$$

where M is the nucleon mass, and

$$\begin{aligned} G &= \left(1 - x\right)^{2TB\cdots} \sim \left(1 - C_+/BM\right)^{2TB} f\left(C_T\right) \\ G &\sim f\left(C_T\right) \exp\left(-\frac{2T}{M} C_+\right) \quad . \end{aligned} \tag{10}$$

This takes the familiar form of a thermodynamic spectrum but with the variable C_+ rather than C_o. The dependence on C_+ [and the factor $f(C_T)$] produce an angular variation which is quite similar to that seen in the data. Furthermore, the dependence of C_+ on the mass produces[6] a difference between the effective temperature for pions (60 MeV) and nucleons (40 MeV) in the same kinetic energy range (0.3-1 GeV) which is again not unlike the data for $T \sim 3.5$.

Let us now turn to QCD, its associated model for hadrons and some possible ramifications for nuclear physics. It is very easy to get a physical understanding of the effects of QCD and confinement. Perhaps the easiest way is to imagine that QCD is an ordinary field theory that was designed by a government committee. Everything works as expected but in reverse.

As an example, one has a picture that the nucleon-nucleon force is due to meson (pion, rho, omega, two-pion, etc) exchange. Since these contributions fall off exponentially at large distances, the longest range part of the force

is due to single pion exchange which is easily evaluated. At shorter distances, these more massive exchanges become more and more complicated and an accurate computation is more and more difficult.

In asymptotically free theories such as QCD, things work the same after a sign change. At short distances (higher momentum transfers) the coupling gets weaker and weaker (as $1/\ell n\, Q^2/\Lambda^2$) and hence perturbation theory is valid. One can expand in the number of gluons involved and even sum the leading terms in this series. At large distances, the coupling constants increase; they increase so fast that the force actually starts to increase as a power of the distance. This is the "confining" potential between colored objects that is expected to grow $\approx$ linearly with the separation. The detailed behavior of the theory in this strong coupling regime and its transition to the perturbative regime is under intense study. It goes without saying that the behavior of the hadronic bound states at large distances is controlled by the strong coupling behavior of the theory.

The potential between a quark-antiquark pair, each of which is a color triplet, has a simple behavior at large and small distances in a color singlet state:

$$V(r) \sim r \qquad (r \text{ large}) \;,$$
$$\sim -\frac{1}{r\,\ell n\, r} \qquad (r \text{ small}) \;. \tag{11}$$

This potential is relevant for mesons and for heavy quark bound states such as the psi, psi-prime, epsilon, and hopefully more. In the nucleon, a bound state of three quarks, two of the quarks form a $\bar{3}$ state ($3 \times 3 = \bar{3} + 6$) which then combines with the third quark to form an overall singlet.

Let us examine some familiar hadronic bound states in the QCD picture[9] (pion, proton, neutron, deuteron, triton) and their basic contents:

$$|\pi\rangle = (q\bar{q})_1 + (q\bar{q} + \text{gluon})_1 + \ldots$$

$$|p\rangle = (uud)_1 + (uud + \text{gluon})_1 + \ldots$$

$$|n\rangle = (udd)_1 + (udd + \text{gluon})_1 + \ldots$$

$$|d\rangle = (uud)_1(udd)_1 + (uud + \text{gluon})_1(udd)_1 + \ldots$$

$$|t\rangle = (uud)_1(udd)_1(udd)_1 + \ldots$$

where the subscript 1 indicates a color singlet state.

The behavior of the structure function for these particles follows from our previous discussion with T = 1 except for an additional spin effect:

$$G_{q/\pi} \sim (1 - x)^{1+1}$$

$$G_{q/p} \sim (1 - x)^{3}$$

$$G_{q/d} \sim (1 - x)^{9+1}$$

$$G_{q/t} \sim (1 - x)^{15} \quad ,$$

where the extra power of $(1 - x)$ arises in those cases in which the initial bound state is bosonic (has an even number of quarks in its basic wave function).

Now as Q^2 (or Q_T^2) increases, where Q is the momentum transfer to the struck quark, the increase in final state phase space allows more and more gluons to be emitted while at the same time the gluon-quark coupling constant is decreasingly logarithmically with Q^2. The momentum taken up by the emitted gluons means that less is available to the quarks so that as Q^2 increases the quark distribution function increases at low x and decreases at high x. The radiative effects of the gluons introduce $\ell n\, Q^2$ and $\ell n\, \ell n\, Q^2$ nonscaling effects in the distribution function itself.

In addition to these log Q^2 effects, there are also a myriad of "higher twist" correction terms which behave as $1/Q^2$ and $1/Q^4$, etc., in addition to the $\ell n\, Q^2$ terns, These arise from mass corrections, M^2/Q^2, finite size corrections $1/R^2Q^2 = \langle k_T^2 \rangle / Q^2$, and coherence effects in the initial and final states. These higher twist terms are not due to some negligible, unphysical, esoteric effects. I remind you that all exclusive scattering and all elastic scattering-scattering processes are pure higher twist.

I would like to finish with mention of a few topics that might prove to be of some interest:

(1) There exists evidence[10] that there is a nonnegligible charm component in the nucleon carrying a reasonable amount of the momentum fraction x. It might be expected that the power law fermi motion in light nuclei, if they were used in a beam, could be a rather copious source of fast forward charm particles.

(2) There has been a recent letter[11] pointing out that photodisintegration of the deuteron in the "classical" energy range below 100 MeV is still not well understood, either experimentally or theoretically. In this note, an ad hoc modification of the deuteron wave function for $r < 1.5$ fermi is used to get agreement. I have not examined this problem in great detail but it is clear that a consistent and proper relativistic treatment has not given (one that explains also electron elastic and inelastic scattering from the deuteron at large Q^2) and the data does not seem all that great either!

(3) The relativistic formulation of the bound state problem allows a proper and invariant treatment of kinematic effects without losing the physical input from the nonrelativistic limit. These kinematic and threshold effects have been well discussed[12] and I shall omit any further consideration here.

(4) Shadowing and rescattering are a subject that still require considerable study in the relativistic case. As far as I know, a general, useful, and convenient formalism to discuss these effects has not yet been given. A relativistic version of the distorted wave born approximation (DWBA) should be very useful. It should take on a quite simple form if one uses a mixed representation for the wave function, i.e., use $\psi^{\pm}(b_T, x)$ the two-dimensional transform of $\psi^{\pm}(k_T, x)$.

(5) The A-dependence and particle production are subjects that have received considerable attention[13] but they are too complicated to adequately review here. I would just remark that the QCD-inspired quark model with color separation and confinement play an important qualitative role in these approaches.

(6) If we want to study the nuclear wave function at extremely small distances, this can be done by studying the effects of the weak interactions and in particular parity violation. If rho and omega exchange play an important role in the nucleon-nucleon force, then since the $W^{\pm}$ and Z^{o} mix with these ordinary vector mesons, there should be a small admixture of opposite parity states in the nucleus. The Compton wave length of the W - Z is $\sim 3 \times 10^{-3}$ fermi so that if this can be studied in detail (such as in polarization experiments with photons) one is examining rather short distances indeed!

(7) The proper treatment of the deuteron will require a treatment of the 6-quark problem. A start has been made in a discussion of this problem in the bag model.[14] The relevant diagrams for the 3-quark (nucleon) and 6-quark states are illustrated in Fig. 2. However, note that the 6-quark state is unstable against the decay into two separated 3-quark bound systems as illustrated in Fig. 3. This separated configuration will dominate the behavior of the wave function at large distances and hence will control the large r properties of the deuteron. We know that in the deuteron the nucleons are outside the range of the force for most of the time. At smaller distances they can interact by ordinary meson exchange, which in this model is the interchange of two quarks as shown in Fig. 4. At much smaller distances, the two bound states "fuse" into the 6-quark configuration and can no longer be cleanly separated into two objects called "nucleons". Thus we see that a full discussion of the deuteron will require (at the very least) a relativistic treatment of configuration mixing.

(8) Penultimately, let me point out an interesting possibility of new types of excited states for the deuteron (or any other nuclei). If the two nucleon configurations (they are color singlets) interact by the exchange of a gluon (which form a color octet) then one gets a new configuration in the deuteron[9] which is composed of two colored octet "nucleons":

$$|d\rangle = a_1 (uud)_1 (udd)_1 + a_8 (uud)_8 (udd)_8 + \ldots \quad .$$

Now these two colored objects will be confined; they will interact via a linearly rising potential (it probably should rise about twice as fast as the $q\bar{q}$ potential). Therefore they should exist only at intermediate distances, within the confining potential. Excited states of the "deuteron" can be formed by these colored baryon objects rattling around in the potential. The excitations should have a larger energy separation than those that are typical of a mesonic $q\bar{q}$ system. It would be very exciting if these new types of excited states that arise from the hidden color degrees of freedom are actually confirmed experimentally.

Finally, I would like to close by quoting Cato's advise to all reviewers, "I think the first wisdom is to hold the tongue".

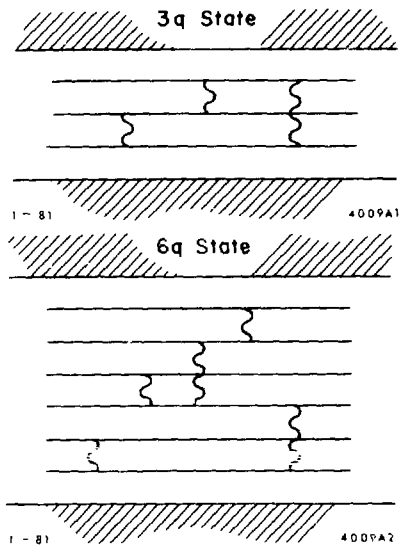

Fig. 2

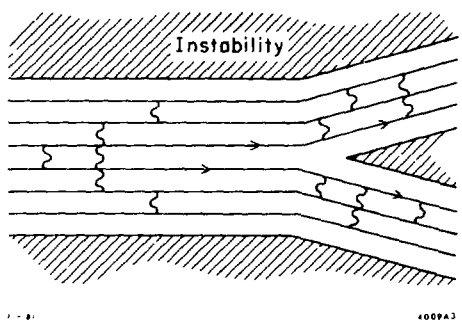

Fig. 3

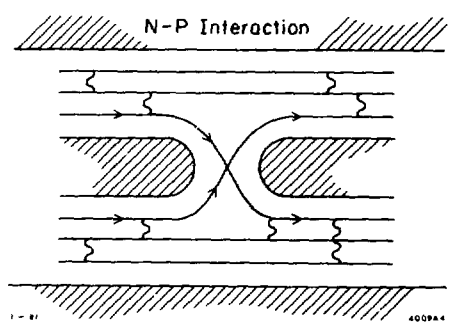

Fig. 4

ACKNOWLEDGMENTS

I wish to thank my colleagues S. Brodsky, J. Gunion, P. Noyes, I. Schmidt and C. Y. Wong for discussions.

REFERENCES (A very abbreviated list)

1. I. A. Schmidt, SLAC report 203 (1977).

2. See appendix in D. Sivers, R. Blankenbecler and S. J. Brodsky, Phys. Rep. 23c (1976).

3. S. Frankel, Phys. Rev. Lett. 38, 1338 (1977);
G. Berlad, A. Dar and G. Eilam, Phys. Rev. D13, 161 (1976);
A. Dar and J. Tran Thanh Van, Phys. Lett. 65B, 455 (1976);
R. D. Amado and R. M. Woloshyn, Phys. Rev. C15, 2200 (1977).

4. M. Chemtob, Nucl. Phys. A314, 387 (1979) and A336, 299 (1979).

5. I. A. Schmidt and R. Blankenbecler, Phys. Rev. D15, 3321 (1977).

6. C. Y. Wong and R. Blankenbecler, SLAC-PUB-2488 (March 1980);
L. S. Schroeder, LBL-10899 (June 1980) and LBL-11103 (July 1980).

7. S. J. Brodsky and R. Blankenbecler, Phys, Rev. D10, 2973 (1974).

8. R. M. Landau and M. Guylassy, Phys. Rev. C19, 149 (1979).

9. See, for example, S. J. Brodsky and G. P. Lepage, SLAC-PUB-2595 (August 1980).

10. S. J. Brodsky, C. Peterson and N. Sakai, SLAC-PUB-2660 (January 1981).

11. E. Hadjimichael and D. P. Saylor, Phys. Rev. Lett. 45, 1776 (1980).

12. I. A. Schmidt and R. Blankenbecler, Phys. Rev. D16, 1318 (1977);
P. V. Landshoff and J. C. Polkinghome, Phys. Rev. D18, 153 (1978);
L. L. Frankfurt and M. I. Strilsman, Nucl. Phys. B148, 107 (1979).
D. Kuzno and M. J. Morovosik, (Oregon U.), IC/80/52(May 1980).

13. For a general discussion and earlier references see A. Capella, U. Sukhatme, Chung-I Tau and J. Tran Thanh Van, Phys. Lett. 81B, 68 (1979);
A. Capella and J. Tran Thanh Van, Phys. Lett. 93B, 146 (1980);
G. Berlad, A. Dar and G. Eilam, Phys. Rev. D22, 1547 (1980).

14. C. Detar, Phys. Rev. D17, 323 (1978) and D19, 1029 (1979);
R. L. Jaffe, Phys. Rev. Lett. 38, 195 and 617 (1977);
C. W. Wong, K. F. Lie and Y. Tzeng, Phys. Rev. C22, 2523 (1980).

INTERNAL SPIN STRUCTURE OF THE PROTON FROM HIGH ENERGY POLARIZED e-p SCATTERING†

by

Vernon W. Hughes*
Yale University, New Haven, Connecticut 06520

ABSTRACT

A review is given of our experimental knowledge of the spin dependent structure functions of the proton, which is based on inclusive high energy scattering of longitudinally polarized electrons by longitudinally polarized protons in both the deep inelastic and resonance regions, and includes preliminary results from our most recent SLAC experiment. Implications for scaling, sum rules, models of proton structure, and the hyperfine structure interval in hydrogen are given. Possible future directions of research are indicated.

INTRODUCTION

The internal spin structure of the proton (and neutron), or the spin dependent structure functions, is a central aspect of nucleon structure. Knowledge of this spin structure is important to the development and testing of theories and models of nucleon structure, as well as to the understanding of spin dependent phenomena involving hadrons, such as polarized hadron-hadron scattering at high energies.

Spin dependent structure functions of the proton can be studied by high energy e-p scattering of polarized electrons by polarized protons,[1] which is especially interesting in the deep inelastic regime where the impulse approximation of e^- scattering from the constituent partons or quarks is valid. However, resonance region scattering at lower energy and momentum transfer is also informative about proton spin structure. Figure 1 indicates the kinematics of polarized e-p inclusive scattering in which the momentum and scattering angle of the scattered electron are measured. The e-p asymmetry, A, which is the normalized difference between the differential scattering cross sections with electron and proton spins antiparallel and parallel, is the quantity measured. Tables 1 and 2 give definitions and relations for the quantities relevant to asymmetry. Thus far only inclusive scattering with longitudinal electron and proton spins has been measured.

YALE-SLAC EXPERIMENT

The Yale-SLAC experiments to measure A were initiated in 1971 with the approval of the SLAC E80 experiment. All the results from this experiment have been published.[2-5] Data-taking for a second experiment

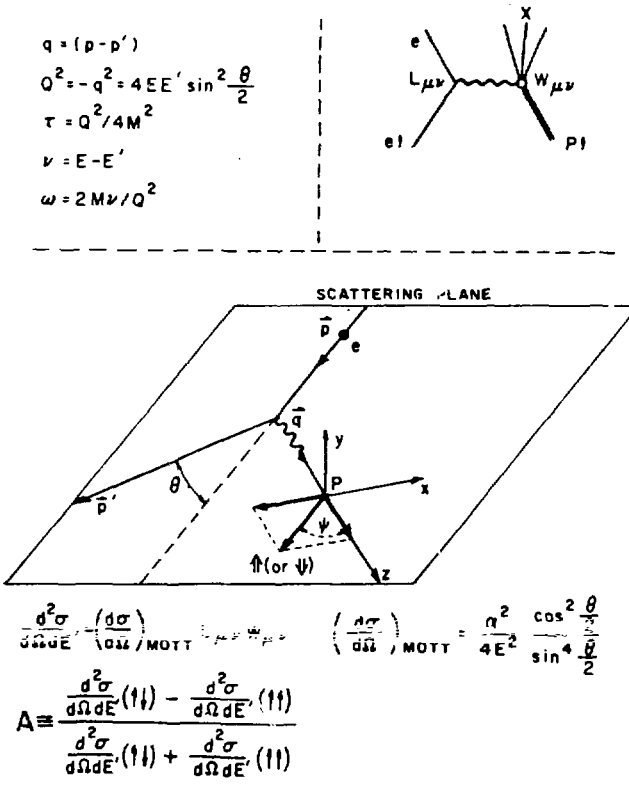

Fig. 1: Kinematics for the scattering of longitudinally polarized electrons by longitudinally polarized protons.

N_2 gas Cerenkov counter, a 4000 wire PWC system, a hodoscope, and a segmented lead glass shower counter. The spectrometer may cover momenta up to 18 GeV/c, and its acceptance $\int d\Omega\, dp/p$ is 0.3 msr with the total momentum acceptance $\Delta p/p$ being about 50%. The momentum resolution of the spectrometer $\delta p/p$ is better than ±1%. For the measurement of the electron polarization P_e by Møller scattering,[9] a new feature was the detection of the two scattered electrons in coincidence. Counting rates and various sources of systematic errors in SLAC E130 are indicated in Table 3.

The kinematic points for which data have been obtained in SLAC E80 and in SLAC E130 are shown in Fig. 4, where proposed data points for a new experiment are also indicated.

Table 1. Cross section and asymmetry for scattering of longitudinally polarized electrons by longitudinally polarized protons.

SLAC E130 was completed in April, 1980, and preliminary results have been reported.[6]

The experimental technique for SLAC E80 has been described in our above publications. The polarized electron source[7] is based on photoionization of spin polarized Li atoms, and the polarized proton target[8] is based on dynamic nuclear polarization using the hydrocarbon butanol. The SLAC 8 GeV/c spectrometer was used as the detector in SLAC E80. The principal new feature of SLAC E130 was the use of a new large acceptance spectrometer. The experimental setup for SLAC E130 is shown in Fig. 2. The new spectrometer is shown in Fig. 3. It utilizes two large dipole magnets (B201 and B81) and a detector system which consists of a 1 m diameter x 4 m long

$$\frac{d^2\sigma}{d\Omega dE'} = \left(\frac{\alpha^2\cos^2\frac{\theta}{2}}{4E^2\sin^4\frac{\theta}{2}}\right)\left[W_2 + 2\tan^2\frac{\theta}{2}\, W_1 \pm 2\tan^2\frac{\theta}{2}\,(E + E'\cos\theta)M G_1 \pm 8EE'\tan^2\frac{\theta}{2}\sin^2\frac{\theta}{2}\, G_2\right]$$

$+(A)$
$-(P)$

$$\frac{d^2\sigma}{d\Omega dE'} = \left(\frac{d\sigma}{d\Omega}\right)_M \left(\frac{1}{\varepsilon(1+\tau/Q^2)}\right) W_1 \left\{1 + \varepsilon R \pm (1-\varepsilon^2)^{1/2}\cos\psi\, A_1 \pm \left[2\varepsilon(1-\varepsilon)\right]^{1/2}\sin\psi\, A_2\right\}$$

$$\varepsilon = \left[1 + 2(1+\nu^2/Q^2)\tan^2\frac{\theta}{2}\right]^{-1}$$

$$R = \sigma_L/\sigma_T;\ \sigma_T = (\sigma_{1/2} + \sigma_{3/2})/2$$

$$A = \frac{d\sigma(\uparrow\downarrow) - d\sigma(\uparrow\uparrow)}{d\sigma(\uparrow\downarrow) + d\sigma(\uparrow\uparrow)}$$

$$A = D(A_1 + \eta A_2)$$

$$D = \frac{E - E'\varepsilon}{E(1+\varepsilon R)} = \frac{(1-\varepsilon^2)^{1/2}\cos\psi}{(1+\varepsilon R)}$$

$$\eta = \frac{\varepsilon(Q^2)^{1/2}}{E - E'\varepsilon} = \left(\frac{2\varepsilon}{1+\varepsilon}\right)^{1/2}\tan\psi \approx \tan\psi$$

$$A_1 = \frac{\sigma_{1/2} - \sigma_{3/2}}{\sigma_{1/2} + \sigma_{3/2}}$$

$$A_2 = \frac{2\sigma_{TL}}{\sigma_{1/2} + \sigma_{3/2}}$$

$|A_1| \le 1;\ |A_2| \le R$ (positivity limits)

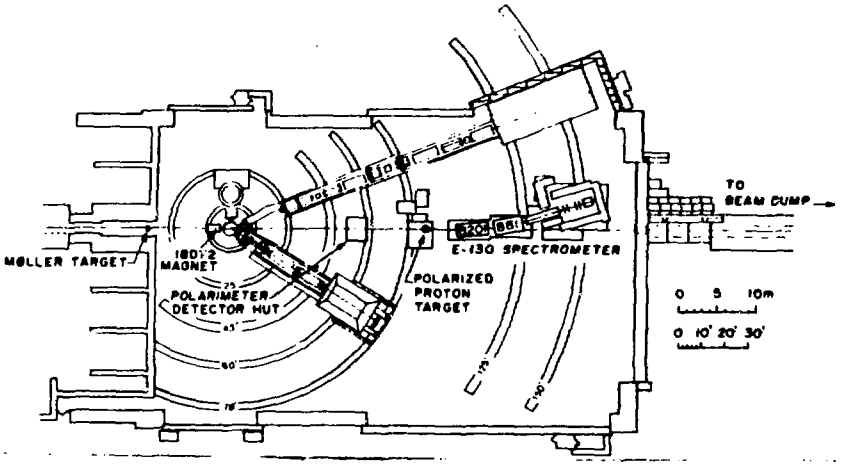

Fig. 2: SLAC E130 experimental set-up in end station A.

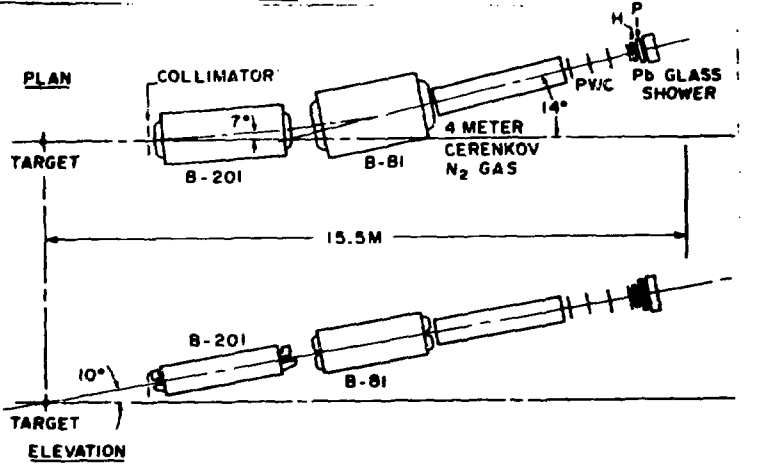

Fig. 3: SLAC E130 spectrometer.

$$W^{\mu\nu}_{[A]} = M\epsilon^{\mu\nu\rho\sigma} q_\rho s_\sigma G_1 + \frac{1}{M}\epsilon^{\mu\nu\rho\sigma} q_\rho \left[(p\cdot q)s_\sigma - (s\cdot q)p_\sigma\right] G_2$$

$$\sigma_{1/2} = \frac{4\pi^2\alpha}{K}(W_1 + M\nu G_1 - Q^2 G_2) \qquad \sigma_L = \frac{4\pi^2\alpha}{K}\left[W_2\left(1+\frac{\nu^2}{Q^2}\right) - W_1\right]$$

$$\sigma_{3/2} = \frac{4\pi^2\alpha}{K}(W_1 - M\nu G_1 + Q^2 G_2) \qquad \sigma_{TL} = \frac{4\pi^2\alpha}{K}\sqrt{Q^2}(MG_1 + \nu G_2)$$

$$\sigma_T = (\sigma_{1/2} + \sigma_{3/2})/2 = \frac{4\pi^2\alpha}{K} W_1 \qquad K = \nu - \frac{Q^2}{2M}$$

IN THE SCALING LIMIT $[\nu, Q^2 \to \infty;\ x \text{ FIXED}]$

$$MW_1(\nu, Q^2) \to F_1(x); \quad \nu W_2(\nu, Q^2) \to F_2(x)$$

$$M^2 \nu G_1(\nu, Q^2) \to g_1(x); \quad M\nu^2 G_2(\nu, Q^2) \to g_2(x)$$

$$A_1 = \frac{\sigma_{1/2} - \sigma_{3/2}}{\sigma_{1/2} + \sigma_{3/2}} = \frac{2x}{F_2}(g_1 - \frac{2Mx}{\nu} g_2)(1+R) \to \frac{2x}{F_2} g_1$$

$$A_2 = \frac{\sigma_{TL}}{\sigma_T} = \frac{\sqrt{Q^2}}{\nu} \frac{2x}{F_2}(g_1 + g_2)(1+R) \to 0$$

$$A_2' = \frac{\nu}{\sqrt{Q^2}} A_2 \simeq \frac{2x}{F_2}(g_1 + g_2)(1+R) \to \frac{2x}{F_2}(g_1 + g_2)$$

FOR THE $\simeq$ EXPRESSIONS FOR A_1, A_2 AND A_2' ALL QUANTITIES EXCEPT R ARE TAKEN IN THE SCALING LIMIT. $(\nu/2Mx \gg 1)$.

Table 2. Some definitions and relations of structure functions and asymmetries.

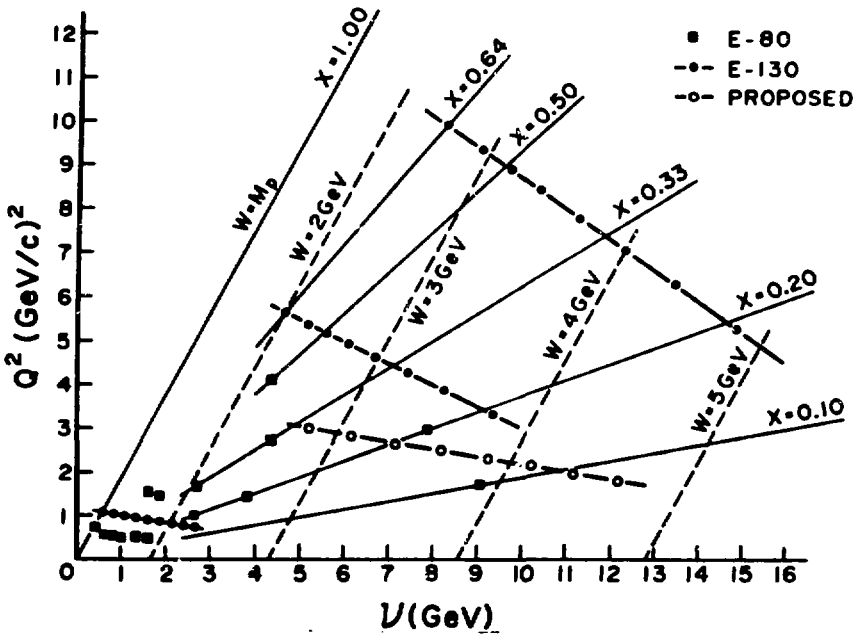

Fig. 4: Kinematic points where data have been taken.

DEEP INELASTIC DATA AND THEIR IMPLICATIONS

All the available deep inelastic asymmetry data are shown in Fig. 5, where the open diamonds are the published SLAC E80 results and the closed squares are the preliminary results for SLAC E130. The E130 results are "on-line" results, which must be checked and refined by off-line analysis. Furthermore radiative corrections are not yet included. All errors are one standard deviation total errors, which include the statistical counting error and systematic errors associated with Pe, P_p and F, added in quadrature. The new E130 data extend considerably our knowledge of the virtual photon-proton asymmetry A/D to higher Q^2 and higher x. A significant verification of the predicted scaling behaviour[10] of A_1

$$A_1(\nu,Q^2)\to A_1(x) \text{ as } \nu,Q^2\to\infty; \quad (1)$$
$$x \text{ fixed}$$

at about the 10% level over the Q^2 range from 1 to 10 $(GeV/c)^2$ is apparent from Fig. 5, where the dashed horizontal lines correspond to the average A_1 values for the three plots.

For Fig. 6 for a given x value data for different Q^2

$$\Delta = \frac{N(\uparrow\downarrow)-N(\uparrow\uparrow)}{N(\uparrow\downarrow)+N(\uparrow\uparrow)}, \quad \text{RAW ASYMMETRY}$$

$$\Delta = P_e P_p F A$$

$$A = \frac{d\sigma(\uparrow\downarrow)-d\sigma(\uparrow\uparrow)}{d\sigma(\uparrow\downarrow)+d\sigma(\uparrow\uparrow)}, \quad \text{INTRINSIC } e\text{-}p \text{ ASYMMETRY}$$

$P_e = 0.8$, $P_p = 0.6$, $F = 0.1$

$\Delta = 0.05\ A$

COUNTING RATE VARIES FROM 0.01 TO 1/PULSE OR 1 TO 100/s.

SOURCE OF ERROR	COMMENT
COUNTING STATISTICS (Δ)	DOMINANT ERROR 1×10^{-3} TO 3×10^{-3} IN Δ 10% TO 30% OF Δ
P_e	$\delta P_e/P_e \sim 5\%$; MÖLLER SCATTERING
P_p	$\delta P_p/P_p \sim 5\%$; NMR
F	$\delta F/F \sim 5\%$; C, CH_2 CROSS SECTIONS
RADIATIVE CORRECTIONS	WHEN COMBINED WITH COUNTING ERROR, OVERALL ERROR IS 1.1 TO 1.5 TIMES COUNTING ERROR
BACKGROUND ASYMMETRY	≤ 1% OF Δ MISIDENTIFIED PIONS FROM PHOTOPION PRODUCTION OFF POLARIZED PROTONS
PEGGY BEAM ASYMMETRIES ENERGY	$<10^{-4}$ IN $\Delta E/E$; MEASURABLE TO $\leq 3\times10^{-5}$
ANGLE	$\leq 10^{-4}$ IN Δ
POSITION	$<10^{-4}$ IN Δ
	$<10^{-4}$ IN Δ

Table 3. Counting rates and sources of error.

have been combined assuming that the A/D values are independent of Q^2. These data are fit by the curve $A_1(x)=(0.90\pm0.05)x^{1/2}$.

The Bjorken sum rule is given in Eq. (2)

$$\int_0^1 [A_1^p F_2^p/(1+R^p) - A_1^n F_2^n/(1+R^n)] \frac{dx}{x} = \frac{1}{3}\left|\frac{g_A}{g_V}\right| = (0.417 \pm 0.003) \qquad (2)$$

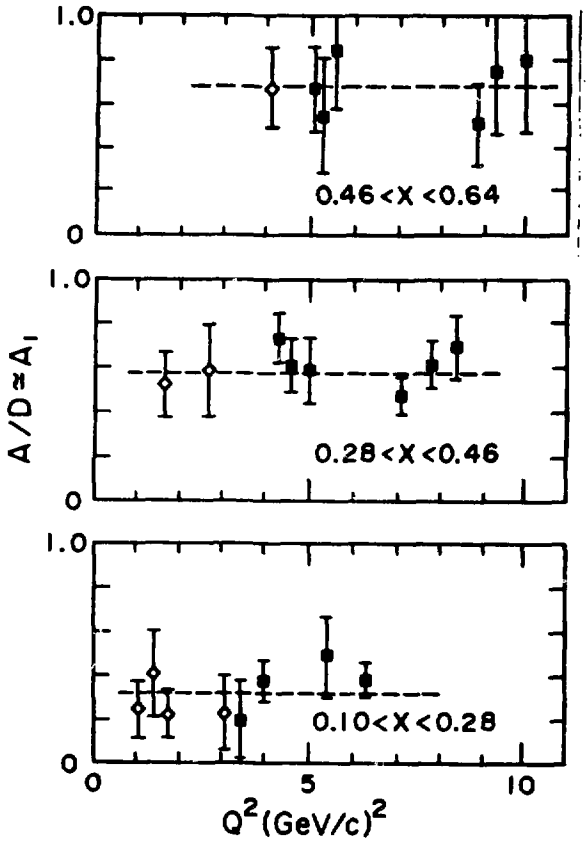

Fig. 5: Measured values of the asymmetry A/D in SLAC E80 (open diamonds) and SLAC E130 (closed squares).

in which quantities are defined in Fig. 1 and Tables 1 and 2; in addition, the superscripts p and n refer to proton and neutron, and g_V and g_A are the vector and axial vector coupling constants for neutron beta decay. The Bjorken sum rule was originally derived[11,12] from commutation relations based on the algebra of currents for the quark model. It can also be derived[13] from quantum chromodynamics (QCD) and is often written

$$\int_0^1 [g_1^p(x) - g_1^n(x)]\, dx = \frac{1}{6}\left|\frac{g_A}{g_V}\right| \qquad (3)$$

In the above forms the sum rule is only valid in the scaling limit.

A comparison of our data with the Bjorken sum rule is indicated in Fig. 7. Values of the quantity $A_1F_2/(1+R)$ are plotted vs x. The solid curve is a plot

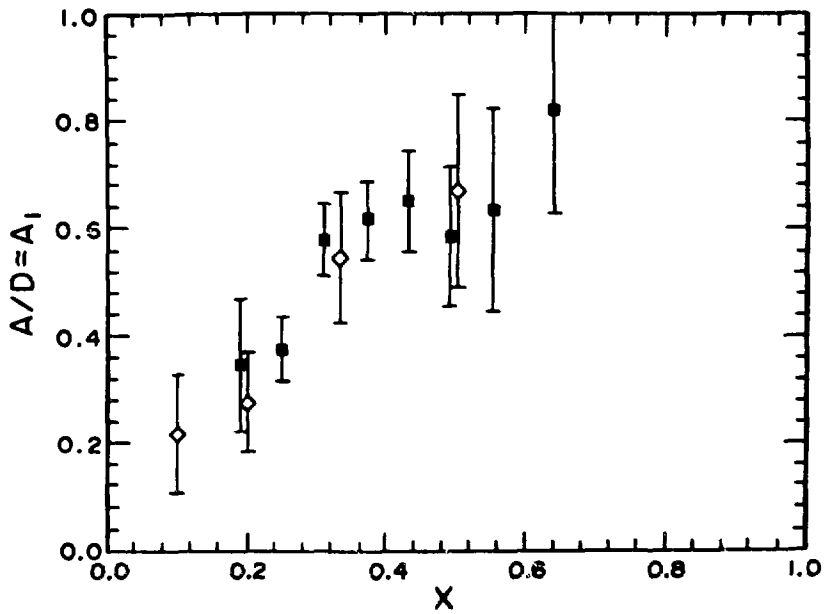

Fig. 6: Measured values of A/D vs x. Points were obtained from Fig. 5 data assuming A/D values are independent of Q^2.

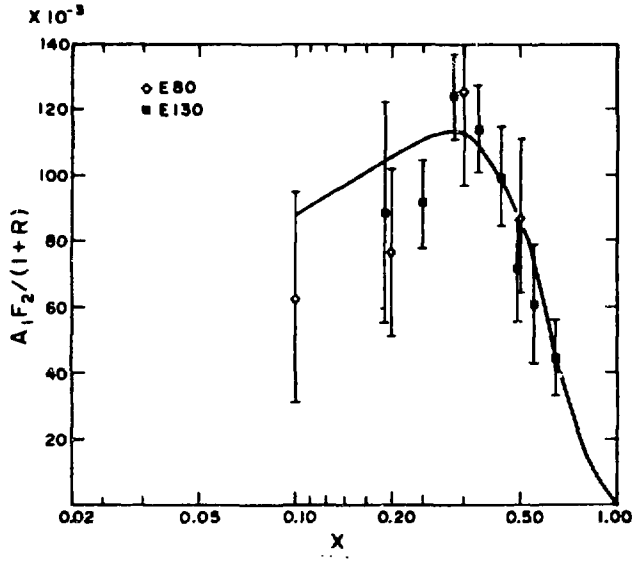

Fig. 7: Experimental values of $A_1F_2^p/(1+R^p)$ vs x, relevant to a test of the Bjorken sum rule.

of the quantity $A_1F_2/(1+R)$ for the proton using the fit to our data of $A_1=0.90x^{1/2}$, $R=0.25$[14] and experimental values[15] of F_2 with $Q^2=4(GeV/c)^2$, which is approximately the mean Q^2 for our data points. The integral under the solid curve in the range of our data from x=0.10 to 0.64 is about 0.23 or about 0.6 of the value predicted by the Bjorken sum rule. Clearly data at lower x are needed, and in addition an extrapolation to low x based on Regge theory can be made.[4] Since there is no experimental information about A_1 for the neutron, the neutron contribution to the integral must be ignored. Our data on A_1^p are clearly consistent with the Bjorken sum rule.

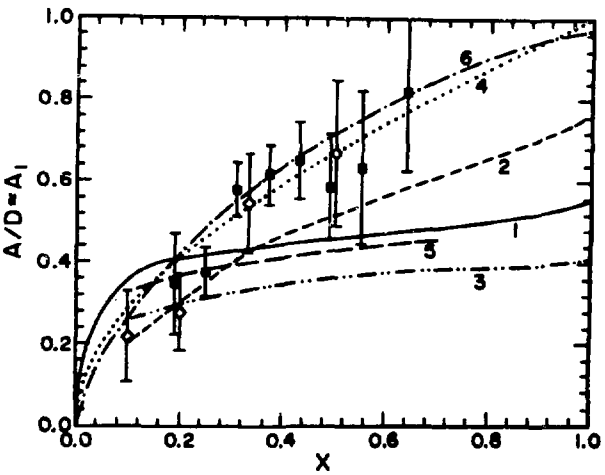

Quantum chromodynamic corrections to the Bjorken sum rule have been calculated. The leading correction in the strong coupling constant $\alpha_s(Q^2)$ is given by:[13,16]

$$\int_0^1 dx(g_1^p-g_1^n) = \frac{1}{6}\left|\frac{g_A}{g_V}\right|\left(1-\frac{\alpha_s}{\pi}\right) \quad (4)$$

in which $\alpha_s = \frac{12\pi}{33-2f}[\ln(Q^2/\Lambda^2)]^{-1}$ where f is the number of quark flavors and Λ is a free parameter. Higher order QCD corrections, including target mass effects,

Fig. 8: Experimental values of A/D ≈ A_1 compared to theoretical predictions for A_1^p. The models are as follows: (1) a relativistic symmetric valence-quark model of the proton [23]; (2) a model incorporating the Melosh transformation which distinguishes between constituent and current quarks [26]; (3) a model introducing nonvanishing quark orbital angular momentum[27,28];(4) an unsymmetrical model[29,30] in which the entire spin of the proton is carried by a single quark in the limit of x=1 ; (5) the MIT bag model of quark confinement[25,31];(6) source theory [32].

have also been evaluated.[17,18,19,20] Significant tests of these QCD corrections require additional experimental data as indicated above.

Another derivative form of the Bjorken sum rule due to Ellis and Jaffe[21] expresses separately a sum rule for the proton and for the neutron in the scaling limit:

$$\int_0^1 dx\ g_1^p = \left|\frac{g_A}{g_V}\right| \frac{(1.78)}{12} \qquad (5)$$

$$\int_0^1 dx\ g_1^n = \left|\frac{g_A}{g_V}\right| \frac{(-0.22)}{12} \qquad (6)$$

As compared to the Bjorken sum rule of Eq. (3), these sum rules involve the additional approximation that strange quarks do not contribute to the polarization asymmetry. According to Eqs. (5) and (6), the neutron contributes about 10% to the Bjorken sum rule.

Comparison of our data on A_1^p with theoretical values provides a major test for our understanding of nucleon structure. The generally accepted theory of quantum chromodynamics involving quarks and gluons has not yet been successfully applied from its own first principles to calculate either spin independent or spin dependent structure functions. However, perturbative QCD does make some important predictions about nucleon structure functions including A_1 for x near 1, which is the high momentum tail of the wavefunction. The models of nucleon structure[22] picture the proton as consisting of three valence quarks, two u quarks and a d quark, together with gluons and a sea of quark-antiquark pairs, and the neutron as two d quarks and a u quark together with gluons and the sea. The early models[23] assumed SU(6) symmetry for the wavefunction. However, experimental data on F_2^n/F_2^p and on A_1^p at large x required that SU(6) symmetry breaking be introduced. The important and unsymmetrical aspect of the wavefunction for the proton (neutron) near x=1, which is predicted by perturbative QCD,[24] is the occurrence with high probability of a single u(d) quark with large x and a diquark with isotopic spin I=0 and spin component S_z=0. Of the various models for the proton wavefunction which are intended to represent the nonperturbative QCD solution perhaps the most basic is the MIT bag model[22,25] which incorporates confinement.

A comparison of our data on $A_1^p(x)$ with various model predictions is shown in Fig. 8. We should remark that some earlier nonquark models of the proton predicted negative values for A_1, but all quark models predict the A_1 is positive.[3,23] Hence our earliest data indicating that A_1 is positive provided a crucial test of the quark model.[3] In the quark model A_1 can be written

$$A_1(x) = \frac{\sum_i e_i^2 \left[q_i^{\uparrow} - q_i^{\downarrow}\right]}{\sum_i e_i^2 \left[q_i^{\uparrow} + q_i^{\downarrow}\right]} \qquad (7)$$

in which the sum is over the quarks i, e_i is the quark i charge, and $q_i^{\uparrow}(q_i^{\downarrow})$ is the probability for quark i to have its spin parallel (antiparallel) to the target nucleon spin. A_1 clearly provides a measure of the probability that the quark spins are aligned with the nucleon spin. Only models 4 and 6 agree well with the experimental data. Curve 4 provides an unsymmetrical model of the quark distributions involving SU(6) breaking, Regge theory at small x, the Melosh transformation, and agreement with the Bjorken sum rule. Curve 6 is based on Schwinger's source theory, which is not a quark model.

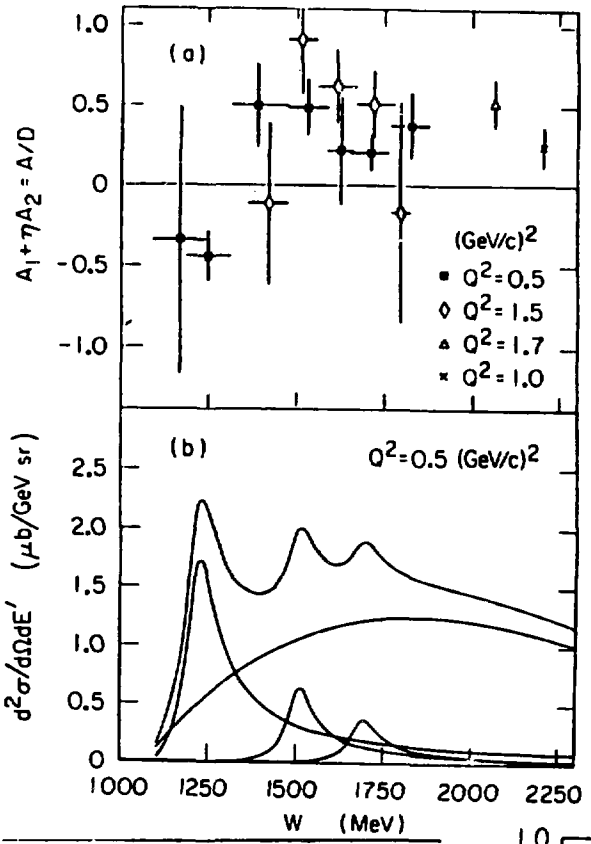

Fig. 9: (a) Asymmetry vs missing mass W. (b) Differential cross section vs W. Also shown is a decomposition into individual resonances and the background.

RESONANCE REGION DATA AND THEIR IMPLICATIONS

The first exploratory experiment at SLAC on polarized e-p scattering in the resonance region, which was a part of E80, has recently been reported.[5] Fig. 9a displays the measured asymmetry values, and Fig. 9b shows the contributions to the differential cross section from resonances and background. Our measured asymmetries A/D are predominantly large and positive throughout the entire range in missing mass W except in the region of the Δ(1232 MeV) resonance, where A/D is expected to be negative because of magnetic dipole excitation. In principle our measured asymmetry values can be predicted from a multipole analysis of complete but unpolarized electroproduction data. Fig. 10 displays the predictions based on a multipole analysis of single pion electroproduction data only, which accounts for about 1/2 of the differential cross section. The agreement between these predictions and our data is rather good, and hence indicates that the net asymmetry contributed by

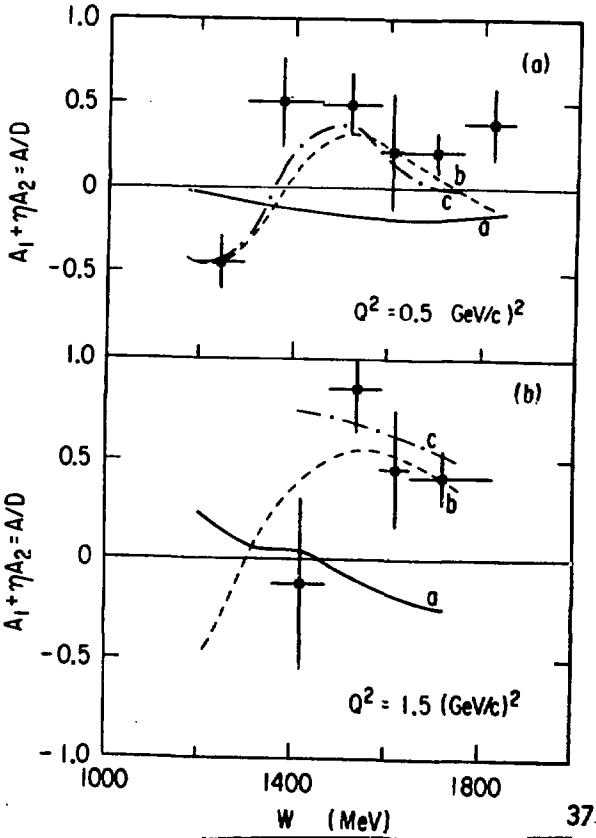

Fig. 10: (a) Asymmetry data at Q^2=0.5 (GeV/c)^2 compared with a multipole analysis performed by Devenish and Gerhardt: curve a, Born terms alone; curve b, Born terms plus Δ(1232); and curve C, Born terms plus all resonances. (b) Same for Q^2=1.5 (GeV/c)^2.

other channels than single pion production cannot be very different from our measured asymmetries. Fig. 11 indicates that scaling applies for our resonance region data except at the $\Delta(1232)$ point, and hence that the spin dependent behaviour is also consistent with a global duality mechanism in analogy to the unpolarized case.

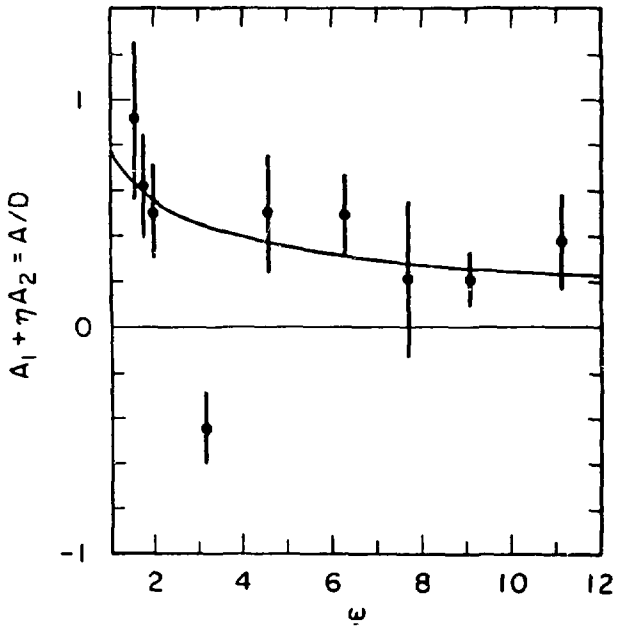

Fig. 11: Asymmetry vs scaling variable ω. The curve $0.78\omega^{-1/2}$ is a fit to deep-inelastic data (W>2 GeV) of SLAC E80. The data points are the resonance-region results (W<2 GeV) of SLAC E80.

THE FUTURE

We turn now to more futuristic aspects. An experiment[33] entitled Son of E130 has been proposed at SLAC to measure A_1(neutron) and A_2 (proton), about which we have no experimental information. Determination of A_1^n can be done by measuring asymmetries for both the deuteron and the proton. Determination of A_2^p can be done by measuring asymmetries in scattering longitudinally polarized electrons by transversely polarized protons, and observing scattered electrons in the plane determined by the directions of the incident electron and the proton polarizations. In

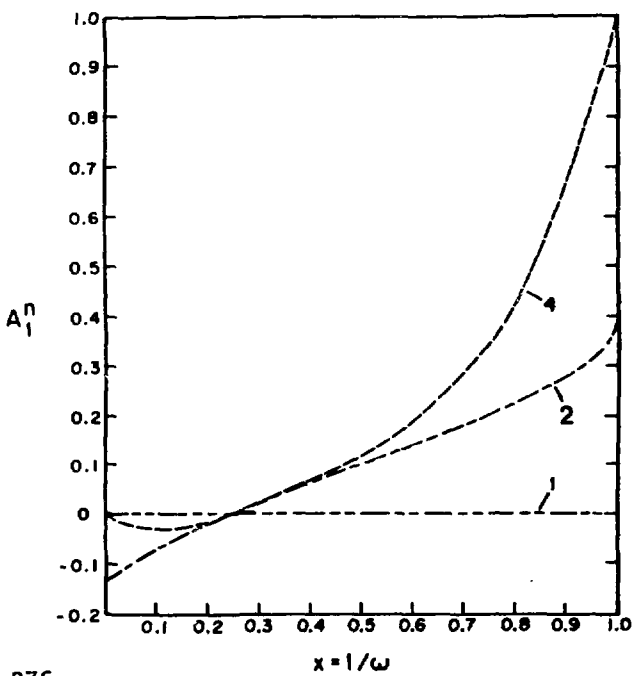

Fig. 12: Theoretical predictions for A_1(neutron). The models are as follows: (1) a relativistic symmetric valence-quark model of the neutron[23]; (2) a model incorporating the Melosh transformation which distinguishes between constituent and current quarks.[26] (4) an unsymmetrical model[29,30] in which the entire spin of the neutron is carried by a single quark in the limit of x=1.

addition, this experiment would determine A_1^p to relatively high precision for values of x as low as 0.07. Both the data on A_1^n and the higher precision data on A_1^p at the lower x values would improve our test of the Bjorken sum rule.

Some theoretical predictions for A_1^n are shown in Fig. 12. On the basis of the spin-isospin part of the SU(6) wavefunction, $A_1^n=0$ for all x (curve 1). Perhaps the most interesting prediction (curve 4) is that of the unsymmetrical model of Carlitz and Kaur which agrees so well with the A_1^p data. It is seen that A_1^n is small over most of the range of x but becomes large at x near 1, where a single quark carries the entire spin of the neutron.

The structure function A_2 arises from an interference between amplitudes for absorption of virtual longitudinal and transverse photons by the proton.[3] In the scaling limit A_2 becomes zero, and there is a positivity bound[34] of $|A_2|<R^{1/2}$. Physically A_2 arises from transverse momenta of the quarks. Fig. 13 shows various theoretical predictions for A_2 for the kinematics of our proposed Son of E130 experiment. The positivity limit of $|A_2|<R^{1/2}$ is 0.5, since the best current value[14] of R in this kinematic range is R=0.25±0.10. Parenthetically, this large experimental value for R, which is expected theoretically to be zero in the scaling limit, poses a problem for QCD theory, which may be related to higher-twist terms; the comparison of theory and experiment for A_2 can be expected to pose a similar problem. In addition, Fig. 13 shows the prediction of the MIT bag model,[25,31] a prediction based on our A_1^p data together with a relation between A_1 and A_2 given by the approximate Wandzura-Wilczek sum rule,[17,35] and a prediction given from $g_2(x)=0$ which is a consequence[23] of SU(6). Data on A_2 are important for comparison with these and other[36] theories for A_2. In addition, data on A_2 are important to our experimental determination of A_1, since we measure $A/D = A_1+\eta A_2$, and we only obtain a value of A_1 provided ηA_2 is sufficiently small. With the positivity bound for A_2, the value of ηA_2 for E80-E130 data is between 0.2 and 0.8 times the experimental one standard deviation error in our determination of A/D.

Further significant tests of the scaling behaviour of A_1 will only come with the availability of additional data on A_1 at higher Q^2, which is planned at CERN by the European Muon Collaboration[37] in the Q^2 range up to about $60(GeV/c)^2$. Fig. 14 shows predictions of scaling violations of g_1 predicted[38] by QCD; they amount to about a 10% variation over the Q^2 range from 2 to $60(GeV/c)^2$ in the accessible range of x, and are of different sign for low and intermediate values of x. Since our measured quantity A_1 is equal to $2xg_1(1+R)/F_2$, the known scaling violations in F_2 must also be considered.

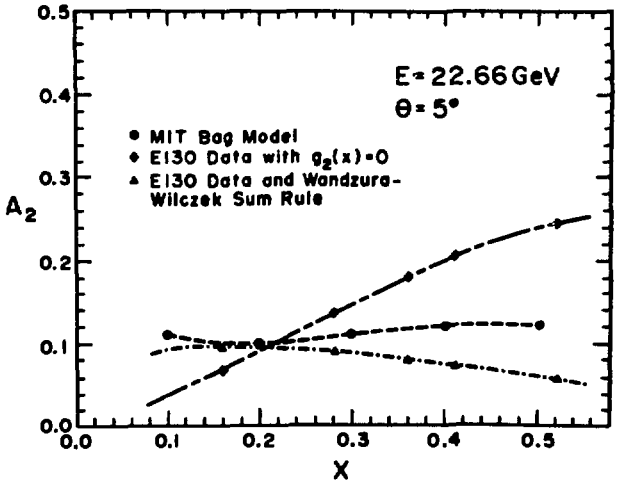

Fig. 13: Theoretical predictions for A_2(proton) for the kinematics of the Son of E130 proposal.

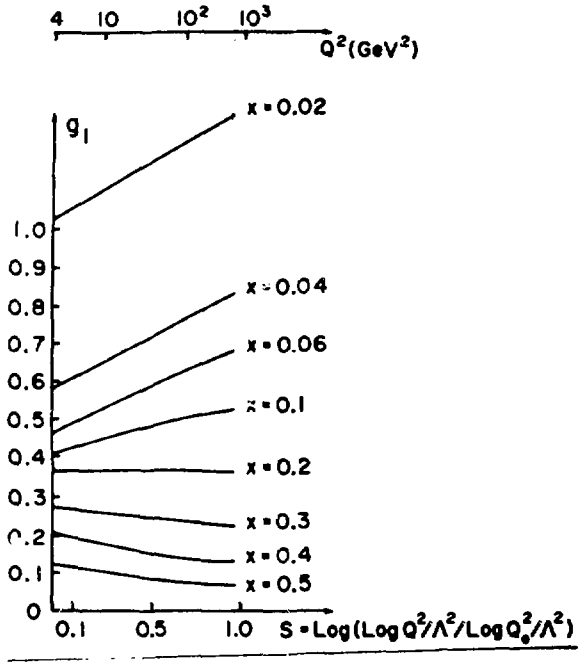

Fig. 14: Theoretical prediction[39] of scaling violation for g_1, with the parameter values Q_o=2 GeV/c and Λ=0.4 GeV/c.

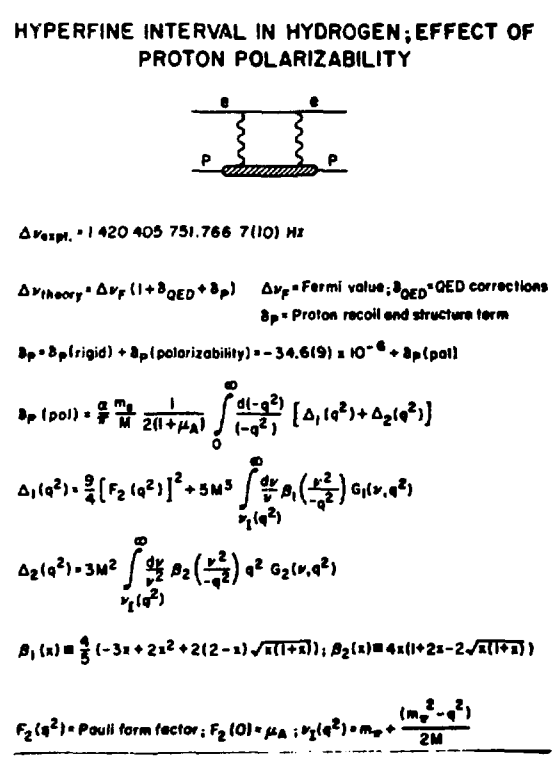

Fig. 15: Hyperfine structure interval $\Delta\nu$ in hydrogen. The Feynman diagram and the expression given for δ_p(pol) indicate the contribution of the spin dependent polarizability of the proton to $\Delta\nu$.

It is well know, in the theory of atomic hyperfine structure[39,40] that a significant contribution to the hfs interval $\Delta\nu$ in hydrogen arises from the spin dependent polarizability of the proton. Figure 15 gives the experimental and theoretical values[41] for $\Delta\nu$. The contribution of the spin dependent polarizability is designated δ_p(pol). The principal theoretical uncertainty in $\Delta\nu$ is due to δ_p(pol), for which a positivity bound $|\delta_p(pol)| \leq 3$ ppm has been calculated.[42] The quantity δ_p(pol) can be expressed[43] in terms of the spin dependent structure functions G_1 and G_2 which are measured in polarized e-p scattering. Using our experimental data for A_1^p and the Wandzura-Wilczek relation,[35] we estimate the total contribution to δ_p(pol) to be $\leq$0.5 ppm from both the deep inelastic and resonance regions above a Q^2 value of ~5(GeV/c)^2. The greatest contribution to δ_p(pol) comes from the small Q^2 region, including the proton resonances. Further experimental data and theoretical work should determine δ_p(pol) to a useful precision.

Finally we emphasize that knowledge of the internal spin structure of the nucleon, apart from its importance to our understanding of nucleon structure, is essential to the interpretation of spin dependent high energy phenomena involving hadrons. These include hadron-hadron scattering[44,45,46,47] the polarized Drell-Yan process,[48,49] and production of polarized W or Z vector bosons in collisions of polarized protons with unpolarized protons in a high energy storage ring.[50,51]

REFERENCES

1. V.W. Hughes, High Energy Physics with Polarized Beams and Polarized Targets, ed. G.H. Thomas (AIP Conference Proceedings No. 51, Argonne, 1978) p. 171.
2. M.J. Alguard, et al., Phys. Rev. Lett. 37, 1258 (1976).
3. M.J. Alguard, et al., Phys. Rev. Lett. 37, 1261 (1976).
4. M.J. Alguard, et al., Phys. Rev. Lett. 41, 70 (1978).
5. G. Baum, et al., Phys. Rev. Lett. 45, 2000 (1980).
6. G. Baum, et al., XX International Conference on High Energy Physics, University of Wisconsin, July 17-23, 1980.
7. M.J. Alguard et al., Nucl. Instrum. Methods 163, 29 (1979).
8. W.W. Ash, High Energy Physics with Polarized Beams and Targets, ed. M.L. Marshak (American Inst. of Physics, New York, 1976) p. 485.
9. P.S. Cooper, et al., Phys. Rev. Lett. 34, 1589 (1975).
10. L. Galfi et al., Phys. Lett. B 31, 465 (1970).
11. J.D. Bjorken, Phys. Rev. 148, 1467 (1966).
12. J.D. Bjorken, Phys. Rev. D 1, 1376 (1970).
13. J. Kodaira, et al., Phys. Rev. D 20, 627 (1979).
14. L.F. Abbott, et al., Phys. Rev. D 22, 582 (1980).
15. A.J. Buras and K.J.F. Gaemers, Nucl. Phys. B 132, 249 (1978).
16. J. Kodaira, et al., Nucl. Phys. B 159, 99 (1979).
17. S. Wandzura, Nucl. Phys. B 122, 412 (1977).
18. J. Kodaira, Nucl. Phys. B 165, 129 (1980).
19. S. Matsuda and T. Uematsu, Nucl. Phys. B 168, 181 (1980).
20. C.S. Lam and B.A. Li, SLAC-PUB-2505, 2506 (1980).
21. J. Ellis and R. Jaffe, Phys. Rev. D 9, 1444 (1974).
22. F.E. Close, "An Introduction to Quarks and Partons:, (Academic Press, London, 1979).
23. J. Kuti and V.W. Weisskopf, Phys. Rev. D 4, 3418 (1971).
24. G.R. Farrar and D.R. Jackson, Phys.Rev. Lett. 35, 1416 (1975).
25. R.L. Jaffe, Phys. Rev. D 11, 1953 (1975).
26. F.E. Close, Nucl. Phys. B 80, 269 (1974).
27. G.W. Look and E. Fischbach, Phys. Rev. D 16, 211 (1977).
28. L.M. Sehgal, Phys. Rev. D 10, 1663 (1974).
29. R. Carlitz and J. Kaur, Phys. Rev. Lett. 38, 673; 1102 (E) (1977).
30. J. Kaur, Nucl. Phys. B 128, 219 (1977)
31. R.J. Hughes, Phys. Rev. D 16, 662 (1977).
32. J. Schwinger, Nucl. Phys. B 123, 223 (1977).
33. V.W. Hughes, et al., SLAC Proposal Son of E130, August 1980.
34. M.G. Doncel and E. de Rafael, Nuovo Cimento 4A, 363 (1971).
35. S. Wandzura and F. Wilczek, Phys. Lett. B 72, 195 (1977).
36. A.S. Joshipura and P. Roy, Phys. Lett. B 92, 348 (1980).
37. E. Gabathuler, CERN Proposal by European Muon Collaboration, 1974.
38. O. Darrigol and F. Hayot, Nucl. Phys. B 141, 391 (1978).
39. S.J. Brodsky and S.D. Drell, Ann. Rev. Nucl. Sci. 20, 147 (1970).
40. A. De Rujula, et al., Phys. Lett. 33B, 605 (1970).
41. E.R. Cohen and B.N. Taylor, Jr. Phys. and Chem. Data 2, 663 (1973).
42. E. De Rafael, Phys. Lett. B37, 201 (1971).
43. R.L. Heimann, Nucl. Phys. B64, 429 (1973).
44. D. Sivers, High Energy Physics with Polarized Beams and Polarized Targets, ed. H.G. Thomas (AIP Conf. Proc. No. 51, 1978) p. 505.
45. J. Babcock, et al., Phys. Rev. D 19, 1483 (1979).
46. K. Hidaka, et al., Phys. Rev. D 19, 1503 (1979).
47. N. Craigie, et al., Phys. Lett. B 96, 381 (1980).

48. J. Soffer and P. Taxil, Phys. Lett. B 85, 404 (1979).
49. K. Hidaka, et al., Phys. Rev. D 21, 1316 (1980).
50. F. E. Paige, et al., BNL-24919, (1978).
51. F. Baldracchini, et al., "A Survey of Polarization Asymmetries Predicted by QCD." Int. Center for Theor. Phys., Trieste, Italy, 1980.

*Co-authored by G. Baum, M. R. Bergström, P. R. Bolton, J. E. Clendenin, N. R. DeBotton, S. K. Dhawan, R. A. Fong-Tom, Y.-N. Guo, V.-R. Harsh, K. Kondo, M. S. Lubell, C.-L. Mao, R. H. Miller, S. Miyashita, K. Morimoto, U. F. Moser, I. Nakano, R. F. Oppenheim, D. A. Palmer, L. Panda, W. Raith, N. Sasao, K. P. Schüler, M. L. Seely, J. Sodja, P. A. Souder, S. J. St Lorant, K. Takikawa, and M. Werlen. University of Bern, University of Bielefeld, KEK, Kyoto University, Peking, SACLAY, SLAC, University of Tsukuba, and Yale University.

†Submitted to Lausanne Conference, December 29, 1980.

The research was supported in part by the U.S. Department of Energy under Contract No. DE-AC02-76ER0 3075, and a John Simon Guggenheim Memorial Foundation Fellowship 1978-1979, V. W. Hughes.

The three strange quark system

by

A. T. Aerts and L. Heller

Theoretical Division

Los Alamos National Laboratory

Los Alamos, New Mexico 87545

A potential model for the heavy three quark system is explained, which results in Coulomb-like two-body and confining three-body interactions between the quarks. Asymptotic freedom effects are included. The application of this potential to the $\Omega^-(s^3)$ system is discussed and its predictions are compared to those of a purely two-body potential model.

Using the Born-Oppenheimer approximation[1] to the MIT bag model[2], we have derived approximate analytic expressions for the spin-independent part of the heavy quark-antiquark potential and the heavy three quark potential[3,4]. Both potentials are calculated from the same equations, the only difference being the number of particles entering in each case, and consequently are described in terms of the same set of parameters. In this adiabatic approximation[1] it is assumed that the glue field and bag surface adjust rapidly compared to the motion of the quarks. They are treated as fixed sources, and the Yang-Mills

equations and bag boundary conditions are solved to lowest order in the quark-gluon coupling constant g. The potential energy obtained in this manner is then put into the Schrödinger equation for the motion of the quarks, thereby obtaining - in the $q\bar{q}$ meson case - wave functions and energy eigenvalues for such mesons as $\Upsilon(b\bar{b})$, $\psi(c\bar{c})$, $\phi(s\bar{s})$, and $F^*(c\bar{s})$. In the q^3 case the only baryon presently available for experimental comparison is the $\Omega^-(s^3)$. In view of the highly similar description of the $q\bar{q}$ and q^3 systems in the MIT bag model this is not a severe restriction.

The comparatively small mass of the s quark needed to fit the ϕ meson, m_s=0.64 GeV, results in that system being somewhat relativistic, with $\langle p^2/m^2\rangle_\phi$=0.56. One begins to suspect the validity of both the Born-Oppenheimer approximation and the use of the non-relativistic Schrödinger equation for systems containing a strange quark, therefore. But consistency between the masses of the ϕ, ψ, and F^* led us to hope that the same approximation could be applied to baryons containing the s quark.

The idea behind our analytic potentials[3,4] is simple. When all quark separations are sufficiently small the bag becomes approximately spherical and an analytic solution is available

$$V_{q\bar{q}}(r) = -\frac{4\alpha_s}{3r} + \left(\frac{2}{3}\right)^{\frac{1}{2}} kr \qquad \text{(1a)}$$

(small separations)

$$V_{q^3}(\bar{x}_1,\bar{x}_2,\bar{x}_3) = -\frac{2}{3}\sum_{i<j}\frac{\alpha_s}{|\bar{x}_i-\bar{x}_j|} + k\rho \qquad \text{(1b)}$$

$\alpha_s=g^2/4\pi$ is the quark-gluon coupling constant, $k\equiv(32\pi B\alpha_s/3)^{\frac{1}{2}}$, and $\rho\equiv\left(\sum_{i<j}(\bar{x}_i-\bar{x}_j)^2/3\right)^{\frac{1}{2}}$ is the hyperspherical radius. B is the MIT bag constant.

For large separations the bag becomes a set of tubes and the potentials are

$$V_{q\bar{q}}(r) = -\frac{4\alpha_s}{3r} + kr + V^o_{q\bar{q}} \qquad (2a)$$

(large separations)

$$V_{q^3}(\bar{x}_1,\bar{x}_2,\bar{x}_3) = -\frac{2}{3}\sum_{i<j}\frac{\alpha_s}{|\bar{x}_i-\bar{x}_j|} + kr_M + V^o_{q^3} \qquad (2b)$$

r_M is the minimized sum of the lengths of the tubes in a Y-shaped bag. (It becomes a V-shape if one of the angles in the quark triangle exceeds 120°.)

We simply join the small and large separations formulae at appropriate values of r_o and ρ_o, and choose $V^o_{q\bar{q}}$ and V_{q^3} to insure that the potentials are continuous. This is called the "global" approximation[3,4].

Note that the confining term in the q^3 case is a pure 3-body potential since ρ and r_M depend on the positions of all three quarks simultaneously.

The validity of the global approximation in the $q\bar{q}$ case has been tested against a numerical solution for the bag which uses more complicated bag shapes[5,6]. This showed that the error in the global approximation is small even in the intermediate region of r, and suggested an optimal choice for the matching radius r_o. We are led to believe, therefore, that the global approximation to V_{q^3} will also be reliable.

The real value in having an analytic approximation to the potential is seen when one tries to incorporate asymptotic freedom effects into the q^3 problem. In the $q\bar{q}$ case there is a simple minded way to include a coupling constant α_s which varies with r. One simply makes the two sources in the bag have a common strength $g(r)=(4\pi\alpha_s(r))^{\frac{1}{2}}$ for any assumed choice of the function $\alpha_s(r)$. This does not in any way complicate the numerical solution[5] which is carried out separately for each value of r. In Ref. 5 a functional form was chosen which conforms to asymptotic freedom in the limit $r\to 0$, viz.,

$$\alpha_s(r) = \frac{12\pi}{33-2n_f} \frac{1}{\ln(\frac{1}{\Lambda^2 r^2}+\gamma)} \qquad (3)$$

It turns out that the resulting potential agrees closely with (1a) and (2a) if we simply replace all α_s's which appear there (including the definition of k) by $\alpha_s(r)$. This will provide the basis for our method of incorporating asymptotic freedom into the q^3 problem.

With the values Λ=0.24 GeV and γ=3.36, good fits were obtained to the $c\bar{c}$ and $b\bar{b}$ spectra and leptonic decay widths. The same value of the bag constant $B^{\frac{1}{4}}$=0.145 GeV was used as in the original MIT fit to the hadrons composed of light quarks[7,8].

In the q^3 case one cannot follow the same simple minded procedure of making the strengths of each quark charge g_i a function of the positions of all the quarks because there are three distances in the problem. On the one hand, one finds that the asymptotic freedom argument also holds (to order g^4) for two quarks at very short separations. The Coulomb term dominates there and consequently the coupling constant in that term would have to assume the value appropriate to that separation. The position of the third quark is irrelevant in this term. On the other hand, the color singlet nature of the state requires that all the strengths g_i be equal. These two constraints can be satisfied in a simple way for the $q\bar{q}$ systems, as described above, but not for the q^3 system. It then proves useful to have an analytic approximation to the potential so that one can put in the expected behavior by hand. We propose[4]

$$V_{q^3}(\bar{x}_1,\bar{x}_2,\bar{x}_3) = -\frac{2}{3}\sum_{i<j}\frac{\alpha_s(|\bar{x}_i-\bar{x}_j|)}{|\bar{x}_i-\bar{x}_j|} + k(\alpha_s(a\rho))\rho \qquad \rho\leq\rho_o$$

(4a)

$$= -\frac{2}{3}\sum_{i<j}\frac{\alpha_s(|\bar{x}_i-\bar{x}_j|)}{|\bar{x}_i-\bar{x}_j|} + k(\alpha_s(a\rho))r_M + V^o_{q^3} \qquad \rho\geq\rho_o$$

(4b)

As seen above, the confining term gets an additional weak ρ dependence, similar to that of the $q\bar{q}$ confining term. Since these terms arise through the confinement mechanism which acts on the system as a whole, α_s will in this case depend on ρ, which for small separations is the only relevant three body variable. The constant a indicates the uncertainty in the precise details of this (effective) dependence, and we expect $(1/3)^{\frac{1}{2}}<a<(3/2)^{\frac{1}{2}}$.

The level splittings of compact systems such as c^3 and b^3 are not very sensitive to the precise choices of a ($\cong$1), or ρ_o ($\cong R_\infty=(8\alpha_s/3\pi B)^{\frac{1}{2}}$). The position of the lowest few excited states shifts about 10 MeV relative to that of the groundstate for a reasonable range of a and ρ_o. Shifts of 10 to 40 MeV occur for the corresponding excitations of the more extended s^3 system. The position of the groundstate level drops upon decreasing a or increasing ρ_o. One can keep it in fixed position, e.g., as in the case of the Ω^-, by increasing the quark mass. Requiring here m_s=0.64 GeV, which fits M(ϕ)=1.02 GeV, one finds an unacceptably small value a$\leq$1/6, for any value of ρ_o. This may be another indication of the slightly relativistic character of the stange quark motion, which, however, is less pronounced in the s^3 system, where $\langle p^2/m^2\rangle\cong.50$.

The first few levels of the Ω^- system have been depicted in Fig. 1. Note that none of the excited states is stable against strong decay. For comparison, the mass spectrum of a purely two body potential has also been given. For this spectrum, we used

$$V_{q^3}(\bar{x}_1,\bar{x}_2,\bar{x}_3) = \frac{1}{2}\sum_{i<j} V_{q\bar{q}}(|\bar{x}_i-\bar{x}_j|) \qquad (5)$$

which was obtained under the assumption[9] that the differences in color eigenstate between the quark-quark and the quark-antiquark systems only leads to and overall factor of 1/2. For $V_{q\bar{q}}$ we used the potential from (1a) and (2a), with asymptotic freedom effects parametrized as in (3), and with m_s adjusted to fit $M(\Omega^-)$=1.672 GeV.

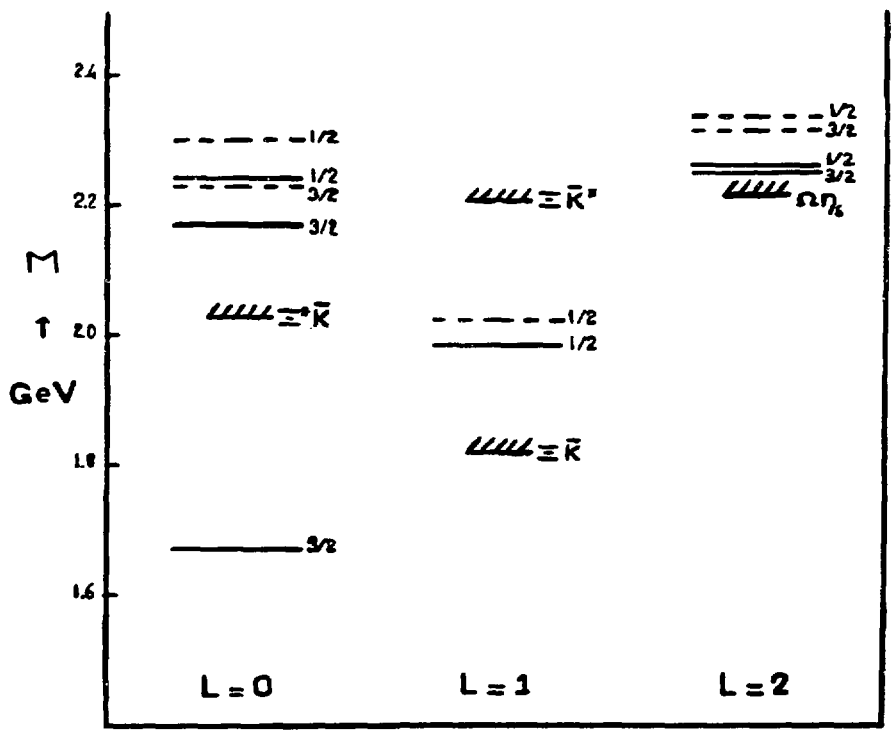

Fig. 1. Comparison of the s^3 mass spectrum, as obtained from the three-quark potential (4), with a=1, $\rho=R_{\infty}$ and m_s=.578 GeV (solid lines), and from the two-body potential (5) with m_s=.504 GeV (dashed lines). The total quarkspin (S=1/2 or 3/2) and orbital angular momentum (L=0,1 or 2) have been given. At convenient places the thresholds for strong two-body decay have been inserted.

References and footnotes

1 P. Hasenfratz, J. Kuti and A. S. Szalay, in: Proc. 10th Rencontre de Moriond (Meribel, France, 1975), ed. J. Tran Thanh Van; P. Gnadig, P. Hasenfratz, J. Kuti and A. S. Szalay, in: Proc. Neutrino '75 IUPAP Conf., Vol. 2 (1975) p. 251; Phys. Lett. 64B, 62 (1976).

2 A. Chodos, R. L. Jaffe, K. Johnson, C. B. Thorn and V. F. Weisskopf, Phys. Rev. D9, 3471, (1974).

3 A. T. Aerts and L. Heller, Phys. Rev. D (1980).

4 A. T. Aerts and L. Heller, in preparation.

5 W. C. Haxton and L. Heller, Phys. Rev. D22, 1198, (1980).

6 Numerical solutions for $q\bar{q}$ have also been obtained by: P. Hasenfratz, R. R. Horgan, J. Kuti and J. M. Richard, Phys. Lett. 95B, 299 (1980), and for q^3 by P. Hasenfratz, R. R. Horgan, J. Kuti and J. M. Richard, Phys. Lett. 94B, 401 (1980).

7 T. A. DeGrand, R. L. Jaffe, K. Johnson and J. Kiskis, Phys. Rev. D12, 2060, (1975).

8 A zeropoint energy term was also included using the same constant as in Ref. 7.

9 See, e.g., D. Robson, Nucl. Phys. A308, 381 (1978).

THE QUARK STRUCTURE OF THE $\Lambda(1405)$ RESONANCE*

P. J. MULDERS
Los Alamos National Laboratory
Theoretical Division
Los Alamos, New Mexico 87545

Submitted to the Workshop "Nuclear and Particle Physics at Energies up to 31 GeV: New and Future Aspects", January 5 - 8, 1981, Los Alamos, New Mexico

ABSTRACT

The interpretation of the $\Lambda(1405)$ resonance as a three-quark baryon resonance belonging to the $[70,1^-]$ multiplet is not quite satisfactory. A large spin-orbit splitting is required to explain the mass difference with the $\Lambda(1520)$ resonance; for none of the other baryon resonances such a large splitting is needed. Also the coupling to the $\bar{K}N$ and the $\pi\Sigma$ channels is not in agreement with SU(6) predictions. The interpretation of the $\Lambda(1405)$ resonance as a four-quark-one-antiquark state appears to create a new problem: where is the $J^P = 1/2^-$ Q^3 baryon resonance in this region. The next resonances with $J^P = 1/2^-$ lie above 1.65 GeV.

We want to investigate if both a Q^3 and a $Q^4\bar{Q}$ state coupling to the I = 0 $\bar{K}N$ S-wave exist in the energy region below 1.6 GeV and if this might explain some of the problems. To accomplish this we use the P-matrix formalism as developed by Jaffe and Low. It provides a connection between scattering of hadrons and bag states. Bag states correspond to poles in the P-matrix. These poles do not necessarily correspond to poles in the S-matrix.

We construct the P-matrix in the coupled $\bar{K}N$-$\pi\Sigma$ I = 0 channel below 1.7 GeV and find not only a pole corresponding to the $\Lambda(1405)$ resonance but also a second pole. We try to find an interpretation for these poles.

* This research was supported by the U. S. Department of Energy

I. INTRODUCTION

In many cases the mass of an unstable state may be calculated while disregarding the decay modes. Examples are the spectra of resonances in baryon-meson (BM) or meson-meson (MM) scattering. These resonances are excitations of three-quark baryonic (B^*) or quark-antiquark (M^*) systems. These states are unstable; they lie above the thresholds of BM or MM channels to which they couple through the strong process of quark-antiquark creation. This coupling can be regarded as a perturbation which does not seriously influence the mass calculated in first order, i.e. neglecting the decay. In other words the width is much smaller than the mass, $\Gamma \ll M$.

Multiquark states like $Q^2\bar{Q}^2$, $Q^4\bar{Q}$, or Q^6 are quite different from the hadron excitations we mentioned above. $Q^4\bar{Q}$ states projected out on the $Q^3 \otimes Q\bar{Q}$ system contain color singlet, $(Q^3)_1(Q\bar{Q})_1$, and color octet, $(Q^3)_8(Q\bar{Q})_8$, components. Calculations involving multiquark states therefore cannot neglect the presence of the decay channel since this channel is often a major component of the "state" itself.

Most analyses of baryon-meson channels parametrize the S-matrix with a set of poles with energies $E=M-i\Gamma/2$ and a smooth background. In the cases where the widths are not too large and the background is stable the different analyses [1,2] yield similar results. The poles are successfully explained as three-quark orbital excitations. The lowest negative parity resonances form a well-established flavor-spin SU(6) multiplet with orbital angular momentum L=1, denoted $[70,1^-]$.

The absence of the $Q^4\bar{Q}$ states is not difficult to understand.

If there is no mechanism to prevent the fission a $Q^4\bar{Q}$ state easily falls apart into a baryon and a meson. A very large width would be required. Jaffe and Low [3] argued that instead of in the S-matrix multiquark states like $Q^4\bar{Q}$ will show up in the P-matrix. Consider e.g. the case that there is only one channel. At a certain distance, say r=b, the baryon-meson system will merge into one bag. Under the assumption that there is no interaction for r>b the relation between the baryon-meson scattering wave function,

$$u(k,r) \sim \sin(kr+\delta) \ , \tag{1}$$

and the calculated $Q^4\bar{Q}$ states in a bag is found using the P-matrix

$$P(k) = b\frac{\left(\frac{\partial u}{\partial r}\right)_b}{u(b)} = kb\cot(kb+\delta) \ . \tag{2}$$

The poles of the P-matrix correspond to solutions for $r \leq b$ with the boundary condition u(b)=0. When the spins of the quarks are neglected this boundary condition is the condition imposed on the quark wave function in a bag; the interior solutions therefore correspond to multiquark states.

Also the ordinary $(Q^3)^*$ baryons show up as poles in the P-matrix through their $Q^4\bar{Q}$ component. From equation (2) it is evident that an S-matrix pole with a small width (δ rises over $\sim\pi$ radians) also yields a P-matrix pole. In this case the difference between the positions of S- and P-matrix poles will not exceed the width.

Jaffe and Low [3] found evidence for P-matrix poles whose energies were not far off from the calculated masses of $Q^2\bar{Q}^2$ states in many meson-meson channels - both the non-exotic like $(\pi\pi)_{I=0}$, $(K\pi)_{I=\frac{1}{2}}$, and the exotic like $(\pi\pi)_{I=2}$, $(K\pi)_{I=3/2}$ -. In baryon-meson

channels the non-exotic $(\pi N)_{I=\frac{1}{2}}$ and $(\pi N)_{I=3/2}$ S-waves and the exotic $(KN)_{I=0}$ and $(KN)_{I=1}$ S-waves have P-matrix poles in reasonable agreement with bag model predictions [4]. In all of the channels mentioned here the results are expected to be reliable, because only short-range forces are important. By short-range we mean distances smaller than the radius of a hadron-bag, ~ 1 fm. An example where long-range effects (π-exchange) clearly do play an important role is the NN channel. The long-range part of the NN potential must be taken into account [5].

II. OUTLAY

In this paper we concentrate on Y=I=0 states with spin-parity $J^P=\frac{1}{2}^-$, denoted $\Lambda(\frac{1}{2}^-)$; for low energies the $\pi\Sigma$ and $\bar{K}N$ S-waves are the most important two-body channels to which they couple. For the $\Lambda(\frac{1}{2}^-)$ states a problem arises, which did not occur in the low-energy P-matrix analyses mentioned in the introduction. In those cases the interpretation of P-matrix poles and the determination of the quark content gave no troubles [3].

For the $\Lambda(\frac{1}{2}^-)$ states S-matrix analyses - or K-matrix analyses [6] - yield a clear pole at 1.405 FeV, just below the $\bar{K}N$ threshold (see fig. 1). This $\Lambda(1405)$ resonance fits in the before mentioned $[70,1^-]$ flavor-spin multiplet. Together with the $\Lambda(3/2^-)$ state at 1520 GeV, a well established resonance in the $\pi\Sigma$-$\bar{K}N$ D03-waves, it then forms a spin-orbit multiplet: the spins of the three quarks combine to $S=\frac{1}{2}$; the orbital angular momentum between the quarks is L=1. In fig. 1

the experimentally well-established S-matrix poles up to 1.7 GeV have been given. In fig. 2 a prediction for the expected negative parity $(Q^3)^*$ states [7] is given together with the predictions for $Q^4\bar{Q}$ states [8]. A $\Lambda(\frac{1}{2}^-)$ state is predicted at 1.42 GeV, degenerate with a $\Sigma(\frac{1}{2}^-)$ state; we will denote these 5-particle states as Λ_5 and Σ_5. They are members of a nonet; three quarks form a flavor singlet and the remaining quark and antiquark make up a nonet; like the ω-ρ system the Λ_5-Σ_5 system is degenerate.

The low energy ($E \leq 1.5$ GeV) P-matrix analysis of Roiesnel [4] indeed shows poles around 1.5 GeV: Λ_5 (1.47) and Σ_5(1.54) - energies given in GeV-. Comparison with fig. 2 makes it tempting to identify these poles as $Q^4\bar{Q}$ states. The $\Lambda(\frac{1}{2}^-)$ pole at 1.47 GeV, however, corresponds to the S-matrix pole at 1.405 GeV. Although there are difficulties with the $(Q^3)^*$ interpretation of the $\Lambda(1405)$ resonance, notably the large spin-orbit splitting between $\Lambda(\frac{1}{2}^-)$ states, the $Q^4\bar{Q}$ interpretation seems to leave us with a missing $\Lambda(\frac{1}{2}^-)$ in the $[70,1^-]$ multiplet.

To investigate the problem above we perform a P-matrix analysis of the coupled $\pi\Sigma$-$\bar{K}N$ S01-wave in the energy region $E \leq 1.7$ GeV. We use the low-energy parametrization of Martin [6] and the phase shift analysis of the RLIC collaboration [2] and we search for poles in the -matrix. We find as the lowest poles a $\Lambda_1(1.49)$ and a $\Lambda_2(1.65)$. To interpret these poles we also perform analyses of the $\pi\Sigma$-$\bar{K}N$ D03-wave, where the other member of the spin-orbit multiplet of three-quark excitations must show up and of the $\pi\Lambda$-$\pi\Sigma$-$\bar{K}N$ S11-wave where the Σ_5 state must show up.

III. RESULTS

If there is no long-range interaction it is especially simple to construct the P-matrix. All we need to know is the S-matrix and radius b at which the baryon-meson system merges into one bag. We will use b = 6.5 GeV^{-1} ≅1.3 fm. Slight variations of b, b~ 6-7 GeV^{-1}, do not have much influence.

1. The πΣ - $\bar{K}N$ S01 Channel (Y=I=0, $J^P=\frac{1}{2}^-$)

In these channels (πΣ ≡ channel 1, $\bar{K}$ N≡ channel 2) we use two different analyses of the data. For the low-energy region (E≦ 1.48 GeV) the reaction matrix (K) is parametrized by the following effective range expansion [6],

$$M = \sqrt{k}\, K^{-1} \sqrt{k} = \begin{pmatrix} 0.32 & -0.182 \\ 0.182 & -0.02 \end{pmatrix} + \begin{pmatrix} 0.4 & -1.5 \\ -1.5 & 2.1 \end{pmatrix} k^2. \qquad (3)$$

The units in the first matrix are GeV, in the second one Gev^{-1}; k is the CM momentum in the channels in GeV; it is a diagonal matrix. The extrapolation of this K-matrix below the $\bar{K}N$ threshold yields a pole in the S-matrix at 1.405 GeV. In order to investigate the channels at higher energies we use the RLIC phase shift analysis for E≧ 1.48 GeV[2]. Assuming only two channels (πΣ and $\bar{K}N$) to be important we easily can construct the S-matrix. This is rescaled such that the sum $|S_{\bar{K}N\to\bar{K}N}|^2$ $+|S_{\bar{K}N\to\pi\Sigma}|^2=1$. The deviation from 1 gives a measure of the reliability. Below 1.65 GeV the sum is ≧ 0.94. In the energy region between 1.45 and 1.50 GeV we use an interpolation between both analyses. The results are not very sensitive to the precise interpolation. Having determined the S-(or K-) matrix we construct the P-matrix (logarithmic derivative at r=b). The results are given in table 1. We determined for each pole

its position and the residue, according to [3]

$$P_{ij} \sim \frac{-b(\frac{ds}{db}o)\lambda_i\lambda_j}{s-s_o} \qquad (4)$$

The residue $\lambda_i\lambda_j$ of the pole then is dimensionless; it factorizes and is proportional to a projection operator on the channels which are included ($\Sigma\ \lambda_i^2 = 1$).

We find two poles up to 1.65 GeV. For higher energies our two-channel approximation is less reliable. At the position of the third pole, 1.71 GeV, the sum of S-matrix elements squared equals 0.81.

Table 1: P-matrix poles in the $\pi\Sigma$ - $\bar{K}N$ channel;

$Y = I = 0;\ J^P = \frac{1}{2}^-$

$\sqrt{s}_o$	$-b(^{ds}o/db)$	$\lambda_{\pi\Sigma}$	$\lambda_{\bar{K}N}$
1.487 GeV	0.68 GeV^2	0.58	0.82
1.651	0.44	-0.81	0.59
1.715	-0.26	-0.99	0.12

2. The $\pi\Sigma$ - $\bar{K}N$ D03 Channel ($Y=I=0, J^P = 3/2^-$)

We investigate these channels ($\pi\Sigma \equiv 1$, $\bar{K}N \equiv 2$) to look where we can expect the three-quark baryonic excitations: $Q^4\bar{Q}$ states do not couple strongly to D-wave channels since all quarks are in S-waves. We use the RLIC phase shift analysis [2] and find the results given in table 2.

Table 2: P-matrix poles in the $\pi\Sigma$-$\bar{K}N$ D03 channel;

$Y=I=0;\ J^P = 3/2^-$

$\sqrt{s}_o$	$-b(^{ds}o/db)$	$\lambda_{\pi\Sigma}$	$\lambda_{\bar{K}N}$
1.564 GeV	0.38 GeV^2	0.68	0.73
1.742	0.59	-0.98	0.21

3. The $\pi\Lambda$-$\pi\Sigma$-$\bar{K}N$ S11 Channel ($Y=0, I=1, J^P=\frac{1}{2}^-$)

These channels ($\pi\Lambda\equiv1$, $\pi\Sigma\equiv2$, $\bar{K}N\equiv3$) are of importance because there are no clear low-lying S-matrix poles found; neither are any three-quark baryon excitations expected. On the other hand degenerate Λ_5 and Σ_5 states are expected from bag model calculations [8]. We therefore expect to see evidence for a $Q^4\bar{Q}$ state both in the $\Lambda(\frac{1}{2}^-)$ and $\Sigma(\frac{1}{2}^-)$ channels.

For the $\Sigma(\frac{1}{2}^-)$ channel a parametrization with a constant M - matrix has been obtained by Martin [7]. The inverse M^{-1} is given by

$$M^{-1} = \frac{1}{\sqrt{k}} K \frac{1}{\sqrt{k}} = \begin{pmatrix} 0.4 & 3.1 & -3.3 \\ 3.1 & 2.9 & -4.7 \\ -3.3 & -4.7 & 5.1 \end{pmatrix} \qquad (5)$$

The units in this matrix are GeV^{-1}. An extrapolation is needed above 1.5 GeV. Assuming this to be valid the P-matrix is constructed and the results are given in table 3.

Table 3: P-matrix poles in the $\pi\Lambda$-$\pi\Sigma$-$\bar{K}N$ S11 channel; Y=0, I=1; $J^P=\frac{1}{2}^-$

$\sqrt{s}_o$	$-b(ds_o/db)$	$\lambda_{\pi\Lambda}$	$\lambda_{\pi\Sigma}$	$\lambda_{\bar{K}N}$
1.543 GeV	0.73 Gev^2	-0.47	-0.59	0.66

IV. DISCUSSION AND CONCLUSION

The P-matrix poles found in our analysis are depicted in fig. 3. Below 1.55 GeV our results are in agreement with the results of Roiesnel [4]. The first encouraging result from our analysis is the fact that there are three $\Lambda(\frac{1}{2}^-)$ poles while there are only two $\Lambda(3/2^-)$ poles. Since the $(Q^3)^*$ states do appear in spin-orbit multiplets (see fig. 2) this means that there is one pole which might be interpreted as a $Q^4\bar{Q}$ state. Furthermore the $\Lambda(\frac{1}{2}^-)$ pole at 1.71 GeV and the $\Lambda(3/2^-)$ pole at 1.74 GeV seem to form a multiplet: they have roughly the same energy; the difference of 30 MeV is comparable with spin-orbit splittings between other baryon resonances. Also the ratio of the couplings to $\pi\Sigma$ and $\bar{K}N$ channels is of the same order.

Among the remaining three Λ poles, two $\Lambda(\frac{1}{2}^-)$ and one $\Lambda(3/2^-)$ pole, we cannot find compelling evidence for another spin-orbit multiplet. The $\Sigma(\frac{1}{2}^-)$ pole does not provide much help either because none of the $\Lambda(\frac{1}{2}^-)$ poles is approximately degenerate with it. Mixing between the $\Lambda(\frac{1}{2}^-)$ states provides the easiest explanation. We note one important fact: the value for $-b(ds_o/db)$ for the lowest $\Lambda(\frac{1}{2}^-)$ pole - just like for the $\Sigma(\frac{1}{2}^-)$ pole - is large compared to the values of the other poles, which is in favor of the interpretation as $Q^4\bar{Q}$ state. If there is mixing we still might expect a large $Q^4\bar{Q}$ component in the lowest $\Lambda(\frac{1}{2}^-)$ state (1.49 GeV).

To get a rought estimate of the mixing we assume that the pure $Q^4\bar{Q}$ state Λ_5 and the pure $(Q^3)^*$ state Λ^* with energies E_5 and E^* are shifted to $E_1 = 1.49$ GeV $= E_5 - \Delta$ and $E_2 = 1.65$ GeV $= E^* = \Delta$. If we take $\Delta = 0.05$ GeV this yields $E_5 = 1.54$ GeV and $E^* = 1.60$

GeV. The energy eigenstates then are the following linear combinations of Λ_5 and Λ^*

$$\begin{aligned} \Lambda_1(1.49) &\sim 0.83\,\Lambda_5 \pm 0.56\,\Lambda^* \\ \Lambda_2(1.65) &\sim 0.56\,\Lambda_5 \mp 0.83\,\Lambda^* \end{aligned} \qquad (6)$$

Of course these numbers should not be taken too seriously. The choice of Δ is only a guess; we think it to be reasonable because it renders a Λ_5 state degenerate with the $\Sigma(\frac{1}{2}^-)$ found at 1.54 GeV and a Λ^* state which forms a spin-orbit multiplet with the $\Lambda(3/2^-)$ found at 1.56 GeV.

Although our analysis is not conclusive on the precise quark structure of the $\Lambda(1405)$ it clearly shows the presence of a $Q^4\bar{Q}$ state in the energy range below 1.65 GeV. It also shows the importance of using the P-matrix. A better result might be expected when we parametrize the P-matrix with a set of poles and compare it with experiment, instead of using the results of analyses which parametrize the S-matrix. One of the advantages is that there is no unitarity constraint as the P-matrix for real energies is real and symmetric.

ACKNOWLEDGEMENTS

I wish to thank L. H. Heller for many helpful discussions and for reading the manuscript. I also wish to thank J. J. de Swart and L. J. Somers at the University of Nijmegen for helpful discussions.

REFERENCES

[1] R. E. Cutkosky, C. P. Forsyth, R. E. Hendrick and R. L. Kelly, Phys. Rev. D20, 2839 (1979); R. E. Cutkosky et al., Phys. Rev. D20, 2804 (1979); G. Höhler, F. Kaier, R. Koch and E. Pietarinen in Handbook of pion-nucleon scattering, ZAED Physics Data 12-1 (1979).

[2] G. P. Gopal et a. (RLIC Collaboration), Nucl. Phys. B119, 362 (1977); M. Alston-Garnjost et al., Phys. Rev. D18, 182 (1978).

[3] R. L. Jaffe and F. E. Low, Phys. Rev. D19, 2105 (1979).

[4] C. Roiesnel, Phys. Rev. D20, 1646 (1979).

[5] E. L. Lomon, private communication.

[6] In the low-energy region ($\leq$1.48 GeV) an analysis using the reaction matrix (K) has been performed by A. D. Martin, Phys. Lett. 65B, 346 (1976).

[7] P. J. Mulders, A. T. Aerts and J. J. de Swart, Phys. Rev. D19 2635 (1979). In fact these are not pure predictions. In this reference the spectrum of N^* and Δ^* resonances has been used to fit three parameters. No spin-orbit interaction has been included. The various fits, however, do not differ very much; see e.g. R. Koniuk and N. Isgur, Phys. Rev. D21, 1868 (1980).

[8] R. L. Jaffe in proceedings of the topical conference on baryon resonances, Oxford 1976, p. 455; P. J. Mulders, A. T. Aerts and J. J. de Swart in proceedings of the meeting on exotic resonancnes, Hiroshima 1978; D. Strottman,, Phys. Rev. D20, 748 (1979); J. J. de Swart, P. J. Mulders and L. J. Somers in proceedings of baryon 1980, Toronto 1980 (to be published).

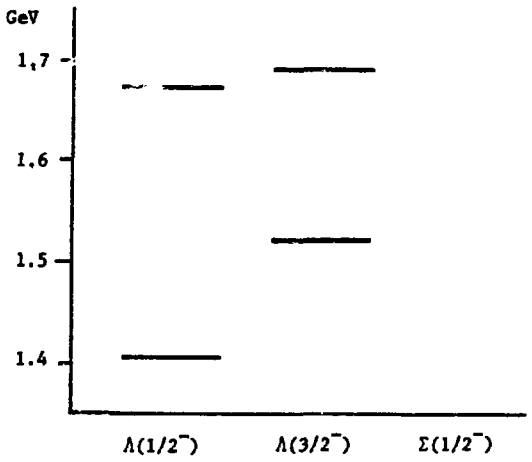

Fig. 1. Poles found in the S-matrix.

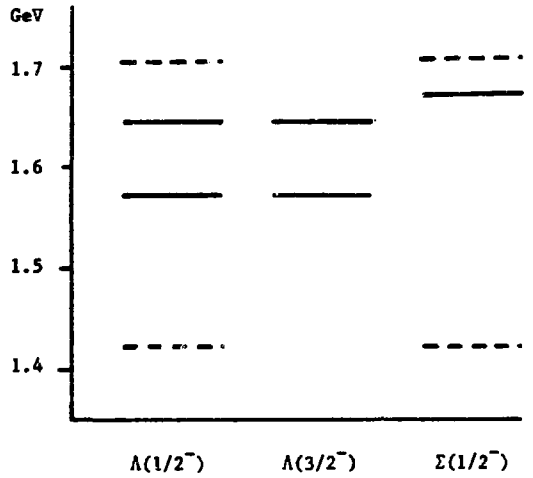

Fig. 2. Predictions for (Q^3) [——] and $Q^4\bar{Q}$ [– – –] states.

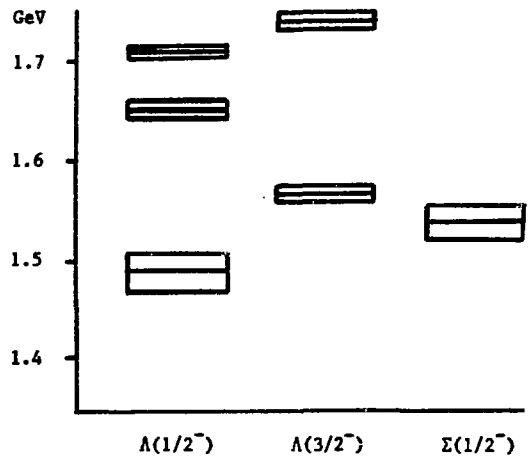

Fig. 3. Poles found in the P-matrix. The three levels for each pole correspond to b = 6.0, 6.5 and 7.0 GeV^{-1} respectively.

JOINING THE QUARK AND HADRON EXCHANGE DESCRIPTIONS OF STRONG INTERACTIONS

by

Earle Lomon
Massachusetts Institute of Technology
Cambridge, Massachusetts

Quark structure of hadrons cannot be ignored in hadron-hadron interactions which already probe the region of asymptotic freedom at relatively low energies. But one cannot compute the full interaction directly with QCD because

- o very high order processes enter at medium and small momentum transfer
- o bag models approximate confinement, and contain no theoretical information on longer range interactions of (unconfined) color singlet pairs.

Our present understanding of nucleon-nucleon and nuclear data implies that nucleon degrees of freedom and hadronic field theory are adequate descriptions for $r \gtrsim 1$ fm. For instance, the parameter free, theoretical Paris potential[1] fits the data without modification of more than a few percent for $r \gtrsim 1$ fm as shown for two parts of the potential, Figs. 1 and 2. All other parts of the potential show relative discrepancies of magnitude between the two cases shown. The total potential fits np and pp data for laboratory energy $E_L < 400$ MeV. For higher energies the dynamic effects of production thresholds must be included. Work by Kloet and Silbar and by Lomon has shown that these can account for data up to $E_L = 800$ MeV, including the "dibaryonic" structures seen. Figures 3 and 4 illustrate the fit obtained to the $^1D_2$ nucleon-nucleon channel. The solid line is the result of a coupled channel calculation; the dotted line and the various points are phase shift solutions. Similar results are obtained for the $^3F_3$ and other partial waves $L \leq 3$. Meson exchange potentials and an energy-independent boundary condition at 0.7 fm are used.

Lattice (or instanton) calculations, compared with bag models to determine a scale, suggest that asymptotic freedom (free quarks and first order gluon exchange) is adequate for $r < 1$ fm. This is illustrated in Fig. 5.[2] It appears that the region of a short range asymptotic freedom approximation may overlap

with the region of a long-range hadron exchange approximation. Therefore a boundary condition (f, P, R-matrix) approach is a promising way to obtain quantitative, parameter-free calculations with useful accuracy. This is the appropriate approach when there are two touching, or overlapping, regions in which different approximate Hamiltonians pertain. Hermiticity, time reversal invariance and causality imply[3]

$$f_{r_o} \equiv r_o P = r_o \frac{\psi'(r_o)}{\psi(r_o)} = f_o + \sum_i \frac{(Res)_i}{s-s_i}$$

$[s_i \text{ real}, (Res)_i > 0]$

$\frac{df}{dE} \leq 0$, and $\frac{df}{dE} = 0$ implies maximum non-locality for $r \leq r_o$

Field theoretical or dispersion calculations show that strong non-locality occurs for 2-meson exchange. Consequently Feshbach, Lomon and others applied the f-matrix method assuming

$$f_{r_o} = \text{constant} \quad r_o \approx \frac{1}{2}\mu^{-1} \quad . \quad \mu = \frac{M_\pi c}{\hbar}$$

In a coupled channel system with f_{ij} = constant, reduction to one channel produces a f_{eff} (one-channel) with cuts and real or complex poles. Poles in the component f_{ij}'s imply "coherent internal states" of which little was known in 1964. This led to the conjecture that such states are at high energy for small r_o, and could be neglected in applications below 1 GeV.

Jaffe and Low,[4] connected the "coherent states" with "primitives": states of completely confined quarks in a bag.

o They noted the important result that, in contrast to S-matrix poles, f-matrix poles stay put when confinement is removed. This is illustrated by Fig. 6.

o Averaging over quark degrees of freedom the two baryon f-matrix has poles at bag state energies when $r_o = b = 1.14\ R$.

As shown in Fig. 7, b is the relative distance between the center-of-mass of the 3-quark nucleon clusters, when all six quarks are confined in a bag of radius R. The ratio of b and R was determined in the free quark and free hadron approximation.

Jaffe and Low also derived the following results

o $\text{Res} = -\, b \frac{dS}{db} = 0 + \text{non-confinement correction}$

They approximated the effect of non-confinement of hadrons by the following Hamiltonian, which completely removes the bag pressure from color singlet pairs:

$$H = H_{bag} - \Lambda_o \frac{4}{3} \pi R^3 B$$

where Λ_o is the projection operator onto color singlet pairs.

o One can express the 6-quark wave function as

$$\psi^{6q} = \sum_i \rho_i^o \, |H_a^i \, H_b^i\rangle + \sum_\mu \rho_\mu^c |C_a^\mu \, C_b^\mu\rangle$$

in terms of uncolored and colored pairs. To obtain branching ratios to the open hadronic channels Jaffe and Low suggest

$$\text{Prob}\,(H_a^i \, H_b^i) = \xi_i^{o\,2} \approx (\rho_i^o)^2/[1 - \sum_\mu (\rho_\mu^c)^2]$$

o J & L ignore long range H-H interactions. Therefore they compare the energies of primitives with zeros of

$$h_\ell^{(2)}(kb) + c^{2i\delta_\ell} \, h_\ell^{(1)}(kb)$$

Good results follow in the meson-meson sector for positions, phase shift slopes and branching ratios-often unrelated to resonances.

o Good results in the meson-baryon sector were obtained by Roiesnel.[5]

o Shatz and Jaffe investigated NN sector. Poor results were found when the long range interaction was ignored.

Bag state energies were predicted by R. L. Jaffe, Aerts, Mulders and deSwart, Austen, Mulders and Rijken.[6]

The vertical scale in the following table is approximately linear with energy.

Expt, M (GeV)	L_{bag} = 0 (GeV)	L_{bag} = 1 (GeV)
$^3S_1 - {}^3D_1 + {}^1S_0$ (1.88)		
		$^1P_1$ (2.11)
$^3P_0$ (2.15)? (Lomon) $^1D_2$ (2.17) (Yokosawa)	$^3S_1 - {}^3D_1$ (2.16)	
		$^3P_1$ (2.20)
	$^1S_0$ (2.24)	$^3P_{0,1,2}$ (2.25)
$^1F_3 + {}^3F_3$ (2.26) (Yokosawa)		
	$^1D_2$ and	$^3P_{0,1,2}$ (2)(2) $^3F_3$ (2.34)
$^3S_1 - {}^3D_1$ (2.35) (Kamae)	$^3D_3 - {}^3G_3$ (2.34)	
or $^3D_3 - {}^3G_3$		
		$^3P_{0,1,2}$ $^1P_1$ (2.43)
		$^3P_{0,1,2}$, $^3F_3$, $^1P_1$, $^1F_3$ (2.47)
$^1G_4$ (2.5) (Yokosawa)		

In the S-matrix comparison above there is only one possible direct correspondence! There is a $^3D_3 - {}^3G_3$ state corresponding to the Kamae resonance. All other bag state energies are too high. The bag state degeneracies do not correspond to the experimental degeneracies. There are many more bag states than shown.

For the f-matrix: it works poorly when the potential for r > b is ignored. It <u>works well</u> when Paris Potential is included for $^1S_0$ & $^3S_1 - {}^3D_1$. It works for these and approximately for higher energy states when coupled channel effects are included (see Fig. 8).

It remains to be seen if the broad higher energy resonances can accurately be related to bag states through f.

In Fig. 8 positions 3 and 4 are the lowest bag state energies for the $^3S_1 - {}^3D_1$ and $^1S_0$ channels, respectively. They are far above the experimentally determined S-matrix poles corresponding to the deuteron (B.E. = 2 MeV) and the $^1S_0$ "anti-resonance" ($E_L \sim 5$ MeV). The f-matrix poles in those two channels computed from phase shifts and ignoring long range interactions are at positions 1 and 2, in better correspondence than the S-matrix poles, but still several hundred MeV distant from the bag state energies. The curves are the zeros of the Paris

potential wave functions in the labeled channels. The $^3S_1$ - $^3D_1$ curve crosses the radius b (dashed line) very close to the bag state energy (position 3). The $^1S_0$ curve crosses b about 100 MeV (c.m) lower than the bag state (position 4). The circles are obtained from the coupled channel long range interactions for $^3S_1$ - $^3D_1$ and make the agreement with the bag state precise.

The Paris potential $^3P_0$, $^1D_2$ and $^3F_3$ curves cross b substantially above the energies of the corresponding bag states (position 5, $^3P_0$; position 6, $^1D_2$ and $^3F_3$). The coupled channel effects improve the agreement if one extrapolates from E_L < 600 MeV. Precise calculations of zeros in the inelastic region are very difficult.

OPEP and TPEP imply that the long range interaction is important in the nucleon-nucleon case. The investigation with the Paris potential and with coupled channel theory confirms this (Lomon, Vinh Mau, Lacombe, Loiseau).

The long range interaction is very important; more than OPEP or Born approximation is needed.

Why does the f_b approach work? How can it be improved?

o b corresponds to full confinement radius R. Hadrons are in separate bags for r > b. In this range the quark structure is hidden and hadronic field theory is expected to be adequate.

o Rapid onset of high order effects in the transition region implies condensation into hadrons for r < b. The à posteriori evidence implies hadronic description good for r $\gtrsim$ 1 fm.

o Asymptotic freedom in QCD is not adequate for $r_q > R - \delta$ $\delta \sim 0.3$ fm but bag model adjusts B to give average effect of confinement with respect to $q\bar{q}$ and q^3 spectra. Residue ($- b \frac{\partial S}{\partial b}$) entirely due to surface effect coming from correction to bag model.

o If $r_o < b - 1.14\delta$ (within transition region) $\frac{\partial S \text{ confined}}{\partial r_o} \neq 0$ and $\Lambda_o \frac{4}{3}\pi R^3 B$ may be dropped.

Reasonable hope: we can match QCD to HFT at r_o = 1.0 - 1.2 fm. (R_q = 0.8 - 1.1 fm). R-matrix theory does not require a physical confinement radius R_q. Mathematical confinement → complete set of states for expansion of true wave-function in interior-match to channel wave functions in exterior.

Extension and improvements:

o Apply to data at all energies, not only at f-poles, using

$$f_{r_o}(E) = \underbrace{f_o + \sum_{i=n+1}^{\infty} \frac{(Res)_i}{s-s_i}}_{\text{approximately constant for } s \ll s_{n+1}} + \sum_{i=1}^{n} \frac{(Res)_i}{s-s_i}$$

This can be applied at $r_o = b$ as in Jaffe-Low. It has been applied without poles at $r_o = \frac{1}{2}\mu^{-1}$. The fact that for the smaller radius $E_L^i > 1$ GeV justifies the success of FL interaction at $E_L \lesssim 300$ MeV and isobar coupling model at $E_L < 900$ MeV. The comparison of constant f-matrix results for small r_o with the Jaffe-Low method using the Paris potential indicates approximate duality for 0.7 fm $< r_o <$ 1.4 fm.

o We must consider influence of colored pairs at $r > r_o$. R-matrix or f-matrix theory can be reduced to open channels:

$$f^o_{eff} = f_{oo} - f_{oc}\,[f_{cc} - \Theta_c(s)]^{-1}\, f_{co}$$

$$\Theta_c(s) \sim \left[\frac{(\psi^{out}_{cc})'}{\psi_{cc}}\right] r_o$$

may be estimated from bag model or quark potential theory.

o Residues calculated from gradients of interior wave functions at surface.

o Matrix calculation will predict branching ratios to open channels

o Corrections possible for center-of-mass motion of quark clusters.

o May improve estimates of r_o as a function of R_q.

These methods can be applied to all strong hadron-hadron interactions, including πN, $\bar{K}N$, and $N\bar{N}$ as well as NN.

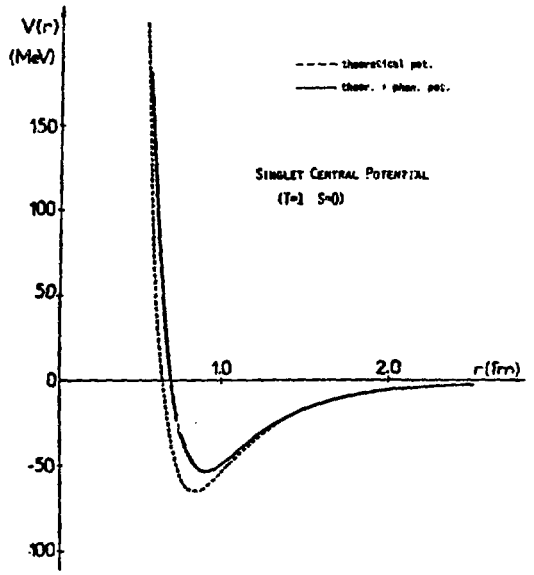

Fig. 1. Paris potential.

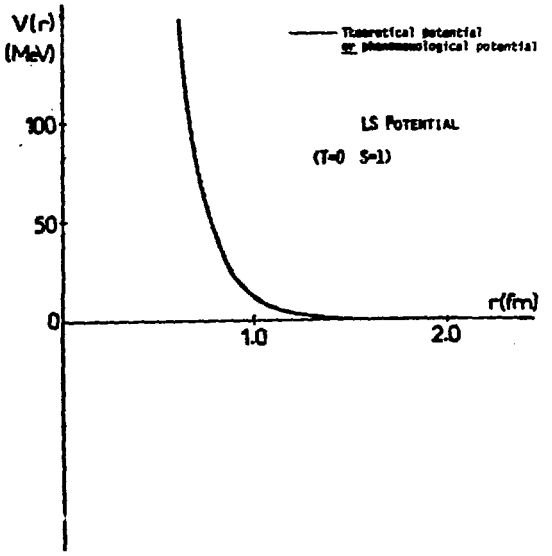

Fig. 2. Paris potential.

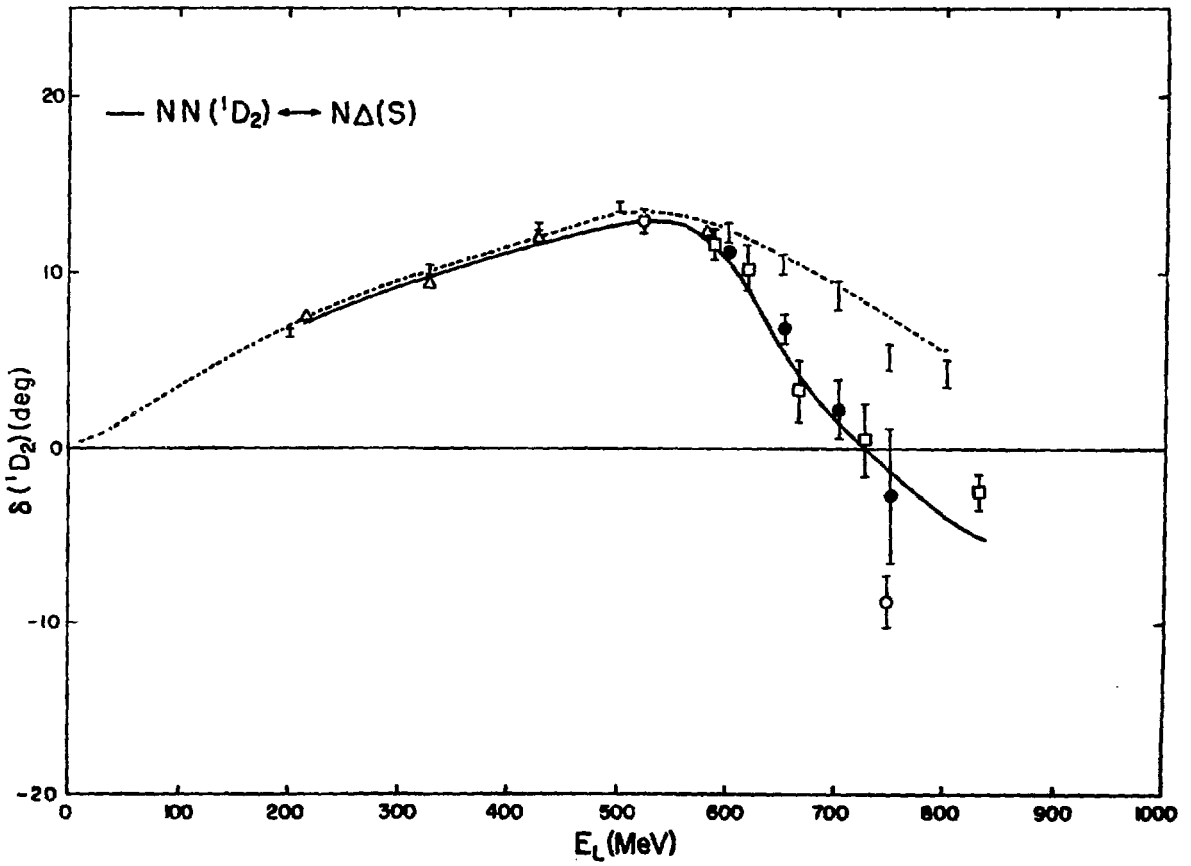

Fig. 3. Coupled channel model (Lomon).

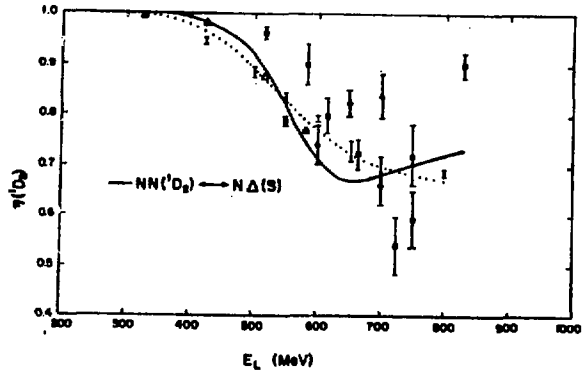

Fig. 4. Coupled channel model (Lomon).

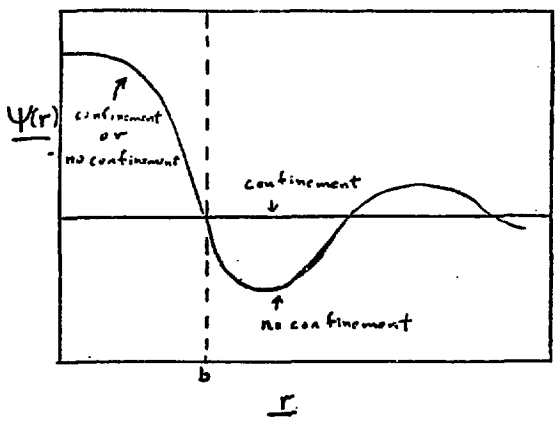

Fig. 6. Effect on wave function of removal of confinement. The confinement is imposed on interior wave function at r = b.

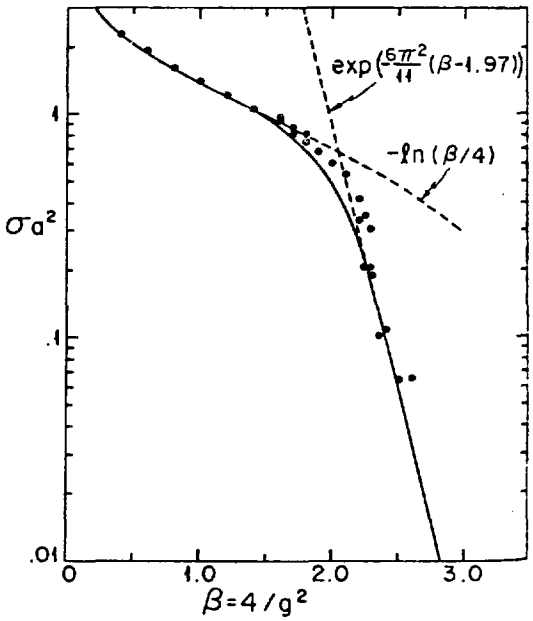

Fig. 5. Coupling strength vs. lattice spacing squared (in units of σ^{-1}). The solid line is C.D.G. solution, the dots are Creutz's data, and the dashed lines are the expected strong- and weak-coupling limits.

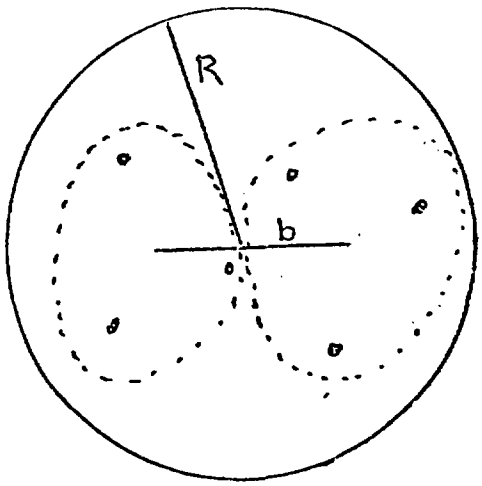

Fig. 7. Two baryon q^3 clusters in a quark bag of radius R. The distance between the center-of-masses of the two clusters is b.

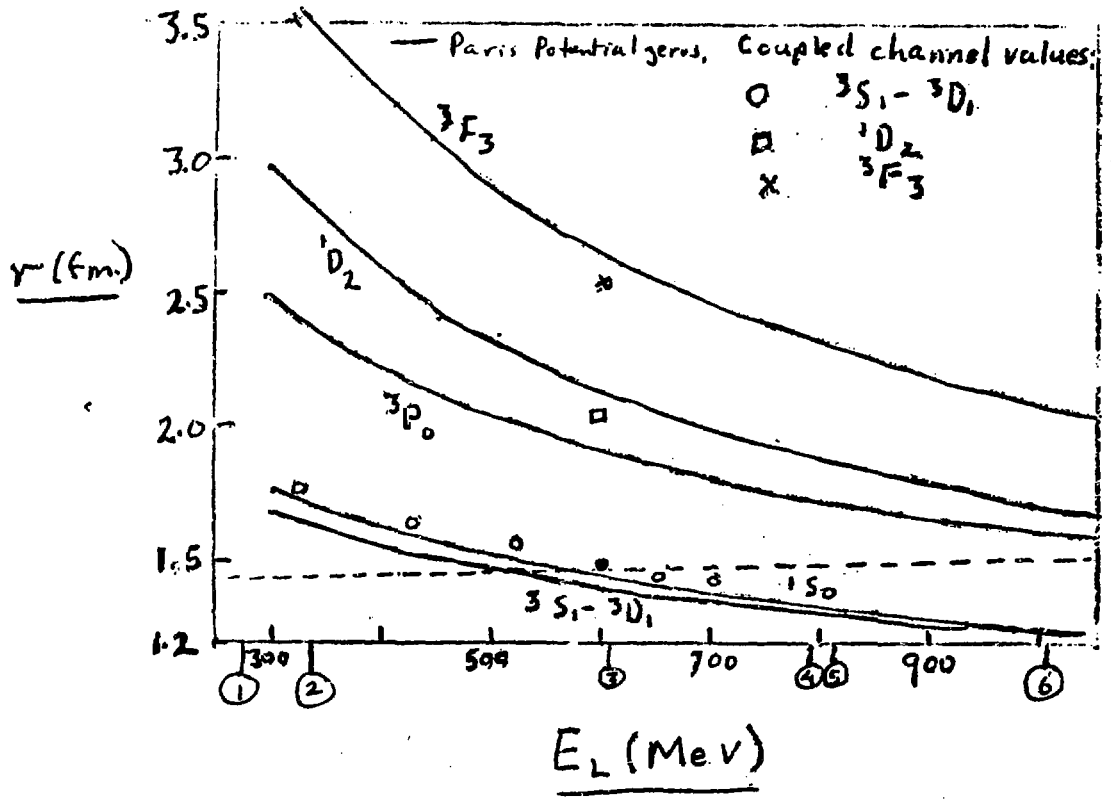

Fig. 8. Comparison of bag state energies with physical states and with f-matrix poles for two long-range interactions.

REFERENCES

1. M. Lacombe et al., Phys. Rev. C21, 861 (1980).

2. M. Creutz, Phys. Rev. Lett. 45, 313 (1980); C. G. Callen, R. F. Dashen, D. J. Gross, Phys. Rev. Lett. 44, 435 (1980).

3. H. Feshbach and E. Lomon, Ann. Phys. 29, 19 (1964).

4. R. L. Jaffe and F. E. Low, Phys. Rev. D19, 2105 (1979).

5. C. Roiesnel, Phys. Rev. D20, 1646 (1979).

6. R. L. Jaffe, Phys. Rev. Lett. 38, 195 (1977); A. Th. M. Aerts, P. J. G. Mulders and J. J. de Swart, Phys. Rev. D17, 260 (1978); Ibid, D21, 2653 (1980); J. J. de Swart, G. Austen, P. J. G. Mulders, and T. A. Rijken, Vancouver meeting talk, 1979.

Supernuclei, Supernuclear Matter & SU(4) Symmetry

by

G. Bhamathi
Theoretical Physics Institute
Department of Physics
University of Alberta
Edmonton, Alberta. T6G 2J1 Canada

ABSTRACT

The possible existence of light supernuclei and the binding of charmed baryons in nuclear matter has been studied using OBEP under SU(4) symmetry. Bound light supernuclei such as C_1N ($I=3/2$, $J=0$), C_1NN($I=2$, $J=1/2$) and C_0NN($I=1$, $J=1/2$, $I=0$, $J=1/2$ and $3/2$) are predicted and the binding of C in nuclear matter is expected to be much stronger than that of baryons.

The discovery of charm quantum number has led to the theoretical study of the strong interaction properties of charmed baryons with other hadrons. We have studied the strong interactions of the charmed baryons with nucleons by using the OBEP model obtained from the SU(4) extension of the unitary symmetric interaction Lagrangian previously used in studying the hyperon-nuclear interactions. We then made use of the low energy scattering parameters thus obtained to study the possible existence of light supernuclei (analogues of hypernuclei) where a charmed baryon plays the same role as a hyperon does in hypernuclei and also the possibility of the charmed baryon being bound to nucleon matter. We present here results obtained for the case of C_0 and C_1 particles.

The OBEP for B_C-N was calculated under full SU(4) symmetry with symmetry breaking introduced only through the use of physical values for the masses of the hadrons. The H_{int} for C_0N and C_1N interactions with pseudoscalar meson exchanges are given by

$$H_{int} = g[2i(1-\alpha)\ \bar{C}_1 x C_1\cdot\pi + \frac{2}{\sqrt{3}}(1-\alpha)\ \bar{C}_1\cdot C_1\eta + \frac{2}{\sqrt{3}}(1-\frac{5}{3}\alpha)\ \bar{C}_0 C_0\eta$$

$$- \frac{1}{\sqrt{6}}(1-4\alpha)\ \bar{C}_1\cdot C_1\eta_c - \frac{1}{\sqrt{6}}(1+\frac{4}{3}\alpha)\eta_c].$$

We obtained the OBEP for the C_0N & C_1N systems in the $I=1/2$ & $3/2$ states assuming the exchange of the scalar, pseudoscalar and vector meson nonets using the coupling constraints obtained by earlier fits to NN & YN scattering data by Brown et al[1]. The OBEP thus obtained were used in the coupled Schrödinger equations for the singlet and triplet S states of the C_1N($I=3/2$) and (C_0N, C_1N $I=1/2$)systems to solve numerically for the scattering length a & effective range r_0. The results displayed in Table I indicate that the C_1N($I=3/2$) system in the $^1s_0$ state is bound whereas there are no bound states in the $I=1/2$ (C_0N, C_1N) system. Next we considered the C_0NN, C_1NN light supernuclei.

Since a solution of the three body coupled equations with OBEP two body interactions involves multiple integral equations. to reduce the problem to a tractable form we made use of equivalent separable potentials of the Yamaguchi type which reproduce the appropriate low energy two body scattering parameters. In solving the C_0NN three body system with the C_0N interaction in the I=1/2 state we had to make a further approximation by neglecting the C_1N interaction in the intermediate state. However the effect of the coupling to the C_1N channel was taken exactly into account while solving for the two body interaction parameters. Similarly where triplet state interaction was involved coupling to the D state through tensor forces was taken into account in determining the two body parameters but had to be neglected in the three body equations. Finally the set of three coupled three body equations in the Schrödinger equivalent form of the Faddeev equations were solved numerically by the Gaussian quadrature method and the binding energies of the C_0NN & C_1NN supernuclei in the various possible spin & isospin states were obtained as displayed in Table II. The results obtained indicate that a fairly strongly bound $_{C^0}H^3$ system is likely to exist with total isospin zero and total spin 1/2 and 3/2. Finally we investigated the possibility of the C_0 particle being bound to nuclear matter similar to the case of a Λ hyperon. Making use of the two body interaction parameters already obtained, in the Bethe-Goldstone equation for C_0 interaction in nuclear matter, we obtained the binding of C_0 in nuclear matter to be in the range of 75-85 MeV. In computing this we found that the estimate depends strongly on the strength of the triplet state interaction as well as on the interchannel coupling strength to the C_1N channel. It may be noted that an earlier estimate [2] of C_0 binding in heavy but finite nuclei gives values of the order of 60 MeV for Pb^{208}.

To summarize, we find that SU(4) OBEP model for C_0N & C_1N interactions leads to the prediction of strongly bound light supernuclei such as $_{C^0}H^3$ as well as a strong binding of C_0 to nuclear matter.

Table I.† a and r_0 variation with r_c

			r_c = 0.46f		r_c = 0.50f	
System	I	J	a	r_0	a	r_0
C_1N	3/2	0	16.12	1.82	-4.55	2.77
C_1N	3/2	1	-2.96	4.71	-2.28	5.54
C_0N	1/2	0	-0.69	5.77	-0.30	16.86
C_0N	1/2	1	5.29	3.71	5.29	3.70

† All quantities are quoted in units of fermi

Table II. Binding and separation energies in MeV.

				r_c = 0.46f		r_c - 0.50f	
System	I_T	J_T	J_{NN}	B.E	S.E	B.E.	S.E
C_1NN	2	1/2	0	0.13	0.13	not bound	
C_0NN	1	1/2	0	5.63	4.98	5.13	4.88
C_0np	0	1/2	1	6.77	4.65	6.33	4.23
C_0np	0	3/2	1	11.53	9.23	11.53	9.23

References

1. J.T. Brown, D.W. Downs & C.K. Iddings. Nucl. Phys. B47, (1972) 138.
2. C.B. Dover & S.K. Kahana. Phys. Rev. Lett. 39, (1977) 1506.

Λ AND Σ HYPERNUCLEAR PHYSICS

by

Peter D. Barnes*
Carnegie-Mellon University, Pittsburgh, PA 15213

ABSTRACT

A general review of progress in hypernuclear physics is given. The current status of the development of the Λ-nucleus shell model is reported together with a discussion of the nuclear spin-orbit force for N, Λ, Λ and Σ nuclei. Natural line width calculations are compared to the data for the strong component of the Λ and Σ nucleus interaction. Calculations of the role of the four fermion weak interaction in the weak decay of Λ hypernuclei are compared to lifetime data. Special topics in two body and few body systems are also reviewed.

Although strange particle physics started about thirty years ago with the discovery of V particles[1] in 1947 and the Λ hyperon[2] in 1952, hypernuclear physics entered its modern phase with the discovery of hypernuclear resonances in 1969 and hypernuclear gamma ray decay in 1971. The advent of high intensity kaon beams and the utilization of counter techniques has accelerated the growth of this field in recent years. Nevertheless the kaon flux limitation is still quite restrictive as will be apparent in the data I will discuss. A large variety of hypernuclear physics problems have now been explored and it is the purpose of this talk to display on one hand the scope of this field and on the other the impact of recent experiments at Brookhaven National Lab and at CERN on our understanding of the underlying physics. However the time constraints of the conference program require that while some subjects can be discussed in detail others will only be sketched. In section II I will begin with the few body hypernuclear systems. After discussing the chief reaction mechanism used to produce hypernuclei in section III, I will proceed to the nuclear structure of lambda hypernuclei in section IV and to sigma hypernuclei in section V.

II. Few Body Systems

The building blocks for constructing hypernuclear systems are, in addition to neutrons and protons, the various long lived strange baryons displayed in Figure 1. We do not consider here the charmed strange baryons. The two lightest S = -1 hyperons, Λ and Σ are the primary subject of this talk. The Cascade and the Omega are more difficult to make and would be expected to have large natural widths in a nuclear system.

The two baryon configurations that can be considered are classified in Figure 2 according to their strangeness S = -1, -2 and -3. The question of whether any of these two baryon systems is bound is of great current interest and revolves around a detailed understanding of the forces of interaction. Our attention is primarily focused on the ΛN and ΣN systems for which some two body phase shift data exists. Furthermore states of both Λ nuclear and Σ nuclear systems have been observed with relatively narrow natural widths. It is of great importance to understand these results in terms of the character of the two body interaction.

A qualitative understanding of the character of the ΛN interaction can be achieved by reviewing the main features of the boson exchange description of the NN interaction:[3]

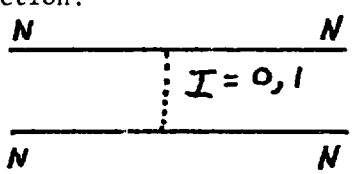

In this case the exchanged bosons can have spin and isospin of zero (scalar) and one (vector). These four contributions to the NN interaction are displayed in Figure 3 and determine the main features of the effective boson exchange potential. The long range one pion part gives the NN interaction

its strong spin-spin and tensor character. The medium range attraction comes from the scalar (σ) and vector (ρ) parts of the two pion exchange while the short range repulsion comes from the three pion (ω) exchange. A major part of the spin-orbit force comes from the vector exchange (ρ and ω) both through the Thomas term and the tensor coupling.

Because the Λ has isospin zero the exchanged bosons in the ΛN interaction are limited to isospin zero, thus eliminating one pion and ρ exchange.

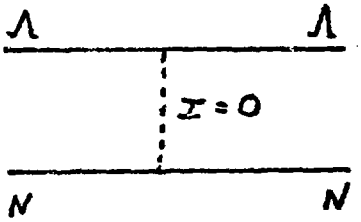

This removes the longest range component of the baryon baryon force. The leading term is now the shorter range spin zero σ exchange, which gives a strong central character to the force. Furthermore the absence of ρ exchange will greatly modify the character of the ΛN spin-orbit force. The short range repulsion generated by ω exchange is retained in the ΛN potential. Thus the ΛN interaction is to be expected to be rather different from the NN interaction with shorter range, and weaker spin dependence.

By comparison the ΣN interaction has all the complexity of the NN system since the Σ has isotopic spin, I = 1.

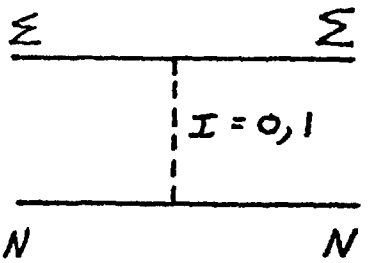

Furthermore since ΛN and ΣN systems only differ by ∿ 80 MeV in mass it is tempting to look for isospin mixing features of the two body force. One might look for change symmetry breaking (CSB) effects such as

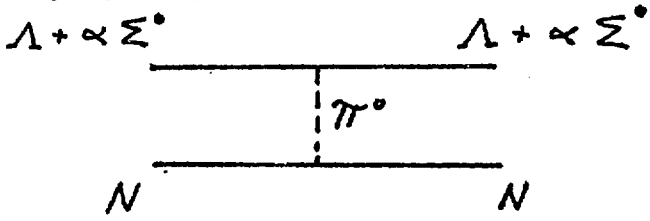

where α characterizes the amplitude of the small isospin breaking amplitude which would contribute to the long range part of the interaction.

Turning now to detailed analysis of the YN potential, Table I summarizes the available total cross section and angular distribution data[4] which is used to generate the YN phase shifts. These in turn can be simulated by an effective meson exchange potential. For example the Nijmegan group[5] has developed a series of potentials from the exchange of nonets of pseudoscalar (π,η,η',K), vector (ρ,ω,ϕ,K^*), and scalar ($\delta'[1255]$, $\varepsilon[760]$, $\varepsilon'[1250]$, and $\chi[1245]$) mesons. Typical scattering length and range parameters obtain for their potential F are shown[4] in Table II. A comparison of these with the corresponding NN parameters indicates the weaker character of the YN interaction.

Will these mesonic forces form two body bound states? There have been various searches reported in the literature of which we will mention three. In the I = 1/2 channel the Nijmegan potential predicts that a resonance like structure should appear in the total elastic cross section of the Λp system at a mass of ∿ 2128 MeV (Figure 4a). This deuteron like structure is just below the Σ^+n threshold. Braun et al.[6] and others have reported a Λp enhancement observed in the $K^-d \to \Lambda p\pi^-$ reaction (see Figure 4b). If

this is a Λp resonance and the coupling to the ΣN channel is small it would have[6] a mass of 2129 ± 0.4 MeV and a width of Γ_0 = 5.9 ± 1.6 MeV. Thus it lies exactly at the $\Sigma^+ n$ threshold (2129.95 MeV).

A search for a $\Sigma^- n$ bound state in the I = 3/2 channel has been attempted at the AGS. May[7] has reported on a search using the $K^- d \rightarrow \Sigma^- n \pi^+$ reaction which found no evidence for such a state.

Bound two baryon systems have also been predicted by Jaffe[7] using color electric forces. He has calculated the total mass for six quark systems confined to a spherical MIT bag. He found that for systems of two u quarks, two d quarks, and two s quarks one could obtain a large binding energy when the quarks are all in relative s states and the like quarks have anti-parallel spins. This is the classic "alpha particle" configuration and might be expected to have large binding for an attractive force due to the large spacial overlap achieved. Figure 5 shows a calculated mass spectrum[4,8] where the lowest spin zero state has a mass of 2170 MeV and thus 60 MeV of binding. Searches for this state at BNL by the Kycia group have thus far been negative.[9]

We turn now briefly to the mass 3, 4 and 5 systems which will be discussed in more detail in the contributed paper of Gibson.[11] Table III summarizes the available binding energy data. The hypertriton is bound by 130 KeV and has $J_\pi = 1/2^+$. However the aligned configuration $J = 3/2^+$ has not been observed. Four states are now known in the mass four system (see Figure 6) as a result of the recent gamma decay work of the Warsaw-Lyon-Cern collaboration.[10] Thus we see that the singlet interaction is more attractive than the triplet by about 1 MeV. Furthermore both the doublets (spin J = 0 and 1) are split in energy. When corrected for the difference in coulomb energy (≈20 KeV) this splitting is ≈300 KeV for the ground state doublet.[11] Recently Gibson

and Lehman[11] have argued that this is consistent with the charge symmetry breaking contribution expected from the Nijmegan potential as long as the $\Lambda N \rightarrow \Sigma N$ coupling is not neglected and a so-called "exact" four body calculation is performed. Gibson also anticipates that inclusion of these effects in a calculation of B_Λ for ${}^{5}_{\Lambda}\mathrm{He}$ will bring the predicted value into line with the small observed value of $B_\Lambda({}^{5}\mathrm{He}) = 3.1$ MeV. This would resolve a long standing problem.

Before turning to the spectroscopy of heavier systems we discuss the general considerations in the production of hypernuclei in charged particle reactions.

III. Production of Hypernuclei

The conversion of neutrons and protons into Λ and Σ hyperons is most conveniently achieved through the charged particle reactions listed in Figure 7. The center of mass cross sections are also listed for an incident kaon momentum of 720 MeV/c. If the nucleon is imbedded in a nucleus the reactions become

$$K^- + A \rightarrow \pi^{\pm} + {}^{\Lambda}_{\Sigma}A^*$$

and has largest yield for natural parity states and especially for $J^\pi = 0^+$ if the pion is detected at zero degrees. The choice of the incident kaon momentum p_K is dictated by the momentum dependence of the elementary cross sections (see the solid curves in Figures 8 and 9) and by the need to avoid excessive recoil momentum, q_Λ, for the hyperon (see the dashed curve in Figures 8 and 9). Many experiments have operated in the range $p_K = 700$-800 MeV/c where the laboratory cross sections at $\theta = 0$ are 1-5 mb/sr and $q_\Lambda < 100$ MeV/c,

q_Σ < 130 MeV/c. Herrera et al.[12] have used $p_K \approx 1700$ MeV/c where the K^- flux is large but this makes severe demands on a charge particle spectrometer. In order to keep q_Σ < 100 MeV/c a short low momentum K beam is now being built at CERN ($p_K \leq 600$ MeV/c)

As an example of such a reaction we consider the formation of hypernuclear $^{12}_{\Lambda}C$. The shell model interpretation of this neutron to lambda conversion is shown in Figure 10*a*. Neutrons in either the $1s_{1/2}$ or $1p_{3/2}$ orbits are converted to Λ's and placed in any of the low lying orbits of the somewhat shallower Λ potential. The largest cross section is achieved when the Λ is given the same quantum numbers as the original neutron. The resulting particle hole (ph) state has spin zero and is referred to as a substitution state. It is observed with large cross section at $\theta = 0$ degrees in recoiless production. Natural parity states for which the particle and hole have different quantum numbers can also be observed, in quasifree production, but have small cross sections. The particle hole multiplets of $^{12}_{\Lambda}C$ are illustrated in Figure 10b together with the expected yields. The ground state has $\Delta\ell = 1$ and is expected to have small yield. The $p_{3/2}$ orbit substitution state ($J^\pi = 0^+$) is expected to be large near zero degrees whereas the natural parity 2^+ state should only appear at larger angles. The s orbit substitution state should have large yield at forward angles but should also be broad due to the spreading width of the deep lying $s_{1/2}^{-1}$ neutron hole state. More complex states can be excited in two step processes and will contribute to a quasifree background.

Mass spectra obtained for $^{12}_{\Lambda}C^*$ using the 800 MeV/c K^- beam at the AGS[13] are shown in Figures 11a and 11b. The $p_{3/2}$ substitution state near 11 MeV is large at $\theta = 0$ but is reduced considerably at $\theta = 15$ degrees. The 1^- ground state stands out very well at the larger angle. The 2^+

state expected near 11 MeV is not resolved in this experiment. Measured angular distributions for these two groups are shown in Figures 12 and 13. Dover et al.[14] have attempted to describe this reaction in a DWIA analysis. They reproduce the shape of the cross section for the ground state very well (dashed curved in Figure 12) but overestimate the cross section by a factor of two. The 11 MeV group is also well described in shape (Figure 13) when they combined the yield from the 0^+ substitution state and the expected but unresolved 2^+ state. Again the observed yield is $\sim$ 40% of the calculated yield. The success of these calculations suggest that the reaction mechanism for this process is fairly well understood.

The excitation spectra of many Λ hypernuclei have now been observed at $\theta = 0$ by the Heidelberg-Saclay-Strasbourg collaboration at CERN.[15] Some cases are summarized in Figure 15 where the yield for each target is plotted against the mass difference

$$M_{HY} - M_A = (m_\Lambda - m_n) - (B_\Lambda - B_n) = 176 \text{ MeV} - \Delta B .$$

The large peaks are the expected $1s_{1/2}$, $1p_{3/2}$, $1p_{1/2}$, $1d_{5/2}$ substitution states. These $\theta = 0$ yields have been analyzed by Bouyssy[16] in terms of the effective number of neutrons that contributed to the Λ conversion process. We can write

$$\left.\frac{d\sigma}{d\Omega}\right|_{\theta=0} = N_{eff}^{\text{total}} \left.\frac{d\sigma}{d\Omega}\right|_{K^- n \to \pi^- \Lambda}$$

where

$$N_{eff}^{total} = \text{effective number of neutrons}$$

$$= N_{eff}^{substitution} + N_{eff}^{quasifree} .$$

When the measured CERN cross sections[15] are expressed in this way, N_{eff}^{total} increases monotonically with nuclear mass from one to five for the entire mass range (see Table IV for some typical results). Bouyssy's calculated yields are in agreement with experiment and indicate that $N_{eff}^{substitution} \simeq 1$ independent of target mass and that it is the quasifree contribution that is increasing (Table IV). The success of both the Bouyssy[16] and the Dover calculations[14] seem to suggest that the main features of the production of Λ hypernuclei are understood both in a qualitative and in a quantitative way.

A convincing demonstration of the existance of Σ hypernuclei was first provided by Bertini et al.[15] for a ^{9}Be target. Figure 15 shows a comparison of states in $^{9}_{\Lambda}$Be to peaks seen 80 MeV up in excitation which they assign to $^{9}_{\Sigma 0}$Be formation. When the data is plotted against the parameter

$$\Delta B = B_n - B_Y = (M_{HY} - M_A) - (m_Y - m_N)$$

as in Figure 15 we see that the Λ is bound by about 3 MeV more than the Σ in $^{9}_{\Sigma}$Be. The width of the Λ and Σ peaks are both about 8 MeV. Similar results have recently been observed[17] at the AGS for a ^{6}Li target (see Figure 16) as reported in the contributed paper by Hungerford at this conference. We will return to a discussion of the width of Σ states at the end of this paper.

IV. Nuclear Structure - Λ

As more and more data on Λ hypernuclei accumulate the broad outlines of the Λ shell model are starting to emerge. Some of these have been anticipated above by looking at the meson exchange character of the force. In this section we first review some crude estimates of the shell model parameters that comes directly from the data, then review some specific shell model calculations before turning to the specific problems of the spin orbit interaction and level widths.

A. General Features

Experimental ground state binding energies, B_Λ, have been known for a long time to increase monotonically with nuclear mass, A, approaching 26 MeV in the limit. Although detailed analysis is very sensitive to the assumed nuclear radius, this suggests that the central shell model potential is of the order of 30 MeV. Furthermore the average shell model orbital spacings can be inferred from the positions of the substitution states (e.g. Figure 14) assuming the multiplet splitting are not large (as confirmed by the ^{12}C data). The orbit spacings obtained by Bertini et al.[18] are shown in Figure 17 and compared to the much larger spacing occurring in the nucleon case.

Information on the $p_{3/2}$ - $p_{1/2}$ spin orbit splitting has been obtained by comparing $^{16}_{\Lambda}O$ to $^{12}_{\Lambda}C$ (Figure 18) by the Bruckner [19]. Figure 19 illustrates the expected low spin levels generated by a Λ in the s and p orbits. The separation of the two low lying 1^- states reflect the 6 MeV spin-orbit splitting known for a p orbit nucleon. Above these are the two $J^\pi = 0^+$ substitution states for the $p_{1/2}$ and $p_{3/2}$ orbits. The later is known to be 11 MeV above the $(s_{1/2}\ p_{3/2}^{-1})\ 1^-$ state

(17 MeV excitation) from $^{12}_{\Lambda}C$ (Figures 11a, 13 and 18). The intense fourth peak in the $^{16}_{\Lambda}O$ spectra is then identified as the $p_{1/2}$ substitution state at 11 MeV excitation. The authors[19] point out that the 6 MeV splitting of the two p substitution states leave no room for a contribution from a Λ spin orbit interaction. They find that it must be $\Delta E_{\Lambda}^{\ell s} \lesssim 0.3$ MeV. The energy splitting is related to the strength of the spin-orbit interaction by:

$$\Delta E^{\ell s} = 1.4\ V^{\ell s}\ (\ell + 1/2)\ A^{-2/3}\ \text{MeV}$$

in the nuclear case. Assuming the same functional dependence for the Λ gives $V_{\Lambda}^{\ell s} \sim 1$ MeV while $V_N^{\ell s} = 20$ MeV. Although this interpretation ignores the role of configuration mixing in these states, the results hold up under more detailed analysis.

Information about the residual interaction is difficult to extract in a simple way from the data. To learn about spin dependent forces one needs to locate, for example, the members of the Λ $s_{1/2}$ doublets[20] and the $(p_{\Lambda}^{+1} p_N^{-1})_J$ multiplets. Since these involve both natural and unnatural parity states they cannot in some cases be excited, muchless resolved, in the (K^-,π^-) reaction. Studies of the gamma decay of hypernuclear levels will become the main tool for identifying these states. We have seen that the Λ spin flip transition is 1 MeV in the 1s orbit in $^{4}_{\Lambda}H$ and $^{4}_{\Lambda}He$. The $(p_{3/2}\ p_{3/2}^{-1})_{J^{\pi}=0^+,2^+}$ states in $^{12}_{\Lambda}C$ were not resolved however their effects on the angular distribution was recognized (Figure 13). The peak shapes indicate a 0^+-2^+ splitting of less than 400 KeV.[13]

Finally there is the possibility of core excitation due to the presence of the Λ. We again take $^{12}_{\Lambda}C$ as an example where the positions and strengths of such states have been calculated by Dalitz and Gal[20] in an intermediate coupling model (Figure 20). Relative yields for exciting these states in the (K^-,π^-) reaction are given in the figure. Notice that the ground state doublet splitting is again estimated at 1 MeV. The 1^- state near 3.3 MeV was not observed in the AGS measurement.[13] It must be <10% of the ground state compared to the 30% predicted.

B. Shell Model Calculations

A variety of detailed shell model calculations have now been reported. Dalitz and Gal[20] have made extensive calculations in an intermediate particle-core coupling model as discussed above. Mujib et al.[21] have fit the known B_Λ values in the p shell using an effective central plus spin dependent, charge independent, ΛN potential. They find that no noncentral or three body forces are needed.

Bouyssy[22] has analyzed all the CERN ($\theta = 0$) spectra using a shell model to generate ph wavefunctions which he then uses in a DWIA calculation of the reaction cross section. He expressed his Λ shell model potential as

$$U_\Lambda(r) = -V_\Lambda^c f(r) + V_\Lambda^{\ell s} \frac{1}{r}\frac{d}{dr} f(r)$$

where the form factor

$$f(r) = [1 + \exp[(r - R)/a)]^{-1}$$

characterizes the nuclear matter distribution. A zero range residual interaction is included with a spin spin force characterized by a strength, α.

$$V_{\Lambda N}(r - r') = -V_0\, \delta(r - r')[1 + \alpha\, \vec{\sigma}_\Lambda \cdot \vec{\sigma}_N] \ .$$

The quantities V_Λ^c, $V_\Lambda^{\ell.s.}$ and α were treated as free parameters and fit to the data. The results are given in Table V and compared to the equivalent nuclear values. The parameter V_0 is connected in a self-consistent way to V_Λ^c. As anticipated $V_\Lambda^c \simeq 32$ MeV and $V_\Lambda^{\ell.s.} \cong 4$ MeV. The sensitivity of this data to α is not large.

A major effort is now underway at BNL to perform a "Cohen and Kurath" type analysis of the Λ nucleus system.[23] The optimum choice of the residual interaction as well as the relative merits of $\bar{L}$-$\bar{S}$ versus j·j coupling are issues of critical importance. One useful test case is the level spectrum of $^{13}_{\Lambda}C$. The states generated in a crude particle plus core coupling model are illustrated in Figure 21. Notice that the splitting of the 11 MeV group will depend on the Λ spin orbit interaction. Figure 22 shows two spectra obtained at the AGS[24] for the $^{13}C(K^-,\pi^-)^{13}_{\Lambda}C^*$ reaction that indicate four $^{13}_{\Lambda}C^*$ levels. These level positions and yields are compared in Figure 23 to a preliminary estimates[20,23] that gives the correct yields but underestimate the splitting of the two strong states. Levels have also been seen[24] in $^{14}_{\Lambda}N$ and $^{18}_{\Lambda}O$ as shown in Figure 24.

A careful analysis of the excitation energies and differential cross sections of this type of detailed and systematic data is required to develop a coherent description of Λ hypernuclei in the framework of the shell model.

We anticipate that this program will ultimately succeed and are primarily interested in how this shell model differs from that required for the nuclear case. In that spirit we now turn to a detailed discussion of the spin orbit interaction and then to level widths.

C. Spin Orbit Force Calculations

There are now four nuclear systems where the spin orbit interaction can be discussed. They involve i) the nucleon, N; ii) the delta, Δ; iii) the lambda, Λ; and iv) the sigma, Σ.

i) In the nucleon case the shell model spin orbit interaction is written in the form

$$U^{\ell\cdot s} = V^{\ell\cdot s} (\vec{\ell}\cdot\vec{s}) \left(\frac{\hbar}{m_\pi c}\right) \frac{1}{r}\frac{df}{dr}$$

where the level positions suggest a strength parameter of $V_N^{\ell\cdot s}$ = 17-20 MeV with the force attractive for the $j = \ell + 1/2$ case. We look for the origin of this force in the two body meson exchange potential. There the major contributions to $v_{NN}^{\ell\cdot s}$ come from the ρ and ω vector meson exchange, the tensor coupling (especially the ρ meson contribution), as well as two pion exchange with excitation of an intermediate Δ (3-10 MeV. OHTA et al.).[25] Beyond the two body contributions there are the exchange forces in the N-nucleus interaction.

ii) In the Δ-nucleus case, Horihawa, Thies and Lenz[26] have recently extracted a phenomenological spin-orbit force from pion-nucleus scattering data. They find

$$V_\Delta^{\ell\cdot s} = -10 - i\ 4 \text{ MeV}$$

with the force attractive for $j = \ell + 1/2$. The meson exchange description of this force is not well developed.

iii) We have seen that the Λ nucleus spin-orbit interaction will be rather different because of the $I = 0$ character of the Λ. Neither the vector exchange nor the tensor coupling of the ρ meson will contribute. Brockmann and Weise[27] have calculated the average isoscalar nuclear field in a Hartree Foch calculation by considering the contribution of σ and ω exchange. They find the scalar and vector two body potentials $v_{\Lambda N}^{s}$ and $v_{\Lambda N}^{v}$ are significantly weaker than the corresponding NN terms

$$V_{\Lambda N}^{s} = \frac{1}{3} V_{NN}^{s}, \quad V_{\Lambda N}^{v} = (0.2 - 0.6)\, V_{NN}^{v} .$$

However they do not use the SU_3 values for the coupling constants. They find that the nuclear central and spin orbit interactions are

$$V_{\Lambda}^{c} \approx \frac{1}{2} V_{N}^{c}, \quad V_{\Lambda}^{\ell\cdot s} \sim \frac{1}{4} V_{N}^{\ell\cdot s} .$$

Noble[28] has recently shown that if the SU_3 prescription for the coupling constants is used in the two body calculation, the resulting large value of the Thomas term in the two body potential is cancelled by the tensor coupling of the ω meson. The resulting two body spin orbit interaction is

$$v_{\Lambda N}^{\ell s} = 2.4 \pm 0.6 \text{ MeV} .$$

iv) Pirner[29] has suggested a different way of estimating the Λ and Σ nucleus interaction. He argues that if the nucleon spin-orbit interaction comes from ρ and ω exchange, it arises from a relatively short range part of the interaction. In that case the underlying quark "bags" are overlapping and a description of the interaction in terms of quark and gluon exchange is appropriate. Thus the baryon nucleus interaction can be discussed in terms of valance quarks outside a multiquark core (see Figure 25). The interaction arises from a quark exchange interaction but because they carry color a gluon exchange is also necessary to preserve the color singlet character of the total system.

The nucleon is made up of three quarks of the u and d flavors. The Λ and Σ are made up of u and d quarks coupled to a s quark. Because the core has zero strangeness only the two u and d quarks can participate in the Λ and Σ nucleus interactions. Thus in the coupling to the average nuclear field:

$$V_\Lambda^c \cong V_\Sigma^c = \frac{2}{3} V_N^c$$

in agreement with table V.

However the Λ and Σ differ in the spin, isospin character of their (ud) diquark

$$\Lambda = s + (ud)_{\substack{S=0 \\ I=0}}$$

$$\Sigma = s + (ud)_{\substack{S=1 \\ I=1}} .$$

This suggests that the Λ spin dependent interactions will be weak:

$$V_\Lambda^{\ell \cdot s} \approx V_\Lambda^{SS} \approx 0 .$$

On the other hand the Σ diquark acts like a spin one object and will give a larger spin-orbit interaction than the nucleon. Pirner suggests[29] that

$$V_{\Sigma}^{\ell\cdot s} \approx \frac{4}{3} V_{N}^{\ell\cdot s} .$$

We will return to this prediction at the end of this paper.

D. Hypernuclear Level Widths

There are two aspects of the Λ-nucleus interaction that contribute to the natural level widths. The strong part of the interaction controls the widths of the observed particle hole states both with respect to the escape width and the spreading width. On the other hand a bound Λ ultimately ends up in the $1s_{1/2}$ orbit and finally decays through a strangeness violating weak decay. Before discussing the latter we review briefly some calculations of the strong interaction widths.

1. Strong Decay

Inspection of the data in figures 11, 14, 15, 18, 22, 24 shows that the widths of ph states measured in the (K^-,π^-) reaction vary from 2-10 MeV. The lower limit is dictated by the experimental mass resolution and the upper limit is determined by the difficulty of identifying a very broad state on top of a background. The natural width of these ph states primarily comes from the partial width for a Λ escaping the nucleus and the spreading width resulting from the coupling of the ph state to the large number of more complicated nuclear excitations that are nearby in energy

$$\Gamma(\Lambda\, n^{-1}) = \Gamma_\Lambda^{\text{escape}}(B_\Lambda) + \Gamma^{\text{spreading}} .$$

Auerbach and VanGiai[30] have performed Hartree Fock calculations of the particle hole excitation spectrum in the continuum for several light nuclei. They include both central and residual interactions for the Λ and extract the Λ escape and spreading widths. The spreading width for deep neutron hole states is not included. Figure 26 shows a comparison of the calculated one particle one hole strength distribution to the yield distribution in the $Li^6(K^-,\pi^-)^6_\Lambda Li$ reaction. The broad peak at $B_\Lambda \simeq -7$ MeV they interpret as the unbound

P orbit substitution state and fit the observed 8 MeV width very well. For this state $\Gamma^{spreading}$ is relatively small and the shape is dominated by the escape width. In their calculation the s orbit substitution peak is large but very narrow compared to the 3 MeV wide peak observed at $B_\Lambda \cong$-14 MeV. In this case the Λ in the $1s_{1/2}$ orbit is bound and it is the spreading width of the deep-lying neutron hole that contributes. They have neglected this effect in their calculation. Overall these calculations suggest that the observed widths can be understood in the context of traditional nuclear structure calculations.

2. Weak Decay

In a bound hypernuclear state, the Λ is trapped in the strong field of the nucleus. Because it receives an effective charge, the Λ can stimulate gamma ray emission and ultimately will end up in the $1s_{1/2}$ orbit. We ignore here the possible existence of metastable states. Having achieved the lowest orbit subsequent strong interactions with the nucleons are restricted to elastic scattering. The final transition to normal nuclei is energetically very favorable ($\Delta M \cong 176$ MeV) but it requires a strangeness violating weak decay. Thus the hypernuclear ground state is expected to have a lifetime characteristic of weak decay, $\sim 10^{-10}$ seconds.

To understand this process we first turn to free Λ decay. The lifetime is 2.63×10^{-10} seconds and is dominated by mesonic decay

$$\Lambda^0 \rightarrow \begin{matrix} p\ \pi^- & (64\%) \\ n\ \pi^0 & (36\%) \end{matrix} + 37 \text{ MeV} .$$

The partial rates for leptonic and photon decay are several orders of magnitude smaller. The center of mass momentum in the final two body state is $q_{CM} \cong 100$ MeV/c with the recoiling nucleon getting ~ 5 MeV. If M_0 and M_1 are the amplitudes for the s wave and p wave contributions to this final state then

$$\Gamma(\Lambda \to p\,\pi^-) = (M_0^2 + M_1^2)q_{CM} .$$

Experiments show that

$$\frac{M_1^2}{M_1^2+M_2^2} = 0.11 \pm 0.02$$

so the decay is dominated by the s wave, parity nonconserving and strangeness nonconserving process.

When the Λ is bound to a nucleus, this mesonic decay mechanism, Γ_M, is modified significantly. On one hand B_Λ = 1-25 MeV so the phase space for the mesonic decay is significantly reduced. On the other hand the recoiling nucleon is so far below the fermi sea ($p_N^{recoil} = 100$ MeV/c, $E_N = 5$ MeV) that Pauli blocking of the low orbits is a significant factor. Both these effects may be small in very light nuclei but should be significant for $A \gtrsim 10$.

There is another decay mode available in a nucleus, however. The Λ can convert to a nucleon in a direct scattering process with no production of a free meson.

$$\Lambda + \{\begin{matrix} p \\ n \end{matrix}\} \to n + \{\begin{matrix} p \\ n \end{matrix}\} + 176 \text{ MeV} .$$

This nonmesonic mode can be thought of (see Figure 27a) as the exchange of one (or more) mesons produced at a weak vertex and absorbed at a strong vertex. Thus the strangeness violation is achieved and the two final nucleons share the 176 MeV released. Dalitz[31] has estimated that the rate for this nonmesonic decay, Γ_{NM}, is about one half the free rate, Γ_Λ, in ^{5}He and increases to twice Γ_Λ for large A nuclei. Adams[32] has worried about the initial and final state interactions and especially about the role of short range correlations that keeps the Λ and nucleon apart (see Figure 27b). In a nuclear matter calculation he finds that $\Gamma_{NM} = 1/2\ \Gamma_\Lambda$ with no correlation but decreases to $\Gamma_{NM} = 0.06\ \Gamma_\Lambda$ with correlations. If Γ_M is also small, this leads to a prediction of very long hypernuclei lifetime.

The experimental data on the weak decay of hypernuclei come primarily from nuclear emulsion and bubble chamber measurements.[34] A pion spectrum observed in the decay of $^4_\Lambda$He is shown in Figure 28. If the four partial decay rates are $\Gamma_M^{\pi^-}$, $\Gamma_M^{\pi^0}$, Γ_{NM}^{p}, Γ_{NM}^{n}, then

$$1/\tau = \Gamma_{total} = \Gamma_M^{\pi^-} + \Gamma_M^{\pi 0} + \Gamma_{NM}^{p} + \Gamma_{NM}^{n}$$

$$= \Gamma_M^{\pi^-} \left[\left(1 + \frac{\Gamma_M^{\pi^0}}{\Gamma_M^{\pi^-}}\right) + \frac{\Gamma_{NM}}{\Gamma_{\pi^-}} \right] .$$

If we assume that in the nucleus the ratio $\Gamma_M^{\pi^0}/\Gamma_M^{\pi^-}$ is to first order still the free value of 0.56, then

$$1/\tau \approx \Gamma_M^{\pi^-} \left[1.56 + \left(\frac{\Gamma_{NM}}{\Gamma_{\pi^-}}\right)\right] .$$

The cases[33] where τ has been measured are shown in Figure 29a. All but one experiment deal with H and He for which both A and B_Λ are too small (see Table 3) to strongly suppress Γ_M. This is supported by the measured values[34] of $\Gamma_{NM}/\Gamma_M{}^{\pi^-}$ shown in Figure 29b which shows a large increase for A > 5. The lifetime of ${}^{16}_{\Lambda}O$ was measured at Berkeley[33] using the recoil distance method and the Bevatron ^{16}O beam. Although the statistics were poor and the background severe they extract a lifetime of $86 \pm 30 \times 10^{-12}$ sec. The limited data[34] on thefraction of neutron stimulated nonmesonic decays is shown in Figure 30.

In summary the contribution of strange currents to the four fermion weak interaction is not well studied. The decay of hypernuclei, Γ_{NM}, is an idea case in which to measure it but better quality and more detailed data is required. The existing data does not seem to support the predictions of Adams.

V. Nuclear Structure - Σ

A. General Features

Although the existence of narrow Σ hypernuclear levels have only recently been discovered[15] the broad outlines of the Σ shell model have started to emerge. States have been observed in ${}^{9}_{\Sigma}Be$ and ${}^{12}_{\Sigma}C$ (reference 15) and ${}^{6}_{\Sigma}Li$ and ${}^{16}_{\Sigma}O$ (reference 17). They have widths comparable to the widths of corresponding Λ hypernuclear states (see Figure 15). The character of the $(\Sigma\, N^{-1})$ particle hole states is somewhat more complicated than the Λ case since the Σ has isotopic spin 1. Thus the resulting configurations can have I = 1/2 or 3/2 and are a mixture of Σ^-, Σ^0, Σ^+ particles with neutron and proton holes. Assuming that the isospin multiplet splittings

are small one can work out the isospin assignments using the two reactions

$$K^- + n \rightarrow \pi^- + \Sigma^0 \quad \Delta I_{Nucleus} = 1/2,\ 3/2$$

$$K^- + p \rightarrow \pi^+ + \Sigma^- \quad \Delta I_{Nucleus} = 3/2$$

for members of the same multiplet in different nuclei. We have seen from ${}^{9}_{\Sigma}Be$ (Figure15) that the Σ binding is about 3 MeV less than the Λ. Bertini has used this data to estimate the central potential well depth[35] and finds $V_{\Sigma}^{c} \approx 21$ MeV. Independently Batty[36] has analyzed the widths and shifts that the nuclear field generate in Σ^- atom x-ray studies and finds that $V_{\Sigma}^{c} \approx 26$ MeV. All this is consistent with a slightly shallower well for the Σ relative to the Λ. We turn now to two topics of particular interests: level widths and the strength of the spin-orbit interaction.

B. Σ Hypernuclear Level Widths

We are concerned here with the Σ in the strong nuclear field which gives the sigma nucleon particle holes states, $(\Sigma^{+1}\ N^{-1})$, an escape width and a spreading width as illustrated in Figure 31. Sigma escape widths will be comparable to Λ escape widths for comparable binding energies. These are of the order of 0-5 MeV. The spreading widths are rather different since the ΣN^{-1} ground state lies $\sim$ 80 MeV up in the ΛN^{-1} spectrum and the ΣN to ΛN coupling cannot in general be neglected.

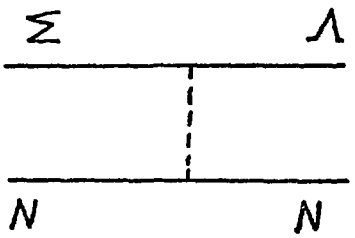

Indeed the Batty analysis of the Σ x-ray data suggests that

$$\Gamma_{\Sigma} = 2\ \mathrm{Im}V_0 = 22\ \mathrm{MeV}$$

for a Σ in the 1s orbit of $^{12}_{\Sigma}C$.

Gal and Dover[37] have used the Watson relation:

$$\Gamma = v\,\sigma\,\rho$$

to make a nuclear matter estimate. Here σ is the ΣN → ΛN conversion cross section at velocity v in nuclear matter of density of ρ. In this and more realistic calculations they find Γ = 20-50 MeV.

$$\Gamma_{1s}^{\Sigma}\ (^{12}C) \sim 22\ \mathrm{MeV}$$

$$\Gamma_{1p}^{\Sigma}\ (^{12}C) \sim 15\ \mathrm{MeV}$$

to which the escape width must be added.

These various estimates are large compared to for example the ∼ 8 MeV width observed in ^{9}Be. Two explanations have been suggested for this discrepancy. Kisslinger[38] points out that in the two body ΣN → ΛN conversion there is in the final state a center of mass momentum of q_{CM} = 290 MeV/c. This large momentum transfer corresponds to short distance in the relative coordinate of the final state. But this is precisely where the hard core aspect of the interaction has reduced the amplitude of the relative wave function. Thus Kisslinger suggests that the Watson formula overestimates the width

for these high momentum transfer processes. He finds that the correlated width is

$$\Gamma_{\Sigma}^{\text{correlated}} \simeq 2 \text{ MeV} .$$

We note that a similar argument would seem to apply to the weak decay process $\Lambda N \rightarrow NN$ which we discussed above. Indeed this is related to the calculation of short range effects by Adams.[32]

A rather different mechanism has been suggested by Gal and Dover.[37] They point out that for low momenta ($q_{\Sigma} < 200$ MeV/c) the Nijmegan potential description of the scattering data predicts that the $\Sigma N \rightarrow \Lambda N$ conversion is dominated by the I = 1/2, $^3S_1$ triplet channel. Thus one may be able to select particular ($\Sigma\ N^{-1}$) states for which the I = 3/2 and $^1S_0$ singlet channel is dominant is which case the $\Sigma N \rightarrow \Lambda N$ coupling would be weak. They find for the I = 3/2 and I = 1/2 P orbit substitution states of $^{12}_{\Sigma}C$ that

$$\Gamma_{I=1/2}^{\text{spreading}} = 21 \text{ MeV} \quad \text{and} \quad \Gamma_{I=3/2}^{\text{spreading}} = 6 \text{ MeV} .$$

to which Γ^{escape} must be added.
Note that in some s orbit substitution states the width may be large because of the width of the deep lying nucleon hole state. As more data accumulates, the relative role of these two different mechanisms will be evaluated.

C. Σ-Spin Orbit Interaction

As we have seen the nuclear spin orbit interaction for a Λ is much smaller than that of the nucleon. This is what we might expect in a boson exchange description of the ΛN interaction and also comes nicely out of

of the quark model arguments of Pirner.[29] The Σ hyperon case is different yet again since it has isospin one. Pirner suggests that it may generate a spin orbit interaction stronger than the nucleon case. It is of great interest therefore to study the $^{16}_{\Sigma}O$ excitation spectrum. Figure 32 shows schematically the positions of the I = 3/2 p orbit substitution states in $^{16}_{\Sigma}O$ under the assumption a) that $V_{\Sigma}^{\ell\cdot s}$ is small and b) that $V_{\Sigma}^{\ell\cdot s} \approx V_{N}^{\ell\cdot s}$ as suggested by Pirner. In the former case one looks for two narrow 0^+ states very much like $^{16}_{\Lambda}O$. In the latter case, these two peaks will coalesce into one narrow state, giving a rather different excitation spectrum. An experiment[17] to look for these states is now in progress at BNL.

In conclusion we see that Λ and Σ hypernuclear spectroscopy has developed significantly over the past several years. A wide variety of problems have been examined in the lab and have provided a strong stimulus for detailed calculations. The issues cover the full range from meson exchange forces, weak interactions, to color electric forces. The major technical problems lie in the area of getting data with better statistics and resolution as well as a wider range of kaon momenta. The physics issues discussed here are varied and fundamental and could play an important role in the research program of a new high intensity proton accelerator.

References

* Work supported in part by USDOE contract DE-AC02-76ERO.3244.A006

1. G. D. Rochester and C. C. Butler, Nature 160 (1947) 855.

2. M. Danysz, J. Pniewski, 1952; see R. H. Dalitz, Rep. Progr. Physics 20 (1957) 163.

3. G. E. Brown, A. D. Jackson, The Nucleon-Nucleon Interaction (Amsterdam: North-Holland) 1976.

4. J. J. de Swart, Nukleonika 25 (1980) 397.

5. M. M. Nagels, T. A. Rijken, and J. J. de Swart, Phys. Rev. D15, 2547 (1977); M. M. Nagels, T. A. Rijken, and J. J. de Swart, Phys. Rev. D20, 1633 (1979).

6. O. Braun, H. J. Grimm, V. Hepp, H. Stroebele, C. Thoel, T. J. Thouw, F. Gandini, C. Kiesling, D. E. Plane, and W. Wittek, Nuc. Phys. B124 (1977) 45.

7. M. May in Proc. Second Int. Topical Conf. on Meson-Nuclear Physics, Houston, 1979, AIPCP#54 (AIP, New York 1979) p. 658.

8. R. L. Saffe, Phys. Rev. Lett. 38 (1977) 195, Errato 38 (1977) 617.

9. A. S. Carroll, I. H. Chiang, R. A. Johnson, T. F. Kycia, K. K. Li, L. S. Littenberg, AGS Experiments #722 and 703.

10. M. Bejidian, A. Filipkowski, J. Y. Grossiord, A. Guichard, M. Gusakow, S. Majewski, H. Piekarz, J. Piekarz, J. R. Pizzi, Phys. Lett. B62 (1976) 62; M. Bedjidian, E. Descroix, J. Y. Grossiord, A. Guichard, M. Gusakow, M. Jacquin, M. J. Kudta, H. Piekarz, J. Piekarz, J. R. Pizzi and J. Pniewski, Phys. Lett. 83B, 252 (1979).

11. J. L. Friar and B. F. Gibson, Phys. Rev. C18, 908 (1978); B. F. Gibson and D. R. Lehman, Phys. Lett. 83B, 289 (1979); Nucl. Phys. A329, 308 (1979); B. F. Gibson and D. R. Lehman, Phys. Rev. C (to be published).

12. J. C. Herrera, J. J. Kolata, H. Kraner, C. L. Wang, R. Allen, D. Gockley, A. Hassan, A. Kanofsky and G. Loro, Phys. Rev. Lett. 40, 158 (1978).

13. R. E. Chrien, M. May, H. Palevsky, R. Sutter, P. Barnes, S. Dytman, D. Marlow, F. Takeutchi, M. Deutsch, R. Cester, S. Bart, E. Hungerford, T. M. Williams, L. S. Pinsky, B. W. Mayes, and R. L. Stearns, Physics Lett. 89b (1979) 31.

14. C. B. Dover, R. H. Dalitz, A. Gal and G. Walker, Physics Lett. 89B (1979) 26.

15. B. Povh, Annual Review of Nuclear and Particle Science 28 (1978) 1; R. Bertini et al., Phys. Letts. 90B (1980) 375.

16. A. Bouyssy, Phys. Lett., to be published and R. Bertini, O. Bing, P. Birien, K. Braune, W. Brückner, H. Catz, A. Chaumeaux, M. A. Faessler, R.-W. Frey, D. Garreta, T. J. Ketel, K. Kilian, B. Mayer, J. Niewisch, B. Pietrzyk, B. Povh, H. G. Ritter and M. Uhrmacher, Nuc. Phys. A, to be published and CERN preprint EP180-159.

17. E. Hungerford, S. Bart, R. Hackenburg, B. Mayes, L. Pinsky, K. Sekharan, R. E. Chrien, M. May, D. Maurizio, H. Pickarz, J. Piekarz, Y. Xu, S. Chen, P. Barnes, B. Bassalleck, R. Eisenstein, R. Grace, P. Pile, R. Reider, W. Wharton, R. Stearns, contribution to this conference and B.A.P.S. (1981).

18. R. Bertini, O. Bing, P. Birien, W. Brückner, H. Catz, A. Chaumeaux, J. M. Durand, M. A. Faessler, T. J. Ketel, K. Kilian, B. Mayer, J. Niewisch, B. Pietrzyk, B. Povh, H. G. Ritter and M. Uhrmacher, Phys. Lets. 83B (1974) 306.

19. W. Brückner, M. A. Faessler, T. J. Ketel, K. Kilian, J. Niewisch, B. Pietrzyk, B. Povh, H. G. Ritter, M. Uhrmacher, P. Birien, H. Catz, A. Chaumeaux, J. M. Durand, B. Mayer, J. Thirion, R. Bertini, O. Bing, Phys. Lett. 79B (1978) 157.

20. R. H. Dalitz and A. Gal, Annals of Physics (N.Y.) 116 (1978) 167; J. D. Walecka, Ann. Physics 83 (1974) 491.

21. F. Mujib, M. Shoeb, Q. N. Usmani, M. Z. R. Khan, J. Phys. G: Nucl. Phys., in print.

22. A. Bouyssy, Phys. Letts. 84B (1979) 41.

23. C. B. Dover, A. Gal, S. Kahana, D. J. Millener, private communication.

24. S. Bart, L. Pinsky, R. Hackenburg, E. Hungerford, D. Marlow, F. Takeutchi, P. Pile, N. Colella, B. Bassalleck, R. Grace, W. Wharton, P. Barnes, M. Deutsch, J. Piekarz, R. L. Stearns, R. Cester, M. May, H. Piekarz, R. E. Chrien, Y. Xu, R. Sutter, H. Palevsky, contribution to Int. Conf. on Nuclear Physics, Berkeley 1979 and the B.A.P.S. (1981).

25. K. Ohta, T. Terasawa, and M. Tokyama, preprint.

26. Y. Horikawa, M. Thies and F. Lenz, to be published in Nuc. Phys. and MIT preprint CTP-#844.

27. R. Brockmann, W. Weise, Phys. Rev. C16 (1977) 1282; R. Brockmann, W. Weise, Phys. Lett. 69B (1977) 167.

28. J. V. Noble, Phys. Letts. 89B (1980) 325.

29. H. J. Pirner, Phys. Lett., to be published.

30. N. Auerbach, N. Van Giai, S. Y. Lee, Phys. Letts. 68B (1977) 225; N. Auerbach, N. Van Giai, Phys. Letts. 90B (1980) 354.

31. R. H. Dalitz, in Proc. Int. Conf. Hyperfragments, St. Cergue (1964) P. 147 (CERN Publication No. 64-1).

32. J. B. Adams, Phys. Rev. 156 (1967) 1611.

33. K. J. Nield, T. Bowen, G. D. Cable, D. A. De Lise, E. W. Jenkins, R. M. Kalbach, R. C. Noggle, A. F. Pifer, Phys. Rev. C13 (1976) 1263 and references therein.

34. G. Keyes et al., Phys. Rev. Letters 20 (1968) 819; G. Keyes, Thesis ANL/HEP 6907 (1969); G. Keyes et al., N.P. 67B, 269 (1973); N. W. Holland, Nuovo Cim. 32 (1964) 48; K. N. Chaudhari et al., Proc. Indian Acad. Sc. 69A (1969) 78; G. Bohm et al., N.P. B16, 46 (1970); R. J. Prem, P. H. Steinberg, P.R. 136, 1803 (1964); C. T. Murphy, Proc. Int. Conf. on Hypernuclear Phys. 1969, Argonne Nat. Lab, p. 438; J. McKenzie, Proc. Int. Conf. on Hyperfragments, Argonne, 1979, p. 403; N. K. Rao, Proc. Indian Acad. Sc. 71A (1970) 100; G. Coremans et al., Nucl. Phys. B16 (1970) 209; H. G. Miller et al., Phys. Rev. 167 (1968) 922; G. Bohm et al., N.P. B23 (1970) 93; J. P. Lagnaux et al., Nucl. Phys. 60 (1964) 97; G. Coremans et al., Bull. Inst. de Phys. de l'Université Libre de Bruxelles, No. 46 (1971); A. Montwill et al., N.P. A234 (1974) 413; D. A. Evans et al., Nuovo Cimento 39, 785 (1965); J. P. Laznaux et al., N.P. 60, 97 (1964).

35. R. Bertini in Meson-Nuclear Physics 1979 (Houston) (AIP Conf. Proc. No. 54, New York 1979) p. 703.

36. C. J. Batty, Phys. Letts. 87B (1979) 324.

37. A. Gal and C. B. Dover, Phys. Review Lett. 44 (1980) 379; A. Gal, Nukleonika 25 (1980) 447.

38. L. S. Kisslinger, Phys. Rev. Lett. 44 (1980).

Table I

YN Cross Section Data

Data		Momentum Range (MeV/c)
$\Lambda p \to \Lambda p$	σ_{el}	135-300 300-1000
$\Lambda p \to \Sigma^0 p$	σ_{inel}	300-1000
$\Sigma^+ p \to \Sigma^+ p$	σ_{el}	145-175
	$d\sigma/d\Omega$	170
$\Sigma^- p \to \Sigma^- p$	σ_{el}	142-167
	$d\sigma/d\Omega$	160
$\Sigma^- p \to \Sigma^0 n$	σ_{inel}	110-160 150-600
$\Sigma^- p \to \Lambda n$	σ_{inel}	110-160
	$d\sigma/d\Omega$	160

Σ^- capture ratio at rest

Table II

Scattering Length and Range Parameters for ΛN

	a_0	r_0	a_1	r_1	
Λp	-2.18	3.19	-1.93	3.35	fm
ΛN	-2.29	3.17	-1.88	3.36	fm
Λn	-2.40	3.15	-1.84	3.37	fm

Table III

Measured Binding Energies, A = 3, 4, 5

A	B_Λ (MeV)	J^π	Configuration
${}^{3}_{\Lambda}H$	0.13 ± 0.05	$1/2^+$	$[{}^{2}H \times \Lambda]_{J = 1/2}$
${}^{3}_{\Lambda}H$	--	$3/2^+$	$[{}^{2}H \times \Lambda]_{J = 3/2}$
${}^{4}_{\Lambda}H$	2.09 ± 0.06	0^+	$[{}^{3}H \times \Lambda]_{J = 0}$
	1.05	1^+	$[{}^{3}H \times \Lambda]_{J = 1}$
${}^{4}_{\Lambda}He$	2.39 ± 0.03	0^+	$[{}^{3}He \times \Lambda]_{J = 0}$
	1.24	1^+	$[{}^{3}He \times \Lambda]_{J = 1}$
${}^{5}_{\Lambda}He$	3.12 ± 0.02	$1/2^+$	$[{}^{4}He \times \Lambda]_{J = 1/2}$

Table IV

Measured and Calculated Values of $N_{effective}$

Target (p_K MeV/c)	N_{eff}^{total} (CERN data)	N_{eff}^{total} (Bouyssy)	$N_{eff}^{substitution}$ (Bouyssy)
$^{7}_{\Lambda}Li$ (720)	1.5 ± 0.4	1.58	1.14
$^{12}_{\Lambda}C$ (720)	1.7 ± 0.4	1.67	1.08
$^{16}_{\Lambda}O$ (720)	1.7 ± 0.6	1.97	1.21
^{40}Ca (790)	2.1 ± 0.8	2.40	1.04
^{209}Bi (640)	5.0 ± 1.8	7.00	1.01

Table V

Λ & N Shell Model Parameters - Bouyssy[22]

Parameter	Λ	N
$V^{central}$	32 ± 2 MeV	50 MeV
$V^{\ell \cdot s}$	4 ± 2 MeV	20 MeV
α (spin-spin)	-0.05 ± 0.1 MeV	0.3 MeV

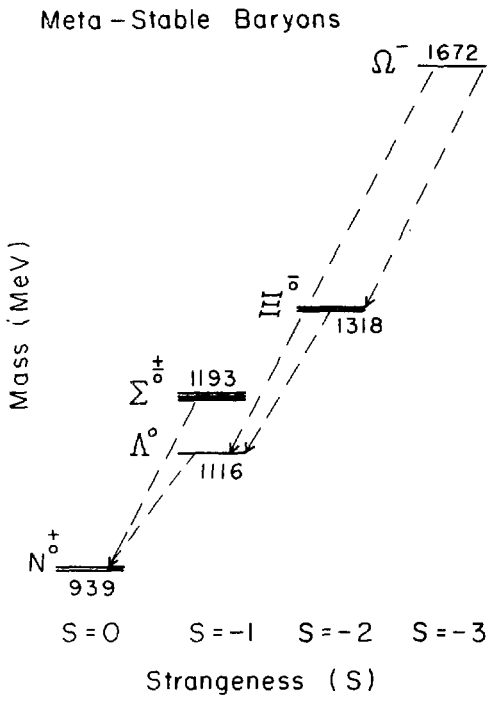

Fig. 1. Mass spectrum and dominant decay modes of non-charmed strange baryons.

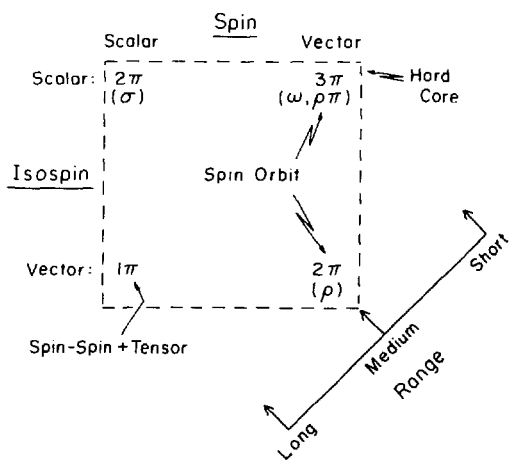

Fig. 3. Schematic description of the NN interaction in terms of the lowest order pion exchange terms.

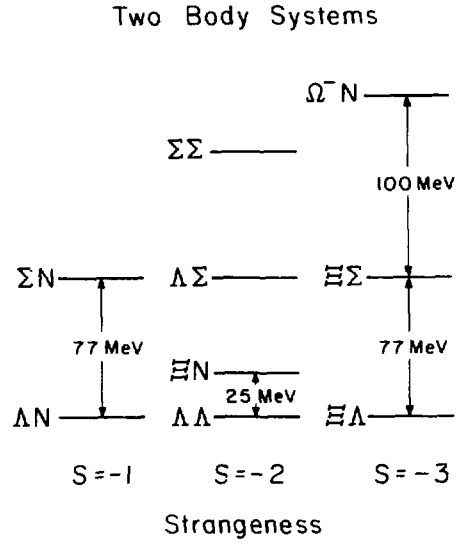

Fig. 2. Mass spectrum of two baryon configurations classified according to strangeness S= -1, -2, -3.

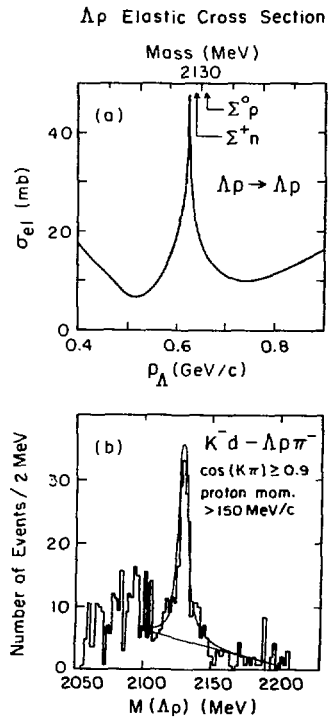

Fig. 4. a) Theoretical prediction[4] for the Λp elastic cross section from the Nijimegan potential, b) Λp enhancement observed in $K^- d \rightarrow \Lambda p \pi^-$ reaction by Braun.[6]

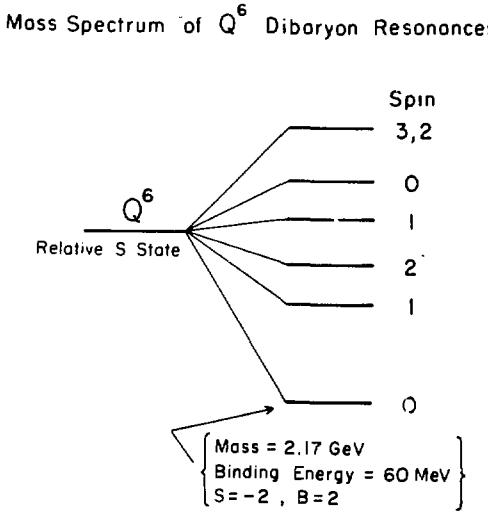

Fig. 5. Calculated spectrum of the Q^6-dibaryon resonances in a spherical bag.[4,8]

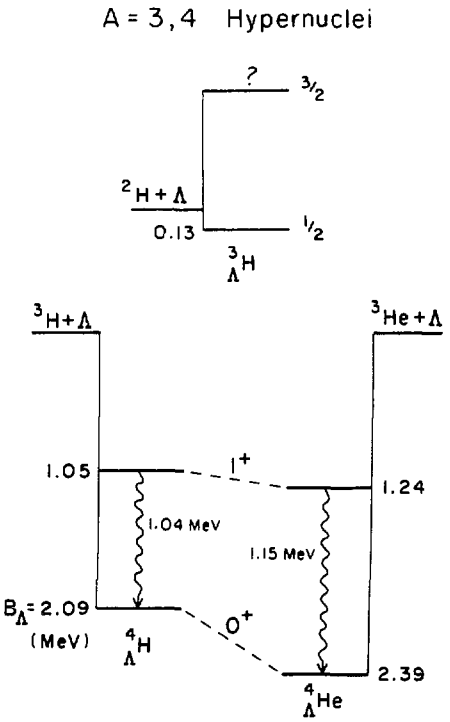

Fig. 6. The level spectra of $^3_\Lambda H$, $^4_\Lambda H$, $^4_\Lambda He$. The measured binding energies, B_Λ, are indicated.

Production of Hypernuclei

Reaction	Cross Section - c.m. (p_K = 720 MeV/c)
$K^- + n \rightarrow \pi^- + \Lambda^\circ$	1.0 mb/sr
$K^- + \begin{cases} n \\ p \end{cases} \rightarrow \pi^- + \begin{cases} \Sigma^\circ \\ \Sigma^+ \end{cases}$	0.3 ~0.1
$K^- + p \rightarrow \pi^+ + \Sigma^-$	0.6

Fig. 7. Reactions and center of mass cross sections for the conversion of nucleons into Λ and Σ hyperons.

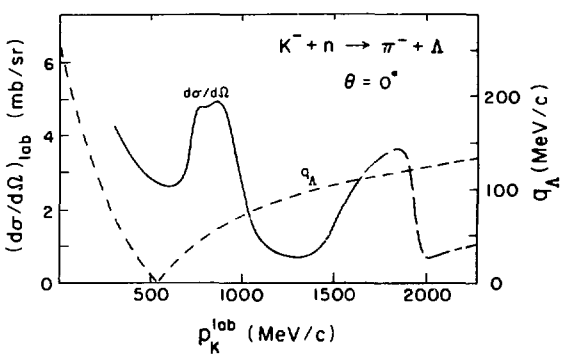

Fig. 8. Dependence of the elementary neutron to Λ conversion cross section (θ=0) in the lab (solid line) and the recoil momentum of the Λ (dashed line) on the incident kaon momentum.

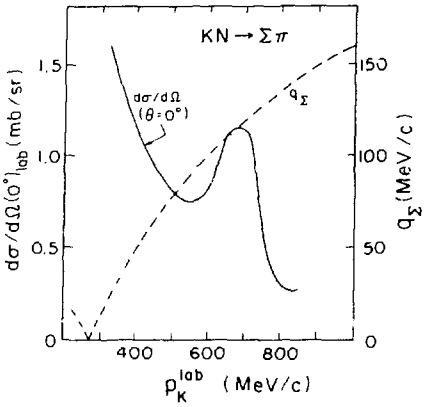

Fig. 9. Dependence of the elementary nucleon to sigma conversion cross section (θ=0) in the lab (solid line) and the recoil momentum of the Σ (dashed line) on the incident kaon

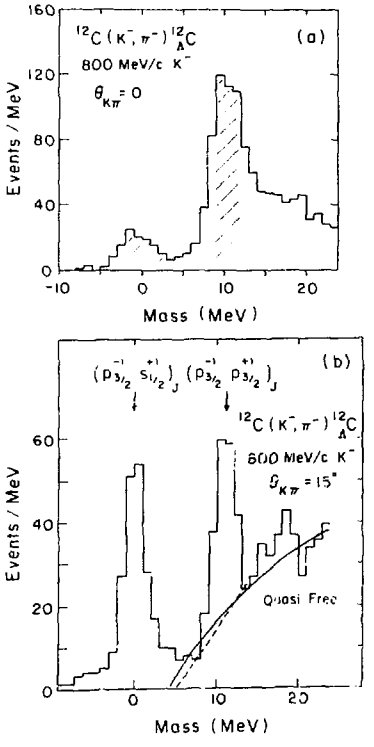

Fig. 11. Mass spectrum observed in the $^{12}C(K^-,\pi^-)^{12}_{\Lambda}C$ reaction at the AGS for a) Θ=0 degrees, b) θ=15 degrees.

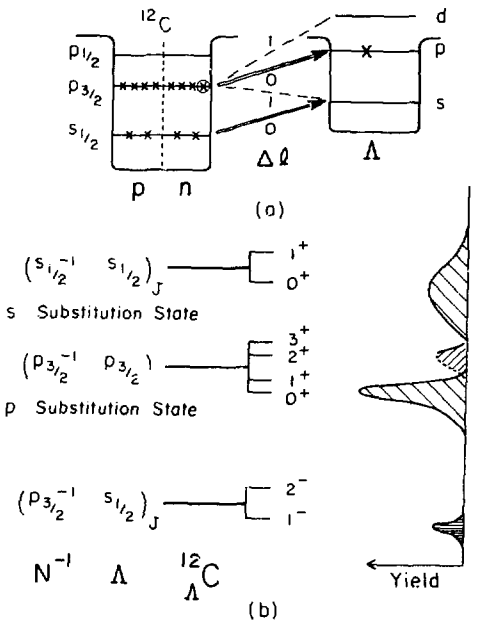

Fig. 10. a) Shell model description of the neutron to Λ conversion process in ^{12}C. b) Configurations and schematic level scheme for $^{12}_{\Lambda}C$. A schematic yield distribution at θ≈0 is shown at the right.

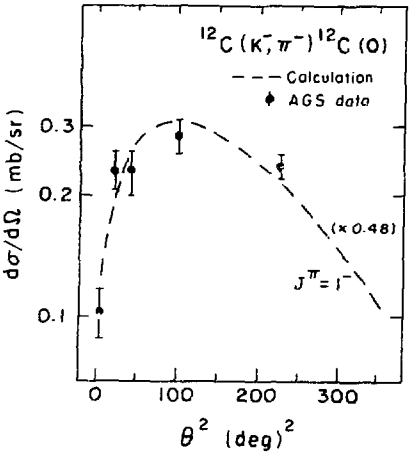

Fig. 12. Comparison of the angular distribution observed for the $^{12}C(K^-,\pi^-)^{12}_{\Lambda}C$ (0) reaction to the DWIA calculation of Dover et al.[14]

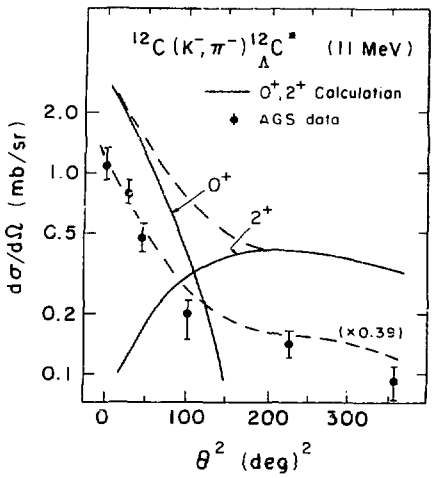

Fig. 13. Comparison of the angular distribution observed for the $^{12}C(K^-,\pi^-)^{12}C^*$ 11 MeV group to the DWIA calculation of Dover et al.[14]

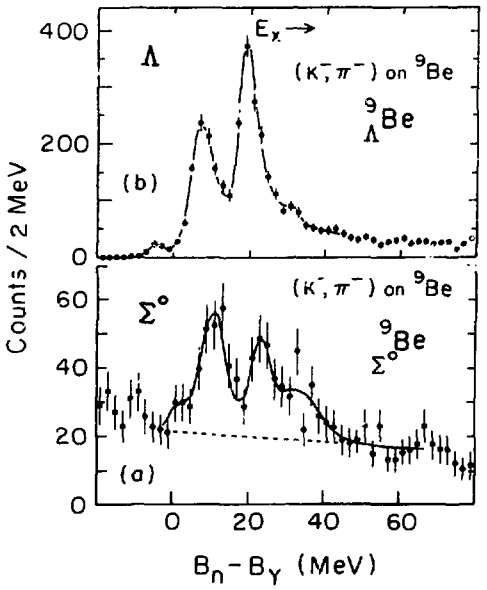

Fig. 15. Comparison of the observed pion spectra from the ^{9}Be(K-,π^-)^{9}Be reaction (θ=0) in the region of Λ formation to that for Σ formation. The ordinate is $\Delta B_{n\gamma}=(M_{H\gamma}-M_A)-(m_\gamma-m_n)=B_n-B_\gamma$.

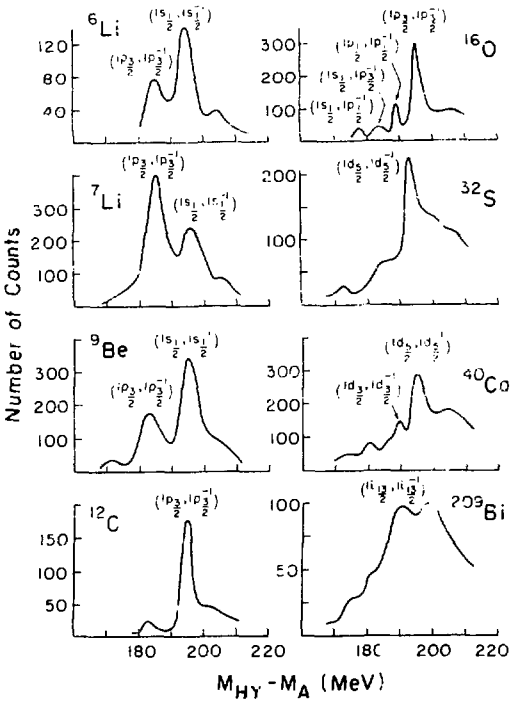

Fig. 14. Schematic representation of Λ hypernuclear spectra observed in mass range from ^{6}Li to ^{209}Bi at θ=0 by the Heidelberg-Saclay-Strasbourg collaboration.[15]

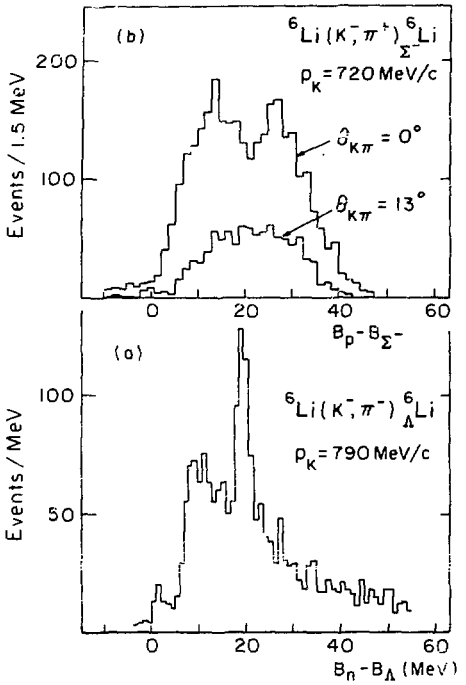

Fig. 16. Comparison of the pion spectrum observed for a) $^6Li(K^-,\pi^+)^6_{\Sigma^-}Li$ to b) that for $^6Li(K^-,\pi^\pm)^6_\Lambda Li$ at θ=0 and p_K= 720 and 790 MeV/c respectively as a function of B_N-B_Y (MeV).

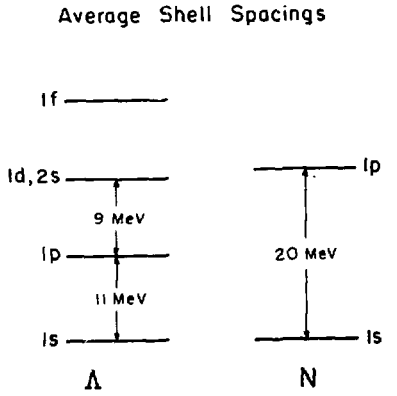

Fig. 17. Average shell spacings for the Λ-nucleus system suggested by the positions of substitution states.[18] The shell spacings for the nucleon-nucleus system are shown for comparison.

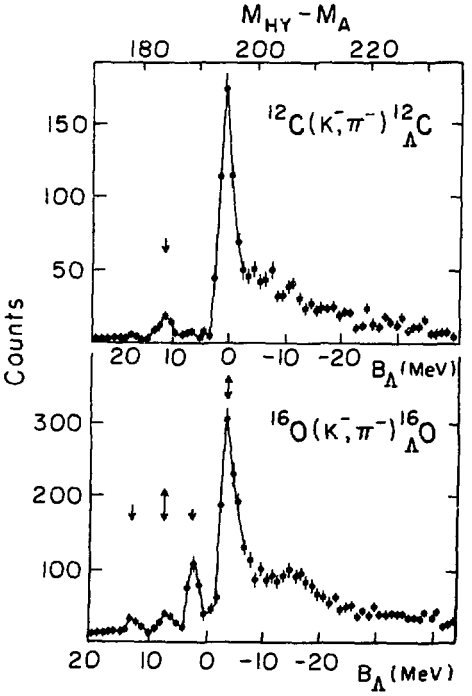

Fig. 18. Comparison of the B_Λ spectrum of a) $^{12}_\Lambda C$ to b) $^{16}_\Lambda O$ for data obtained at CERN.[19]

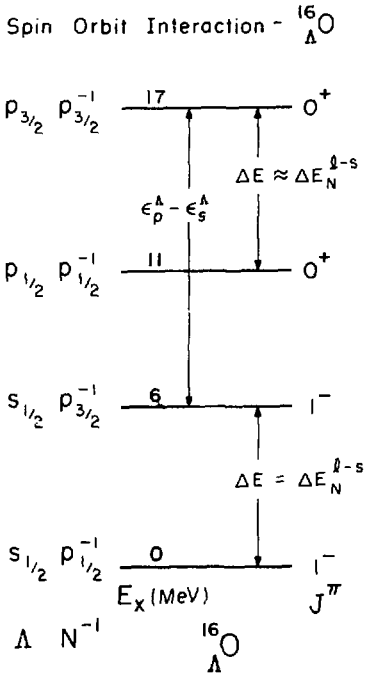

Fig. 19. Schematic level scheme for $^{16}_{\Lambda}O$.

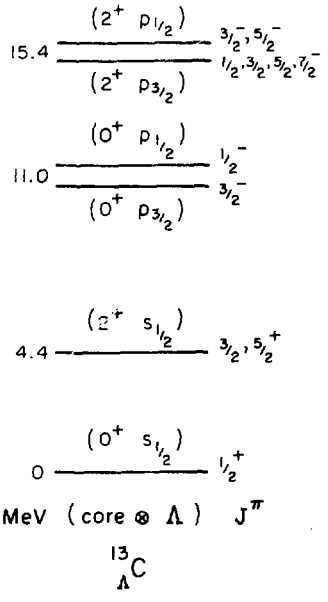

Fig. 21. Schematic level scheme for $^{13}_{\Lambda}C$ for a Λ particle coupled to a ^{12}C core.

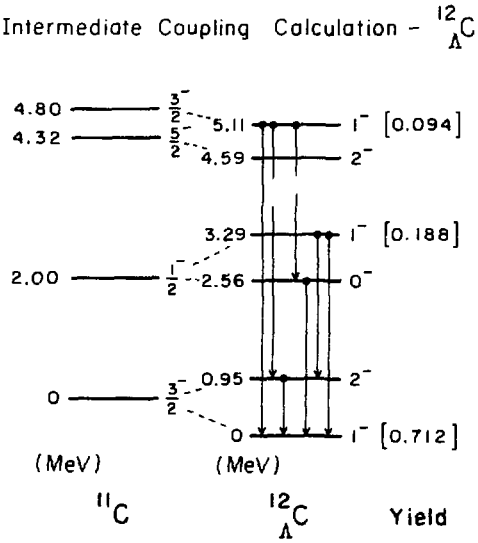

Fig. 20. Level scheme and yields calculated for $^{12}_{\Lambda}C$ by Dalitz and Gal[20] in an intermediate coupling model.

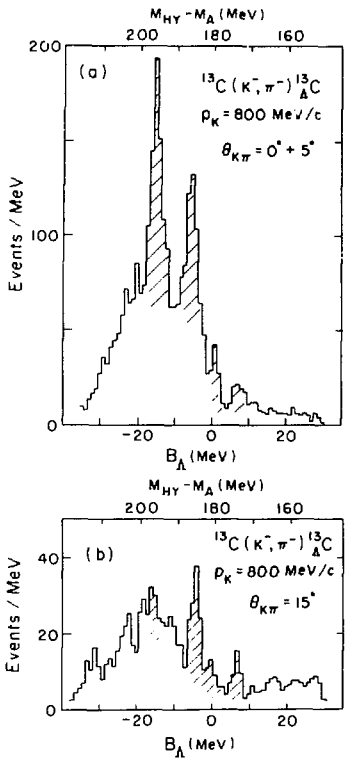

Fig. 22. Pion spectrum obtained[17] for the $^{13}C(K^-,\pi^-)^{13}_{\Lambda}C$ reaction at a) $\theta \sim 2$ degrees and b) $\theta = 15$ degrees at BNL.

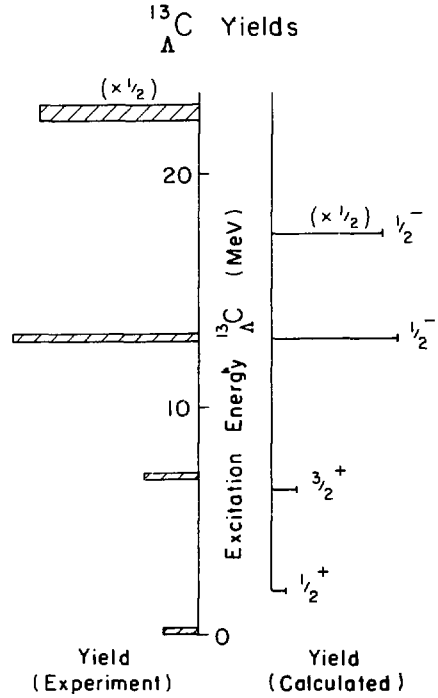

Fig. 23. Comparison of yields measured[17] at BNL for states in ^{13}C to those estimated in calculations by Dalitz and Gal[20] and by Dover et al.[23]

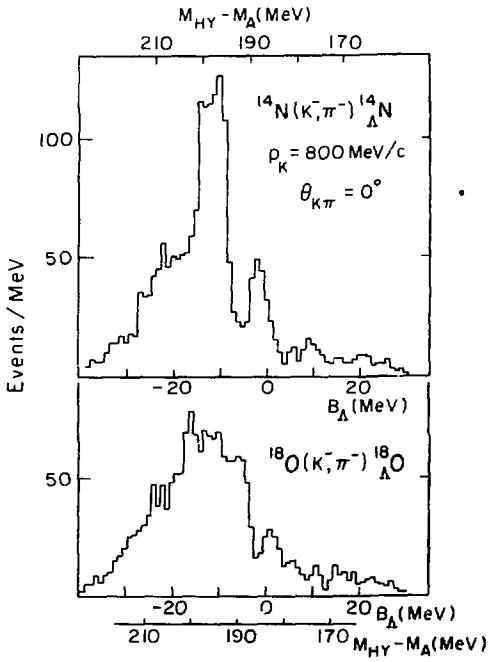

Fig. 24. Pion spectrum obtained for the (K,π) reaction at θ=0 for targets of ^{14}N and ^{16}O.

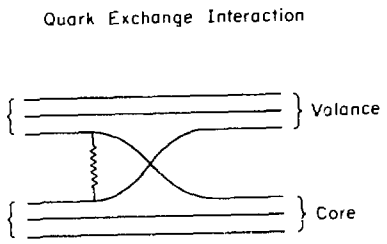

Fig. 25. Quark exchange description of the baryon-Y-nucleus interaction.

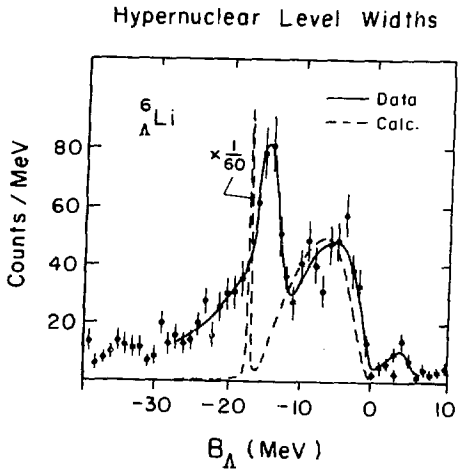

Fig. 26. Excitation spectrum of the $^6_\Lambda$Li system. The solid line is drawn through the data. The dashed line is the strength distribution of ph states calculated by Auerbach and Gial.[30]

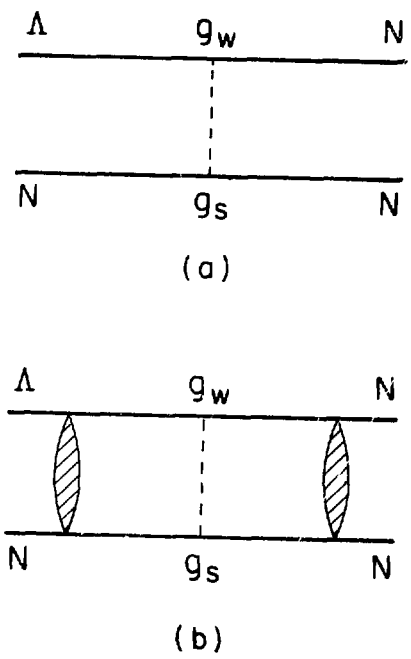

Fig. 27. Contribution to the Λ nucleus weak decay process from strangeness nonconserving ΛN scattering, a) without and b) with initial and final state scattering.

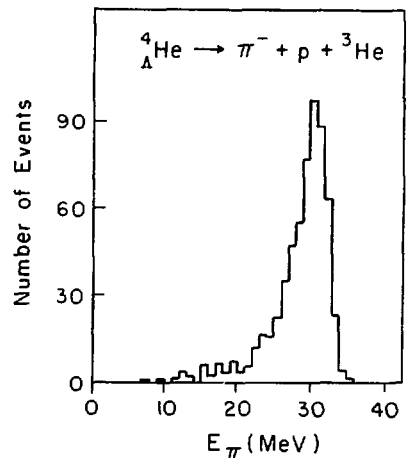

Fig. 28. Measured delayed pion spectrum obtained in emulsion measurements[34] for the $^4_\Lambda He \rightarrow \pi^- + p + {}^3He$ reaction.

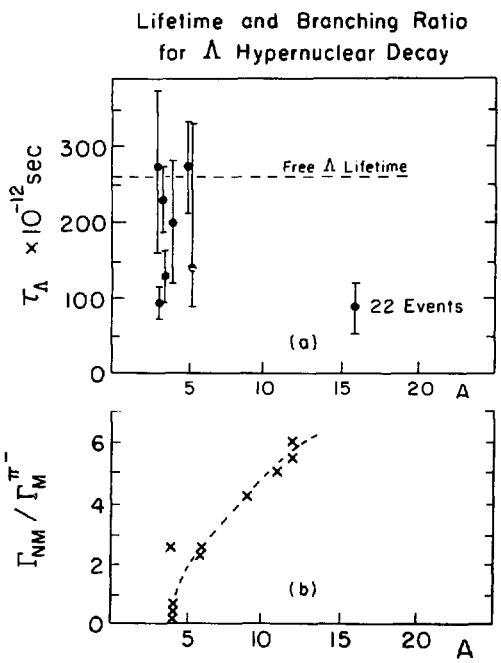

Fig. 29. Nuclear mass dependence of a) measured hypernuclear lifetimes (obtained using the recoil distance method) and b) the branching ratio for nonmesonic to π^- decay.

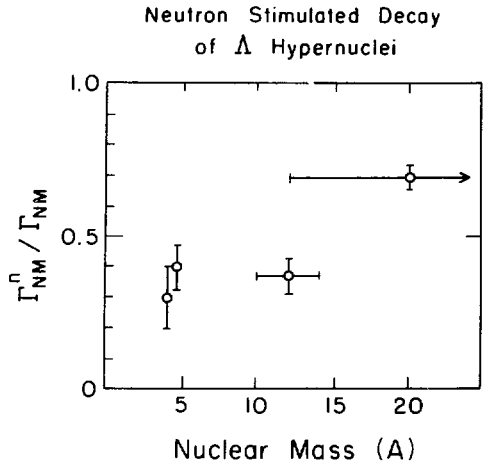

Fig. 30. Fraction of nonmesonic decay events in which the Λ scatters from a neutron.

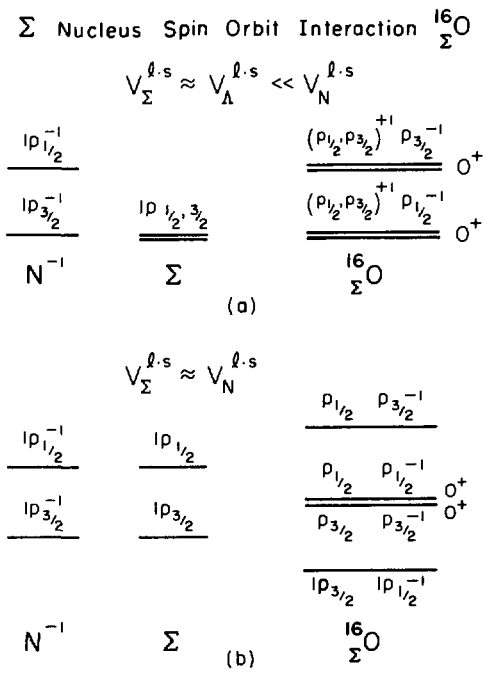

Fig. 32. Schematic level scheme for $^{16}_{\Sigma}O$ in the limit of a) $V_\Sigma^{\ell\cdot s}=0$ and $V_\Sigma^{\ell\cdot s}\approx V_N^{\ell\cdot s}$. The assumed single particle level spacings are shown at the left.

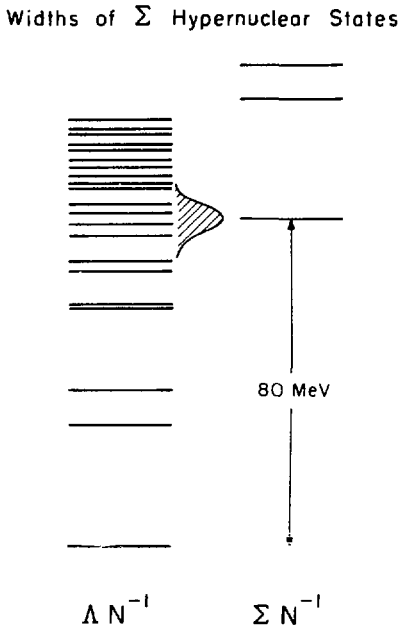

Fig. 31. Schematic level scheme for ΛN^{-1} and ΣN^{-1} particle hole states and the spreading width resulting from ΣN-ΛN coupling.

PRELIMINARY REPORT ON AN EXPERIMENT TO OBSERVE Σ HYPERNUCLEI IN THE 1p SHELL NUCLEI

by

E. V. Hungerford, S. Bart, R. Hackenburg, B. Mayes, L. Pinsky, K. Sekharan
University of Houston, Houston, Texas*

R. Chrien, M. May, D. Maurizio,
H. Piekartz, J. Piekartz, Ying-Ting Xu, Chip-Ing Chen,
Brookhaven National Laboratory, Upton, Long Island, New York†

P. Barnes, B. Bassalleck, R. Eisenstein,
R. Grace, P. Pile, R. Reider, W. Wharton
Carnegie Mellon University, Pittsburgh, Pennsylvania#

R. Stearns
Vassar College, Poughkeepsie, New York

ABSTRACT

An experiment designed to observe sigma hypernuclei in ^{6}Li and ^{16}O is in progress on the LESBI line at the Brookhaven AGS. The reaction (K^-,π^+) is used, which populates only the highest isospin states in the Σ hypernucleus. The intrinsic spectrometer resolution and finite size of the target provide an energy resolution in the excitation energy spectrum of approximately 3 MeV (FWHM). Preliminary data are interesting and may be used to extract information on the Σ-nucleus well depth and the expected Σ-hypernucleus level structure.

*Supported by US DOE Contract DE-AS05-36ER03948.

†Supported by US DOE Contract EY-76-C-02-0016.

#Supported by US DOE Contract DE-AC02-76ER0-3244.

A STUDY OF THE T = 3/2 ΣN INTERACTION

by

A.S. Rosenthal

TRIUMF, 4004 Wesbrook Mall, Vancouver, B.C., Canada V6T 2A3

One boson exchange models of the ΣN interactions have been studied, preparatory to a full investigation of Σ-hypernuclei. The simplest channel is T = 3/2 where the strong decay ΣN → ΛN is isospin forbidden and in which there is the outstanding problem of a possible Σ^-n bound state. Standard analyses[1] proceed by fitting meson coupling constants to NN and the small amount of ΛN and ΣN data, a procedure which involves a large number of free parameters. This analysis has used the OBEP with recent parameters derived from meson-baryon scattering, an independent source of information.[2] The couplings are in many cases quite different from the fitted values of Ref. 1. I find that at low energies all Σ^-n channels are repulsive except for the $^1S_0$ whose depth depends strongly on 0^+ meson exchange. Two models have been considered:

A. A single 0^+ nonet with masses at the Particle Data values. There are two free parameters, the εNN coupling and the F/D ratio. The former is fixed in fits to S-wave NN scattering and the latter has been varied to the ΣN data.

B. A pair of 0^+ nonets, one (called 0_1^+) at ~800 MeV including the S* and δ, and another (0_2^+) at ~1400 MeV including the ε and κ as suggested by bag models. There are five free parameters: ε_1NN, κ_1NN, ε_2NN and the two F/D ratios.

With model B one can fit the low energy data in more than one way and predictions are ambiguous. In model A, however, adequate fits to data are possible only in a very restricted parameter range. None of these fits allow a bound Σ^-n and they all predict a strongly repulsive $^3S_1$ channel so that such a model is unlikely to bind the Σ^-nn system. These results lead us to expect that even for the lightest Σ-hypernuclei one will be concerned with the full complications of a coupled channels problem.

---

1. M.M. Nagels, *et al.*, Phys. Rev. [illegible] (1979).

2. R.A.W. Bradford [illegible]

REMARKS ON THE S-SHELL Λ-HYPERNUCLEI

by

B. F. Gibson
Theoretical Division
Los Alamos Scientific Laboratory
Los Alamos, New Mexico 87545

and

D. R. Lehman
Department of Physics
The George Washington University
Washington, D. C. 20052

ABSTRACT

The complexities of the s-shell Λ-hypernuclei ($A \leq 5$) are explored. Difficulties associated with attempts to describe the hyperon-nucleon (YN) interaction in all such Λ-hypernuclei by simple, effective Λp and Λn potentials are examined. The explicit A dependence of the effective YN interaction due to ΛN-ΣN coupling and isospin differences among the 'nuclear core' states is investigated. The necessity of using exact four-body theory to calculate small charge-symmetry-breaking effects (in the A=4 system) using ΛN potentials fitted to free ΛN scattering data is emphasized. Possible use of s-shell hypernuclear binding energies to help distinguish among candidate YN potential parameterizations is discussed.

I. INTRODUCTION

The light (s-shell) hypernuclei provide a unique opportunity for the in-depth study of few-body bound states of baryons other than just the neutron and proton as well as a rich source of information about the basic hyperon-nucleon (YN) force. The hypertriton ($^{3}_{\Lambda}$H) binding energy places important restrictions upon the strength of the dominant spin-singlet component of the ΛN-ΣN interaction.

The A=4 isodoublet ground state energies are not consistent with a charge symmetry hypothesis for the YN interaction. The A=4 (spin-flip) excited states are very sensitive to the ΛN-ΣN coupling in the spin-triplet channel. The anomalously small ground state binding energy of ${}^{5}_{\Lambda}$He provides important information about the strength of the basic ΛN component of the YN force as well as the size of the tensor coupling in the triplet channel. (The ground and excited states of ${}^{6}_{\Lambda\Lambda}$He, the only tripley closed ls-shell nucleus known, should provide useful knowledge about the ΛΛ force and the possible existence of a di-Λ; unfortunately the data are very limited.)

In this brief report, we wish to emphasize a few of the interesting aspects of 'exact' calculations for the A=2,3,4,5 Λ-hypernuclei: 1) Simple effective force models of the ΛN potential (neglecting explicit Λ-Σ conversion) fitted to free ΛN scattering data are not valid except (with minor caveats) for the A=3 and 4 ground states. 2) The small size of the charge-symmetry-breaking (CSB) energy difference in the A=4 ground state isodoublet requires exact 4-body calculations in order to utilize or extract information about the nature of the CSB aspect of the YN force. 3) The tensor nature of the nucleon-nucleon (NN) spin-triplet force is important and should be included in meaningful hypernuclear calculations. 4) The 'suppression', that results from the reduced strength of the ΛN-ΣN coupling potential when the trinucleon core is restricted to isospin T=1/2, is significant in understanding the excitation energy between the ground and first excited states in the A=4 system. 5) Extension of this idea to the A=5 hypernucleus, which is built upon a strongly bound T=0 nuclear 'core', indicates why one should expect an anomaly in the ${}^{5}_{\Lambda}$He binding. 6) A combination of model calculations for A=3,4,5 Λ-hypernuclei should help one discriminate among various proposed OBE model parametrizations of the YN force.

We discuss first the YN two-body interaction as a simple ΛN effective force model and as a coupled ΛN-ΣN system. Our use of the separable potential approximation is explained. We then discuss in order the A=3, 4, and 5 hypernuclear systems. We close with a brief summary.

II. THE YN INTERACTION

Lack of precision data on YN scattering is a severe limitation in our characterization of that interaction. Courageous efforts have been made to parametrize potentials using 1) a combined analysis of all of the existing YN data and the extensive NN data and 2) various symmetry assumptions concerning

meson coupling in an OBE potential model of the YN and NN interactions.[1-4] We shall consider the consequences of some of these models in the following sections, but first we examine the model that results when the YN force is assumed to be independent of explicit ΛN-ΣN coupling. This model has been extensively employed in the literature in s-shell hypernuclear studies.

Such a phenomenological approach is based upon the following spin-isospin decomposition of the effective ΛN central potential (neglecting for the moment any CSB difference between Λp and Λn interactions):

$$\Lambda N: \quad V_{YN} = \bar{V}^{s}_{\Lambda N} , \bar{V}^{t}_{\Lambda N}$$

$$^{3}_{\Lambda}H: \quad V_{YN} = \frac{3}{4}\bar{V}^{s}_{\Lambda N} + \frac{1}{4}\bar{V}^{t}_{\Lambda N}$$

$$^{4}_{\Lambda}H: \quad V_{YN} = \frac{1}{2}\bar{V}^{s}_{\Lambda N} + \frac{1}{2}\bar{V}^{t}_{\Lambda N}$$

$$^{4}_{\Lambda}H^{*}: \quad V_{YN} = \frac{1}{6}\bar{V}^{s}_{\Lambda N} + \frac{5}{6}\bar{V}^{t}_{\Lambda N}$$

$$^{5}_{\Lambda}He: \quad V_{YN} = \frac{1}{4}\bar{V}^{s}_{\Lambda N} + \frac{3}{4}\bar{V}^{t}_{\Lambda N} ,$$

where it has been assumed that the singlet interaction is stronger than the triplet interaction.[5,6] Here, the YN subscript indicates that the potential describes the general hyperon-nucleon (ΛN-ΣN) interaction. Implicit in the above effective potential description is the assumption[7] that the ΛN-ΣN coupling in the YN interaction is identical in each system regardless of the isospin of the (A-1) nucleons forming the nuclear 'core'; i.e., one has assumed that the 2x2 matrix potential

$$V^{i}_{YN} = \begin{pmatrix} V^{i}_{\Lambda N} & V^{i}_{XN} \\ V^{i}_{XN} & V^{i}_{\Sigma N} \end{pmatrix} , \quad i = s,t$$

can be represented by a unique effective one-channel potential $\bar{V}^{i}_{\Lambda N}$ for A=2,3,4,5. Such is not the case.

Let us define the free interaction to be of the form

$$V^{s}_{YN} = \begin{pmatrix} V^{s}_{\Lambda N} & V^{s}_{XN} \\ V^{s}_{XN} & V^{s}_{\Sigma N} \end{pmatrix} , \qquad V^{t}_{YN} = \begin{pmatrix} V^{t}_{\Lambda N} & V^{t}_{XN} \\ V^{t}_{XN} & V^{t}_{\Sigma N} \end{pmatrix} .$$

(We note that the ΛN elastic scattering is dominated by the triplet interaction, since $\sigma = (\sigma^{s} + 3\sigma^{t})/4.$) For the $^{3}_{\Lambda}H$ system, where the np pair is restricted to be in the S=1,T=0 'deuteron' state, the relevant potentials are

$$V^s_{YN} = \begin{pmatrix} V^s_{\Lambda N} & 0 \\ 0 & 0 \end{pmatrix} \quad , \qquad V^t_{YN} = \begin{pmatrix} V^t_{\Lambda N} & 0 \\ 0 & 0 \end{pmatrix} ;$$

i.e., there is no Λ-Σ conversion unless one allows for the np T=1 'excited' state in the formalism. This is a consequence of the T=0 nature of the ${}^3_\Lambda H$ ground state (the Λ and the deuteron each being T=0 objects); the Σ has T=1 and must couple to the T=1 singlet np state to produce a hypernucleus with total T=0. For the A=4 hypernuclei, the $J^\pi=0^+$ ground state potentials are

$$V^s_{YN} = \begin{pmatrix} V^s_{\Lambda N} & -\frac{1}{3} V^s_{XN} \\ -\frac{1}{3} V^s_{XN} & V^s_{\Sigma N} \end{pmatrix}, \quad V^t_{YN} = \begin{pmatrix} V^t_{\Lambda N} & V^t_{XN} \\ V^t_{XN} & V^t_{\Sigma N} \end{pmatrix}$$

and the $J^\pi=1^+$ excited state potentials are

$$V^s_{YN} = \begin{pmatrix} V^s_{\Lambda N} & V^s_{XN} \\ V^s_{XN} & V^s_{\Sigma N} \end{pmatrix}, \quad V^t_{YN} = \begin{pmatrix} V^t_{\Lambda N} & \frac{1}{5} V^t_{XN} \\ \frac{1}{5} V^t_{XN} & V^t_{\Sigma N} \end{pmatrix}$$

(see for example, Refs. 8 and 9). In neither case is the coupling of the Λ-Σ system to a composite T=1/2 object the same as is the coupling to an elementary nucleon constituent. The singlet potential differs from the free interaction in the A=4 ground state. The triplet potential differs from the free interaction in the A=4 excited state. In each case the ΛN-ΣN coupling strength is reduced, weakening the YN interaction relative to its free strength. For the ${}^5_\Lambda He$ system, the situation is similar to that encountered with the hypertriton. A T=0,S=0 assumption for the four-nucleon 'core' (the alpha particle is bound by 28 MeV) leads to potentials of the same form as in the case of ${}^3_\Lambda H$:

$$V^s_{YN} = \begin{pmatrix} V^s_{\Lambda N} & 0 \\ 0 & 0 \end{pmatrix} \quad , \qquad V^t_{YN} = \begin{pmatrix} V^t_{\Lambda N} & 0 \\ 0 & 0 \end{pmatrix} ;$$

i.e., there is again no ΛN-ΣN coupling unless one allows for even parity, T=1 'excited' states of the alpha-like core in the formalism.[10] (Note that this does not mean that we assume a rigid, non-distorted alpha-core model; however, the formalism must be extended if coupling of T=1 and T=0 four-nucleon states is to be permitted.)

It is clear that in principle the YN interactions acting in each of the five systems (ΛN, ${}^3_\Lambda H$, ${}^4_\Lambda H$, ${}^{4*}_\Lambda H$, and ${}^5_\Lambda He$) cannot be represented by single, unique $\bar{V}^s_{\Lambda N}$

and $\bar{V}^t_{\Lambda N}$ effective potentials. In practice, one finds experimentally[11] that $V^s_{XN}\simeq 0$, so that effective potential representation of the free YN interactions is 'reasonable' when dealing with the A=4 ground states, where $V^t_{YN}({}^4_\Lambda H) \equiv V^t_{YN}(\Lambda N$ scattering). However, the triplet interactions involved in ${}^3_\Lambda H$, ${}^4_\Lambda H^*$, and ${}^5_\Lambda He$ calculations differ from the free case (i.e., the coefficient of V^t_{XN} is not unity as in free scattering), and the free effective triplet potential $\bar{V}^t_{\Lambda N}$ should not be used in those calculations.[7] ${}^3_\Lambda H$ is a possible exception since the ΛN interaction in that ground state is 3/4 singlet and $V^s_{XN}\simeq 0$ experimentally. The importance of including ΛN-ΣN coupling in calculations involving these hypernuclei has been previously noted; see, for example, Refs. 8,9,12,13, and 14.

In the numerical calculations referred to below, we assume that effective ΛN interactions $\bar{V}^{s,t}_{\Lambda N}$ (i.e., one-channel ΛN potentials determined from the free ΛN scattering parameters) can be used to describe the coupled ΛN-ΣN hyperon-nucleon system. Thus, we are restricted to estimates of the ${}^3_\Lambda H$, ${}^4_\Lambda H$ and ${}^4_\Lambda He$ ground-state energies. As just noted, this is not an entirely correct procedure in the case of ${}^3_\Lambda H$; however, since the average ΛN interaction is 3/4 singlet and only 1/4 triplet, and since the binding is weak, we shall assume that the error produced by this procedure is small. We shall also neglect in the ${}^3_\Lambda H$ case the tensor nature of the ΛN triplet force, which tends to compensate for our neglect of explicit ΛN-ΣN coupling in that channel.[14]

We use a separable potential representation of both the NN and YN interactions in all of our numerical calculations in order to have a consistent model with which to carry out the exact 4-body calculations. We use rank one potentials of the form

$$V_i = -\frac{\lambda_i}{2\mu} g_i(\vec{k})\, g_i(\vec{k}') \quad , i = s,t \ ,$$

where $g_i = (k^2 + \beta_i^2)^{-1}$ if there is no tensor component and where

$$g_t = g_c + \frac{S_{ij}}{\sqrt{8}} g_T$$

$$g_c = (k^2 + \beta_c^2)^{-1}$$

$$g_T = \xi_T k^2 (k^2 + \beta_T^2)^{-2}$$

$$S_{ij} = 3\, \vec{\sigma}_i\cdot\hat{k}\, \vec{\sigma}_j\cdot\hat{k} - \vec{\sigma}_i\cdot\vec{\sigma}_j$$

in the case of a tensor force in the spin-triplet channel. The quantity μ is the appropriate two-body reduced mass. The low-energy ΛN scattering parameters which we use to determine our separable-potential parameters are listed in Table I.

TABLE I.

The ΛN scattering lengths and effective ranges in fm for the YN potential models A-F.

Model	Ref.	$a^s_{\Lambda p}$	$r^s_{\Lambda p}$	$a^t_{\Lambda p}$	$r^t_{\Lambda p}$	$a^s_{\Lambda n}$	$r^s_{\Lambda n}$	$a^t_{\Lambda n}$	$r^t_{\Lambda n}$
A	1	-2.16	2.03	-1.32	2.31	-2.67	2.04	-1.02	2.55
B	2	-2.11	3.19	-1.88	3.16	-2.47	3.09	-1.66	3.33
D	3	-1.77	3.78	-2.06	3.18	-2.03	3.66	-1.84	3.32
F	4	-2.18	3.19	-1.93	3.35	-2.40	3.15	-1.84	3.37

TABLE II.

Separable potential parameters and properties for the NN interactions.

Spin	Model(ref.)	a_i(fm)	r_i(fm)	P_D	Q(fm^2)	λ_i(fm^{-3})	β_i(fm^{-1})	ξ_T	β_T(fm^{-1})
t	GL(16)	5.423	1.761	0.	-	0.3815	1.406	0.	-
t	P_4(15)	5.397	1.727	0.04	0.282	0.24310	1.3134	1.6894	1.5283
t	P_7(15)	5.397	1.722	0.07	0.283	0.14297	1.2412	4.4949	1.9476
s	GL(16)	-17.0	2.84	-	-	0.1323	1.130	-	-

TABLE III.

Hypertriton Λ-separation energy in MeV for YN models A-F as a function of P_D in the np triplet interaction.

YN Model	GL	P_4	P_7
A	0.90	0.56	0.35
B	0.37	0.22	0.13
D	0.12	0.06	0.03
F	0.37	0.23	0.13

These are taken from the meson exchange theoretic potentials developed by Nagels, Rijken, and deSwart.[1-4] Mass differences in the isomultiplets as well as symmetry breaking exchanges were included in a combined analysis of NN, Λp, $\Sigma^{\pm}$p, etc. data. The NN low energy scattering parameters as well as resulting potential parameters are listed in Table II.[15,16]

III. THE HYPERTRITON

$^{3}_{\Lambda}$H ($J^{\pi}=0^{+}$, T=0) is the lightest of the bound hypernuclei having a Λ-separation energy $B_{\Lambda} = B(^{3}_{\Lambda}H) - B(^{2}H) \simeq 0.13 \pm 0.05$ MeV.[17] Because the Λ-binding is weak, it was originally assumed that the loose structure would make B_{Λ} insensitive to the short range (high-momentum) character of the YN force and the tensor nature of the triplet component.[12] As noted above, we also assumed that explicit ΛN-ΣN coupling could be omitted since it was included implicitly by using the physical low-energy ΛN scattering parameters to construct the potentials. It was later pointed out that, while repulsion in the YN force and explicit ΛN-ΣN coupling were not large effects, neglecting the tensor nature of the np triplet force was a significant omission.[18] Because the average ΛN interaction is 3/4 singlet, we have neglected the tensor nature of the ΛN triplet interaction. This tends to slighty overestimate B_{Λ} but should be compensated for by our neglect of explicit ΛN-ΣN coupling in that channel which tends to underestimate B_{Λ}.[12,14] The fact that there is little or no ΛN-ΣN coupling in the dominant singlet YN interaction should ensure that our model calculations are reasonable.[11] We summarize in Table III values of $B_{\Lambda}(^{3}_{\Lambda}H)$ for the various YN potentials models with and without including the explicit tensor force nature of the np spin-triplet force. (For details of the equations used, see Refs. 12 and 19.)

Model A clearly overbinds $^{3}_{\Lambda}$H regardless of the np triplet force used. This is a result of the comparatively small values ($\leq$ 2.5 fm) for the effective ranges of the ΛN potentials in that model, as noted in Ref. 12. Although the value of B_{Λ} differs among models B,D, and F by 0.1-0.2 MeV, none of these models is obviously incorrect. (B_{Λ} for P_D=0 is not considered to be realistic, and we do not consider B_{Λ} for model D to lie significantly outside the experimental limits.) The B_{Λ} from model D are systematically smaller than those of models B and F, because the average (3/4 singlet plus 1/4 triplet) effective range is larger; $r_0 > r_0'$ implies $B_3 < B_3'$.[20] Models B and F produce very similar values of B_{Λ} because their average singlet scattering lengths and effective ranges are similar; they would produce different values of ΔB_{Λ} in the $^{4}_{\Lambda}$He-$^{4}_{\Lambda}$H isodoublet

system where differences in the Λp and Λn triplet scattering lengths and effective ranges are significant.

A recent estimate of B_Λ using a sum of local Yukawa forms (including short range repulsion) to represent the model F ΛN interaction and the Reid-soft-core potential for the np triplet interaction by Narumi, Ogawa, and Sunami gave a value of 0.17 MeV.[21] This agrees very well with our 0.13 MeV estimate for model F using an np potential model with $P_D = 7\%$, and it lends credence to the accepted use of rank one separable potentials to represent baryon-baryon interactions phenomenologically. The agreement here and for the well known case of the triton illustrates the point that the important aspects of the interactions for relatively weakly bound systems are the low-energy scattering parameters and not the short range behavior of nor the off-shell behavior generated by the potentials.

IV. THE A=4 ISODOUBLET

The latest experimental estimates of the Λ-separation energies for these $J^\pi = 0^+$ ground states are[17]

$$B_\Lambda({}^4_\Lambda\text{He}) = B({}^4_\Lambda\text{He}) - B({}^3\text{He}) \simeq 2.42 \pm 0.04 \text{ MeV}$$
$$B_\Lambda({}^4_\Lambda\text{H}) = B({}^4_\Lambda\text{H}) - B({}^3\text{H}) \simeq 2.08 \pm 0.06 \text{ MeV} .$$

Because we do not solve the complete set of tensor force equations for each model (we treat the YN triplet potentials in a central force approximation and use the truncated t-matrix approximation[22] for the NN triplet force), we consider the Λ-separation energy difference $\Delta B_\Lambda \simeq 0.34 \pm 0.07$ MeV to be a better measure of model consistency. This ΔB_Λ reflects true charge symmetry breaking in the YN interaction; simple considerations of Coulomb energies in the A=3 and 4 nuclear systems suggest that ΔB^C_Λ, the additional Coulomb energy in ${}^4_\Lambda$He due to compression of the '^{3}He core', is small and of opposite sign.[23] It is this Coulomb corrected quantity $\Delta B_\Lambda \simeq 0.36$ MeV that we estimate for each of the YN potentials defined by the low-energy scattering parameters in Table I.

The exact coupled two-variable integral equations that must be solved for the A=4 hypernuclear problem when the NN and YN interactions are represented by separable potentials are described in detail in Ref. 24. The integral equations are solved numerically without resort to separable expansions of the kernels. The resulting solutions possess the characteristics of true few-body calculations: for an attractive potential with a negative scattering length, $|a| > |a'|$ implies that V is more attractive than V' in two-body, three-body, and four-body

calculations, whereas $r > r'$ implies that V is more attractive than V' in a two-body calculation, but less attractive in three-body and four-body calculations. Even though this picture is an oversimplification in terms of scattering length and effective range, it is possible to understand ΔB_Λ from each of the models in Table I qualitatively in terms of the low-energy scattering parameters of the various models.

In our numerical calculations, we assume that effective ΛN interactions $\bar{V}^{s,t}_{\Lambda N}$ (i.e., one channel ΛN potentials determined from the free ΛN scattering parameters) can be used to describe the coupled ΛN-ΣN hyperon-nucleon system. As noted above, this can be justified for the $J^\pi = 0^+$ ground state (but not for the $J^\pi = 1^+$ excited states), where the triplet interaction is unmodified from its free form

$$V^t_{YN} = \begin{pmatrix} V^t_{\Lambda N} & V^t_{XN} \\ V^t_{XN} & V^t_{\Sigma N} \end{pmatrix} \simeq \bar{V}^t_{\Lambda N} \quad .$$

Since $V^s_{XN} \simeq 0$ in the singlet interaction,

$$V^s_{YN} = \begin{pmatrix} V^s_{\Lambda N} & -\frac{1}{3} V^s_{XN} \\ -\frac{1}{3} V^s_{XN} & V^s_{\Sigma N} \end{pmatrix} \simeq \bar{V}^s_{\Lambda N}$$

is also a good approximation. Thus, the effects of Λ-Σ conversion upon the ΛN potential parameters, including charge symmetry breaking due to meson mixing, $\Sigma^{\pm,0}$ mass differences, etc., are taken into account implicitly, but there are no explicit Σ-channels in the calculation.[24]

The Λp and Λn potential averages appropriate to ${}^4_\Lambda\mathrm{He}$ and ${}^4_\Lambda\mathrm{H}$ are

$${}^4_\Lambda\mathrm{He}: \quad V^t_{\Lambda N} = V^t_{\Lambda p} \qquad\qquad {}^4_\Lambda\mathrm{H}: \quad V^t_{\Lambda N} = V^t_{\Lambda n}$$

$$V^s_{\Lambda N} = \frac{1}{3} V^s_{\Lambda p} + \frac{2}{3} V^s_{\Lambda n} \qquad\qquad V^s_{\Lambda N} = \frac{1}{3} V^s_{\Lambda n} + \frac{2}{3} V^s_{\Lambda p} \quad .$$

Instead of using the two potential formula to obtain the required potentials, we used the excellent approximation of scattering length and effective range averages

$$a^{-1}_{\Lambda N} = \frac{1}{3} a^{-1}_{\Lambda p} + \frac{2}{3} a^{-1}_{\Lambda n}$$

$$r_{\Lambda N} = \frac{1}{3} r_{\Lambda p} + \frac{2}{3} r_{\Lambda n}$$

to parametrize the ΛN singlet interaction, etc. The resulting potential

parameters are listed in Table IV. The NN potential parameters for the model calculations were chosen to be the P_7 model; the triton binding energy is 7.05 MeV in the truncated t-matrix approximation which is only 7% below the complete model result.[22]

The results of our ${}^4_\Lambda$He-${}^4_\Lambda$H binding energy difference calculations are tabulated in Table V.[25] Because the singlet potentials are averages of Λn and Λp potentials, most of the charge symmetry breaking results from the triplet interaction differences (see Table IV). It is clear that differences between triplet scattering lengths and effective ranges for the ${}^4_\Lambda$He and ${}^4_\Lambda$H systems are very similar for models B and D. Thus one anticipates similar values of ΔB_Λ for models B and D, and these values are not inconsistent with experiment. Model A has an even larger difference in scattering length values ($\Delta a \sim -0.3$ fm vs. -0.2 fm for models B and D) and effective range values ($\Delta r \sim -0.25$ fm vs. -0.15 fm). Hence ΔB_Λ for model A is expected to be larger than that for models B and D, as is the case; it is probably outside the limits set by the experimental values. The perhaps surprisingly large model A value of ΔB_Λ results from the small values of the effective ranges in that model, which produce large values of $B_\Lambda({}^4_\Lambda\text{He})$ and enhance CSB differences. We pointed out above that these small effective ranges of the model A singlet interactions are primarily responsible for the value of $B_\Lambda({}^3_\Lambda\text{H})$ being inconsistent with experiment. It is clear from the effective ranges in Table I that model F is a much more charge symmetric model than models A,B, or D. In fact, the model F ${}^4_\Lambda$He and ${}^4_\Lambda$H scattering lengths and effective ranges in Table IV show very little difference between the two singlet sets or the two triplet sets. Thus, one anticipates a small value of ΔB_Λ, one which is too small to be consistent with the experimental binding energy difference.

Since we have used a central potential approximation in representing the ΛN triplet interaction, we have overestimated ΔB_Λ for each of the models. Although this is a non-negligible effect, we have previously shown[24] that it would not alter the conclusions drawn above and that it would bring our model D result into closer agreement with the experimental value of $\Delta B_\Lambda = 0.36$ MeV. We constructed a tensor force YN triplet potential (of the same form as that of our np triplet potential) fitted to the model D triplet phase shift and mixing parameter up to laboratory momenta of 300 MeV/c. We made the same truncated t-matrix approximation in the complete set of 4-body equations as noted above for the NN channel. Our estimate of ΔB_Λ for model D was reduced from 0.43 MeV to 0.37 MeV; see Ref. 24

TABLE IV.

Potential parametrizations and their low energy properties for the interaction averages appropriate to each A=4 hypernucleus.

Model	System	Spin	$\lambda(fm^{-3})$	$\beta(fm^{-1})$	a(fm)	r(fm)
A	$\Lambda N(^{4}_{\Lambda}He)$	s	0.4787	1.8891	-2.48	2.04
		t	0.4348	1.9660	-1.32	2.31
	$\Lambda N(^{4}_{\Lambda}H)$	s	0.4957	1.9217	-2.31	2.03
		t	0.3819	1.9608	-1.02	2.55
B	$\Lambda N(^{4}_{\Lambda}He)$	s	0.1578	1.3634	-2.34	3.12
		t	0.1670	1.4229	-1.88	3.16
	$\Lambda N(^{4}_{\Lambda}H)$	s	0.1532	1.3527	-2.32	3.16
		t	0.1542	1.4128	-1.66	3.33
D	$\Lambda N(^{4}_{\Lambda}He)$	s	0.1099	1.2549	-1.94	3.70
		t	0.1581	1.3846	-2.06	3.18
	$\Lambda N(^{4}_{\Lambda}H)$	s	0.1093	1.2607	-1.85	3.74
		t	0.1484	1.3785	-1.84	3.32
F	$\Lambda N(^{4}_{\Lambda}He)$	s	0.1532	1.3527	-2.32	3.16
		t	0.1421	1.3531	-1.93	3.35
	$\Lambda N(^{4}_{\Lambda}H)$	s	0.1525	1.3558	-2.25	3.18
		t	0.1428	1.3632	-1.84	3.37

TABLE V.

The A=4 binding energy difference ΔB_{Λ} for each of the YN models discussed in the text in the central potential approximation for the ΛN interaction.

Model	ΔB_{Λ}
A	1.32
B	0.47
D	0.43
F	0.19

for details.

In the ${}^{3}_{\Lambda}H$ and ${}^{4}_{\Lambda}He$-${}^{4}_{\Lambda}H$ calculations discussed, we have used exact few-body equations based upon separable potential approximations to the YN and NN interactions. Could one have done as well for ΔB_Λ with a simpler effective 2-body model? The answer is no. We have explicitly demonstrated this for one standard 2-body formalism:[24] in the procedure outlined by Dalitz and Downs[26] the 2-body ΛN potentials are folded with the nuclear core density to produce a Λ-${}^{3}He$ (or Λ-${}^{3}H$) effective 2-body potential which is then inserted into the Schrodinger equation to determine the Λ-separation energy. (Radial compression of the nuclear core is easily accommodated by altering the radius of the core density.) Using this formalism, we found ΔB_Λ(2-body) to be between 0.21 and 0.24 MeV, depending upon the core compression permitted, for model D.[24] This is about 1/2 that obtained (0.43 MeV) for model D using the exact 4-body theory and the identical ΛN potentials. This can be understood in terms of the characteristics of true few-body calculations outlined above and the scattering lengths and effective ranges listed in Table IV. For model D the ${}^{4}_{\Lambda}He$ and ${}^{4}_{\Lambda}H$ singlet scattering lengths and effective ranges are very similar and contribute little to the CSB difference. On the other hand, $|a_t({}^{4}_{\Lambda}He)| > |a_t({}^{4}_{\Lambda}H)|$ implies that ΔB_Λ (with $\Delta r^t_{\Lambda N}=0$) > 0, whereas $r_t({}^{4}_{\Lambda}He) < r_t({}^{4}_{\Lambda}H)$ implies that ΔB_Λ(with $\Delta a^t_{\Lambda N}=0$) < 0 in an effective 2-body formalism but > 0 in an exact 4-body formalism. Thus, the model D $\Delta a^t_{\Lambda N}$ and $\Delta r^t_{\Lambda N}$ produce compensating effects in an effective 2-body calculation but reinforce each other in a true 4-body calculation.

The spin-flip $J^\pi=1^+$ state energies are not calculable in terms of the free interactions unless one has coupled ΛN-ΣN potentials with which to work. While the singlet potential is the same in this case as the free V^s_{YN} (whether or not $V^s_{XN}\simeq 0$), the equality does not hold for the triplet potential where

$$V^t_{YN} = \begin{pmatrix} V^t_{\Lambda N} & \frac{1}{5} V^t_{XN} \\ \frac{1}{5} V^t_{XN} & V^t_{\Sigma N} \end{pmatrix} \simeq \bar{V}^t_{\Lambda N}(A=4^*)$$

One must explicitly alter the coefficient of the V^t_{XN} coupling potential and recompute the effective $\bar{V}^t_{\Lambda N}(A=4^*)$ potential to use in our one-channel, effective potential formalism. The resulting $\bar{V}^t_{\Lambda N}(A=4^*)$ will be considerably weaker than the free $\bar{V}^t_{\Lambda N}$. In fact, the use of $\bar{V}^t_{\Lambda N}$ in calculating the binding energy of the $J^\pi=1^+$ states would result in the conclusion that these were the ground states of the A=4 system and not the 0^+ states. Therefore, it is not possible in simple

model calculations to use the $0^+ \rightarrow 1^+$ transition energies to determine the spin dependence of the effective ΛN potential; a unique single-channel potential representation is not an adequate description of the physics. Σ-suppression in the A=4 excited states is a very important effect.

V. THE $^{5}_{\Lambda}$He ANOMALY

The possibility that Σ-suppression (actually suppression of the Λ-Σ conversion) is responsible for the anomalously small Λ-separation energy in $^{5}_{\Lambda}$He has been the subject of speculation for some time.[27] Shell model and variational[5,6] estimates of $B_{\Lambda}(^{5}_{\Lambda}\mathrm{He})$ are of the order of 5-6 MeV compared to an experimental[17] value of approximately 3.1 MeV when one uses effective ΛN spin-dependent potentials fitted to the binding energy of $^{3}_{\Lambda}$H and the average of $^{4}_{\Lambda}$He and $^{4}_{\Lambda}$H. However, the wave function is actually of the form[10]

$$a\{\,|^{4}\mathrm{He},T=0\rangle \times |\Lambda,T=0\rangle\,\}^{T=0} \quad + \quad b\{\,|^{4}\mathrm{He}^{*},T=1\rangle \times |\Sigma,T=1\rangle\,\}^{T=0} \ .$$

The even parity T=1 states of ^{4}He have large excitation energies relative to the ground state which should strongly suppress the ΛN-ΣN coupling. The isospin structure is very reminiscent of the hypertriton, where conversion of the Λ to a Σ requires that the Σ couple to the $d^{*}(T=1)$ state of the np pair and not the d(T=0) state in order that the total isospin of the $^{3}_{\Lambda}$H system be T=0.

A first estimate of this is possible in a simple A=5 calculation. If one assumes that the T=0, four-nucleon core is the only allowed isospin state, then one need only use the $V^{t}_{\Lambda N}$ element of V^{t}_{YN} in the calculation. The difference in $B_{\Lambda}(^{5}_{\Lambda}\mathrm{He})$ in that approximation compared to the same calculation using the effective potential approximation of the free interaction $\bar{V}^{t}_{\Lambda N}$ would provide an upper limit on the effect of Σ-suppression for a given potential model.

VI. CONCLUSIONS

In summary, we have tested separable potential approximations to four of the hyperon-nucleon potential models of Nagels, Rijken, and deSwart in exact 3-body calculations of $B_{\Lambda}(^{3}_{\Lambda}\mathrm{H})$ and exact 4-body calculations of ΔB_{Λ} for the $^{4}_{\Lambda}$He - $^{4}_{\Lambda}$H isodoublet. We find model A, which overbinds $^{3}_{\Lambda}$H, to overestimate ΔB_{Λ}. Models B and D appear to be consistent with the experimental value of ΔB_{Λ} (and give reasonable $^{3}_{\Lambda}$H binding energies). We find model F, which is consistent with $B_{\Lambda}(^{3}_{\Lambda}\mathrm{H})$, to underestimate ΔB_{Λ} for the A=4 system; this result is understood in terms of the

small differences between the singlet Λp and Λn scattering lengths and effective ranges in that model.

We emphasize that exact formalisms are required when dealing with small quantities such as ΔB_Λ; effective 2-body calculations have been shown to underestimate exact 4-body results by a factor of 2. Formalisms which treat properly the ΛN-ΣN coupling are required to account for the Σ-suppression that separates the $J^\pi=1^+$ states from the 0^+ ground states by an MeV and that produces the anomalously small Λ-separation energy $B_\Lambda(^5_\Lambda\mathrm{He})$.

Finally, we point out that similar ΛN-ΣN coupling effects should be apparent in the $^4_\Sigma$He and $^5_\Sigma$He decay widths. The Λ-Σ conversion should be uninhibited in the former case leading to a broad width, whereas the T=1 nature of $^5_\Sigma$He will require a 'core' state transition from T=0 to T=1 when the Σ converts to a Λ which should lead to an inhibited transition and correspondingly narrower width.

ACKNOWLEDGMENTS

The work of BFG was performed under the auspices of the U. S. Department of Energy, that of DRL was supported in part by the U. S. Department of Energy. We wish to thank the Clinton P. Anderson Meson Physics Facility (LAMPF) for making available their VAX computing facilities.

REFERENCES

1. M. M. Nagels, T. A. Rijken, and J. J. deSwart, Ann. Phys. (N.Y.) 79, 338 (1973).

2. M. M. Nagels, T. A. Rijken, and J. J. deSwart, in 'Few Particle Problems in the Nuclear Interaction,' ed. by I. Slaus, S. Moszkowski, R. P. Haddock, and W. T. van Oers (North-Holland, Amsterdam, 1972) pp. 41-45.

3. M. M. Nagels, T. A. Rijken, and J. J. deSwart, Phys. Rev. D15, 2547 (1977).

4. M. M. Nagels, T. A. Rijken, and J. J. deSwart, Phys. Rev. D20, 1633 (1979).

5. R. C. Herndon and Y. C. Tang, Phys. Rev. 153, 1091 (1967); 159, 853 (1967); 165, 1093 (1968).

6. R. H. Dalitz, R. C. Herndon, and Y. C. Tang, Nucl. Phys. B47, 109 (1972).

7. B. F. Gibson and D. R. Lehman, 'A Qualitative Discussion of the YN Interaction for Λ-hypernuclei with $A\leq 4$,' Phys. Rev. C (to be published).

8. B. F. Gibson, A. Goldberg, and M. S. Weiss, Phys. Rev. C6, 741 (1972); C8, 837 (1973).

9. J. Dabrowski, Phys. Rev. C8, 835 (1973).

10. B. F. Gibson, Lecture Notes in Physics (Springer Verlag) 82, 302 (1978).

11. See, for example, Ref. 3 or S. Wycech, Acta Phys. Pol. B3, 307 (1972).

12. B. F. Gibson and D. R. Lehman, Phys. Rev. C10, 888 (1974); 14, E2346 (1976).

13. L. H. Schick and A. J. Toepfer, Phys. Rev. 170, 946 (1968).

14. J. Dabrowski and E. Fedorynska, Nucl. Phys. A210, 509 (1973).

15. A. C. Phillips, Nucl. Phys. A107, 209 (1968).

16. B. F. Gibson and D. R. Lehman, Phys. Rev. C11, 29 (1975).

17. M. Juric, G. Bohm, J. Klabuhn, U. Krecker, F. Wysotzki, G. Coremans-Bertrand, J. Sacton, G. Wilquet, T. Cantwell, F. Esmael, A. Montwill, D. H. Davis, D. Kielczewska, T. Pniewski, T. Tymieniecka, and J. Zakrzewski, Nucl. Phys. B52, 1 (1973).

18. B. F. Gibson and D. R. Lehman, Phys. Rev. C11, 2092 (1975); L. H. Schick, Phys. Rev. C11, 2089 (1975).

19. B. F. Gibson and D. R. Lehman, Phys. Rev. C22, 2024 (1980).

20. B. F. Gibson and G. J. Stephenson, Jr., Phys. Rev. C11, 1448 (1975).

21. H. Narumi, K. Ogawa, and Y. Sunami, Prog. Theor. Phys. 63, 533 (1980).

22. B. F. Gibson and D. R. Lehman, Phys. Rev. C18, 1042 (1978).

23. J. L. Friar and B. F. Gibson, Phys. Rev. C18, 908 (1978).

24. B. F. Gibson and D. R. Lehman, Phys. Lett. 83B, 289 (1979); Nucl. Phys. A329, 308 (1979).

25. B. F. Gibson and D. R. Lehman, 'Comparative $^{4}_{\Lambda}$He-$^{4}_{\Lambda}$H Binding Energy Differences for Four Meson-Theoretic YN Potential Models,' Phys. Rev. C (to be published).

26. R. H. Dalitz and B. W. Downs, Phys. Rev. 111, 967 (1958).

27. A. R. Bodmer, Phys. Rev. 141, 1387 (1966); B. F. Gibson, A. Goldberg, and M. S. Weiss, in 'Few Particle Problems in the Nuclear Interaction,' ed. by I. Slaus, S. Moszkowski, R. P. Haddock, and W. T. van Oers (North-Holland, Amsterdam, 1972) p. 188; and Ref. 14.

ON THE UNCERTAINTY IN THE K^+-NUCLEUS INTERACTION BELOW 1 GEV†

Stephen R. Cotanch
North Carolina State University, Raleigh, N. C. 27650

ABSTRACT

Corrections to the first-order, multiple scattering K^+-optical potential are investigated through simple model calculations. For lab energies up to 1GeV rough theoretical error bounds are determined for each of the following effects: form factor momentum dependence (off-shell behavior), angle transformation of kaon-nucleon (KN) t-matrix, additional elementary KN partial wave amplitudes, and different phenomenological KN phase shifts.

INTRODUCTION

The pioneering kaon-nucleus experiments recently performed by the Carnegie-Mellon, Houston, and Brookhaven collaboration[1] motivates a more detailed treatment of the K-nucleus interaction. To this end, the current work focuses on furthering our understanding of the K^+-optical potential by examining a number of effects which have been found important in pion-nucleus scattering. The study, which is briefly summarized in the next two sections, will be described in full detail elsewhere[2].

DETAILS OF THE STUDY

Within the framework of standard multiple scattering formalism (first-order, impulse approximation), the uncertainty in the theoretical K^+-optical potential is assessed by investigating four separate effects: 1) the momentum dependence of the form factor (related to off-shell behavior of the KN interaction; 2) angle transformation of elementary t-matrix from KN to KA c.m.; 3) including higher KN partial waves (d and f); 4) different sets of empirical KN amplitudes.

The percent size effect for items 1) and 2) is determined by comparing cross sections from different potentials with a reference cross section which is computed using a Kissingler form with parameters, b_o and b_1, determined from s and p wave Martin amplitudes (see ref. 3 for details). Item 1, the form factor momentum dependence, was examined by comparing the Kissingler form to two other potentials, a local Laplacian[4] and a simple s-wave model[5] which has been used[5] for similar studies in K^- scattering. The s-wave model combines all amplitudes into a single, effective coefficient, $b_o = \sum_\ell b_\ell$, and involves no gradiant operators. For item 2, the angle-transformation prescription of Landau, Phatak, and Tabakin[6] was adopted (also Kisslinger form). This transformation mixes and renormalizes the b_ℓ coefficients, however, $\sum_\ell b_\ell$ is preserved. Only s and p wave KN amplitudes were used in the study of these two items and therefore calculations were restricted to below $E_{lab} \leq .5$ GeV.

Items 3 and 4 were examined within the context of the s-wave model. The importance of including higher partial wave KN amplitudes (item 3) was determined by computing cross section percent change introduced by the addition of Martin d and f waves. For item 4 cross sectons predicted (again s-wave model) using BGRT amplitudes were compared to the reference cross sections obtained from Martin

†Work supported in part by the U. S. Department of Energy

amplitudes (note: BGRT includes $s_{1/2}$, $p_{1/2}$, $p_{3/2}$, $d_{3/2}$, $d_{5/2}$ while Martin includes $s_{1/2}$, $p_{1/2}$, $p_{3/2}$, $d_{3/2}$, $d_{5/2}$, $f_{5/2}$). This part of the investigation spanned the energy region E_{lab} = .1 to 1 GeV.

RESULTS AND CONCLUSIONS

The study was performed for elastic scattering from ^{12}C (see ref. 3 for model parameters). Table I list the range of percent change, as a function of lab energy, introduced by each of the four items. The percentages were extracted by comparing peak differential elastic cross sections (total cross sections gave nearly identical percentages).

TABLE I. Percent Change in $K^{+}-^{12}C$ Elastic Cross Section

Item	.1 to .5 GeV	.5 to 1.0 GeV
1. momentum dependence	-1 to -6	not investigated
2. angle transformation	+2 to +8	not investigated
3. d and f wave amplitudes	+2 to +20	+21 to +26
4. Martin vs. BGRT	-11 to -37	-7 to +5

The table reveals that both momentum dependence and angle-transformation effects are small (less than 10%). The dominant effects are clearly generated by the KN amplitudes where at low energies the uncertainty in the KN interaction introduces as much as a 40% effect. This of course has been known for sometime. At higher energies, however, Martin and BGRT amplitudes give similar results (to within 10%). As one might expect, the importance of including d and f waves is readily apparent at higher energies. Even at lower energies, .4 to .5 GeV, this effect can be important.

In summary, below .5 GeV the momentum dependence of the form factor (loosely, off-shell behavior) is found to be slight and angle-transformation effects are small. Both effects are easily over-shadowed by the uncertainty in the KN interaction. Above .5 GeV the uncertainty diminishes, however, it is essential to include d and f wave KN amplitudes. Until more precise KN amplitudes are available this would appear to be a favorable energy region for nuclear structure studies.

REFERENCES

1. R. Eisenstein, in Proceedings of the Kaon Factory Workshop, edited by M. K. Craddock (Vancouver, 1979), p. 75.
2. S. R. Cotanch, to be published.
3. S. R. Cotanch, Nucl. Phys. A308, 253 (1978).
4. H. K. Lee and H. McManus, Nucl. Phys. A167, 257 (1971).
5. A. S. Rosenthal and F. Tabakin, Phys. Rev. C (press).
6. R. H. Landau, S. C. Phatak, and F. Tabakin, Ann. of Phys. 78, 299 (1973).

A HIGH INTENSITY ACCELERATOR FACILITY

by

Lee C. Teng
Fermilab*, P.O. Box 500, Batavia, IL 60510

I. INTRODUCTION

Discussions of high energy versus high intensity were pursued vigorously as far back as 1955 at the Midwestern Universities Research Association.[1] The heated dispute at the time was focused on a contest between the merits of one against the other. Now 25 years later the ever rising energy will soon reach 2 TeV in the $\bar{p}p$ colliding beams at Fermilab, equivalent to a fixed target beam energy of some 2000 TeV, and a consistent standard model of elementary particles and their interactions evolved as a consequence. There is no more doubt that the energy frontier should be advanced with all vigor. It is, therefore, doubly significant and convincing when interests are mounting for a high intensity proton accelerator facility at some modest energy.

The need for such a facility has been well documented by the interesting new physics reported at this and other workshops and symposia.[2] An energy between 10 and 20 GeV would be adequate for most of the experiments envisioned. Much above 20 GeV we enter the energy range which is serviced by the so-called high energy accelerators. The unique requirement for this "medium" energy facility is the high intensity. As usual, the intensity desired is the higher the better limited only by practical considerations, but some two orders of magnitude higher than that now available is considered sufficient and justification enough for a new facility. We choose for discussion here an energy of 16 GeV (rather arbitrary) and an average beam current of 100 μA (6×10^{14}sec^{-1}). The practical considerations leading to this choice of beam current are:

(a) At 16 GeV and 100 μA the beam power is 1.6 MW. To accelerate such a beam one needs ~3 MW of rf power or ~6 MW of ac power. This large power

*Operated by the Universities Research Association, Inc., under contract with the U.S. Department of Energy.

consumption for rf alone implies rather high operating cost for the facility. Furthermore, the cost of the rf supply, typically $3/watt, is already about $10 million.

(b) Targetting the 1.6 MW beam, although possible, is not trivial. To go much beyond this would make targetting extremely difficult.

(c) An intensity of 100 μA is about two orders of magnitude higher than that available from existing accelerators. It will be seen later that this high intensity is close to the limiting capability of an inexpensive type of accelerator, the fast cycling synchrotron. To get much higher intensity one must take a step toward a more costly type of accelerator.

The potential of such a proton beam for physics can be illustrated by the following considerations.

(a) With primary beam on target, taking a rather large beam cross-sectional area of 1 cm^2, hence a conservative beam flux of $6x10^{14}cm^{-2}sec^{-1}$, and a 1 mole target we get a luminosity of

$$L = (6x10^{23})x(6x10^{14}cm^{-2}sec^{-1}) = 3.6x10^{38}cm^{-2}sec^{-1}$$

which is very large indeed compared to the $<10^{31}cm^{-2}sec^{-1}$ available from colliding beams. Moreover, the reaction cross-sections considered here are likely to be much larger than those of the events studied on the colliders.

(b) For secondary beams we take as an example kaon beams at 1 and 2 GeV/c. This was studied in 1976.[3] Taking forward production and an acceptance solid angle of 24 msr (5^o semi-cone angle) we get

	Number per GeV/c per sec	
Momentum	K^+	K^-
1 GeV/c	$1.4x10^{12}xE_T$	$0.4x10^{12}xE_T$
2 GeV/c	$1.6x10^{12}xE_T$	$0.6x10^{12}xE_T$

where E_T is the targetting efficiency. These are, again, very high intensities.

II. GENERAL CONSIDERATIONS

A. Type of Accelerator

(1) Linac is capable of the highest intensity. For application as source of spallation neutrons for breeding fissile fuels or for neutron damage studies

intensities as high as 300 mA have been contemplated. On the other hand, it is also the most costly. At the current unit cost of about 10 eV per dollar, a 16 GeV linac would cost well over $1 billion.

(2) Microtron[4] and FFAG[5] (Fixed-Field Alternating Gradient ring accelerator) are both capable of this and, perhaps, higher intensities. But a great deal of R&D is required before the construction of either type of accelerator can proceed. Furthermore, although not to the extreme as the linac, these accelerators still tend to be rather costly.

(3) Fast cycling synchrotron is straightforward and the most inexpensive, but is limited in intensity. To get an average intensity of 6×10^{14} protons/sec we need 1×10^{13} p/pulse at a 60 Hz pulse rate. Normally this is close to the limit of the capability of a fast cycling synchrotron. However, if one can use the 800 MeV LAMPF as injector this intensity is easily obtainable.

The space charge limited proton number in a synchrotron is given by

$$N = \frac{2\,\Delta\nu}{r_p}\,\beta^2\gamma^3\,\varepsilon = (1.17\times10^{18}\,\mathrm{m}^{-1})\varepsilon$$

where

r_p = classical radius of proton = 1.54×10^{-18}m

$\Delta\nu$ = allowable tune shift = 0.2

$\beta^2\gamma^3$ = relativistic kinematic factor = 4.5 (at 800 MeV)

ε = beam emittance.

Thus to get $N = 10^{13}$ one needs an emittance of only $\varepsilon = 8.5\times10^{-6}$m $= 2.7\pi$ mm-mrad which is quite easily contained in a synchrotron. On the other hand, if instead of 800 MeV the injection is from a conventional 200 MeV Alvarez linac, the $\beta^2\gamma^3$ factor is down by a factor of ~8. The beam emittance, hence the magnet aperture must then be increased by a factor 8. Although possible, this requires a substantially more expensive magnet system.

Aside from this simple space charge detuning there are many other high intensity effects causing instability in the beam. But experiences show that all these effects are either avoidable or curable at intensities of 1 or 2×10^{13} p/pulse.

B. Synchrotron Features

The only choices requiring discussion are the type and peak field of the magnet system.

(1) We choose conventional instead of superconducting magnets. In the first place, the highest ramp-rate obtained for any superconducting magnet is about $\frac{1}{2}$ Hz. To obtain 6×10^{14} p/sec this requires 1.2×10^{15} p/pulse, much too high for beam stability and for the stability of the superconducting magnets against quenching by stray beam.

Even if, somehow, one were able to keep the magnets superconducting when pulsed at 60 Hz, the ac loss in these magnets will be entirely too high. If the Fermilab Tevatron magnets were used for 16 GeV the ac loss would be ~8.5 kJ/cycle or ~500 kW at 60 Hz. To remove this heat at 4 K one needs approximately 150 MW of electrical power to run the refrigerator. For this reason also, it is impractical to pulse a superconducting magnet ring at rates much higher than 1 Hz.

(2) The peak field B should not be too high. This is because:

(a) magnet cost $\propto$ magnet volume
$\propto$ cross-sectional area x length $\propto B^2 \times \frac{1}{B} \propto B$

(b) power supply cost $\propto$ stored energy in magnet
$\propto$ energy density x aperture x length
$\propto B^2 \times 1 \times \frac{1}{B} \propto B$ (for fixed aperture).

Hence the cost of both the magnets and their power supplies goes down as B is reduced. This should, however, be compromised with the rising cost of the synchrotron tunnel and utilities in the tunnel which is roughly proportional to the ring circumference. In addition, the cost of the rf cavities being proportional to the voltage is also proportional to the circumference. (The cost of the rf supply is, however, proportional to the power.) A nearly optimal compromise is $B \cong 7$ kG.

We will use combined function magnets. This eliminates the need of space for quadrupoles, hence leads to a smaller circumference of the ring.

C. Spill-Stretcher Ring

For slow beam spill we will need a separate spill-stretcher ring. This ring will have the same circumference as the synchrotron and will be installed in the same tunnel either above or below the synchrotron. This ring will be operated dc at 16 GeV and is hence ideal for the application of superconducting magnets.

It should be emphasized that superconductors are basically not capable of pulsed operation. The chief and crucial advantage of superconducting magnets

is the more than 200-fold power savings compared to conventional magnets when operated dc. The factor ~2 in maximum field over that of conventional magnets is nice but certainly not critical.

III. SYNCHROTRON DESIGN PARAMETERS

A. Ring Magnet Lattice

We shall split a focusing-defocusing cell in the middle of the focusing magnet to insert a long straight section and adjust the magnet gradients to give a phase advance per cell $\mu \cong 90^{o}$. These choices will facilitate injection and extraction of the beam. For a high intensity synchrotron clean injection and extraction are essential to keep induced radioactivity low so that hands-on maintenance is possible after prolonged periods of operation. After some cutting and fitting we come to the following cell structure and beam containment parameters. The cell shown is obviously very much stylized. Small gaps between all magnets are needed to accommodate coil ends, correction magnets, beam sensors, etc. However, for the present only the roughest zeroth order approximate values of the parameters are necessary.

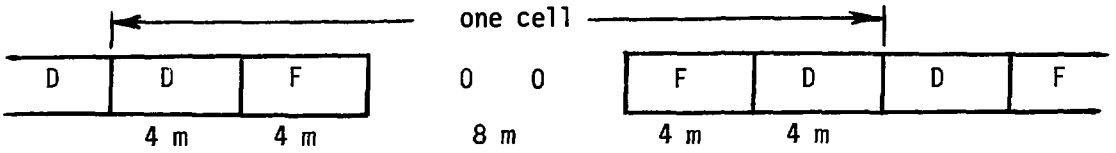

Length of DFOOFD cell = 24 m — No. of cells = 32

Ring circumference ($2\pi R$) = 768 m — Radius (R) = 122 m

Total magnet length ($2\pi\rho$) = 512 m — Bending radius (ρ) = 81.5 m

	Initial	Final
Kinetic energy (T)	800 MeV	16 GeV
Bending field (B)	0.60 kG	6.9 kG
Revolution frequency (F)	0.33 MHz	0.39 MHz

Field gradients (B'/B) = $\pm 2.7\ m^{-1}$

Phase advance/cell (μ) = 93^{o} — Tune (ν) = $8\frac{1}{4}$

		β_h (horizontal)	β_v (vertical)
Amplitude function	Mid DD	7.3 m	43 m
	Mid OO	23 m	8.8 m
	Max. D	15 m	43 m
	Max. F	24 m	25 m

B. Magnet Aperture and Space Charge Limit

We shall assume a conservative good-field aperture of 60 mm(h) x 40 mm (v). Taking the maximum β_v = 43 m we get for the minimum vertical beam emittance

$$\varepsilon_v = \pi \frac{(20\,\text{mm})^2}{43\,\text{m}} = 9.3\,\pi\,\text{mm-mrad}$$

or a corresponding space charge limit of

$$N = 3.4 \times 10^{13}.$$

This enables us to adopt a more conservative pulse rate of 30 Hz. To get an intensity of 100 μA we will need 2×10^{13} p/pulse, still comfortably within the space charge limit. All other high intensity beam instabilities should still be avoidable or curable. The magnet cross-section will look roughly as shown below and the power consumption by the magnets will be about 2.5 MW.

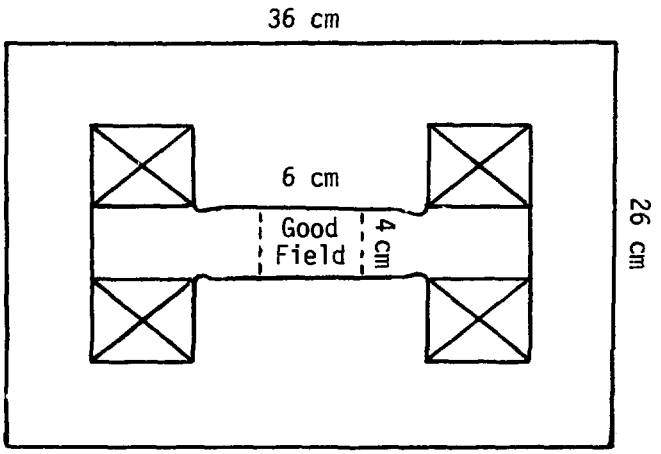

C. Radiofrequency System

To get the cleanest injection and capture we adopt the synchronous injection/capture scheme in which the synchrotron rf frequency is synchronized to the bunch frequency of the beam from the injector. Assuming LAMPF is used as the injector the beam bunch frequency is then, 200 MHz (201.25 MHz to be exact). The synchrotron rf frequency at injection should then be 200 MHz or an integral fraction. We choose a frequency of $\frac{200\ \text{MHz}}{4}$ = 50 MHz because one needs the 20 nsec time interval between beam bunches for time-of-flight experiments. Also 50 MHz is a good frequency in regard to the availability of

power tubes and ferrites. Thus we have

Harmonic number = h = 153

Injection rf frequency = $f_i = hF_i = 50.3$ MHz

Final rf frequency = $f_f = hF_f = 59.6$ MHz

Range of frequency modulation = $\frac{\Delta f}{f} \cong 18\%$

Pulse rate = P = 30 Hz

Max. energy gain per turn = $\left(\frac{dT}{dn}\right)_{max} = 2\pi R \left(\frac{dp}{dt}\right)_{max}$

$= 2\pi R \times \pi P \times (p_f - p_i) = 3.7$ MeV/turn

Highest synchronous phase = $\phi_s = 60^o$

Max. peak rf voltage per turn = $\frac{3.7 \text{ MV}}{\sin 60^o} = 4.3$ MV.

The most straightforward hence the most reliable cavity is the 180^o single drift-tube double-gap cavity shown below. The amount of ferrite needed for the 18% frequency modulation is not very large and a shunt resistance of ~100 kΩ should be obtainable.

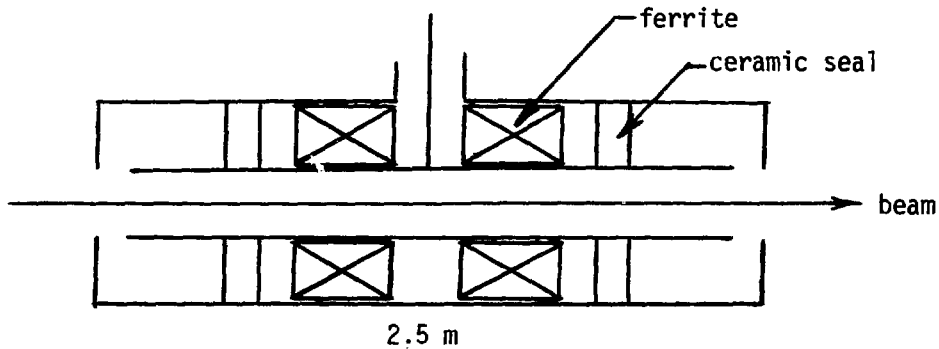

A peak voltage of 80 kV should be easy. With some pushing 160 kV may be attainable. At 80 kV/cavity we will need 54 cavities or 27 straight sections with 2 cavities in each straight section. The cavity loss will be 32 kW/cavity or 1.7 MW total.

D. Injector Requirements

LAMPF is capable of a peak current of 12 mA when every one of the 200 MHz rf buckets is filled. With only one of every 4 buckets filled one gets only 3 mA or 5.5×10^{10} p/turn injected. Thus for 1×10^{13} p one needs to inject 180 turns corresponding to a pulse length of 0.54 msec and a circulating current of 180 x 3 mA = 0.54 A in the synchrotron. For 2×10^{13} p one needs 360 turns,

1.08 msec, and 1.08 A. With charge-exchange injection of H^- ions these large numbers of turns can be injected as has been demonstrated on the ANL-ZGS.[6]

E. Spill-Stretcher Ring

As was mentioned above superconducting coils could be used for this dc ring. But since the magnetic field does not have to be high one can still use the iron-yoke to shape the field. If we place two 3 m dipoles per cell the field strehgth only has to be 18.5 kG, still below the saturation of iron. The ideal cross-sectional geometry of the dipole is, then, the picture frame shown below.

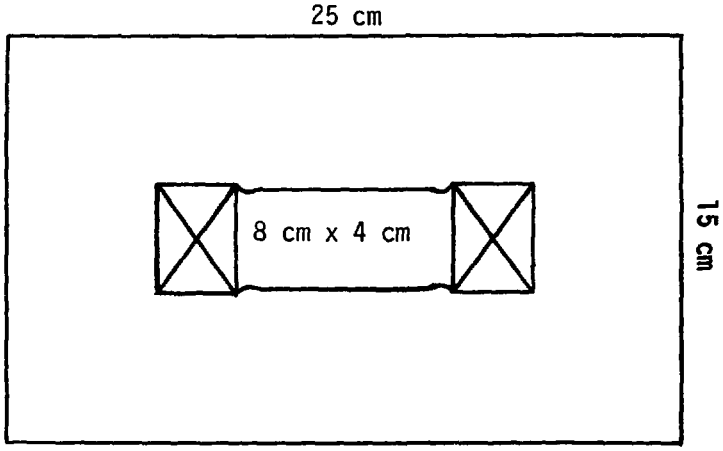

The lattice now should have separated functions with dipoles and quadrupoles (represented as lenses) arranged as shown in the figure below.

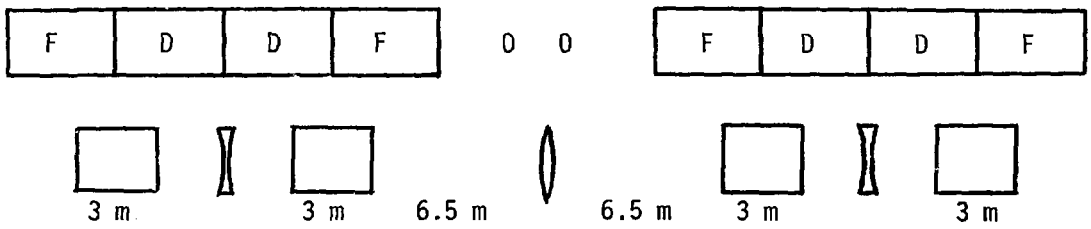

The long straight section is now 13 m long (disregarding the quadrupole in the middle) which should be adequate for a 4π detector surrounding future colliding beams in the middle of the straight section.

The 16 GeV beam is fast injected, say, vertically from the synchrotron in one turn and slow extracted horizontally by, say, half-integer resonant extraction in $\frac{1}{30}$ sec. This way one should get a spill duty-factor close to 100%.

No rf is needed in principle. However some minimal rf at fixed frequency or with a very small range of frequency modulation may be advantageous for keeping some control over the beam during the slow extraction.

IV. COST ESTIMATE

The very crude cost estimate given below is no more than an educated guess since no detailed quantitative analysis was done. The estimates are conservative, some contingency may be considered included.

	M$	
Fast Cycling Synchrotron		
Magnet and P.S. Systems	20	
RF System	15	
Control and Diagnostics Systems	5	
Miscellaneous	10	
Vacuum, Injection, Extraction Transport, etc.		
Conventional Facilities	30	
		80
Spill-Stretcher Ring		20
	TOTAL	100

V. FUTURE OPTIONS

Other than additions and improvements to secondary and tertiary beams and to a variety of targets one can consider:

$\bar{p}p$ colliding beams in the stretcher ring

pp or ep colliding beams between the stretcher ring and the synchrotron.

In addition, the synchrotron can of course always be used as injector into a much higher energy accelerator.

This investigation was initiated at the prompting of Darragh Nagle. The synchrotron described resembles closely that outlined by him[7] in 1979. Technologically this is a realistic but unique and challenging project. When many hundred millions of dollars have been spent on gambles at the high energy frontier it is only sensible and wise to devote some resources on the high intensity territory where sober and intelligent evaluation has already indicated an abundance of interesting physics.

REFERENCES

1. See e.g. R.L. Cool, A. Wattenberg, T. Ypsilantis and A. Roberts, MURA Reports 469, 473 (1959), and "Proposal for a High Intensity Accelerator," MURA, submitted 1962 revised 1963.

2. Summer Study on Kaon Physics, BNL, 1976.

   Workshop on Intermediate Energy Physics, CERN, 1977.

   Seminar on the Kaon-Nuclear Interaction and Hyernuclei, Zvenigorod, 1977.

   Workshop on the AGS Fixed Target Programs, BNL, 1978.

   Working Seminars on Physics in the 10-20 GeV Region, LAMPF, 1979.

   Kaon Factory Workshop, TRIUMF, 1979

   Meeting on Hypernuclear and Low-Energy Kaon Physics, Warsaw, 1979.

   Workshop on Low- and Intermediate-Energy Kaon-Nuclear Physics, Rome, 1980.

   Series of International Symposia on High Energy Physics with Polarized Beams and Polarized Targets, 1974-1980.

   Series of International Conferences on High Energy Physics and Nuclear Structures, LASL, No. 8 in 1979.

3. L.C. Teng, Proceedings of the Summer Study Meeting on Kaon Physics and Facilities, Brookhaven (BNL 50579) p. 189 (1976).

4. A. Roberts, Ann. of Physics. 4, p. 115 (1958).

5. K.R.Symon, D.W. Kerst, L.W. Jones, L.J. Laslett and K.M. Terwilliger. Phys. Rev. 103, No. 6, p. 1837 (1956).

6. C.W. Potts, IEEE Trans. on Nucl.Sci. NS-24, No. 3, p. 1385 (1977).

7. D.E. Nagle, Proceedings of TRIUMF Kaon Factory Workshop (TRI 79-1) p. 197 (1979)

A SPECULATIVE TEN-YEAR PLAN FOR NUCLEAR PHYSICS AT LAMPF

by

H.A. Thiessen

ABSTRACT

Recent results in nuclear physics at LAMPF are reviewed. Possibilities for several projects are briefly discussed, including a new low-energy pion spectrometer, a high-intensity polarized ion source, and utilization of the proton storage ring as a 1.5 GeV d.c. electron machine during the several months of each year that LAMPF is down. Some detailed proposals for facilities for nuclear physics at a high-intensity 30 GeV proton machine are discussed, and a second-order design for a kaon beam for use with the (K^-, π^-) reaction is given.

I. MOTIVATION

I would like to start by reviewing the present status of nuclear physics research at LAMPF and other medium-energy facilities, treating all of the elementary probes, namely

$$\gamma,\ e^{\pm},\ \mu^{\pm},\ \pi^{\pm},\ K^{\pm},\ p^{\pm},\ \ldots\ .$$

In particular, I would like to look for possibilities for facilities improvements which maximize the utilization of existing hardware, thereby minimizing costs.

A. Protons

Starting with the heaviest probe, the proton, I would like to remind the reader of the many recent publications from HRS in the area of

1. Neutron Radii[1]
2. Giant Resonances[2]
3. Inelastic Scattering[3]
4. Nucleon-Nucleon Experiments.[4]

These experiments take advantage of the high resolution ($\sim$ 45 keV at 500 MeV) and great flexibility of the HRS and the beams available from LAMPF. In the near future, you will see results in two new classes of experiments, namely, spin flip experiments utilizing the focal plane polarimeter[5] and continuum experiments.[6] The present limitations on this work are: 1) the availability of running time;

2) the polarized beam intensity; 3) the duty factor, which limits the possibilities for coincidence work; and 4) the resolution. In the next few years, we expect improvements in (2)-(4) above, including a possible factor of two improvement in resolution resulting from elimination of drifts and more careful tuning. The running time at HRS is limited by the six months per year during which LAMPF is in production status. Only a significant change in the funding level for LAMPF can change this.

The program of nucleon-nucleon experiments in Area B has been particularly successful in the past year. Among the recent results are precision proton-proton scattering experiments at 800 MeV, and the very successful program of experiments performed during the past summer at energies from 330 to 800 MeV including the $\Delta\sigma_L$, $\Delta\sigma_T$, and $K_{nn}(90^\circ)$ using polarized beams and polarized targets.[7] Work in this area suffers form a lack of running time, marginal manpower, and a limited intensity of polarized neutrons. The 100 μA polarized H^- source being studied by Cornelius, York, and Hinds would make possible a big improvement in polarized neutron flux.[8]

B. Antiprotons

For a review of recent work with antiprotons, I refer the reader to the excellent talks presented Tuesday p.m. at this Workshop. If we are to provide antiproton beams at the High-Intensity Machine (HIM), then we should be prepared to construct an antiproton accumulator and, most likely, another ring for acceleration/deceleration and cooling. As a rough figure, $\$ 35 \times 10^6$ at today's prices might be sufficient to build a system which could compete with LEAR at CERN.[9] The production of antiprotons and the operation of an antiproton facility will have significant impact on the design of HIM, not considered in Dr. Teng's excellent talk this morning.

In our planning for an antiproton physics program, we should consider using the $\bar{p}$ beam in HRS and Area B. These experimental areas are already ideally suited for use with low-energy nucleon beams which might result from an improved version of LEAR at a high-intensity machine. We should make every possible effort to obtain high-quality polarized antiprotons for this purpose. For more details of a $\bar{p}$ experimental program, see the talks of the Tuesday p.m. session.[10]

C. Kaons

For a detailed discussion of kaon-nuclear physics, I refer the reader to Dr. Eisenstein's talk at this Workshop.[11] There are two groups presently performing experiments in this field, one at Brookhaven, and one at CERN. Both are studying (K^-, π^-) reactions and, in particular, are looking for states in which a Σ is bound in the residual nucleus. The idea behind these experiments is that recently the spin-orbit force between a Λ and a nucleon has been found to be nearly zero. This follows naturally from a quark model[12] in which the strange quark in the Λ does not couple to the remainder of the quarks in the nucleus. The remaining non-strange quarks in the Λ are in a state of relative $J = 0$, hence cannot have a spin-orbit interaction with the nucleus. On the other hand, the non-strange quarks in the Σ are in a state of relative $J = 1$, hence should have a large spin-orbit force. The study of the spectra of Σ hypernuclei should be a sensitive test of this idea.

Other important experiments in this field include (K^+, K^+), which, as Dr. Eisenstein discussed, should be a sensitive, strongly interacting probe of the nuclear interior; (π^+, K^+), which will be studied soon at Brookhaven[13] and will search for the "stretched states" of hypernuclei with higher counting rate than (K^-, π^-); and (K^-, K^+) which populates doubly strange hypernuclear states. All of these reactions have low counting rates and background problems, and would become

much more useful tools if new beam lines and spectrometers were available at a high-intensity machine.

D. Pions

Pion scattering near resonance energies (180 MeV) at EPICS has been one of the most productive programs at LAMPF. The comparison of π^+ and π^- is an extremely sensitive tool for measuring isospin mixing and for picking out neutron or proton components of particle-hole wave functions. Recent reviews have been given by Morris[14] and Thiessen[15]. Low-energy pion scattering has been studied by groups at LAMPF[16] and TRIUMF[17]. The low-energy comparison of π^+ and π^- has been hampered by the lack of a good spectrometer and beam-line combination -- such a facility could be constructed at one of the meson factories in the near future and, indeed, several groups are actively working on this problem.[18] Even EPICS, with 10^8 π^+/s and 2×10^7 π^-/s, and resolution of 140 keV, is clearly limited in its ability to do inelastic scattering even to moderately strong states. A much improved version of EPICS with 10^9 π^+ and π^- per second could be built at a high-intensity machine.

A unique opportunity to study high-energy pion-nucleus scattering will occur at a high-intensity machine. In Fig. 1 are shown the π^+p and π^-p total cross-sections. In the region from 500 MeV to 1000 MeV the cross-section is roughly an order of magnitude smaller than at 200 MeV, yet large differences exist between π^+ and π^-. The smaller cross-section will make the impulse approximation more accurate. The larger momentum transfer at small angles will make experiments easier to analyze in multiple scattering theories. This region of pion energy has never been explored with adequate resolution and adequate counting rate for nuclear physics studies (see Eisenstein's talk for the only exception to this statement). It should be possible to make beams of 10^9 π^+ and π^- per second if a high-energy version of EPICS were constructed at a high-intensity machine. Such a facility could also be used for (K^+, K^+) and would be an outstanding addition to the available facilities for nuclear structure studies.

E. Muons

The Workshop on Program Options in Intermediate-Energy Physics held at Los Alamos in 1979 [19] considered the needs of the muon physics program. Of the recommendations of the panel on electroweak interactions, the easiest to implement is the pulsed π-μ beam at the proton storage ring. An additional muon channel and provision for a Gatchina-type curved crystal spectrometer near the beam stop are being considered. The long shutdown of LAMPF, required to install any large new facility on Line A, is difficult to justify at this time.

F. Electrons, Positrons, and Photons

Electron, positron, and photon beam experiments can benefit from a 2 GeV d.c. electron machine. Proposals for such a machine are being actively prepared by several groups.[20] I would like to suggest that here at LAMPF we already have most of the expensive parts of such a machine, either in existence or under construction, if one is willing to settle for 1.46 GeV. By this I mean that the momentum of a 1.46 GeV electron is the same as that of an 800 MeV proton. For an accelerator, I would propose some sort of low duty cycle linac injected into the proton storage ring, which would be used as a stretcher. The extracted beam could then be sent back through the injection line and through a short section of new beam line, and then into Line X for use in HRS (Area C) or Area B. The HRS spectrometer has a demonstrated resolution of about 60 keV for 800 MeV and 40 keV for 500 MeV protons. This translates into 70 keV for 1.46 GeV electrons and 50 keV for 1 GeV electrons. Improvements in the power supplies and beam tuning which are already under way should improve the resolution by roughly a factor of two. In

Fig. 2 is shown a plan of the LAMPF experimental areas with the linac and beam transport system roughly sketched in.

In order to construct such a facility, it would be necessary to purchase a 1.5 GeV electron linac and construct a building to house it, add r.f. cavities to PSR, and add a transport line in the switchyard which connects Line X and Line D. If more than one spectrometer is desired, of course this must be added. It might be possible to construct a tagged photon facility somewhere in Line D or in Area B. Operating the electron machine should be possible for most of the six months per year that LAMPF has historically been turned off. It would be possible to maintain Area A and the LAMPF accelerator while the electron machine is in operation. Because of the much lower power bill expected for running such a machine, it should require only a modest increase in the LAMPF operating budget to operate an electron machine for six months out of each year.

No detailed calculations have been done to demonstrate the technical feasibility of this idea. Clearly the accelerator deserves careful study before a serious proposal can be made. In addition, the experimental areas required also deserve attention. But even without such detailed work, it is obvious that the utilization of existing buildings, of HRS, of the PSR magnet ring, and of the installed utilities and services at the LAMPF site must make significant cost reductions compared with any other proposal for a similar machine. The availability of operators and support personnel would also mean that savings in operating costs would be possible.

I would therefore like to ask if any of you present at this Workshop would like to help turn this idea into a serious proposal?

II. POSSIBLE TIMESCALE

I have tried to make an estimate of the dates when it would be possible to do some of the projects indicated above. In most cases these are only guesses based on my personal intuition, but these might serve as a guide to more careful study. The schedule is listed in Table I.

TABLE I

TIMETABLE FOR LAMPF IMPROVEMENTS

Date	Project	Purpose
1983	Portable pion spectrometer	Pion scattering and reactions
1984	Laser polarized source	High-intensity (100 μA) polarized negative ion beam
1986	Proton storage ring	Neutrons, neutrinos, pulsed muons
1987	d.c. electron machine	Multipurpose
1988	High-intensity 30 GeV proton machine	Multipurpose
1990	Antiproton system for above	Multipurpose

III. A DISPERSED, SEPARATED KAON BEAM FOR (K^-, π^-)

I would like to report the results of some work performed at CERN during the past few months. The goal of this work was to make a feasibility study for a beam line and spectrometer which could be used at a High-Intensity Machine to study the (K^-, π^-) reaction. For the purpose of this study, I assumed that such a machine will produce 6×10^{14} p/s (100 μA) at 30 GeV, that the duty factor will be nearly 100%, that the beam will have a 50 MHz microstructure, that timing with the r.f. will be possible, and that it will be reasonable for 1×10^{14} p/s to interact in a kaon-producing target.

It is clear that a target station for such a beam will have a serious power problem, as ∿ 500 kW will be dissipated. However, most of the power will go to the beam stop in the form of high-energy pions and muons. A target consisting of a 3 mm thick by 5 cm wide platinum wheel, similar to the carbon wheel targets in use at LAMPF, will be able to handle the beam power. It is clear that conventional magnets must be used in the early part of the beam. To maintain symmetry, the whole line should be conventional. Considering the troubles discovered with the separator for EPICS, the separator should be well shielded and should be located as far as possible from the production target and beam stop.

The requirements of the experiment are: beam intensity as high as possible, with detectors in the beam near the (K^-, π^-) target. This dictates that the pion contamination in the kaon beam be less than 1:1 in order that the detectors use their available dead time analyzing mostly kaons. A reasonable compromise choice for the kaon momentum is 700 MeV/c -- the factors influencing this choice are momentum transfer in the (K^-, π^-) reaction, kaon yield, feasibility of separation, and resolution. Resolution of 10^{-3} seems to be a reasonable choice. Time-of-flight compared with the r.f. is required in order to clean up the kaon trigger.

The design of a pion spectrometer for this purpose is straightforward. Many existing spectrometers could be used. A unique possibility at LAMPF is the use of the EPICS spectrometer. The two dipoles (without the quadrupole triplet) would be ideally suited for this purpose. If we get the high-intensity machine, the EPICS users would most likely be willing to give up EPICS to work with kaons and/or high-energy pions. In any case, manpower, including users, must be conserved, and it will not be possible to do all experiments simultaneously. Thus I consider it reasonable to plan to use the EPICS spectrometer for this purpose.

For a beam line, I propose that a dispersed beam, similar to EPICS, but bending in the horizontal plane, would be appropriate. The dispersed beam would eliminate the need for detectors at an intermediate focus, which would otherwise be a rate limitation. With a 3 mm target (and a smaller beam spot) the resolution could be of the order of 0.1% with 3 cm/% dispersion. Software corrections could be used for any aberrations affecting resolution and for the first-order corrections required for time-of-flight.

The most difficult problem is K-π separation. Several recently constructed kaon beams, including LESBI and LESBII at Brookhaven and k_{25} at CERN, have had π:k ratios of 10:1 or worse. The explanations given (without proof) have been variously decays of hadrons near the production target (e.g. $K^0 \rightarrow 2\pi$), production or scattering of pions in the walls of the vacuum system, and imperfect optics. I believe that optics problems can be corrected if they exist, and that the other proposed sources can be eliminated if one chooses to make an image of the target upstream of the separator. A slit placed at this location can clean up any halo and should make possible a substantial improvement in the action of a downstream separator. This has the additional advantage of locating the separator further from the production target than has usually been the case. A design using conventional magnets is presented in the Appendix. This system is approximately 15 m long, has $\Delta\Omega\Delta p/p$ of 20 msr %, has resolution of 0.1%, and yields roughly 10^7 K^- of

700 MeV/c per 10^{14} interacting protons. A detailed calculation is required in order to attempt to estimate the π:K ratio. I expect that it will approach 1:1 for this design.

Note: In the question period, someone asked about kaon decay after the last magnet. The decay length for kaons is 5.3 m at 700 MeV/c. It is not possible for decays in the last 1.2 m (from the middle of the last bend) of the proposed design to contribute a large number of pions. A second objection was that the last K beam built at the Bevatron[21] had two stages of separation, yet had a π:K ratio of 18:1. We should study this result carefully, since it could indicate that we have not considered all possible sources of trouble. However, the authors point out that because of mechanical problems, the beam was never properly tuned. Also the kaon yield at the 6 GeV Bevatron energy is much lower than at 30 GeV -- the π:K ratio at the target will be much worse at Bevatron energies. After looking at the sketch of the design for this beam, I wonder if it is possible for high-energy pions to penetrate the apparatus and scatter into the final target. It appears that massive shielding should be provided around the beam pipe after the first bend in order to prevent penetration and rescattering.

IV. A HIGH-ENERGY K AND π BEAM AND SPECTROMETER

It is possible to construct a system similar to EPICS[22] designed for kaons and pions up to 1 GeV/c. Such a system of modest $\Delta\Omega\Delta p/p$ -- say 10 msr % -- could have 10^9 π^+ or π^-/s and 10^7 K^+/s. Resolution of 1 or 2 parts in 10^4 should be possible. Kaon separation is not a crucial question, since for pion scattering (π^+, K^+) and (K^+, K^+), good particle identification after the spectrometer would be sufficient to eliminate background. A Fitch-type[23] Čerenkov counter can be designed to separate pions from kaons in a large phase-space beam. Such a system would have more than 3× more kaon flux than the present pion flux at SUSI at SIN today;[24] it will certainly be possible to have an exciting program of kaon inelastic scattering with such a system. Pion scattering -- especially π^+/π^- comparison -- could be done ∿ 50× faster than at EPICS. Perhaps, for the pion case, we could trade intensity for better resolution. This, combined with the better transparency of the nucleus to 700 MeV/c pions and the larger available pion flux, should result in an extremely effective program of pion scattering at a high-intensity machine.

V. CONCLUSION

We have seen that a series of improvements to LAMPF, including the construction of a low-energy pion spectrometer, a more intense polarized ion source, and a pulsed pion/muon beam, are possible in the next five years. A 1.5 GeV d.c. electron machine and experimental areas might be constructed from major components already existing on the LAMPF site. A 30 GeV, high-intensity machine provides numerous opportunities for nuclear physics experiments including (K, K′), (π, π'), (K^-, π^-), (π^+, K^+), and (K^-, K^+). Two spectrometer systems are proposed: a 700 MeV/c well-separated beam and spectrometer for (K^-, π^-); and a 1 GeV/c version of EPICS for (K, K′), (π, π'), and (π^+, K^+). These facilities will ensure a bright future for nuclear physics at LAMPF in the decade to come.

REFERENCES

1. G.W. Hoffmann, in "Workshop on Nuclear Structure with Intermediate Energy Probes," Los Alamos, January 1980, LA-8303-C, p. 99.

2. T.A. Carey, W.D. Cornelius, N.J.D. Giacomo, J.M. Moss, G.S. Adams, J.B. McClelland, G. Pauletta, C. Whitten, M. Gazzaly, N. Hintz and C. Glashausser, Phys. Rev. Lett. 45, 239 (1980).

3. For a recent review, see N. Hintz, in "Proceedings of LAMPF Users Group Meeting," October 1980, to be published. A typical recent paper is M.L. Barlett, J.A. McGill, L. Ray, M.M. Barlett, G.W. Hoffmann, N.M. Hintz, G.S. Kyle, M.A. Franey and G. Blanpied, Phys. Rev. C 22, 1168 (1980).

4. A. Wriekat, G.S. Adams, M. Bleszynski, S.M. Haji-Saerd, G. Igo, J.B. McClelland, G. Pauletta, C.A. Whitten, Jr., M.M. Gazzaly and N. Tanaka, Phys. Lett. 97B, 33 (1980).

5. J.M. Moss, private communication.

6. G.W. Hoffmann and C. Glashausser, private communication.

7. See "Proceedings of Conference on Polarization Phenomena," Santa Fe, New Mexico, August 1980, to be published; and "Proceedings of International Symposium on High-Energy Physics with Polarized Beams and Polarized Targets," Lausanne, Switzerland, September 1980, to be published.

8. W. Cornelius, private communication.

9. P. Lefèvre, D. Möhl and G. Plass, in "Proceedings of International Conference on High-Energy Accelerators," CERN, Geneva, 1980 (Birkhäuser, Basle, 1980), p. 819. See also CERN/PS/DL-80-13.

10. See also K. Kilian, "Possibilities in Low-Energy Antiproton Physics at LEAR," in "Proceedings of LAMPF Users Group Meeting," October 1980, to be published.

11. R. Eisenstein, in Proceedings of this Workshop.

12. H. Pirner, Phys. Lett. 85B, 190 (1979).

13. H.A. Thiessen et al., "The (π^+, K^+) Reaction: A New Tool for the Study of Hypernuclear Structure," Brookhaven AGS experiment # 758.

14. C.L. Morris, in "Workshop on Nuclear Structure with Intermediate Energy Probes," Los Alamos, January 1980, LA-8303-C, p. 57.

15. H.A. Thiessen, Nucl. Phys. A335, 329 (1979).

16. M.A. Moinster et al., Phys. Rev. C 18, 2678 (1978).

17. R.R. Johnson, T. Masterson, B. Bassaleck, W. Gyles, T. Marks, K.L. Erdman, A.W. Thomas, D.R. Gill, E. Rost, J.J. Kraushaar, J. Alster, C. Sabev, J. Arvieux and M. Krell, Phys. Rev. Lett. 43, 844 (1979).

18. A group at TRIUMF under Dick Johnson in constructing a spectrometer from salvaged magnets, a Karlsruhe/Neuchâtel Collaboration (Egger and Kluge) has ordered a new spectrometer for SIN, and a U of Va/LAMPF Collaboration under Klaus Ziock is studying a proposal for a new spectrometer at LAMPF.

19. "Proceedings of the Workshop on Program Options in Intermediate Energy Physics," Los Alamos, August 1979, LA-8335-C, p. 49.

20. Proposals for a high energy electron accelerator are being prepared by a U. of Va group under J. McCarthy, by Argonne National Laboratory, and by the Bates Laboratory.

21. C. Leeman, R. Morgado and R. Sah, "A New High Intensity K-Beam at the Bevatron," LBL-3369 (1975).

22. H.A. Thiessen, "A Proposal For EPICS: A High Resolution Beam and Spectrometer For Nuclear Structure Studies With Pions," LA-4534-MS, unpublished.

23. D.M. Ritson, "Techniques of High-Energy Physics" (Interscience, New York, 1961).

24. The presently usable flux of π^+ and π^- at SUSI is limited to 3×10^6/s. This limitation results from counting rate problems in the hodoscope or proportional chambers located at the intermediate focus of the beam line. Q. Ingram, private communication.

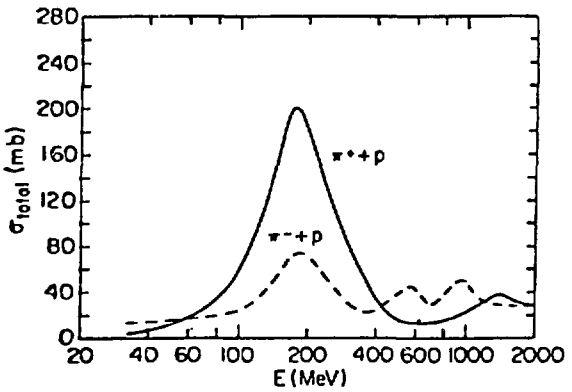

Fig. 1

The pion-nucleon total cross-section versus pion energy. The solid curve is π^+-p, the dashed curve is π^--p.

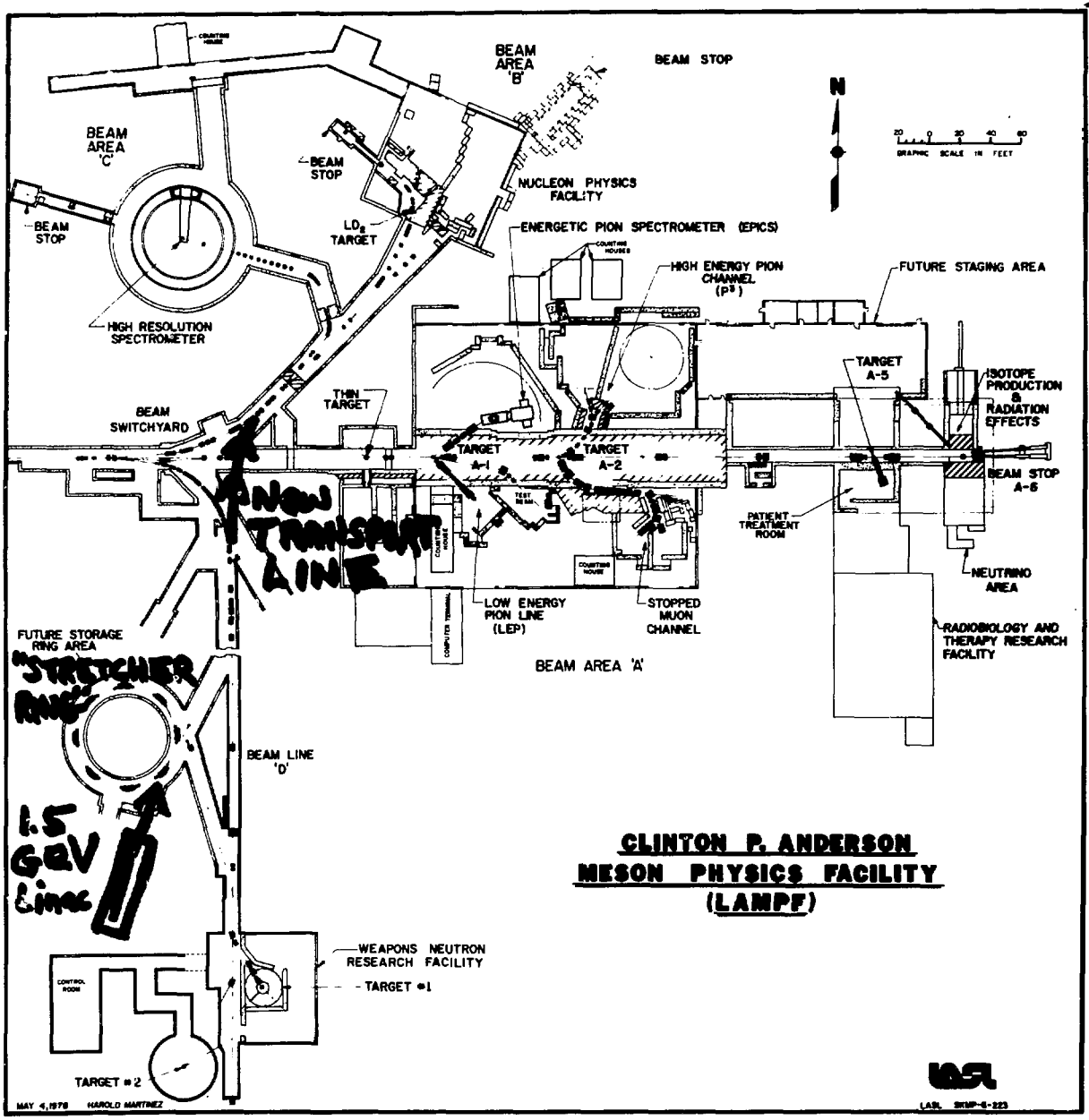

Fig. 2

LAMPF experimental areas plan showing possible use of the proton storage ring as a 1.5 GeV electron accelerator providing a beam for experiments at HRS and in Area B

APPENDIX - DISPERSED SEPARATED BEAM

A. TRANSPORT INPUT DECK

```
1.  0.15  40.  0.1  25.  0.  2.  0.7  'BEAM';
3.  0.78514  'DRIFT';
16.  1.  0.16530E-03  'EPS1'
16.  5.  8.  'GAP';
16.  7.  0.4  'K1';
16.  8.  4.4  'K2';
2.  -25.  'ROT1';
4.  1.7  18.  0.  'BEND1';  '75 DEGREES';
2.  -25.  'ROT2';
3.  0.4  'DRIFT';
5.  0.5  -9.3789  10.  'QUAD';
18.  0.1  -.02022  1.;  'SEXTUPOLE IN DRIFT';
5.  0.5  9.21037  10.  'QUAD';
3.  0.5  'DRIFT';  'TO Y FOCUS';
3.  0.2  'DRIFT;  TO X FOCUS';
3.  0.9  'DRIFT';
5.  0.25  11.23610  10.  'QUAD';
18.  0.1  -0.01517  1.0  'SEXTUPOLE';
5.  0.5  -10.13987  10.  'QUAD';
3.  0.1  'DRIFT';
5.  0.25  11.23610  10.  'QUAD';
3.  0.9  'DRIFT';  'HALF SEPARATOR';
3.  0.9  'DRIFT';  'HALF SEPARATOR';
5.  0.25  11.23610  10.  'QUAD';
3.  0.1  'DRIFT';
5.  0.50  -10.13987  10.  'QUAD';
18.  0.1  +.01521  1.  'SEXTUPOLE';
5.  0.25  11.23610  10.  'QUAD';
3.  0.9  'DRIFT';  'X FOCUS';
3.  0.2  'DRIFT';  'Y FOCUS';
3.  0.5  'DRIFT';
5.  0.5  9.21037  10.  'QUAD';
18.  0.1  +.00755  1.  'SEXTUPOLE';
5.  0.5  -9.37389  10.  'QUAD';
3.  0.4  'DRIFT';
16.  1.  0.27895E-4  'EPS2';
2.  -25.  ROT3;
4.  1.7  18.  0.  'BEND';  '75 DEGREES'
2.  -25.  'ROT4';
3.  0.78514  'DRIFT';  'KAON SCATTERING TARGET';
```

B. TRANSPORT MATRIX-INPUT TO OUTPUT

```
-1.0   0.     0.     0.     0.    2.90
22.8  -1.0    0.     0.     0.  -33.0
 0.    0.    -1.0    0.     0.    0.
 0.    0.   -15.6   -1.0    0.    0.
 3.3  -0.29   0.     0.    +1.0  -7.48
 0.    0.     0.     0.     0.    1.0
```

C. SECOND ORDER X MATRIX-INPUT TO OUTPUT

```
1.11 -6.812E-04
1.12 -3.124E-03  1.22 -3.170E-04
1.13  0.         1.23  0.         1.33 5.123E-02
1.14  0.         1.24  0.         1.34 7.527E-03  1.44 -2.502E-07
1.15  0.         1.25  0.         1.35 0.0        1.45  0.         1.55 0
1.16 -1.447E-01  1.26  9.687E-03  1.36 0.0        1.46  0.         1.56 0  1 66 2.316E-01
```

D. OUTPUT BEAM SIZE (SECOND ORDER)

X	5.85 cm
θ	81.0 mrad
Y	0.76 cm
ϕ	26.3 mrad
L	19.9 cm
δ	2.0%
length	15.37 m

ANTINUCLEON TIME-SEPARATED BEAMS (TSB)*

T. E. Kalogeropoulos
Department of Physics, Syracuse University, Syracuse, New York 13210

The work which was performed at the AGS in search of a narrow bunched proton beam is summarized. The encouraging results lead to the concept and design of a time separated antiproton beam. This beam is more intense and of higher luminosity than any of the past, present and projected antiproton beams.

I. INTRODUCTION

This work has been motivated initially by interest in $\bar{N}N$ interactions at low energies. Antiproton beams present serious experimental problems at low energies because of ionization losses. To bypass them, it was proposed[1] the use of antineutrons and to tag their energy by time of flight (TOF). This requires knowledge of the time at production.

It was proposed to extract the protons from the AGS while maintaining the RF power during flat top and thus be able to define the production time. It was generally assumed and observed in neutrino experiments that the width of the proton bunches would be too wide ($\sim$ 50 ns) for TOF. It was also thought that a 'continuum' of protons may be present between bunches which could impose serious problems in identifying the antineutrons.

We report briefly here our work using an RF structured external beam at the AGS and give the references for further details. Further, we present their consequences for an antiproton time separated beam (TSB) which compares favorably to other antiproton beams up to $\sim$ 10 GeV/c.

II. TIME STRUCTURE

The time structure of the slow extracted beam, while maintaining the RF power during flat top, has been measured[2] by time delay coincidences of 14 GeV/c π^- signals. The results are:

- Bunch width (FWHM) is (3-5)ns,
- Intensity drops (Fig. 1) exponentially with time constant 1.7 ns,
- Bunches are separated by 220 ns.

The surprisingly small width has been interpreted[3] as a consequence of the characteristics of resonance extraction which is used in the slow ($\sim$ 1 sec) extracted beam. It has been further suggested that adjustments of the chromatic parameters may produce even much smaller widths.

---

*Contribution to the Workshop on "Nuclear and Particle Physics at Energies up to 31 GeV: New and Future Aspects", Los Alamos National Laboratory, January 5-8, 1981.

Work supported by the National Science Foundation, Washington, D. C.

III. LOW ENERGY ANTINEUTRON TAGGING

We designed a simple detector (Fig. 2) to identify antineutrons[4]. This detector has been placed in a forward neutral beam 71° downstream of the production target (Fig. 3). The detector is an array of scintillation counters around a polyethelene target. The trigger for antineutrons was based on multiplicity ($\geq$ 3).

Fig. 4 shows the distribution of antineutrons as a function of time of arrival (at 0 and 220 ns the β = 1 particles arrive). The events between $\sim$ 1.0 to 0.3 GeV/c have the expected characteristics (angular and multiplicity distributions) for $\bar{N}N$ annihilations. These events correspond to $\sim 10^{14}$ interacting protons. Their production is in reasonable agreement with the predictions based on the production of antiprotons at very high energies ($x \simeq 1$) and charge symmetry in the pp cm system.

In spite of the small fraction of antineutrons at these low energies ($\sim 10^{-6} - 10^{-8}$) and the simplicity of detection, it is impressive their easy identification. Further, the resolution in $\bar{N}N$ mass (Fig. 5) is unprecedented and clearly this technique, if there are narrow $\bar{N}N$ resonances near threshold, can play a unique role.

This technique is effective for non relativistic antineutrons. In order to get good resolution at higher energies large distances are required which result to unacceptable small fluxes.

IV. TIME SEPARATED ANTINUCLEON BEAMS

The previous work leads naturally to the concept of the antiproton time separated beam. It consist of a series of focusing-defocusing quadripoles (transfer channel) which transmit a momentum band of charged particles to large distances from the point of production without a loss of intensity (for stable particles). Such a beam has already been designed by Brown[5].

Figs. 6, 7, 8 compare the fluxes, luminosities and event rate for the interesting rare $\bar{p}p \to e^+e^-$ reaction. From the flux point of view the TSB beam is superior and can easily be improved by special magnet designs particularly in the front section which images the target into the transfer channel. The power required for the long ($\sim$ 1 Km) transfer channel is typical of conventional beams while the cost is reasonable: $\sim \$10^6$/Km.

We would like to emphasize, however, that in comparing this beam with others, one should keep in mind that the momentum bite is large ($\sim \pm$ 4%). Thus, if one is interested in studying a narrow state, for example the J/ψ, then an appropriately large target will be required in order that all antiprotons will go over its mass.

An antiproton TSB will provide antideuterons as well. We estimate using known[6] $\bar{d}$ production that few thousands $\bar{d}$/sec will be also present.

If a LH_2 target is inserted at the end of the $\bar{p}$ TSB then the charge exchange reaction ($\sim$ 10% of total) which has a large forward peak can provide an antineutron beam. The knowledge of the $\bar{p}$ energy, the $\bar{p}p \to \bar{n}n$ vertex and the $\bar{n}$ interaction at the detector provide the $\bar{n}$-momentum accurately. Such antineutron beams can be made to yield fluxes of $\sim (10^{-2} - 10^{-3})$ the $\bar{p}$ flux or similar to the fluxes obtained for antiprotons with conventional beams (Fig. 5).

REFERENCES

1. T. E. Kalogeropoulos, AGS proposal 625, 1973.
2. A. Fainberg and T. E. Kalogeropoulos, BNL-18938 report (unpublished) 1974.
3. M. Q. Barton, BNL-19076 report (unpublished) 1974.
4. T. Brando, A. Fainberg T. E. Kalogeropoulos, D. Michael and G. Tzanakos, Nuclear Instruments and Methods (In Press).
5. H. Brown EP and S Division Technical Report No 90, BNL, 1980.
6. Dorfan et al., Physical Review Letters 14, 1003 (1965).

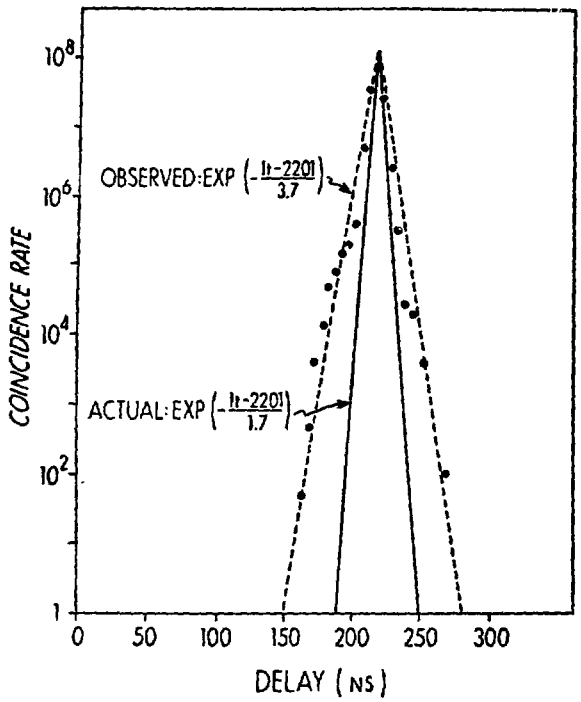

Fig. 1. The proton intensity as a function of the time from the previous bunch. Dots are the data. Since this distribution is the result of convolution of two distributions the actual bunch intensity has a time constant of 1.7 ns.

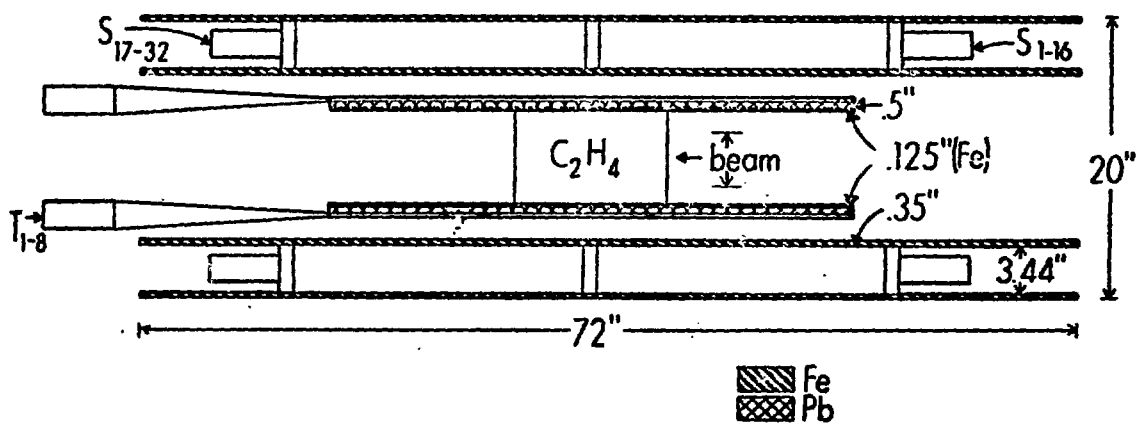

Fig. 2. The antineutron detector. The liquid scintillator counters (S_{1-32}) measure the multiplicity, azimuthal and forward/backward asymmetries. The signals from these counters were required to be in coincidence with the corresponding plastic scintillator counters (R_{1-8}).

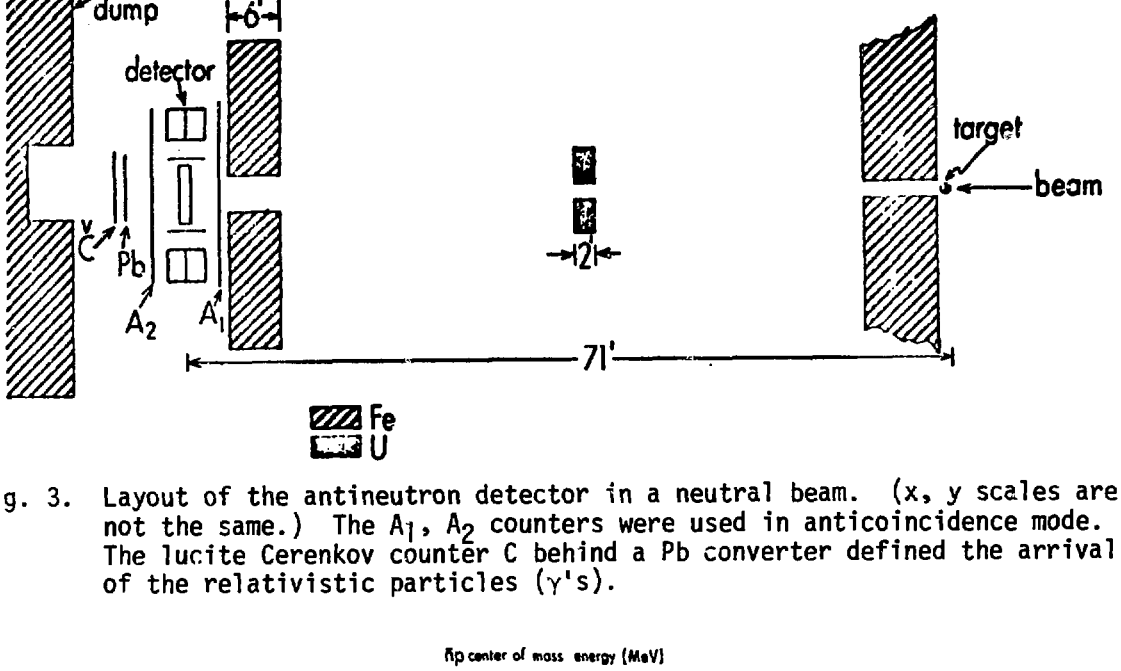

Fig. 3. Layout of the antineutron detector in a neutral beam. (x, y scales are not the same.) The A_1, A_2 counters were used in anticoincidence mode. The lucite Cerenkov counter C behind a Pb converter defined the arrival of the relativistic particles (γ's).

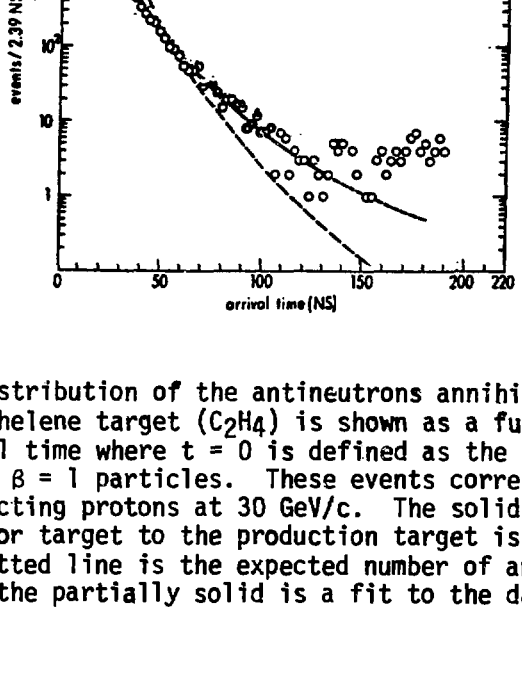

Fig. 4. The distribution of the antineutrons annihilating in the polyethelene target (C_2H_4) is shown as a function of the arrival time where t = 0 is defined as the time of arrival of the $\beta = 1$ particles. These events correspond to $\sim 10^{14}$ interacting protons at 30 GeV/c. The solid angle of the detector target to the production target is 20 μster. The dotted line is the expected number of antineutrons while the partially solid is a fit to the data.

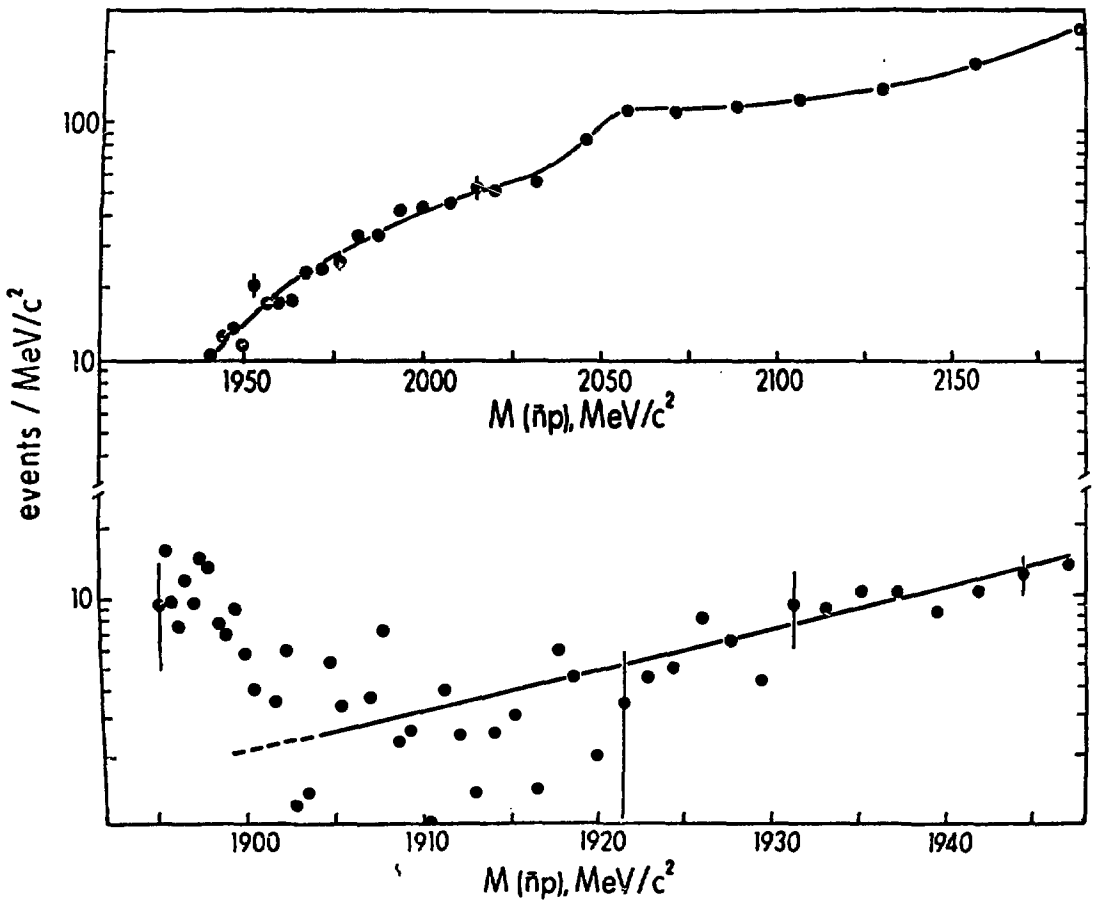

Fig. 5. The distribution of the antineutrons as a function of the $\bar{n}p$ invariant mass. Since each point corresponds to the resolution it is clear that high mass resolutions can be achieved, particularly if the distance is increased and the time resolution improved.

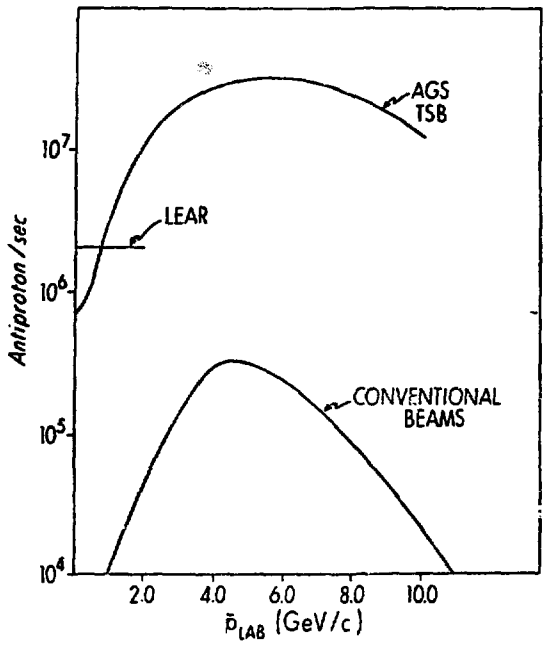

Fig. 6. A comparison of the antiproton fluxes for a TSB at the AGS, LEAR and in conventional beams. Maximum corresponding to the total (10^{13} ppp) proton flux available at AGS (PS).

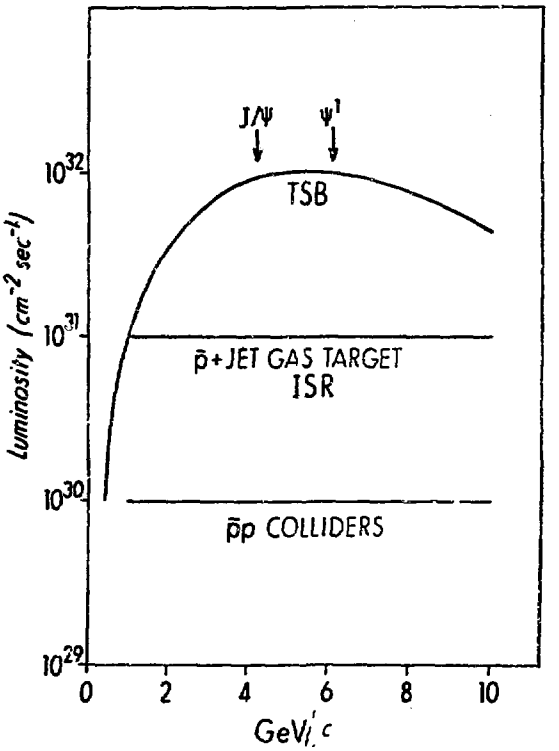

Fig. 7. Expected luminosities for TSB and 1 m of liquid hydrogen target antiproton in the ISR and a Jet gas target and $\bar{p}p$ colliders.

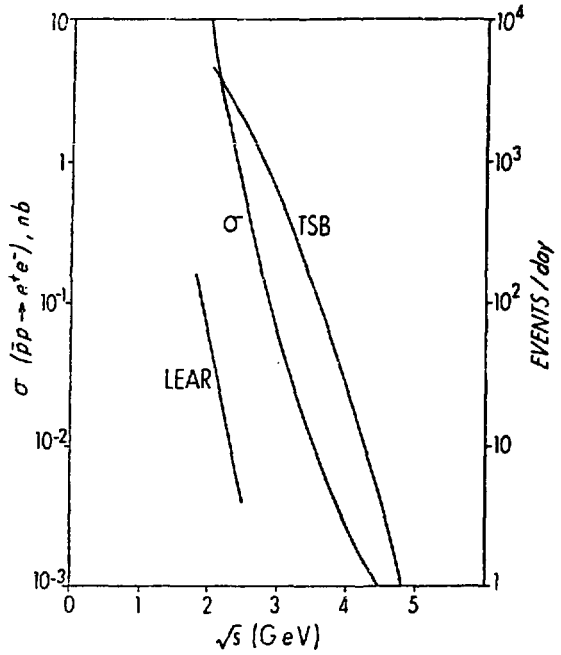

Fig. 8. Event rates for the rare reaction $p\bar{p} \to e^+e^-$ in the designed TSB at the AGS and for an approved experiment at LEAR as a function of the $p\bar{p}$ invariant mass.

NEUTRON OSCILLATIONS

H. L. Anderson

Los Alamos National Laboratory

As Cy Hoffman made clear in the preceeding talk there is no reason to believe that baryon number should be a good quantum number. No violation of this conservation law has yet been seen. However, we are living in a period when it has become popular and important to look for ways in which the symmetries and their corresponding conservation laws might be broken. In fact, there now exist a plethoria of theories, the so-called unified theories in which baryon number emerges unconserved. In particular, for some theories, $\Delta B = 2$ is allowed at a level that should make a process like $n \rightleftarrows \bar{n}$ observable in the laboratory. This paper discusses how a practical test of such theories might be made.

Neutron-Antineutron Conversion

The physics involved in the process $n \rightleftarrows \bar{n}$ with $\Delta B = 2$ is analogous to the process $K^0 \rightleftarrows \overline{K^0}$ with $\Delta S = 2$. The neutron and antineutron may be treated as components of a two component system. The system which may start out at $t = 0$ as a pure neutron amplitude will, if unperturbed as time goes on, build up an appreciable antineutron amplitude. The time available for the conversion is limited by neutron beta decay, whose mean life is 1000 seconds.

In the unperturbed case, e.g. in the absence of magnetic fields. The transitions between the two states of the system is given by a 2 x 2 matrix.

$$\begin{pmatrix} M & \delta m \\ \delta m & M \end{pmatrix}$$

where M is the nucleon mass, the same for n as for $\bar{n}$, and δm is the

perturbation energy through which the transition $n \rightleftarrows \bar{n}$ proceeds. Glashow's estimate,[1] $\delta m < 10^{-21}$ eV, emphasizes how small the interaction is.

In practice, the masses of n and $\bar{n}$ are not exactly the same because of the presence of the earth's magnetic field. We write $\Delta M = \mu H$ and recognize that the magnetic moment, while the same in magnitude, has opposite signs for n and $\bar{n}$. Thus, the matrix operator is written.

$$\begin{pmatrix} M + \Delta M & \delta m \\ \delta m & M - \Delta M \end{pmatrix}$$

It is a straight-forward matter to diagonalize this matrix and obtain the familiar expression for the evolution of the system in time. This is an oscillating behavior which several of the previous speakers in this workshop have discussed in connection with either $K^0 \rightleftarrows \overline{K^0}$ or neutrino oscillation experiments.

If we test the composition of the beam by interposing a target which can distinguish n from $\bar{n}$, the probability that we will find $\bar{n}$ after a flight time t is given by

$$P_{\bar{n}}(t) = \frac{1}{2}\left(\frac{\delta m}{\Delta M}\right)^2 \left(1 - \cos \frac{2\Delta M t}{\hbar}\right) e^{-\lambda t}$$

the last factor $e^{-\lambda t}$ takes into account the reduction in amplitude due to neutron beta decay. In a field of 0.5 gauss, $\Delta M = 3 \times 10^{-12}$ eV, much larger than δm. Thus the conversion is highly suppressed in the presence of a magnetic field. However, with

$$\frac{2\Delta M t}{\hbar} \ll 1 \qquad \text{and} \qquad \lambda t \ll 1$$

We obtain a field independent expression,

$$P_{\bar{n}}(t) = \left(\frac{t}{\tau}\right)^2$$

where $\tau = \hbar/\delta m$ is the mixing time and is a measure of the strength of the $\Delta B = 2$ interaction.

Unified Theories

Not all unified theories allow $\Delta B = 2$. In fact, the SU(5) grand unification group in which the $SU(2)_2 \times U(1)$, the electroweak group of Weinberg-Salam, and $SU(3)_c$, the strong interaction color group, are embedded together has $\Delta(B - L) = 0$ as a conservation law. This allows proton decay but not neutron oscillations. On the other hand there is a large class of theories, among them the Pati-Salam Theories, in which $\Delta B = 2$ processes can occur with mixing times that are accessible to experiment. Estimates of the mixing time given by Glashow[1] and Marshak[2] are of the order of $\tau \approx 10^6$ seconds. Terry Goldman has been studying this question in more detail and has given

$\tau = 10^{7\pm2}$ seconds.

Thus, it appears that neutron oscillations are complementary to proton decay in providing the necessary evidence to help decide which of the multitude of unified theories might have some relevance to nature.

The following chart, due to Chang[3] is a useful way of displaying how the outcome of proton decay or neutron oscillation experiments can help decide which of the theories might have some validity.

TABLE 1

Proton Decay	$n \to \bar{n}$	Theory	
yes	no	GUT	SU(5) type grand unified theory
yes	yes	EUT	extended unified theory
no	yes	PUT	partial unified theory
no	no	???	unified theory unknown

Experimental Limit

The $n \to \bar{n}$ process can take place in a nucleus and then give rise to a striking signature, the release of 2 GeV in energy when the $\bar{n}$ annihilates with another nucleon in that nucleus. There is an emission, 4-5 pions on average, some of which may be π^+ which escape absorption and decay to μ^+. Such $\pi \to \mu$ decays have been looked at by Reines[4] in a deep mine experiment and have been used to set a limit of $\sim 10^{30}$ years for proton decay.[5] To the extent that the branching ratio for the production of π^+ in proton decay is not very different from that in $\bar{n}$ annihilation we can take the same lifetime to apply to either type of nucleon instability. We can make a rough estimate of this lifetime by calculating the transition rate using Fermi's Golden Rule.

$$w = \frac{2\pi}{\hbar} |H|^2 \frac{dN}{dE}$$

where H is the transition matrix element = δm x an overlap integral, and dN/dE is the number of states per unit energy interval.

Using plausible values, a level spacing of 1 GeV, a mixing time of 10^6 seconds, and taking into account that the overlap between two nucleons in a nucleus will be of the order of 1/100 (Mohapatra and Marshak[2] estimate), we obtain $1/w = 7 \times 10^{29}$ years. Thus, specific theories aside, an experiment on neutron oscillation that sets a mixing time $> 10^6$ seconds will establish a new limit for nucleon stability.

$n \to \bar{n}$ Conversion Experiment

To observe the conversion $n \to \bar{n}$ we arrange to have a large number of neutrons moving as slowly as possible over a long evacuated drift space in which the magnetic field is kept low. The interaction of $\bar{n}$ with the target produces the spectacular signature of $\bar{n}n$ or $\bar{n}p$ annihilation, the emission of

4-5 pions, on average, with the release of 2 GeV in energy. The event rate may be written,

$$\nu_{n\to\bar{n}} = \left(\frac{\ell/v}{\tau}\right)^2 FT\epsilon$$

where ℓ is the drift length, v is the appropriate average neutron velocity,* τ is the mixing time, F is the total number of neutrons per second seen by the target, T is the time of observation and ϵ is the detection efficiency. In a practical experiment with ℓ = 10 meters, v = 1556 m/s (thermal neutrons), $\tau = 10^6$ seconds, $F = 10^{12}$ neutrons/sec, T = 8.64×10^4 seconds (1 day) and ϵ = 0.8, we can expect 2.8 events/day for a mixing time of 10^6 seconds.

To my knowledge there are 4 proposals to look for this process. An experiment at Grenoble[6] uses the cold neutron beam from that reactor. This experiment has modest sensitivity, 10 events in 100 days for a mixing time of 10^6 seconds. However, this is an approved experiment at Grenoble and scheduled to run in the fall 1981. Its sensitivity could be increased by increasing the size of and the investment in the detector.

The experiment proposed at Oak Ridge[7] is more ambitious. The plan is to extract a large flux of neutrons from the Oak Ridge Research Reactor which operates at 50 MW. This experiment can give 400 events/day for 10^6 second mixing time. One problem here is how to handle the radiation problems when the 1m x 1m opening which will be used as the neutron source is exposed. This proposal is awaiting funding.

*Strictly speaking we need $(\overline{1/v^2})$, in which case v = 1556 m/s for a Maxwellian distribution with T = 293^0 K.

The experiment at Pavia[8] also uses a reactor. This is only 250 kilowatts but the thermal column is arranged to provide an efficient thermal neutron source. The sensitivity appears to be comparable to Grenoble.

The KEK proposal[9] is to use the external proton beam from the booster and have this strike a high neutron yield spallation target. The neutrons emerging at right angles from the target will be cooled in a cold (liquid methane?) moderator. The plan has not been sufficiently developed to say what sensitivity can be obtained.

Experiment at Los Alamos

At Los Alamos two neutron sources are available. The best experiment could be done using the neutrons from the beam dump of the Los Alamos LINAC. Unfortunately, this presently serves a different purpose and has so much steel and concrete around it that it would be a major effort to redesign the beam dump to install a proper moderator and openings that would be suitable for an intense cold neutron beam. However, the WNR[10] (Weapons Neutron Research) facility does provide a means for using 20 μa from the LAMPF accelerator for slow neutron production. With an idealized moderator 10^{12} thermal neutrons per second could be delivered to a 1 meter diameter target with a 10 meter flight path. These are just the conditions discussed above which give an event rate of 2.8 events/day for a 10^6 second mixing time. An important advantage in using a pulsed neutron source from an accelerator is that the time of flight separates the neutrons from the capture gamma rays that are produced in the course of thermalizing the neutrons. The detector can be gated off while the gamma rays, traveling at the speed of light are arriving, and gated on when the much slower neutrons are arriving at the target.

I have devoted most of my effort to date to the design of an experiment that uses the Omega West Reactor. This is a continuous source of neutrons but

its steady output and reliable operation over long periods of time are valuable features if long running times turn out to be required to push the sensitivity for a given detector as far as possible.

The Omega West Reactor operates at 8 megawatts and produces about 2.5 x 10^{17} neutrons/sec. In Figure 1 I show an arrangement which could serve for an $n \rightleftarrows \bar{n}$ oscillation experiment. We would remove most of the thermal column, but leave enough, 75 cm, to thermalize the neutrons from the core. The number of neutrons emerging from the front face of this shortened thermal column is 1.5 x 10^{15} neutrons/sec. This refers to the flux emitted from the full 1.2 m x 1.2 m area.

A detector mounted directly in front of the thermal column of the reactor with a 1 meter diameter target and at 10 meters distance would give 2.6 events/day for a 10^6 second mixing time.[11] Unfortunately, the control room for the reactor is in that direction and the radiation levels from neutron capture gamma rays and from fast neutrons and gamma rays from the reactor core would be difficult to handle.

We show a solution in which the direction of the beam is turned 90^0 by means of a graphite reflector. With the same 1 meter diameter target and detector we get 6.5 x 10^{11} neutrons/sec[11] and an event rate of 0.9/day, 35% of the 0^0 arrangment.

We show a cylindrical detector[12] surrounding the target in which concentric layers of iron and scintillator serve as a calorimeter. The scintillators are viewed at both ends with photomultiplier tubes for accurate timing of the $\bar{n}$ annihilation shower.

Note the use of Li^6D for the target and for the liner of the cylindrical drift tube near the detector. We use the high absorption cross-section of Li^6 for thermal neutrons to remove the neutrons of the beam with

a minimum of capture gamma ray production. The branching ratio for the (n,γ) process in Li^6D is 1/23000 of the total absorption. Without the Li^6D the number of capture gamma rays produced at the detector would be of the same order as the neutron flux. With Li^6D the number of capture gamma rays would be 23000 times less or about 3×10^7 per second. More worrisome are the capture gamma rays which accompany the neutrons coming from the graphite reflector. These amount to about 6% of the neutron flux. We take advantage of the small angle with which they enter the detector. We line the inside cylindrical surface of the detector with a 1.2 cm thick layer of lead. Because of the oblique angle of incidence only a small fraction, 10^{-3} of these γ's enter the detector. This number is manageable because the amount of energy deposited by these γ-rays in a 20 ns time gate is only a small fraction of the energy deposited by the annihilation shower. By setting a threshold well above the level of the capture γ background we can detect the presence of the large energy deposition of the annihilation without difficulty. Thus the large pulse expected as the signature of $\bar{n}$ in the beam is used to trigger the readout of time and pulse height from each scintillator in the detector array.

It remains to distinguish clearly the cosmic ray events which are also capable of producing a several hundred MeV pulse in the calorimeter. These also cause triggers and we have to depend on a detailed analysis of time and pulse height information from the detector array to distinguish events which come from inside and not from the outside of the detector.

We reduce the number of charged particle cosmic ray events, mainly high energy muons, by a scintillator array surrounding the calorimeter that acts as a veto. It is important to prevent a self-veto, so enough iron is interposed

between the calorimeter and the cosmic ray veto to range out most of the possible charged pions from the annihilation before they can reach the veto.

Cosmic ray neutrons may enter the calorimeter without setting the veto. We reduce the number of these with a suitable concrete shield and depend on the information detail from the scintillator array in the detector to distinguish a possible neutron produced shower from the annihilation event. By these means we expect to reduce the number of cosmic ray events that can simulate the $\bar{n}$ annihilation signature to less than 1 per 100 days.

An important advantage of the $n \rightleftarrows \bar{n}$ experiment of over proton decay is that the neutron beam can be turned off and a detailed study of the cosmic ray events made. We can use direct observation of the cosmic rays to teach us how to identify them. We can also nullify the effect by turning on the magnetic field. The $n \rightleftarrows \bar{n}$ effect is easily destroyed if the magnetic field in the drift tube is not maintained at the 10^{-4} - 10^{-3} gauss level. Thus, an effect, if seen would be easy to verify.

Since presenting this report we have studied the possibility of using a 30 cm x 30 cm port in the reactor that can view the center of the thermal column quite close to the reactor core. This makes accessible a thermal neutron flux of 10^{13} neutrons/cm^2/sec at right angles to the axis of the thermal column. The event rate for a detector similar to the one described above, is 14 events/day. With the cosmic ray background reduced sufficiently we should be able to have a sensitivity of 1 event/100 days for a 3×10^7 second mixing time.

I thank W. S. C. Williams, A. Lundby, S. Fukui, L. Schwarz, and J. Solem for helpful discussions.

References

1. S. L. Glashow, "The Future of Elementary Particle Physics," 1979 Cargese Summer Institute, Harvard Preprint HUTP-79/A059.
2. R. N. Mohapatra and R. E. Marshak, "Phenomenology of Neutron-Antineutron Oscillations,"Virginia Polytechnic Institute Preprint VPI-HEP-80/4 and CCNV-HEP-80/7 (1980).
3. L. N. Chang, Talk given at the VPI Workshop on "Weak Interaction as Probes of Unification," Blacksburg, VA, Dec. 4-6, 1980.
4. J. Learned, F. Reines, and A. Soni, Phys. Rev. Lett. 43, 907 (1979).
5. For a review see M. Goldhaber, P. Langacker, and R. Slansky, "Is the Proton Stable?" Science 210, 851 (1980).
6. Milla Baldo-Ceolin, "Search for Neutron-Antineutron Oscillations," Talk presented at "Astrophysics and Elementary Particles, Common Problems," Rome, February 21-23, 1980.
7. Glenn Young, Talk given at VPI Workshop on "Weak Interaction as Probes of Unification," Blacksburg, VA, December 4-6, 1980.
8. S. Ratti, Talk given at VPI Workshop on "Weak Interaction as Probes of Unification," Blacksburg, VA, December 4-6, 1980.
9. T. Kamai, Talk given at VPI Workshop on "Weak Interaction as Probes of Unification," Blacksburg, VA, December 4-6, 1980.
10. I am indebted to John Moses, Los Alamos National Laboratory, P Division, for pointing this out to me.
11. Calculations by R. J. McKee, Los Alamos National Laboratory, P Division.
12. I thank J. C. Peng, Los Alamos National Laboratory, P Division, for suggesting a cylindrical type of detector.

Figure Caption

Figure 1: Arrangement at the Los Alamos Omega West Reactor for a neutron-antineutron experiment. Part of the thermal column is removed. A large graphite reflector deflects the neutrons at right angles. The drift distance is 8.7 m, the detector diameter is 1 m. A cylindrical iron-scintillator sandwich calorimeter will trigger on $\bar{n}$ annihilation in the Li^6D target. Time and pulse height information in the calorimeter hodoscope identifies cosmic ray triggers. The drift space is lined with a mu metal shield to keep the magnetic field under 10^{-4} gauss. The vacuum is maintained better than 10^{-5} Torr.

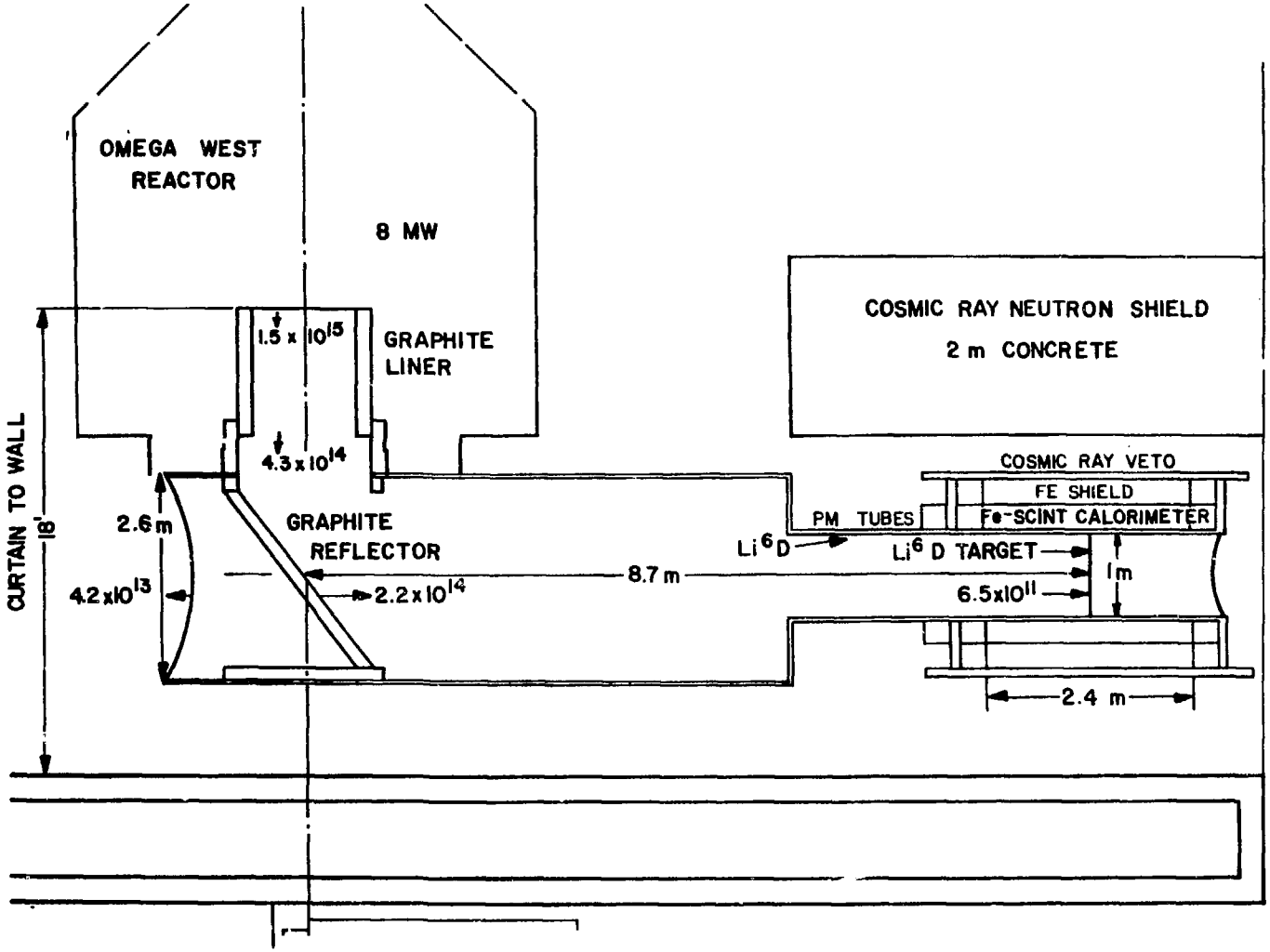
OMEGA WEST
REACTOR
8 MW
COSMIC RAY NEUTRON SHIELD
2 m CONCRETE
1.5 x 10^15
GRAPHITE
LINER
4.3 x 10^14
CURTAIN TO WALL
18'
2.6 m
GRAPHITE
REFLECTOR
4.2 x 10^13
2.2 x 10^14
8.7 m
COSMIC RAY VETO
FE SHIELD
PM TUBES
Fe-SCINT CALORIMETER
Li^6 D
Li^6 D TARGET
6.5 x 10^11
1 m
2.4 m

RESULTS OF A FIRST ROUND 150 MeV ν_μ OSCILLATION EXPERIMENT AND IMPLICATIONS FOR FUTURE LAMPF EXPERIMENTS

B. Cortez, J. LoSecco* and L. Sulak*
Harvard University, Cambridge, Massachusetts 02138

A. Soukas, W. Weng
Brookhaven National Laboratory, Upton, New York 11973

We report on a sensitive search for neutrino oscillation. A pure ν_μ beam of low energy was constructed at the Brookhaven AGS. The appearance of any ν_e in the beam would signify oscillations. To maximize sensitivity the energy of the neutrino beam was reduced to 150 MeV. The existing neutrino beam line and a 30T liquid scintillation calorimeter used in previous νp scattering experiments [1] were utilized.

As described elsewhere in the conference [2], for the case of two neutrino mixing a pure ν_μ beam will have a ν_e fraction

$$\frac{\nu_e}{\nu_e+\nu_\mu} = \frac{\sin^2 2\theta}{2} \left(1 - \cos \frac{\Delta^2 \ell}{2E_\nu}\right)$$

where ℓ is the distance travelled, $\Delta = \sqrt{m_1^2-m_2^2}$ is the difference of neutrino masses, and θ is the mixing angle. Sensitivity to small Δ requires large ℓ and small E. A proton beam momentum of 1.5 GeV/c is used to maximize pion flux and facilitate electron/muon separation by total visible energy cuts. The observed e/μ ratio is compared to the expected number as a function of Δ and θ. Systematic errors in the calculation cancel out. A limit on oscillations at $\Delta \sim$lev and maximal mixing can be set, and implications for future dedicated experiments can be drawn.

We made extensive calculations of the expected event rate. It can be divided into three parts - pion production in the target, horn focusing, and neutrino interactions in the detector.

We rely on Cochran, et al.[3] for π^+ production by protons of 730 MeV. We use a target of pyrolytic graphite to maximize the event rate. The

target is 40 cm long, compared to an interaction length of 25 cm. It has a diameter of 2 cm to minimize pion reabsorption which peaks at these energies. The pion interaction length is ∿20cm so much of the forward flux is attenuated. The beam energy is 810 MeV to compensate for dE/dX losses in the target. This is below the kaon production threshold, thus reducing the contamination of ν_e. The only ν_e background comes from muon decay in the tunnel, which contributes less than 1% of the event rate.

Cochran, measured the pion flux for angles greater than 15^o. However, it is primarily the pions from less than 10^o that contribute to the neutrino flux in the detector, since the larger angle pions hit the walls of the tunnel before decaying. We have linearly extrapolated Cochran's results to 0^o; $\frac{d\sigma}{d\Omega}$ is 30% larger than at 15^o, assuming dominance of Δ in π^+ production.

The pions are traced through the magnetic focusing horn, which bends π^+ forward. The π^+ can then decay into $\mu+\nu_\mu$ in the tunnel. The total flux of neutrinos at the detector is increased by a factor of 4 by the horn and the event rate is increased by a factor of 6, due to the hardening of the spectrum. Figure 1 shows the angular distribution of the π^+, originally, after absorption in the target, and after horn focusing. Figure 2 is a plot of the neutrino energy spectrum at the detector, 150 m from the production target, which peaks at 170 MeV.

The detector is primarily CH_2 and the neutrinos interact on carbon as $\nu_\mu C \rightarrow \mu^- + X$. The cross section for $\nu_\mu n \rightarrow \mu^- p$ on free neutrons, valid at higher energies, overestimates the carbon scattering, since nuclear effects are important at 50 MeV kinetic energy. The nuclear transition $n \rightarrow p$ is Pauli suppressed. We will somewhat arbitrarily sum the cross section of Smith and Moniz [4] for a Fermi gas model with the calculations by two groups [5),6)] (ODW) for scattering into specific excited nuclear final states. The flux averaged cross section is $3.8 \times 10^{-39} cm^2$/nucleus of which 1.0×10^{-39} comes from ODW. These cross sections are plotted in figure 3. Figure 4 is the result of multiplying flux by cross section. The event rate peaks at 210 MeV, which would appear as 105 MeV of visible energy from a ν_μ interaction. A total visible energy decision at 150 MeV will be effective in separating ν_μ (E<150 MeV) from ν_e (E>150 MeV) interactions.

The expected number of ν_μ events in the absence of oscillations is 5 [7] down by a factor of 10^4 from normal 30 GeV operation of the AGS. We estimate the total systematic errors at present to be large. They can (and should) be reduced for future experiments by measurement of the pion yields from the actual targets, and by better calculation of the neutrino cross sections with more refined models.[8]

We accumulated data for 7.2×10^{18} POT (60 sec live time). The detector was enabled for 18μsec while the beam was present and for the same time midway between bursts (called the cosmic gate) to independently monitor the cosmic ray background. A total of 2×10^6 triggers were recorded.

The detector is shown in figure 5. It is optically separated into 216 cells, viewed at each end by photomultiplier tubes. Energy deposition and event position are reconstructed. Four drift chamber planes above the detector are used as a software veto for cosmic rays, etc. To reject entering cosmic rays, we require that the event be totally contained in the calorimeter, outside of the shaded region in figure 5. The average detection efficiency for muon neutrino events is ∿40% and for electron neutrino events ∿25%, using a simulation based on the SLAC electron gamma shower program EGS.

We divide the events into two categories, make containment cuts, and scan by hand to eliminate entering cosmic ray events that penetrate the veto unnoticed. Category A is muon neutrino candidates, where we require $25 < E_{vis} < 150$ MeV. There are still several hundred beam events, presumably induced by skyshine neutrons. We can separate ν_μ from this background by requiring the delayed coincidence characteristic of a stopping muon decaying into on electron. We detect this signature with 60% efficiency, as measured by a sample of stopping cosmic rays. After this requirement there are 10 beam and 10 cosmic gate events in Category A. Category B is electron neutrino candidates where we require $150 < E_{vis} < 300$ MeV. 13 beam and 16 cosmic events pass this cut.

Muon neutrino experiments of 150 MeV on carbon targets have not been constructed before. Confirmation of our estimates of event rate is both necessary for this experiment and for predicting rates at future experiments in similar configuration.

If we examine the fine time structure of the beam events with respect to the RF timing of the beam, a peak is visible which is characteristic of neutrinos from pions made in the target. Slow neutrons or cosmic rays would show no timing structure. After background subtraction, the signal is 3±2 events compared with 1.2 expected events.

Since ν_e candidates would deposit significantly more energy than ν_μ they are essentially free of any beam related neutron background (which is low energy). The RF timing distribution for ν_e events is flat and the in time excess is 0±2 events. There are no events with signatures expected for electron showers of this energy. There is no evidence for ν_e.

We can use these observations to set limits on neutrino oscillation parameters. We calculate the expected ratio ν_e/ν_μ as a function of Δ and θ. The error in this ratio is small because the normalization cancels out. Since most of the ν_μ's oscillate away at $\Delta \sim 1$eV, this ratio can be greater than 10. We use the analysis of James and Roos[9] to arrive at a 68% CL for an expected ratio of 3. Figure 6 shows the region in the Δ,θ plane where oscillations are rejected at Δ=1.1 eV for maximal mixing.

Proposals for second generation experiments[10] have been submitted at BNL and LASL. The product of proton flux times fiducial mass should be at least a factor of 100 larger than that described here if reasonable event rates are to be expected in these experiments. Given the large unanticipated neutron background in this experiment, the large duty cycle at LAMPF may require massive shielding and/or a storage ring. In principle, the limit on Δ can be extended to $\sim$0.2eV at maximal mixing in future experiments based on extending the rate measured and calculated in this work.

*Present address: University of Michigan, Ann Arbor, Michigan, 48109

References

1. "Observation of Elastic Neutrino-Proton Scattering", W. Kozanecki and "Antineutrino Proton Elastic Scattering", J. B. Strait, Harvard University Theses, May 1978.

2. A. Mann, Invited Paper, "Neutrino Mass Oscillations".

3. D. Cochran, et al., Phys. Rev. D6, 3084 (1972).

4. R. A. Smith and E. J. Moniz, Nucl. Phys. B43, 605 (1972).

5. J. S. O'Connell, et al., Phys. Rev. C6, 719 (1972).

6. H. Uberall, et al., Phys. Rev. C6, 1911 (1972).

7. The original proposal expected 100 ν_μ events. Only 35% of the requested beam was received. The fiducial volume, pion production, and neutrino cross sections were overestimated.

8. There are new efforts to calculate neutrino cross sections in carbon. Private communication, T. W. Donnelly and H. Uberall.

9. F. James and M. Roos, Nucl. Phys. B172, 475 (1980).

10. T. Dombeck, et al.; T. Y. Ling, et al., proposals submitted to LAMPF to construct 150 MeV ν_μ beam. R. Galik et al., proposal submitted to BNL.

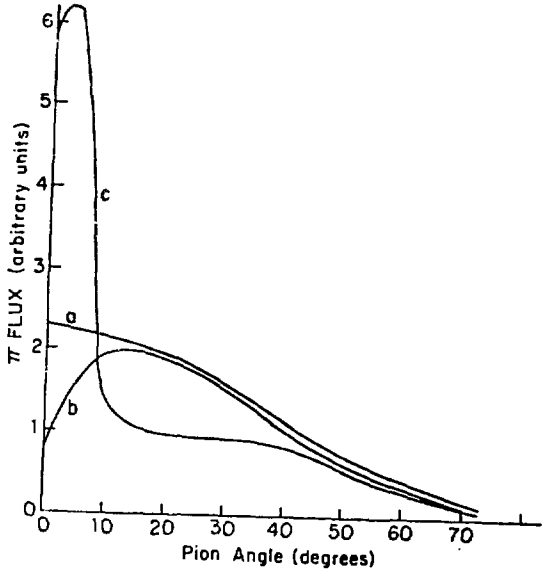

Fig. 1. π^+ angular distributions (for $T_{\pi+} > 200$ MeV). a) thin target distribution, b) + attenuation in target, c) + horn focusing.

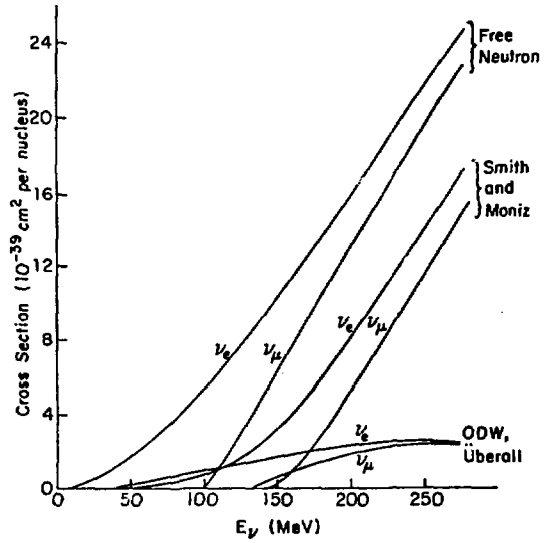

Fig. 3. ν_μ and ν_e cross sections on carbon.

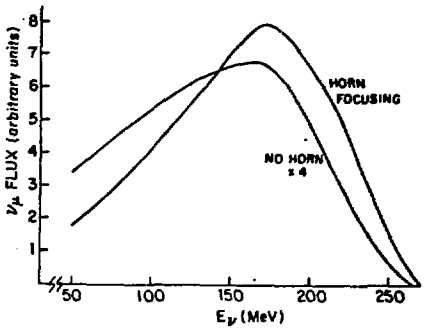

Fig. 2. Neutrino flux at detector. (Total flux = 1.4×10^{-10} ν/cm^2 incident proton.)

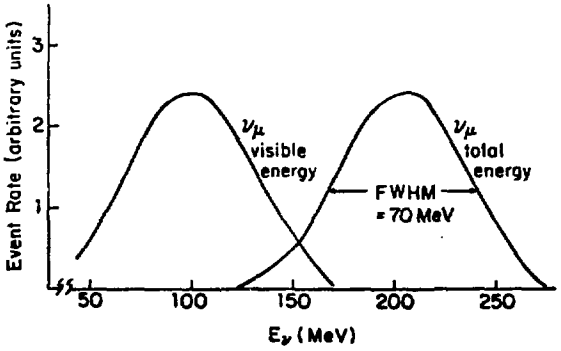

Fig. 4. Event rate spectrum vs. total energy and visible energy.

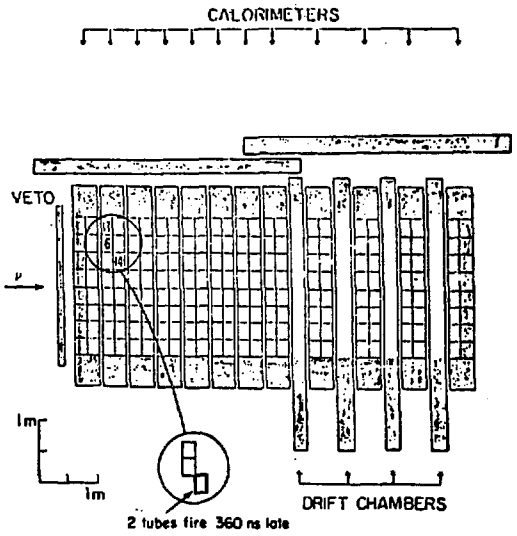

Fig. 5. Run 6066, event 1414.

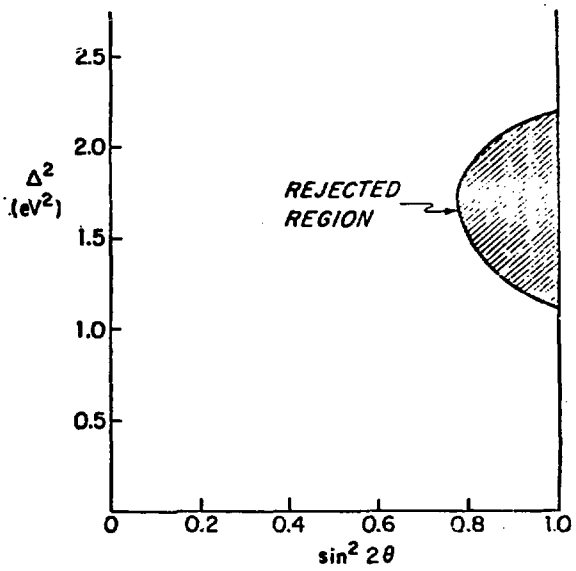

Fig. 6. Limits on $\nu_\mu \rightarrow \nu_e$ oscillations set by this experiment. 68% CL.

NORMAL MUON DECAY AND THE LOS ALAMOS TPC PROJECT

by

W. Wayne Kinnison

Los Alamos National Laboratory*

Los Alamos, New Mexico 87545

ABSTRACT

The Los Alamos National Laboratory high-statistics muon decay experiment, which utilizes a time projection chamber (TPC) for the detector, is described. The anticipated improvement in the experimental limits on the weak interaction coupling constants and their possible theoretical implications are presented. The discussion concludes with a status report on the experiment.

This talk is about a new high statistic muon decay experiment. The experiment is being conducted by a collaboration consisting of the Los Alamos National Laboratory, The University of Chicago, the National Research Council of Canada, and Carlton University, Ottawa, Canada, and it will take place here at LAMPF (Exp. 455). After a brief description of the apparatus, an equally brief summary of the present ideas on muon decay will be presented. The talk will conclude with a status report on the experiment

The experiment will measure the positron spectrum from polarized, positive muons decaying at rest:

$$\mu^+ \rightarrow e^+ + \nu_e + \bar{\nu}_\mu \ .$$

The positron momentum vector magnitude and direction with respect to the muon polarization vector will be determined for each of the 10^8 muon decays to be collected. The momentum analysis will cover the range from about 1 MeV/c to the end-point of 52.8 MeV/c. The angular measurements will be from about 4° to about 176°. A time projection chamber (TPC) will be used as the detector. This type of detector has several advantages: a) It will give a large solid angle of acceptance (nearly 4π over the entire angular and momentum range); b) Its operating gas will be a low-mass stopping target, which will result in reduced multiple scattering and external bremsstrahlung of the decay positrons; c) It will give very high resolution measurements of all kinematic variables; d) The associated magnetic field will help to hold the muon polarization.

A plan drawing of the apparatus is given in Fig. 1. The magnet produces a very uniform magnetic field over a region 70-cm long by 1.3-m diameter. The TPC is sensitive over a region 60-cm long (i.e., the drift direction) by 1.2-m diameter. The time projection readout consists of 21 modules. Each module has 15 wires spaced 1-cm apart. Each wire has 17 pads 0.8 x 0.8 cm^2 under it. The resulting 5355 analog pad signals go through a multiplexing system which produces an analog OR of 35 pad signals. The multiplexer outputs are then sent to 8-bit flash analog-to-digital encoders[1] which digitize and store the pad information in 40-ns-wide time buckets. All wire signals are stored in 40-ns time

buckets as well. The encoded pad information under a single wire allows the determination of where the trajectory, projected onto the readout plane crosses, that sense wire. The timing information from the wires determines the height of the trajectory above the wire. We, therefore, will have a full three-dimensional view of the positron track as well as that of the incoming muon. This time projection principle has already been described in somewhat more detail by C. Hargrove.[2] The experiment will operate in a mode which allows only one muon into the chamber at a time. This is accomplished by reducing the beam flux to a few thousand per second and using a fast beam deflector to turn off the beam as soon as a muon has entered the chamber. The entering muon is detected by a 20-mil plastic scintillator in the beam. This scintillator is connected, through fiber optics, to two 3/4-in photomultiplier tubes outside of the magnet.[3] If a pulse in the center module of the TPC readout is then detected after an appropriate delay (4 to 8 μs), indicating that the muon stopped in the central region of the detector, the event will be accepted. If the delayed pulse is at the wrong time, the beam is turned back on to try for another muon stop. The deflector cycling time and drift times in the TPC are such that up to 30 tries per accelerator macropulse may occur. The beam tune will be such that an acceptable stop will almost be assured during one of these tries over the time of the macropulse.

To get an idea of the resolutions which can realistically be expected, I will now present the results which have been obtained on our prototype TPC. This prototype has a drift distance equal to that of the full detector and a backplane made of one of the modules which will be used in the full detector, i.e., 15 wires and 255 pads. For these measurements, 2-MeV β rays from a Ru^{106} source, hardened by a 2-mm-thick Al absorber,

were used to produce tracks in the TPC. The resolutions, which are dominated by multiple scattering in the 50-50 Ar-CH_4 gas mixture, were σ_z (the drift direction) equal to about 0.1 cm, and σ_y (the direction parallel to the wires) equal to about 800 μm. This was determined with tracks drifting a length of 40 cm. Even if the position resolutions were assumed to be this wide over the entire muon decay spectrum (which will not be the case because multiple scattering will decrease with increased energy), we would then expect a momentum resolution of about 1.5% over the entire spectrum or 0.8% for events having a positron energy greater than 42 MeV.

The rest of this talk will describe what potential improvements this experiment can make in our understanding of the weak interaction process. The phenomenological V-A weak interaction Hamiltonian is given by[4]

$$H_{\text{leptonic}} = \frac{G_F}{\sqrt{2}} \{[\bar{\psi}_e \gamma^\alpha (1 - \gamma_5)\psi_\mu][\bar{\psi}_{\nu_\mu} \gamma_\alpha (1 - \gamma_5)\psi_{\nu_e}] + \text{h.c.}\}, \qquad (1)$$

where G_F is the Fermi constant. Also, the most general expression for the positron decay spectrum from polarized positive muons at rest, summed over all positron polarizations and neutrino energies, and to first order in m_e/m_μ is[4]

$$dN = \frac{d^3\vec{p}}{(2\pi)^4} \frac{m_\mu^2}{12} A \{12(1 - x) + \frac{4}{3}\rho(8x - 6) + 24\eta \frac{m_e}{m_\mu} \frac{(1 - x)}{x} \qquad (2)$$

$$+ \xi \cos\theta[4(1-x) + \frac{4}{3}\delta(8x-6)]\} .$$

In this expression, $\vec{p}$ and m_e are the positron momentum and mass, respectively, m_μ is the muon mass, A is a constant related to the weak

interaction coupling constants (and thus G_F). Also, $x = (2E/m_\mu)$, where E is the positron energy and θ is the angle between the positron momentum vector and the muon polarization. As can be seen from Eq. (2), the spectrum is determined by four constants--ρ, η, ξ, and δ. ρ describes the shape of the high-energy end of spectrum (i.e., $x \to 1$); η describes the low-energy end (i.e., $x \to 0$); ξ determines the asymmetry with respect to θ; δ gives the energy-dependence of this asymmetry. Table I gives the V-A predictions for all of these parameters as well as the current experimental measurements.[5] Also shown in Table I are the expected errors that a full maximum likelihood analysis of this experiment will be able to produce.[6] Table II gives the present and anticipated limits on the weak interaction coupling constants (in units of g_V) which can be determined from these Michel parameters. These coupling constants are found by a method due to Derenzo.[7] As can be seen from the table, the present limits allow up to about 30% deviation from a pure V-A interaction. This experiment should reduce this allowed departure to less than about 5%.

Another way to view this test of V-A is to assume an interaction Hamiltonian of the following form:

$$H_{\text{leptonic}} = \frac{G_F}{\sqrt{2}} \left(\left[\bar{\psi}_e \left[\gamma^\alpha - (1 + \varepsilon)\gamma^\alpha \gamma_5 \right] \psi_\mu \right] \right.$$

$$\left. \left[\bar{\psi}_{\nu_\mu} \gamma_\alpha (1 + \gamma_5) \psi_{\nu_e} \right] + \text{h.c.} \right) . \qquad (3)$$

In Eq. (3), the departure from a pure V-A form is described by the complex number ε. This Hamiltonian predicts[8]

$$\rho = \delta = \frac{3}{4} \tag{4a}$$

$$\xi \approx 1 - \frac{1}{2}|\varepsilon|^2 \tag{4b}$$

$$\eta \approx \frac{1}{2}\mathrm{Re}\varepsilon \tag{4c}$$

Figure 2(a) shows the allowed values for ε based on the current knowledge of the Michel parameters. Also shown in the figure is the region allowed by an experiment (currently running at SIN) which measures the transverse polarization of the positrons from muon decay.[9] Figure 2(b) shows the allowed values which can be anticipated from the results of our experiment.

A weak interaction theory which includes charged right-handed as well as the usual charged left-handed W bosons would result in a Hamiltonian of the form[8]

$$H_{\text{leptonic}} = \frac{G_F}{\sqrt{2}}\{[\bar{\psi}_e \gamma^\alpha (1 - \gamma_5) \psi_{\nu_e}][\bar{\psi}_{\nu_\mu} \gamma_\alpha (1 - \gamma_5)\psi_\mu](1 - \delta) \tag{5}$$

$$+ \delta[\bar{\psi}_e\gamma^\alpha (1 + \gamma_5) \psi_{\nu_e}][\bar{\psi}_{\nu_\mu}\gamma_\alpha (1 + \gamma_5)\psi_\mu] + \text{h.c.}\} .$$

Such a theory predicts that

$$\rho = \delta = \frac{3}{4} \tag{6a}$$

$$\xi \approx 1 - 2|\delta|^2 \approx [1 - 4(\frac{M_L}{M_R})^4] \tag{6b}$$

$$\eta = 0 \tag{6c}$$

where M_L and M_R are the masses of the left-handed and right-handed bosons, respectively. The current limit on the right-handed boson mass is $M_R > 270$ GeV/c^2 (90% confidence), which is primarily determined by the current measurement of ξ.[9] The current mmeasurement will be able to improve this limit to $M_R > 600$ GeV/c^2. This will be a higher limit than anything to be expected from high-energy physics in the near future.

In conclusion, an experiment at LAMPF will soon be underway which would contribute to a greater understanding of weak interaction phenomenology. At this time, the magnet is in place with mapping and shimming to begin this month (January 1981), and both the electronics and TPC have recently moved from the prototype stage to the production stage. We anticipate taking test data beginning this summer and our first production data this fall.

REFERENCES

1. TRW Model TDC1007J Monolithic Video A/D Converter from TRW LSI Products, P.O. Box 1125, Redondo Beach, CA 90278.

2. C. Hargrove, "Rare π and μ Decays," these proceedings.

3. M.-J. Yang, K. Gabriel, W. W. Kinnison, H. S. Matis, and H. L. Anderson, "Fiber-Optics Light Guides for Thin Scintillators," Los Alamos National Laboratory report LA-UR-80-3120 (October 1980).

4. A. M. Sachs and A. Sirlin, "Muon Decay," in Muon Physics, V. W. Hughes and C. S. Wu, Eds. (Academic Press, New York, 1974), Vol. II, Chapter V, pp 49-81.

5. Particle Data Group, "Review of Particle Properties," Rev. Mod. Phys. 52, S65-S66 (1980).

6. R. J. McKee, "Extraction of the Michel Parameters from Muon Decay by Maximum Likelihood," Los Alamos National Laboratory report LA-7966 (1979).

7. S. H. Derenzo, "Measurements of the Low-Energy End of the μ^+ Decay Spectrum," Phys. Rev. 181, 1854 (1969).

8. F. Corriveau, J. Egger, W. Fetscher, H.-J. Gerber, K. Johnson, H. Kaspar, H. J. Mahler, M. Salzman, and F. Scleck, "Polarization of the Positrons in the Decay of Polarized Muons," SIN Newsletter 12, 24 (1979).

9. M. A. B. Beg, R. V. Bundy, R. Mohaptra, and A. Sirlin, "Manifest Left-Right Symmetry and Its Experimental Consequences," Phys. Rev. Lett. 38, 1252 (1977).

TABLE I

THE MICHEL PARAMETERS

Parameter	V-A	Current Value	Expected Limits
ρ	$\frac{3}{4}$	0.752 ± 0.003	± 0.00023
η	0	-0.12 ± 0.21	± 0.0061
ξ	1	0.972 ± 0.013	± 0.00099
δ	$\frac{3}{4}$	0.755 ± 0.009	± 0.00064

TABLE II

THE LIMITS ON THE WEAK INTERACTION COUPLING CONSTANTS

Constant	Present Limit	Expected Limit
Avial Vector	$0.76 < g_A < 1.20$	$0.988 < g_A < 1.052$
Tensor	$g_T < 0.28$	$g_T < 0.027$
Scaler	$g_S < 0.33$	$g_S < 0.048$
Pseudoscaler	$g_P < 0.33$	$g_P < 0.048$
Vector-Axial Vector Phase	$\tau_{VA} = 180° \pm 15°$	$\tau_{VA} = 180° \pm 2.6°$

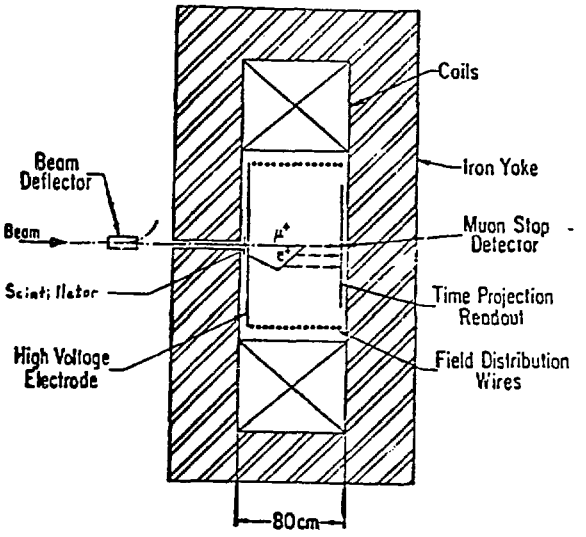

Fig. 1. Plan view of the experimental apparatus.

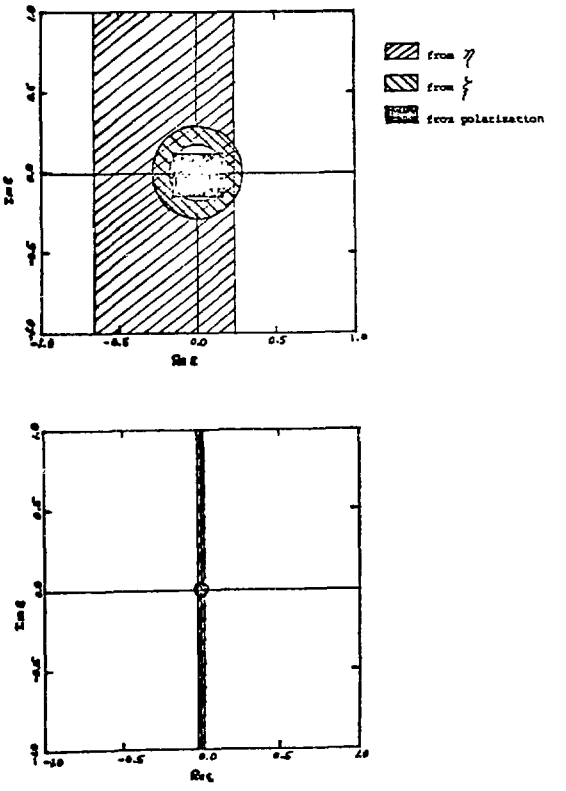

Fig. 2. Allowed values for ϵ.

a) The limits due to the current limits on the Michel parameters.

b) The range due to anticipated limits of this experiment.

THE SEARCH FOR MUON NUMBER VIOLATION AT LAMPF

by

Cyrus M. Hoffman
Los Alamos National Laboratory

The first topic I would like to discuss is why it is so interesting to search for violation of lepton number and baryon number. Conservation laws fall into two categories: those which are related to space-time displacements and rotations, (such as conservation of energy and momentum) and those which are not (such as conservation of electric charge, lepton number and baryon number). Conservation of electric charge is related to gauge invariance of the electromagnetic field and its associated massless gauge boson, the photon. It can be shown[1] that lepton (or baryon) number cannot be associated with a massless gauge boson without violating the Eötvös experiment which demonstrates the equality of inertial mass and gravitational mass. As a result, an exact conservation law for lepton (or baryon) number is absurd.[2] A gedanken experiment will help illustrate the point.

Consider a region of space from which you are excluded from making observations (a black hole would be such a region but we need not have black holes for this gedanken experiment). If we place a charged object in this region, can we tell that the charge of the region has changed? Yes we can, since the memory of the charge is preserved in the electric field which pervades all space outside the region. If we place a lepton in this region, can we tell that the lepton number of the region has changed? No, we cannot, the lepton leaves no trace at all.

Since an exact conservation law for lepton number and for baryon number do not make sense, it is clear that one should search for violations as well as one can, independent of any theoretical prediction. It is always possible that one of these numbers can be conserved "by accident." For example, in the Weinberg-Salam model[3] with two generations, lepton number is conserved due to the accident of the masslessness of the neutrinos.

Having decided that it is appropriate to search for lepton number violation, it is now fair to discuss how this is done. There are two basic methods.

a) Direct searches for processes which manifestly violate lepton number. Examples are:

$$\mu^+ \to e^+\gamma$$
$$\mu^+ \to e^+e^+e^-$$
$$\mu^+ \to e^+\gamma\gamma$$
$$\mu^-Z \to e^-Z$$
$$\mu^-Z \to e^+Z'$$

The nonobservation of these processes is what led to the postulation of the concept and conservation law of lepton number[4] and the suggestion of distinct ν_e and ν_μ.

b) Neutrino oscillations.

Which of these methods is more sensitive? We don't know! The existence of one of these processes would necessarily imply the existence of the others, though not necessarily at detectable levels. If the mass differences between neutrinos are very small, neutrino oscillations will be quite hard to observe, yet the rate for $\mu \to e\gamma$ (for example) could be as large as its present limit. On the other hand, if $\Delta^2 \simeq 1(ev)^2$, neutrino oscillations could be observable while the rate for $\mu \to e\gamma$ could be infinitesimal. Hence, both types of experiments should be pursued as vigorously as possible.

A group from Los Alamos, Stanford and Chicago is planning to search for processes $\mu^+ \to e^+\gamma$, $\mu^+ \to e^+e^+e^-$ and $\mu^+ \to e^+\gamma\gamma$ in a large modularized sodium iodide (NaI) detector known as the Crystal Box. A list of participants is shown in Table I. A schematic view of the apparatus is shown in Fig. 1. The detector consists of the array of NaI crystals which surround 36 scintillation counters, a 700-wire cylindrical drift chamber and a thin target in which μ^+'s stop and decay. There will be 360 crystals measuring 6.3 x 6.3 x 30.5 cm each viewed by a photomultiplier and 36 crystals measuring 6.3 x 6.3 x 70 cm, viewed by two photomultipliers. The detector totals approximately 2 tons of NaI. The detector has a solid angle of 60% of 4π for the detection of one particle and about 25% of 4π for the detection of a 3-body decay.

The plans are to search for the rare decays, $\mu^+ \to e^+\gamma$, $\mu^+ \to e^+e^+e^-$ and $\mu^+ \to e^+\gamma\gamma$ simultaneously with a μ^+ stopping rate of 5×10^5/s (average). The muon stopping rate is limited by pile-up in the NaI and by the requirement that the trigger rate be manageable. This rate implies that one is sensitive to branching ratios as low as 10^{-11} in reasonable running times (10^6 s) provided

TABLE I

PARTICIPANTS AND INSTITUTIONS

Los Alamos National Laboratory

Richard Bolton
J. David Bowman
Harold S. Butler
Roger Carlini
Martin D. Cooper
Minh Duong-Van
James S. Frank
Cyrus M. Hoffman
Gary E. Hogan
W. Wayne Kinnison
Robert J. Macek
Howard S. Matis
Richard E. Mischke
Darragh E. Nagle
Vern D. Sandberg
Gary H. Sanders
Robert A. Williams
Richard L. Talaga

Stanford University

Robert Hofstadter
E. Barrie Hughes
Steve Wilson

University of Chicago

Dave Grosnick
S. Courtenay Wright

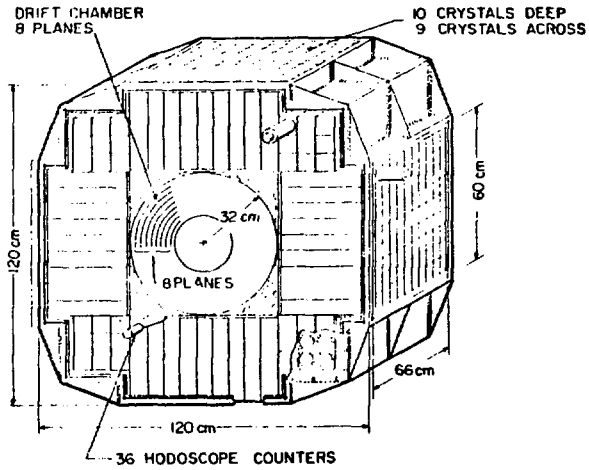

Fig. 1. Schematic diagram of the crystal box.

that background processes can be eliminated to at least that level. The major source of backgrounds is the chance coincidence of e^+'s and γ's from the decays of several muons. The backgrounds are eliminated by requiring the detected particles to be in time coincidence and by imposition of conservation of energy and momentum: good background rejection depends on good timing, position, and energy resolutions. With the resolutions assumed in our proposal, shown in Table II, the backgrounds are suppressed to below the 10^{-11} level for each of the processes. For that reason, we plan to run long enough to take data for 3×10^6 seconds and achieve sensitivities of $\sim 7 \times 10^{-12}$ for the three-body decays and $\sim 10^{-11}$ for $\mu^+ \rightarrow e^+\gamma$.

We have performed extensive tests on various components of the detector[4] to measure what resolutions can be achieved. These tests involved prototype detectors and e^+'s from the test channel and P^3 channel at LAMPF. In almost all cases, the achieved resolutions also shown in Table II, are significantly better than what we assumed in the proposal.

The crystals are currently being produced at Harshaw, and stacking in the large, hermetically sealed box, should commence shortly. We expect delivery of the crystals in April of this year and plan to instrument one quadrant for tests in the muon beam this spring; the scintillation counters will be installed for

TABLE II

CRYSTAL BOX RESOLUTIONS

System	Quantity	Resolution Assumed in Proposal	Resolution Achieved
NaI	Ee,Eγ	$\frac{\delta E}{E}$ = 0.06(FWHM) @ 50 MeV	$\frac{\delta E}{E}$ = 0.058(FWHM)
	t	1 ns (FWHM)	0.4 ns (FWHM)
	Δx	2 cm (FWHM)	∿3.5 cm (FWHM)
Scintillator	Δt	1 ns (FWHM)	0.35 ns (FWHM)
Drift Chamber	Δx	200 μM (RMS)	≤150 μM (RMS)

these tests. The entire detector will be instrumented for tests this summer; the drift chamber will be tested separately this summer. We intend to mate the drift chamber and the NaI for data taking commencing this fall.

There are several other measurements which could be made with the Crystal Box following the search for the rare muon decays. Some of these are listed in Table III together with the principal physics interests.

Finally, I show in Fig. 2 how the limits for muon-number violating processes have improved with time. Although we have been concerned with the length of time it has taken to mount the Crystal Box experiment, it is clear from Fig. 2 that the longer we wait, the better our experiment becomes!

TABLE III

OTHER PROCESSES THAT CAN BE STUDIED WITH THE CRYSTAL BOX

Process	Interest	Reference
$\pi^0 \to 3\gamma$	C-violation	a
$\pi^0 \to \nu\nu'$	Gauge-Models, Neutrino Mass	b
$\pi^0 \to e^+e^-\gamma$	π^0 Form Factor	c
$\pi^+ \to e^+\nu_e\gamma$	Axial Form Factor	d
$\pi^0 \to e^+e^-$	Gauge-Models Leptoquarks	e

a) V. L. Highland, L. B. Auerbach, N. Haik, W. K. McFarlane, R. J. Macek, J. C. Pratt, J. Sarracino, and R. D. Werbeck, Phys. Rev. Lett. 44, 628 (1980).

b) P. Herczeg and C. M. Hoffman, LA-UR-80-1778 (1980) and submitted to Phys. Lett., T. Kalogeropoulos, J. Schechter and J. Valle, Phys. Lett 86B, 72 (1979), and D. E. Nagle, private communication.

c) J. Fischer, P. Extermann, O. Guisan, R. Mermod, L. Rosselet, R. Sachot, P. Bloch, G. Bunce, B. Devaux, A. M. Diamant-Berger, N. Do-Duc, G. Marel and R. Turlay, Phys. Lett. 73B, 359 (1978).

d) See e.g., SIN experiment 78-13.1, J. P. Perroud, Spokesman.

e) J. Fischer et al., Phys. Lett. 73B, 364 (1978); LAMPF Experiment #222, R. E. Mischke, Spokesman; CERN Experiment #SC-77, J. D. Davies, Spokesman; P. Herczeg, Phys. Rev. D16, 712 (1977).

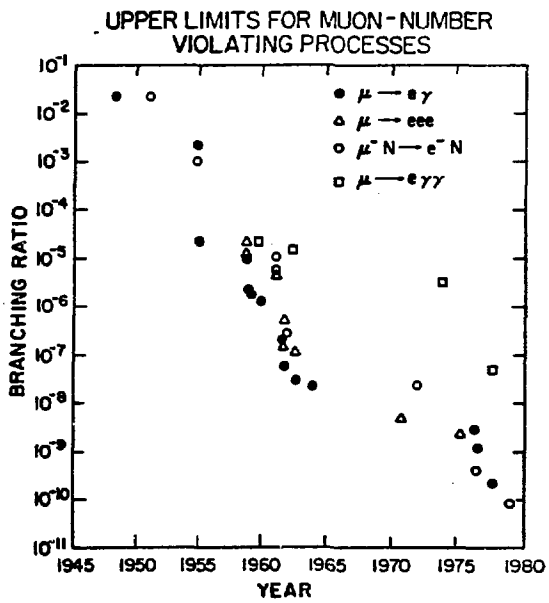

Fig. 2. Upper limits for various muon number violating processes as a function of time.

REFERENCES

1. T. D. Lee and C. N. Yang, Phys. Rev. 98, 1501 (1955).

2. A. de Rujula, H. Georgi and S. L. Glashow, Phys. Rev. D12, 147 (1975).

3. S. Weinberg, Phys. Rev. Lett. 19, 1264 (1967); A. Salam in Elementary Particle Theory, ed. by N. Svartholm (Almquist and Forlag, Stockholm, 1968), p. 367.

4. The timing resolutions are discussed in G. H. Sanders, G. Hart, G. Hogan, J. S. Frank, C. M. Hoffman, H. S. Matis and V. D. Sandberg, Nucl. Instr. and Meth. (to be published). The drift chamber is discussed in R. D. Bolton, R. D. Carlini, M. D. Cooper, M. Duong-Van, J. S. Frank, H. S. Matis, R. E. Mischke, V. D. Sandberg, J. P. Sandoval and R. L. Talaga, to be submitted to Nucl. Instr. and Meth.

Can Exotic Phenomena be Induced in Low Energy Antiproton-Nucleus Collisions?

R. M. DeVries and N. J. DiGiacomo

Physics Division
Los Alamos Scientific Laboratory
Los Alamos, NM 87545

It appears that nuclear reactions (induced by light or heavy-ions) are dominated by nucleon-nucleon (N-N) collisions at least to the 10% level in σ_R 1). Therefore studies of $\bar{p}$-Nucleus ($\bar{p}$-n) interactions are likely to reveal fascinating new aspects of nuclear science because the $\bar{N}$-N interaction is radically different from the N-N case, particularly at low incident energies (E_i<500 MeV). First of all, low energy $\bar{N}$-N elastic scattering is quite forward peaked while N-N systems exhibit fairly isotopic angular distributions. Secondly, there are two new components to σ_T which do not exist in the N-N case: a) charge exchange, which is always <5% of σ_T, and b) annihilation which is large (see Fig. 1), particularly at low incident energies.

Thus in order to predict what might happen in $\bar{p}$-n collisions it would be appropriate to assume that a $\bar{p}$ interacts, with a nucleus, first of peripherally and eventually annihilates on a nucleon in the target nucleus. Because the annihilation cross section is so large it might be assumed that the $\bar{p}$ usually disappears in the stratosphere of the target. However, as is shown in another paper submitted to this conference (DiGiacomo and DeVries), the strong real attraction thought to exist in the p-n system and the Pauli blocking of the (predominantly) backward scattered nucleon in each $\bar{p}$-N collision cause a reasonable fraction of the incident p's to be transmitted into at least the nuclear

half-density point. The forward peaked $\bar{p}$-N elastic angular distributions insure that small impact parameter p's will drive in towards the center of target until they annihilate.

The annihilation of a $\bar{p}$ on a nucleon can occur into a staggering number of different channels[2]) unless the incident energy is very low. In that case π production predominates[3]) and, in fact, about 45% of the annihilation cross section goes into the production of 5 π's (see Fig. 2). If these π's were statistically distributed we might expect the average kinetic energy to be:

$$[938+938-5(139)]/5 = 236 \text{ MeV}$$

In fact experimental measurements of the π energy spectrum (averaged over all pion production possibilities) indicate an average energy of about 238 MeV[4]) as shown in Fig. 2. Notice that the spectrum looks fairly statistical. It should be realized that even if the p annihilation occurred at a very low asymptotic incident energy, the strong real attractive potential would tend to focus the π's forward towards the center of the nucleus.

Before we consider the π-N interactions we must worry about intermediate mass mesonic states which might carry some of the π's out of the target nucleus without interactions. The ρ meson (mass 765 MeV) "consists" primarily of two π's and has a fairly sizeable production cross section in p-N annihilations[3]) but lives only $\sim 5\times10^{-24}$ sec. so it will quickly decay and allow the π's to interact on their own. The η (mass 549 MeV, $T = 2\times10^{-19}$ sec.) and the ω (mass 783 MeV, T =

5.4×10^{-23} sec.)"consist" of 3π's and live for long enough times to carry their π's outside the target nucleus. However, the η is very weakly produced in p-N collisions and the ω production constitutes only about 5% of all (at rest) annihilations[3,5].

Thus we can continue our scenario and assume that there exist 5π's with a statistical energy distribution of average value 238 MeV. These π's are produced at the half density point (or deeper) in the nucleus and are focussed (at least partly) towards the center of the nucleus. These π's will be strongly absorbed onto the nucleons in the target nucleus via the $\Delta(3,3)$ resonance. Alternatively it is possible to imagine that 5Δ's are coherently produced directly in the annihilation process. In any case, these Δ's will decay in a relatively short distance inside the target nucleus. The emitted π's will likely be absorbed onto target nucleons again so that a significant fraction of annihilation energy is transferred to the nucleons of the target nucleus.

Since the incident $\bar{p}$ kinetic energy can be quite low, there is only a small amount of linear momentum to be conserved and leading particles would not be expected (at least for fairly small impact parameters). Thus it appears likely that $\bar{p}$ + n collisions will allow 1000 or more MeV to be dumped into a nucleus. The resultant nuclear conditions should be unique. It is certainly possible that such conditions would tell us about properties of nuclear matter which are presently unknown.

The critical question, in our opinion, is how much of the initial annihilation energy can be reasonably expected to be deposited onto the nucleons in the target nucleus. We are presently attempting internucleon cascade calculations starting with 5π's and the annihilation energy

released inside of a nucleus in order to answer this question. We note that we recently discovered a paper[6] which considers $\bar{p}$-n interactions from a different basis, but arrives at similar conclusions.

Clearly $\bar{p}$-n experimental studies are in order. We are planning such experiments, probably using our 360^{o} magnetic spectrometer system[7]. It would seem reasonable to compare the π and N experimental angular distributions and energy spectra with internucleon cascade calculations in which no exotic phenomena are included.

References

1) R. M. DeVries and J. C. Peng, Phys. Rev. C22, 1055 (1980); N. J. DiGiacomo, R. M. DeVries and J. C. Peng, Phys. Rev. Letts. 45, 527 (1980).

2) A list of all possible $\bar{p}$-N annihilation channels occupies four pages in: $\bar{N}$-N and $\bar{N}$-D Interaction Compilation, Berkeley Particle Data Group, LBL-58, 1972.

3) R. Armenteros and B. French in High Energy Physics, Vol IV, Academic Press, New York, 1969.

4) J. Roy, Proc. IV Int. Sym. on $\bar{N}N$ Interactions, Syracuse University, 1975.

5) Maglic, et al., Phys. Rev. Letts. 7, 178 (1961).

6) J. Rafelski, Phys. Letts. 91B, 281 (1980).

7) LAMPF proposals #591 and #592.

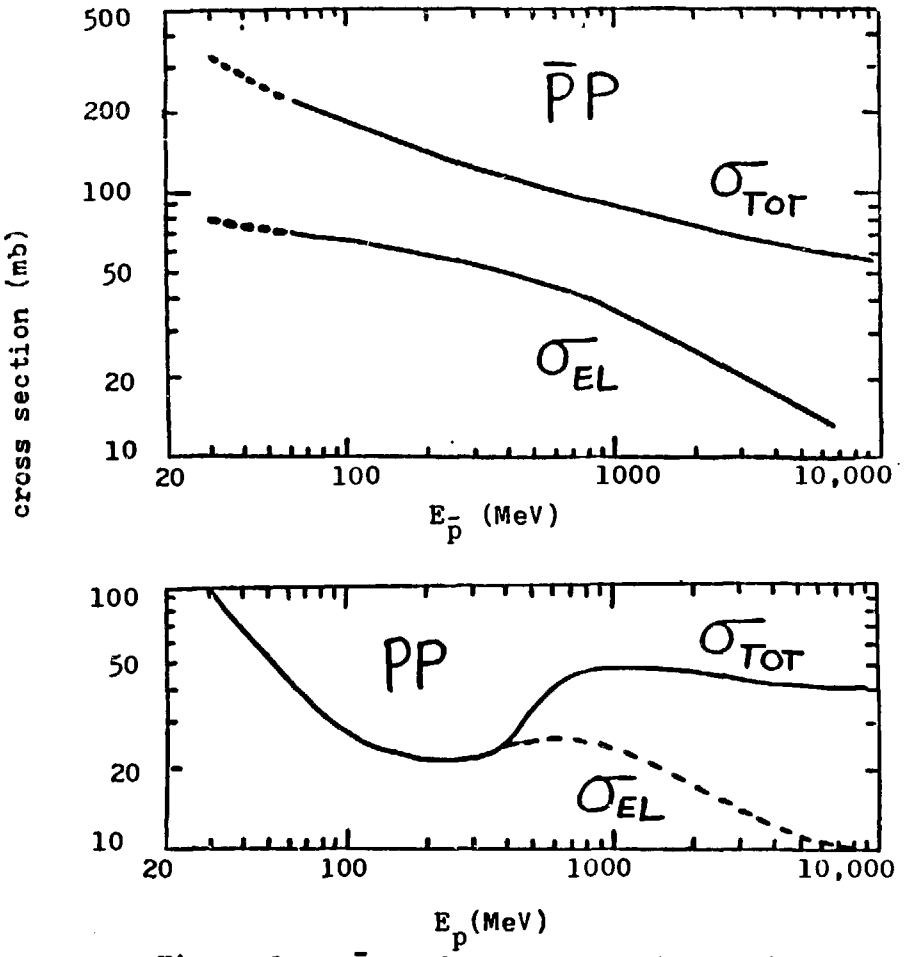

Figure 1a: $\bar{p}p$ and pp total and elastic cross sections vs. projectile lab energy

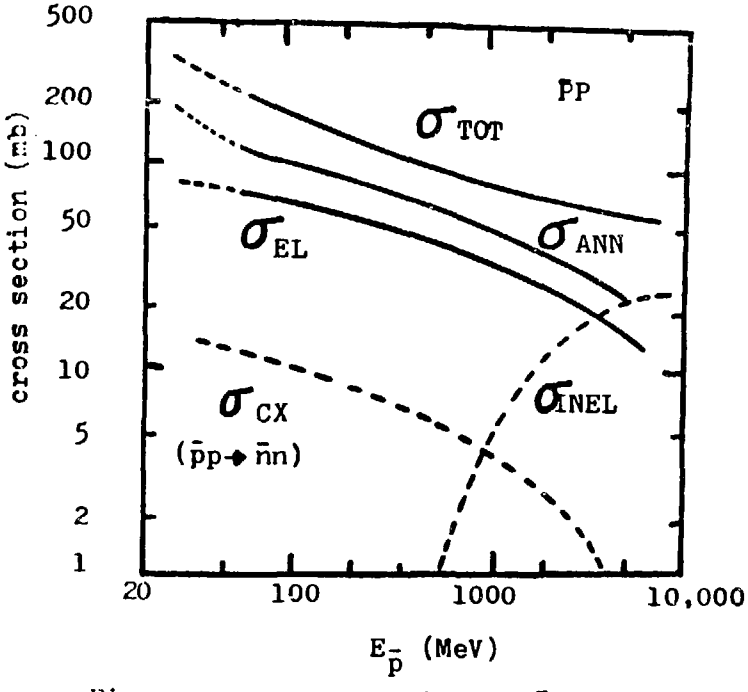

Figure 1b: Composition of $\bar{p}p$ total cross section as a function of projectile lab energy

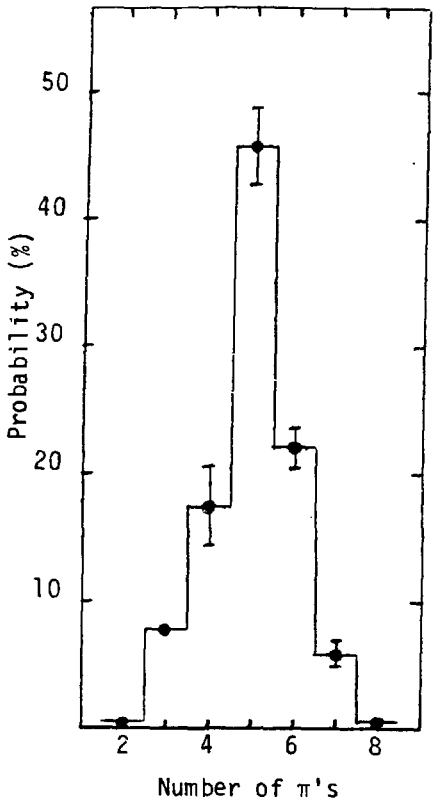

Fig. 2a: Probabilities for π emission in $\bar{p}$ + p annihilations at rest

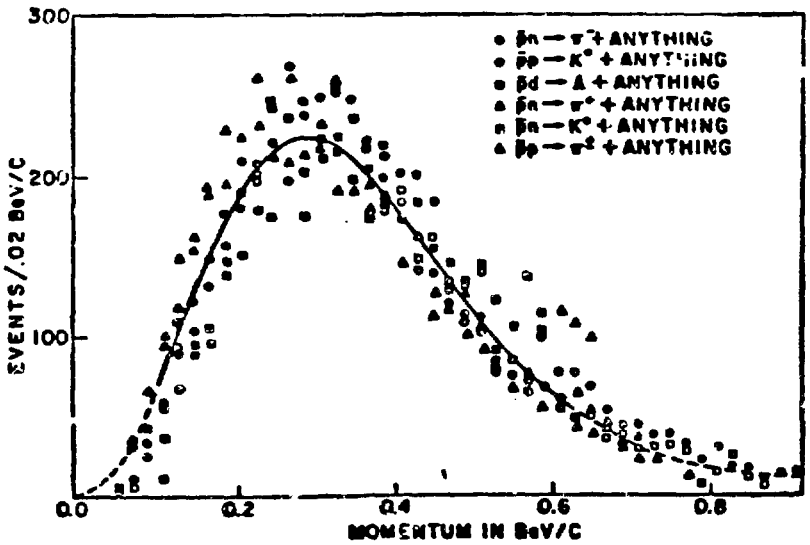

Fig. 2b: Momentum distribution for annihilation products.

THE EFFECTS OF STRONG ATTRACTION IN ANTIPROTON-NUCLEUS SCATTERING *

N. J. DiGiacomo and R. M. DeVries

Physics Division
Los Alamos National Laboratory
Los Alamos, N.M., USA 87545

Introduction

Since the observation of the antiproton 25 years ago, much theoretical and experimental consideration has been given to the interaction of anti-nucleons with nucleons and deuterons. [1,2] To this day aspects of the interaction, such as the annihilation process and the existence of bound states and resonances, stand as interesting unsolved problems.

Suprisingly, $\bar{N}N$ studies have not engendered parallel investigations of $\bar{p}$ nucleus ($\bar{p}A$) scattering. Little quantitative information exists for the $\bar{p}A$ system, particularly at energies below 1 GeV. To this end we discuss means of obtaining quantitative insight into the $\bar{p}A$ interaction by examining the sensitivity of the total reaction cross section (σ_R) to the strength and energy dependence of the attraction.

The $\bar{p}$ nucleus data

Below 1 GeV incident $\bar{p}$ energy, there exists exactly one limited angular distribution for $\bar{p}$ + C averaged over a broad energy range[3], a few σ_R data at 430 MeV[4] and some antiprotonic atom ($\bar{p}$ atom) measurements[5,6,7].

Consider first the $\bar{p}$ atom data. These experiments support the existence of strong attraction and absorption. Analyses assume optical potentials which follow the nuclear density shape and have strengths which

* supported by the U.S. Department of Energy

vary from $V_o + iW_o = (70 + i\ 210)$ MeV to $(250 + i\ 100)$ MeV. The strength of the $\bar{N}N$ optical potential[8,9,10] in all probability indicates that simple folding calculations will not provide a believable alternative to the uncertain potential derived from $\bar{p}$ atom data. Clearly, quality elastic scattering data would be of utmost utility. Such data are, however, at least 3 years away. One eagerly awaits the high quality, high intensity (10^6/sec) variable energy $\bar{p}$ beam from LEAR (low energy antiproton ring)[11] at CERN.

Insights into the $\bar{p}A$ interaction

Recently, Auerbach et al.[12] examined the possibility of resonances in $\bar{p}A$, given the uncertainties of the interaction. The present authors chose a somewhat different tact in order to gain insight into the $\bar{p}A$ interaction.

We developed[13] a method of obtaining information about the strong attraction in $\bar{p}A$ scattering by comparing total reaction cross section data with a model for σ_R that allows quantitative identification of the role of the attraction and its strength and energy dependence. The model successfully describes σ_R for pA scattering over an energy range from 15 MeV to 1 GeV[14] (see Fig 1) by including the effects of Pauli blocking, Fermi motion and the Coulomb and real nuclear potentials in a prescription based on the optical limit of Glauber theory. By extending the model to $\bar{p}A$ scattering, the problem of constructing an imaginary $\bar{p}A$ potential from poorly understood $\bar{N}N$ annihilation potential is avoided, i.e. nuclear absorption is calculated from the measured $\sigma_T^{\bar{N}N}$ and $\sigma_{el}^{\bar{N}N}$ data. Perhaps most importantly, the necessary σ_R data can be obtained at existing facilities, such as LESB I,II (low energy separated beam) at the AGS.

The form and strength of the real potential is, as noted, quite uncertain. In our opinion, a promising approach to predicting the strength and energy dependence of the $\bar{p}A$ real potential involves the relativistic field theory (RFT) of Walecka[15]. Recent success in the application of the RFT to the pA optical potential systematics[16,17] has motivated application to the $\bar{p}A$ system[17]. Indeed, an early form of the RFT was used by Duerr and Teller[18,19] 25 years ago in examining $\bar{p}A$ scattering. The RFT predicts a very strong attraction (600-700 MeV) with a relatively constant energy dependence. The $\bar{p}$ predictions result essentially from changing the sign of the vector potential in the RFT from that found for the pA system. The sensitivity of σ_R to the strong attraction allows one to test the RFT predictions by comparison of the calculations to σ_R data. It seems reasonable, then, to use the RFT prediction to demonstrate the sensitivity of the σ_R calculations to the attraction.

Details of the model for σ_R can be found in ref. 14. What follows is a cursory review, emphasizing salient features of the pA calculations.

$$\sigma_R(E) = 2\pi\int bdb[\,1 - \exp(-\chi(b,E))] \qquad 1)$$

$$\chi(b,E) = 2\int_{rmin} ds\,[\,\rho_p(r)\sigma^{pp}_{eff}(K(r)) + \rho_n(r)\sigma^{pn}_{eff}(K(r))] \qquad 2)$$

$$K(r) = \frac{1}{\hbar c}(2mc^2(\,T - V(r))^{1/2}, \qquad V(r) = V_{Coul}(r) + V_{real}(r) \qquad 3)$$

$$\sigma^{pp}_{eff}(K(r)) = \frac{1}{V}\int dR_1\,\frac{2k}{K}\,\sigma^{pp}_T(k)\int_{free}\frac{d\Omega}{4\pi}, \qquad 4)$$

The σ_R is calculated by integrating over impact parameter (b) where each trajectory ($\chi(b,E)$) is determined by a numerical path integration, given V(r). This has the effect of attracting/repulsing flux from the nucleus as well as determining K(r), the local collision momentum between the projectile and the individual target nucleons. The cross section for the individual collisions is modified from the free cross section due to Fermi averaged Pauli blocking effects. The σ_{eff}^{pp} and σ_{eff}^{pn} are calculated via a geometrical construction. Equation 4 represents the average over the local momenta while the integral over $d\Omega'$ is the Pauli blocking factor. Let us now outline the changes necessary to adapt the model for pA σ_R to consider the $\bar{p}$A scattering.

As noted, in contrast to the nucleon-nucleon system, the $\bar{N}N$ total cross section has a large nonelastic component at all energies. This alters the calculation of the Pauli blocking in a manner which requires as input both the antiproton-proton (neutron) total $\sigma_T^{\bar{p}p}$ ($\sigma_T^{\bar{p}n}$) and elastic $\sigma_e^{\bar{p}n}$ ($\sigma_e^{\bar{p}n}$) cross sections. Useful $\sigma_T^{\bar{p}p}$ and $\sigma_e^{\bar{p}p}$ data are available above approximately 40 MeV incident $\bar{p}$ energy.[2] Although $\sigma_T^{\bar{p}n}$ and $\sigma_T^{\bar{p}n}$ (obtained from $\bar{p}d$ data) data are more sparse, enough are available to ascertain that, to 10%, $\sigma_T^{\bar{p}n} \approx \sigma_T^{\bar{p}p}$ and $\sigma_e^{\bar{p}n} \approx \sigma_e^{\bar{p}p}$.

The Coulomb potential, of course, changes sign and becomes attractive. This has the effect of drawing flux to the nucleus and increasing the reaction cross section.

The most complex change involves the calculation of the target Fermi averaged Pauli blocking. Only the final state nucleon (not the antiproton)

in an elastic scattering ($\bar{p}+p \to \bar{p}+p$ or $\bar{p}+n \to \bar{p}+n$) is blocked, in contrast to the nucleon-nucleus system in which both final state nucleons are subject to exclusion. Also, as stated, for the $\bar{p}p$ system only a fraction of σ_T is elastic ($\sigma_e^{\bar{p}p} \approx 1/3\ \sigma_T^{\bar{p}p}$). A strong reduction in the blocking for the $\bar{p}$+A system is thus expected. An interesting difference between the $\bar{p}p(\bar{p}n)$ and $pp(pn)$ systems alters this conclusion, however. The nucleon-nucleon center of mass elastic angular distribution is essentially isotropic at energies below a few hundred MeV, while the $\bar{p}p(\bar{p}n)$ scattering is forward peaked even at the lowest energies, becoming more so as the energy increases (Fig 2). We modify our geometric model of the Pauli blocking to include this fact by constraining the final state elastically scattered $\bar{p}$ (p or n) to scatter into a limited forward (backward) solid angle. This region is chosen such that 95% of the experimentally observed cross section falls within the cone. Examination of the data[2] allows the following parameterization of the cutoff angle (in degrees) in the antiproton-nucleon center of mass as a function of the antiproton center of mass momentum K (in fm^{-1}):

$$\theta_{cutoff} = 17 + \frac{125}{K} - \frac{38}{K^2} \quad . \qquad 5)$$

This effect tends to extend the Pauli blocking influence to higher $\bar{p}$ incident energies, for as the $\bar{p}$ energy increases, the $\bar{p}+p,n$ collisions occur at higher K. The increased forward peaking then yields a smaller allowed solid angle. The Pauli blocking of the final state nucleon in the charge exchange reaction $\bar{p}+n \to \bar{n}+p$ ($\sigma_{cx}^{\bar{p}n}$) is neglected, because $\sigma_{cx}^{\bar{p}n}/\sigma_T^{\bar{p}n} \leq 5\%$. The results of the $\bar{p}$+A calculations, including all above effects but with no real nuclear potential, are shown in Fig. 3 as the solid curve, along with the existing data.[4,20,21,22] The effects of the Pauli blocking on the effective cross sections is shown in Fig. 4.

We next consider the effect of including the strong attraction. We use a Woods-Saxon form for the potential with a range and diffusivity the same as observed in empirical analyses of nucleon-nucleus elastic scattering. It is felt[17] that the range of the $\bar{p}$+A potential will, if anything, be slightly larger than this. The dashed curves in Fig. 3 result from the assumption of a strength V_o = 650 MeV with a constant energy and mass dependence. This strength and a relative constancy with energy and mass is a prediction of the RFT. The dash-dot curve in the upper left of Fig. 3 depicts V_o = 325 MeV, while the dot-dashed curve in the upper right of Fig. 1 reflects a linear energy dependence for the real strength, namely, V_o = 650 (1 -.001 $E_{\bar{p}}$) MeV up to 1 GeV and then V_o = 0.

In Fig.5 light is shed on the details of the $\bar{p}$+A interaction within this model. The upper figure shows the absorption probability versus impact parameter (b) for 100 MeV $\bar{p}$ (and p) on copper. It is clear that the strong real potential draws flux from far beyond the actual surface. As previously noted, the attractive real potential also increases the $\bar{p}$+p,n interaction momentum. This is very important at lower energies, where the free cross sections are rapidly decreasing with energy, because the resulting $\sigma_T^{\bar{p}p,n}$ are then much smaller. This effect, along with the Pauli blocking, leads to a sort of transparency. To demonstrate this (in the lower part of Fig.5) we show the absorption as a function of position along a diameter for a b=0 trajectory $\bar{p}$ (and p) at 100 MeV on copper. This quantity reflects the local absorption at a given point within the nucleus. Note that the $\bar{p}$ is not as strongly absorbed as one might first suspect, although, more in fact than a proton. For example, approximately 75% of the $\bar{p}$'s penetrate to the half density point of 4.8 fm before interacting, compared to 90% of the protons. Thus, though σ_R is quite large, a given $\bar{p}$

can penetrate a reasonable distance into the nucleus. In Fig (6) the sensitivity of the transparency is investigated as a function of projectile energy and potential strength. It is interesting to note that, while within the model σ_R increases rapidly at low energies, the penetration of individual antiprotons remains high. This has important ramifications for the use of the antiproton as a probe of nuclei, given the multitude of interesting and unusual reactions it can initiate[2].

References

1. Proc. V European Sumposium on $\bar{N}N$ Interactions, Bressanone, Italy (1980). Proc. IV International Symposium on $\bar{N}N$ Interactions Vols. I, II, Syracuse University (1975). Proc. III European Symposium on $\bar{N}N$ Interactions, Stockholm, Pergamon Press, Oxford (1976). These provide excellent background reading of the subjest of $\bar{N}N$ physics.
2. $\bar{N}N$ and $\bar{N}D$ Interactions Compilation, Berkeley Particle data group LBL-58, May 1972.
3. L. E. Agnew et al., Phys. Rev. 118 1371 (1960).
4. O. Chamberlain et al., Phys. Rev. 102 1637 (1956).
5. P. D. Barnes et al., Phys. Rev. Lett. 29 1132 (1972).
6. P. Roberson et al., Phys. Rev. C16 1945 (1978).
7. H. Poth et al., Nucl. Phys. A294 435 (1977).
8. C. B. Dover and J. M. Richard, Ann. Phys. 121 70 (1979).
9. C. B. Dover and J. M. Richard, Phys. Rev. C21 1466 (1980).
10. T. Ericson in Proc. III European Symposium on $\bar{N}N$ Interactions, Stockholm, Pergamon Press, Oxford, p. 3, (1976).
11. R. Bersa et al., LEAR letter of intent, CERN,PSCC 179-55.
12. E. H. Auerbach, C. B. Dover and S. H. Kahana, BNL preprint, BNL-28585 (1980).

13. N. J. DiGiacomo, LASL preprint LA-UR 80-2773 (1980).

14. N. J. DiGiacomo, R. M. DeVries and J. C. Peng, Phys. Rev. Lett. , 45 527 (1980).

15. D. Walecka, Ann. Phys. 83 491 (1974).

16. M. Jaminon, C. Mahaux and P. Rochus, Phys. Rev. C22 2027 (1980).

17. J. Boguta, to be published and private communication 1980.

18. H. P. Duerr, Phys. Rev. 103 469 (1956).

19. H. P. Duerr and E. Teller, Phys. Rev. 101 494 (1956).

20. U. P. Gorin et al., Yad. Phys. 18, 336 (1973), Sov. J. Nucl. Phys., 18, 173 (1974).

21. J. C. Allaby et al., Yad. Phys. 12, 538 (1970), Sov. J. Nucl. Phys. 12, 295 (1971).

22. R. J. Abrams et al., Phys. Rev. D4, 3235 (1971).

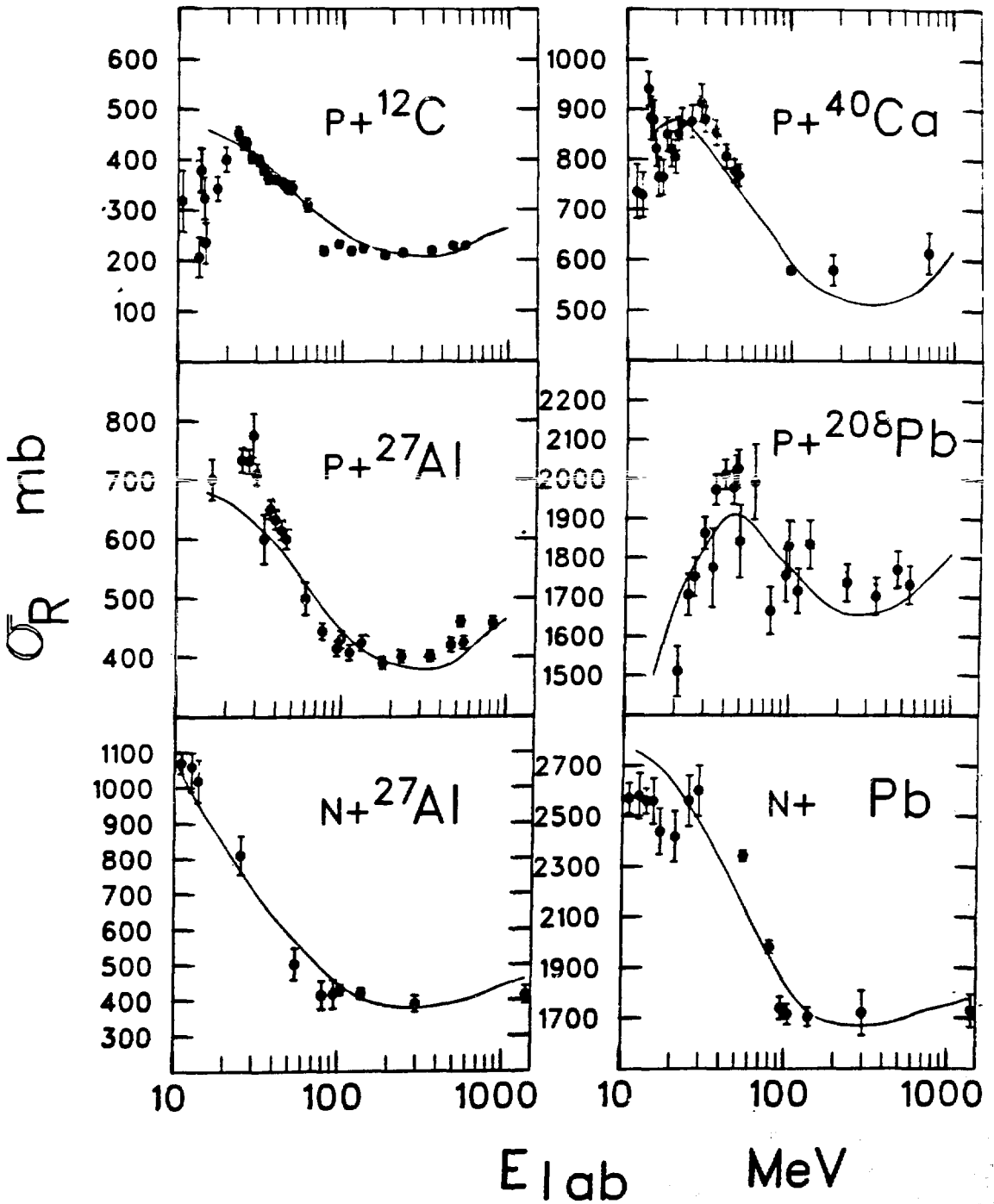

Figure 1 : Proton-nucleus and neutron-nucleus total reaction cross sections. The calculation is that of Ref. 14.

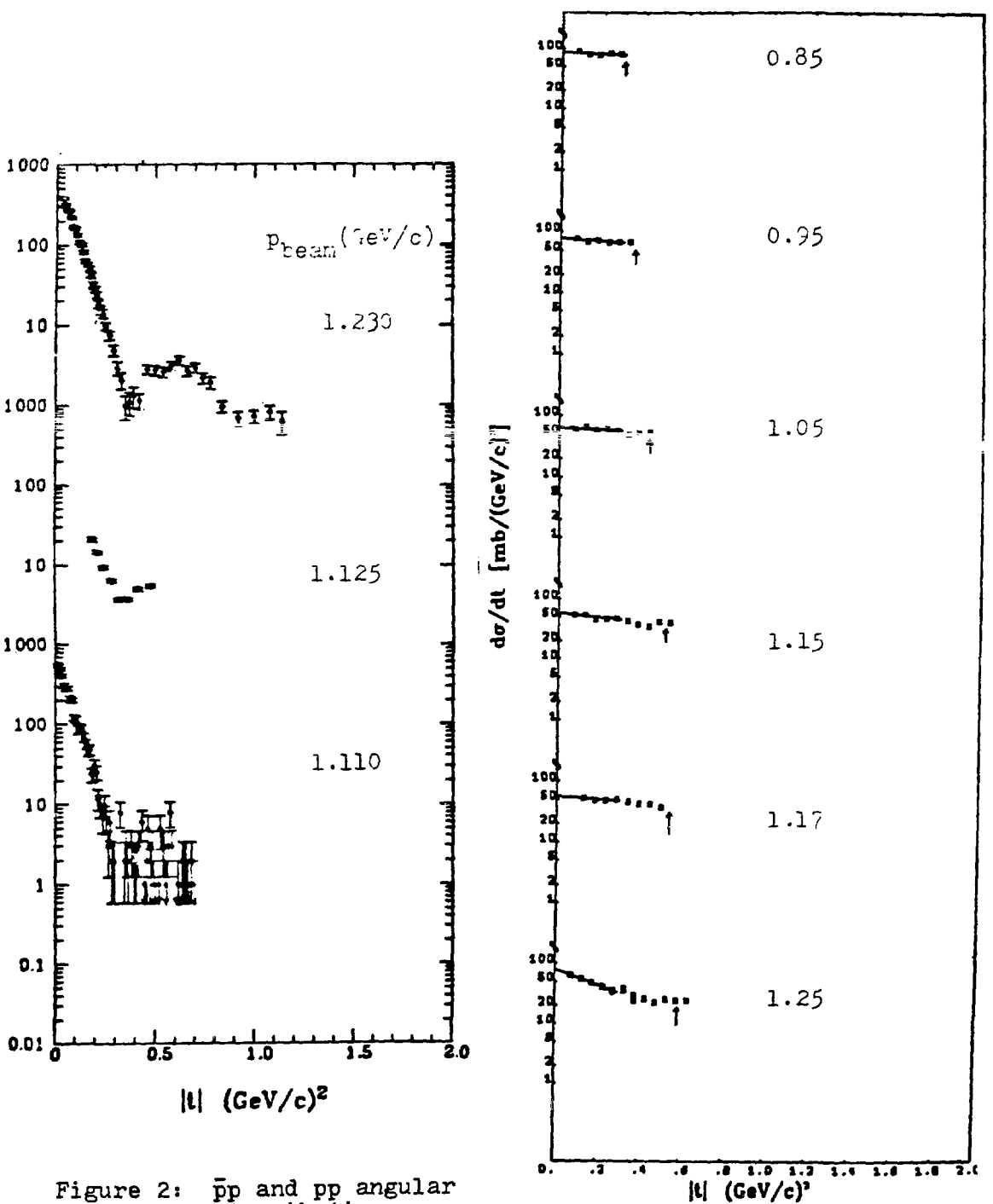

Figure 2: $\bar{p}p$ and pp angular distributions

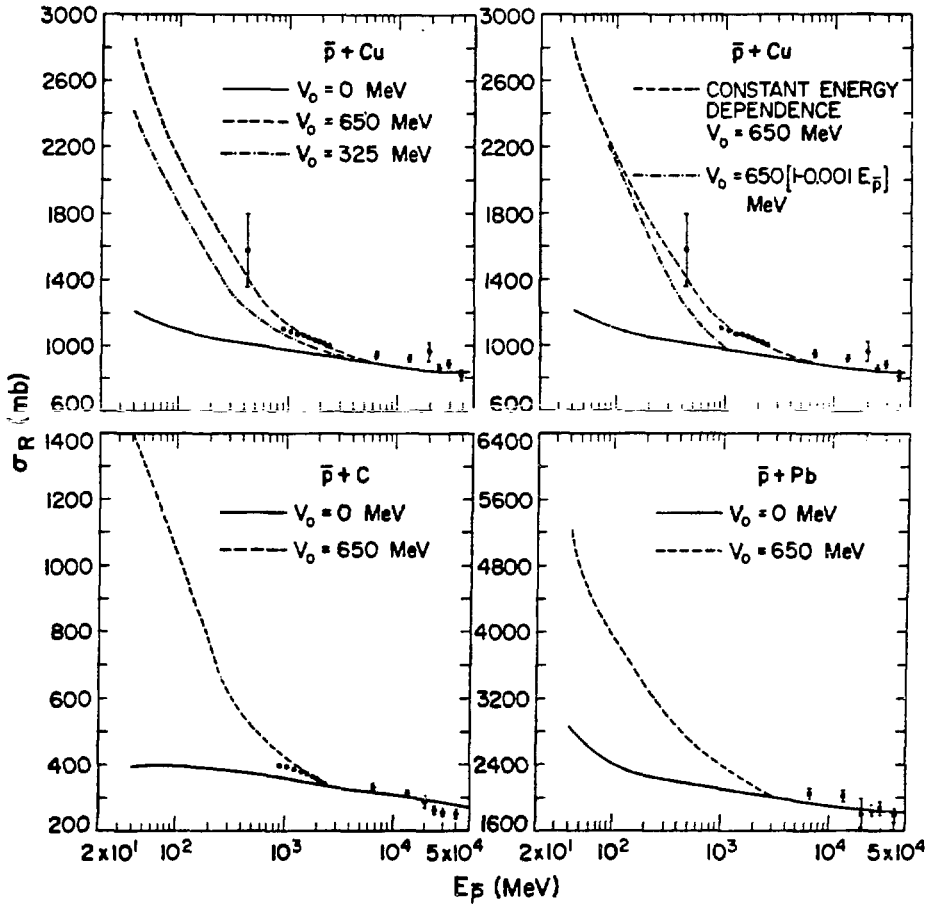

Figure 3: The $\bar{p}$-nucleus σ_R versus incident lab energy. The solid curves reflect full calculations (see text) but with no real optical potential. The dashed and dashed-dot curves include the real potential in a Woods-Saxon form with $R = 1.21\,A^{1/3}$ fm and a = .77 fm and energy dependence as given in the figure.

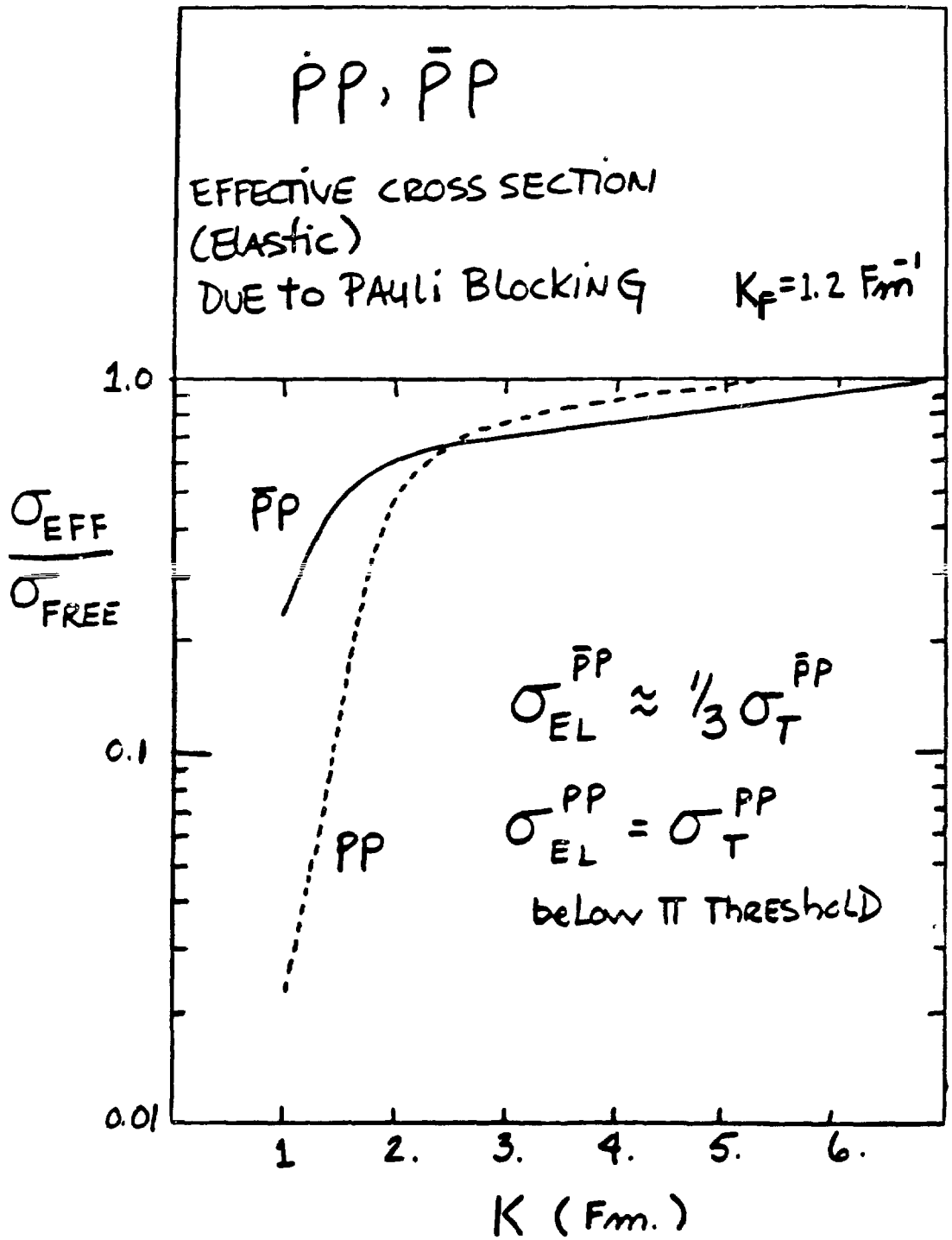

Figure 4: Effective $\bar{p}p$ & pp cross sections due to Pauli blocking (see text). K is relative momentum of collision (see Eqn 3).

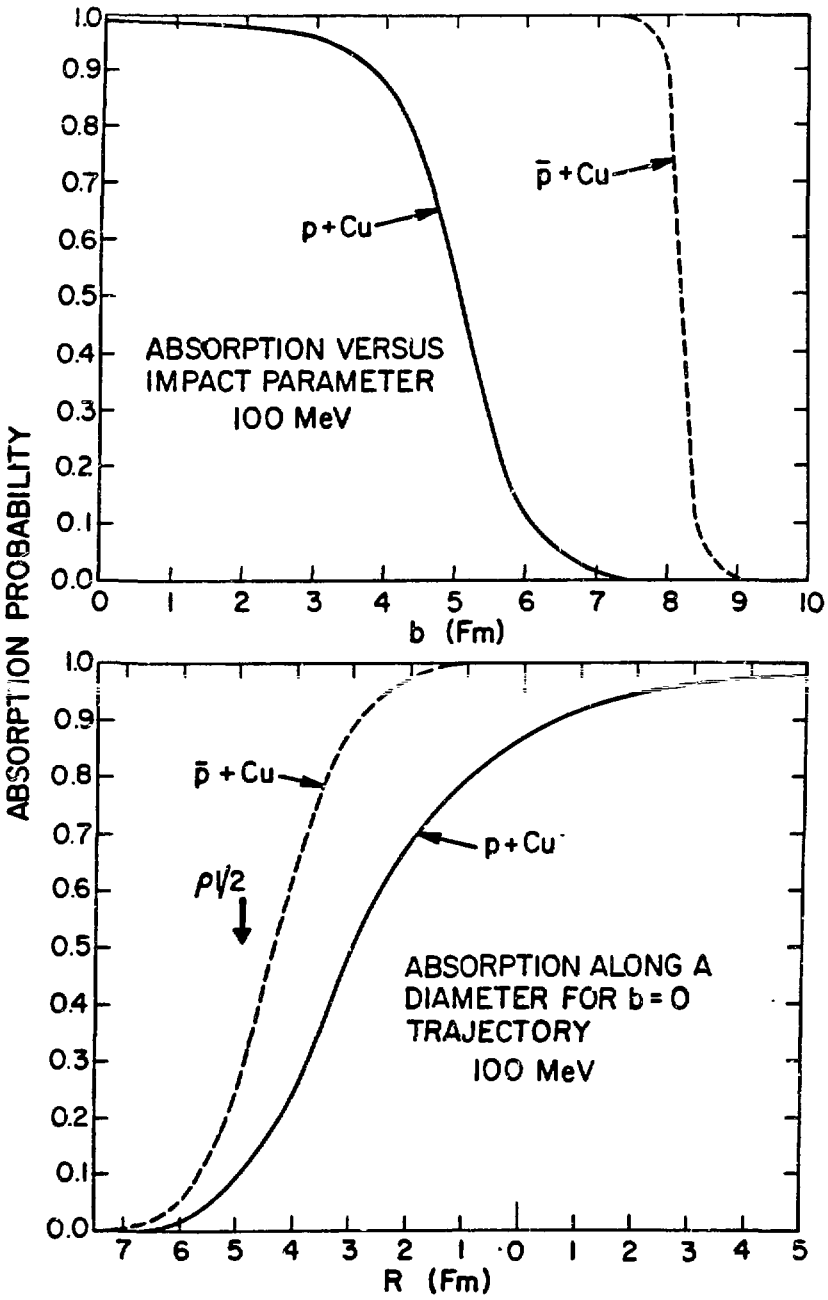

Figure 5: The upper figure shows absorption probability versus impact parameter for $\bar{p}$ and p on Cu at 100 MeV. In the lower figure the absorption probability versus position along a nuclear diameter for b=0 trajectory $\bar{p}$ and p and Cu at 100 MeV (asymptotic energy) is plotted. The radius marked $\rho_{1/2}$ is the half density point.

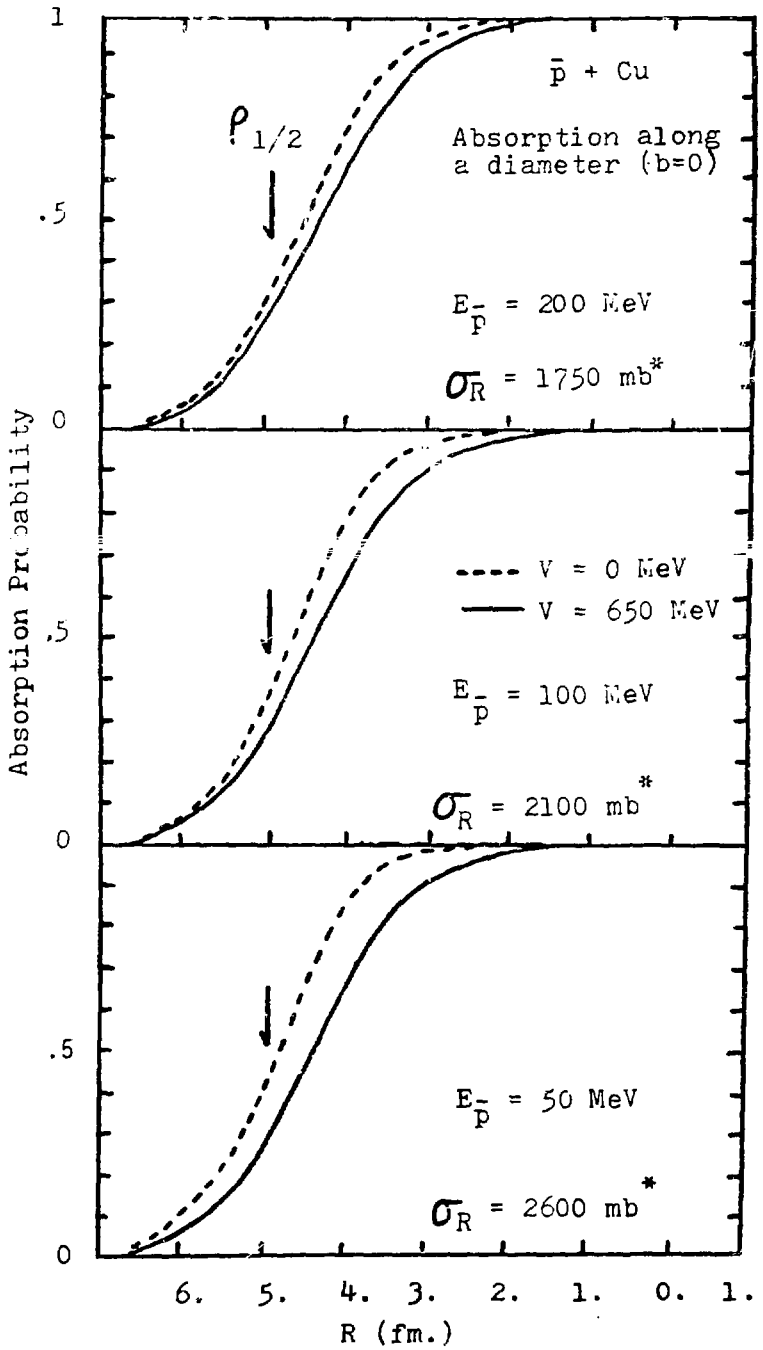

Figure 6 : Sensitivity of $\bar{p}$ penetration to energy and real potential strength. (see Fig 6b for explanation of plot)
* calculated with V = 650 MeV.

RECENT RESULTS AND PHYSICS AT A FUTURE HIGH INTENSITY FACILITY OF E $\lesssim$ 31 GeV

By

Ernest M. Henley
Institute for Nuclear Theory and Department of Physics
University of Washington, Seattle, Washington 98195

I. INTRODUCTION

You will note that the title of my talk refers to a high intensity facility. I hope that this nomenclature will become more prevalent and that the name Kaon Factory will disappear from our vocabulary. A high intensity facility produces a large number of p's, π's, K's and hopefully also p's. So why call it a Kaon Factory?

There is no way in which I can summarize this conference, with its many interesting and though provoking talks. What follows is a partial and biased overview with some personal comments. I apologize for omissions ahead of time.

Yesterday, we heard a fine summary from Lee Teng on the subject of what a 16 GeV, 100μA facility might look like and is likely to cost. The technology is clearly in hand for building and designing such a facility; his proposal was a fast cycling proton synchrotron which would use LAMPF as an injector and produce copious secondary (e.g. $K^{\pm}$) beams. The physics which might be carried out with such an accelerator is based on our present knowledge and some extrapolation therefrom. It is therefore not surprising that this workshop featured summaries of both types of considerations

The advent of medium energy high intensity facilities has led to high precision investigations with pions as well as nucleons. Whereas such investigations have concentrated on nuclei and nuclear structure, the next high energy accelerator is likely, I believe, to be used more for investigations of nucleon and meson structure. Thus, it is most fitting that particle and nuclear physicists get together at workshops such as this one. The investigation of nucleon structure is an area not unrelated to nuclear physics. The confinement of quarks due to many gluon exchanges is a non-local, difficult many-body problem, even harder than ones we deal with in nuclear physics. The "long range" QCD confining force dominates the structure of baryons and mesons. Particle physicists are likely to bypass this important investigation of confinement in their thrust to shorter distances and higher energies, where the physics is simpler. With a higher energy and high intensity accelerator we should be able to make important contributions to a better understanding of confinement and particle structure.

There is another difference between today and a decade or so ago. At the present time much of the experimental physics that is being carried out or planned, is done on the basis of theoretical considerations. The development of the quark-parton model and of QCD for strong forces, of the electro-weak theories of Weinberg and Salam, and more recently of global or grand unification schemes have suggested, and continue to suggest, numerous experimental investigations.

We heard about some of these tests at this conference. The advent of a high intensity high energy accelerator is likely to reverse again the role of theoretical and experimental physicists.

II. HADRONIC STRUCTURE, QCD, QUARK-PARTON MODELS

What we know from QCD is that there is a weak (1/r) gluon exchange force between quarks at short distances. The large distance confining (r^n, $n \simeq 1$) force is not understood. Beyond the confining region there might exist the remnant of a multigluon field. As we heard from R. Hwa, this Van der Waals force could fall off as r^{-n}, $n \geq 7$, and might be detectable. R. Hwa also pointed out that the gluon field is responsible for turning current quarks into constituent quarks (valons). It was stressed by R. Blankenbecler and R. Hwa that it is important to use the correct variables, e.g. use of the infinite momentum frame, in order to obtain a simple physical description. In the absence of a theory for confinement, bag models are used to provide tractable mathematical descriptions. There is a rich spectroscopy of baryons and mesons, which only has been partially explored so far. As we heard from R. Kelly it may well be that these resonances investigated by πN and KN scatterings do not belong to pure configurations of SU(6). Further, it appears that more detailed aspects of the inter-quark forces are required to understand the spectroscopy; for instance spin-orbit forces must be included. These features have a familiar ring to nuclear physicists. Future studies of meson-baryon interactions and resonances with π and K beams should help shed light on these effective quark-quark forces.

Further information on the structure of hadrons can be obtained from photon and electron scattering experiments. V. Hughes gave us a summary of what has been learned so far from polarized electron-polarized proton scattering. Because of the high energy and high momentum transfers involved, the infinite momentum frame is used here. The distribution of (polarization) spin in a proton can come from the spins of the valence quarks, the spins of the sea quarks, from orbital angular momenta, or even from gluons. The SLAC results suggest that when one quark carries most of the momentum ($x \to 1$) of the nucleon it also is responsible for its spin or polarization. This suggests that the other two quarks form a singlet configuration in this region. R. Blankenbecler pointed out that this is also the region for which the quark distribution is understood best with a behavior $\propto (1-x)^n$, with $n = 3$ for baryons and 2 for mesons, and 10 for deuterium. The probability for quarks of high momenta decreases rapidly for heavier nuclei. Clearly more detailed information from electron scattering, such as $\vec{e}\,\vec{d}$ scattering, can be extremely useful. (See Fig. 1a.) Information can also be obtained from e^+e^- annihilation into hadrons and perhaps from lepton pair production experiments such as $\pi p \to \ell^+\ell^- X$ (Drell-Yan process) with polarized beams or targets. (See Figs. 1b and 1c.)

There is little doubt that these high energy processes probe the underlying quark structure of nucleons.

III. THE NN, $\bar{N}N$, ΛN, ΣN....AND OTHER B-B SYSTEMS

Do nuclear forces probe the quark structure of nucleons? To what extent can we understand the B-B (B = baryon) forces in terms of quark-quark forces? How can we search for the underlying quark constituents in these processes? Is the meson exchange force a residue of strong color QCD forces? Can QCD explain

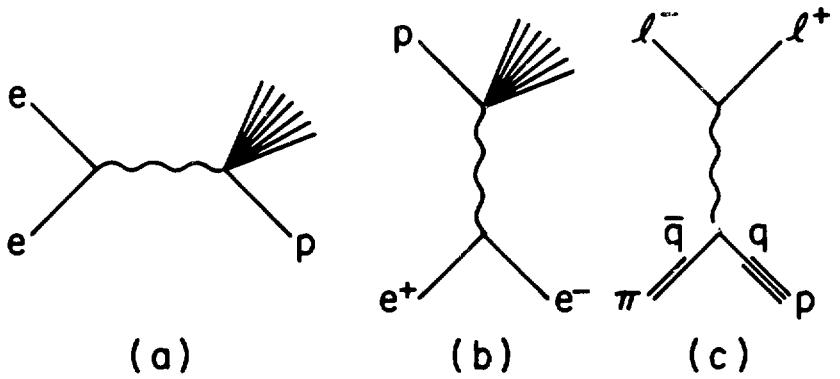

Fig. 1
Probes of nucleon structure: (a) electron scattering, (b) electron-positron annihilation into a proton and other hadrons, (c) lepton-pair production in πp collisions.

why meson exchange forces are successful? What is the spectroscopy of dibaryons and of the baryon-antibaryon system? These questions were raised, but most of them cannot be answered at the present time. A higher energy high intensity accelerator would help.

A. Kerman pointed out the anaology of the interaction of two nucleon bags to the α-α interaction, with strong internal but weak external forces and the need for simple collective variables. We note again that our experience in describing nuclear structure should be helpful in understanding the quark structure of nucleons and baryonic forces. The ΛN and ΣN, $\Lambda\Lambda$, ... forces may be related more simply to those of the NN system in a quark model than in meson theories. For instance, P. Barnes mentioned how the strength of the central, and the weak tensor and spin-orbit ΛN forces can be understood due to a Λ structure as a singlet (ud) coupled to a spin ½ s quark. The Σ would then have a larger spin-orbit force than the N-one as (ud) couple to spin 1. This explanation is not unique but a test of the ΣN spin-orbit force clearly would be of interest.

The BB system, strange and nonstrange, is expected to have a rich spectroscopy. Can this spectroscopy be understood more simply in terms of meson exchanges and resonances, or in terms of 6 quarks? W. Kloet presented the theory and H. Spinka the experimental evidence for resonances in the NN system. Of the various resonances observed in the past, only the $^3F_3$ in pp scattering appears to be surviving. The S = -1 and -2 systems, remain to be explored - only the ΛN one has been studied in any detail, but other ones are likely to be interesting. For instance, as pointed out by P. Barnes, the exotic $\Lambda\Lambda$ system is predicted to be strongly bound, in the $^1S_0$ state. This system has uds quarks in a filled (ℓ = 0) s-state and is analogous to ^{4}He.

In meson theory, the $\bar{N}N$ force can be related to the NN one by G-conjugation, but it also has open annihilation channels. Since $N\bar{N}$ annihilation occurs when these particles are close together, we must have overlapping bags in this case.

Thus the annihilation might be sensitive to the underlying quark structure and to bag dynamics. In Seattle, we find that the $p\bar{p}$ annihilation and scattering data are very sensitive to the bag radius. The $\bar{N}N$ force has been studied both as a $3q3\bar{q}$ or, $2q2\bar{q}$, system, and via meson exchange forces. In both cases a rich spectroscopy of the $B\bar{B}$ system are predicted. R. Tripp reviewed the experimental evidence for these disappearing resonances, but as he pointed out the last word has not been said and future experiments with polarized particles, for instance, at the type of accelerator we are projecting here, may find a whole nest of resonances; in other words the present data may well hide many individual resonances with well defined angular momenta and decay channels. Indeed I also believe that this may be the case and that the $\bar{N}N$ system may yield valuable information about the connection between quark models and meson exchange models. P. Dalpiaz outlined the rich research program which soon will be undertaken at LEAR; it includes scattering and annihilation cross section measurements, studies of $\bar{p}p$ atoms, production of hypernuclei, vector mesons, lepton pairs and other exotic systems, including the study of individually trapped $\bar{p}$'s. There is a rich field of investigation here which is quite different than the NN system. T. Kalogeropoulos argued that a competitive separated $\bar{p}$ beam could be built at the AGS, but so far there has not been enough interest in such a beam to turn it into a reality.

IV. HEAVIER BARYONIC SYSTEMS (NUCLEI)

There remains great interest in studying the nucleus with p, π, K^+, and K^- probes at higher energies. To what extent can such probes be considered as q's or/and $\bar{q}$'s passing through a sea of quarks? R. Eisenstein and A. Thiessen reviewed our present knowledge of pion and kaon scattering and P. Barnes discussed the formation and properties of hypernuclei.

In the former case, considerable effort has gone into understanding pion scattering from nuclei. R. Eisenstein reviewed the various approaches and stressed the importance of the $\Delta(1232)$. The dynamics of the Δ-hole (doorway state) has received considerable attention recently and this approach has proven to be fruitful. The importance of pion absorption and production in elucidating the dynamics of pion nuclear interactions was pointed out. Nuclear spectroscopic studies with pions were reviewed. A. Thiessen pointed out that in addition to low energy and Δ resonance scattering, the use of higher energy (e.g. 600 MeV/c) pions could be helpful in separating the π-n from the π-p interaction. The nucleus is also more transparent to pions at energies above the Δ resonance. The difference between the K^+ and K^- interaction with nuclei was stressed by both R. Eisenstein and P. Barnes. The production of hypernuclei in (K^-, π^-) reactions, and some of the properties of the interactions of Λ's with nuclei were reviewed by A. Thiessen and P. Barnes. Λ hypernuclear spectroscopy has progressed considerably in the past decade. Much work remains to be done, especially for other hypernuclei such as Σ and double $\Lambda\Lambda$ ones. We heard a little about these subjects.

The use of the nucleus as a target may also help to establish its underlying quark structure. For instance, can the A dependence of high energy particle production from nuclear targets be understood in terms of a sea of quarks?

V. ELECTROWEAK AND GRAND UNIFIED THEORIES

The past decade has seen the verification of the remarkable unification of the electromagnetic and weak forces. Cabibbo reviewed this theory for us and pointed out the importance of more precise experiments to test it in detail. Whereas this theory has but one constant (the ratio of charged to neutral boson masses) the grand unified theories (GUT) have a large number of parameters. So our work is cut out for us to determine these parameters in order to test the validity of various theories. Precision experiments are required. I will give but a few examples.

CP violation is still not understood. The most popular model today is that of Kobayashi and Maskawa, but experimental data do not yet allow us to differentiate between this model and others such as the superweak theory. Proposed and possible experiments in K decays to differentiate between these models were reviewed by B. Winstein.

There are 3 colors and 3 generations of quarks. At least 3 generations are required in the Kobayashi-Maskawa model to obtain a meaningful CP violating phase. Since then there also must be, and are, 3 generations of leptons, we can expect CP to be violated among the leptons as well. Such CP violation remains to be discovered.

In modern gauge theories of weak and strong interactions, there is no reason for baryons and lepton number conservation. The hunt is on for rare generation changing and baryon- or lepton-number violation. The present status of muon number violating decays was reviewed by C. Hargrove. As pointed out by Cy Hoffman, the sensitivity of experiments is increasing logarithmically with time but no violation has been discovered as yet. Another consequence of the lack of generation number conservation is neutrino oscillations which occur if, in addition, some neutrinos (ν's) are massive. A review of neutrino oscillation work and of attempts to measure neutrino masses was presented by A. Mann who also pointed out the importance of such searches for astrophysics. His review made it clear that neutrino investigations remain highly interesting even at very low energies. A. Hahn and E. Pasierl reviewed some present results obtained at Grenoble and Savannah River reactors. Soni also discussed an analysis of these data. Although the two experiments are not consistent with each other within one standard deviation (1σ), they do overlap at the 2σ level. The indications for ν oscillations remain very imprecise, but continuing investigations are likely to lead to more accurate results. H. Anderson discussed a possible experiment on n-$\bar{n}$ oscillations to test baryon number conservation.

The experiments on weak interactions are immensely rich in information and can test our understanding of electro-weak as well as unified models. However at energies $\lesssim$ 31 GeV, the effective strength of the interaction is $G\,Q^2/4\pi \sim 10^{-3}$ (G is the weak interaction constant and Q is a measure of the momentum transfer). Since CP violation is weaker than this strength by a factor of 100 or more, it is clear that high precision and high intensities are required. For such experiments, the type of accelerator under discussion would clearly be valuable.

VI. CONCLUSION

Recent theoretical and experimental investigations have shown the value and necessity of searches for rare events and of high precision experiments. For such investigations a high intensity and higher energy accelerator which

can produce new beams such as kaons and antiprotons should be very helpful. At the present time there are more questions than answers. Thus, we do not understand the connection between nuclear physics as we have known it, with meson exchange forces, and the quark-parton model with QCD forces. We do not understand quark confinement. We do not understand the connection of the electroweak and QCD forces. Although there are conjectures and theories, experimental proof is required. Our grasp of weak forces and of nuclear structure should prove helpful in proposing theoretical answers. A high intensity higher energy accelerator should be helpful in providing the required experimental confirmation.